UNIVERSITÉ DU QUÉBEC À MONTRÉAL

ARYLATION CUPRO-CATALYSÉE DE COURTS PEPTIDES CONTENANT L'HISTIDINE AVEC DES TRIARYLBISMUTHINES

THÈSE

PRÉSENTÉE

COMME EXIGENCE PARTIELLE

DU DOCTORAT EN CHIMIE

PAR

HWAI-CHIEN CHAN

AOUT 2022

REMERCIEMENTS

Voilà le moment tant attendu...

Je ne peux commencer l'écriture de cette thèse sans remercier avec beaucoup d'émotions mon grand maître spirituel, guide suprême et accessoirement professeur : Alexandre, aka le Lex. Comment assez te remercier ? Tout d'abord, je te suis reconnaissant de m'avoir accueilli au sein ton groupe et de m'avoir donné cette opportunité inouïe de faire partie du club des PhD. Je te suis reconnaissant pour ta confiance et ton soutien sans failles que tu as pu placer en moi. Je te suis reconnaissant pour chaque jour où j'ai appris quelque chose de nouveau et qui me permet de m'endormir un peu plus intelligent chaque jour (je parle allemand maintenant). Je te suis reconnaissant d'avoir su me conseiller tout le long de ces années de thèse qui ont été d'une facilité presque insolente, certainement grâce à ta supervision sans égale. Et finalement, je te remercie pour tous les moments de joie et de bonne humeur que j'ai pu passer durant ma thèse, on remettra ça à Toronto si un jour j'y vais. Alex, un grand merci !

Après avoir verser quelques larmes, je souhaite remercier mes grands frelons du labo Ahmed, aka Memed et Adrien, aka le Dryxte. Ces quatre années ont été fortes en émotion et c'est évidemment grâce à vous. Je vous aime mes frérots. Ahmed on t'attend de l'autre côté. Je n'oublie pas de remercier chaleureuseument mes sœurettes, Yarelys, aka Yaré et Bianca, aka Bibi, aka cheveux rouges. Merci d'avoir été mon public numéro onu et de rire à pleins poumons à toutes mes blagues bonnes comme mauvaises. Je remercie également toutes les personnes qui m'ont supporté plus ou moins longtemps durant ces années, je pense à toi Léa, à toi Emy et à toi Anna. À tous les membres de la famille Gagnon, je vous remercie !

Par la suite, je souhaite remercier particulièrement Gwilherm Evano qui sans lui toute cette histoire de thèse n'aurait jamais eu lieu. Si un jour tu lis cette thèse, sache que tu as ma reconnaissance éternelle et je te remercie d'avoir eu confiance en moi alors que j'étais encore qu'un chimiste à l'état de larve (je suis encore sous cette forme). Je remercie également mon superviseur de stage Benoît de Boeck qui a su réveiller en moi la curiosité d'un chercheur. Sache que je ne t'ai pas oublié et que notre rencontre a eu une résonance certaine dans ma vie de chimiste.

Je ne peux pas conclure sans remercier toute l'équipe de l'UQÀM qui a contribué de près ou de très près à la réussite de cette thèse. Je pense à Steve Bourgault et son équipe, merci à vous d'être si généreux et de nous laisser utiliser vos appareils indispensables à la réussite de toute thèse (j'avoue c'est moi qui est cassé les portes de la balance du futur), à Alexandre Arnold, merci de t'efforcer chaque jour à maintenir la RMN

opérationnelle, à Luc, merci de te soucier tous les jours du niveau d'azote pour notre boîte à gant, à Sophie, merci d'être l'unique personne à qui mon mandarin reste utile, à Charlotte, merci pour ton génie et qui sans toi notre labo aurait déjà déposé le bilan, à Chantal, merci d'avoir toujours le sourire même à l'ouverture du magasin pour me réapprovisionner en glace sèche, et évidemment à MC, merci d'avoir partagé avec moi trois ans de ma vie à m'enivrer d'ester de banane, inoubliable.

Je remercie évidemment tous les membres de ma famille qui ont cru en moi depuis le tout début, merci au daron, au frérot et ma sœur, pour votre soutien financier et émotionnel. Ah oui c'est vrai, une petite pensée toute particulière à Trang qui sans elle, ces années auraient été bien tristes alors merci pour tes bons petits plats. Mais nan je rigole, on ne peut même plus rigoler… Merci pour ton amour et ton soutien qui ont fortement contribué à la réussite de cette thèse.

Merci à tous, tcho bye !

DÉDICACE

À ma mère,

TABLE DES MATIÈRES

LISTE DES FIGURES

LISTE DES TABLEAUX

LISTE DES ABRÉVIATIONS, DES SIGLES ET DES ACRONYMES

ADN : Acide désoxyribonucléique

AIRCAR : Ribonucléotide 5-aminoimidazole-4-carboxamide

ATP : Adénosine triphosphate

CMD : Déprotonation métallique concertée

CS : Carnosine synthétase

Dba : Dibenzylidèneacétone

DCM : Dichlorométhane

DHP : Dihydropyridine

DIPEA : *N*,*N*-Diisopropyléthylamine

DMF : *N*,*N*-Diméthylformamide

DMSO : Diméthylsulfoxyde

EF2 : Facteur d'élongation 2

FAO : Food and Agriculture Organization of the United Nations (Organisation des Nations Unies pour l'Alimentation et l'Agriculture)

FDA : US Food Drug Administration (Administration américaine des denrées alimentaires et des médicaments)

FG : Formyl glutamate

FIG : Formimino glutamate

Hol-P : Histidinol phosphate

IAP : Imidazoleacetol phosphate

IGP : Imidazoleglycérol phosphate

MT : Méthyl transférase

m-CPBA : Acide *m*-chloroperbenzoïque

NAD : Nicotinamide adénine dinucléotide

NBS : N-bromosuccinimide

NMP : *N*-méthyl-pyrrolidone

PRATP : Phosphoribosyl-ATP

PRFAR : Ribonucléotide phosphoribosyle formimino-5-aminoimidazole-4-carboxamide

ProFAR : Ribonucléotide prophosphoribosyle formimino-5-aminoimidazole-4-carboxamide

PRPP : Phosphoribosylpyrophosphate

RPECV : Répulsion des paires d'électrons de la couche de valence

SAM : S-adénosylméthionine

SPSS : Synthèse de Peptides sur Support Solide

TBHP : Hydroperoxyde de tertbutyle

TFA : Acide trifluoroacétique

Tp : Température pièce

RÉSUMÉ

L'histidine est une membre du groupe très fermé des acides aminés essentiels. Essentiel parce qu'elle est cruciale dans bon nombre de processus biologiques, mais également parce qu'elle n'est pas synthétisée par l'organisme. Ses fonctions s'étendent sur un large panel d'actions : elles peuvent par exemple passer par une simple dégradation métabolique afin de fournir les produits utiles dans d'autres processus ou alors être impliquées dans la structure complexe des chaînes peptidiques aboutissant à des protéines aux implications diverses. Ses différentes caractéristiques font qu'une quelconque modification structurelle de l'histidine peut avoir des conséquences considérables sur l'ensemble de l'organisme. Toutefois, si bien contrôlée et maitrisée, la modification de l'histidine peut avoir des effets bénéfiques et dont toute une discipline s'est développée autour de ce but unique.

En parallèle, depuis ses débuts dans les années 80, la chimie du bismuth a vu son implication croître dans de nombreuses réactions. Une diversité de bon augure, puisque comparé à ses homologues métalliques, le bismuth reste bon marché et présente en plus une toxicité bien moindre. Ces aspects font du bismuth un métal de choix pour l'incorporer dans des réactions chimiques, notamment dans des modifications de l'histidine.

Cette thèse s'inscrit dans la lignée des modifications spécifiques catalysées au cuivre de l'histidine à travers l'usage d'organobismuthines. L'essence de ces modifications repose sur l'arylation de la chaîne latérale de l'histidine, qu'elle soit isolée ou au sein d'une séquence peptidique. À la suite du développement de la méthode, une observation surprenante d'arylation de la chaîne principale a été découverte et sera présentée en détail à travers ce modeste manuscrit.

Mots clés : Histidine • Triarylbismuthines • Arylations sélectives • Petits peptides • Catalysée au cuivre

ABSTRACT

Histidine belongs to the very select group of essential amino acids. Essential because it is crucial in many biological processes but also because it is not synthesized by the organism. Its fonctions extend over a wide range of actions: it can for instance, be involved into a simple metabolic degradation in order to provide useful products for other processess or be involved in the complex structure of peptide chains leading to proteins with various implications. Theses different characteristics mean that any structural modification of histidine can have considerable consequences for the whole organism. However, if well controlled and mastered, modification of histidine can have beneficial effects and an entire discipline has been developed around this single aim.

At the same time, since its beginnings in the 80s, bismuth chemistry has seen its involvement grow in numerous reactions. This diversity augur well since compared to its metallic counterparts, bismuth remain in one hand, inexpensive and in the other hand, has much lower toxicity. These aspects make bismuth a metal of choice for incorporating it in chemical reactions, espcially in histidine modifications.

This thesis is in line with the specific copper-catalyzed modifications of histidine through the use of organobismuthines. The essence of these modifications relies on the arylation of the side chain of histidine, whether isolated or within a peptide sequence. Following the development of the method, a surprising observation of main chain arylation was discovered and will be presented in detail throughout this modest manuscript.

Keywords : Histidine • Triarylbismuthines • Selective arylations • Small peptides • Copper catalyzed

INTRODUCTION

La chimie des peptides a connu plusieurs grandes révolutions au cours de l'histoire. Une première a eu lieu à l'université de Toronto dans les années 1920, grâce aux travaux remarquables des Nobélisés Frederick Banting et John J. R. Macleod, ainsi que de leurs étudiants Charles H. Best et James B. Collip. En effet, leurs travaux portant sur l'insuline ont permis d'apporter une réponse majeure aux malades du diabète. Leur découverte est d'autant plus importante lorsqu'on s'aperçoit des chiffres endémiques du nombre de diabétiques dans le monde. Ce n'est qu'après une trentaine d'années, que l'insuline a pu être complètement séquencée grâce aux travaux de Frederick Sanger, prix Nobel de chimie en 1958.[1] Une petite révolution dans la chimie des peptides mais à l'impact considérable puisqu'il amorcera le séquençage de l'ADN ainsi que les travaux du Robert B. Merrifield avec sa synthèse de peptides sur support solide (SPSS). Cette invention de 1963 le récompensera du prix Nobel de chimie en 1984 et marquera une deuxième révolution majeure en chimie des peptides.[2] En effet, la SPSS est d'une importance et d'un avantage si grand qu'après 60 ans d'évolution technologique, le principe même de cette méthode de synthèse artificielle reste inchangé et est tout autant utilisé. À la suite de ces grandes découvertes et inventions, la chimie peptidique vit actuellement sa troisième révolution. Effectivement, depuis ces dernières décennies, le nombre de peptides à usage thérapeutique ne cesse de croître au fil des années en passant de l'insuline, unique peptide à caractère pharmaceutique, à plus de 80 peptides à ce jour approuvés par la FDA (US Food Drug Administration), ce qui représente 8% des médicaments mis sur le marché.[3, 4] Il est évident qu'une telle présence ne peut être due par le simple caractère naturel des acides aminés que composent les peptides, mais également aux astucieuses modifications chimiques de ces derniers. En effet, l'utilisation de peptides non-naturels a joué un rôle crucial dans l'amélioration et l'optimisation des effets thérapeutiques des peptides. Dans la littérature, il existe à ce jour une quantité appréciable de méthodes permettant la synthèse de peptides non naturels. Ces derniers peuvent être obtenus selon trois grandes catégories de méthodes, à savoir par la synthèse classique non initiée par des acides aminés, par le recours à des acides aminés non-naturels ou alors par la modification post-synthétique du peptide.

Par le passé, notre groupe de recherche a rapporté de nouvelles méthodes de modification peptidique par l'arylation chemosélective de la chaîne latérale des peptides du tryptophane ou de la tyrosine. Au cours de ces précédents travaux, différents acides aminés ont été soumis aux conditions d'arylation nouvellement établies et l'histidine a présenté une affinité remarquable. C'est dans cette optique que s'est inscrite l'essence même de mes travaux de recherches. En effet, dans le but de fournir une suite logique et complémentaire à ces travaux, mes recherches se sont appuyées comme précédemment, sur l'utilisation de triarylbismuthines catalysée au cuivre afin de modifier des peptides contenant l'histidine.

Les résultats obtenus à l'issue de ces recherches seront décrits après une mise en contexte de l'importance de l'histidine au sein des peptides naturels, de l'état de l'art des modifications de l'histidine et de ses applications dans différents domaines. Un bref historique de la chimie du bismuth et ses applications dans les modifications de peptides sera également présenté avant l'insertion des dites publications qui formeront le cœur central de cette thèse.

CHAPITRE 1

L'HISTIDINE, DE L'ACIDE AMINE AUX PEPTIDES

Dans ce chapitre, il sera question de l'importance de l'histidine dans sa globalité. Comprendre comment l'histidine est synthétisée chez les différentes espèces tout en décrivant son rôle à travers les bactéries, les plantes ainsi que les animaux. On y énumérera quelques particularités de sa réactivité biochimique et chimique tout en apportant les détails qu'ont pu découvrir les chimistes à son égard.

1.1 L'histidine au quotidien

Découvert indépendamment pour la première fois par Albrecht Kossel et Sven G. Hedin en 1896, l'acide 2-amino-3-(1H-imidazol-4-yl)propanoïque, plus communément appelé histidine, est l'acide aminé dont sa chaîne latérale est pourvue d'un imidazole. Parce qu'elle participe dans une multitude de mécanismes biologiques, l'histidine est d'une importance cruciale chez tout être vivant, mais semble être d'une importance tout aussi fondamentale en chimie aux vues de ses propriétés chimiques particulières.

1.1.1 Chez les êtres vivants

L'alimentation chez les êtres humains régit son unique apport en histidine car elle a la particularité d'être synthétisée chez tous les procaryotes, champignons et plantes, mais pas chez les animaux. La biosynthèse de l'histidine se déroule en 10 étapes et engage une multitude d'enzymes propres à chaque espèce. Elle débute par la condensation du phosphoribosylpyrophosphate (PRPP) avec de l'ATP (Adénosine triphosphate) pour former le phosphoribosyl-ATP (PRATP) avant d'être hydrolysé en ribonucléotide prophosribosyle formimino-5-aminoimidazole-4carboxamide (ProFAR) sous l'action de deux hydrolases successives. Une isomérase initie l'ouverture du phosphoribosyle conduisant au ribonucléotide phosphoribosyle formimino-5-aminoimiadazol-4-carboxamide (PRFAR) qui entraîne, grâce à l'IGP synthase et une glutamine, la formation de ribonucléotide 5-aminoimidazole-4-carboxamide (AICAR) et de l'imidazoleglycérol phosphate (IGP). Le AICAR est recyclé en ATP alors que l'IGP subit une déshydratation sous l'effet d'une enzyme conduisant à l'imidazoleacetol phosphate (IAP). Par la présence d'une aminotransférase et de glutamate, l'IAP passe sous la forme d'histidinol phosphate (Hol-P) qui est rapidement déphosphorylé en histidinol. Catalysé par l'histidinol déshydrogénase, ce dernier est finalement oxydé par deux NAD^+ en histidine (Figure 1-1).[5, 6]

Figure 1-1 Biosynthèse générale de l'histidine. Adaptée de [5]

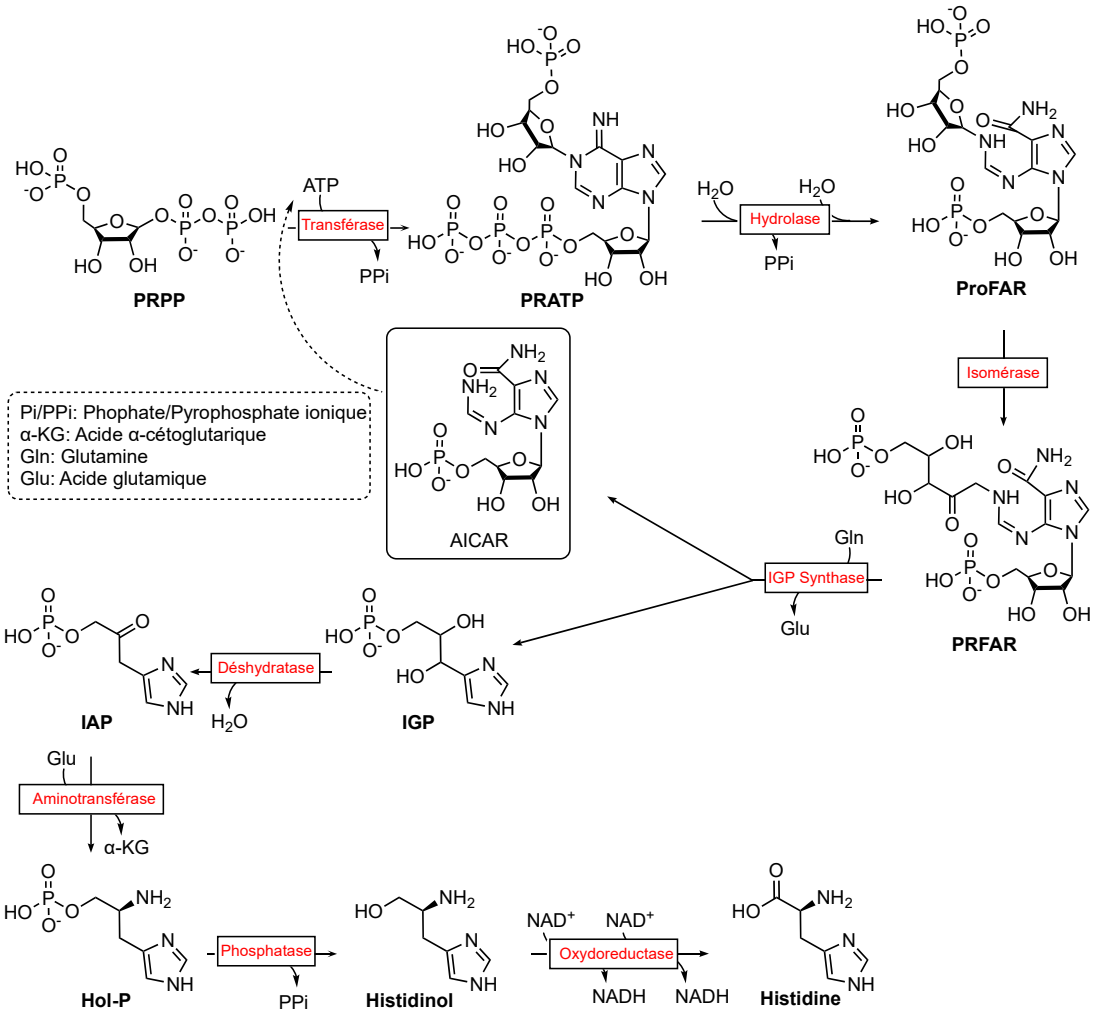

Chez les bactéries la biosynthèse de l'histidine est hautement conservée et se classe au quatrième rang des processus amino-synthétiques les plus gourmands en énergie, après la synthèse du tryptophane, de la phénylalanine et de la tyrosine.[7] Ce processus est tellement énergivore que la plupart des bactéries ont su développer une capacité à se servir uniquement de l'histidine présente dans son environnement dans un but totalement économique. L'évolution a même abouti à la mutation de certaines souches de bactéries en espèces auxotrophes, c'est-à-dire, incapables de synthétiser l'histidine par leur propre moyen et de devoir dépendre d'un hôte. Ces derniers ont la particularité d'être souvent pathogène pour l'humain, on peut y trouver par exemple, le *Mycobacterium genitalium* responsable d'urétrites,[8, 9] l'*Helicobacter pylori* responsable de gastrites et d'ulcères à l'estomac ou bien encore l'*Haemophilus influenzae*, qui lui est responsable de pharyngites.[9] Bien entendu, bien que la biosynthèse de l'histidine soit un processus hautement conservé, chaque espèce de bactérie possède une affinité aux acides aminés qui lui est propre afin de croître et/ou de développer une résistance à son milieu. Par exemple, *Escherichia coli* peut n'utiliser

que la serine, l'aspartate, la cystéine, la glycine, le glutamate et l'alanine comme unique source d'azotes et de carbones pour se développer et essaye d'éviter les milieux trop concentrés en valine et en leucine. Par opposition, l'espèce *Staphylococcus aureus* a souvent besoin de valine, de proline, d'arginine et de cystéine pour proliférer.[10] De manière complémentaire à la biosynthèse, l'*Histidine Utilization* (Hut) *system* est la voie catabolique de l'histidine chez les bactéries. Ce processus est tout autant conversé qu'universel et débute par l'action de l'histidase sur l'histidine conduisant à l'urocanate en libérant de l'ammoniac. L'urocanase va ensuite catalyser la formation du propionate d'imidazolone avant l'ouverture du cycle imidazolone par l'IPase pour former du formimino glutamate (FIG). À cette étape, deux voies sont possibles en fonction des espèces. Une première voie permet la formation directe en glutamate et d'un formamide par l'action d'une FIGase. Alors qu'une deuxième voie passe d'abord par la formation du formyl glutamate (FG) avant d'aboutir au glutamate tout en éliminant de l'ammoniac et du formaldéhyde (Figure 1-2).[11]

Figure 1-2 *Histidine Utilization system* : voie métabolique de l'histidine chez les bactéries. Adaptée de [11]

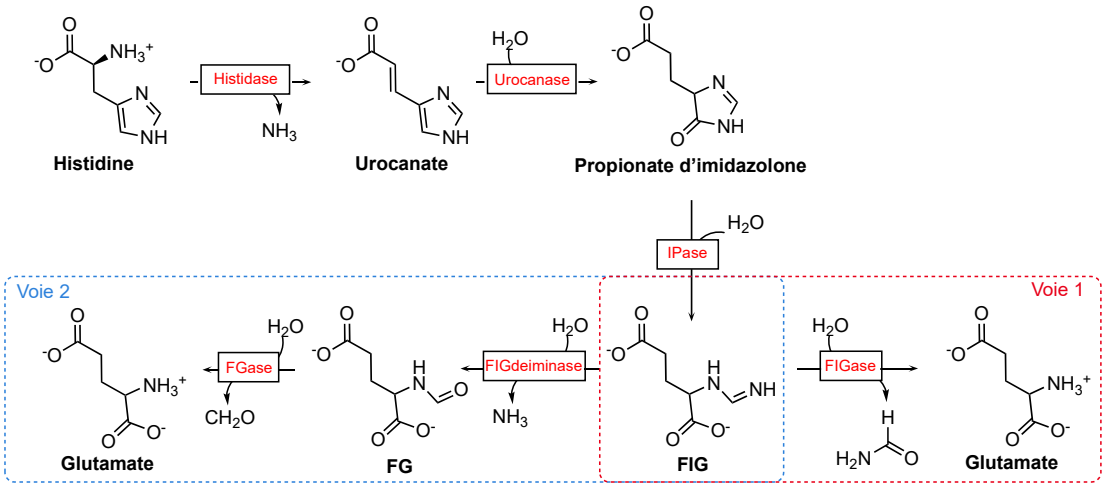

Chez les plantes, la production d'histidine s'effectue dans les chloroplastes et joue un rôle crucial dans la croissance et le développement de la plante. Des travaux effectués sur l'arabette de Thalius ont permis de démontrer qu'en faisant des *knockdowns* de différents gènes des enzymes responsables de la biosynthèse de l'histidine, il était possible d'observer différents phénotypes de silique (fruit de la plante). En effet, le désamorçage du gène *hisn2-1* conduit à la formation de siliques blanches et/ou atrophiées, tandis que celui du gène *hisn8* mène à la présence de siliques immatures. L'apport en solution riche en histidine a permis de sauver partiellement les siliques juvéniles, concluant ainsi de l'importance de l'histidine dans le développement et la croissance des plantes.[12] L'histidine, de par la nature de ses fonctions chimiques, possède une forte affinité au zinc, cobalt, cuivre et nickel et joue un rôle supplémentaire crucial dans la régulation et le transport de ces métaux lourds potentiellement toxiques. Effectivement, face à la présence

de ces métaux provenant de sols souillés, les plantes ont su développer une réponse défensive qui consiste en la synthèse accrue d'histidine, qui envoyée dans les racines vont complexer les métaux avant de les transporter jusqu'aux feuilles afin de les stocker sans danger.[13, 14] Ces complexes sont formés par la co-coordination de deux histidines avec le métal, dont l'azote de l'amine, l'azote de l'imidazole ainsi que l'oxygène du carbonyle de chacun des résidus formant le trident chélatant. La nature du métal influence le caractère cristallographique du complexe. La chélation d'un atome de cuivre, de nickel ou de cobalt par l'histidine suivra un système cristallin orthorhombique alors qu'un atome de zinc préférera un système tétragonal (Figure 1-3).[15, 16]

Figure 1-3 Complexes de métal avec l'histidine obtenus par cristallographie

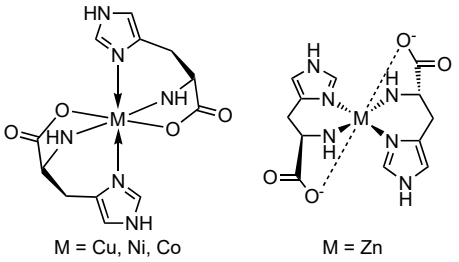

Chez les animaux, de manière assez similaire, l'histidine va jouer un rôle fondamental à la fois dans la croissance et le développement, mais également dans le transport et la séquestration des différents métaux. Par ailleurs, d'après l'Organisation des nations unies pour l'alimentation et l'agriculture (FAO), il est recommandé pour un adulte de consommer de 8 à 12 mg/kg d'histidine par jour.[17] Il est possible de la retrouver en grande quantité dans la viande rouge et dans le poisson sous forme libre ou protéique. L'importance de l'histidine peut également être soulignée à travers différentes voies cataboliques. Une première voie permet l'élimination de l'excès d'histidine par l'action d'une transaminase et d'un pyruvate pour la transformer en imidazole lactate, afin d'être éliminée par les urines plus facilement. Une deuxième voie consiste en la décarboxylation de l'histidine en histamine, un neurotransmetteur responsable des réponses immunitaires ainsi que de la régulation physiologique dans l'intestin. Une troisième voie possible est sa transformation en acide urocanique, un chromophore s'accumulant dans l'épiderme jouant un rôle protecteur dans la photocarcinogénèse.[18] Et enfin, les deux dernières voies possibles seraient sa transformation en ansérine soit par l'intermédiaire du méthylhistidine, soit par l'intermédiaire du carnosine. À savoir que l'ansérine et la carnosine sont des actrices dans les réactions inflammatoires du sang et

pourraient retarder la maladie d'Alzheimer chez les personnes âgées si consommées en plus grande quantité (Figure 1-4).[19]

Figure 1-4 Les voies cataboliques de l'histidine. MT : Méthyl transférase ; CS : Carnosine synthétase. Adaptée de [17]

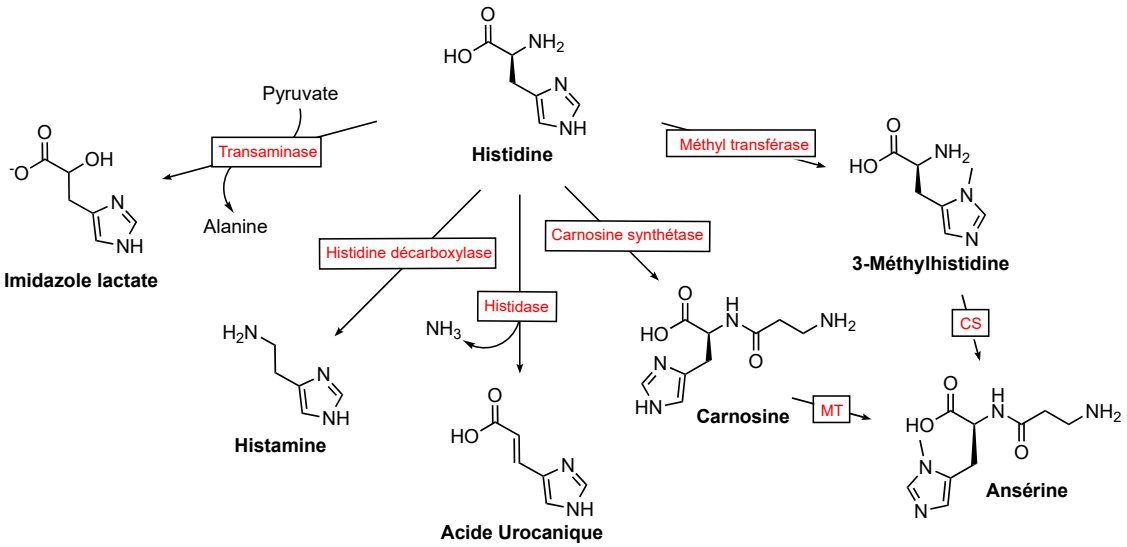

D'autres recherches sur différentes espèces ont également démontré l'utilité de l'histidine. Notamment chez les poissons, une alimentation riche en histidine va non seulement avoir un impact sur la taille des spécimens mais également sur la prévention de la cataracte, une maladie souvent observée dans les pisciculture.[20-22] Chez les rongeurs, une quantité accrue d'histidine ingérée conduit à une satiété plus rapide sûrement due à l'action neurologique de l'histamine.[23, 24] Chez les poules d'élevage, un régime enrichi en histidine induit une augmentation du taux en carnosine et en ansérine dans les muscles, ce qui peut être perçu comme une amélioration de la qualité de la viande.[25] Finalement chez les vaches laitières, un tel régime augmenterait la production de lait.[26]

Au-delà de l'importance de l'histidine en tant qu'acide aminé libre, l'histidine joue un rôle plus important encore dans le domaine des peptides et des protéines. Ceci est facilement compréhensible lorsqu'on s'aperçoit de sa forte sensibilité au pH. En effet, le pKa de sa chaîne latérale d'environ 6 permet à l'histidine d'endosser les caractéristiques d'un ampholyte ; puisqu'à bas pH elle sera donneuse de protons sous sa forme cationique doublement protonée, et à pH physiologique elle sera accepteuse de protons sous sa forme neutre mono-protonée. Petite particularité à pH physiologique, l'histidine peut se présenter sous la forme de deux tautomères, le tautomère protoné N^{τ} et le tautomère protoné N^{π} (Figure 1-5A).[27] Ainsi, l'histidine se retrouve souvent au niveau des sites actifs des protéines ou des sites catalytiques de différents enzymes et se classe première en tant que résidu le plus enclin à être impliqué dans les mécanismes catalytiques. Elle

intervient le plus souvent dans les hydrolases et oxydoréductases, moins souvent dans le cadre des lyases et transférases et plus rarement dans les cas d'isomérases et ligases (Figure 1-5B).[28] Au niveau des sites catalytiques, l'histidine est souvent accompagnée par deux autres acides aminés pour ainsi former ce qu'on appelle une triade catalytique. Il en existe plusieurs types, mais la triade Ser-His-Asp de la chymotrypsine est certainement la plus connue. Elle catalyse des protéolyses en aval des résidus tyrosine, tryptophane, phénylalanine, méthionine et leucine. Son mécanisme d'action débute à la suite de l'augmentation du pKa de l'histidine par l'aspartate par le biais d'un pont hydrogène. S'en suit l'activation de la serine qui va alors attaquer le carbonyle du substrat formant ainsi l'hémiacétal anionique. L'ester se forme en cassant le lien amide et l'histidine cationique se retrouve de nouveau neutre. Cette dernière va donc pouvoir activer une molécule d'eau qui va effectuer une réaction de saponification de l'ester, rétablissant ainsi la triade catalytique de départ (Figure 1-5C).[29] Les autres triades impliquant l'histidine, telles que les triade Cys-His-Asp, Cys-His-Ser et Ser-His-His, constituent également le site catalytique d'autres protéases et possèdent un mécanisme d'action similaire.

Figure 1-5 A – Histidine cationique et neutre ainsi que ses tautomères. B – Propension catalytique de 10 acides aminés selon les familles d'enzymes. C – Mécanisme d'action de la triade Ser-His-Asp de la chymotrypsine.

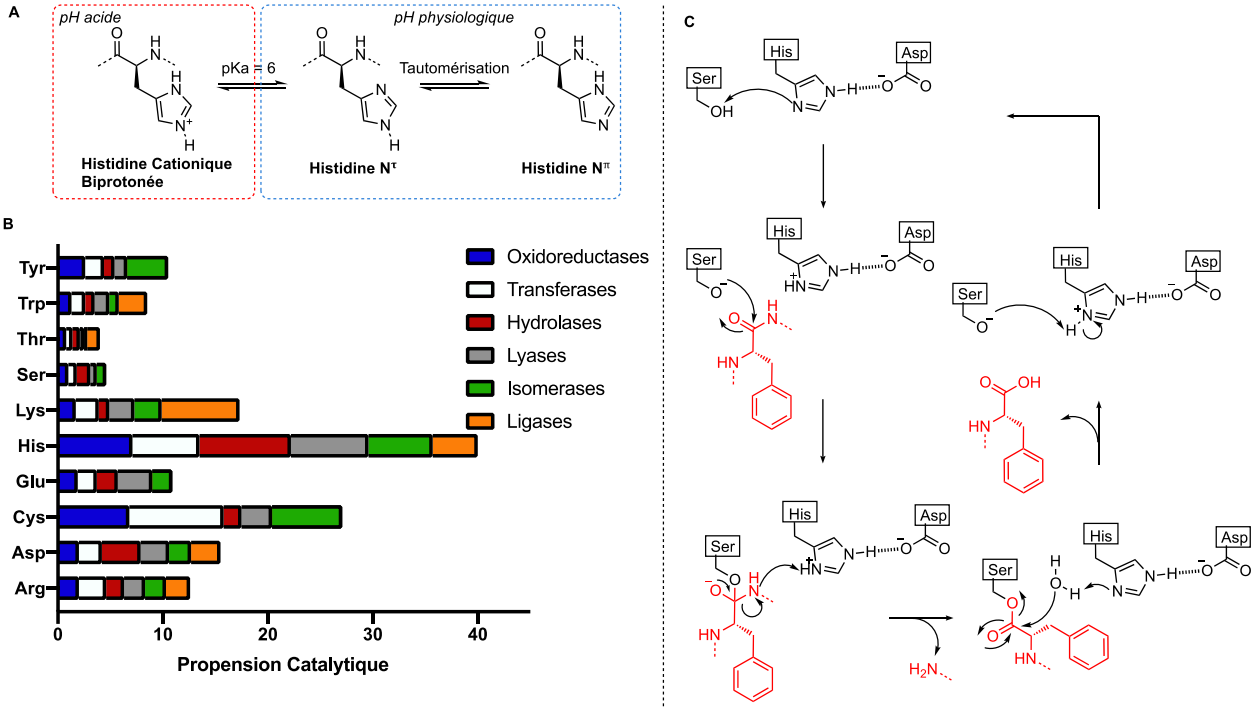

L'histidine est donc un acide aminé essentiel, car indispensable au développement chez tous les êtres vivants, non seulement par elle-même, mais également parce qu'elle est le précurseur de plusieurs composés à caractère immunologique. De plus, de par sa richesse chimique, elle se retrouve souvent au cœur de

mécanismes catalytiques dans de nombreux enzymes aux rôles diversifiés. Du fait de ce rôle bien précis, l'absence ou la modification structurelle de l'histidine conduirait à une perte certaine de l'activité de l'enzyme. En chimie médicinale, il n'est pas rare de souhaiter réduire l'activité d'une protéine et pour cela il est inévitable de passer par des modifications chimiques.

1.1.2 Chez les chimistes

Avant de voir comment modifier l'histidine, il est intéressant d'abord de pouvoir la synthétiser. Dans le but de mieux comprendre l'origine de la vie, la synthèse de l'histidine a été décrite pour la première fois en 1987 par Shen qui a fait condenser de l'érythrose avec du formamidine pour former tout d'abord de l'imidazole-4-acétaldéhyde qui va par la suite le transformer en histidine à travers la réaction de Strecker avec un rendement global de 4% (Figure 1-6).[30]

Figure 1-6 Synthèse de l'histidine à partir d'érythrose

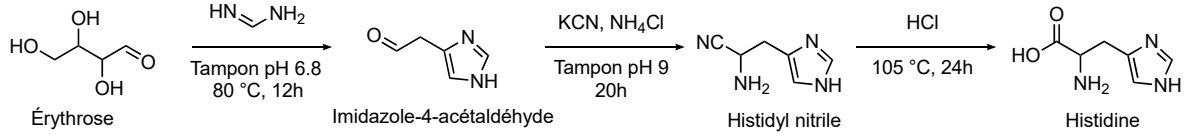

La demande en histidine dans le monde ne cesse de grandir et son marché global a été évalué à 252 millions de dollars en 2022 et pourrait valoir 354 millions d'ici 2028.[31] Il est évident que la synthèse classique d'histidine n'est pas assez rentable à l'échelle industrielle et c'est à ce titre que les méthodes actuelles de production d'histidine se font majoritairement par fermentation de souches bactériennes.[32, 33] De plus, c'est parce que l'histidine est souvent utilisée en tant qu'additif alimentaire que les groupes agroalimentaires sont les plus grands demandeurs en histidine. L'industrie pharmaceutique participe également à la prospérité du marché, mais pour des objectifs cette fois-ci tout autre, comme son utilisation en tant que catalyseur mais également de sa modification structurelle.

1.2 L'histidine, catalyseur de la réaction d'aldolisation

L'utilisation d'acides aminés comme catalyseur dans la réaction d'aldolisation a remarquablement été étudié par MacMillan. Les acides aminés permettent de se passer à la fois de l'utilisation de métaux de transition et de devoir préactiver le carbonyle en énolate (Figure 1-7A).[34] Outre la proline, plusieurs groupes de recherche ont activement exploré l'activité catalytique des différents acides aminés, incluant l'histidine. Bien qu'efficaces, ces différentes recherches montrent cependant une profonde limitation dans la diversité des aldéhydes utilisables et n'abrogent pas des limitations pratiques et chimiques.[35-39] En effet, les grandes limites persistantes sont la nécessité d'ajouter lentement le carbonyle nucléophile, dit donneur, par le biais

d'un pousse-seringue afin d'éviter les sous-produits d'homoaldolisation et qu'un carbonyle non-énolisable ne puisse jouer uniquement le rôle d'accepteur. Ce n'est que grâce aux études de Mahrwald que l'histidine a pu se différencier des autres acides aminés et enfin apporter une réponse valable à ces deux problématiques, car elle permet de réaliser la réaction en *one-pot* et de synthétiser des aldols à centre quaternaire jusque-là impossibles (Figure 1-7B).[40-42]

Figure 1-7 A – Aldolisation catalysée par une proline ; B – Versatilité de l'aldolisation catalysée par l'histidine

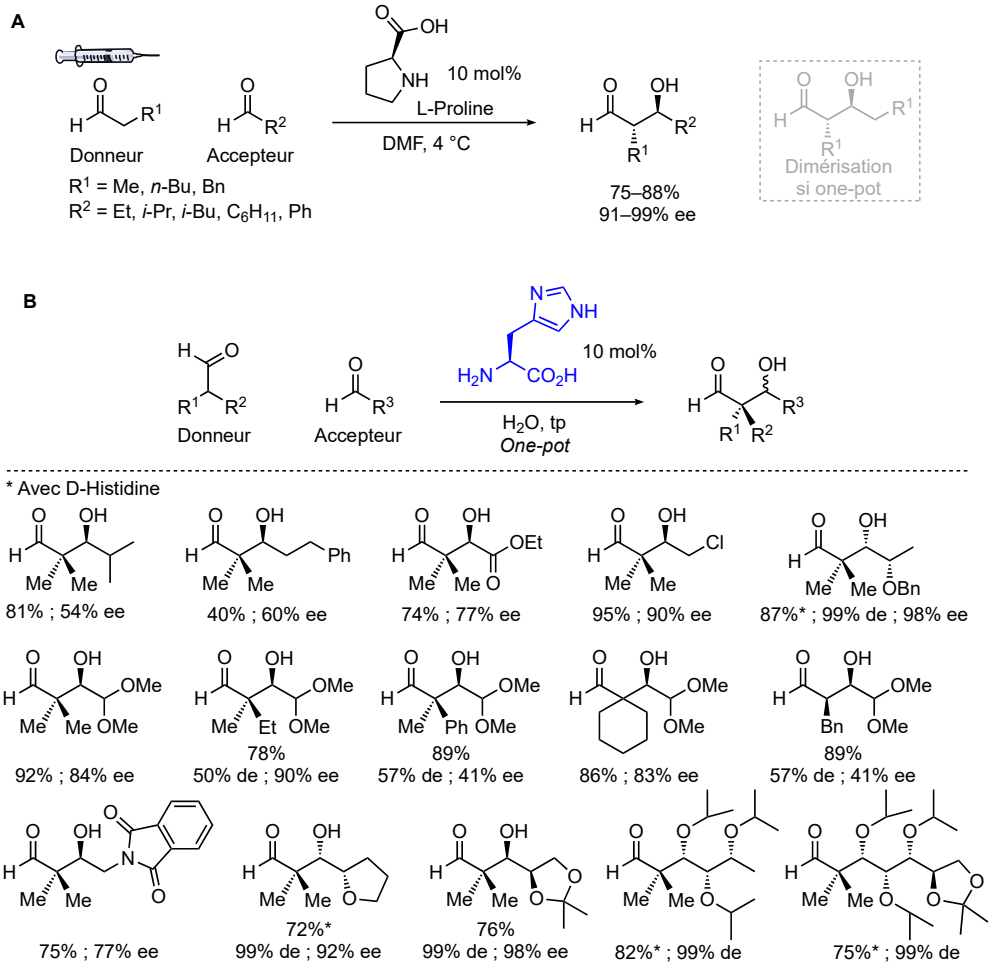

Si jusque-là l'emploi de l'histidine semble être l'équivalent pratique de la proline, une différence sur la stéréochimie du produit formé existe selon l'acide aminé utilisé. En effet, de son côté la proline favorise la formation d'un produit anti parce que son mécanisme passe par un état de transition chaise de Zimmerman-Traxler favorisant l'attaque nucléophile sur la face Ré du carbonyle accepteur.[43] Tandis que dans le cadre de l'histidine, l'état de transition de type « Zimmerman-Traxler » provient du pont hydrogène formé avec l'imidazole bloquant le carbonyle dans une configuration décalée minimisant les interactions gauches. Le

carbonyle accepteur ainsi bloqué subit une attaque nucléophile sur sa face Ré conduisant à la formation du produit syn (Figure 1-8).[44]

Figure 1-8 Mécanismes de l'aldolisation catalysée par la proline (gauche) et par l'histidine (droite)

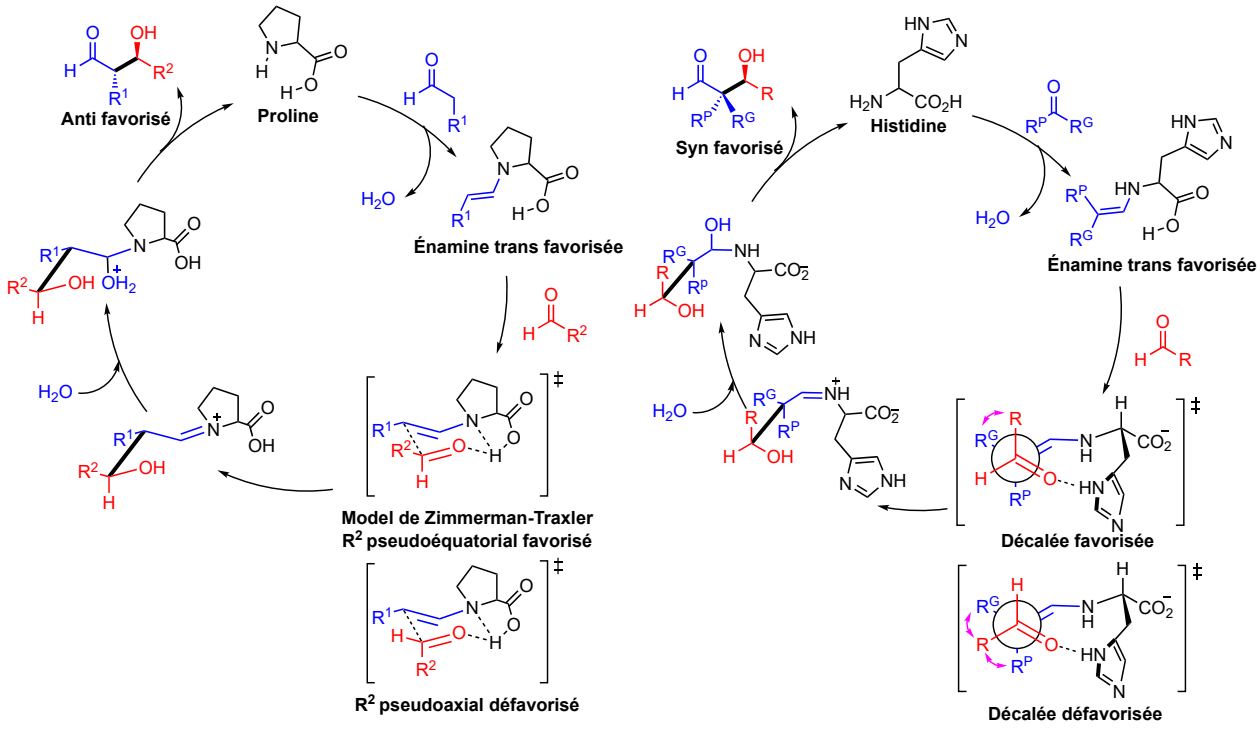

Apporter des modifications structurelles à l'histidine, comme un groupement protecteur sur l'azote terminal, inhibe totalement la réaction d'aldolisation. Ceci démontre à un certain point l'importance de chaque fonction chimique pour une activité donnée. Sur ce principe même, plusieurs groupes ont mené des études sur la modification spécifique de l'histidine et parfois son impact sur son environnement.

1.3 Les modifications synthétiques de l'histidine

1.3.1 Alkylations et groupements protecteurs

Les premières modifications que l'on peut apporter sur l'histidine sont l'ajout de groupements dits protecteurs au niveau de l'acide carboxylique, de l'amine terminale ainsi que de la position N^{τ}. Ces modifications sont assez triviales puisque l'histidine se retrouve le plus souvent reliée à d'autres acides aminés et la position N^{τ} est suffisamment nucléophile pour être facilement occupée par divers groupements par simples réactions de substitution. À l'inverse, les groupements protecteurs ou la présence d'un groupement alkyle à la position N^{π} sont pour le coup beaucoup moins fréquents et méritent d'être soulignés. Une méthode robuste largement utilisée permet l'obtention d'un groupement alkyle à cette position, mais il

est néanmoins nécessaire de protéger la position N^{τ} au préalable. Ainsi les alkyles, allyles ainsi que les benzyles sont tous compatibles avec des rendements excellents.[45, 46] De manière tout à fait similaire, des groupements protecteurs d'éthers peuvent également être installés (Figure 1-9A).[47-50] Ces groupements protecteurs ont non seulement l'avantage d'être compatibles à la synthèse peptidique sur support solide, mais confèrent également le pouvoir d'empêcher totalement la racémisation de la molécule. En effet, l'azote N^{π} est parfaitement situé pour arracher un proton en alpha du carbonyle et un groupement quelconque à ce niveau inhiberait totalement ce genre de phénomène (Figure 1-9B).[51]

Figure 1-9 A – Alkylation de la position N^{π} de l'histidine ; B – Mécanisme de la racémisation de l'histidine

[a] R_2–Br ou R_2–I, Et_3N, DMF, tp ou 50 °C, 36–72h; [b] R_2–OH, Tf_2O, DIPEA, DCM, -75 °C à tp, 16h; [c] Me_3OCH_2Cl, CCl_4/DCM; [d] Adom-Cl, DCM, tp, 8h; [e] $BnOCH_2Cl$, Et_2O, tp. puis Et_3N, MeOH; [f] MBom-Cl, DCM, tp, 4h

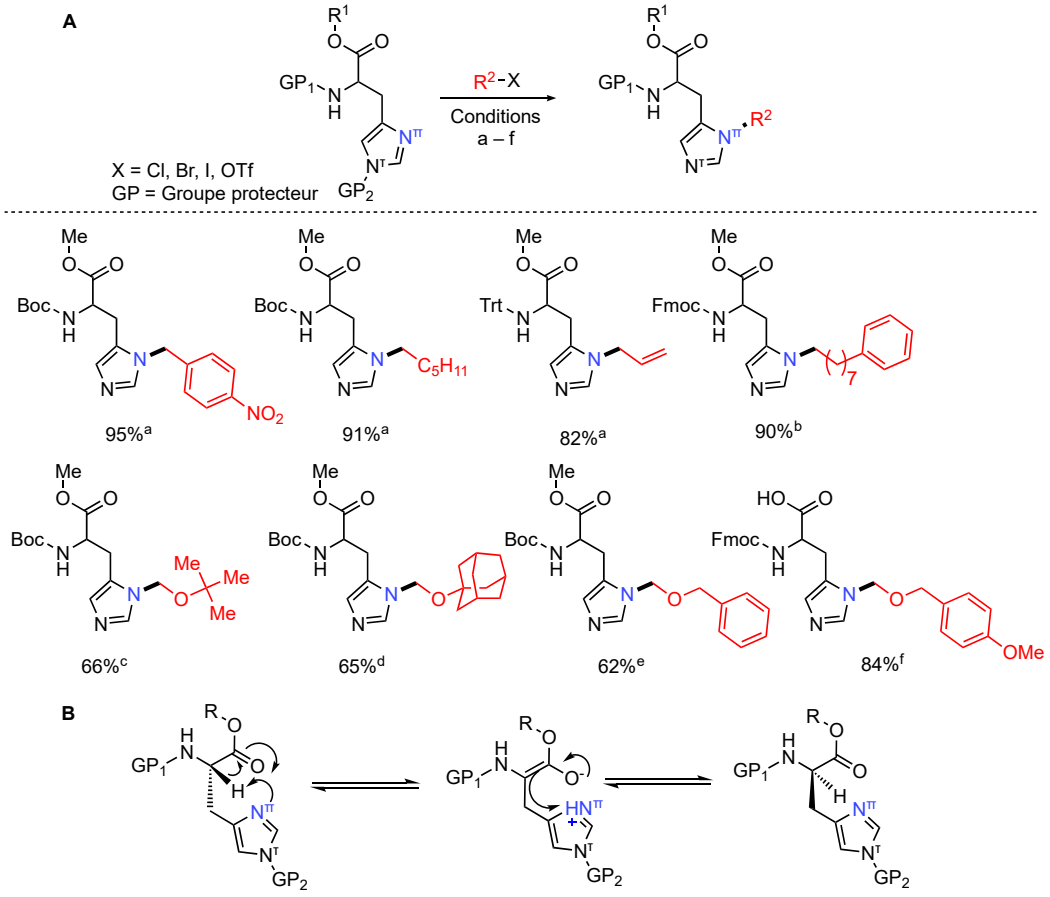

Dans le cadre d'une étude de synthèse asymétrique, une équipe a réussi à additionner un alkyle chiral sur la position N^{π} par le biais d'une ouverture d'époxydes. Mais n'ayant pas protégé la position N^{τ}, les résultats obtenus démontrent que l'alkylation de l'azote N^{π} reste grandement défavorisée sans trop de surprise avec un ratio (*S,R*)-Nτ:(*S,S*)-Nτ:(*S,S*)-Nπ:(*S,R*)-Nπ de 28:18:1:5 (Figure 1-10).[52]

Figure 1-10 Étude asymétrique de l'alkylation des azotes de l'imidazole de l'histidine

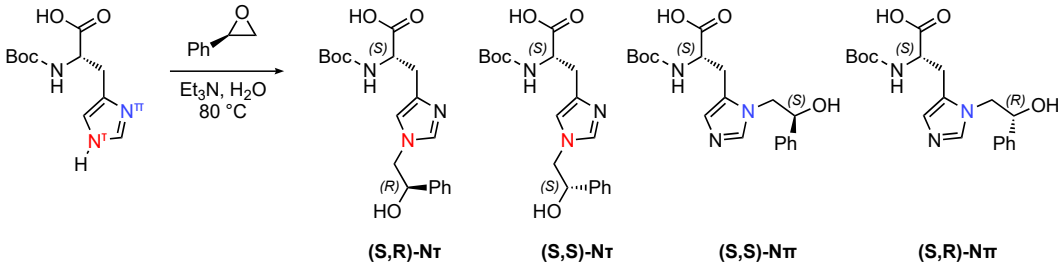

Dans ce cadre bien précis, l'espèce dialkylée n'est qu'un intermédiaire obligatoire à l'obtention du produit N^{π}-monoalkylé désiré. Cependant, il existe dans la nature des théonellamides, une famille de peptides aux propriétés antifongiques isolée d'éponges de mer, qui comportent une histidine cationique dont ses deux azotes de sa chaîne latérale sont alkylés (Figure 1-11A).[53] Dans une optique similaire, le groupe de Bang a réussi à synthétiser et isoler l'histidine doublement alkylée et de l'utiliser par la suite dans la synthèse d'un lipo-peptidomimétique, un peptide aux propriétés antimicrobiennes (Figure 1-11B).[54]

Figure 1-11 A – Structure du Théonellamide A ; B – Synthèse d'un lipo-peptidomimétique

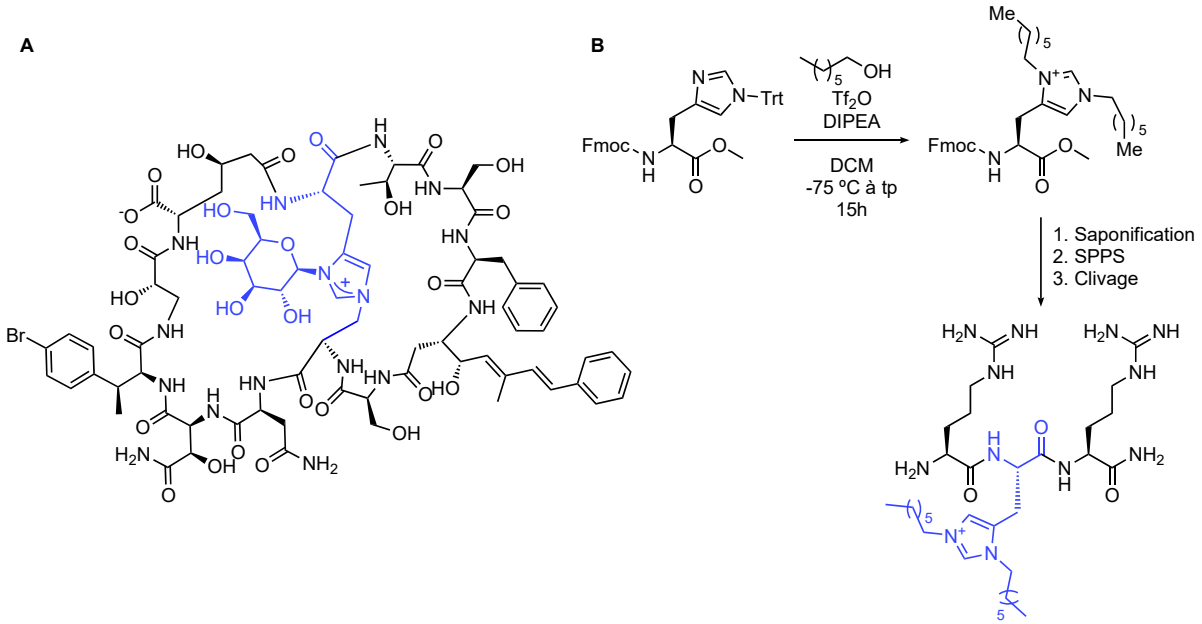

L'alkylation chimiosélective de l'imidazole à la position N^{π} au sein d'un petit peptide est possible et a été découverte par hasard par le groupe de Burke aux États-Unis. En mettant en présence l'histidine N^{τ}-protégée d'un pentapeptide sur support solide dans les conditions réactionnelles de Mistunobu, ils ont découvert que l'azote N^{π} s'est retrouvé alkylé.[55] Ils ont tout d'abord pensé que la présence de la thréonine O-phosphorylée située à un résidu de distance jouait un rôle dans le mécanisme réactionnel, mais la nécessité d'un deuxième

équivalent de « réactifs de Mistunobu » pour que l'azote N^{π} se retrouve alkylé ainsi que la présence de l'alkyle sur le groupement phosphate sur le produit final, ont permis de démontrer le contraire (Figure 1-12A).[46] Le groupe ne s'est pas arrêté à l'étude mécanistique et a poursuivi leurs travaux en étudiant l'activité inhibitrice de cette nouvelle molécule sur la polo-like kinase 1 (Plk1), une protéine jouant un rôle dans la mitose et la méiose. En ce faisant, ils ont découvert qu'en ajoutant un macrocycle au peptide reliant l'imidazole de l'histidine à l'amide terminal il était possible d'améliorer son caractère inhibiteur contre Plk1 en passant d'un IC_{50} de 150 à 44 nM (Figure 1-12B).[56]

Figure 1-12 A – Alkylation à la position N^{π} de l'histidine sur un pentapeptide ; B – Propriétés inhibitrice de Plk1 des peptides contenant l'histidine N^{π} alkylé et N^{τ} macrocyclisés

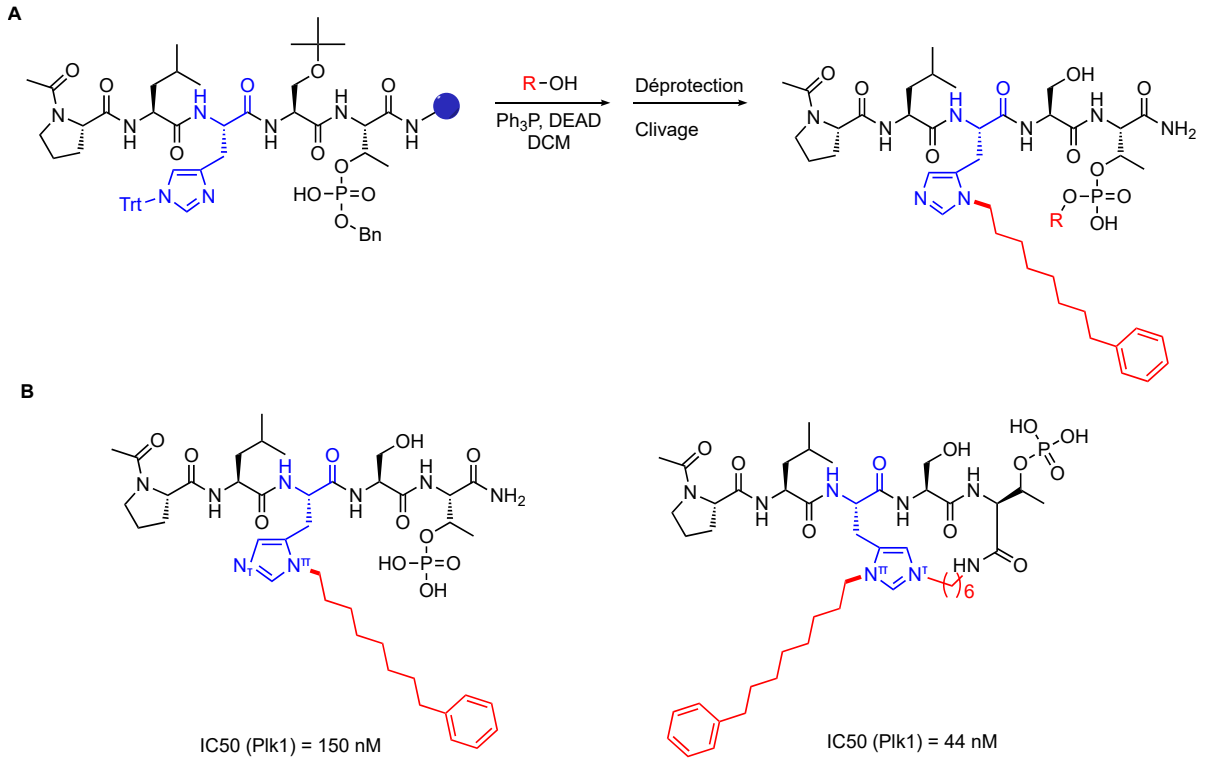

Bien que peu manifestes, les carbones C^2 et C^5 de l'imidazole peuvent être également alkylés. En 1984, Cohen a rapporté les premières réactions d'alkylation qui ont été effectuées par photochimie et de ce fait, un mélange inévitable de produits d'alkylation C^2 et C^5 a été obtenu. Toutefois, les résultats obtenus montrent que l'alkylation sur le carbone C^5 se trouve plus favorisée par rapport au carbone C^2 dû au fait de la différence de densité électronique et des traces de produit doublement alkylé.[57] Un peu plus tard, la réaction sur un tripeptide a donné des résultats assez similaires avec un rendement total de 70% donnant toujours le produit d'alkylation C^5 majoritaire (Figure 1-13).[58]

Figure 1-13 A – Phototrifluorométhylation de l'histidine protégée ; B – Phototrifluorométhylation du tripeptide NH_2-Pro-His-Glp

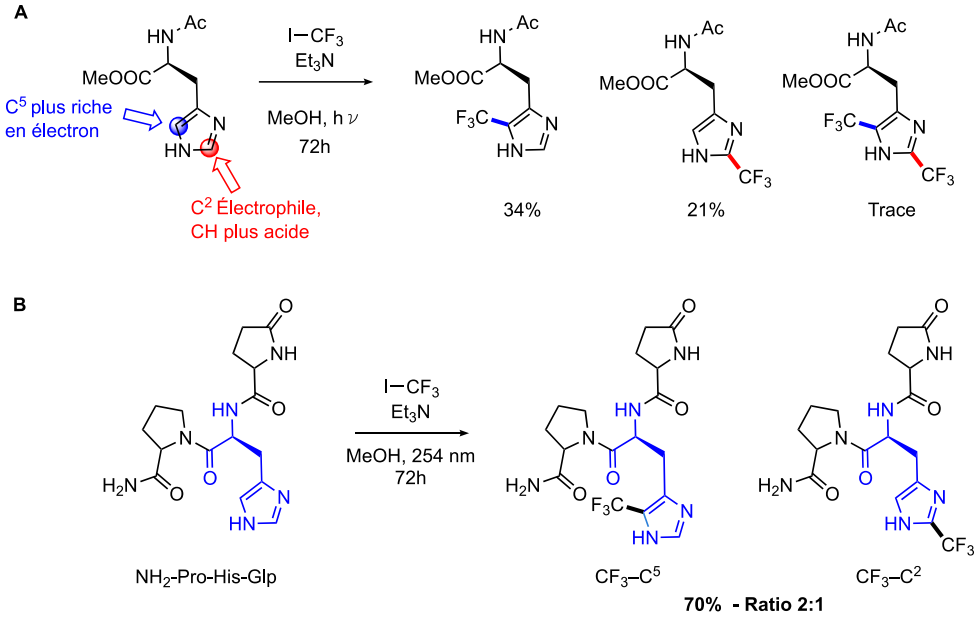

Ce n'est que sept années plus tard, qu'en s'inspirant des travaux du groupe de Minisci,[59] ce même groupe de recherche a réussi à installer un plus large panel d'alkyles de manière régiosélective sur le carbone C^2 le plus électrophile. Ces nouvelles conditions de réaction permettent de se passer de lumière et d'utiliser le nitrate d'argent comme agent radicalaire d'acides carboxyliques (Figure 1-14).[60]

Figure 1-14 C^2-Alkylation de l'imidazole de l'histidine protégée dans les conditions de Minisci

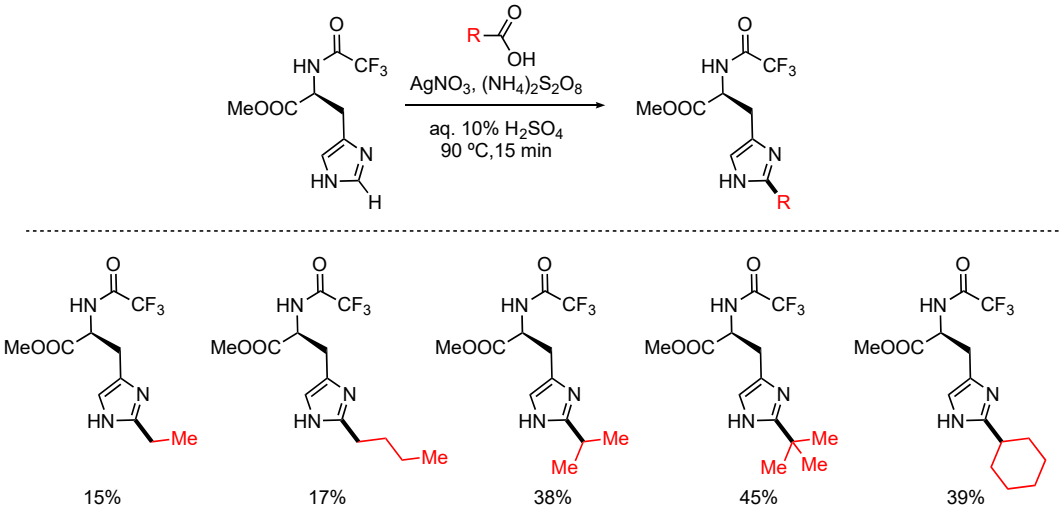

Chez les archaeas et les eucaryotes, la biosynthèse de la diphtamide s'effectue à travers une réaction d'alkylation C^2-sélective de l'histidine du facteur d'élongation 2 (EF2), une protéine jouant un rôle crucial

dans la synthèse de protéines. Il est accepté que la réaction se fasse de manière radicalaire et soit catalysée par cinq protéines Dph où la S-adénosylméthionine (SAM) fournit le groupement alkyle (Figure 1-15).[61]

Figure 1-15 Biosynthèse de la diphthamide. Adapté de [61]

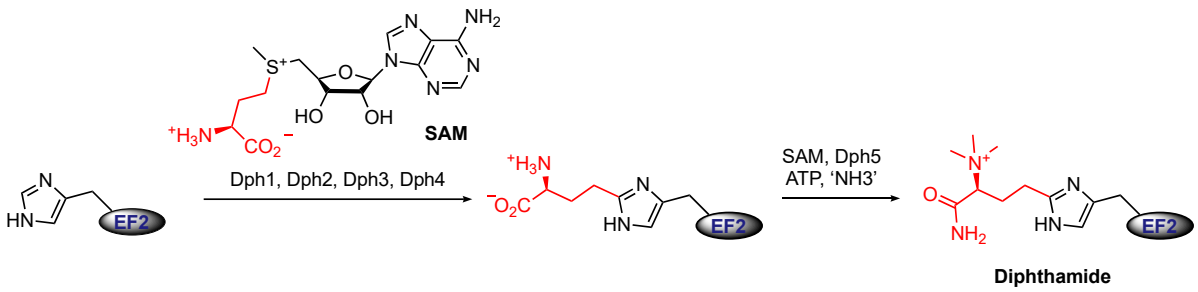

Ce n'est que très récemment, à la même année, que deux groupes de recherche sont parvenus à alkyler sélectivement l'imidazole de l'histidine à la position C^2 sur des peptides plus ou moins longs. Ces travaux impressionnent tant par leur versatilité que par leur robustesse mais adoptent toutefois des stratégies différentes. L'un utilise de la lumière bleue et des dérivés d'alkyles de dihydropyridine (DHP) comme couple initiateur radicalaire,[62] alors que l'autre utilise des sels d'alkylsulfonates et de l'hydroperoxyde de *tert*-butyle (TBHP) (Figure 1-16).[63] Leurs travaux remarquables sur l'alkylation de l'histidine montrent qu'elle fonctionne sur plus de dix peptides non-protégés différents, mais ne seront pas mentionnés ici par souci de concision.

Figure 1-16 A – C^2-Alkylation sélective de l'histidine dans le saralasin par lumière bleue et DHP [62]; B – C^2-Alkylation sélective de l'histidine d'un peptide par l'utilisation de sels de sulfonates et de TBHP [63]

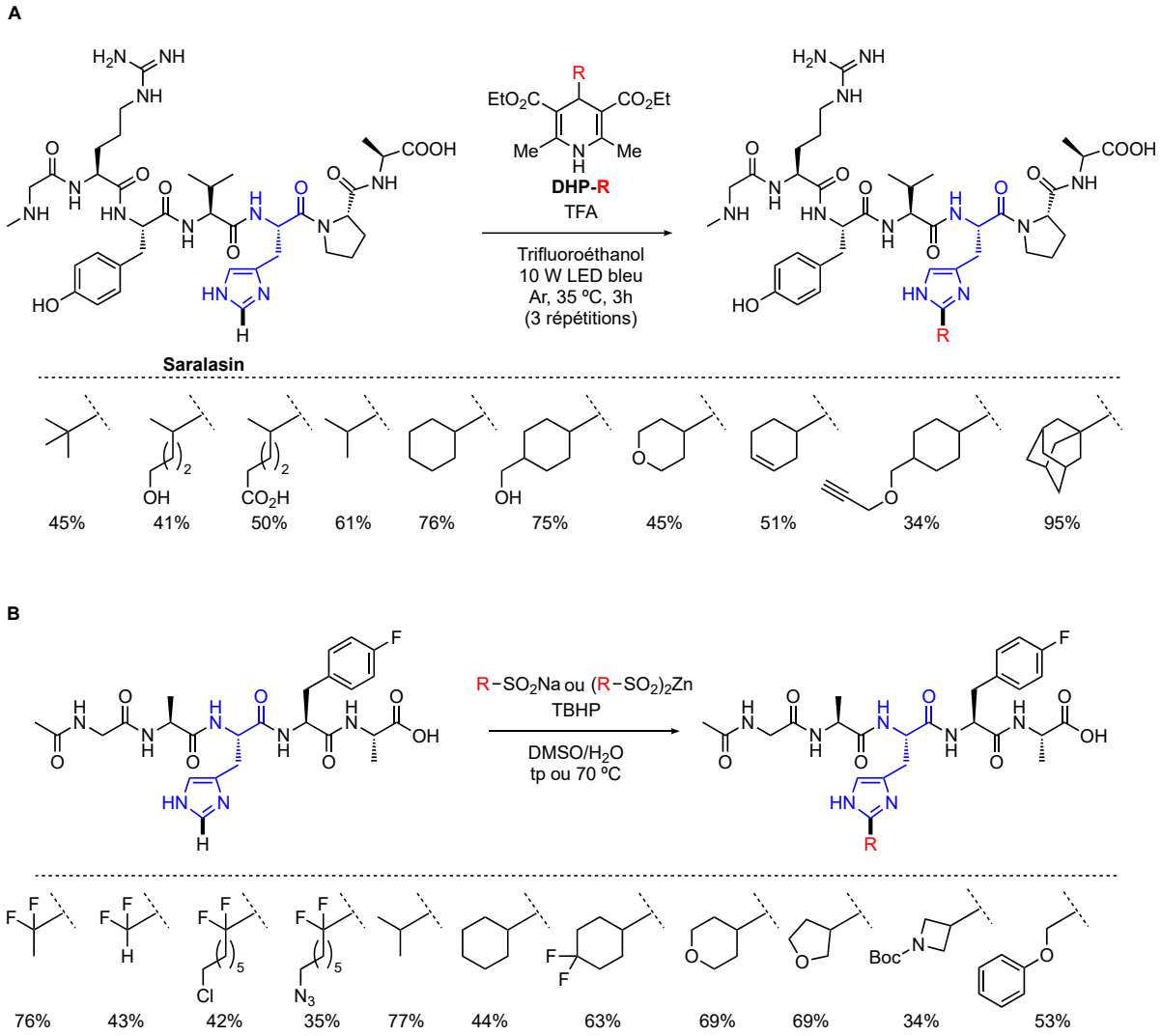

À ce jour, aucun exemple d'alkylation sélective à la position C^5 de l'imidazole de l'histidine n'a été rapporté dans la littérature. Cependant, bien que sporadique, la modification de cette position par oxydation peut être mentionnée.

1.3.2 Oxydation de la chaîne latérale de l'histidine

Isolé pour la première fois par Charles Joseph Tanret en 1909, l'ergothionéine est un acide aminé naturel non-protéinogène synthétisé par le champignon *Claviceps purpurea*.[64] Sa structure chimique est simplement une histidine oxydée par une fonction thione à sa position C^2 de l'imidazole et une triméthylamine sur son azote terminal. Sa synthèse très instable et difficile à isoler, il a longtemps été l'objet d'étude pour les chimistes dans la quête de sa préparation en laboratoire. Ce n'est qu'en 1951, que sa

synthèse a été rapportée pour la première fois par le groupe de Heath.[65] Une longue voie synthétique de six étapes qui à partir de méthyle ester histidine passe par une ouverture de l'imidazole par du chlorure de benzoyle, suivit de sa fermeture et de l'installation du thione grâce au thiocyanate de potassium. L'ergothionéine est par la suite obtenue par méthylation de l'azote terminal sur l'intermédiaire carboéthoxythiohistidine suivie d'une étape de déprotection (Figure 1-17A). Beaucoup plus tard, le groupe de Yadan a eu l'idée d'incorporer la source de soufre directement à la première étape, à travers l'utilisation du chlorothioformate de phényle, ce qui a permis d'obtenir, sans intermédiaire, le mercaptohistidine et d'écourter la synthèse de deux étapes (Figure 1-17B).[66]

Figure 1-17 Synthèse de la L-ergothionéine : A – Thiocyanate comme source de soufre ; B – Chlorothioformate de phényle comme source de soufre

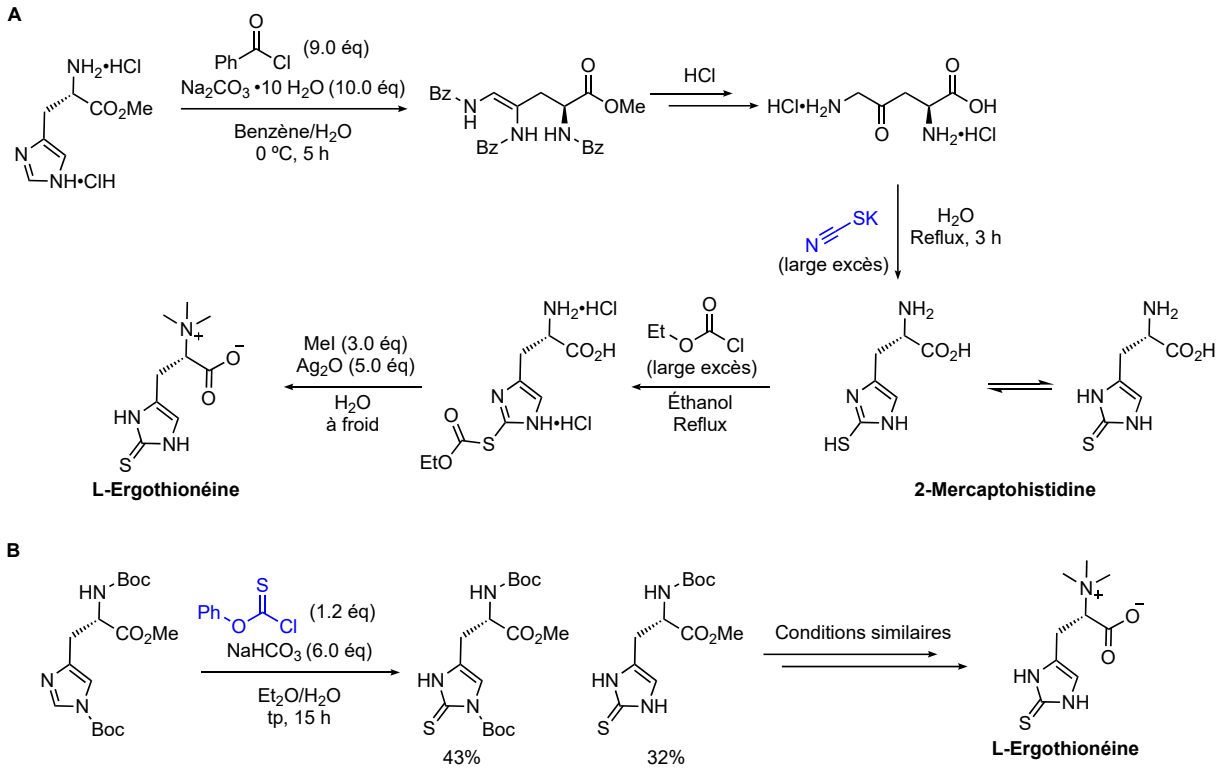

Récemment, en s'inspirant de la voie biosynthétique de l'ergothionéine, ce même groupe de recherche a proposé une nouvelle voie de synthèse de l'ergothionéine. En effet, ce dernier est produit par les champignons à partir de l'histidine en quatre étapes dont la première serait la triméthylation de l'amine terminale grâce à une molécule de SAM catalysée par une méthyltransférase, l'EgtD. L'hercynine ainsi formée, est convertie en hercynine cystéinesulfoxyde à l'aide de deux enzymes (EgtB et EgtC) et du γ-glutamylcystéine. Cet intermédiaire est finalement clivé en ergothionéine par une dernière enzyme, le EgtE (Figure 1-18A). Ainsi, en partant directement de l'hercynine, en remplaçant le γ-glutamylcystéine et

la protéine EgtE par une simple cystéine en milieu acide et bromé, et par de l'acide mercaptopropionique respectivement, ils ont réussi à mimer la biosynthèse de l'ergothionéine avec un rendement global de 52% (Figure 1-18B).[67] Curieusement, en employant les mêmes conditions de réaction mais en remplaçant cette fois la cystéine par de l'acide thioacétique, la position C^2 est épargnée et a laissé place à la thiocylation sélective de la position C^5 de l'imidazole (Figure 1-18C). Ce phénomène est encore mal compris à ce jour, mais ils proposent un mécanisme à travers lequel l'état de transition bromospirolactone pourrait se faire attaquer préférentiellement à la position C^2 par un nucléophile dit dur comme la cystéine, et en position C^5, par un nucléophile dit mou tel que l'acide thioacétique (Figure 1-18D).[68]

Figure 1-18 A – Voie biosynthétique de l'ergothionéine ; B – Synthèse de l'ergothionéine à travers l'utilisation de la cystéine ; C – C^5-thiolisation à partir de l'hercynine et d'acide thioacétique ; D – Mécanisme proposé de la sélectivité C^2/C^5

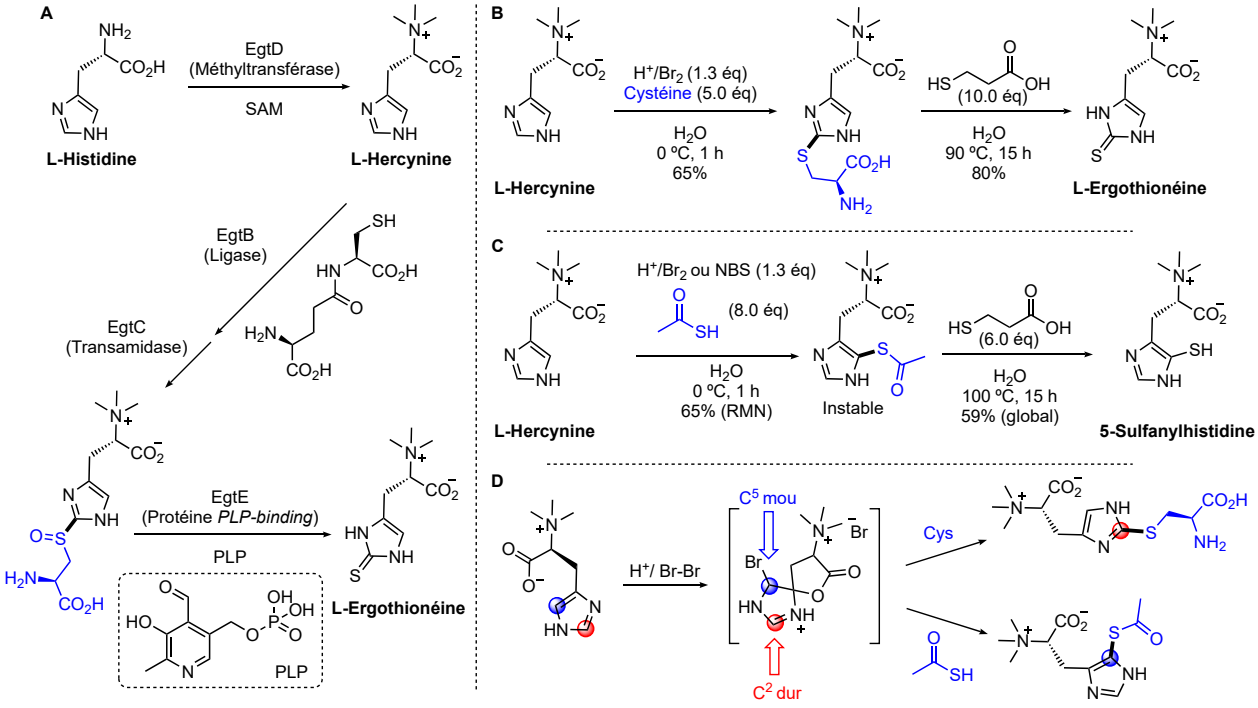

Présentant un intérêt essentiellement limité à la compréhension biomécanistique, l'histidine peut également s'oxyder par la présence d'oxygène via une réaction de Diels-Alder photocatalysée par le biais d'un intermédiaire endoperoxyde.[69] En effet, des preuves d'histidines oxydées ont été observées sur l'anticorps monoclonal IgG1[70] et il semblerait que les efforts scientifiques ont été placés sur l'étude mécanistique du phénomène et non sur l'exploitation éventuelle de ce genre de composés dans le domaine synthétique (Figure 1-19).

Figure 1-19 Mécanisme proposé de l'oxydation de l'histidine observée sur l'anticorps monoclonal IgG1. Image tirée de [70]

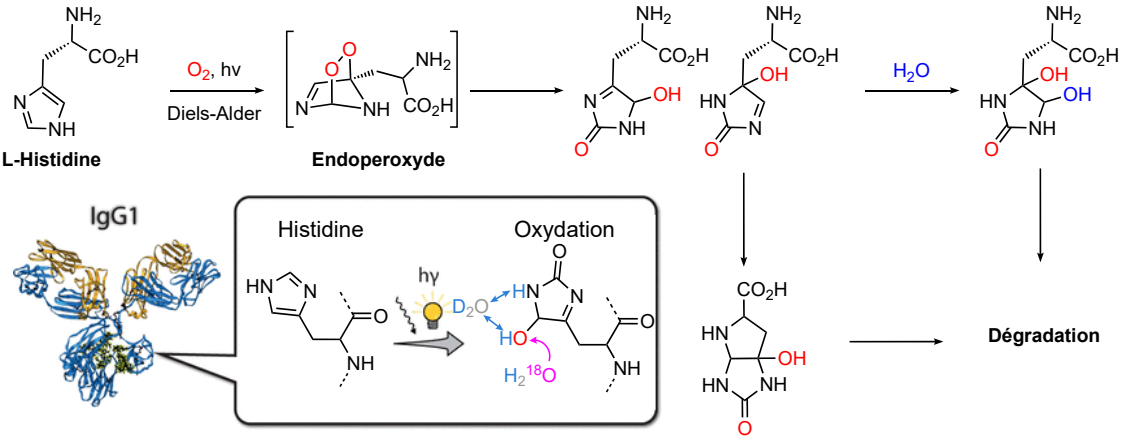

Les modifications de l'histidine par alkylation ont largement été rapportées dans la littérature, mais celles-ci restent toutefois modestes face aux méthodes d'arylation d'histidine décrites dans les revues scientifiques.

1.3.3 Méthodes d'arylation de la chaîne latérale de l'histidine

Comme précédemment, l'imidazole de la chaîne latérale peut être arylé soit sur les azotes N^{π} et N^{τ}, soit sur les carbones C^2 et C^5. Dans le cadre de ces deux dernières, à ce jour uniquement deux méthodes d'arylation directe ont été rapportées dans la littérature : une par réaction radicalaire et une autre par activation C–H. La méthode radicalaire s'inspire des conditions de Minisci vues plus tôt, mais en utilisant cette fois-ci l'acide boronique à la place de l'acide carboxylique. De la même façon, l'arylation est sélective sur le carbone le plus électrophile C^2 et sans trop de surprise, les groupements aromatiques appauvris en électrons donnent des rendements nettement moins bons que leurs homologues riches en électrons (Figure 1-20).[71] Aujourd'hui, aucune autre méthode d'arylation, que ce soit à la position C^2 ou C^5 par voie radicalaire n'a encore été rapportée.

Figure 1-20 C^2-Arylation de l'imidazole de l'histidine protégée dans les conditions radicalaires de Minisci

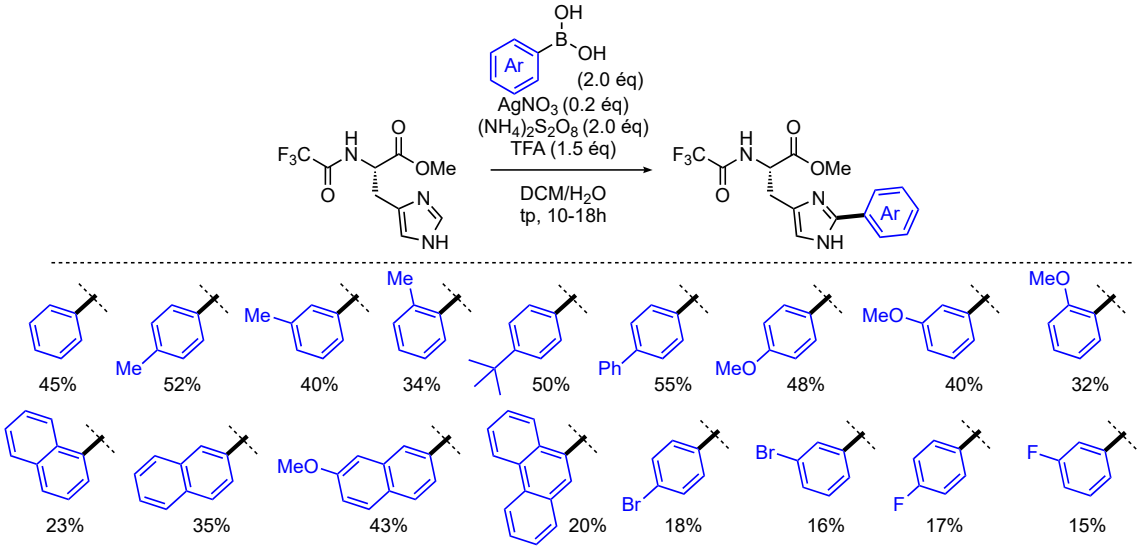

Plus tard, ce même groupe de recherche a élaboré la deuxième méthode d'arylation par C–H activation, plus robuste et versatile avec des rendements bien plus appréciables. La position C^5 a pu être sélectivement arylée en mettant en présence l'histidine protégée avec une quantité catalytique de palladium et de ligand phosphoré, de carbonate de potassium et d'acide pivalique comme le couple de déprotonation métallique concertée (CMD) dans du diméthylformamide (DMF) aux micro-ondes à 140 ºC (Figure 1-21A).[72] De manière assez surprenante, ils ont par la suite découvert qu'en ajoutant du cuivre(I) dans les conditions, cela permettait de changer complètement la régiosélectivité de l'arylation, passant cette fois sur le carbone C^2 de l'imidazole (Figure 1-21B).[73] La régiosélectivité peut s'expliquer par le mécanisme de la réaction. Sans la présence de cuivre, un mécanisme classique d'activation C–H dans lequel se succède une addition oxydante du palladium, une CMD et une élimination réductrice, pourrait expliquer la sélectivité de l'arylation du carbone C^5. Dans le cas opposé, le cuivre formerait d'abord l'organocuprate au niveau du carbone le plus acide suivi d'une transmétallation qui aboutirait à l'élimination réductrice, donnant le produit C^2-arylé (Figure 1-22).

Figure 1-21 A – C^5-Arylation sélective de l'imidazole de l'hisitine protégée ; B – C^2-Arylation sélective de l'imidazole de l'hisitine protégée par C–H activation

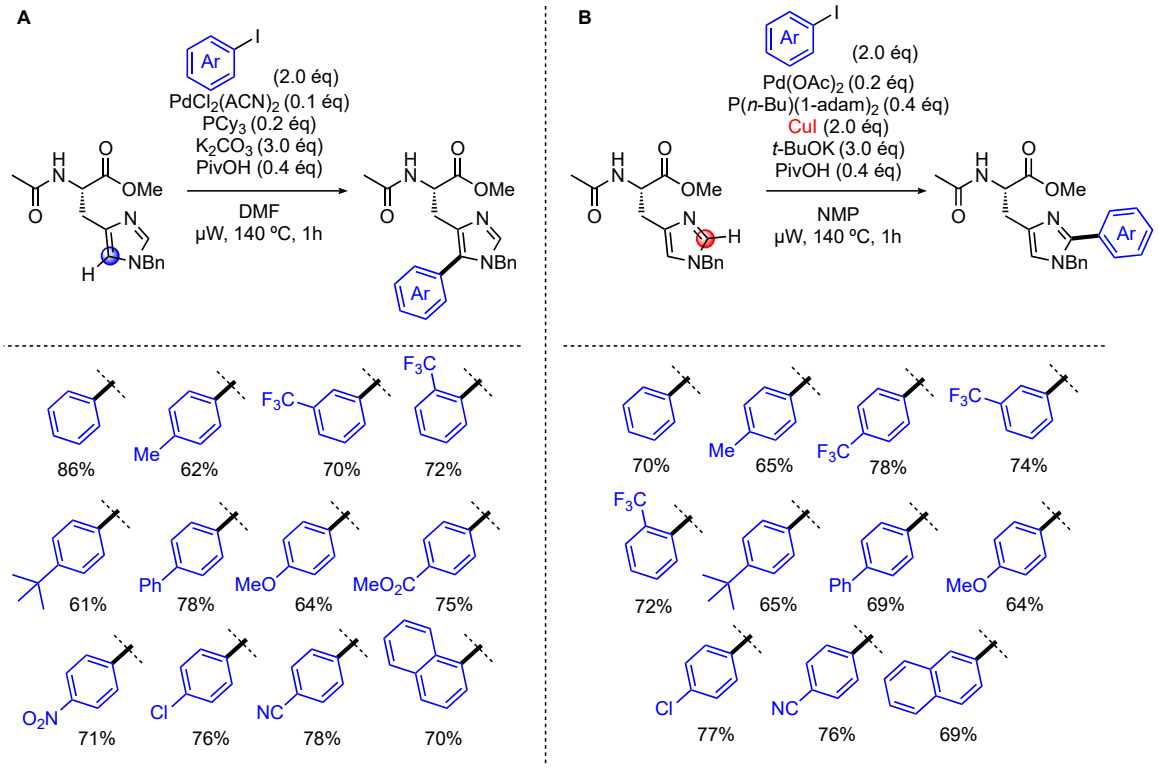

Figure 1-22 Mécanismes proposés tentant d'expliquer la régiosélectivité de l'arylation par C–H activation

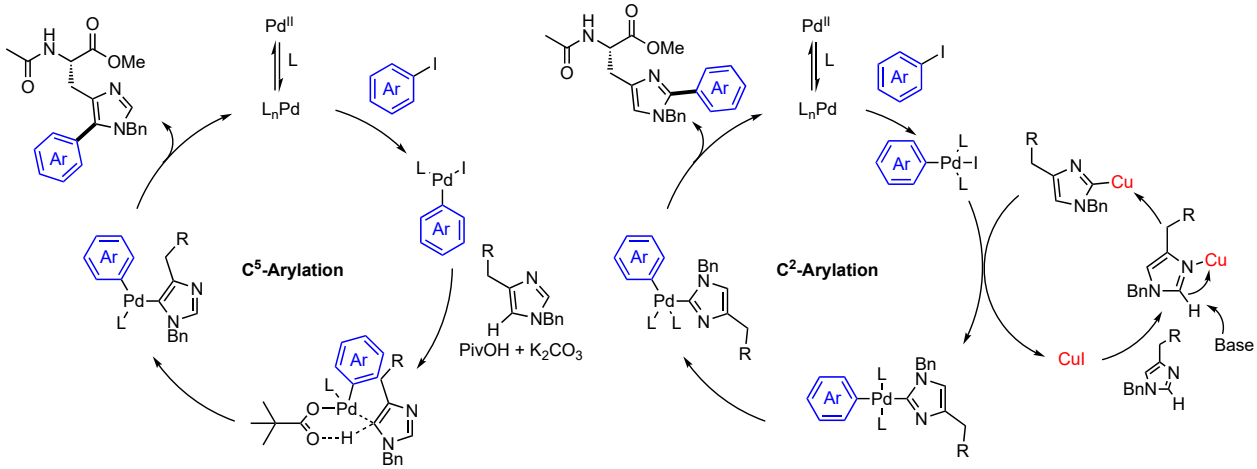

Une autre méthode indirecte, plus ancienne, était effectuée par couplage de Suzuki-Miyaura sur l'histidine préalablement bromée en position C^5 à l'aide du N-bromosuccinimide (NBS). Malgré le fait que cette méthode soit bien moins explorée, elle permet néanmoins d'apporter une réponse favorable sur la tolérance d'un groupement hétéroaromatique (Figure 1-23).[74]

Figure 1-23 C^5-Arylation indirecte par couplage Suzuki-Miyaura

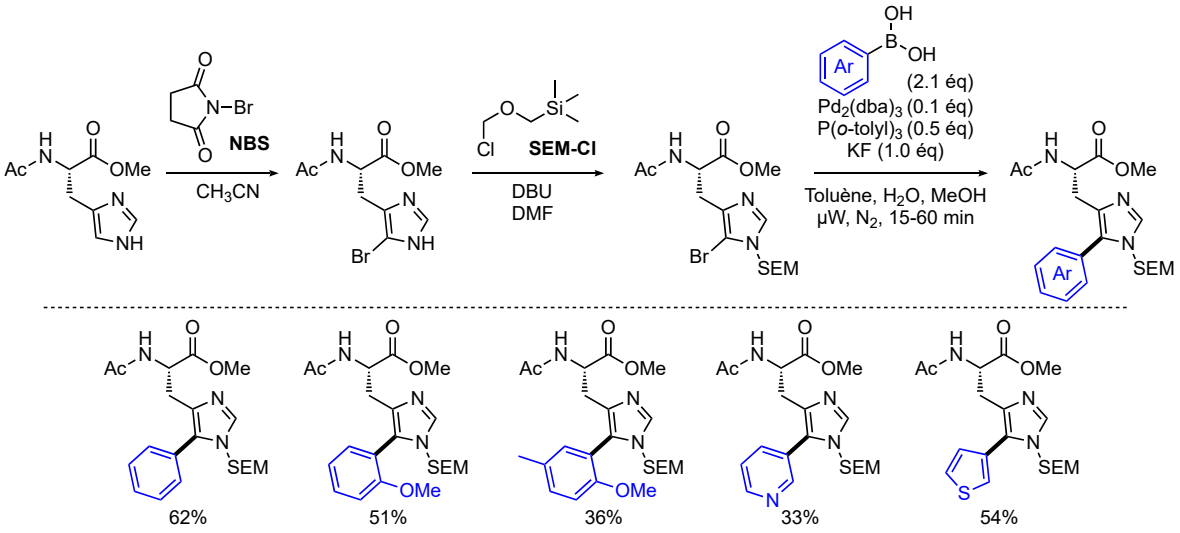

Pour ce qui est des méthodes de N-arylation de l'imidazole de l'histidine, il en existe un nombre plus conséquent et chronologiquement, les pionniers dans ce domaine exploitaient l'avantage du caractère nucléophile de l'azote N^{τ} pour réaliser différentes modifications. En effet, les premiers signes d'histidine arylée ont été rapportés dans les années 50 où une méthode de substitution nucléophile aromatique (SN_{Ar}) donnait un mélange d'histidine $N^{terminal}$-arylée et N^{τ}-arylée en mettant en présence l'histidine avec du fluorodinitrobenzene.[75, 76] Plus tard, Merrifield proposa de protéger d'abord l'azote terminal afin d'obtenir exclusivement l'arylation de l'imidazole (Figure 1-24A).[77] La nécessité de la présence d'un groupement électro-attracteur ainsi qu'un halogène sur le cycle aromatique rend inévitablement la méthode très limitée en termes de diversité de groupements. Par la suite, dans le cadre d'études biochimiques, soit très loin de l'objectif de modification, l'histidine s'est retrouvée arylée par une attaque nucléophile, mais cette fois sur des composés « pro-aromatiques » tels que l'époxyde bromocyclohexadiène[78] et l'orthoquinone (Figure 1-24B).[79] En plus de l'inconvénient de devoir les préparer, la diversité des groupements aromatiques reste toujours très limitée. Il aura fallu attendre les travaux du groupe de Konopelski pour voir les prémices d'une diversité des groupements aromatiques installables sur l'histidine. En effet, en s'inspirant du couplage croisé organoplomb/cuivre développé par Barton,[80, 81] ils ont réussi à installer des cycles aromatiques à la fois enrichis et appauvris en électrons et même de coupler l'imidazole de l'histidine avec la chaîne latérale d'une tyrosine protégée en ayant un rendement convenable (Figure 1-24C).[82-84]

Figure 1-24 A – N$^{\tau}$-Arylation par SN_{Ar} ; B – N$^{\tau}$-Arylation par attaque nucléophile sur un pro-aromatique ; C – N$^{\tau}$-Arylation par couplage croisé de Barton

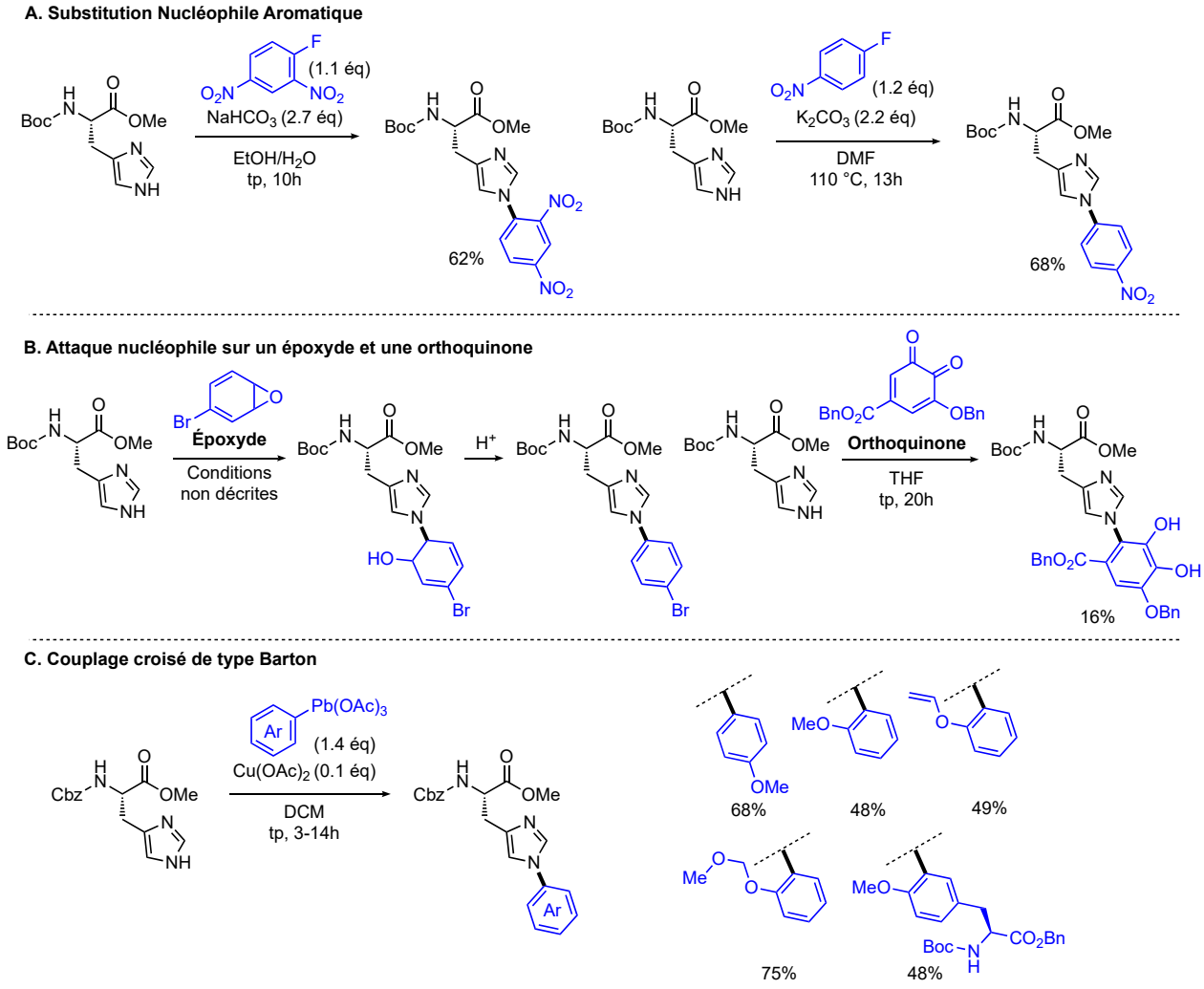

Conscient des problèmes de toxicité liés aux organoplombs et basé sur les travaux de Buchwald relatifs aux arylations de l'imidazole,[85] Hanzlik réussi non sans peine à obtenir des nouveaux dérivés aromatiques de l'histidine en la mettant en présence d'halorgénures d'aryle, d'une quantité catalytique de cuivre(I) avec de la phénanthroline et du dibenzylidèneacétone (Dba) comme ligands et du carbonate de césium en guise de base dans un mélange xylène/DMF à 115 °C (Figure 1-25A).[86] Très proche des conditions optimales, il semblerait que l'activation de la liaison N–H de l'imidazole de l'histidine par simple chauffage n'était pas suffisante et qu'un chauffage par micro-onde était la clé, comme le démontre Jain à travers ses études. En effet, en y changeant le cuivre et le ligand et en chauffant simplement par micro-ondes, ces travaux remarquables impressionnent tant par la diversité des groupements aromatiques tolérés que par les rendements obtenus. Effectivement, toutes les positions (para, meta, ortho) des substituants sur le cycle

aromatique sont tolérées, qu'ils soient électrons donneurs ou accepteurs. De plus, les groupements hétéroaromatiques sont également applicables (Figure 1-25B).[87]

Figure 1-25 A – Transposition des conditions d'arylation de l'imidazole dans le cadre de l'histidine ; B – N^{τ}-Arylations de l'imidazole de l'histidine protégée par couplage de type Ullman-Goldberg chauffées par micro-onde

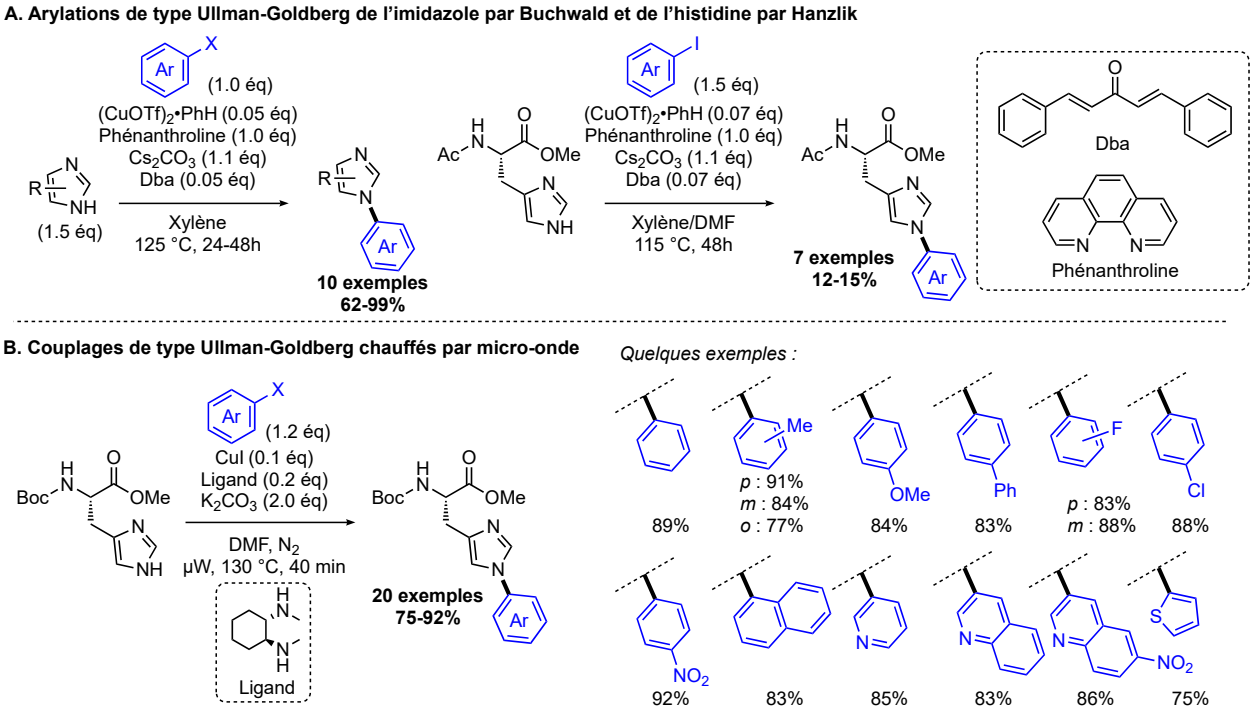

Une méthode alternative à celle par couplage de Ullman-Goldberg a été décrite par Campagne qui permet l'arylation de l'imidazole par un couplage croisé de Chan-Lam-Evans. Ces conditions ont l'avantage de se faire à une température plus douce et de se passer de solvant anhydre. En contrepartie, les cycles hétéroatomiques ne sont plus compatibles dans ces circonstances (Figure 1-26).[88]

Figure 1-26 Nᵗ-Arylation de l'imidazole de l'histidine protégée par un couplage Chan-Lam-Evans

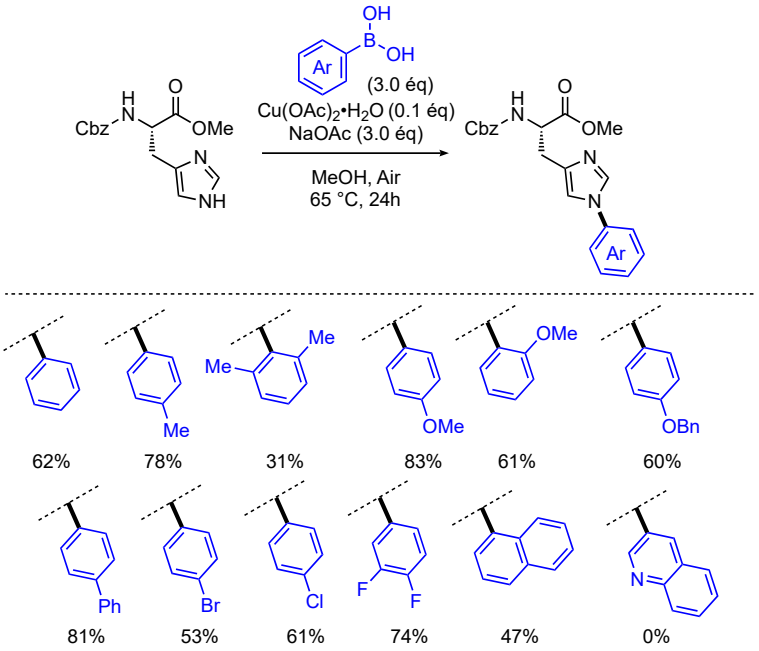

À ce jour, aucune méthode ne mentionne l'arylation régiosélective de la position Nᵖ de l'imidazole de l'histidine. Cependant, une méthode par photochimie proposée par Nicewicz peut apporter un semblant de réponse, mais malheureusement le manque de régiosélectivité rend cette dernière moins intéressante et reste encore sous explorée (Figure 1-27).[89]

Figure 1-27 N-Arylations par réaction photochimique

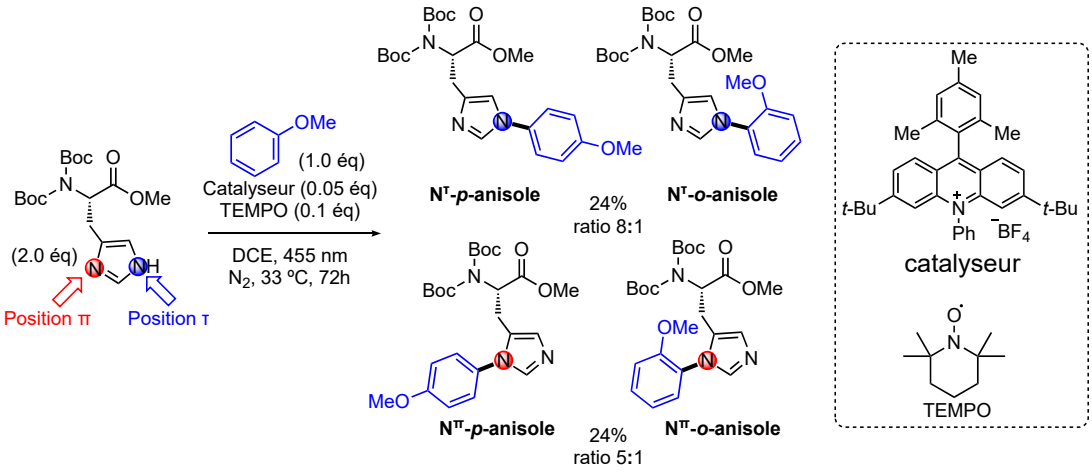

Il a été démontré qu'il était néanmoins possible de combiner deux méthodes d'arylations régiosélectives afin d'obtenir l'histidine doublement arylée à la fois à la position C^2 et Nᵗ. Pour ce faire, la position C^2 est

d'abord arylée avec les conditions de Minisci avant d'effectuer un couplage de type Ullman-Goldberg sur l'azote N^{τ} de manière complètement régiosélective (Figure 1-28).[90]

Figure 1-28 Double arylation de l'imidazole par réactions successives régiosélectives

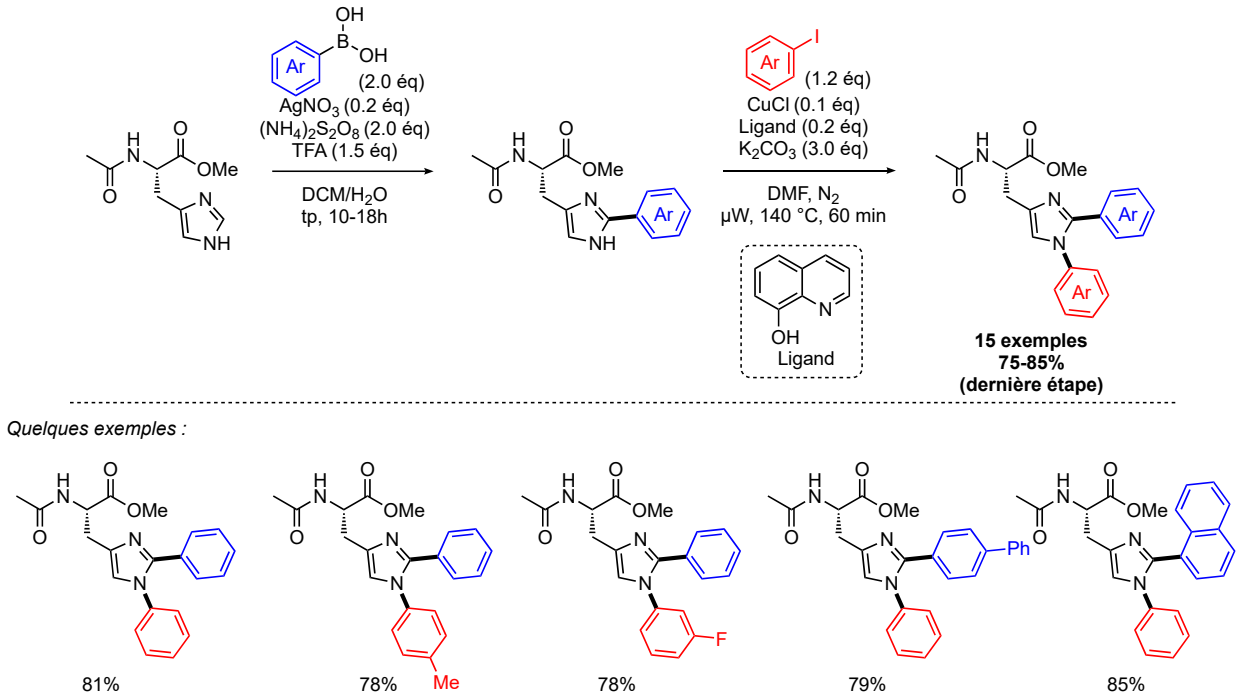

Ces derniers résultats datant de 2017 clôturent à ce jour les recherches autour de la modification de l'histidine et concluent par une remarquable preuve de la versatilité et de la diversité de sa chimie.

En parallèle à ces études, d'autres groupes ont proposé des méthodes de modification pour d'autres acides aminés, tels que le tryptophane ou encore la tyrosine. Ces études ne seront pas détaillées dans le cadre de cette thèse, mais il serait incongru de ne pas mentionner que notre groupe de recherche a participé à l'enrichissement méthodologique des modifications de ces deux acides aminés à travers l'utilisation d'organobismuthines.[91, 92]

CHAPITRE 2

LES BISMUTHINES, UN NOUVEL OUTIL

Dans ce chapitre il sera question tout d'abord d'appréhender les différentes facettes du bismuth avant de survoler ses multiples utilisations dans différents domaines d'application. En revanche, le domaine de la chimie de synthèse sera un peu plus détaillé et on verra comment le bismuth organique a su trouver sa place parmi les métaux de transition déjà fort employés dans ce secteur.

2.1 Les généralités

Identifié pour la première fois par Claude François Geoffroy en 1753, le bismuth est un métal du tableau périodique des éléments portant le numéro atomique 83 avec une configuration électronique [Xe] $4f^{14}5d^{10}6s^{2}6p^{3}$. Étant le dernier élément naturel de la famille des pnictogènes, soit la colonne 15 du tableau, il a longtemps été considéré comme le métal le plus lourd non radioactif. Toutefois, des chercheurs de l'institut d'astrophysique spatiale d'Orsay ont démontré que le bismuth émettait finalement des particules alpha lors de sa désintégration en thallium et en l'hélium avec une demi-vie de $1{,}9 \times 10^{19}$ années. Une demi-vie plus grande que l'âge de la Terre elle-même explique ainsi pourquoi il est considéré comme stable.[93] À peu près deux fois plus abondant que l'or dans la croûte terrestre, le bismuth se trouve généralement sous la forme de minerai de bismuthinite (Bi_2S_3) et de bismite (Bi_2O_3). Son isolation élémentaire provient le souvent du débismuthage du plomb par des procédés pyrométallurgiques dont la Chine intervient comme le premier producteur au monde suivit du Laos et de la Corée du Sud.[94]

Parce que le bismuth partage des similitudes physiques avec ses proches voisins, il a longtemps été confondu avec le plomb ou l'antimoine. Cependant contrairement à ces derniers, le bismuth montre une toxicité tout de même moindre et présente même des propriétés thérapeutiques.[95] En effet, sous la forme de sous-salicylate dans le Pepto-Bismol®, de sous-citrate dans le Zantac® ou de sous-nitrate dans le Mammol®, ces principes actifs à base de bismuth sont utilisés comme un antiacide qui permet de soulager soit les brûlures et les ulcères de l'estomac, soit les démangeaisons causées par des piqûres ou de l'eczéma. De plus, usant des capacités chalcophile du bismuth (aime à se lier fortement au soufre), le groupe de Nitsche a récemment démontré qu'un peptide bismobicycliqué pouvait avoir un effet bénéfique contre les protéases du virus Zika (ZikaPro) et du Nil occidental (WNVPro) (Figure 2-1).[96] Ses formidables propriétés doivent toutefois être nuancées, puisque lorsqu'accumulé dans l'organisme, le bismuth peut néanmoins provoquer des effets indésirables comme des néphropathies, des encéphalopathies, des ostéoporoses ou encore des hépatites.[97]

Figure 2-1 Exemples de composés contentant du Bismuth aux propriétés thérapeutiques

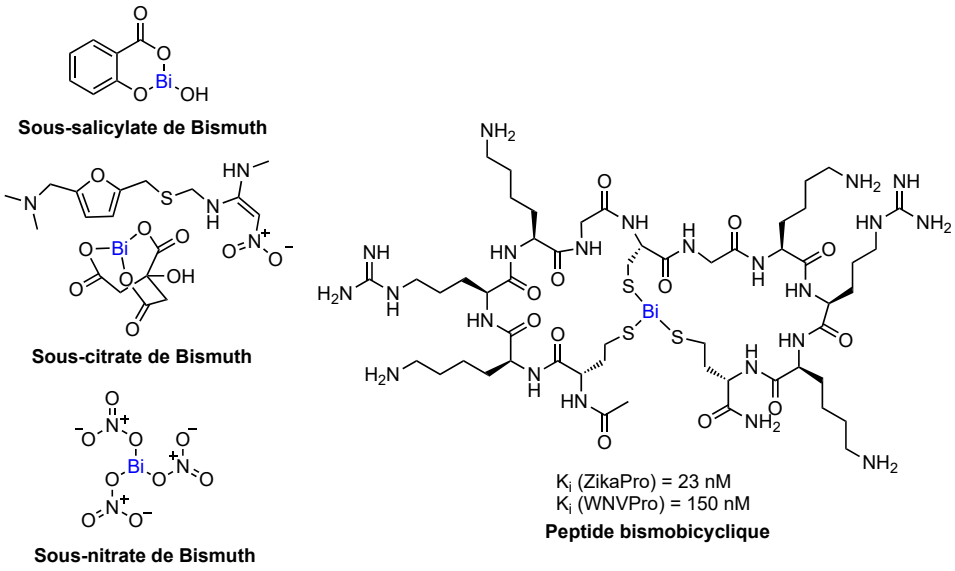

Outre le domaine pharmaceutique, deux autres domaines se disputent également les ressources de bismuth à savoir le domaine de la chimie des matériaux et la chimie en synthèse organique. Dans le premier cas, c'est parce qu'il partage des propriétés physiques communes avec le plomb que le bismuth est devenu très rapidement son équivalent non toxique. Le plomb est ainsi remplacé par le bismuth dans les peintures, les écrans pararayons X ou encore dans les alliages métalliques qui en comportaient comme les tuyauteries ou les munitions de chasse. D'autres applications existent mais ne seront pas détaillées dans le cette thèse pour des raisons évidentes de concision. En revanche, dans le cadre de la chimie en synthèse organique, le bismuth et ses applications vont être vus un peu plus en détail.

2.2 Les organobismuthines, leurs synthèses et applications

2.2.1 Synthèse des organobismuthines trivalents

On nomme par organobismuthines une espèce qui comporte au moins une liaison Bi–C. Ses formes stables se distinguent d'une part par les bismuths trivalents d'état d'oxydation +3, et d'une autre part par les pentavalents d'état d'oxydation +5. Les bismuths trivalents sont les plus documentés et se différencient selon s'ils sont trialkylés ou triarylés. Au-delà de la différence structurelle, les trialkylbismuthines sont liquides et pyrophoriques, alors que les triarylbismuthines sont solides et tout à fait stables à l'air. Ceci s'explique par la présence du doublet non-liant du bismuth fortement polarisé dans le cas des alkylbismuthines et qui est complètement diffus par résonance grâce aux groupements aromatiques dans le cas des arylbismuthines. Par des techniques de cryo-cristallisation et/ou cristallisation classique, les structures des alkyles et aryles bismuths ont pu être analysées en détail. Tous deux adoptent une géométrie

pyramidale trigonale avec des distances et des angles qui varient selon les groupements (Figure 2-2). On peut s'apercevoir que les angles de C–Bi–C sont nettement inférieurs à la valeur théorique de 109,5 ° établie selon la théorie de la répulsion des paires d'électrons de la couche de valence (RPECV). Ce phénomène particulier peut s'expliquer par les effets relativistes du bismuth qui sans rentrer dans les détails quantiques, permettent au doublet d'électrons libres de se localiser préférentiellement dans son orbitale 6s plutôt que dans l'orbitale hybridée sp^3, ce qui a pour conséquence un angle de liaison réduit.[98]

Figure 2-2 Structures cristallographiques de quelques organobismuthines trivalents

Tiré de : [a] Schulz[99] ; [b] Hoge[100] ; [c] Bučinský[**Erreur! Référence de lien hypertexte non valide.**] ; [d] Gagnon[102]

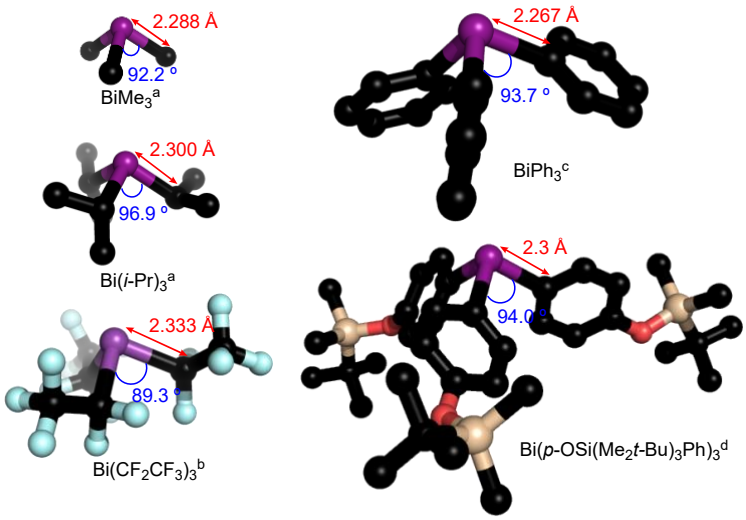

Bien que moins faciles à isoler, les trialkylbismuthines seront les premières à être synthétisées. En effet, le professeur Löwig mentionnera en 1850 qu'en appliquant les mêmes conditions de synthèse des organoantimoines, il était possible d'obtenir le triéthylbismuth, sans plus de détails.[103] Cette synthèse sera détaillée deux ans plus tard par Breed où il indiquera qu'en chauffant de l'idoéthane avec un alliage de bismuth et potassium il était possible d'obtenir le produit désiré.[104] Fortement inspiré par cette méthode, en 1887 Michaelis et Polis rapporteront la première synthèse de triarylbismuthines. Pour ce faire, ils ont chauffé du bromobenzène avec un alliage de bismuth et sodium pour obtenir le triphénylbismuth attendu.[105] À ce jour, la méthode la plus répandue est celle de l'utilisation d'un organomagnésien sur un sel de trihalogénobismuthine. Cette dernière datant du début du 20ième siècle reste aujourd'hui la plus simple à mettre en place et permet à la fois d'obtenir des trialkyl-[106, 107] et des triarylbismths.[108-110] Loin d'être la seule méthode disponible, d'autres groupes ont utilisé d'autres organométaux. Le Tableau 2-1 en liste quelques-uns sans être exhaustif.

Tableau 2-1 Organométaux compatibles à la synthèse d'organobismuthines

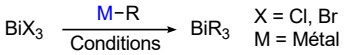

Auteurs	Organométaux	Bismuthines	Auteurs	Organométaux	Bismuthines
Marquardt [111]	Me_2Zn, Et_2Zn	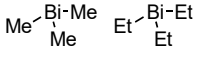	Fisher et Schreiner [112]	NaCp	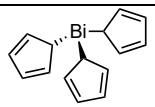
Hilpert, Dimart et Grüttner [113]	Al_4C_3	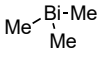	Dickson et West [114]	$LiAlEt_4$	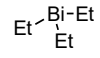
Hilpert et Grüttner [115]	$HgPh_2$	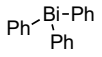	Naumann et Tyrra [116]	$Cd(CF_3)_2$	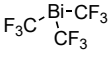
Zakharkin et Okhlobystin [117]	AlR_3	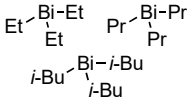	Whitmire, Roesky et al.[118]	Li(*p*-CF_3Ph)	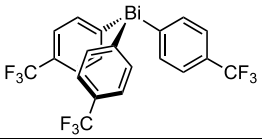

Lors des synthèses des organobismuthines rapportées précédemment, un composé d'halogénure de diorganobismuth est souvent décrit comme étant un sou-produit. Ce dernier issu de la conversion partielle du trihalogénobismuth, peut être obtenu plus systématiquement en ajoutant simplement un ou deux équivalents d'organolithien par rapport au sel de bismuth, comme le décrit Breunig.[119] D'autre part, il est également possible d'obtenir ces espèces en faisant réagir du diéthyléthérate de trifluorure de bore, du bromure d'hydrogène ou encore du diiode avec du triarylbismuth conduisant respectivement au fluorure,[120] au bromure,[121] ou à l'iododure de diarylbismuth.[122, 123] Une méthode par dismutation conduit également aux mêmes espèces et semble être la méthode la plus utilisée. Elle consiste en la simple mise en réaction du triarylbismuth avec son équivalent trihalogéné. La subtilité de cette dernière méthode est qu'une addition lente du sel de bismuth à une solution de triarylbismuth donnera bien l'espèce monohalogénée correspondante mais que l'addition d'ordre contraire conduira au dihalogénure d'arylbismuth.[124] L'existence de ces espèces a permis l'emergence de nouveaux organobismuths trivalents dits hétéroleptiques. En effet, en ajoutant du naphtylmagnésien sur le bromure de diphénylbismuth,[125] Challenger réussit la première synthèse d'un tel organobismuth et inspirera par la suite plusieurs groupes soit à travers les mêmes conditions,[124, 126] soit à travers des turbo Grignard,[127] soit à travers des organolithiens.[128] En poussant le concept un peu plus loin, il est possible d'obtenir des organobismuths hétéroleptiques dits mixtes, ainsi nommés car le bismuth porte à la fois des groupements aromatiques et alkyliques. Ces espèces sont sensibles à l'air mais ne sont pas pyrophoriques comme leurs homologues trialkyliques.[119, 129] Par ailleurs, l'utilisation d'une stratégie dans laquelle les deux cycles aromatiques sont liés par une fonction portant un caractère datif conduit à des organobismuthines trivalents hypervalents et

permet d'avoir des bismuthines tout à fait stables à l'air. Cette stratégie est encore peu explorée, seuls quelques exemples ayant été rapportés dans la littérature à ce jour (Figure 2-3).[130-132] Ce phénomène d'hypervalence se caractérise par la faculté du bismuth à enfreindre la règle de l'octet et à accepter davantage d'électrons, ce qui mène parfois à des bismuths pentavalents.

Figure 2-3 Voies de synthèse des halogénures de bismuth et leurs transformations

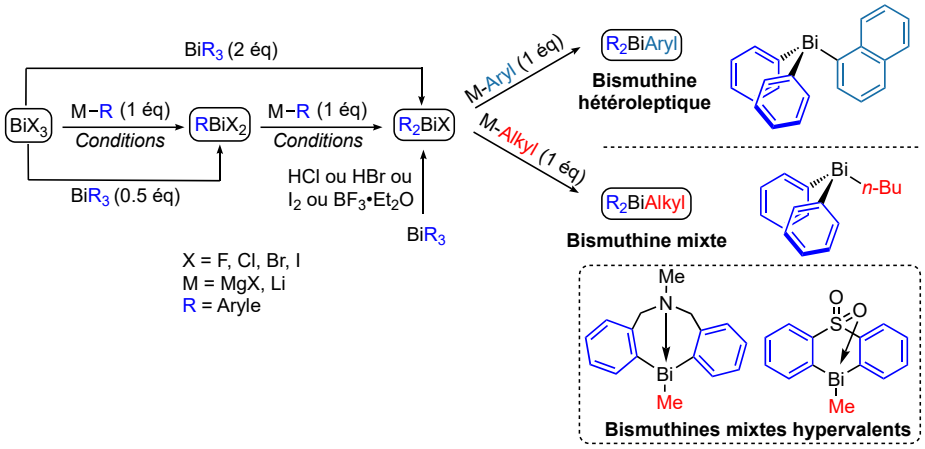

2.2.2 Synthèse des organobismuthines pentavalents

Les bismuths pentavalents présentent généralement une géométrie bipyramidale à base trigonale[133] et comme leurs homologues trivalents, les dérivés alkyliques sont sensibles à l'air et peu stables à température ambiante contrairement aux aromatiques correspondants. Pour ces derniers, il est possible de trouver dans la littérature autant de méthodes de synthèse que de dérivés mais elles ont en commun le fait qu'il est souvent nécessaire de passer par un intermédiaire trivalent. Les premières synthèses de tels bismuths ont été mentionnées par Michaelis et Polis en 1887, avec leurs triphényldihalogénobismuthines préparées en faisant simplement passer du chlore gazeux ou en ajoutant une solution de dibrome à une solution refroidie de triphénylbismuth pour obtenir respectivement l'espèce pentavalente dichlorée et/ou dibromée correspondante sous forme de précipités blancs.[105] Cette méthode de synthèse sera imitée par de nombreux groupes[110, 134] et l'inconvénient du dichlore gazeux sera vite détourné par l'utilisation plus pratique du chlorure de sulfuryle,[124, 135, 136] et par du dichlorure d'iodobenzène dans les cas les plus spécifiques.[137] Pour ce qui est des autres homologues halogénés, le fluorure correspondant a pu être obtenu à partir du triphényldichlorobismuth mis en présence de fluorure de sodium[138] ou de fluorure d'argent,[139] ou alors obtenu directement en oxydant le bismuth trivalent avec du difluorure de xénon.[140-142] Malheureusement, malgré les tentatives, les bismuths pentavalents iodés restent encore absents de la littérature. Dans un autre registre, il est également possible d'obtenir des dicarboxylates de triarylbismuthines soit à partir du dichlorure d'arylbismuth(V) décrit plus haut mit en présence d'un carboxylate,[143, 144] ou bien directement

à partir de triarylbismuthines à travers une oxydation par un peracide.[145-151] Les méthodes pour obtenir ces espèces sont diverses et variées, et ne seront pas présentées en détail dans cette thèse. Bien que très peu référencés dans la littérature, les bismuths pentavalents homo- et hétéroleptiques peuvent s'obtenir assez facilement en ajoutant un organolithien sur des dérivés halogénés correspondants. Wittig et Clauß seront les premiers à rapporter le pentaphénylbismuthine en 1952,[152] qui inspirera par la suite les travaux de l'équipe de Seppelt avec leurs bismuthines pentavalentes hétéroleptiques. Curieusement, les pentaarylbismuthines adoptent généralement une structure plutôt pyramidale à base carrée et non plus bipyramidale trigonale comme ses homologues halogénés. Le tritolyl-*o*-difluorobismuthine endosse le rôle d'exception avec sa structure bipyramidale (Figure 2-4).[142, 153]

Figure 2-4 Méthodes de synthèse des halogénures de triarylbismuthines et pentaarylbismuthines

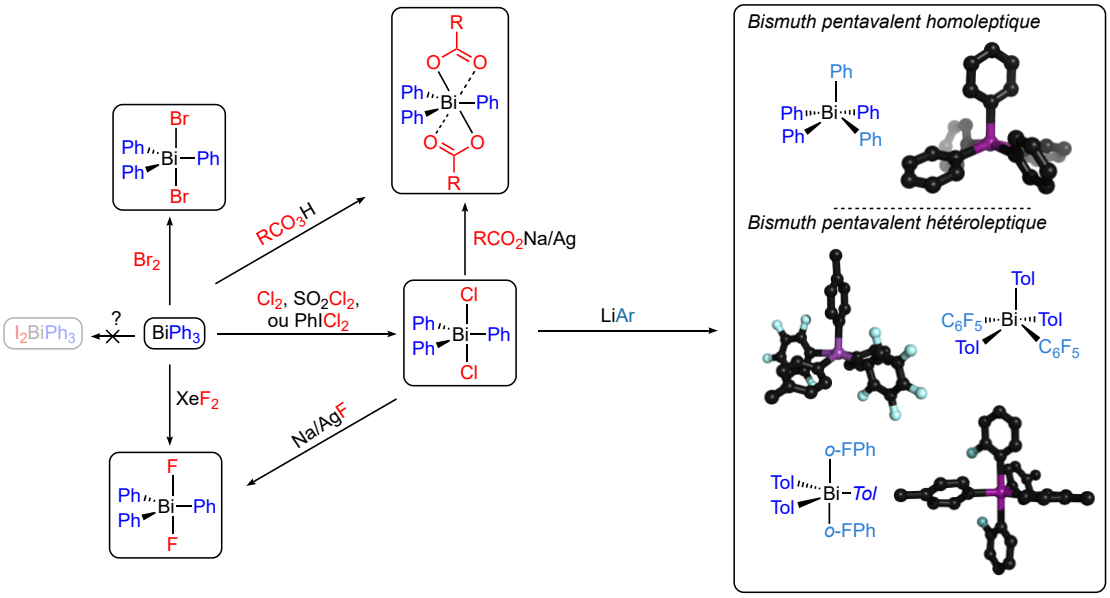

Bien que très instables à température ambiante, il est également possible d'oxyder les trialkylbismuthines. En 1986, une analyse par ^{19}F-RMN de Maurer a permis de caractériser des traces du tributyldifluorobismuthine obtenu par oxydation de l'alkylbismuth correspondant avec du pentafluorure d'iode (IF_5).[154] Plus tard, grâce à des analyses cristallographiques par Wallenhaeur et de Seppelt, des preuves supplémentaires ont pu être apportées. En effet, ils ont réussi à synthétiser et à caractériser la première pentaméthylbismuthine en passant par un intermédiaire chloré de triméthylbismuthine.[155] De manière assez surprenante, la structure géométrique du pentaméthylbismuth reste bipyramidale et n'adopte pas la structure pyramidale comme le pentaphénylbismuth (Figure 2-5).

Figure 2-5 Synthèses d'halogénures de trialkylbismuthines et du pentaméthylbismuthine

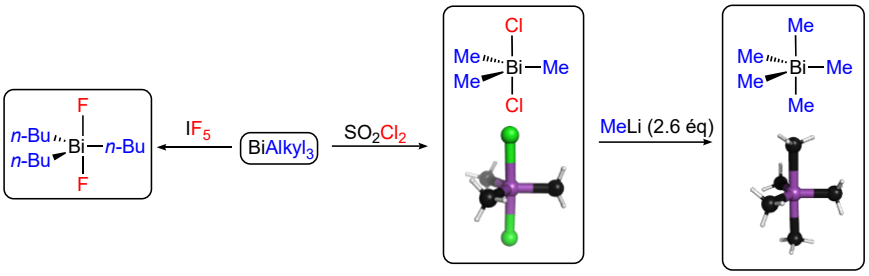

Les préparations des organobismuthines sont parfois des défis synthétiques et font souvent l'objet d'études cristallographiques. Outre l'élégance des clichés des rayons X, les organobismuthines proposent également une richesse réactionnelle appréciable.

2.2.3 Réaction d'alkylation par les alkylbismuthines

Certainement pour des raisons de stabilité, les réactions de transfert du groupement alkyle des bismuthines ne sont pas très communes. Toutefois, le groupe de Naumann réussit, sans l'aide d'un métal de transition à transférer le groupement trifluorométhyle du bismuth(III) correspondant en position α du chlorure de benzoyle pré-activé avec de la pyridine.[156] Par la suite, ils ont découvert qu'en utilisant l'acétate de cuivre(II) il était possible de trifluorométhyler à la fois une énamine et une aniline *N*,*N*-dialkylée. Sur cette dernière, un mélange de produits ortho et para est cependant obtenu avec un ratio 1,7 pour 1 (Figure 2-6A).[157] Par la suite, l'équipe de Tanaka a développé des conditions d'alkylation catalysée au palladium en utilisant des organobismuthines hypervalents. Grâce à cette stratégie, les problèmes pyrophoriques relatifs aux alkylbismuths sont jugulés, mais vraisemblablement en raison de la réaction parasite potentielle d'élimination β-hydrure des palladiums, seuls les dérivés méthylés et insaturés du bismuth sont proposés. Leurs conditions permettent ainsi de méthyler des pseudo-halogénures et halogénures d'aryle avec une quantité catalytique de palladium, avec ou sans base dans du *N*-méthyl-pyrrolidone (NMP) (Figure 2-6B).[130, 158, 159] En s'inspirant de ces travaux, Gagnon a proposé d'appliquer les conditions avec son tricyclopropylbismuthine dont les résultats montrent une grande versatilité avec une tolérance aux hétérocycles jusque-là non vérifiée.[160] Par ailleurs, en s'orientant avec les conditions d'arylation au cuivre de Barton–Finet–Chan[161], il a démontré qu'il était également possible d'utiliser le tricyclopropylbismuth pour *N*-cycloprolyper facilement des lactames, des imides, des indolidinones, des oxazolidinones, des azoles ou encore des indoles (Figure 2-6C).[162]

Figure 2-6 A – Trifluorométhylation du chlorure de benzoyle, d'énamines et d'aniline ; B – Méthylation d'halogénure d'aryles ; C – Cyclopropylation d'halogénures d'aryles et N-cyclopropylation de lactames, d'azoles et d'indoles

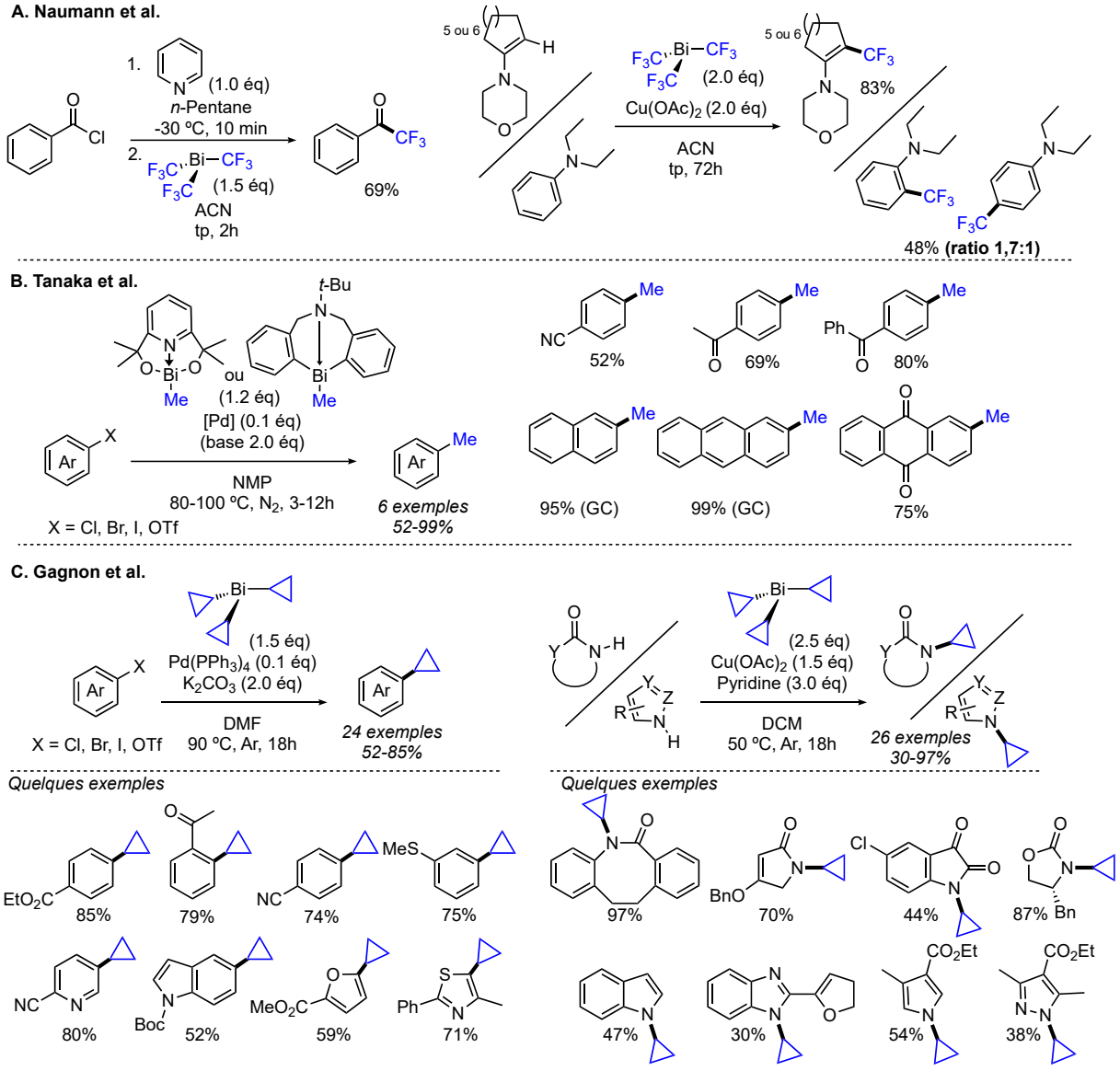

Pendant les études de cyclopropylation catalysée au palladium, l'équipe de Gagnon s'est aperçu avec surprise que leurs conditions permettaient de transférer le groupement éthyle du triéthylbismuthine avec un bon rendement de 81% sans pour autant être impacté par l'élimination β-hydrure tant redoutée. Ainsi, encouragés par ces résultats, ils ont par la suite soumis une variété d'alkylbismuths à différents halogénures d'aryles le tout en maintenant des rendements appréciables (Figure 2-7).[163]

Figure 2-7 Alkylation d'halogénures d'aryles pallado-catalysées

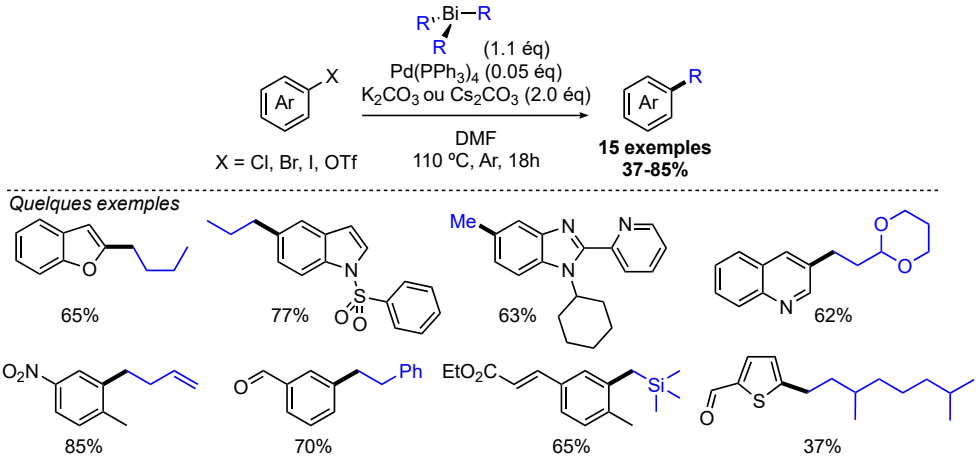

Ces exemples concluent avec virtuosité les dernières réactions rapportées à ce jour d'alkylations par l'utilisation de trialkylbismuthines. Toutefois, bien que très anecdotique, la méthylation à travers un alkylbismuth pentavalent est possible. L'unique exemple disponible dans la littérature est mentionné par Mukaiyama et Sakurai avec la méthylation de l'acide para-toluènesulfonique à partir du méthylbismacycle hypervalent oxydé au préalable avec de l'acide *m*-chloroperbenzoïque (*m*-CPBA) (Figure 2-8).[131]

Figure 2-8 Méthylation de l'acide p-toluènesulfonique par le dicarboxylate de méthylbismacycle

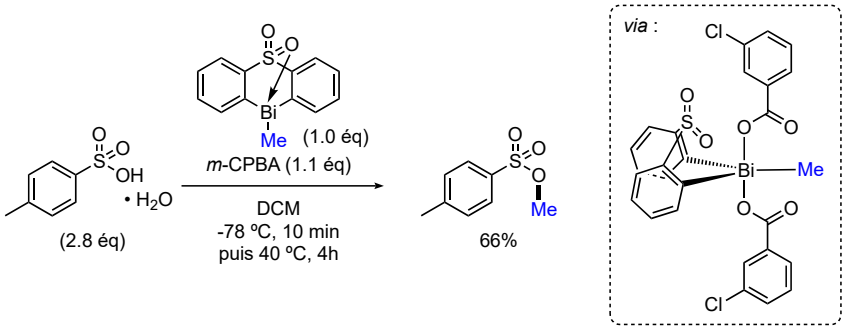

Avant d'embarquer dans les réactions d'arylation, il est nécessaire de mentionner que les méthodes d'arylation à partir d'organobismuthines sont légion dans la littérature et il serait inconvenant de mentionner l'ensemble des stratégies existantes. Ainsi, il sera présenté dans un premier temps une brève sélection des méthodes d'arylation à travers l'usage des arylbismuths trivalents avant de poursuivre dans un deuxième temps celles avec les pentavalents.

2.2.4 Réaction d'arylation par des arylbismuthines trivalentes

Les conditions de transfert d'alkyles vues précédemment peuvent s'appliquer dans le cadre des aryles de manière quasi systématique. En effet, les chlorures d'acyles peuvent se faire aryler à partir d'un arylbismuth trivalent avec une quantité catalytique de palladium. Les prémices de ces travaux ont été effectuées par Barton et ont inspiré un grand nombre de groupes.[145] Notamment, l'équipe de Rao a non seulement su démontrer la grande robustesse de la méthode, mais également qu'une quantité substoechiométrique de triarylbismuth était suffisante puisque les trois aryles sont transférables.[164-168] Suzuki est passé par l'usage d'une arylbismuthine hypervalente[132] alors que les équipes de Tsai[169] et Cai[170] ont proposé des catalyseurs sur support solide contenant du palladium facilement recyclable (Figure 2-9A). Le couplage croisé catalysé au palladium avec des halogénures d'aryles reste remarquablement efficace. Le groupe de Tanaka a ouvert la voie en 1999 en couplant des aryltriflates avec le dialcoolate de méthylbismuth hypervalent.[158] Par la suite, accompagné de Rao,[171-174] ils ont participé activement au développement de la technique en couplant une variété importante de dérivés halogénés aromatiques tels que des thiophènes,[175] des furanes[176], des benzofuranes[177] ou encore des pyridines.[178] À ces travaux sont ajoutés les couplages avec des diazines, des benzopyridines et benzodiazines par les équipes de Condon[179] et de Gagnon.[180, 181] Pour conclure cette partie, des catalyseurs sur support solide ont également été développés par Wang et peuvent être ajoutés à cette liste déjà assez dense (Figure 2-9B).[182] Les couplages croisés au cuivre donnent également accès avec grande facilité aux produits de *N*- et *O*-arylation. Les méthodes de cette dernière ont été beaucoup plus étudiées dans le cadre des bismuths pentavalents, mais il reste intéressant de mentionner que la première et unique *O*-arylation à partir d'un triarylbismuth a été observée par Barton en 1987. Pour ce faire, il a mis en réaction du 3,5-di-*t*-butylphénol avec du triphénylbismuth avec une quantité catalytique d'acétate de cuivre(II) et de la triéthylamine dans du dichlorométhane à température ambiante pendant 24 heures et a observé le produit *O*-phénylé avec un rendement de 25%. Ce rendement a pu être légèrement amélioré en ajoutant une quantité stœchiométrique de cuivre.[183] Ce n'est que plus récemment que cette méthode a été explorée plus en détail par Gagnon et les résultats montrent qu'autant les phénols substitués que les phénols appauvris en électrons sont acceptés.[91, 184] Dans la même lignée, ces mêmes conditions permettent également d'aryler des alcools primaires et secondaires avec des rendements sensiblement similaires (Figure 2-9C).[185] En vue du caractère nucléophile accru des amines, les méthodes de *N*-arylations sont possibles et présentent sans trop de surprise, de bien meilleurs rendements. C'est à travers les études mentionnées plus tôt de 1987 que Barton a usé de l'avantage nucléophilique des azotes pour effectuer ce type d'arylation.[183] En utilisant une quantité catalytique de cuivre dans du dichlorométhane à température ambiante, il a réussi à aryler des azotes d'anilines, d'amines primaires et secondaires en terminant par des hydrazines et hydrazones. Hormis des changements mineurs tels que le nombre d'équivalents de cuivre ou l'ajout d'une base, ses conditions semblaient déjà être les conditions optimales puisqu'elles ont été largement utilisées. En effet, en passant par les arylations des pipéridines de

Banfi en 1994,[186] des amides de Chan en 1996,[161] des hydrazines de Kikugawa[187] et de Ragnarsson en 2000,[188] des imides de Hügel en 2006,[189] des hydrazones de Mäeorg en 2007[190] et des indoles et azoles de Gagnon en 2014, ces mêmes conditions ont toujours été préférées (Figure 2-9D).[191]

Figure 2-9 A – Arylations pallado-catalysées de chlorures d'acyles ; B – Arylations pallado-catalysées d'halogénures d'aryles ; C – *O*-Arylations cupro-catalysées de phénols et d'alcools ; D – *N*-Arylations cupro-catalysées d'azotes

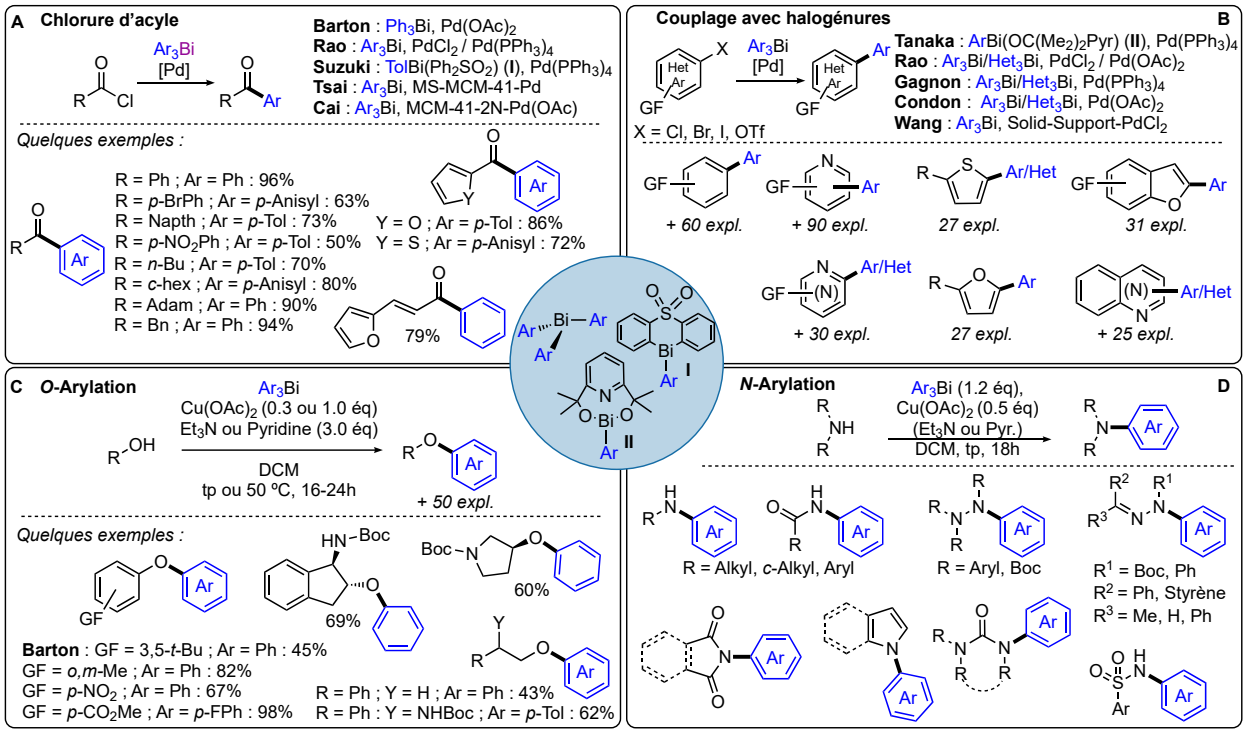

Cette sélection personnelle reflète en somme bien l'étendue du spectre des applications des triarylbismuthines en chimie de synthèse. Bien que déjà très dense, les réactions engageant des bismuthines trivalentes sont relativement moins nombreuses si comparées à celles qui passent par des homologues pentavalents. En effet, ces dernières ont eu le droit à une quinzaine d'années de plus de développement depuis leurs premières applications dans des réactions de transfert.

2.2.5 Réactions d'arylation par des arylbismuthines pentavalentes

Historiquement, la première réaction de transfert d'aryle a été découverte inopinément par Barton en 1980. En effet, en étudiant les capacités oxydantes des bismuths pentavalents, il s'est aperçu qu'en oxydant la quinine avec le carbonate de triphénylbismuth, il obtenait bien la quinone correspondante mais avec un groupement phényle additionnel en position alpha. Dans cette même publication, il a poursuivi ses recherches et réussi avec l'aide d'une base en sus, à aryler des stéroïdes carbonylés et un naphtol en position

alpha du carbonyle et de l'alcool, respectivement.[192] Fort de ces découvertes, il a conduit des études plus approfondies sur l'arylation de phénols et des carbonyles en utilisant une diversité de bismuths pentavalents. Ces premières études sur le phénol étaient d'une grande importance puisqu'elles permettent de mettre en lumière une régiosélectivité différente selon la nature du bismuth ainsi que le pH du milieu réactionnel. En effet, un bismuth de type triphénylé (Ph_3BiX_2) ou tétraphénylé pentavalent (Ph_4BiX) orientera plutôt vers une *O*-arylation en milieu acide ou neutre, et plutôt vers une C^{ortho}-arylation en milieu basique. D'un autre côté, un bismuth de type pentaphénylé (Ph_5Bi) n'étant pas stable, ne s'utilise uniquement qu'en milieu neutre et donnera systématiquement le produit d'*ortho*-arylation correspondant.[124, 193, 194] Les phénols substitués avec un groupement électroattracteur en position *para* font office de singularités à cette règle puisque leurs arylations donneront invariablement le produit éthéré même à pH basique avec n'importe quel type de bismuth (Figure 2-10A). Cette particularité n'est pas très bien comprise à ce jour, mais l'isolation de l'intermédiaire phénolate de bismuth permet de confirmer que le mécanisme d'action ne passe pas par un mécanisme de type S_N2 comme proposé en milieu acide mais qu'il emprunte une voie alternative conduisant au produit de *O*-arylation (voir voie 2, Figure 2-10B).[195]

Figure 2-10 A – Influence de la nature du bismuth pentavalent sur l'arylation régiosélective de dérivés phénols selon le pH ; B – Mécanismes proposés expliquant la régiosélectivité

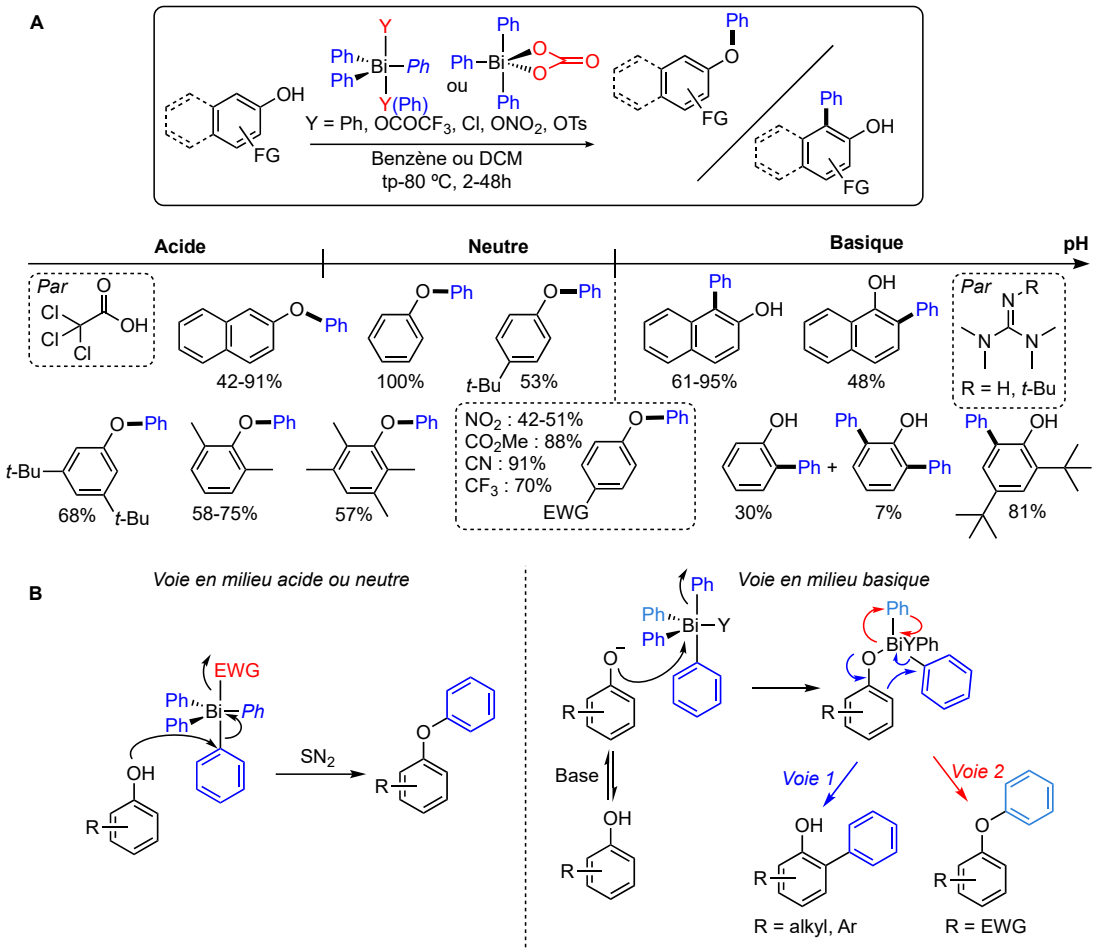

Dans le cadre des carbonyles, les résultats obtenus avec le phénol permettent d'anticiper avec plus ou moins de justesse la régiosélectivité de l'arylation. En effet dans un environnement basique, l'arylation des carbonyles s'effectue plus généralement en position alpha mais cette fois-ci, un environnement neutre semble suivre le même schéma et orienter également en alpha, toutefois avec des rendements nettement inférieurs. Des conditions acides ont été étudiées uniquement dans le cadre de diones et montrent la formation de quelques produits éthérés (Figure 2-11).[196]

Figure 2-11 α-Arylation de carbonyles par des bismuths pentavalents en milieu neutre et basique et *O*-arylation en milieu acide. Milieu : ^{A} = acide, ^{N} = neutre, ^{B} = basique

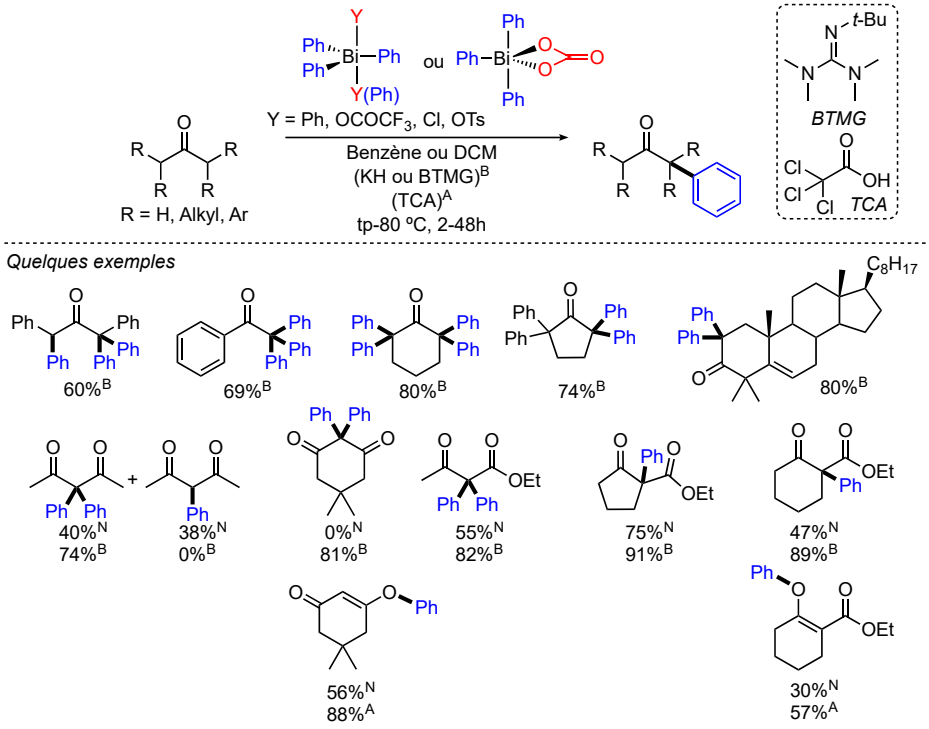

Le pouvoir d'insérer un groupement aryle régiosélectivement uniquement avec un bismuth pentavalent et surtout sans l'intervention d'un autre métal est un avantage incontestable de cette méthode. Cependant, la limitation de transférer uniquement un seul des groupements aromatiques parmi les trois (quatre ou cinq), apporte une certaine limitation à cette méthode en termes d'économie d'atomes. Cette faiblesse a pu être surmontée grâce aux travaux de Finet en 2000 qui, en utilisant des bismacycles pentavalents, a réalisé l'incroyable prouesse de maintenir la réactivité et la régiosélectivité des conditions déjà établies et d'en plus de pouvoir récupérer le sous-produit de bismacycle qui peut être réutilisé après de simples étapes de réactivation.[197] Plus récemment, ces travaux ont été repris et remarquablement approfondis dans le cadre des phénols par Ball en 2020 (Figure 2-12).[151]

Figure 2-12 *C*-Arylations régiosélectives par l'usage de bismacycles pentavalents

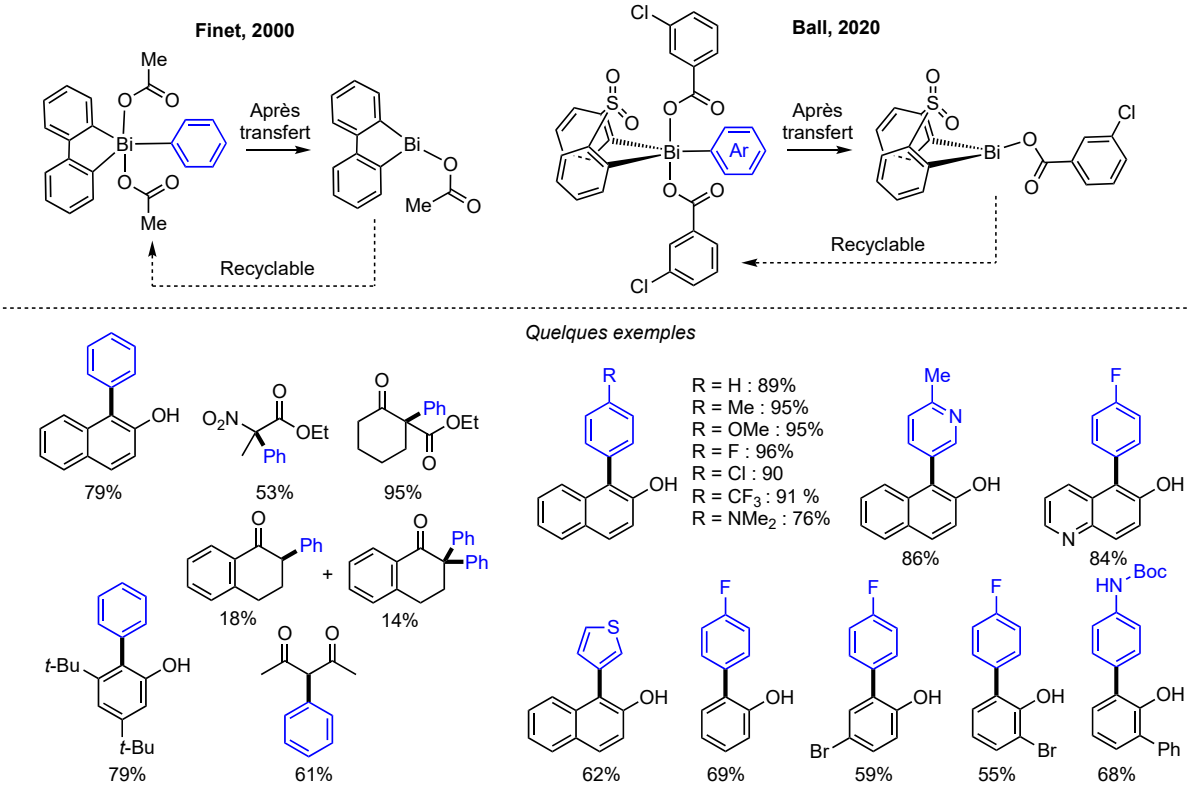

À l'image des bismuths trivalents, il est possible d'utiliser les bismuthines pentavalentes afin d'effectuer des réactions de *N*-[198-201] et *O*-arylation[202-205] cupro-catalysées. Mais la véritable force des bismuths pentavalents réside dans le fait de pouvoir effectuer ce genre de transfert sans l'intermédiaire d'un quelconque métal de transition. Les réactions avec le phénol en démontrent une partie, mais il est possible de trouver dans la littérature des arylations d'alcools plus simples et de diols, aisément en présence de bismuths pentavalents dans du solvant au reflux.[206-208] Les résultats obtenus montrent une efficacité de transfert raisonnable sur les alcools primaires, moyenne sur les secondaires et totalement nulle sur les tertiaires (Figure 2-13A). En revanche, dans le cadre des *N*-arylations, les résultats connus à ce jour sont beaucoup moins favorables à des conditions sans cuivre, mais peuvent toutefois être mentionnés. Dans ses travaux sur la *O*-arylation d'alcools, Barton a essayé ses conditions sur des amides, des imides et un indole.[196, 207] Les produits de *N*-arylations ont bel et bien été obtenus avec des rendements plutôt moyens, à l'exception de l'indole, où le produit de C^3-arylation a été observé majoritairement (Figure 2-13B). Curieusement, la littérature récente ne fait mention d'aucune autre méthode d'arylation à la position C^3 d'un indole à travers l'unique usage d'un organobismuth. Nonobstant, grâce à l'aide d'une catalyse au cuivre et un blocage de la position azotée, il est possible d'obtenir des produits de C^3-arylation avec de bien meilleurs résultats.[209]

Figure 2-13 A – *O*-Arylation d'alcools et de diols à partir de bismuths pentavalents ; B – *N*-Arylation d'amides, d'imides et d'indoles à partir du trifluoroacétate tétraphénylbismuth.

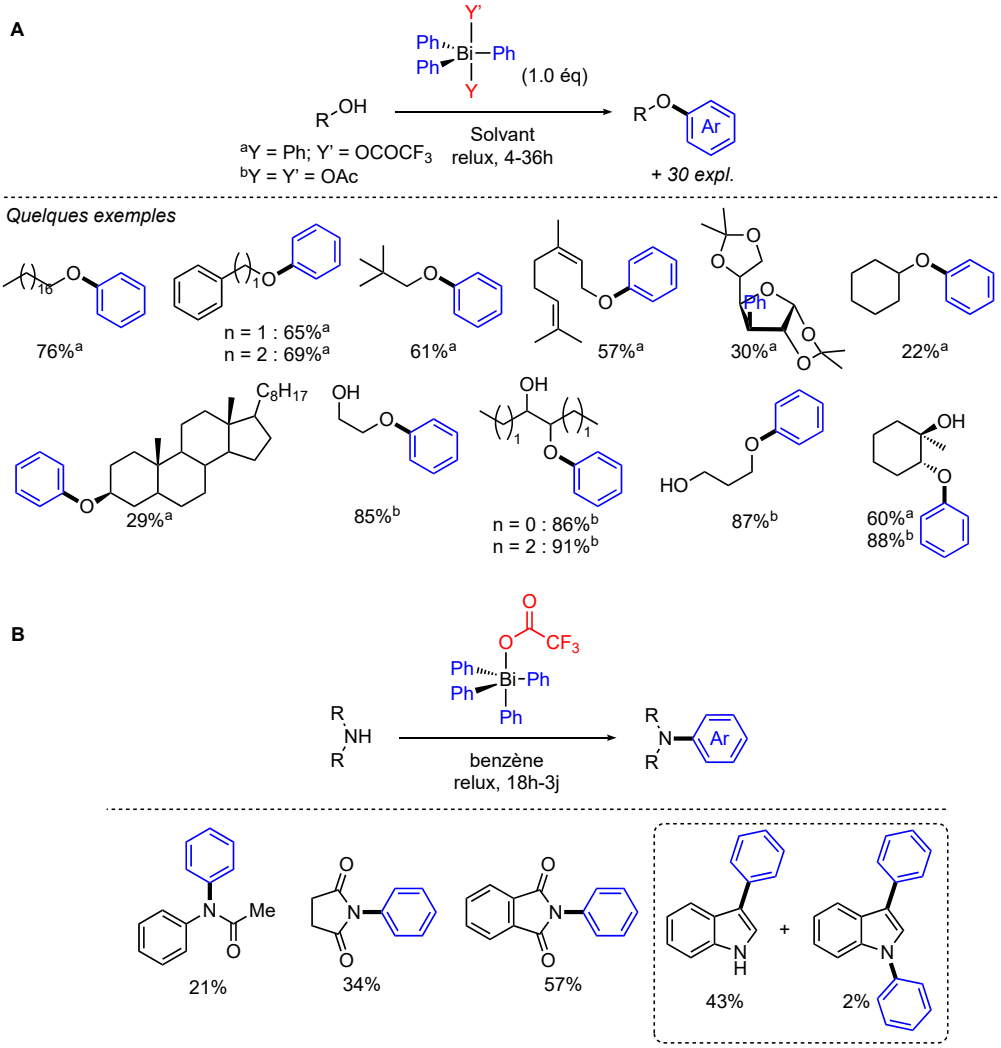

À travers ce chapitre, il a été possible d'appréhender les différentes facettes du bismuth à la fois en tant que métal mais surtout en tant que réactifs en chimie organique. Toutefois, à cette étape de lecture, il se peut qu'il soit déroutant de ne percevoir aucun lien concret entre l'histidine et le bismuth, mais comme mentionné à la fin du chapitre précédent, notre groupe de recherche a utilisé des bismuths trivalents afin de modifier sélectivement la chaîne latérale de différents acides aminés dans de petits peptides. Ces travaux marquent les premières phases de la genèse de cette thèse.

LE BISMUTH AU SERVICE DES MODIFICATIONS DE PEPTIDES

Les arylations de la chaîne latérale d'acides aminés par des bismuths trivalents ont été rapportées pour la première fois en 2020 par notre groupe de recherche. Les conditions développées permettent d'aryler efficacement l'oxygène du phénol de la tyrosine[91] et l'azote de l'indole du tryptophane[92] contenus dans de petits peptides. Au détour du développement de ces méthodes, les conditions d'arylation s'avéraient être également efficaces sur l'imidazole de l'histidine, une découverte fortuite sans précédent et aux applications potentiellement intéressantes (voir Figure 3-1). En effet, les techniques d'arylation vues dans le premier chapitre, bien que très fournies, ne présentent aucun cas d'arylation d'histidine au sein d'un peptide. Ce genre de modification post-synthétique est non seulement très recherchée en chimie médicinale où une modification structurelle de peptides peut avoir des effets thérapeutiques intéressants, mais la modification sélective de l'histidine est également un outil extrêmement convoité en biochimie avec les différentes étiquettes bio-marquantes aux vertus diverses. Mais avant toutes ambitions d'applications concrètes, il est nécessaire de passer par la recherche fondamentale dont cette thèse va essayer d'y apporter une petite pierre et ainsi enrichir cet immense édifice.

Figure 3-1. Résultat d'arylation d'un tripeptide contenant l'histidine durant les études précédentes

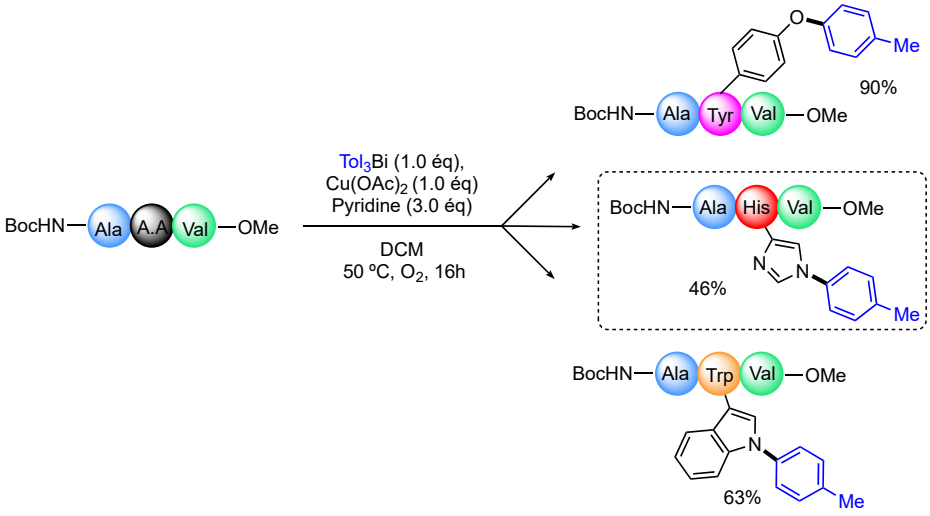

CHAPITRE 3

COPPER-PROMOTED N-ARYLATION OF THE IMIDAZOLE SIDE CHAIN OF PROTECTED HISTIDINE BY USING TRIARYLBISMUTH REAGENTS

3.1 Introduction

Ce chapitre présentera les résultats issus du développement d'une nouvelle méthode d'arylation de l'imidazole de l'histidine sous forme protégée ou peptidique utilisant des triarylbismuthines. En passant par des étapes d'optimisation et des études établissant les limites de la méthode, il a été possible de démontrer que non seulement l'arylation de l'histidine était robuste en tolérant une grande variété de dérivés aromatiques, mais également que la méthode présente une grande spécificité à l'histidine comparée à ses homologues nucléophiles.

3.2 Article issu de ces travaux

Chan, H.-C., Bueno, B., Le Roch, A. and Gagnon, A. (**2021**). Copper-Promoted N-Arylation of the Imidazole Side Chain of Protected Histidine by Using Triarylbismuth Reagents. *Chemistry – A European Journal*, *27*(53), 13330-13336. https://doi.org/10.1002/chem.202102186

Copper-Promoted N-Arylation of the Imidazole Side Chain of Protected Histidine by Using Triarylbismuth Reagents

Hwai-Chien Chan,[a] Bianca Bueno,[a] Adrien Le Roch,[a] and Alexandre Gagnon*[a]

[a] Université du Québec à Montréal
Département de chimie
C.P. 8888, Succursale Centre-Ville
Montréal, Québec, Canada, H3C 3P8
E-mail: gagnon.alexandre@uqam.ca

This paper is dedicated to our colleague and dear friend Prof. Victor Snieckus for his exceptional lifetime contribution to organic Chemistry

Abstract: The N-arylation of the side chain of histidine by using triarylbismuthines is reported. The reaction is promoted by copper(II) acetate in dichloromethane at 40 °C under oxygen in the presence of diisopropylethylamine and 1,10-phenanthroline and allows the transfer of aryl groups with substituents at any position of the aromatic ring. The reaction shows excellent functional group tolerance and is applicable to dipeptides where the histidine is located at the N terminus. A histidine-guided backbone N–H arylation was observed in dipeptides where the histidine occupies the C terminus.

Bismuth is the heaviest stable non-radioactive element of the periodic table.[1] Contrary to its neighboring elements, this heavy metal shows relatively low toxicity, as exemplified by medicinal ingredients that contain inorganic bismuth salts.[2] Due to its borderline behavior as a metal and a classic pnictogen, bismuth compounds have served both as Lewis acids and bases.[3]

Triarylbismuthines are versatile organometallic reagents that have been used in a wide range of transition metalcatalyzed reactions.[4] Our group reported a portfolio of coppercatalyzed methods for the arylation of NH-containing

heterocycles,[5] phenols[6] and amino alcohols[7] that involve triarylbismuthines. Recently, we transposed some of these protocols to the arylation of the side chain of tryptophan[8] and tyrosine.[9] In the course of our studies, we found that the side chain of histidine was considerably reactive under those conditions, resulting in the N-arylation of the imidazole moiety.[9] This observation was in agreement with reports from Finet and more recently Jadhav showing that imidazole can be smoothly arylated by triarylbismuthines in the presence of copper salts.[10] Motivated by these results, we decided to further investigate this reaction. Various methods have been reported for the N-arylation of the side chain of histidine, usually in their N,O-diprotected form. While the arylation can in principle occur at the proximal N(π) or distal N(τ) atom of the imidazole ring in **A**, the vast majority of these methods result in the arylation of the sterically more accessible N(τ) position to deliver product **B** (Scheme 1).[11]

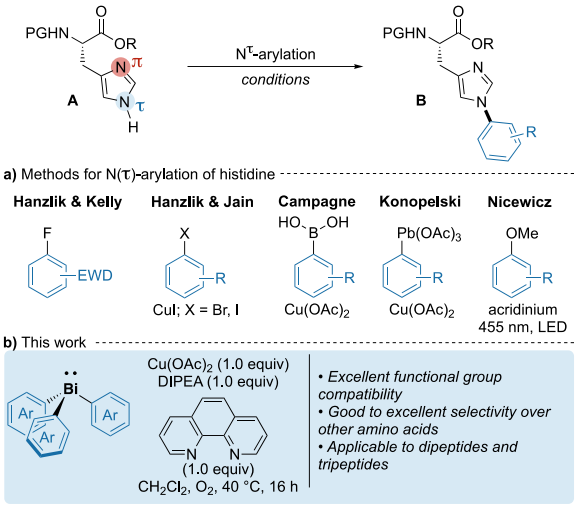

Scheme 1. Methods for the N(τ)-arylation of the side chain of histidine.

The first procedures leading to the arylation of the side chain of histidine relied on an SNAr reaction with aryl fluorides, as shown first by Hanzlik[12] and then by Kelly.[13] However, like most SNAr reactions, these methods require very high temperatures and/ or the presence of electron-withdrawing groups on the aryl substrate. Hanzlik and Jain developed two copper(I)-catalyzed protocols to arylate the side chain of histidine using aryl bromides and iodides.[14] While their methods show excellent scope, high temperatures are required. Using a Chan-Evans-Lam approach, Campagne reported an efficient procedure to arylate the imidazole side chain of histidine.[15] Although the reaction operates under air at a moderate temperature, limited functional groups were introduced on the aryl moiety. Histidine has also been arylated using aryl lead triacetates, as shown by Konopelski, but the toxicity associated with lead reagents considerably limits the use of the method.[16] Recently, Nicewicz performed the arylation of histidine according to a photoredox protocol that involves an aryl methyl ether under irradiation at 455 nm in the presence of an acridinium photosensitizer.[17] However, a mixture of arylation products at N(π) and N(τ) connected to the ortho and para position of anisole was obtained.

There is an interest for general methods that lead to the modification of amino acids, not only in medicinal chemistry where peptides are used as lead compounds, but also in chemical biology where arylated amino acids have been found to play a role in biochemical processes.[18] Even though procedures exist to arylate the side chain of histidine, additional methods that operate under smooth conditions while offering excellent functional group compatibility are still highly desirable. In this context, we would like to report herein our investigation into the copper(II)-promoted arylation of histidine using triarylbismuth reagents.

We commenced our work by optimizing the conditions for the arylation of the imidazole side chain of Boc-protected histidine methyl ester **1a** with tri(4-tolyl)bismuth **2a** (Table 1). Using the conditions that we reported for the arylation of the side chain of tyrosine,[9] we obtained the desired product in 81% yield (entry 1). After testing a few organic bases, we identified N,N-diisopropylethylamine (DIPEA) as a suitable replacement for the undesirable pyridine and found that the reaction could be performed at 40 °C with only 1.0 equivalent of DIPEA (entries 2 to 4). With the objective of improving the yield, we added ligands **L1–L5** and found that 1,10-phenanthroline **L4** and bathophenanthroline **L5** provided the best improvement in the yield of the reaction (entries 5 to 9). Using **L4** as the ligand, we verified the necessity of performing the reaction under oxygen and found a considerable drop in the yield when replacing it by air or argon (entry 10 and 11). Conducting the reaction in other solvents led to the identification of THF and acetonitrile as suitable replacements for dichloromethane (entries 12 to 14). A complete loss of reactivity was observed upon performing the reaction at room temperature, demonstrating the importance of heat (entry 15). Minimal impact on the yield was observed upon reducing the catalyst loading to 0.7 equivalent or lowering the reaction time to 4 h (entry 16 and 17).

We then investigated the scope of the reaction using various triarylbismuth reagents (Scheme 2). To maximize the yields, we used conditions from entry 8 in Table 1. Our results show that the reaction tolerates substituents at any position of the aromatic ring (**3a–d**), is unaffected by electronic effects (**3e–i**), is compatible with a broad range of functional groups (**3j–q**), allows the transfer of a naphthyl unit (**3r**) and functions with Cbz and Fmoc protecting groups (**3s**, **t**). We performed some entries in acetonitrile (yields indicated in brackets) and observed that the transfer proceeded efficiently with the electronically poor 4-fluorophenyl group (**3f**) but not with the electronically rich 4-methoxyphenyl (**3e**) or sterically encumbered 2-tolyl (**3c**). Also, while the efficiency was preserved with Cbz-protected histidine (**3s**), a dramatic drop was observed with the Fmoc counterpart (**3t**).

Table 1. Optimization of the reaction conditions for the copper-promoted N-arylation of the imidazole side chain of N-Boc histidine methyl ester **1a** using tri(4-tolyl)bismuth **2a**.[a]

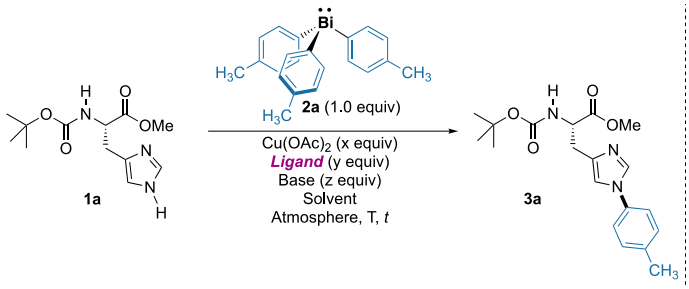

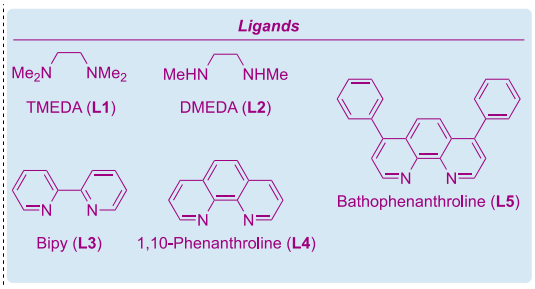

Entry	$Cu(OAc)_2$ (x equiv)	Ligand (y equiv)	Base (z equiv)	Solvent	Atmosphere	T (°C)	*t* (h)	Yield **3a** (%)[b]
1	1.0 equiv	–	Pyridine (3.0 equiv)	CH_2Cl_2	O_2	50	16	81
2	1.0 equiv	–	Et_3N (3.0 equiv)	CH_2Cl_2	O_2	50	16	72
3	1.0 equiv	–	DIPEA (3.0 equiv)	CH_2Cl_2	O_2	50	16	82
4	1.0 equiv	–	DIPEA (1.0 equiv)	CH_2Cl_2	O_2	40	16	84
5	1.0 equiv	**L1** (1.0 equiv)	DIPEA (1.0 equiv)	CH_2Cl_2	O_2	40	16	37
6	1.0 equiv	**L2** (1.0 equiv)	DIPEA (1.0 equiv)	CH_2Cl_2	O_2	40	16	72
7	1.0 equiv	**L3** (1.0 equiv)	DIPEA (1.0 equiv)	CH_2Cl_2	O_2	40	16	85
8	1.0 equiv	**L4** (1.0 equiv)	DIPEA (1.0 equiv)	CH_2Cl_2	O_2	40	16	99
9	1.0 equiv	**L5** (1.0 equiv)	DIPEA (1.0 equiv)	CH_2Cl_2	O_2	40	16	99
10	1.0 equiv	**L4** (1.0 equiv)	DIPEA (1.0 equiv)	CH_2Cl_2	Air	40	16	88
11	1.0 equiv	**L4** (1.0 equiv)	DIPEA (1.0 equiv)	CH_2Cl_2	Argon	40	16	42
12	1.0 equiv	**L4** (1.0 equiv)	DIPEA (1.0 equiv)	DMF	O_2	40	16	87
13	1.0 equiv	**L4** (1.0 equiv)	DIPEA (1.0 equiv)	THF	O_2	40	16	99
14	1.0 equiv	**L4** (1.0 equiv)	DIPEA (1.0 equiv)	MeCN	O_2	40	16	98
15	1.0 equiv	**L4** (1.0 equiv)	DIPEA (1.0 equiv)	MeCN	O_2	r.t.	16	0
16	0.7 equiv	**L4** (0.7 equiv)	DIPEA (1.0 equiv)	MeCN	O_2	40	16	93
17	1.0 equiv	**L4** (1.0 equiv)	DIPEA (1.0 equiv)	MeCN	O_2	40	4	93

[a] Reaction performed in a sealed tube placed in an oil bath at the indicated temperature and under the specified atmosphere. [b] Yield of isolated pure product. DMF = N,N-dimethylformamide. THF = tetrahydrofuran.

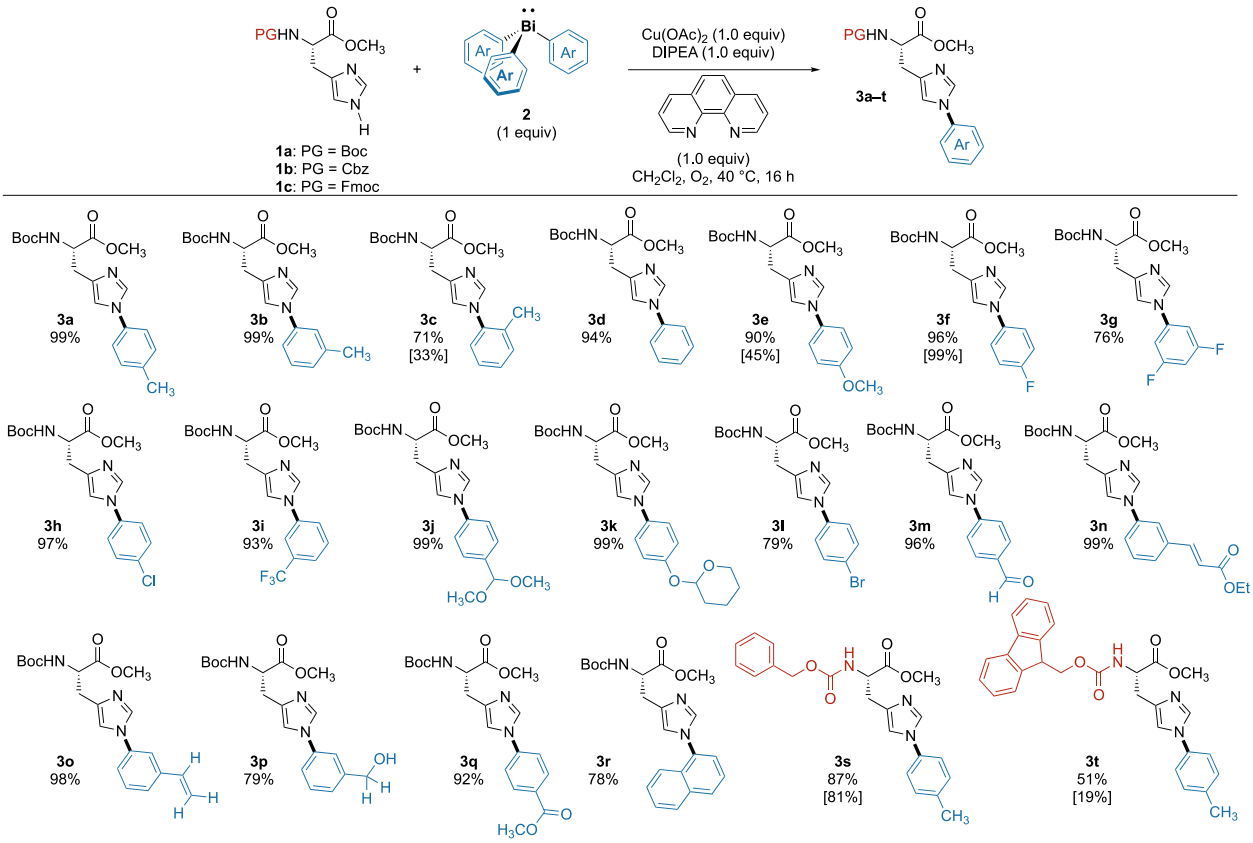

Scheme 2. Scope of the N-arylation of the side chain of N-protected histidine methyl esters **1a–c**. Yields are for isolated pure products; yields in brackets are for reactions performed in MeCN instead of CH_2Cl_2.

Before transposing our protocol to histidine-containing peptides, we sought to evaluate the relative reactivity of amino acids possessing a nucleophilic side chain under our newly optimized conditions (Figure 1).

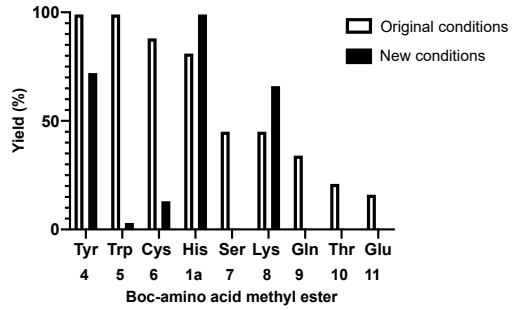

Figure 1. Arylation of amino acids possessing a nucleophilic side chain. Original conditions: amino acid N-Boc methyl ester (1.0 equiv), $(p\text{-Tol})_3Bi$ (1.0 equiv), $Cu(OAc)_2$ (1.0 equiv), pyridine (3.0 equiv), CH_2Cl_2, O_2, 50 °C, 16 h.[9] New conditions: amino acid N-Boc methyl ester (1.0 equiv), $(p\text{-Tol})_3Bi$ (1.0 equiv), $Cu(OAc)_2$ (1.0 equiv), DIPEA (1.0 equiv), 1,10-phen (1.0 equiv), CH_2Cl_2, O_2, 40 °C, 16h. Numbers refer to the N-Boc methyl ester amino acids substrates.

Under our original conditions, N-Boc tyrosine methyl ester **4** and N-Boc tryptophan methyl ester **5** were almost equally reactive, followed by N-Boc cysteine methyl ester **6** and N-Boc histidine methyl ester **1a** (Figure 1, white bars).[9] This lack of differentiation in reactivity was expected to lead to issues of chemoselectivity during the arylation of histidine-containing peptides. Under our new conditions (Figure 1, black bars), a dramatic change in the order of reactivity between the amino acids was observed: N-Boc histidine methyl ester 1a was now the most reactive amino acid, followed by N-Boc tyrosine methyl ester **4** and N-Boc lysine methyl ester **8**. N-Boc tryptophan methyl ester **5** and NBoc cysteine methyl ester **6** were found to be poorly reactive under these new conditions: indeed, N-Boc tryptophan methyl ester **5** gave the arylated product in only 12% yield with 88% recovered starting material while N Boc cysteine methyl ester **6** gave the desired product in 19% along with 59% recovered starting material. N-Boc serine methyl ester **7**, N-Boc glutamine methyl ester **9**, N-Boc threonine methyl ester **10** and N-Boc glutamic acid mono methyl ester **11** were all recovered intact. While it is difficult to explain this drastic change in ranking of amino acids between the original and the new conditions, it must be hypothesized that the lower reaction temperature combined with the presence of the 1,10-phenanthroline ligand are necessarily responsible for this phenomenon. Further mechanistic and theoretical studies will be needed to better understand the difference in reactivity under both sets of conditions.

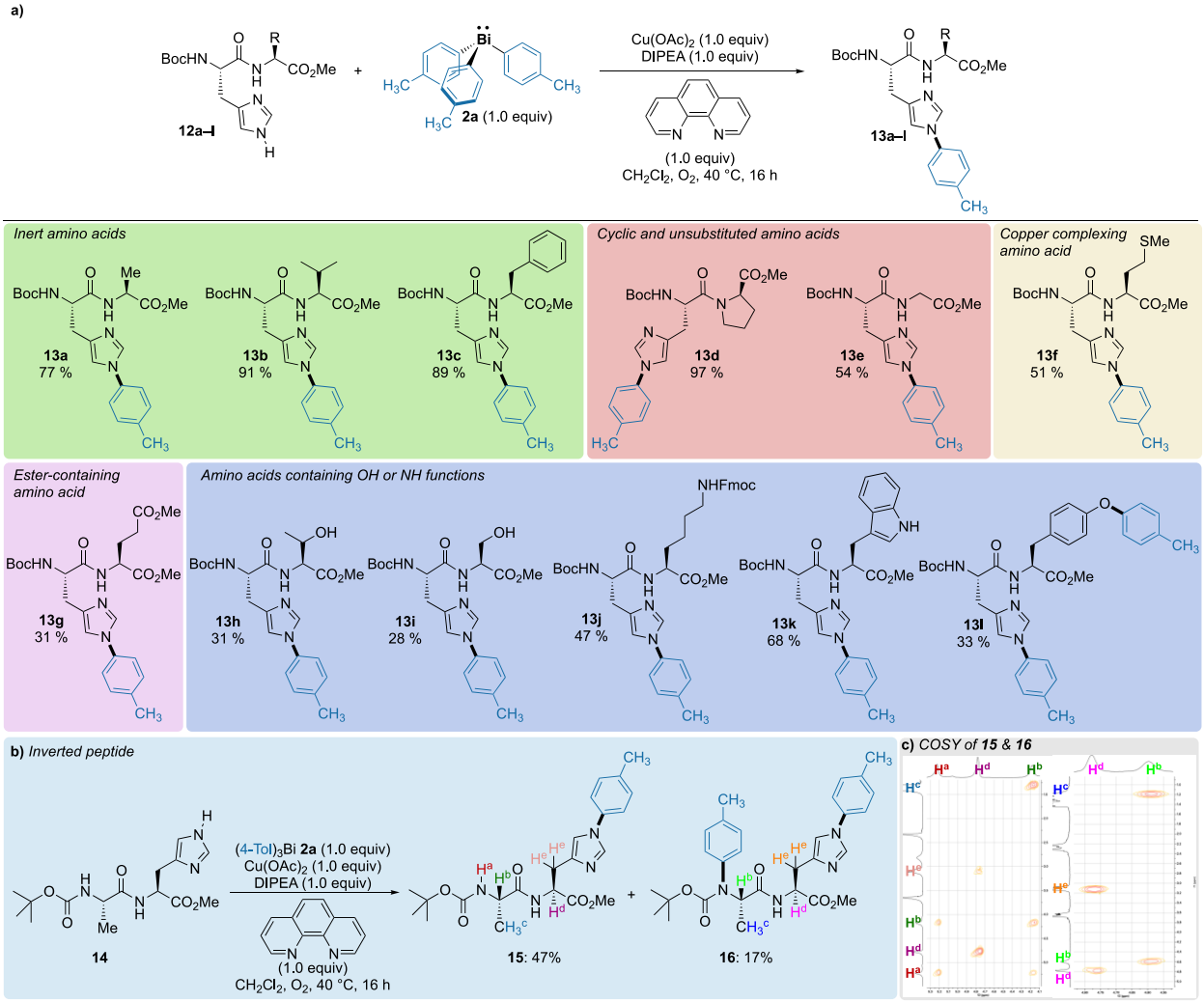

Scheme 3. a) N-Arylation of histidine-containing dipeptides **12a–l**. b) Double histidine and backbone N-arylation of "inverted" Boc-Ala-His-OMe. Yields of isolated pure products. c) COSY spectra of product **15** and **16** (full spectra in Supporting Information).

Having established the order of reactivity of protected amino acids under our arylating conditions, we explored the chemoselectivity in the context of histidine-containing dipeptides where histidine occupies the N-terminal position (Scheme 3a). Thus, dipeptides **12a–l** were prepared by conventional methods (see the Supporting Information for details) and were reacted with tri(4-tolyl)bismuth **2a** under our optimized conditions. In the event, good to excellent yields were obtained with dipeptides where histidine is connected to an inert or cyclic amino acid (**13a–d**). Lower yields were obtained when the histidine is connected to an unsubstituted glycine residue (**13e**), a copper-complexing methionine (**13f**) or an estercontaining amino acid (**13g**). Using bathophenanthroline instead of phenanthroline resulted in similar yields for **13a** (78%) and 13f (54 %), motivating us to pursue with the simpler phenanthroline ligand. The arylation of Boc-His-Thr-OMe and Boc-His-Ser-OMe gave the products of histidine arylation **13h** and **13i** in low yields, even though N-Boc threonine et serine methyl esters were found to be unreactive under these conditions in our amino acids study (Figure 1c, f). The results suggest that the arylation of amino acids in peptides greatly depends on the immediate environment. However, as anticipated from our amino acid studies, Boc-His-Trp-OMe provided exclusively product **13k** from arylation on the histidine residue while Boc-His-Tyr-OMe led to the diarylated product **13l**.

To verify if the position of the histidine in the dipeptide has an impact on the outcome of the reaction, Boc-Ala-His-OMe **14** was submitted to our arylation reaction (Scheme 3b). Firstly, we found that the product of imidazole N-arylation **15** was formed in lower yield than in the complementary dipeptide Boc-His-Ala-OMe **13a**, suggesting that the position of histidine in the dipeptide affects the yield of the reaction. Secondly, product **16** where two aryl groups are transferred was isolated in 17% yield. 2D NMR analysis showed that the second aryl group had been introduced on the N–H backbone of alanine, thus the amino acid preceding histidine (so-called n-1 residue; Scheme 3c). This type of N–H backbone arylation has previously been reported by Ball in the copper- and nickel-catalyzed arylation of peptides using boronic acids.[19] We sought to gain some understanding about this copper-catalyzed histidinedirected backbone N–H arylation involving triarylbismuth reagents.

To prevent the arylation of the histidine, we prepared dipeptide **17** where the imidazole ring is protected with a trityl group (Scheme 4). When submitted to our arylation conditions, peptide **17** provided the corresponding product of N–H arylation **18a** in a modest 68% yield. This yield was increased to 84% simply by raising the temperature to 50°C. Rapid investigation of the scope of this transformation indicated that aryl groups with electron donating (**18b**) and withdrawing (**18c**) substituents could be efficiently transferred using this protocol. However, we found that the presence of a substituent in ortho position was not accepted, possibly due to exacerbated steric congestion generated by the tert-butyloxycarbonyl protecting group (**18d**).

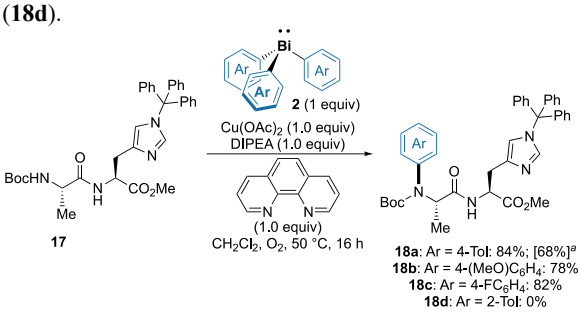

Scheme 4. Histidine-directed N–H backbone arylation of Boc-Ala-His(Nτ-Trt)-OMe **17**. Yield of isolated pure products. [a] Performed at 40 °C instead of 50 °C.

To determine if the reaction is guided by the histidine residue or simply proceeds on the terminal NHBoc moiety, we submitted Boc-Ala-Val-His(Trt)-OMe **19a** to our conditions where a histidine-directed process should lead to the arylation of the central n-1 valine residue (Scheme 5a). In the event, no reaction was observed and the starting material was recovered intact. To make sure that the reaction was not inhibited by the sterically encumbered isopropyl residue at R_2, we submitted the "reverse" tripeptide Boc-Val-Ala-His(Trt)-OMe **19b** to our conditions but again, no reaction was observed. The histidine was then moved to the central position, as shown in Boc-Ala-His (Trt)-Val-OMe **21**, and in this case, the product of arylation at the n-1 position **22** was isolated in 83% yield (Scheme 5b). Finally, to confirm our hypothesis that the imidazole ring acts as a directing group, we prepared tripeptide **23** where the histidine is replaced by a phenyl alanine (Scheme 5c). As anticipated, product of arylation **24** could not be detected and the starting peptide **23** was recovered in 83% yield. Altogether, these results suggest that: 1) the arylation is guided by the histidine; 2) the arylation proceeds at the n-1 position, that is, one residue before the histidine; 3) the arylation occurs only if the n-1 position is also the NHBoc terminus. These results can be best explained by an ATCUN-like motif (amino terminal Cu and Ni) where the copper center is chelated by the imidazole moiety and the peptide backbone (Scheme 5d).[20] In the case of 19a or 19b, formation of the putative copper(III) species would lead to a severe steric clash between the NHBoc and the aryl group (complex i) thus preventing the arylation process. Moreover, the complex would not be able to avoid this steric hindrance since rotation around the C–N or C–C bond would lead to conformers with steric repulsion between R_1 and R_2 (species ii) or R_1 and the Ar group (species iii). On the contrary, in the case of **21**, formation of an ATCUN-like intermediate iv where the copper center is simultaneously chelated by the imidazole, the internal amide, the terminal NBoc and the aryl group would be less hindered and thus allowed, leading to the arylation product **22**.

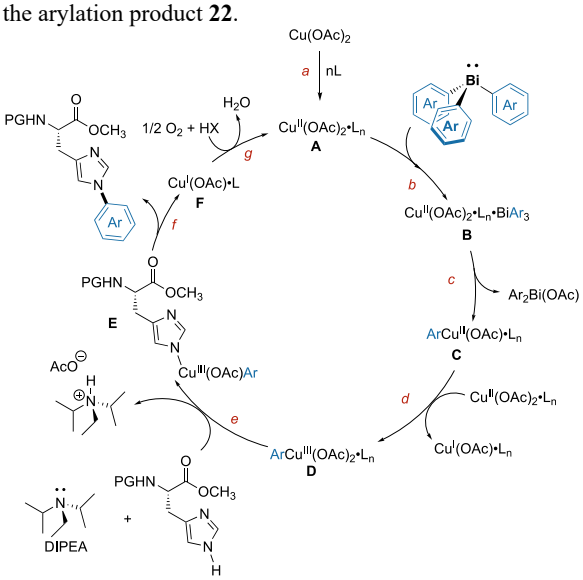

Scheme 6. Proposed mechanism for the N-arylation of the imidazole side chain of histidine. L=1,10-phenanthroline.

The proposed mechanism for the arylation of the imidazole side chain of histidine begins by the complexation of cupric acetate by phenanthroline to give species **A** (Scheme 6, step a). Complexation of the triarylbismuth to this species would then generate species **B** (step b) on which transmetalation of the aryl group from Bi to Cu^{II} would occur (step c) to give species **C** concomitantly with diarylbismuth acetate. Disproportion between the copper(II) complex **C** and copper(II) diacetate would provide the copper(III) intermediate **D** along with copper(I) acetate (step d). Complexation of the imidazole ring of histidine to copper and deprotonation by DIPEA would then lead to the key intermediate **E** where a copper(III) center is simultaneously ligated to the imidazole ring, the aryl group and an acetate (step e). Reductive elimination would provide the desired Narylated product along with cuprous acetate (species F, step f). Oxidation of this copper(I) species by oxygen would regenerate the initial copper(II) catalyst. This mechanism is based on the mechanism proposed for the Chan-Evans-Lam reaction and involves a 2:1 ratio of $Cu(OAc)_2$:Ar_3Bi.[21] Based on our previous results, we exclude a mechanism where copper diacetate oxidizes the triarylbismuth species to its pentavalent triarylbismuth diacetate counterpart.[22] The mechanism for the arylation of the NH backbone of peptides would presumably be similar except that it would proceed through the ATCUN complex iv presented in Scheme 5.

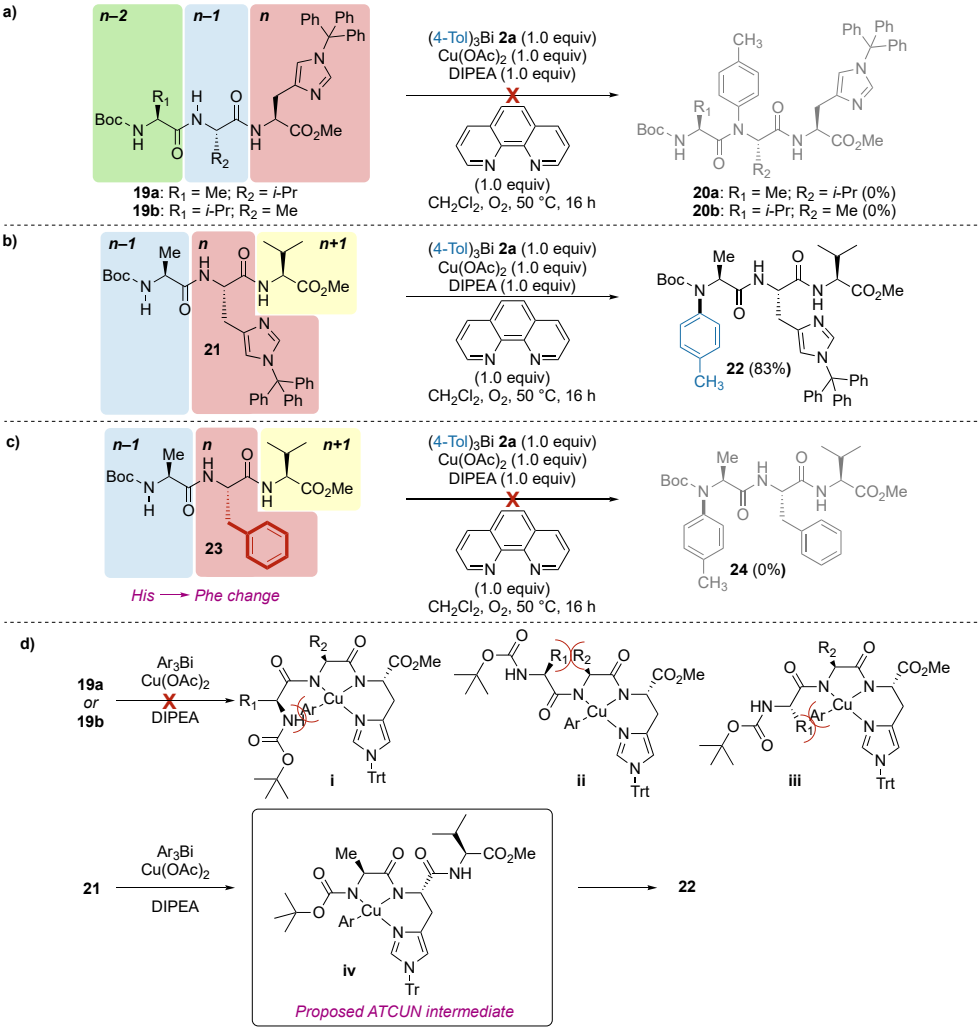

Scheme 5. a) Attempted backbone NH arylation of tripeptides where histidine occupies the C-terminal position. b) Successful backbone NH-arylation of tripeptides where histidine occupies the central position. c) Attempted backbone NH-arylation of tripeptide where the histidine is replaced by a nonchelating phenyl alanine residue. d) Proposed ATCUN models to explain the difference in reactivity between tripeptides **19a**,**b** and **21**. Yields are of isolated pure products.

Finally, we verified that the trityl group could be chemoselectively removed under mild conditions, a process which was achieved by stirring **22** in a 9:1 mixture of acetic acid and water at 60°C for 1.5 h to afford **25** in quantitative yield (Scheme 7).

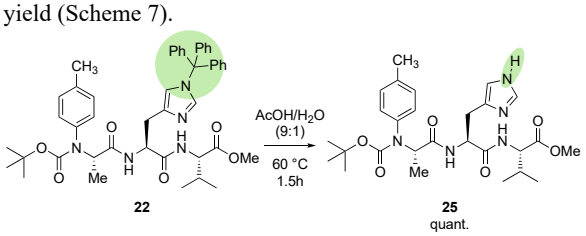

Scheme 7. Selective trityl removal in arylated peptide **22**.

In conclusion, we have developed a protocol to arylate the imidazole side chain of histidine by using triarylbismuthines. The reaction is promoted by cupric acetate, uses 1,10-phenanthroline as a ligand and DIPEA as the base, and operates in dichloromethane at 40°C under an oxygen atmosphere. The reaction is insensitive to electronic or steric effects, shows excellent functional group compatibility, and can be performed with Boc, Cbz or Fmoc protecting groups. The protocol was applied to histidine-containing dipeptides where histidine is at the N terminus. Chemoselective arylation on the histidine residue was obtained in most cases, except when histidine was connected to a tyrosine. Dipeptides where the histidine is at the C terminus resulted in imidazole and N–H backbone arylation. Protection of the imidazole with a trityl group led to exclusive backbone arylation. The arylation occurs at the n-1 position when this position is also the N-terminal position. Chemoselective removal of the trityl group was accomplished under mild conditions.

Acknowledgements

This work was supported by the Natural Sciences and Engineering Research Council of Canada (NSERC), by the Centre in Green Chemistry and Catalysis (CGCC) and by Boehringer Ingelheim Pharmaceuticals Inc. through a

Scientific Advancement grant. We would like to thank Prof. Steve Bourgault for useful discussions and advice.

Conflict of Interest

The authors declare no conflict of interest.

Keywords: copper catalysis • histidine • imidazole • N-arylation • organobismuthines

[1] R. Mohan, *Nat. Chem.* **2010**, *2*, 336.
[2] a) M. Kowalik, J. Masternak, B. Barszcz, *Curr. Med. Chem.* **2019**, *26*, 729–759; b) Y. Yang, R. Ouyang, L. Xu, N. Guo, W. Li, K. Feng, L. Ouyang, Z. Yang, S. Zhou, Y. Miao, *J. Coord. Chem.* **2015**, *68*, 379–397; c) D. M. Keogan, D. M. Griffith, Molecules **2014**, *19*, 15258 15297; d) J. A. R. Salvador, S. A. C. Figueiredo, R. M. A. Pinto, S. M. Silvestre, *Future Med. Chem.* **2012**, *4*, 1495–1523; e) G. G. Briand, N. Burford, *Chem. Rev.* **1999**, *99*, 2601–2658.
[3] a) A. Gagnon, E. Benoit, A. Le Roch, *Sci. Synth. Knowl. Uptades* **2018**, *4*, 1–111 b) A. Gagnon, J. Dansereau, A. Le Roch, *Synthesis* **2017**, *49*, 1707–1745.
[4] a) S. Condon, C. Pichon, M. Davi, *Org. Prep. Proced. Int.* **2014**, *46*, 89–131; b) S. Shimada, M. L. N. Rao, *Top. Curr. Chem.* **2012**, *311*, 199–228; c) H. Suzuki, T. Ikegami, Y. Matano, *Synthesis* **1997**, *3*, 249–267.
[5] P. Petiot, J. Dansereau, A. Gagnon, *RSC Adv.* **2014**, *4*, 22255–22259.
[6] C. Crifar, P. Petiot, T. Ahmad, A. Gagnon, *Chem. Eur. J.* **2014**, *20*, 2755–2760.
[7] a) P. Petiot, J. Dansereau, M. Hébert, I. Khene, T. Ahmad, S. Samaali, M. Leroy, F. Pinsonneault, C. Y. Legault, A. Gagnon, *Org. Biomol. Chem.* **2015**, *13*, 1322–1327; b) T. Ahmad, J. Dansereau, M. Hébert, C. Grand-Maître, A. Larivée, A. Siddiqui, A. Gagnon, *Tetrahedron Lett.* **2016**, *57,* 4284–4287.
[8] A. Le Roch, H.-C. Chan, A. Gagnon, *Eur. J. Org. Chem.* **2020**, *36*, 5815–5819.
[9] A. Le Roch, M. Hébert, A. Gagnon, *Eur. J. Org. Chem*. **2020**, *33*, 5363–5367.
[10] a) B. D. Jadhav, S. K. Pardeshi, *RSC Adv.* **2016**, *6*, 14531–14537; b) A. Y. Fedorov, J.-P. Finet, *Tetrahedron Lett.* **1999**, *40*, 2747–2748.
[11] To the best of our knowledge, there are two reports of arylation of histidine at the proximal nitrogen: a) L. Aurelio, R. T. C. Brownlee, A. B. Hughes, *Org. Lett.* **2002**, *4*, 3767–3769; b) L. Aurelio, J. S. Box, R. T. C. Brownlee, A. B. Hughes, M. M. Sleebs, *J. Org. Chem.* **2003**, *68*, 2652–2667.
[12] R. Bambal, R. P. Hanzlik, *J. Org. Chem.* **1994**, *59*, 729–732.
[13] S. Deechongkit, S.-L. You, J. W. Kelly, *Org. Lett.* **2004**, *6*, 497–500.
[14] a) K. K. Sharma, M. Mandloi, R. Jain, *Org. Biomol. Chem.* **2016**, *14*, 8937–8941; b) K. K. Sharma, M. Mandloi, R. Jain, *Eur. J. Org. Chem*. **2017**, *5*, 984–988; c) W. Yue, S. I. Lewis, Y. M. Koen, R. P. Hanzlik, Bioorg. *Med. Chem. Lett.* **2004**, *14*, 1637–1640.
[15] C. DalZotto, J. Michaux, E. Martinand-Lurin, J.-M. Campagne, Eur. *J. Org. Chem.* **2010**, *20*, 3811–3814.
[16] a) G. I. Elliott, J. P. Konopelski, *Org. Lett.* **2000**, *20*, 3055–3057; b) M. E. Mahoney, A. Oliver, Ó. Einarsdóttir, J. P. Konopelski, *J. Org. Chem.* **2009**, *74*, 8212–8218; c) Y. R. Landaverry, K. N. White, M. M. Olmstead, Ó. Einarsdóttir, J. P. Konopelski, *Heterocycles* **2006**, *70*, 147–152; d) K. N. White, I. Sen, I. Szundi, Y. R. Landaverry, L. E. Bria, J. P. Konopelski, M. M. Olmstead, Ó. Einarsdóttir, *Chem. Commun.* **2007**, 3252–3254.
[17] a) N. A. Romero, K. A. Margrey, N. E. Tay, D. A. Nicewicz, *Science* **2015**, *349*, 1326–1330; b) N. E. S. Tay, D. A. Nicewicz, *J. Am. Chem. Soc.* **2017**, *139*, 16100–16104.
[18] a) I. Avan, C. D. Hall, A. R. Katritzky, *Chem. Soc. Rev.* **2014**, *43*, 3575–3594; b) A. A. Kaspar, J. M. Reichert, *Drug Discovery Today* **2013**, *18*, 807–817.
[19] a) J. Ohata, M. B. Minus, M. E. Abernathy, Z. T. Ball, *J. Am. Chem. Soc.* **2016**, *138*, 7472–7475; b) K. Hanaya, M. K. Miller, Z. T. Ball, *Org. Lett*. **2019**, *21*, 2445–2448.
[20] a) B. K. Maiti, N. Govil, T. Kundu, J. J. G. Moura, *iScience* **2020**, *23*, 101792; b) Y. Jin, M. A. Lewis, N. H. Gokhale, E. C. Long, J. A. Cowan, *J. Am. Chem. Soc.* **2007**, *129*, 8353–8361; c) L. W. Donaldson, N. R. Skrynnikov, W.-Y. Choy, D. R. Muhandiram, B. Sarkar, J. D. Forman-Kay, L. E. Kay, *J. Am. Chem. Soc.* **2001**, *123*, 9843–9847.
[21] a) S. D. McCann, S. S. Stahl, *Acc. Chem. Res*. **2015**, *48*, 1756–1766; b) A. Casitas, X. Ribas, *Chem. Sci.* **2013**, *4*, 2301–2318.
[22] M. Hébert, P. Petiot, E. Benoit, J. Dansereau, T. Ahmad, A. Le Roch, X. Ottenwaelder, A. Gagnon, *J. Org. Chem.* **2016**, *81*, 5401–5416.

3.3 Informations supplémentaires

Les informations supplémentaires concernant les protocoles expérimentaux, les caractérisations et les spectres RMN ^{1}H et ^{13}C des composés synthétisés sont disponible en Annexe A et sur https://chemistry-europe.onlinelibrary.wiley.com/doi/10.1002/chem.202102186.

3.4 Contributions des auteurs à l'article

L'auteur de la thèse, et premier auteur de l'article, a réalisé une petite partie de la table d'optimisation des conditions (Table 1), la préparation de la moitié des triarylbismuths pour le schéma 2 et le reste des réactions pour les schémas 3 à 7 ainsi que pour la figure 1. Ceci inclut l'ensemble de la synthèse des dipeptides et tripeptides. L'auteur a également rédigé l'ensemble de la partie expérimentale, le traitement des spectres RMN et a contribué à l'écriture de l'article, la recherche bibliographique affiliée et la préparation des figures.

La seconde auteure, Bianca Bueno, a contribué à la majorité des réactions d'optimisation de la table 1 ainsi que l'intégralité des réactions pour le schéma 2. Elle a également fait la relecture et la correction de la partie expérimentale.

Le troisième auteur, Adrien Le Roch, a contribué à l'initiation du projet avec des réactions démontrant la compatibilité des conditions à l'arylation de l'histidine.

L'auteur de correspondance, le Professeur Alexandre Gagnon, a effectué la rédaction du corps de l'article ainsi que le processus de soumission de celui-ci et a aidé l'auteur principal dans la relecture de la partie expérimentale.

CHAPITRE 4

ON THE COPPER-PROMOTED BACKBONE ARYLATION OF THE HISTIDINE-CONTAINING PEPTIDES USING TRIARYLBISMUTHINES

4.1 Introduction

Suites aux développements des réactions d'arylation de l'imidazole de l'histidine, il a été possible de démontrer que la position du résidu au sein du peptide avait une importance sur la régiospécificité lors du transfert de l'aryle. En effet, un acide aminé précédant l'histidine au sein d'un di- ou tripeptide possède un azote alpha ($N^{terminal}$) suffisamment actif pour se faire aryler. Une observation très peu documentée dans la littérature et qui a été jugée intéressante à investiguer davantage.

4.2 Article issu de ces travaux

Chan, H.-C. and Gagnon, A. (**2022**). On the Copper-Promoted Backbone Arylation of Histidine-Containing Peptides using Triarylbismuthines. *Synthesis*. https://doi.org/10.1055/a-1786-6578

On the Copper-Promoted Backbone Arylation of Histidine-Containing Peptides using Triarylbismuthines

Hwai-Chien Chan[a] and Alexandre Gagnon*[a]

[a] Université du Québec à Montréal
Département de chimie
C.P. 8888, Succursale Centre-Ville
Montréal, Québec, Canada, H3C 3P8
E-mail: gagnon.alexandre@uqam.ca

This paper is dedicated to the memory Dr. Michael Boŝ for his remarkable contribution to the pharmaceutical industry in the Montreal area and his friendship.

Abstract We report herein our detailed investigation on the histidine-directed backbone arylation of histidine-containing peptides using triarylbismuth reagents. The reaction proceeds on the backbone NH of the amino acid that precedes the histidine, the so-called n–1 position. The protocol is applicable to dipeptides where the histidine is located at the C-terminus and to tripeptides where the histidine occupies the central position. The transformation is promoted by copper(II) acetate in the presence of phenanthroline (Phen) and diisopropylethylamine in dichloromethane at 50 °C under oxygen. An excellent scope was observed for the triarylbismuthines. In all cases, the imidazole ring of the histidine is protected with a trityl group to prevent the arylation of the side chain. An ATCUN-like model is proposed to explain the observed results.

Key words triarylbismuthines, histidine, peptides, backbone arylation, copper catalysis

Organobismuth compounds are versatile organometallic species that can be easily accessed from

inexpensive and low-toxic bismuth trichloride.[1] Originally pioneered by Barton, Finet, and Dodonov in the 1980s,[2] these species have recently seen a remarkable renaissance with the work of Burford,[3] Dóstal,[4] Lichtenberg,[5] L. T. Ball,[6] and Cornella,[7] who greatly contributed to demonstrating their unique properties and expanding their synthetic utility. Our own interest in organobismuth chemistry resulted in the development of a series of metal-catalyzed reactions which led to the construction of C–C,[8] C–N,[9] C–O,[10] and C–S bonds.[11]

Amino acids and peptides, long considered as poor choices for drug discovery, are now gaining traction in medicinal chemistry due to their non-planarity and their ability to form strong and selective interactions with various biological targets.[12] As a consequence, multiple methods tomodify amino acids and peptides have appeared in the literature over the past decade.[13] In addition to giving access to potential drug candidates, many of these methods also allow the chemoselective installation of small organic groups that help modulate the biophysical properties of the peptide or investigate the role played by specific residues in the peptide's activity.

Recently, we published three papers on the arylation of the side chain of tryptophan,[14] tyrosine,[15] and histidine[16] using triarylbismuthines. In the course of our studies on the arylation of histidine-containing peptides, we found that
the histidine residue was capable of directing the arylation on the backbone of a dipeptide at the so-called n–1 position (Scheme 1, A → C). To prevent the arylation of the side chain of the histidine, the imidazole ring was protected with a trityl group.

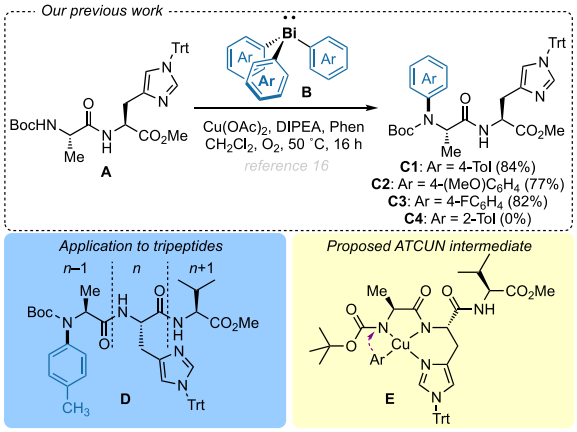

Scheme 1. Our work on the copper-catalyzed histidine-directed backbone arylation of peptides using triarylbismuthines (Phen = phenanthroline)

Our result was in line with that of Z. T. Ball, who observed similar results during the nickel/copper-catalyzed arylation of histidine-containing peptides using arylboronic acids.[17] Ball's method was remarkably powerful due to its the ability to selectively arylate large proteins at the position preceding the histidine.

As a preliminary investigation on the copper-catalyzed histidine-directed backbone arylation of peptides using triarylbismuthines, we found that the reaction was not affected by electronic effects on the aryl ring (**C1–3**), but was completely inhibited by substituents in the ortho position (**C4**) (see Scheme 1). Using Boc-Ala-His(Trt)-Val-OMe to test this manifold, we also discovered that the backbone arylation proceeded only when the *n–1* residue was located at the N-terminus of the peptide, delivering the arylated product **D**. To explain these results, the ATCUN-like (amino terminal copper and nickel) model **E** was proposed (Scheme 1).[18]

Hoping that our method could be complementary to Ball's method, where the amino acid which is arylated does not have to be at the terminal position,[17] and to other methods which indiscriminately arylate the N terminus of peptides,[19] we decided to undertake a thorough investigation of this intriguing copper-promoted histidine-directed backbone arylation of peptides.

Having not demonstrated the scope of the n–1 amino acid in the reaction **A** → **C** above, we began by arylating dipeptides **1a–k** using tris(4-tolyl)bismuth (**2a**) under our previously reported conditions (Scheme 2).[16] In the event, fair to good yields were obtained in cases where the N-terminal amino acid was an alanine (**3a**), a leucine (**3b**), a phenylalanine (**3c**), a glycine (**3d**), or a methionine (**3e**). However, a low yield was obtained for N-Boc-Val-His(Trt)-OMe (**3f**), presumably due to severe steric congestion between the aryl, the tert-butyloxycarbonyl, and the isopropyl group. Chemoselective backbone arylation occurred in dipeptide **3g**, which contains an Fmoc-protected lysine, albeit in low yield. Submitting Boc-Ser-His(Trt)-OMe to our conditions provided the diarylation product **3h** in modest yield. To our surprise, a reversal of chemoselectivity was observed for Boc-Thr-His(Trt)-OMe, where preferential arylation of the OH moiety on the threonine side chain occurred (**3i**).

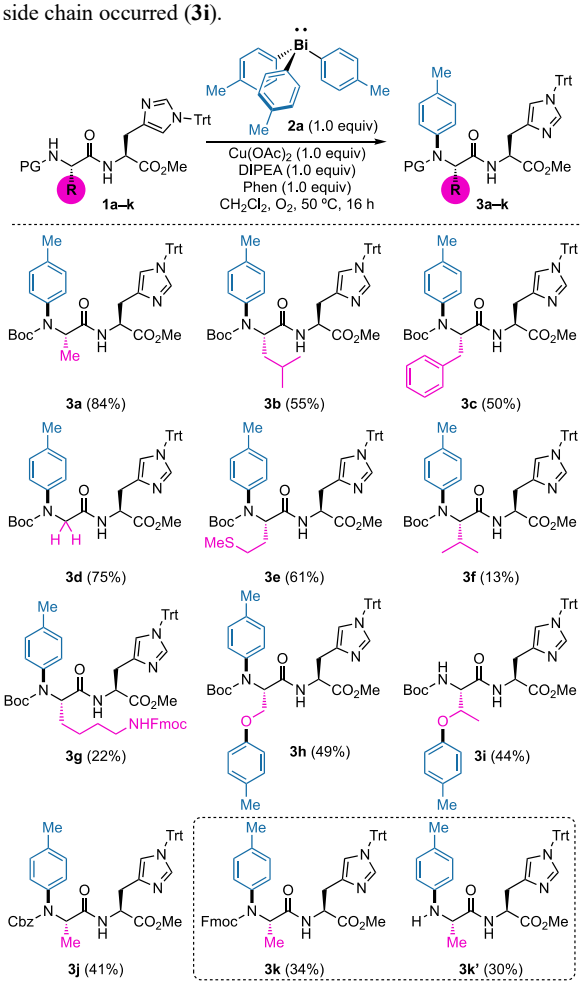

Scheme 2. Scope of the N-terminal amino acid in the histidine-directed backbone arylation of histidine-containing dipeptides

The backbone arylation proceeded less efficiently on peptides protected at the N-terminal with a benzyloxy carbonyl (compare **3j** with **3a**) or a fluorenylmethoxycarbonyl (compare **3k** with **3a**) group (Scheme 2). Unexpectedly, in the case of Fmoc-Ala-His(Trt)-OMe, we also isolated a considerable amount of the unprotected arylated product **3k′**. These two examples indicate that while the arylation can be performed with Cbz-, Fmoc-, and Boc-protected peptides, it is more efficient with the latter.

Having already explored the scope of the aryl group with dipeptides (cf. products **C1–4**), we decided to study the arylation of Boc-Ala-His(Trt)-Val-OMe (**4a**) using various triarylbismuthines (Scheme 3). As predicted from our studies on dipeptide A, we found that the reaction operates reasonably well with *para*- and *meta*-substituted or unsubstituted aryl groups, but not with *ortho*-substituted ones (**5a–ad**). Electron-rich and -deficient aryl groups were transferred in comparable yields (**5ae–af**). However, a low yield was observed with p-(trifluoromethyl)phenyl (**5ag**), while no product could be isolated with 3,5-difluorophenyl (**5ah**). The process tolerates halogens as well as various functional groups (**5ai–an**), offering points of entry for further diversification. A naphthyl group was also transferred in modest yield (**5ao**).

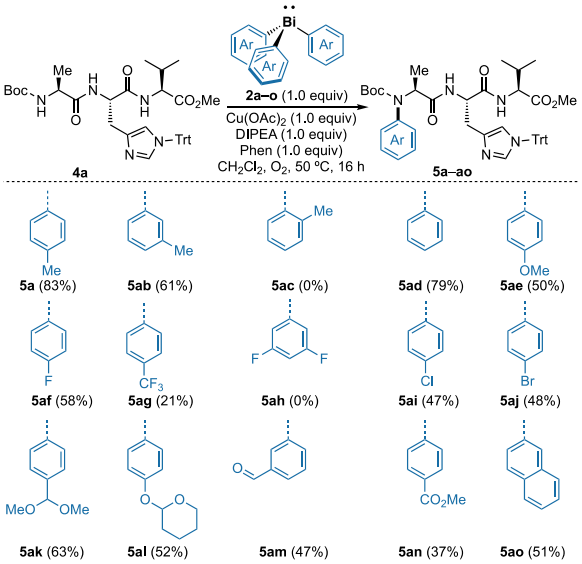

Scheme 3. Scope of the triarylbismuthines in the arylation of Boc-Ala-His(Trt)-Val-OMe

We then moved our focus to the C-terminal *n+1* residue of tripeptides **4a–f** (Scheme 4), with the assumption that this position, as it is remote from the arylation site, should not have a dramatic impact on the efficiency of the process, unless it has a reactive side chain. As anticipated, tripeptides bearing a glycine (**5b**), a phenylalanine (**5c**), a methionine (**5d**), or a proline (**5e**) at the *n+1* position gave similar yields as the original valine-containing tripeptide (**5a**). As expected from compound **3h**, the presence of a serine at the *n+1* position resulted in the formation of the double arylation product **5f**. This product was accompanied by a small amount of mono-arylated product on the serine residue, suggesting that the diarylation proceeds first on the serine and then on the terminal NH.

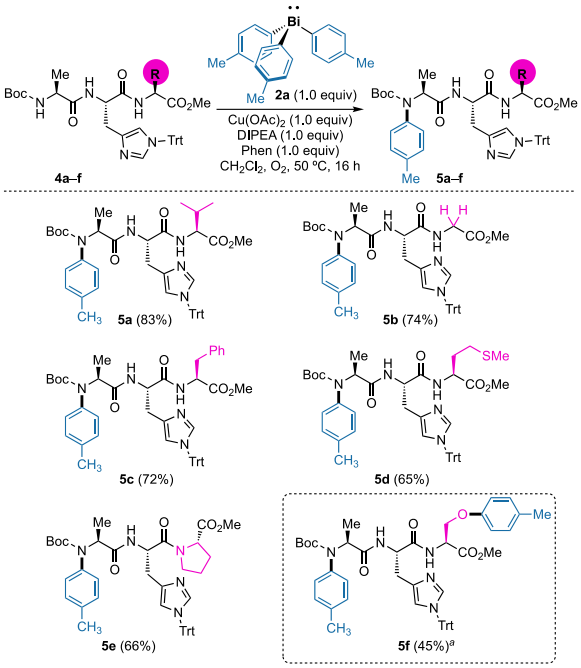

Scheme 4. Scope of the C-terminal *n+1* amino acid in the backbone N–H arylation of tripeptides. [a] Accompanied by 6% of the mono-arylated product on serine.

Using tripeptides **4g–j**, we then evaluated the impact of the amino acid at the *n–1* position on the arylation process (Scheme 5). As anticipated, because the arylation proceeds on the NH backbone at that location, we observed a much greater influence from this residue than the one at the *n+1* position. For instance, a simple, although slightly more encumbered phenylalanine led to a lower yield of the desired product than an alanine (**5g** vs **5a**). The yield could be improved to 46% by using 1.5 equivalents of each reagent.

Arylation of Boc-Gly-His(Trt)-Val-OMe and Boc-Met-His(Trt)-Val-OMe afforded the respective products **5h** and **5i** in slightly higher yields than **5g**, but still lower than **5a** (Scheme 5). As predicted from **3h** and **5f**, arylation of Boc-Ser-His(Trt)-Val-OMe **4j** exclusively provided the product of double arylation **5j**.

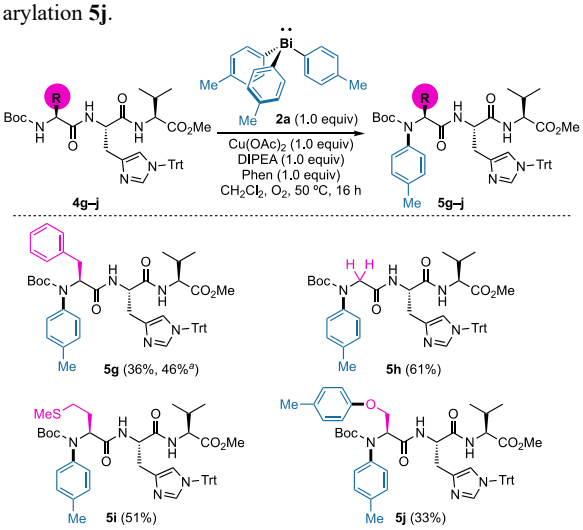

Scheme 5. Scope of the N-terminal *n–1* amino acid in the backbone N–H arylation of tripeptides. a Reaction performed with **2a** (1.5 equiv), $Cu(OAc)_2$, DIPEA, Phen.

In our previous paper,[16] we observed that tripeptides **6a**,**b**, where the histidine is at the C-terminal *n* position, failed to deliver the desired product of backbone arylation **7a**,**b** at *n–1* (Scheme 6). To explain these results, we proposed the ATCUN model **E**, where steric congestion between the side chain residues R^1 and R^2 of the amino acids at the *n–1* and *n–2* positions prevents the formation of the copper(III) intermediate, thus shutting down the arylation process. This led us to conclude that the histidine-directed backbone arylation proceeds on the amino acid preceding the histidine *only* if this residue is *also* at the N-terminal position.

To test this hypothesis, we submitted tripeptides 6c and **6d**, where a glycine at *n–1* or *n–2* is expected to reduce the congestion and therefore permit the arylation reaction. In the event, the unreacted peptides were recovered intact (Scheme 6), suggesting that our model is either incorrect or that the release of steric congestion is still not sufficient to allow the formation of the presumed intermediate **E**. Therefore, we then tested tripeptide Boc-Gly-Gly-His(Trt)-OMe (**6e**) under our conditions and obtained the desired backbone arylation product **7e** in 13% yield. The yield could be increased to 25% by using 1.5 equivalents of tritolylbismuth, copper acetate, DIPEA, and phenanthroline. Comparison of the HSQC $^1H–^{15}N$ NMR spectra between **6e** and **7e** showed the disappearance of the hydrogen on the central glycine, thus confirming that the arylation proceeded at the *n-1* position, that is, left from the histidine (Scheme 6B). Despite the low yields, these results appear to support our model **E**, leading us to slightly revise our original conclusion: the histidine-directed backbone arylation occurs at the amino acid preceding the histidine if this residue is located at the N-terminal position or if it is part of a Gly-Gly-His triad.

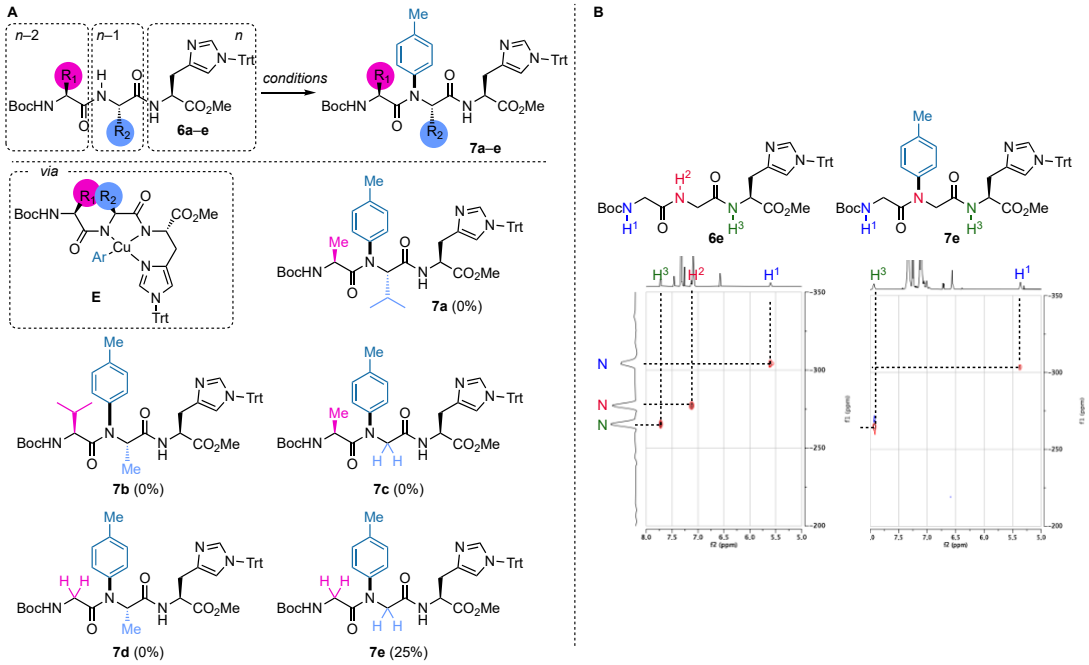

Scheme 6. (A) Studies aimed at testing the ATCUN model **E** for the histidine-directed backbone arylation of tripeptides where the histidine occupies the C-terminal position. Reagents and conditions: Tol_3Bi (1.5 equiv), $Cu(OAc)_2$ (1.5 equiv), DIPEA (1.5 equiv), Phen (1.5 equiv), CH_2Cl_2, O_2, 50 °C, 16h. (B) HSQC $^1H–^{15}N$ spectra of **6e** and **7e** (full spectra in Supporting Information, SI).

To explore the limit of our method, we submitted tetrapeptide Boc-Ala-His(Trt)-Val-Gly-OMe (**8**) to our conditions and obtained the corresponding product **9** in 64% yield, indicating that the process is poorly affected by elongation of the peptide on the C-terminus (Scheme 7). However, we believe that the limit of our procedure has been reached due to solubility issues associated with higher peptides in dichloromethane. Previous attempts at changing the solvent resulted in drastic erosion in the yield of the reaction. To further increase the versatility of our method, we developed conditions to selectively remove each protecting group in **5a** (Scheme 7). The ester could easily be saponified using lithium hydroxide in a 3:1 mixture of methanol and water, resulting in **10**, which was directly coupled with glycine methyl ester by using HATU, to generate **9** in 61% yield over two steps. The ıH NMR spectrum of **9** obtained via the coupling of 10 was identical to that obtained through the arylation of **8**, confirming that the tolyl group was installed on the alanine residue on **8**. The trityl group was selectively removed by treating 5a with acetic acid in water at 60 °C for 1.5 hours, providing **11** in quantitative yield. Selective removal of the tert-butyloxycarbonyl group could be accomplished by treating **5a** with trifluoroacetic acid in dichloromethane at 0 °C for 45 minutes, affording **12** in 69% yield.

In conclusion, we developed a histidine-directed backbone arylation of peptides using triarylbismuthines. The reaction is catalyzed by cupric acetate and operates in dichloromethane at 50 °C under oxygen in the presence of phenanthroline as the copper ligand and diisopropylethylamine as the base. The reaction proceeds on the backbone of dipeptides and tripeptides at the amino acid preceding the histidine only when it occupies the N-terminal position. The arylation of the backbone of tripeptides where the histidine is located at the C-terminus is possible only with the Gly-Gly-His triad. In all cases, the imidazole of the histidine is protected with a trityl group to prevent the arylation of the side chain. Good scope was observed for the triarylbismuth, except for ortho-substituted ones. The protocol was applied to one tetrapeptide. Conditions were developed for the selective removal of each protecting group. The reaction is presumed to proceed via an ATCUN-like

intermediate, where the copper metal is complexed simultaneously by the imidazole ring and two amide bonds.

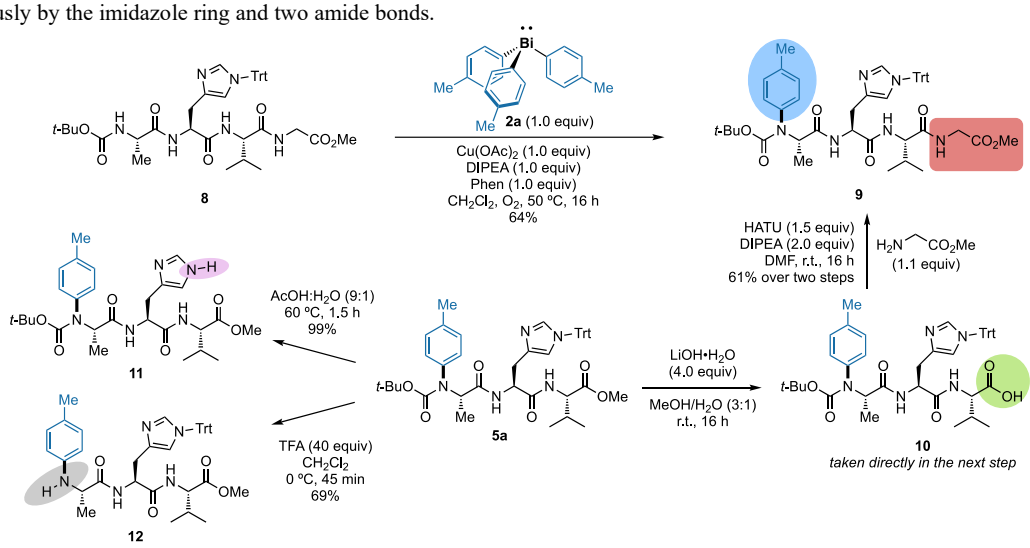

Scheme 7. Histidine-directed backbone arylation of tetrapeptide **8** and further derivatization of tripeptide **5a**

Conflict of Interest

The authors declare no conflict of interest.

Funding Information

This work was supported by the Natural Sciences and Engineering Research Council of Canada (NSERC), the Centre in Green Chemistry and Catalysis (CGCC), and Boehringer Ingelheim Pharmaceuticals Inc. through a Scientific Advancement Grant.

Acknowledgment

We would like to thank Bianca Bueno, Ahmed Fnaiche, and Yarelys Elena Augusto Jimenez for proofreading the manuscript. We would like to acknowledge Cédric Gros for his assistance in the synthesis of selected peptides and Dr. Alexandre Arnold for his help with the NMR experiments.

Supporting Information

Supporting information for this article is available online at https://doi.org/10.1055/a-1786-6578.

References

(1) (a) Gagnon, A.; Benoit, E.; Le Roch, A. *Sci. Synth., Knowl. Updates* **2018**, *4*, 1. (b) Gagnon, A.; Dansereau, J.; Le Roch, A. *Synthesis* **2017**, *49*, 1707. (c) Condon, S.; Pichon, C.; Davi, M. *Org. Prep. Proced. Int.* **2014**, *46*, 89. (d) Shimada, S.; Rao, M. L. N. *Top. Curr. Chem.* **2012**, *311*, 199. (e) *Bismuth-Mediated Organic Reactions*, In *Topics in Current Chemistry*, Vol. *311*; Ollevier, T., Ed.; Springer: Berlin, **2012**.
(2) (a) Barton, D. H. R.; Lester, D. J.; Motherwell, W. B.; Papoula, M. T. B. J. *Chem. Soc., Chem. Commun.* **1980**, 246. (b) Barton, D. H. R.; Bhatnagar, N. Y.; Finet, J.-P.; Motherwell, W. B. *Tetrahedron* **1986**, *42*, 3111. (c) Barton, D. H. R.; Finet, J.-P.; Khamsi, J. *Tetrahedron Lett.* **1987**, *28*, 887. (d) Dodonov, V. A.; Gushchin, A. V.; Brilkina, T. G. *Zh. Obshch. Khim.* **1985**, *55*, 2514.
(3) (a) Gray, P. A.; Burford, N. Coord. *Chem. Rev.* **2016**, *324*, 1. (b) Robertson, A. P. M.; Burford, N.; McDonald, R.; Ferguson, M. J. *Angew. Chem. Int. Ed.* **2014**, *53*, 3480.
(4) (a) Kremláček, V.; Hejda, M.; Rychagova, E.; Ketkov, S.; Jambor, R.; Růžička, A.; Dostál, L. Eur. J. *Inorg. Chem.* **2021**, 4030. (b) Hejda, M.; Jirásko, R.; Růžička, A.; Jambor, R.; Dostál, L. *Organometallics* **2020**, *39*, 4320. (c) Vránová, I.; Dušková, T.; Erben, M.; Jambor, R.; Růžička, A.; Dostál, L. *J. Organomet. Chem.* **2018**, *863*, 15. (d) Vránová, I.; Alonso, M.; Jambor, R.; Růžička, A.; Erben, M.; Dostál, L. *Chem. Eur. J.* **2016**, *22*, 7376. (e) Vránová, I.; Alonso, M.; Lo, R.; Sedlák, R.; Jambor, R.; Růžička, A.; De Proft, F.; Hobza, P.; Dostál, L. *Chem. Eur. J.* **2015**, *21*, 16917. (f) Vránová, I.; Jambor, R.; Růžička, A.; Jirásko, R.; Dostál, L. *Organometallics* **2015**, *34*, 534. (g) Urbanová, I.; Jambor, R.; Růžička, A.; Jirásko, R.; Dostál, L. *Dalton Trans.* **2014**, *43*, 505. (h) Dostál, L.; Novák, P.; Jambor, R.; Růžička, A.; Císařová, I.; Jirásko, R.; Holeček, J. *Organometallics* **2007**, *26*, 2911.
(5) (a) Ramler, J.; Fantuzzi, F.; Geist, F.; Hanft, A.; Braunschweig, H.; Engels, B.; Lichtenberg, C. *Angew. Chem. Int. Ed.* **2021**, *60*, 24388. (b) Lichtenberg, C. *Chem. Commun.* **2021**, *57*, 4483. (c) Ramler, J.; Wüst, L.; Rempel, A.; Wolz, L.; Lichtenberg, C. *Organometallics* **2021**, *40*, 832. (d) Hanft, A.; Radacki, K.; Lichtenberg, C. *Chem. Eur. J.* **2021**, *27*, 6104. (e) Oberdorf, K.; Grenzer, P.; Wieprecht, N.; Ramler, J.; Hanft, A.; Rempel, A.; Stoy, A.; Radacki, K.; Lichtenberg, C. *Inorg. Chem.* **2021**, *60*, 19086. (f) Mukhopadhyay, D. P.; Schleier, D.; Wirsing, S.; Ramler, J.; Kaiser, D.; Reusch, E.; Hemberger, P.; Preitschopf, T.; Krummenacher, I.; Engels, B.; Fischer, I.; Lichtenberg, C. *Chem. Sci.* **2020**, *11*, 7562. (g) Ramler, J.; Krummenacher, I.; Lichtenberg, C. *Angew. Chem. Int. Ed.* **2019**, *58*, 12924.
(6) (a) Senior, A.; Ball, L. T. *Synlett* **2021**, *32*, 235. (b) Ruffell, K.; Ball, L. T. *Trends Chem.* **2020**, *2*, 867. (c) Jurrat, M.; Maggi, L.; Lewis, W.; Ball, L. T. *Nature Chem.* **2020**, *12*, 260.
(7) (a) Planas, O.; Wang, F.; Leutzsch, M.; Cornella, J. *Science* **2020**, *367*, 313. (b) Pang, Y.; Leutzsch, M.; Nöthling, N.; Katzenburg, F.; Cornella, J. *J. Am. Chem. Soc.* **2021**, *143*, 12487. (c) Planas, O.; Peciukenas, V.; Cornella, J. *J. Am. Chem. Soc.* **2020**, *142*, 11382.
(8) (a) Dansereau, J.; Gautreau, S.; Gagnon, A. *ChemistrySelect* **2017**, *2*, 2593. (b) Benoit, E.; Dansereau, J.; Gagnon, A. *Synlett* **2017**, *28*, 2833. (c) Petiot, P.; Gagnon, A. *Heterocycles* **2014**, *88*, 1615. (d) Petiot, P.; Gagnon, A. *Eur. J. Org. Chem.* **2013**, 5282. (e) Gagnon, A.; Albert, V.; Duplessis, M. *Synlett* **2010**, *19*, 2936. (f) Gagnon, A.; Duplessis, M.; Alsabeh, P.; Barabé, F. *J. Org. Chem.* **2008**, *73*, 3604.

(9) (a) Petiot, P.; Dansereau, J.; Gagnon, A. *RSC Adv.* **2014**, *4*, 22255. (b) Gagnon, A.; St-Onge, M.; Little, K.; Duplessis, M.; Barabé, F. *J. Am. Chem. Soc.* **2007**, *129*, 44.
(10) (a) Ahmad, T.; Dansereau, J.; Hébert, M.; Grand-Maître, C.; Larivée, A.; Siddiqui, A.; Gagnon, A. *Tetrahedron Lett.* **2016**, *57*, 4284. (b) Petiot, P.; Dansereau, J.; Hébert, M.; Khene, I.; Ahmad, T.; Samaali, S.; Leroy, M.; Pinsonneault, F.; Legault, C. Y.; Gagnon, A. *Org. Biomol. Chem.* **2015**, *13*, 1322. (c) Crifar, C.; Petiot, P.; Ahmad, T.; Gagnon, A. *Chem. Eur. J.* **2014**, *20*, 2755.
(11) Benoit, E.; Bueno, B.; Choinière, C.; Gagnon, A. J. *Organomet. Chem.* **2019**, *893*, 72.
(12) (a) Sawyer, T. K. *Renaissance in Peptide Drug Discovery: The Third Wave, In Peptide-Based Drug Discovery and New Therapeutics*; The Royal Society of Chemistry: London, **2017**, 1–34. (b) Lee, A. C.-L.; Harris, J. L.; Khanna, K. K.; Hong, J.-H. *Int. J. Mol. Sci.* **2019**, *20*, 2383. (c) Ding, Y.; Ting, J. P.; Liu, J.; Al-Azzam, S.; Pandya, P.; Afshar, S. *Amino Acids* **2020**, *52*, 1207. (d) Blaskovich, M. A. T. *J. Med. Chem.* **2016**, *59*, 10807. (e) Goldflam, M.; Ullman, C. G. *Front. Chem.* **2015**, *3*, 69. (f) Kaspar, A. A.; Reichert, J. M. *Drug Discovery Today* **2013**, *18*, 807. (g) Avan, I.; Hall, C. D.; Katritzky, A. R. *Chem. Soc. Rev.* **2014**, *43*, 3575.
(13) (a) Zhang, C.; Vinogradova, E. V.; Spokoyny, A. M.; Buchwald, S. L.; Pentelute, B. L. *Angew. Chem. Int. Ed.* **2019**, *58*, 4810. (b) Ohata, J.; Martin, S. C.; Ball, Z. T. *Angew. Chem. Int. Ed.* **2019**, *58*, 6176. (c) Malins, L. R. *Aust. J. Chem.* **2016**, *69*, 1360. (d) Miller, M. K.; Ball, Z. T. *Isr. J. Chem.* **2021**, *61*, 387. (e) Noisier, A. F. M.; Brimble, M. A. *Chem. Rev.* **2014**, *114*, 8775. (f) Sengupta, S.; Mehta, G. *Tetrahedron Lett.* **2017**, *58*, 1357. (g) deGruyter, J. N.; Malins, L. R.; Baran, P. S. *Biochemistry* **2017**, *56*, 3863. (14) Le Roch, A.; Chan, H.-C.; Gagnon, A. *Eur. J. Org. Chem.* **2020**, 5815.
(15) Le Roch, A.; Hébert, M.; Gagnon, A. *Eur. J. Org. Chem.* **2020**, 5363.
(16) Chan, H.-C.; Bueno, B.; Le Roch, A.; Gagnon, A. *Chem. Eur. J.* **2021**, *27*, 13330.
(17) (a) Hanaya, K.; Miller, M. K.; Ball, Z. T. *Org. Lett.* **2019**, *21*, 2445. (b) Ohata, J.; Minus, M. B.; Abernathy, M. E.; Ball, Z. T. *J. Am. Chem. Soc.* **2016**, *138*, 7472.
(18) (a) Maiti, B. K.; Govil, N.; Kundu, T.; Moura, J. J. G. *iScience* **2020**, *23*, 101792. (b) Jin, Y.; Lewis, M. A.; Gokhale, N. H.; Long, E. C.; Cowan, J. A. *J. Am. Chem. Soc.* **2007**, *129*, 8353. (c) Donaldson, L. W.; Skrynnikov, N. R.; Choy, W.-Y.; Muhandiram, D. R.; Sarkar, B.; Forman-Kay, J. D.; Kay, L. E. *J. Am. Chem. Soc.* **2001**, *123*, 9843.
(19) (a) Ohata, J.; Ball, Z. T. *Chem. Commun.* **2017**, *53*, 1622. (b) Miller, M. K.; Wang, H.; Hanaya, K.; Zhang, O.; Berlaga, A.; Ball, Z. T. *Chem. Sci.* **2020**, *11*, 10501.
(20) Hébert, M.; Petiot, P.; Benoit, E.; Dansereau, J.; Ahmad, T.; Le Roch, A.; Ottenwaelder, X.; Gagnon, A. *J. Org. Chem.* **2016**, *81*, 5401.
(21) Koshizuka, M.; Makino, K.; Shimada, N. *Org. Lett.* **2020**, *22*, 8658.

4.3 Informations supplémentaires

Les informations supplémentaires concernant les protocoles expérimentaux, les caractérisations et les spectres RMN ^{1}H et ^{13}C des composés synthétisés sont disponible en Annexe B

4.4 Contributions des auteurs à l'article

L'auteur de la thèse, et premier auteur de l'article, a réalisé l'ensemble des réactions. L'auteur a également rédigé la partie expérimentale, le traitement des spectres RMN et a contribué à l'écriture de l'article, la recherche bibliographique affiliée et la préparation des figures.

L'auteur de correspondance, le Professeur Alexandre Gagnon, a effectué la rédaction du corps de l'article ainsi que le processus de soumission de celui-ci et a aidé l'auteur principal dans la relecture de la partie expérimentale.

CONCLUSION

À travers cette thèse il a été possible de faire un peu plus connaissance avec l'histidine en y apprenant comment elle était produite et métabolisée ainsi que ses implications dans les divers processus biologiques. Par la suite, il a été possible de voir que son groupement imidazole pouvait être amené à des modifications naturelles et artificielles. Ces dernières ont été détaillées et présentent un champ large de possibilité avec les travaux remarquables à la fois d'alkylation et d'arylation. D'un autre côté, le bismuth a été présenté comme un métal relativement récent dans le domaine de la chimie de synthèse et mérite une attention toute particulière au vu du fort potentiel qu'il présente. Cette thèse a tenté de le prouver en ajoutant un outil supplémentaire à l'arsenal des modifications post-synthétiques de peptides et de l'histidine elle-même. La méthode développée permet d'aryler l'imidazole de l'histidine avec une compatibilité avec des groupements aromatiques enrichis ou appauvris en électrons et avec des substituants à toutes les positions. De plus, il a été démontré que l'histidine présentait une capacité à diriger l'arylation sur l'azote du résidu placé juste avant elle.

La durée d'une thèse étant évidemment trop courte, il n'a pas été possible d'explorer toutes les facettes des organobismuths et des études supplémentaires peuvent encore être effectuées. En effet, étudier le comportement des organobismuthines dans le cadre de peptides plus longs est une perspective intéressante. La synthèse sur support solide des peptides faciliterait grandement la préparation de tels peptides et l'étape d'arylation pourrait éventuellement s'effectuer entre deux phases d'élongation. Une autre limite assez sensible dans l'utilisation des triarylbismuths est qu'un seul des groupements aryle parmi les trois n'est transférable. Cette limitation pourrait être éventuellement contournée en passant par une stratégie employant des bismacycles hypervalents (voir figure 4-1).

Figure 4-1. Perspectives sur l'étude du comportement des organobismuthines sur de longs peptides synthétisés sur support solide

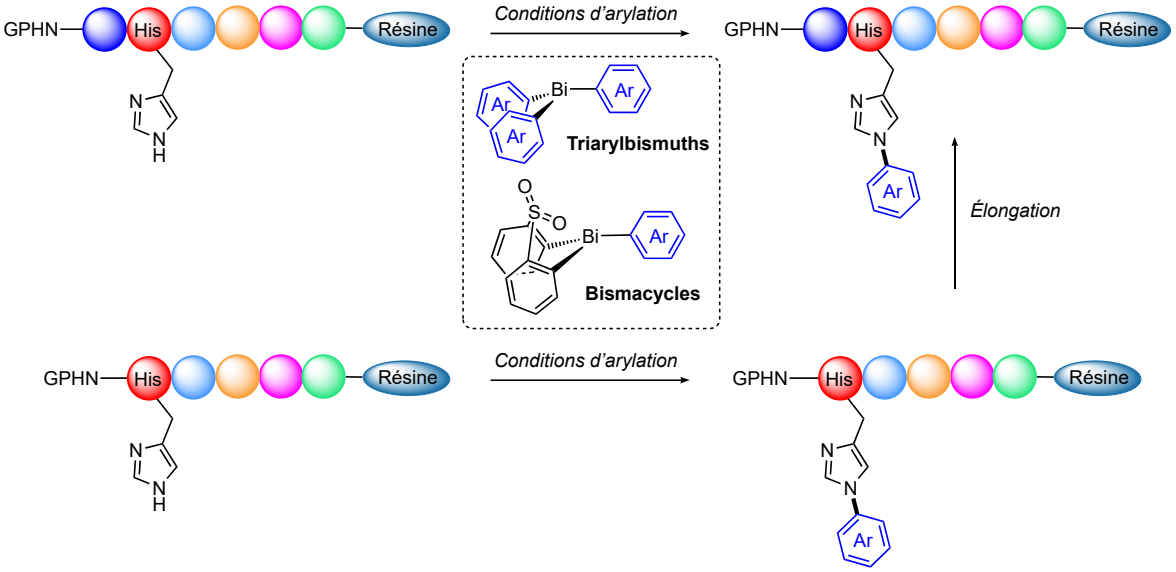

BIBLIOGRAPHIE

1. Sanger, F. (**1988**). Sequences, sequences, and sequences. *Annu Rev Biochem*, *57*, 1-28. https://doi.org/10.1146/annurev.bi.57.070188.000245
2. Merrifield, R. B. (**1963**). Solid Phase Peptide Synthesis. I. The Synthesis of a Tetrapeptide. *Journal of the American Chemical Society*, *85*(14), 2149-2154. https://doi.org/10.1021/ja00897a025
3. Muttenthaler, M., et al. (**2021**). Trends in peptide drug discovery. *Nature Reviews Drug Discovery*, *20*(4), 309-325. https://doi.org/10.1038/s41573-020-00135-8
4. Albericio, F. and Kruger, H. G. (**2012**). Therapeutic peptides. *Future Medicinal Chemistry*, *4*(12), 1527-1531. https://doi.org/10.4155/fmc.12.94
5. Stepansky, A. and Leustek, T. (**2006**). Histidine biosynthesis in plants. *Amino Acids*, *30*(2), 127-42. https://doi.org/10.1007/s00726-005-0247-0
6. Alifano, P., et al. (**1996**). Histidine biosynthetic pathway and genes: structure, regulation, and evolution. *Microbiological reviews*, *60*(1), 44-69. https://doi.org/10.1128/mr.60.1.44-69.1996
7. Akashi, H. and Gojobori, T. (**2002**). Metabolic efficiency and amino acid composition in the proteomes of Escherichia coli and Bacillus subtilis. *Proceedings of the National Academy of Sciences of the United States of America*, *99*(6), 3695-3700. https://doi.org/10.1073/pnas.062526999
8. Fraser, C. M., et al. (**1995**). The minimal gene complement of Mycoplasma genitalium. *Science*, *270*(5235), 397-403. https://doi.org/10.1126/science.270.5235.397
9. Juliao, P. C., et al. (**2007**). Histidine auxotrophy in commensal and disease-causing nontypeable Haemophilus influenzae. *Journal of bacteriology*, *189*(14), 4994-5001. https://doi.org/10.1128/JB.00146-07
10. Liu, Y.-K., et al. (**2020**). Single amino acid utilization for bacterial categorization. *Scientific Reports*, *10*(1), 12686. https://doi.org/10.1038/s41598-020-69686-5
11. Bender, R. A. (**2012**). Regulation of the histidine utilization (hut) system in bacteria. *Microbiology and molecular biology reviews : MMBR*, *76*(3), 565-584. https://doi.org/10.1128/MMBR.00014-12
12. Muralla, R., et al. (**2007**). Genetic Dissection of Histidine Biosynthesis in Arabidopsis. *Plant Physiology*, *144*(2), 890-903. https://doi.org/10.1104/pp.107.096511
13. Riyazuddin, R., et al. (**2022**). A Comprehensive Review on the Heavy Metal Toxicity and Sequestration in Plants. *Biomolecules*, *12*(1). https://doi.org/10.3390/biom12010043
14. Krämer, U., et al. (**1996**). Free histidine as a metal chelator in plants that accumulate nickel. *Nature*, *379*(6566), 635-638. https://doi.org/10.1038/379635a0
15. Fraser, K. A. and Harding, M. M. (**1967**). The crystal and molecular structure of bis(histidino)nickel(II) monohydrate. *Journal of the Chemical Society A: Inorganic, Physical, Theoretical*, 415-420. https://doi.org/10.1039/J19670000415
16. Kretsinger, R. H., Cotton, F. A., and Bryan, R. F. (**1963**). The crystal and molecular structure of di-(l-histidine)-zinc(II) dihydrate. *Acta Crystallographica*, *16*(7), 651-657. https://doi.org/10.1107/S0365110X63001705
17. Moro, J., et al. (**2020**). Histidine: A Systematic Review on Metabolism and Physiological Effects in Human and Different Animal Species. *Nutrients*, *12*(5), 1414. https://doi.org/10.3390/nu12051414
18. Schwarz, T. (**2005**). Mechanisms of UV-induced immunosuppression. *The Keio Journal of Medicine*, *54*(4), 165-171. https://doi.org/10.2302/kjm.54.165
19. Katakura, Y., et al. (**2017**). Anserine/Carnosine Supplementation Suppresses the Expression of the Inflammatory Chemokine CCL24 in Peripheral Blood Mononuclear Cells from Elderly People. *Nutrients*, *9*(11), 1199. https://doi.org/10.3390/nu9111199

20. Michelato, M., et al. (**2017**). Dietary histidine requirement of Nile tilapia juveniles based on growth performance, expression of muscle-growth-related genes and haematological responses. *Aquaculture*, *467*, 63-70. https://doi.org/10.1016/j.aquaculture.2016.06.038
21. Breck, O., et al. (**2003**). Cataract preventative role of mammalian blood meal, histidine, iron and zinc in diets for Atlantic salmon (Salmo salar L.) of different strains. *Aquaculture Nutrition*, *9*(5), 341-350. https://doi.org/10.1046/j.1365-2095.2003.00269.x
22. Remø, S. C., et al. (**2014**). Dietary histidine requirement to reduce the risk and severity of cataracts is higher than the requirement for growth in Atlantic salmon smolts, independently of the dietary lipid source. *British Journal of Nutrition*, *111*(10), 1759-1772. https://doi.org/10.1017/S0007114513004418
23. Kasaoka, S., et al. (**2004**). Histidine supplementation suppresses food intake and fat accumulation in rats. *Nutrition*, *20*(11), 991-996. https://doi.org/10.1016/j.nut.2004.08.006
24. Ookuma, K., et al. (**1989**). Hypothalamic sites of neuronal histamine action on food intake by rats. *Brain Research*, *490*(2), 268-275. https://doi.org/10.1016/0006-8993(89)90244-8
25. Haug, A., et al. (**2008**). Increased broiler muscle carnosine and anserine following histidine supplementation of commercial broiler feed concentrate. *Acta Agriculturae Scandinavica, Section A — Animal Science*, *58*(2), 71-77. https://doi.org/10.1080/09064700802213545
26. Doelman, J., et al. (**2008**). The Effects of Histidine-Supplemented Drinking Water on the Performance of Lactating Dairy Cows. *Journal of Dairy Science*, *91*(10), 3998-4001. https://doi.org/10.3168/jds.2008-1131
27. Li, S. and Hong, M. (**2011**). Protonation, tautomerization, and rotameric structure of histidine: a comprehensive study by magic-angle-spinning solid-state NMR. *Journal of the American Chemical Society*, *133*(5), 1534-1544. https://doi.org/10.1021/ja108943n
28. Holliday, G. L., Mitchell, J. B. O., and Thornton, J. M. (**2009**). Understanding the Functional Roles of Amino Acid Residues in Enzyme Catalysis. *Journal of Molecular Biology*, *390*(3), 560-577. https://doi.org/10.1016/j.jmb.2009.05.015
29. Ekici, O. D., Paetzel, M., and Dalbey, R. E. (**2008**). Unconventional serine proteases: variations on the catalytic Ser/His/Asp triad configuration. *Protein science : a publication of the Protein Society*, *17*(12), 2023-2037. https://doi.org/10.1110/ps.035436.108
30. Shen, C., et al. (**1987**). Prebiotic synthesis of imidazole-4-acetaldehyde and histidine. *Origins of life and evolution of the biosphere*, *17*(3), 295-305. https://doi.org/10.1007/BF02386469
31. MarketWatch. (2022, 24 Février 2022). Histidine Market Size, Share 2022 Global Companies,Growth Status, Consumption, Drivers, Top Leading Countries, Trends, Forces Analysis, Revenue, Challenges and Global Forecast to 2028. Récupéré le 6 Avril 2022 de https://www.marketwatch.com/press-release/histidine-market-sizeshare-2022-global-companiesgrowth-status-consumption-drivers-top-leading-countries-trends-forces-analysis-revenue-challenges-and-global-forecast-to-2028-2022-02-24
32. Ikeda, M., *Amino Acid Production Processes*, in *Microbial Production of l-Amino Acids*, R. Faurie, et al., Editors. 2003, Springer Berlin Heidelberg: Berlin, Heidelberg. p. 1-35.
33. Wu, H., et al. (**2020**). Highly Efficient Production of l-Histidine from Glucose by Metabolically Engineered Escherichia coli. *ACS Synth Biol*, *9*(7), 1813-1822. https://doi.org/10.1021/acssynbio.0c00163
34. Northrup, A. B. and MacMillan, D. W. C. (**2002**). The First Direct and Enantioselective Cross-Aldol Reaction of Aldehydes. *Journal of the American Chemical Society*, *124*(24), 6798-6799. https://doi.org/10.1021/ja0262378
35. Amedjkouh, M. (**2005**). Primary amine catalyzed direct asymmetric aldol reaction assisted by water. *Tetrahedron: Asymmetry*, *16*(8), 1411-1414. https://doi.org/10.1016/j.tetasy.2005.02.031
36. Tsogoeva, S. B. and Wei, S. (**2005**). (S)-Histidine-based dipeptides as organic catalysts for direct asymmetric aldol reactions. *Tetrahedron: Asymmetry*, *16*(11), 1947-1951. https://doi.org/10.1016/j.tetasy.2005.04.027

37. Córdova, A., et al. (**2006**). Direct Asymmetric Intermolecular Aldol Reactions Catalyzed by Amino Acids and Small Peptides. *Chemistry – A European Journal*, *12*(20), 5383-5397. https://doi.org/10.1002/chem.200501639
38. Amedjkouh, M. (**2007**). Aqua-organocatalyzed direct asymmetric aldol reaction with acyclic amino acids and organic bases with control of diastereo- and enantioselectivity. *Tetrahedron: Asymmetry*, *18*(3), 390-395. https://doi.org/10.1016/j.tetasy.2007.01.025
39. Hayashi, Y., et al. (**2008**). The Effectiveness of Proteinogenic Amino Acids in the Asymmetric Aldol Reaction in DMSO and Aqueous DMSO. *Synlett*, *2008*(10), 1565-1570. https://doi.org/10.1055/s-2008-1077789
40. Markert, M., Scheffler, U., and Mahrwald, R. (**2009**). Asymmetric Histidine-Catalyzed Cross-Aldol Reactions of Enolizable Aldehydes: Access to Defined Configured Quaternary Stereogenic Centers. *Journal of the American Chemical Society*, *131*(46), 16642-16643. https://doi.org/10.1021/ja907054y
41. Scheffler, U. and Mahrwald, R. (**2011**). Asymmetric Organocatalyzed Direct Aldol Additions of Enolizable Aldehydes. *Synlett*, *2011*(12), 1660-1667. https://doi.org/10.1055/s-0030-1260813
42. Scheffler, U. and Mahrwald, R. (**2012**). Histidine-Catalyzed Asymmetric Aldol Addition of Enolizable Aldehydes: Insights into its Mechanism. *The Journal of Organic Chemistry*, *77*(5), 2310-2330. https://doi.org/10.1021/jo202558f
43. Armstrong, A., et al. (**2014**). The Houk–List transition states for organocatalytic mechanisms revisited. *Chemical Science*, *5*(5), 2057-2071. https://doi.org/10.1039/C3SC53416B
44. Lam, Y.-h., et al. (**2012**). Stereoselectivities of Histidine-Catalyzed Asymmetric Aldol Additions and Contrasts with Proline Catalysis: A Quantum Mechanical Analysis. *Journal of the American Chemical Society*, *134*(14), 6286-6295. https://doi.org/10.1021/ja2118392
45. Kim, B. M., Park, J. S., and Cho, J. H. (**2000**). Preparation of N(π)-alkyl- histamine and histidine derivatives through efficient alkylation followed by deprotection using activated silica gel. *Tetrahedron Letters*, *41*(51), 10031-10034. https://doi.org/10.1016/S0040-4039(00)01792-5
46. Qian, W., Liu, F., and Burke, T. R. (**2011**). Investigation of Unanticipated Alkylation at the N(π) Position of a Histidyl Residue Under Mitsunobu Conditions and Synthesis of Orthogonally Protected Histidine Analogues. *The Journal of Organic Chemistry*, *76*(21), 8885-8890. https://doi.org/10.1021/jo201599c
47. Colombo, R., Colombo, F., and Jones, J. H. (**1984**). Acid-labile histidine side-chain protection: the N(π)-t-butoxymethyl group. *Journal of the Chemical Society, Chemical Communications*(5), 292-293. https://doi.org/10.1039/C39840000292
48. Okada, Y., et al. (**1996**). Amino acids and peptides. Part 45. Development of a new Nπ-protecting group of histidine, Nπ-(1-adamantyloxymethyl)histidine, and its evaluation for peptide synthesis. *Journal of the Chemical Society, Perkin Transactions 1*(17), 2139-2143. https://doi.org/10.1039/P19960002139
49. Brown, T. and Jones, J. H. (**1981**). Protection of histidine side-chains with π-benzyloxymethyl- or π-bromobenzyloxymethyl-groups. *Journal of the Chemical Society, Chemical Communications*(13), 648-649. https://doi.org/10.1039/C39810000648
50. Hibino, H., Miki, Y., and Nishiuchi, Y. (**2012**). Synthesis and application of Nα-Fmoc-Nπ-4-methoxybenzyloxymethylhistidine in solid phase peptide synthesis. *J Pept Sci*, *18*(12), 763-9. https://doi.org/10.1002/psc.2464
51. Jones, J. H., Ramage, W. I., and Witty, M. J. (**1980**). Mechanism of racemisation of histidine derivatives in peptide synthesis. *Int J Pept Protein Res*, *15*(3), 301-3. https://doi.org/10.1111/j.1399-3011.1980.tb02581.x
52. Jágr, M., et al. (**2007**). Synthesis and Characterization of Styrene Oxide Adducts with Cysteine, Histidine, and Lysine in Human Globin. *Chemical Research in Toxicology*, *20*(10), 1442-1452. https://doi.org/10.1021/tx700057t

53. Espiritu, R. A., et al. (**2013**). Interaction between the Marine Sponge Cyclic Peptide Theonellamide A and Sterols in Lipid Bilayers As Viewed by Surface Plasmon Resonance and Solid-State 2H Nuclear Magnetic Resonance. *Biochemistry*, *52*(14), 2410-2418. https://doi.org/10.1021/bi4000854
54. Ahn, M., et al. (**2013**). Discovery of novel histidine-derived lipo-amino acids: Applied in the synthesis of ultra-short antimicrobial peptidomimetics having potent antimicrobial activity, salt resistance and protease stability. *European Journal of Medicinal Chemistry*, *68*, 10-18. https://doi.org/10.1016/j.ejmech.2013.07.008
55. Liu, F., et al. (**2011**). Serendipitous alkylation of a Plk1 ligand uncovers a new binding channel. *Nature Chemical Biology*, *7*(9), 595-601. https://doi.org/10.1038/nchembio.614
56. Hymel, D., et al. (**2018**). Histidine N(τ)-cyclized macrocycles as a new genre of polo-like kinase 1 polo-box domain-binding inhibitors. *Bioorganic & Medicinal Chemistry Letters*, *28*(19), 3202-3205. https://doi.org/10.1016/j.bmcl.2018.08.018
57. Kimoto, H., Fujii, S., and Cohen, L. A. (**1984**). Photochemical trifluoromethylation of some biologically significant imidazoles. *The Journal of Organic Chemistry*, *49*(6), 1060-1064. https://doi.org/10.1021/jo00180a021
58. Labroo, V. M., Labroo, R. B., and Cohen, L. A. (**1990**). Direct photochemical trifluoromethylation of histidine-containing peptides. *Tetrahedron Letters*, *31*(40), 5705-5708. https://doi.org/10.1016/S0040-4039(00)97937-1
59. Minisci, F., et al. (**1971**). Nucleophilic character of alkyl radicals—VI: A new convenient selective alkylation of heteroaromatic bases. *Tetrahedron*, *27*(15), 3575-3579. https://doi.org/10.1016/S0040-4020(01)97768-3
60. Jain, R., et al. (**1997**). Regiospecific alkylation of histidine and histamine at C-2. *Tetrahedron*, *53*(7), 2365-2370. https://doi.org/10.1016/S0040-4020(96)01193-3
61. Zhang, Y., et al. (**2010**). Diphthamide biosynthesis requires an organic radical generated by an iron–sulphur enzyme. *Nature*, *465*(7300), 891-896. https://doi.org/10.1038/nature09138
62. Chen, X., et al. (**2019**). Histidine-Specific Peptide Modification via Visible-Light-Promoted C–H Alkylation. *Journal of the American Chemical Society*, *141*(45), 18230-18237. https://doi.org/10.1021/jacs.9b09127
63. Noisier, A. F. M., et al. (**2019**). Late-Stage Functionalization of Histidine in Unprotected Peptides. *Angewandte Chemie International Edition*, *58*(52), 19096-19102. https://doi.org/10.1002/anie.201910888
64. Tanret, M. C. (**1909**). Sur une base nouvelle retirée du seigle ergoté, l'ergothionéine *Compt. Rend.*, *149*, 222-224.
65. Heath, H., Lawson, A., and Rimington, C. (**1951**). 488. 2-Mercaptoglyoxalines. Part I. The synthesis of ergothioneine. *Journal of the Chemical Society (Resumed)*(0), 2215-2217. https://doi.org/10.1039/JR9510002215
66. Xu, J. and Yadan, J. C. (**1995**). Synthesis of L-(+)-Ergothioneine. *The Journal of Organic Chemistry*, *60*(20), 6296-6301. https://doi.org/10.1021/jo00125a014
67. Erdelmeier, I., et al. (**2012**). Cysteine as a sustainable sulfur reagent for the protecting-group-free synthesis of sulfur-containing amino acids: biomimetic synthesis of l-ergothioneine in water. *Green Chemistry*, *14*(8), 2256-2265. https://doi.org/10.1039/C2GC35367A
68. Daunay, S., et al. (**2016**). Short protecting-group-free synthesis of 5-acetylsulfanyl-histidines in water: novel precursors of 5-sulfanyl-histidine and its analogues. *Organic & Biomolecular Chemistry*, *14*(44), 10473-10480. https://doi.org/10.1039/C6OB01870J
69. Méndez-Hurtado, J., et al. (**2012**). Theoretical Study of the Oxidation of Histidine by Singlet Oxygen. *Chemistry – A European Journal*, *18*(27), 8437-8447. https://doi.org/10.1002/chem.201103680
70. Amano, M., et al. (**2014**). Detection of Histidine Oxidation in a Monoclonal Immunoglobulin Gamma (IgG) 1 Antibody. *Analytical Chemistry*, *86*(15), 7536-7543. https://doi.org/10.1021/ac501300m

71. Mahindra, A. and Jain, R. (**2012**). Regiospecific Direct C–H Arylation at the 2-Position of l-Histidine Using Arylboronic Acids. *Synlett*, *23*(12), 1759-1764. https://doi.org/10.1055/s-0031-1290381
72. Mahindra, A., Bagra, N., and Jain, R. (**2013**). Palladium-Catalyzed Regioselective C-5 Arylation of Protected l-Histidine: Microwave-Assisted C–H Activation Adjacent to Donor Arm. *The Journal of Organic Chemistry*, *78*(21), 10954-10959. https://doi.org/10.1021/jo401934q
73. Mahindra, A. and Jain, R. (**2014**). Regiocontrolled palladium-catalyzed and copper-mediated C–H bond functionalization of protected l-histidine. *Organic & Biomolecular Chemistry*, *12*(23), 3792-3796. https://doi.org/10.1039/C4OB00430B
74. Cerezo, V., et al. (**2007**). Synthesis of 5-arylhistidines via a Suzuki–Miyaura cross-coupling. *Tetrahedron*, *63*(42), 10445-10453. https://doi.org/10.1016/j.tet.2007.08.010
75. Ramachandran, L. K. and McConnell, W. B. (**1955**). Synthesis of (L) α-2,4-Dinitrophenylhistidne. *Nature*, *176*(4489), 931-932. https://doi.org/10.1038/176931a0
76. Zahn, H. and Pfannmüller, H. (**1956**). α-2,4-Dinitrophenylhistidin. *Angewandte Chemie*, *68*(1), 40-41. https://doi.org/10.1002/ange.19560680108
77. Chillemi, F. and Merrifield, R. B. (**1969**). Use of Nim-dinitrophenylhistidine in the solid-phase synthesis of the tricosapeptides 124-146 of human hemoglobin .beta. chain. *Biochemistry*, *8*(11), 4344-4346. https://doi.org/10.1021/bi00839a018
78. Bambal, R. and Hanzlik, R. P. (**1994**). Synthesis of N.epsilon.-(p-Bromophenyl)-L-lysine and N.tau.-(p-Bromophenyl)-L-histidine as Models for Adducts of Bromobenzene 3,4-Oxide to Protein. Observation of an Unusual Pd-Catalyzed N.tau. to N.pi.-Aryl Substituent Migration. *The Journal of Organic Chemistry*, *59*(4), 729-732. https://doi.org/10.1021/jo00083a011
79. Feldman, K. S., Quideau, S., and Appel, H. M. (**1996**). Galloyl-Derived Orthoquinones as Reactive Partners in Nucleophilic Additions and Diels−Alder Dimerizations: A Novel Route to the Dehydrodigalloyl Linker Unit of Agrimoniin-Type Ellagitannins. *The Journal of Organic Chemistry*, *61*(19), 6656-6665. https://doi.org/10.1021/jo961043u
80. Barton, D. H. R., et al. (**1987**). Phenylation of aromatic and aliphatic amines by phenyllead triacetate using copper catalysis. *Tetrahedron Letters*, *28*(27), 3111-3114. https://doi.org/10.1016/S0040-4039(00)96298-1
81. Barton, D. H. R., et al. (**1989**). Arylation of amines by aryllead triacetates using copper catalysis. *Tetrahedron Letters*, *30*(11), 1377-1380. https://doi.org/10.1016/S0040-4039(00)99469-3
82. Elliott, G. I. and Konopelski, J. P. (**2000**). Complete *N*-1 regiocontrol in the formation of *N*-arylimidazoles. Synthesis of the active site His-Tyr side chain coupled dipeptide of cytochrome c oxidase. *Organic Letters*, *2*(20), 3055-7. https://doi.org/10.1021/ol006271w
83. Cappuccio, J. A., et al. (**2002**). Modeling the Active Site of Cytochrome Oxidase: Synthesis and Characterization of a Cross-Linked Histidine−Phenol. *Journal of the American Chemical Society*, *124*(8), 1750-1760. https://doi.org/10.1021/ja011852h
84. White, K. N., et al. (**2007**). Synthesis and structural characterization of cross-linked histidine–phenol Cu(ii) complexes as cytochrome c oxidase active site models. *Chemical Communications*(31), 3252-3254. https://doi.org/10.1039/B703835F
85. Kiyomori, A., Marcoux, J.-F., and Buchwald, S. L. (**1999**). An efficient copper-catalyzed coupling of aryl halides with imidazoles. *Tetrahedron Letters*, *40*(14), 2657-2660. https://doi.org/10.1016/S0040-4039(99)00291-9
86. Yue, W., et al. (**2004**). Synthesis of Nτ-arylhistidine derivatives via direct N-arylation. *Bioorganic & Medicinal Chemistry Letters*, *14*(7), 1637-1640. https://doi.org/10.1016/j.bmcl.2004.01.058
87. Sharma, K. K., Mandloi, M., and Jain, R. (**2016**). Regioselective copper-catalyzed N(1)-(hetero)arylation of protected histidine. *Organic & Biomolecular Chemistry*, *14*(38), 8937-8941. https://doi.org/10.1039/C6OB01753C
88. DalZotto, C., et al. (**2010**). Chan–Lam–Evans Coupling of Cbz-Protected Histidines. *European Journal of Organic Chemistry*, *2010*(20), 3811-3814. https://doi.org/10.1002/ejoc.201000591

89. Romero, N. A., et al. (**2015**). Site-selective arene C-H amination via photoredox catalysis. *Science*, *349*(6254), 1326-1330. https://doi.org/doi:10.1126/science.aac9895
90. Sharma, K. K., Mandloi, M., and Jain, R. (**2017**). Regioselective Access to 1,2-Diarylhistidines through the Copper-Catalyzed N1-Arylation of 2-Arylhistidines. *European Journal of Organic Chemistry*, *2017*(5), 984-988. https://doi.org/10.1002/ejoc.201601566
91. Le Roch, A., Hébert, M., and Gagnon, A. (**2020**). Copper-Promoted O-Arylation of the Phenol Side Chain of Tyrosine Using Triarylbismuthines. *European Journal of Organic Chemistry*, *2020*(33), 5363-5367. https://doi.org/10.1002/ejoc.202000790
92. Le Roch, A., Chan, H.-C., and Gagnon, A. (**2020**). Copper-Promoted N-Arylation of the Indole Side Chain of Tryptophan Using Triarylbismuthines. *European Journal of Organic Chemistry*, *2020*(36), 5815-5819. https://doi.org/10.1002/ejoc.202000667
93. de Marcillac, P., et al. (**2003**). Experimental detection of α-particles from the radioactive decay of natural bismuth. *Nature*, *422*(6934), 876-878. https://doi.org/10.1038/nature01541
94. Garside, M. (2022, 1 Avril 2022). Major countries in bismuth mine production from 2010 to 2021. Récupéré le 15 Avril 2022 de https://www.statista.com/statistics/264975/production-of-bismuth/
95. DiPalma, J. R. (**2001**). Bismuth Toxicity, Often Mild, Can Result in Severe Poisonings. *Emergency Medicine News*, *23*(3), 16.
96. Voss, S., Rademann, J., and Nitsche, C. (**2022**). Peptide–Bismuth Bicycles: In Situ Access to Stable Constrained Peptides with Superior Bioactivity. *Angewandte Chemie International Edition*, *61*(4), e202113857. https://doi.org/10.1002/anie.202113857
97. Slikkerveer, A. and de Wolff, F. A. (**1989**). Pharmacokinetics and Toxicity of Bismuth Compounds. *Medical Toxicology and Adverse Drug Experience*, *4*(5), 303-323. https://doi.org/10.1007/BF03259915
98. Berger, R. J., et al. (**2012**). Relativistic effects in triphenylbismuth and their influence on molecular structure and spectroscopic properties. *Phys Chem Chem Phys*, *14*(44), 15520-4. https://doi.org/10.1039/c2cp43471g
99. Schulz, S., et al. (**2013**). Solid-State Structures of Trialkylbismuthines BiR3 (R = Me, i-Pr). *Organometallics*, *32*(19), 5445-5450. https://doi.org/10.1021/om400730r
100. Solyntjes, S., et al. (**2017**). Pentafluoroethyl Bismuth Compounds. *Chemistry – A European Journal*, *23*(7), 1557-1567. https://doi.org/10.1002/chem.201604910
101. Bučinský, L., Jayatilaka, D., and Grabowsky, S. (**2016**). Importance of Relativistic Effects and Electron Correlation in Structure Factors and Electron Density of Diphenyl Mercury and Triphenyl Bismuth. *The Journal of Physical Chemistry A*, *120*(33), 6650-6669. https://doi.org/10.1021/acs.jpca.6b05769
102. Ahmad, T., et al. (**2016**). Preparation of 3-O-aryl chloramphenicol derivatives via chemoselective copper-catalyzed O-arylation of (1R,2R)-(−)-N-BOC-2-amino-1-(4-nitrophenyl)-1,3-propanediol using triarylbismuthines. *Tetrahedron Letters*, *57*(38), 4284-4287. https://doi.org/10.1016/j.tetlet.2016.08.021
103. Löwig, C. and Schweizer, E. (**1850**). Ueber Stibäthyl, ein neues antimonhaltiges organisches Radical. *Liebigs Ann.*, *75*(3), 315-355. https://doi.org/10.1002/jlac.18500750307
104. Breed, D. (**1852**). Bismaethyl, ein neues wismuthhaltiges organisches Radical. *Liebigs Ann.*, *82*(1), 106-111. https://doi.org/10.1002/jlac.18520820109
105. Michaelis, A. and Polis, A. (**1887**). Ueber Wismuthtriphenyl und einige Derivate desselben. *Ber. Dtsch. Chem. Ges*, *20*(1), 54-57. https://doi.org/10.1002/cber.18870200110
106. Schaefer, K. and Hein, F. (**1917**). Optische Untersuchungen über die Konstitution von Wismutverbindungen. *Zeitschrift für anorganische und allgemeine Chemie*, *100*(1), 249-303. https://doi.org/10.1002/zaac.19171000110
107. Gilman, H. and Nelson, J. F. (**1937**). Relative Reactivities of Organometallic Compounds. XVI. Detection of the —SH Group. *Journal of the American Chemical Society*, *59*(5), 935-937. https://doi.org/10.1021/ja01284a049

108. Pfeiffer, P. and Pietsch, H. (**1904**). 718. Zur Darstellung der Phenylverbindungen der Elemente der Phosphorgruppe. *Berichte der deutschen chemischen Gesellschaft*, *37*(4), 4620-4623. https://doi.org/10.1002/cber.19040370468
109. Challenger, F. (**1913**). 70. Organic derivatives of bismuth (Preliminary note.). *Proceedings of the Chemical Society, London*, *29*(412), 65-80. https://doi.org/10.1039/PL9132900065
110. Supniewski, J. V. and Adams, R. (**1926**). Organic Bismuth Compounds. I. Preparation of Tricarboxy-Triphenylbismuth Dichlorides and Certain Nitro-Triaryl Bismuth Compounds. *Journal of the American Chemical Society*, *48*(2), 507-517. https://doi.org/10.1021/ja01413a031
111. Marquardt, A. (**1887**). Ueber Wismuthalkyle. *Berichte der deutschen chemischen Gesellschaft*, *20*(1), 1516-1523. https://doi.org/10.1002/cber.188702001332
112. Fischer, E. O. and Schreiner, S. (**1960**). Cyclopentadienylverbindungen des Wismuts und Antimons. *Chemische Berichte*, *93*(6), 1417-1424. https://doi.org/10.1002/cber.19600930628
113. Hilpert, S., Ditmar, M., and Grüttner, G. (**1913**). Über die Methylierung von Metallen durch Einwirkung von Aluminiumcarbid auf die gelösten Salze derselben. *Berichte der deutschen chemischen Gesellschaft*, *46*(3), 3738-3741. https://doi.org/10.1002/cber.191304603163
114. Dickson, R. and West, B. (**1962**). The Reactions of Lithium Tetraethylaluminate with Some Halides of Group IV and VB Elements. *Australian Journal of Chemistry*, *15*(4), 710-718. https://doi.org/10.1071/CH9620710
115. Hilpert, S. and Grüttner, G. (**1913**). Über die gegenseitige Verdrängung der Metalle aus ihren Phenyl-Verbindungen. *Berichte der deutschen chemischen Gesellschaft*, *46*(2), 1675-1687. https://doi.org/10.1002/cber.19130460265
116. Naumann, D. and Tyrra, W. (**1987**). The preparations and properties of tris(perfluoroorgano)bismuth compounds Bi(Rf)3 (Rf = CF3, C2F5, n-C3F7, n-C4F9, n-C6F13, n-C8 F17, C6F5). *Journal of Organometallic Chemistry*, *334*(3), 323-328. https://doi.org/10.1016/0022-328X(87)80094-3
117. Zakharkin, L. I. and Okhlobystin, O. Y. (**1959**). Synthesis of organometallic compounds from trialkylaluminums and metal salts. *Bulletin of the Academy of Sciences of the USSR, Division of chemical science*, *8*(11), 1853-1858. https://doi.org/10.1007/BF00914756
118. Whitmire, K. H., et al. (**1991**). Sterically crowded aryl bismuth compounds: synthesis and characterization of bis{2,4,6-tris(trifluoromethyl)phenyl} bismuth chloride and tris{2,4,6-tris(trifluoromethyl)phenyl} bismuth. *Journal of Organometallic Chemistry*, *402*(1), 55-66. https://doi.org/10.1016/0022-328X(91)80081-T
119. Althaus, H., et al. (**1999**). Synthesis and Characterization of R2BiCl and RBiCl2 [R = CH(SiMe3)2]. *Organometallics*, *18*(3), 328-331. https://doi.org/10.1021/om9806444
120. Suzuki, H., Murafuji, T., and Azuma, N. (**1993**). Synthesis and first X-ray structure analysis of a stabilized chiral chlorobismuthine: fixation of molecular geometry induced by the intramolecular coordination of a sulfonyl group. *Journal of the Chemical Society, Perkin Transactions 1*(10), 1169-1175. https://doi.org/10.1039/P19930001169
121. Bras, P., Van Der Gen, A., and Wolters, J. (**1983**). Synthesis of metallochiral triorganobismuthines. *Journal of Organometallic Chemistry*, *256*(1), C1-C4. https://doi.org/10.1016/S0022-328X(00)99311-2
122. Suzuki, H. and Murafuji, T. (**1992**). A new general method for the synthesis of chiral triarylbismuthines based on the intramolecular coordination by a sulfonyl group. *Journal of the Chemical Society, Chemical Communications*(16), 1143-1144. https://doi.org/10.1039/C39920001143
123. Matano, Y., Miyamatsu, T., and Suzuki, H. (**1996**). A New Convenient Synthesis of Triarylbismuthanes Bearing Three Different Aryl Groups by the Grignard Arylation of Unsymmetrical Diarylbismuth Triflate−Hexamethylphosphoric Triamide (HMPA) Complexes. *Organometallics*, *15*(7), 1951-1953. https://doi.org/10.1021/om9509709

124. Barton, D. H. R., et al. (**1986**). Pentavalent organobismuth reagents. Part vi. Comparative migratory aptitudes of aryl groups in the arylation of phenols and enols by pentavalent bismuth reagents. *Tetrahedron*, *42*(12), 3111-3122. https://doi.org/10.1016/S0040-4020(01)87378-6
125. Challenger, F. (**1914**). CCVII.—Organo-derivatives of bismuth. Part I. The preparation and properties of some tertiary aromatic bismuthines and their halogen derivatives. *Journal of the Chemical Society, Transactions*, *105*(0), 2210-2218. https://doi.org/10.1039/CT9140502210
126. Gilman, H. and Yablunky, H. L. (**1941**). Unsymmetrical Organobismuth Compounds. *Journal of the American Chemical Society*, *63*(1), 207-211. https://doi.org/10.1021/ja01846a048
127. Caires, C. C. and Guccione, S. (**2008**). Synthesis, Structure, and Reactivity of Borate Ester Coordinated Organobismuth Compounds. *Organometallics*, *27*(4), 747-752. https://doi.org/10.1021/om7009792
128. Rahman, M. M., Matano, Y., and Suzuki, H. (**1997**). Sodium Diarylbismuthide as a Reagent for the Bismuthanation of Reactive Arenes. Application to the Synthesis of Mixed Triarylbismuthanes Bearing a Substituent Group Incompatible with Grignard and Organolithium Reagents. *Organometallics*, *16*(15), 3565-3568. https://doi.org/10.1021/om9701377
129. Steinseifer, F. and Kauffmann, T. (**1980**). The Diphenylbismuthyl Group—A Potential New Auxiliary Group in Organic Synthesis. *Angewandte Chemie International Edition in English*, *19*(9), 723-724. https://doi.org/10.1002/anie.198007231
130. Yamazaki, O., et al. (**2004**). Palladium-Catalyzed Cross-Coupling Reaction of Organobismuth Compounds with Aryl and Alkenyl Chlorides. *Synlett*(11), 1921-1924. https://doi.org/10.1055/s-2004-831298
131. Sakurai, N. and Mukaiyama, T. (**2007**). A New Preparative Method of Aryl Sulfonate Esters by Using Cyclic Organobismuth Reagents. *Heterocycles*, *74*(1), 771-790. https://doi.org/10.3987/COM-07-S(W)63
132. Suzuki, H., Murafuji, T., and Azuma, N. (**1992**). Synthesis and reactions of some new heterocyclic bismuth-(III) and -(V) compounds. 5,10-Dihydrodibenzo[b,e]bismine and related systems. *Journal of the Chemical Society, Perkin Transactions 1*(13), 1593-1600. https://doi.org/10.1039/P19920001593
133. Hawley, D. M. and Ferguson, G. (**1968**). The stereochemistry of some organic derivatives of Group VB elements. Part II. The crystal and molecular structure of triphenylbismuth dichloride. *Journal of the Chemical Society A: Inorganic, Physical, Theoretical*, 2539-2543. https://doi.org/10.1039/J19680002539
134. Jensen, K. A. (**1943**). Über die räumliche Konfiguration der Verbindungen vom Typus R3PX2, R3AsX2, R3SbX2 und R3BiX2. *Zeitschrift für anorganische und allgemeine Chemie*, *250*(3-4), 257-267. https://doi.org/10.1002/zaac.19432500305
135. Moon, H. W. and Cornella, J. (**2022**). Bismuth Redox Catalysis: An Emerging Main-Group Platform for Organic Synthesis. *ACS Catalysis*, *12*(2), 1382-1393. https://doi.org/10.1021/acscatal.1c04897
136. Finet, J.-P. and Fedorov, A. Y. (**2006**). Tris(polymethoxyphenyl)bismuth derivatives: Synthesis and reactivity. *Journal of Organometallic Chemistry*, *691*(11), 2386-2393. https://doi.org/10.1016/j.jorganchem.2006.01.022
137. Ikegami, T. and Suzuki, H. (**1998**). A Stabilized Triarylbismuthane Imide: Synthesis and First X-ray Structure Analysis. *Organometallics*, *17*(6), 1013-1017. https://doi.org/10.1021/om970996v
138. Sharutin, V. V., et al. (**2002**). Synthesis and Structure of Triphenylbismuth Difluoride. *Russian Journal of General Chemistry*, *72*(1), 44-45. https://doi.org/10.1023/A:1015328925333
139. Rahman, A. F. M. M., et al. (**2004**). Effect of π-accepting substituent on the reactivity and spectroscopic characteristics of triarylbismuthanes and triarylbismuth dihalides. *Journal of Organometallic Chemistry*, *689*(21), 3395-3401. https://doi.org/10.1016/j.jorganchem.2004.07.055
140. Matano, Y., Begum, S. A., and Suzuki, H. (**2001**). A New Synthesis of Triarylbismuthanes via Directed Ligand Coupling of Oxazoline-Substituted Tetraarylbismuthonium Salts: Synthesis of

Polystyrenes Bearing the Diarylbismuthino Group. *Synthesis*(7), 1081-1085. https://doi.org/10.1055/s-2001-14565
141. Tyrra, W. and Naumann, D. (**1989**). On pentavalent perfluoroorgano bismuth compounds. *Canadian Journal of Chemistry*, *67*(11), 1949-1951. https://doi.org/10.1139/v89-303
142. Schmuck, A. and Seppelt, K. (**1989**). Strukturen von Pentaarylbismut-Verbindungen. *Chemische Berichte*, *122*(5), 803-808. https://doi.org/10.1002/cber.19891220502
143. Goel, R. G. and Prasad, H. S. (**1970**). Organobismuth compounds. I. Studies on triphenylbismuth(V) derivatives, Ph_3BiX_2. *Canadian Journal of Chemistry*, *48*(16), 2488-2493. https://doi.org/10.1139/v70-421
144. Gilman, H. and Yale, H. L. (**1951**). Some New Pentavalent Salts of Triarylbismuth Compounds. *Journal of the American Chemical Society*, *73*(9), 4470-4471. https://doi.org/10.1021/ja01153a518
145. Arnauld, T., Barton, D. H. R., and Doris, E. (**1997**). The chemistry of pentavalent organobismuth reagents. New preparative methods for aryl bismuth (V) carboxylates and sulfonates. *Tetrahedron Letters*, *38*(3), 365-366. https://doi.org/10.1016/S0040-4039(96)02305-2
146. Sharutin, V. V., Sharutina, O. K., and Senchurin, V. S. (**2013**). Synthesis and structure of tri-m-tolylbismuth dicarboxylates. *Russian Journal of Inorganic Chemistry*, *58*(12), 1470-1474. https://doi.org/10.1134/S003602361401015X
147. Ong, Y. C., et al. (**2014**). Stability and toxicity of heteroleptic organometallic Bi(V) complexes towards Leishmania major. *Dalton Trans*, *43*(34), 12904-16. https://doi.org/10.1039/c4dt00957f
148. Andreev, P. V., et al. (**2015**). Synthesis and structure of triphenylbismuth bis(3-phenylprop-2-enoate). *Crystallography Reports*, *60*(4), 517-520. https://doi.org/10.1134/S1063774515040057
149. Moiseev, D. V., et al. (**2005**). Study of homo- and cross-coupling competition in the reaction of triarylbismuth(V) dicarboxylates with methyl acrylate in the presence of a palladium catalyst. *Journal of Organometallic Chemistry*, *690*(16), 3652-3663. https://doi.org/10.1016/j.jorganchem.2005.04.051
150. Sinclair, P. J., et al. (**1995**). Preparation and in vitro activity of aryl ether derivatives of the FK-506 related immunosuppressive macrolides ascomycin and L-683,742. *Bioorganic & Medicinal Chemistry Letters*, *5*(10), 1035-1038. https://doi.org/10.1016/0960-894X(95)00161-L
151. Jurrat, M., et al. (**2020**). Modular bismacycles for the selective C–H arylation of phenols and naphthols. *Nature Chemistry*, *12*(3), 260-269. https://doi.org/10.1038/s41557-020-0425-4
152. Wittig, G. and Clauß, K. (**1952**). Pentaphenyl-wismut. *Justus Liebigs Annalen der Chemie*, *578*(1), 136-146. https://doi.org/10.1002/jlac.19525780116
153. Schmuck, A., Seppelt, K., and Pyykkö, P. (**1990**). Structure and Color of Substituted Pentaphenylbismuth. *Angewandte Chemie International Edition in English*, *29*(2), 213-215. https://doi.org/10.1002/anie.199002131
154. Frohn, H. J. and Maurer, H. (**1986**). Beiträge zur chemie des iodpentafluorids Teil V. IF_5 als oxidatives fluorierungsmittel für elementorganika des arsens, antimons und bismuts: selektivität und methodische grenzen. *Journal of Fluorine Chemistry*, *34*(1), 129-145. https://doi.org/10.1016/S0022-1139(00)81932-6
155. Wallenhauer, S. and Seppelt, K. (**1994**). Methylbismuth(V) Compounds. *Angewandte Chemie International Edition in English*, *33*(9), 976-978. https://doi.org/10.1002/anie.199409761
156. Kirij, N. V., et al. (**1994**). Synthesis and characterization of aryl(trifluoromethyl)bismuth compounds $(R\text{-}C_6H_4)_{3-n}Bi(CF_3)_n$ [R=H, 4-CH_3, 4-CF_3, 3-F, 4-F; n=1 and 2] and the reactions of $(C_6H_5)_{3-n}Bi(CF_3)_n$ [n=0–3] with benzoylpyridinium chloride. *Journal of Fluorine Chemistry*, *69*(3), 219-223. https://doi.org/10.1016/0022-1139(94)03134-7
157. Kirij, N. V., et al. (**2000**). $Bi(CF_3)_3/Cu(OCOCH_3)_2$ — a new system for the synthesis of 2-trifluoromethylcycloalkan-1-ones, trifluoromethylanilines and phenyl(trifluoromethyl)sulfane. *Journal of Fluorine Chemistry*, *106*(2), 217-221. https://doi.org/10.1016/S0022-1139(00)00339-0
158. Rao, M. L. N., Shimada, S., and Tanaka, M. (**1999**). Palladium Complex-Catalyzed Cross-Coupling Reaction of Organobismuth Dialkoxides with Triflates. *Organic Letters*, *1*(8), 1271-1273. https://doi.org/10.1021/ol990941k

159. Rao, M. L. N., et al. (**2002**). Cross-coupling reaction of organobismuth dialkoxides with aryl bromides and iodides catalyzed by $Pd(PPh_3)_4$. *Journal of Organometallic Chemistry*, *659*(1), 117-120. https://doi.org/10.1016/S0022-328X(02)01716-3
160. Gagnon, A., et al. (**2008**). Palladium-catalyzed cross-coupling reaction of tricyclopropylbismuth with aryl halides and triflates. *The Journal of Organic Chemistry*, *73*(9), 3604-7. https://doi.org/10.1021/jo702377h
161. Chan, D. M. T. (**1996**). Promotion of reaction of N-H boths with triarylbismuth and cupric acetate. *Tetrahedron Letters*, *37*(50), 9013-9016. https://doi.org/10.1016/S0040-4039(96)02116-8
162. Gagnon, A., et al. (**2007**). Direct N-Cyclopropylation of Cyclic Amides and Azoles Employing a Cyclopropylbismuth Reagent. *Journal of the American Chemical Society*, *129*(1), 44-45. https://doi.org/10.1021/ja0676758
163. Gagnon, A., Albert, V., and Duplessis, M. (**2010**). Csp^3-Csp^2 Palladium-Catalyzed Cross-Coupling Reaction of Trialkylbismuth Reagents with Aryl, Heteroaryl, and Vinyl Halides and Triflates. *Synlett*, *2010*(19), 2936-2940. https://doi.org/10.1055/s-0030-1259023
164. Rao, M. L. N., Venkatesh, V., and Jadhav, D. N. (**2006**). An atom-efficient palladium-catalyzed cross-coupling reaction of triarylbismuths with acid chlorides: synthesis of diaryl and alkyl aryl ketones. *Tetrahedron Letters*, *47*(39), 6975-6978. https://doi.org/10.1016/j.tetlet.2006.07.129
165. Rao, M. L. N., Venkatesh, V., and Banerjee, D. (**2007**). Atom-efficient cross-coupling reactions of triarylbismuths with acyl chlorides under Pd(0) catalysis. *Tetrahedron*, *63*(52), 12917-12926. https://doi.org/10.1016/j.tet.2007.10.047
166. Rao, M. L. N., Venkatesh, V., and Jadhav, D. N. (**2008**). A palladium catalyzed atom-efficient cross-coupling reactivity of triarylbismuths with α,β-unsaturated acyl chlorides. *Journal of Organometallic Chemistry*, *693*(15), 2494-2498. https://doi.org/10.1016/j.jorganchem.2008.05.012
167. Rao, M. L. N., Giri, S., and Jadhav, D. N. (**2009**). Pd-catalyzed synthesis of α-aryl ketones through couplings of α-arylacetyl chlorides with triarylbismuths as multi-coupling nucleophiles. *Tetrahedron Letters*, *50*(45), 6133-6138. https://doi.org/10.1016/j.tetlet.2009.08.074
168. Rao, M. L. N., Jadhav, D. N., and Venkatesh, V. (**2009**). Pd(0)/C-catalyzed cross-couplings of acyl chlorides with triarylbismuths as atom-efficient sub-stoichiometric multi-coupling reagents. *Tetrahedron Letters*, *50*(29), 4268-4271. https://doi.org/10.1016/j.tetlet.2009.05.003
169. Chen, J.-Y., et al. (**2009**). Coupling of acyl chlorides with triarylbismuths catalyzed by palladium bipyridyl complex anchored on nanosized MCM-41: A recyclable and atom-efficient catalytic process for the synthesis of diaryl and alkyl aryl ketones. *Journal of Molecular Catalysis A: Chemical*, *307*(1), 88-92. https://doi.org/10.1016/j.molcata.2009.03.014
170. Zhao, H., Yin, L., and Cai, M. (**2013**). A Phosphane-Free, Atom-Efficient Cross-Coupling Reaction of Triarylbismuths with Acyl Chlorides Catalyzed by MCM-41-Immobilized Palladium Complex. *European Journal of Organic Chemistry*, *2013*(7), 1337-1345. https://doi.org/10.1002/ejoc.201201432
171. Rao, M. L., et al. (**2001**). Palladium-catalyzed cross-coupling reaction of triarylbismuths with aryl halides and triflates. *Organic Letters*, *3*(25), 4103-5. https://doi.org/10.1021/ol016885g
172. Rao, M. L. N., Banerjee, D., and Jadhav, D. N. (**2007**). Palladium catalyzed atom-efficient cross-coupling reactions of triarylbismuths with aryl iodides and aryl triflates. *Tetrahedron Letters*, *48*(38), 6644-6647. https://doi.org/10.1016/j.tetlet.2007.07.107
173. Rao, M. L. N., Banerjee, D., and Jadhav, D. N. (**2007**). Palladium catalyzed atom-efficient cross-coupling reactions of triarylbismuths with aryl bromides. *Tetrahedron Letters*, *48*(15), 2707-2711. https://doi.org/10.1016/j.tetlet.2007.02.068
174. Rao, M. L. N., Jadhav, D. N., and Banerjee, D. (**2008**). A new palladium catalyzed protocol for atom-efficient cross-coupling reactions of triarylbismuths with aryl halides and triflates. *Tetrahedron*, *64*(24), 5762-5772. https://doi.org/10.1016/j.tet.2008.04.011
175. Rao, M. L. N., Banerjee, D., and Dhanorkar, R. J. (**2011**). Synthesis of Functionalized 2-Arylthiophenes with Triarylbismuths as Atom-Efficient Multicoupling Organometallic

Nucleophiles under Palladium Catalysis. *Synlett*, *2011*(09), 1324-1330. https://doi.org/10.1055/s-0030-1260554
176. Rao, M. L. N., Awasthi, D. K., and Talode, J. B. (**2012**). Mono- and Biscouplings Using Triarylbismuths for the Atom-Efficient Arylations of Functionalized Furans under Palladium Catalysis. *Synlett*, *23*(13), 1907-1912. https://doi.org/10.1055/s-0032-1316567
177. Rao, M. L. N., Awasthi, D. K., and Talode, J. B. (**2012**). Palladium-catalyzed cross-couplings of functionalized 2-bromobenzofurans for atom-economic synthesis of 2-arylbenzofurans using triarylbismuth reagents. *Tetrahedron Letters*, *53*(21), 2662-2666. https://doi.org/10.1016/j.tetlet.2012.03.059
178. Rao, M. L. N. and Dhanorkar, R. J. (**2014**). Triarylbismuthanes as Threefold Aryl-Transfer Reagents in Regioselective Cross-Coupling Reactions with Bromopyridines and Quinolines. *European Journal of Organic Chemistry*, *2014*(24), 5214-5228. https://doi.org/10.1002/ejoc.201402455
179. Urgin, K., et al. (**2013**). Pd-Catalyzed Chemoselective Cross-Coupling Reaction of Triaryl- or Triheteroarylbismuth Compounds with 3,6-Dihalopyridazines. *European Journal of Organic Chemistry*, *2013*(1), 117-124. https://doi.org/10.1002/ejoc.201200977
180. Petiot, P. and Gagnon, A. (**2013**). Palladium-Catalyzed Cross-Coupling Reaction of Functionalized Aryl- and Hetero-arylbismuthanes with 2-Halo(or 2-Triflyl)-azines and -diazines. *European Journal of Organic Chemistry*, *2013*(24), 5282-5289. https://doi.org/10.1002/ejoc.201300850
181. Hébert, M., et al. (**2016**). Synthesis of Highly Functionalized Triarylbismuthines by Functional Group Manipulation and Use in Palladium- and Copper-Catalyzed Arylation Reactions. *The Journal of Organic Chemistry*, *81*(13), 5401-16. https://doi.org/10.1021/acs.joc.6b00767
182. Zhou, W.-J., et al. (**2010**). Reusable, Polystyrene-Resin-Supported, Palladium-Catalyzed, Atom-Efficient Cross-Coupling Reaction of Aryl Halides with Triarylbismuths. *European Journal of Organic Chemistry*, *2010*(3), 416-419. https://doi.org/10.1002/ejoc.200901210
183. Barton, D. H. R., Finet, J.-P., and Khamsi, J. (**1987**). Copper salts catalysis of N-phenylation of amines by trivalent organobismuth compounds. *Tetrahedron Letters*, *28*(8), 887-890. https://doi.org/10.1016/S0040-4039(01)81015-7
184. Crifar, C., et al. (**2014**). Synthesis of highly functionalized diaryl ethers by copper-mediated O-arylation of phenols using trivalent arylbismuth reagents. *Chemistry*, *20*(10), 2755-2760. https://doi.org/10.1002/chem.201303684
185. Petiot, P., et al. (**2015**). Copper-catalyzed O-arylation of N-protected 1,2-aminoalcohols using functionalized trivalent organobismuth reagents. *Organic & Biomolecular Chemistry*, *13*(5), 1322-1327. https://doi.org/10.1039/c4ob02497d
186. Banfi, A., et al. (**1994**). Synthesis of Substituted N-Arylpiperidines via Organobismuth Derivatives. *Synthesis*, *1994*(08), 775-776. https://doi.org/10.1055/s-1994-25569
187. Aoki, Y., et al. (**2000**). N-Phenylation of N-Arylaminophthalimides with Triphenylbismuth and Cupric Acetate: A Convenient Synthesis of 1-Aryl-1- Phenylhydrazines. *Synthetic Communications*, *30*(1), 131-140. https://doi.org/10.1080/00397910008087300
188. Loog, O., Mäeorg, U., and Ragnarsson, U. (**2000**). Synthesis of Hydrazines with Aromatic Substituents Using Triarylbismuth Reagents. *Synthesis*, *2000*(11), 1591-1597.
189. Hügel, H. M., Rix, C. J., and Fleck, K. (**2006**). Comparison of Copper(II) Acetate Promoted N-Arylation of 5,5-Dimethyl Hydantoin and Other Imides with Triarylbismuthanes and Aryl Boronic Acids. *Synlett*, *2006*(14), 2290-2292. https://doi.org/10.1055/s-2006-949638
190. Starkov, P., et al. (**2007**). Copper-catalyzed N-arylation of carbamate-protected hydrazones with organobismuthanes. *Tetrahedron Letters*, *48*(7), 1155-1157. https://doi.org/10.1016/j.tetlet.2006.12.071
191. Petiot, P., Dansereau, J., and Gagnon, A. (**2014**). Copper-catalyzed N-arylation of azoles and diazoles using highly functionalized trivalent organobismuth reagents. *RSC Advances*, *4*(42), 22255-22259. https://doi.org/10.1039/C4RA02467B

192. Barton, D. H. R., et al. (**1980**). Obsevations on the cleavage of the bismuth–carbon bond in Bi compounds: a new arylation reaction. *Journal of the Chemical Society, Chemical Communications*(5), 246-247. https://doi.org/10.1039/C39800000246
193. Barton, D. H. R., et al. (**1980**). Comparative arylation reactions with pentaphenylbismuth and with triphenylbismuth carbonate. *Journal of the Chemical Society, Chemical Communications*(17), 827-829. https://doi.org/10.1039/C39800000827
194. Barton, D. H. R., et al. (**1985**). Pentavalent organobismuth reagents. Part 2. The phenylation of phenols. *Journal of the Chemical Society, Perkin Transactions 1*(0), 2657-2665. https://doi.org/10.1039/P19850002657
195. Barton, D. H. R., et al. (**1987**). The chemistry of pentavalent organobismuth reagents: Part X. Studies on the phenylation and oxidation of phenols. *Tetrahedron*, *43*(2), 323-332. https://doi.org/10.1016/S0040-4020(01)89960-9
196. Barton, D. H. R., et al. (**1985**). Pentavalent organobismuth reagents. Part 3. Phenylation of enols and of enolate and other anions. *Journal of the Chemical Society, Perkin Transactions 1*(0), 2667-2675. https://doi.org/10.1039/P19850002667
197. Fedorov, A. Y. and Finet, J.-P. (**2000**). Synthesis and reactivity of pentavalent biphenyl-2,2′-ylenebismuth derivatives. *Journal of the Chemical Society, Perkin Transactions 1*(22), 3775-3778. https://doi.org/10.1039/B006307J
198. Barton, D. H. R., Finet, J.-P., and Khamsi, J. (**1986**). Metallic copper catalysis of N-arylation of amines by triarylbismuth diacylates. *Tetrahedron Letters*, *27*(31), 3615-3618. https://doi.org/10.1016/S0040-4039(00)84863-7
199. Barton, D. H. R., Finet, J.-P., and Khamsi, J. (**1989**). N-phenylation of amino acid derivatives. *Tetrahedron Letters*, *30*(8), 937-940. https://doi.org/10.1016/S0040-4039(00)95284-5
200. Tšubrik, O., et al. (**2004**). Arylation of diversely substituted hydrazines by tri- and pentavalent organobismuth reagents. *Tetrahedron*, *60*(38), 8363-8373. https://doi.org/10.1016/j.tet.2004.07.020
201. Fedorov, A. Y. and Finet, J.-P. (**1999**). N-Phenylation of azole derivatives by triphenylbismuth derivatives/cupric acetate. *Tetrahedron Letters*, *40*(14), 2747-2748. https://doi.org/10.1016/S0040-4039(99)00287-7
202. Barton, D. H. R., Finet, J.-P., and Pichon, C. (**1986**). The catalytic effect of copper ions in the phenylation reaction of david and thieffry. *Journal of the Chemical Society, Chemical Communications*(1), 65-66. https://doi.org/10.1039/C39860000065
203. Kazuhiro, I., Kentarou, F., and Teruaki, M. (**2006**). Copper(II)-catalyzed O-Phenylation of Tertiary Alcohols with Organobismuth(V) Reagents. *Chemistry Letters*, *35*(6), 612-613. https://doi.org/10.1246/cl.2006.612
204. Sheppard, G. S. (**1999**). Copper(II) Pivalate/Oxone: An Improved Promoter System for Aryl Transfer via Organo-Bismuth Reagents. *Synlett*, *1999*(08), 1207-1210. https://doi.org/10.1055/s-1999-2816
205. Teruaki, M., Naoto, S., and Kazuhiro, I. (**2006**). Copper(II)-catalyzed O-Phenylation of Alcohols with Organobismuth(V) Reagents: A Convenient Method for the Synthesis of Simple tert-Alkyl Phenyl Ethers. *Chemistry Letters*, *35*(10), 1140-1141. https://doi.org/10.1246/cl.2006.1140
206. David, S. and Thieffry, A. (**1981**). Selective phenylation in mild conditions of one hydroxy group in glycols with triphenylbismuth diacetate: A new specific glycol reaction. *Tetrahedron Letters*, *22*(50), 5063-5066. https://doi.org/10.1016/S0040-4039(01)92420-7
207. Barton, D. H. R., et al. (**1987**). The chemistry of pentavalent organobismuth reagents. Part 8. Phenylation and oxidation of alcohols by tetraphenylbismuth esters. *Journal of the Chemical Society, Perkin Transactions 1*(0), 251-259. https://doi.org/10.1039/P19870000251
208. David, S. and Thieffry, A. (**1983**). Conversion of one hydroxy group in a diol to a phenyl ether with triphenylbismuth diacetate, a new glycol reaction showing strong axial preference in six-membered rings. *The Journal of Organic Chemistry*, *48*(4), 441-447. https://doi.org/10.1021/jo00152a007

209. Barton, D. H. R., Finet, J.-P., and Khamsi, J. (**1988**). Copper catalysed phenylation of indoles by triphenylbismuth BIS-trifluoroacetate. *Tetrahedron Letters*, *29*(10), 1115-1118. https://doi.org/10.1016/S0040-4039(00)86664-2

Annexe A

Informations supplémentaires

Copper-Promoted N-Arylation of the Imidazole Side Chain of Protected Histidine by Using Triarylbismuth Reagents

SUPPORTING INFORMATION

Copper-Promoted *N*-Arylation of the Imidazole Side Chain of Protected Histidine using Triarylbismuth Reagents

Hwai-Chien Chan, Bianca Bueno, Adrien Le Roch, Alexandre Gagnon*

Département de chimie
Université du Québec à Montréal
C.P. 8888, Succ. Centre-Ville, Montréal, Québec, Canada, H3C 3P8
gagnon.alexandre@uqam.ca

1. General information

Unless otherwise indicated, all reactions were run under ambient atmosphere in non-flame dried glassware. For reactions performed under oxygen, 99.6% extra dry oxygen was used. Unless otherwise stated, commercial reagents were used without further purification. Triarylbismuthines were prepared according to Hébert et al.[i] Anhydrous solvents were obtained using a MBRAUN (model MB-SPS 800) encapsulated solvent purification system. The evolution of reactions was monitored by analytical thin-layer chromatography using silica gel 60 F254 precoated plates. Flash chromatography was performed employing 220 mesh silica (Silicycle) using the indicated solvent system according to standard techniques. Nuclear magnetic resonance spectra ^{1}H were recorded on a BrukerAvance-III 300MHz spectrometer or a BrukerAvance-III 600MHz and ^{13}C were recorded on a BrukerAvance-III 75MHz spectrometer or a BrukerAvance-III 150MHz. Chemical shifts for ^{1}H-NMR spectra are recorded in parts per million from tetramethylsilane with the solvent resonance as the internal standard (chloroform, δ 7.26 ppm). Data are reported as follows: chemical shift, multiplicity (s = singlet, d = doublet, t = triplet, q = quartet, p = quintuplet, m = multiplet, dd = doublet of doublet, dt = doublet of triplet, dq = doublet of quartet, tt = triplet of triplet, td = triplet of doublet, s(br) = broad singlet), coupling constant *J* in Hz and integration. Chemical shifts for ^{13}C-NMR spectra are recorded in parts per million from tetramethylsilane using the central peak of deuterochloroform (77.16 ppm) as the internal standard. All ^{13}C-NMR spectra were obtained with complete proton decoupling. IR spectra were recorded on a Thermo Scientific Nicolet 6700 PT-IR from thin films and are reported in reciprocal centimeters (cm^{-1}). Melting points were measured using Büchi M560 melting point apparatus in open capillaries.

[i] Hébert, M.; Petiot, P.; Benoit, E.; Dansereau, J.; Ahmad, T., Le Roch, A.; Ottenwaelder, X.; Gagnon, A. *J. Org. Chem.* **2016**, *81*, 5401–5416

2. Triarylbismuthines (2) used in this work

The organobismuthines used in this publication are illustrated in **Figure S1.** The procedures for synthesis of these organobismuthines can be found in the following references: [a] P. Petiot, A. Gagnon, *Eur. J. Org. Chem.*, **2013**, 5282; [b] P. Petiot, J. Dansereau, A. Gagnon, *RSC Adv.*, **2014**, 4, 22255; [c] D. H. R. Barton, N. Y. Bhatnagar, J.-P. Finet and W. B. Motherwell, *Tetrahedron*, **1986**, *42*, 3111; [d] R. Ding, C.-S. Ge, Y.- J. Chen, D. Wanga, C.-J. Li, *Tetrahedron Lett.*, **2002**, *43*, 7789; [e] M. H.bert, P. Petiot, E. Benoit, J. Dansereau, T. Ahmad, A. Le Roch, X. Ottenwaelder, A. Gagnon, *J. Org. Chem.*, **2016**, *81*, 5401; [f] X. Marset, J. Torregrosa-Crespo, R. M. Martínez-Espinosa, G. Guillena, D. J. Ramón, *Green Chem.*, **2019**, *21*, 4127.

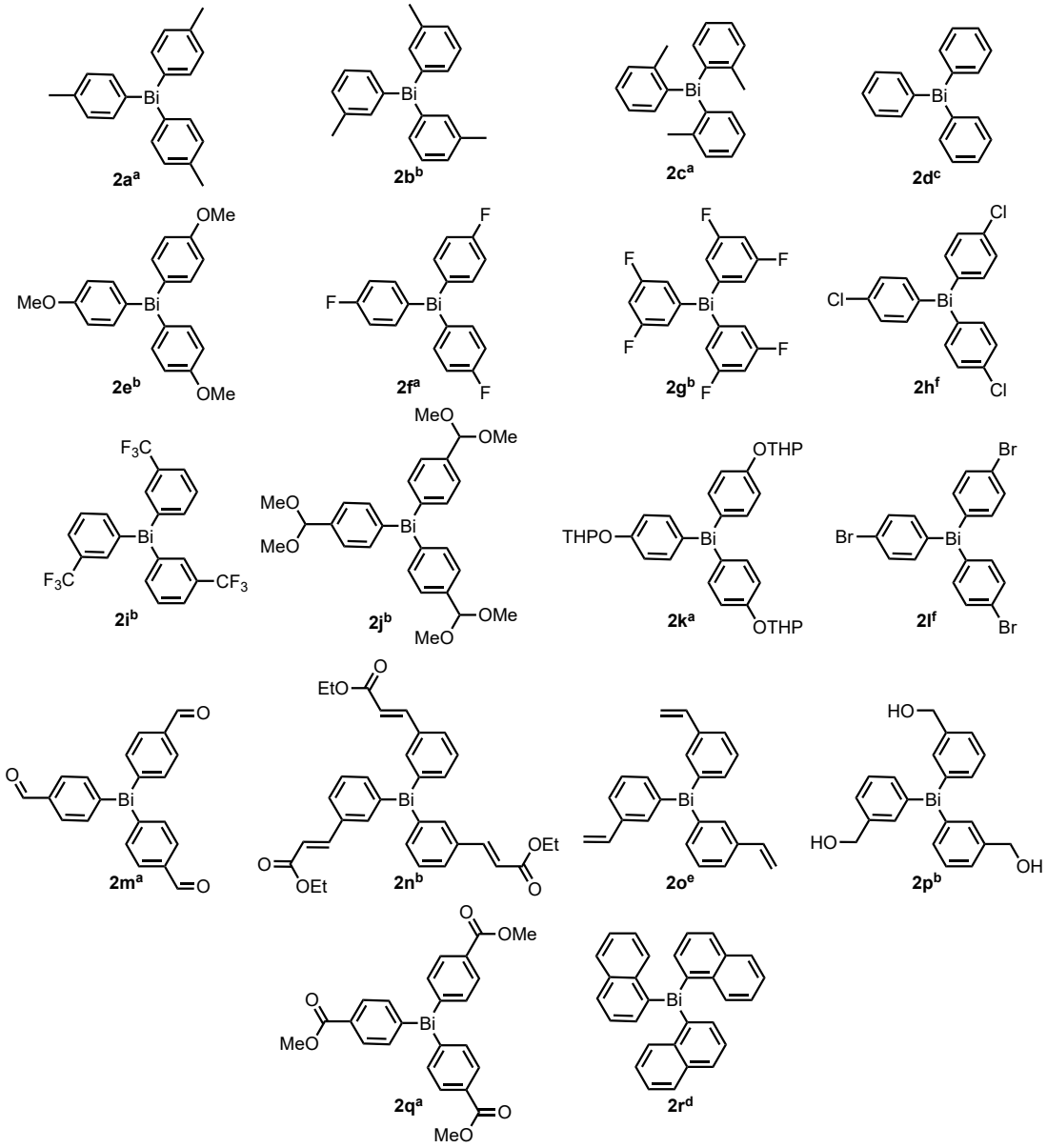

Figure S1. Functionalized organobismuthines used in this publication

3. General procedure for the optimization of the reaction conditions for the coupling between Boc–His–OMe (1a) and tri(4-tolyl)bismuth (2a)

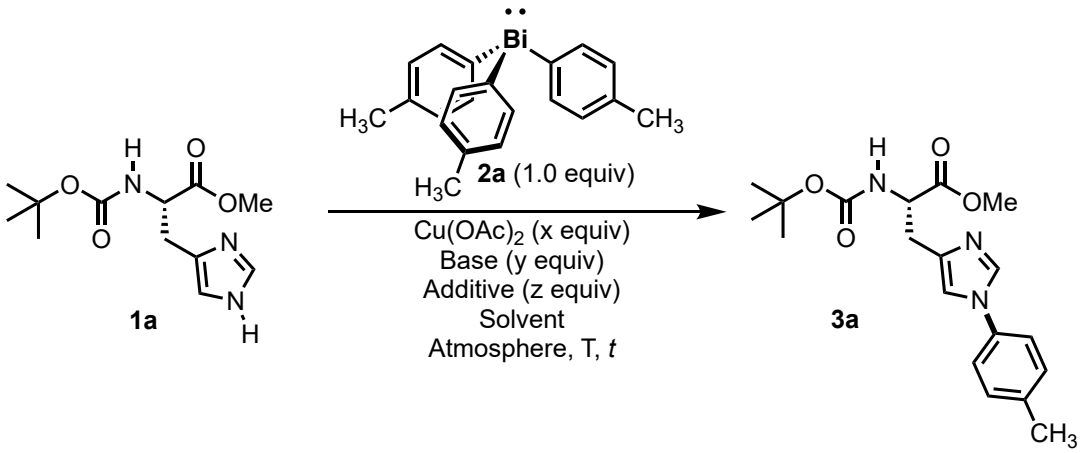

Manuscript, Table 1: In a sealed tube, the base (y equiv) was added to a mixture of the *N*-protected *L*-histidine methyl ester **1a** (1.0 equiv), tri(4-tolyl)bismuthine **2a** (1.0 equiv), copper(II) acetate (x equiv) and additive (z equiv) in CH_2Cl_2 (0.1 M). The mixture was stirred at the corresponding temperature under the corresponding atmosphere for 4 or 16 hours. The solvent was evaporated under reduce pressure and the residue was purified on silica gel chromatography system (2% MeOH/CH_2Cl_2) to afford **3a** as a yellow thick oil. See section 4 for complete characterization of **3a**.

4. General procedure for the coupling between N-protected histidine methyl ester (1a) and triarylbismuthines (2)

Manuscript, Scheme 2: In a sealed tube, *N*,*N*-diisopropylethylamine (25.5 µL, 0.15 mmol, 1.0 equiv) was added to the *N*-protected *L*-histidine methyl ester **1a** (0.15 mmol, 1.0 equiv), the corresponding triarylbismuthine **2** (0.15 mmol, 1.0 equiv), copper(II) acetate (27 mg, 0.15 mmol, 1.0 equiv) and phenanthroline (27 mg, 0.15 mmol, 1.0 equiv) in CH_2Cl_2 (0.1 M). Oxygen was bubbled in the reaction mixture before stirred in an oil bath set at 40 °C for 16 hours. The solvent was evaporated under reduce pressure and the residue was purified on silica gel chromatography using the corresponding eluent system to afford desired pure product **3a**–**r**.

Methyl N^{α}-(*tert*-butoxycarbonyl)-N^{τ}-(4-tolyl)-*L*-histidinate (3a)

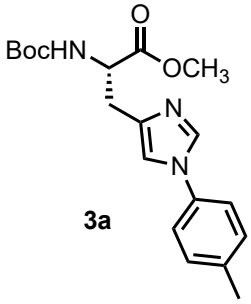

3a

The general procedure was followed starting from (*L*)-Boc–His–OMe **1a** (40.0 mg) and tri(4-tolyl)bismuthine **2a** (72 mg). The crude material was purified on silica gel (2% MeOH/CH_2Cl_2) to afford **3a** as a yellow thick oil (53 mg, 99%): $\mathbf{R_f}$ = 0.46 (5% MeOH/CH_2Cl_2); **^{1}H-NMR (300 MHz, $CDCl_3$)** δ 7.73 (s(br), 1H), 7.28 – 7.17 (m, 4H), 7.04 (s(br), 1H), 5.90 (d, *J* = 6.5 Hz, 1H), 4.59 (s(br), 1H), 3.70 (s, 3H), 3.29 – 2.89 (m, 2H), 2.37 (s, 3H), 1.42 (s, 9H); **^{13}C-NMR (75 MHz, $CDCl_3$)** δ 172.7, 155.7, 137.6, 134.9, 130.5, 121.3, 79.8, 53.6, 52.3, 30.4, 28.4, 21.0; **IR (ATR)/$\bar{\nu}$ (cm^{-1}):** 3350, 3129, 2973, 2928, 1741, 1703, 1521, 1483, 1365, 1251, 1159, 1051, 1019, 813; **HRMS (ESI)** calcd. for $[C_{19}H_{25}N_3O_4 + H]^+$: 360.1918, found 360.1922.

Methyl N^{α}-(*tert*-butoxycarbonyl)-N^{τ}-(3-tolyl)-*L*-histidinate (3b)

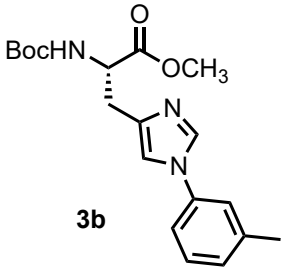

3b

The general procedure was followed starting from (*L*)-Boc–His–OMe **1a** (40 mg) and tri(3-tolyl)bismuthine **2b** (72 mg). The crude material was purified on silica gel (2% MeOH/CH_2Cl_2) to afford **3b** as a yellow thick oil (53 mg, 99%): $\mathbf{R_f}$ = 0.44 (5% MeOH/CH_2Cl_2); **^{1}H-NMR (600 MHz, $CDCl_3$)** δ 7.82 (s(br), 1H), 7.33 (t, *J* = 7.7 Hz, 1H), 7.17 – 7.10 (m, 3H), 7.08 (s(br), 1H), 5.89 (d, *J* = 7.2 Hz, 1H), 4.60 (s, 1H), 3.71 (s, 3H), 3.23 – 3.02 (m, 2H), 2.40 (s, 3H), 1.42 (s, 9H); **^{13}C-NMR (150 MHz, $CDCl_3$)** δ 172.6, 155.7, 140.2, 137.1, 129.8, 128.4, 122.0, 118.4, 79.8, 53.5, 52.4, 30.3, 28.4, 21.5; **IR (ATR)/$\bar{\nu}$ (cm^{-1}):** 3241, 3127, 3106, 2970, 2950, 2926, 1743, 1697, 1614, 1594, 1538, 1506, 1436, 1363, 1158, 1069, 1048, 1030, 985, 854, 786, 691; **HRMS (ESI)** calcd. for $[C_{19}H_{25}N_3O_4 + H]^+$: 360.1918, found 360.1923.

Methyl N^{α}-(*tert*-butoxycarbonyl)-N^{τ}-(2-tolyl)-*L*-histidinate (3c)

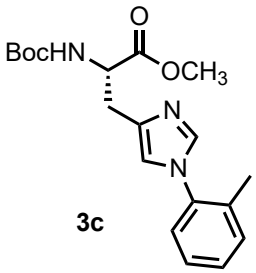

3c

The general procedure was followed starting from (*L*)-Boc–His–OMe **1a** (40 mg) and tri(2-tolyl)bismuthine **2c** (72 mg). The crude material was purified on silica gel (2% MeOH/CH_2Cl_2) to afford **3c** as a yellow oil (38 mg, 71%): $\mathbf{R_f}$ = 0.51 (3% MeOH/CH_2Cl_2); **^{1}H-NMR (300 MHz, $CDCl_3$)** δ 7.53 (s(br), 1H), 7.38 – 7.28 (m, 2H), 7.28 – 7.24 (m, 1H), 7.18 (d, *J* = 7.6 Hz, 1H), 6.84 (s(br), 1H), 5.93 (d, *J* = 7.8 Hz, 1H), 4.65 – 4.55 (m, 1H), 3.71 (s, 3H), 3.23 – 3.01 (m, 2H), 2.15 (s, 3H), 1.43 (s, 9H); **^{13}C-NMR (75 MHz, $CDCl_3$)** δ 172.6, 155.7, 136.5, 133.9, 131.5,

129.1, 127.0, 126.5, 79.8, 53.7, 52.3, 30.3, 28.5, 17.7; **IR (ATR)/$\bar{\nu}$ (cm^{-1}):** 3357, 2974, 2930, 1744, 1708, 1501, 1436, 1391, 1365, 1163, 1022, 992, 969, 761, 719; **HRMS (ESI)** calcd. for $[C_{19}H_{25}N_3O_4 + H]^+$: 360.1918, found 360.1929.

Methyl *N*$^{\alpha}$-(*tert*-butoxycarbonyl)-*N*$^{\tau}$-(phenyl)-*L*-histidinate (3d)

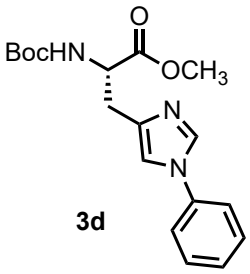

3d

The general procedure was followed starting from (*L*)-Boc–His–OMe **1a** (40 mg) and triphenylbismuthine **2d** (66 mg). The crude material was purified on silica gel (2% MeOH/CH_2Cl_2) to afford **3d** as a yellow oil (48 mg, 94%): **R_f** = 0.46 (5% MeOH/CH_2Cl_2); **^{1}H-NMR (600 MHz, $CDCl_3$)** δ 7.86 (s(br), 1H), 7.49 – 7.40 (m, 2H), 7.36 – 7.29 (m, 3H), 7.09 (s(br), 1H), 5.89 (d, *J* = 7.5 Hz, 1H), 4.59 (s(br), 1H), 3.70 (s, 3H), 3.21 – 3.03 (m, 2H), 1.41 (s, 9H); **^{13}C-NMR (150 MHz, $CDCl_3$)** δ 172.5, 155.7, 138.3, 137.1, 135.2, 130.0, 127.7, 121.3, 116.1, 79.8, 53.5, 52.4, 30.2, 28.4; **IR (ATR)/$\bar{\nu}$ (cm^{-1}):** 3382, 3012, 2971, 2951, 1741, 1698, 1600, 1500, 1435, 1391, 1365, 1157, 1055, 753, 692; **HRMS (ESI)** calcd. for $[C_{18}H_{23}N_3O_4 + H]^+$: 346.1761, found 346.1775.

Methyl *N*$^{\alpha}$-(*tert*-butoxycarbonyl)-*N*$^{\tau}$-(4-methoxyphenyl)-*L*-histidinate (3e)

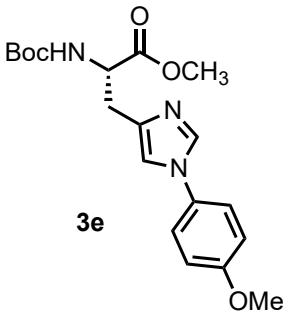

3e

The general procedure was followed starting from (*L*)-Boc–His–OMe **1a** (40 mg) and tri(4-methoxyphenyl)bismuthine **2e** (79 mg). The crude material was purified on silica gel (2% MeOH/CH_2Cl_2) to afford **3e** as a yellow oil (50 mg, 90%): **R_f** = 0.34 (5% MeOH/CH_2Cl_2); **^{1}H-NMR (600 MHz, $CDCl_3$)** δ 7.77 (s(br), 1H), 7.24 (d, *J* = 8.8 Hz, 2H), 7.00 (s(br), 1H), 6.95 (d, *J* = 8.8 Hz, 2H), 5.90 (d, *J* = 7.2 Hz, 1H), 4.58 (s, 1H), 3.81 (s, 3H), 3.70 (s, 3H), 3.19 – 3.11 (m, 1H), 3.11 – 3.04 (m, 1H), 1.41 (s, 9H); **^{13}C-NMR (150 MHz, $CDCl_3$)** δ 172.5, 159.1, 155.7, 137.9, 135.3, 130.4, 123.1, 116.6, 115.0, 79.8, 55.7, 53.5, 52.3, 30.2, 28.4; **IR (ATR)/$\bar{\nu}$ (cm^{-1}):** 3373, 3263, 3134, 2975, 2841, 1741, 1693, 1606, 1518, 1436, 1390, 1250, 1160, 1126, 1069, 1028, 983, 970, 835, 756; **HRMS (ESI)** calcd. for $[C_{19}H_{25}N_3O_5 + H]^+$: 376.1867, found 376.1879.

Methyl N^{α}-(*tert*-butoxycarbonyl)-N^{τ}-(4-fluoroyphenyl)-*L*-histidinate (3f)

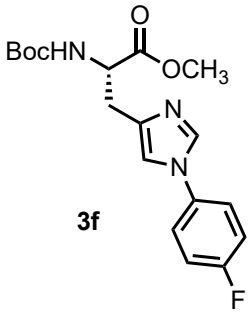

3f

The general procedure was followed starting from (*L*)-Boc–His–OMe **1a** (40 mg) and tri(4-fluorophenyl)bismuthine **2f** (74 mg). The crude material was purified on silica gel (3% MeOH/CH_2Cl_2) to afford **3f** as a yellow oil (52 mg, 96%): $\mathbf{R_f}$ =0.33 (5% MeOH/CH_2Cl_2); **^{1}H-NMR (600 MHz, $CDCl_3$)** δ 7.85 (s(br), 1H), 7.36 – 7.28 (m, 2H), 7.14 (t, *J* = 8.4 Hz, 2H), 7.04 (s(br), 1H), 5.87 (d, *J* = 7.2 Hz, 1H), 4.59 (s, 1H), 3.71 (s, 3H), 3.21 – 3.03 (m, 2H), 1.40 (s, 9H) ; **^{13}C-NMR (150 MHz, $CDCl_3$)** δ 172.5, 161.8 (d, *J* = 246.7 Hz), 155.7, 133.4, 123.4 (d, *J* = 8.4 Hz), 116.9 (d, *J* = 23.0 Hz), 79.8, 53.4, 52.4, 30.2, 29.7, 28.4 **; ^{19}F-NMR (282 MHz, $CDCl_3$)** δ -113.7 **; IR (ATR)/$\bar{\nu}$ (cm^{-1}):** 3125, 2980, 2932, 2850, 1744, 1701, 1515, 1437, 1391, 1366, 1226, 1159, 1058, 1022, 839, 818, 753, 665; **HRMS (ESI)** calcd. for $[C_{18}H_{22}FN_3O_4 + H]^+$: 364.1667, found 364.1683.

Methyl N^{α}-(*tert*-butoxycarbonyl)-N^{τ}-(3,5-difluorophenyl)-*L*-histidinate (3g)

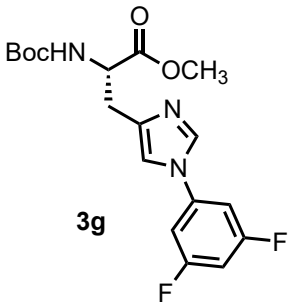

3g

The general procedure was followed starting from (*L*)-Boc–His–OMe **1a** (40 mg) and tris(3,5-difluorophenyl)bismuthine **2g** (82 mg). The crude material was purified on silica gel (2% MeOH/CH_2Cl_2) to afford **3g** as a yellow solid (43 mg, 76%): $\mathbf{R_f}$ = 0.77 (5% MeOH/CH_2Cl_2); **m.p.**= 129 – 131 °C; **^{1}H-NMR (300 MHz, $CDCl_3$)** δ 7.84 (s, 1H), 7.07 (s(br), 1H), 6.98 – 6.86 (m, 2H), 6.80 (tt, *J* = 8.7, 2.2 Hz, 1H), 5.78 (d, *J* = 7.5 Hz, 1H), 4.60 (s(br), 1H), 3.72 (s, 3H), 3.34 – 2.81 (m, 2H), 1.42 (s, 9H); **^{13}C-NMR (75 MHz, $CDCl_3$)** δ 172.5, 165.3 (d, *J* = 14.1 Hz), 162.0 (d, *J* = 14.3 Hz), 155.7, 104.613 (d, *J* = 28.6 Hz), 104.612 (d, *J* = 9.1 Hz), 103.3, 103.0, 102.6, 79.9, 53.3, 52.4, 30.4, 28.4; **^{19}F-NMR (282 MHz, $CDCl_3$)** δ -106.3 ; **IR (ATR)/$\bar{\nu}$ (cm^{-1}):** 3253, 3134, 3110, 2959, 2931, 2851, 1742, 1692, 1626, 1605, 1540, 1506, 1477, 1435, 1364, 1285, 1260, 1220, 1162, 1127, 1067, 994, 851, 836, 758, 674; **HRMS (ESI)** calcd. for $[C_{18}H_{21}F_2N_3O_4 + H]^+$: 382.1573, found 382.1580.

Methyl N^{α}-(*tert*-butoxycarbonyl)-N^{τ}-(4-chlorophenyl)-*L*-histidinate (3h)

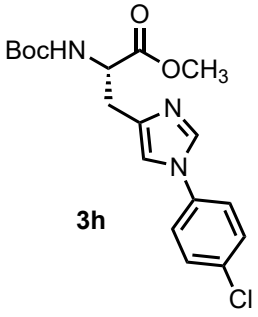

3h

The general procedure was followed starting from (*L*)-Boc–His–OMe **1a** (40 mg) and tri(4-chlorophenyl)bismuthine **2h** (81 mg). The crude material was purified on silica gel (2% MeOH/CH_2Cl_2) to afford **3h** as a thick yellow oil (55 mg, 97%): $\mathbf{R_f}$ = 0.76 (5% MeOH/CH_2Cl_2); **^{1}H-NMR (300 MHz, $CDCl_3$)** δ 7.78 (s, 1H), 7.41 (dt, *J* = 9.3, 2.4 Hz, 2H), 7.27 (dt, *J* = 9.4, 2.4 Hz, 2H), 7.04 (s(br), 1H), 5.84 (d, *J* = 7.5 Hz, 1H), 4.58 (s(br), 1H), 3.70 (s, 3H), 3.23 – 2.98 (m, 2H), 1.40 (s, 9H); **^{13}C-NMR (75 MHz, $CDCl_3$)** δ 172.6, 155.7, 135.7, 133.3, 130.1, 122.5, 79.8, 53.4, 52.4, 30.4, 28.4; **IR (ATR)/$\bar{\nu}$ (cm^{-1}):** 3375, 2977, 1743, 1705, 1504, 1436, 1392, 1365, 1306, 1250, 1210, 1161, 1096, 1014, 991, 968, 829, 754; **HRMS (ESI)** calcd. for $[C_{18}H_{22}ClN_3O_4 + H]^+$: 380.1372, found 380.1376.

Methyl N^{α}-(*tert*-butoxycarbonyl)-N^{τ}-(3-(trifluoromethyl)phenyl)-*L*-histidinate (3i)

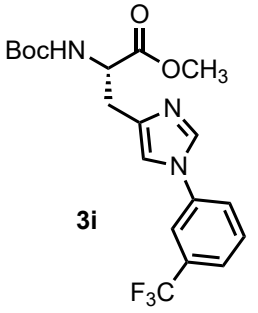

3i

The general procedure was followed starting from (*L*)-Boc–His–OMe **1a** (40 mg) and tri(3-(trifluoromethyl)phenylbismuthine **2i** (96 mg). The crude material was purified on silica gel (2% MeOH/CH_2Cl_2) to afford **3i** as a yellow oil (57 mg, 93%): $\mathbf{R_f}$ = 0.7 (5% MeOH/CH_2Cl_2); **^{1}H-NMR (600 MHz, $CDCl_3$)** δ 7.99 (s, 1H), 7.65 – 7.53 (m, 4H), 7.15 (s, 1H), 5.83 (d, *J* = 7.4 Hz, 1H), 4.60 (s, 1H), 3.71 (s, 3H), 3.20 – 3.06 (m, 2H), 1.40 (s, 9H); **^{13}C-NMR (150 MHz, $CDCl_3$)** δ 172.4, 155.7, 139.0, 137.5, 135.2, 132.7 (q, *J* = 131.7 Hz), 130.9, 124.5, 124.4 (q, *J* = 14.4 Hz), 123.4 (q, *J* = 1084.5 Hz), 118.20 (q, *J* = 14.7 Hz), 115.9, 79.9, 53.3, 52.4, 30.2, 28.4 ; **^{19}F-NMR (282 MHz, $CDCl_3$)** δ -62.88; **IR (ATR)/$\bar{\nu}$ (cm^{-1}):** 2977, 2934, 1744, 1705, 1619, 1599, 1505, 1437, 1392, 1366, 1322, 1166, 1125, 1098, 1068, 1021, 803, 756, 697; **HRMS (ESI)** calcd. for $[C_{19}H_{22}F_3N_3O_4 + H]^+$: 414.1635, found 414.1648.

Methyl N^{α}-(*tert*-butoxycarbonyl)-N^{τ}-(4-(dimethoxymethyl)phenyl)-*L*-histidinate (3j)

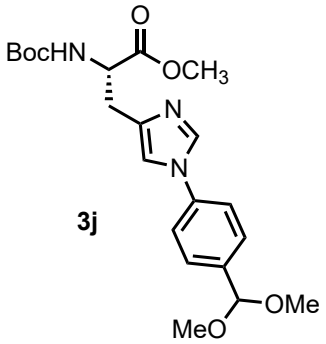

3j

The general procedure was followed starting from (*L*)-Boc–His–OMe **1a** (40 mg) and tri(4-(dimethoxymethyl)phenyl)bismuthine **2j** (98 mg). The crude material was purified on basified silica gel (2% MeOH/CH_2Cl_2) to afford **3j** as a yellow oil (62 mg, 99%): $\mathbf{R_f}$ = 0.45 (5% MeOH/CH_2Cl_2); **^{1}H-NMR (600 MHz, $CDCl_3$)** δ 7.79 (s, 1H), 7.53 (d, *J* = 8.4 Hz, 2H), 7.32 (d, *J* = 8.5 Hz, 2H), 7.06 (s, 1H), 5.86 (d, *J* = 8.0 Hz, 1H), 5.40 (s, 1H), 4.58 (X of ABX, *J* = 12.7, 5.2 Hz, 1H), 3.70 (s, 3H), 3.31 (s, 6H), 3.13 (A of ABX, *J* = 14.8, 5.7 Hz, 1H), 3.08 (B of ABX, *J* = 14.7, 4.9 Hz, 1H), 1.40 (s, 9H) ; **^{13}C-NMR (150 MHz, $CDCl_3$)** δ 172.5, 155.7, 137.7, 137.1, 135.2, 128.5, 120.9, 115.9, 102.3, 79.8, 53.5, 52.8, 52.3, 30.3, 28.4, 8.7 **; IR (ATR)/$\bar{\nu}$ (cm^{-1}):** 2937, 2831, 1744, 1705, 1613, 1522, 1489, 1436, 1366, 1206, 1614, 1101, 1054, 985, 969, 818, 753; **HRMS (ESI)** calcd. for $[C_{21}H_{29}N_3O_6 + H]^+$: 420.2129, found 420.2138.

Methyl N^{α}-(*tert*-butoxycarbonyl)-N^{τ}-(4-((tetrahydro-2H-pyran-2-yl)oxy)phenyl)-*L*-histidinate (3k)

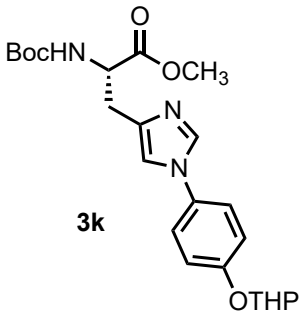

3k

The general procedure was followed starting from (*L*)-Boc–His–OMe **1a** (40 mg) and tri(4-((tetrahydro-2H-pyran-2-yl)oxy)phenyl)bismuthine **2k** (110 mg). The crude material was purified on basified silica gel (2% MeOH/CH_2Cl_2) to afford **3k** as a yellow oil (66 mg, 99%): $\mathbf{R_f}$ = 0.47 (5% MeOH/CH_2Cl_2); **^{1}H-NMR (600 MHz, $CDCl_3$)** δ 7.69 (s(br), 1H), 7.21 (dt, *J* = 9.7, 2.5 Hz, 2H), 7.10 (dt, *J* = 9.7, 2.6 Hz, 2H), 6.99 (s(br), 1H), 5.90 (d, *J* = 7.4 Hz, 1H), 5.41 (t, *J* = 3.1 Hz, 1H), 4.57 (s, 1H), 3.85 (ddd, *J* = 12.0, 9.2, 2.1 Hz, 1H), 3.69 (s, 3H), 3.62 – 3.56 (m, 1H), 3.19 – 2.98 (m, 2H), 2.02 – 1.92 (m, 1H), 1.88 – 1.81 (m, 2H), 1.73 – 1.63 (m, 2H), 1.62 – 1.54 (m, 1H), 1.41 (s, 9H); **^{13}C-NMR (150 MHz, $CDCl_3$)** δ 172.6, 156.5, 155.7, 131.2, 122.8, 117.6, 96.6, 79.7, 62.1, 53.5, 52.3, 30.3, 29.7, 28.4, 25.1, 18.7; **IR (ATR)/$\bar{\nu}$ (cm^{-1}):** 2946, 2874, 1747, 1709, 1515, 1456, 1436, 1365, 1237, 1201, 1166, 1109, 1074, 1035, 958, 919, 835, 752; **HRMS (ESI)** calcd. for $[C_{23}H_{31}N_3O_6 + H]^+$: 446.2286, found 446.2293.

Methyl N^{α}-(*tert*-butoxycarbonyl)-N^{τ}-(4-bromophenyl)-*L*-histidinate (3l)

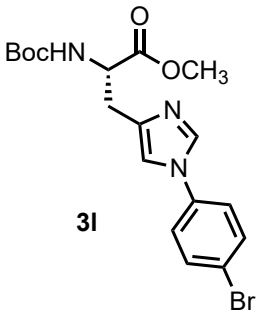

3l

The general procedure was followed starting from (*L*)-Boc–His–OMe **1a** (40 mg) and tri(4-bromophenyl)bismuthine **2l** (101 mg). The crude material was purified on silica gel (2% MeOH/CH_2Cl_2) to afford **3l** as a thick yellow oil (50 mg, 79%): **R_f** = 0.67 (5% MeOH/CH_2Cl_2); **^{1}H-NMR (600 MHz, $CDCl_3$)** δ 7.88 (s, 1H), 7.58 (d, *J* = 8.6 Hz, 2H), 7.24 (d, *J* = 8.7 Hz, 2H), 7.06 (s, 1H), 5.84 (d, *J* = 7.7 Hz, 1H), 4.66 – 4.51 (m, 1H), 3.71 (s, 3H), 3.15 (A of ABX, *J* = 14.6, 4.8 Hz, 1H), 3.10 (B of ABX, *J* = 14.7, 4.1 Hz, 1H), 1.41 (s, 9H); **^{13}C-NMR (150 MHz, $CDCl_3$)** δ 172.5, 155.7, 136.1, 133.2, 122.8, 121.2, 79.9, 53.4, 52.4, 30.2, 28.4; **IR (ATR)/$\bar{\nu}$ (cm^{-1}):** 2979, 1744, 1701, 1500, 1436, 1365, 1161, 1068, 1010, 966, 826, 752; **HRMS (ESI)** calcd. for $[C_{18}H_{22}BrN_3O_4 + H]^+$: 424.0867, found 424.0876.

Methyl N^{α}-(*tert*-butoxycarbonyl)-N^{τ}-(4-formylphenyl)-*L*-histidinate (3m)

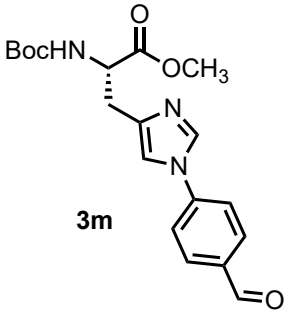

3m

The general procedure was followed starting from (*L*)-Boc–His–OMe **1a** (40 mg) and tri(4-formylphenyl)bismuthine **2m** (78 mg). The crude material was purified on silica gel (3% MeOH/CH_2Cl_2) to afford **3m** as a yellow oil (53 mg, 96%): **R_f** = 0.37 (5% MeOH/CH_2Cl_2); **^{1}H-NMR (300 MHz, $CDCl_3$)** δ 10.00 (s, 1H), 8.02 – 7.92 (m, 3H), 7.52 (d, *J* = 8.5 Hz, 2H), 7.18 (s, 1H), 5.81 (d, *J* = 8.0 Hz, 1H), 4.70 – 4.50 (m, 1H), 3.70 (s, 3H), 3.20 – 2.98 (m, 2H), 1.39 (s, 9H); **^{13}C-NMR (75 MHz, $CDCl_3$)** δ 190.6, 172.5, 155.6, 141.4, 135.1, 131.7, 120.9, 79.9, 53.3, 52.4, 30.4, 28.4; **IR (ATR)/$\bar{\nu}$ (cm^{-1}):** 3358, 3125, 2980, 2849, 2742, 1744, 1698, 1605, 1519, 1486, 1436, 1392, 1366, 1305, 1206, 1164, 1059, 1023, 966, 835, 752; **HRMS (ESI)** calcd. for $[C_{19}H_{23}N_3O_5 + H]^+$: 374.1711, found 374.1724.

Ethyl (*S*,*E*)-3-(3-(4-(2-((*tert*-butoxycarbonyl)amino)-3-methoxy-3-oxopropyl)-1*H*-imidazol-1-yl)phenyl)acrylate (3n)

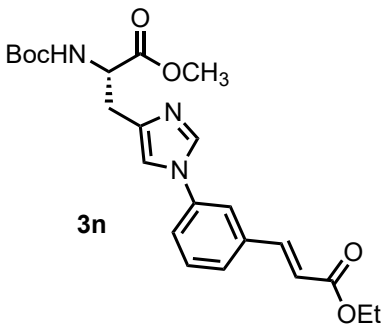

3n

The general procedure was followed starting from (*L*)-Boc–His–OMe **1a** (40 mg) and triethyl 3,3',3''-(bismuthanetriyltris(benzene-3,1-diyl))(2*E*,2'*E*,2''*E*)-triacrylate **2n** (109 mg). The crude material was purified on silica gel (2% MeOH/CH_2Cl_2) to afford **3n** as a yellow oil (65 mg, 99%): **R_f**= 0.45 (5% MeOH/CH_2Cl_2); **^{1}H-NMR (600 MHz, $CDCl_3$)**

δ 7.90 (s(br), 1H), 7.65 (d, *J* = 16.0 Hz, 1H), 7.52 – 7.44 (m, 3H), 7.35 (d, *J* = 7.1 Hz, 1H), 7.13 (s(br), 1H), 6.47 (d, *J* = 16.0 Hz, 1H), 5.86 (d, *J* = 6.8 Hz, 1H), 4.60 (s, 1H), 4.25 (q, *J* = 7.1 Hz, 2H), 3.71 (s, 3H), 3.24 – 3.00 (m, 2H), 1.41 (s, 9H), 1.32 (t, *J* = 7.1 Hz, 3H); **^{13}C-NMR (150 MHz, $CDCl_3$)** δ 172.5, 166.5, 155.7, 142.8, 137.7, 136.5, 130.6, 127.0, 122.7, 120.5, 120.4, 79.8, 60.8, 53.4, 52.4, 30.3, 28.4, 14.3; **IR (ATR)/$\bar{\nu}$ (cm^{-1}):** 2980, 1705, 1640, 1589, 1499, 1366, 1307, 1162, 1027, 983, 860, 753; **HRMS (ESI)** calcd. for $[C_{23}H_{29}N_3O_6 + H]^+$: 444.2129, found 444.2131.

Methyl *N*$^{\alpha}$-(*tert*-butoxycarbonyl)-*N*$^{\tau}$-(3-vinylphenyl)-*L*-histidinate (3o)

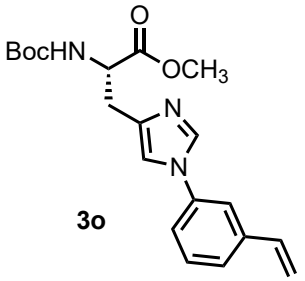

3o

The general procedure was followed starting from (*L*)-Boc–His–OMe **1a** (40 mg) and tri(3-vinylphenyl)bismuthine **2o** (77 mg). The crude material was purified on silica gel (2% MeOH/CH_2Cl_2) to afford **3o** as a yellow oil (54 mg, 98%): **R_f** = 0.57 (5% MeOH/CH_2Cl_2); **^{1}H-NMR (600 MHz, $CDCl_3$)** δ 7.87 (s(br), 1H), 7.41 – 7.34 (m, 2H), 7.33 (s, 1H), 7.20 (d, *J* = 7.5 Hz, 1H), 6.70 (dd, *J* = 17.6, 10.9 Hz, 1H), 5.91 (d, *J* = 6.5 Hz, 1H), 5.79 (d, *J* = 17.5 Hz, 1H), 5.33 (d, *J* = 10.9 Hz, 1H), 4.59 (s(br), 1H), 3.70 (s, 3H), 3.19 – 2.99 (m, 2H), 1.40 (s, 9H); **^{13}C-NMR (150 MHz, $CDCl_3$)** δ 172.5, 155.6, 139.6, 137.5, 135.6, 130.1, 125.4, 120.5, 119.0, 115.9, 79.7, 53.4, 52.3, 30.2, 28.3; **IR (ATR)/$\bar{\nu}$ (cm^{-1}):** 2979, 1744, 1705, 1607, 1585, 1498, 1436, 1392, 1366, 1162, 1055, 1023, 991, 915, 751; **HRMS (ESI)** calcd. for $[C_{20}H_{25}N_3O_4 + H]^+$: 372.1918, found 372.1930.

Methyl *N*$^{\alpha}$-(*tert*-butoxycarbonyl)-*N*$^{\tau}$-(3-(hydroxymethyl)phenyl)-*L*-histidinate (3p)

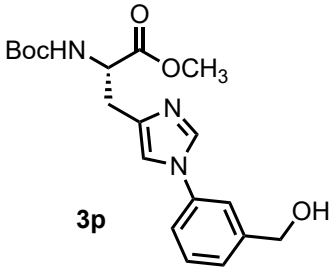

3p

The general procedure was followed starting from (*L*)-Boc–His–OMe **1a** (40 mg) and tri(3-(hydroxymethyl)phenyl)bismuthine **2p** (79 mg). The crude material was purified on silica gel (3% MeOH/CH_2Cl_2) to afford **3p** as a yellow oil (44 mg, 79%): **R_f** = 0.45 (10% MeOH/CH_2Cl_2); **^{1}H-NMR (300 MHz, $CDCl_3$)** δ 7.72 (s(br), 1H), 7.46 – 7.28 (m, 3H), 7.18 (d, *J* = 7.8 Hz, 1H), 7.06 (s, 1H), 5.83 (d, *J* = 8.0 Hz, 1H), 4.73 (s, 2H), 4.61 – 4.49 (m, 1H), 4.30 (s, 1H), 3.70 (s, 3H), 3.16 – 2.97 (m, 2H), 1.40 (s, 9H); **^{13}C-NMR (75 MHz, $CDCl_3$)** δ 172.6, 155.7, 143.9, 137.2, 135.2, 130.0, 125.8, 119.9, 119.4, 116.0, 79.9, 64.0, 53.6, 52.4, 29.8, 28.4; **IR (ATR)/$\bar{\nu}$ (cm^{-1}):** 3310, 2920, 2850, 1741, 1699, 1499, 1456, 1436, 1365, 1249, 1214, 1160, 1052, 1022, 785; **HRMS (ESI)** calcd. for $[C_{19}H_{25}N_3O_5 + H]^+$: 376.1867, found 376.1884.

Methyl (*S*)-4-(4-(2-((*tert*-butoxycarbonyl)amino)-3-methoxy-3-oxopropyl)-1*H*-imidazol-1-yl)benzoate (3q)

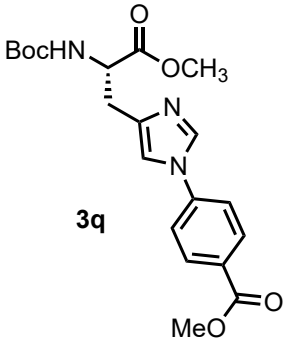

3q

The general procedure was followed starting from (*L*)-Boc–His–OMe **1a** (40 mg) and trimethyl 4,4',4''-bismuthanetriyltribenzoate **2q** (91 mg). The crude material was purified on silica gel (2% MeOH/CH_2Cl_2) to afford **3q** as a white solid (55 mg, 92%): $\mathbf{R_f}$ = 0.34 (5% MeOH/CH_2Cl_2); **m.p.**= 50 – 52 °C; **^{1}H-NMR (300 MHz, $CDCl_3$)** δ 8.11 (dt, *J* = 8.9, 2.0 Hz, 2H), 7.84 (s, 1H), 7.40 (dt, *J* = 9.0, 2.0 Hz, 2H), 7.12 (s, 1H), 5.83 (d, *J* = 8.0 Hz, 1H), 4.69 – 4.47 (m, 1H), 3.91 (s, 3H), 3.70 (s, 3H), 3.20 – 3.01 (m, 2H), 1.40 (s, 9H); **^{13}C-NMR (75 MHz, $CDCl_3$)** δ 172.5, 166.0, 155.6, 140.5, 135.1, 131.6, 129.0, 120.3, 115.4, 79.8, 53.4, 52.4, 30.4, 29.7, 28.4; **IR (ATR)/$\bar{\nu}$ (cm^{-1}):** 3341, 2919, 2843, 1708, 1609, 1520, 1485, 1435, 1365, 1281, 1210, 1162, 1111, 1056, 1017, 966, 855, 769, 694; **HRMS (ESI)** calcd. for $[C_{20}H_{25}N_3O_6 + H]^+$: 404.1816, found 404.1820.

Methyl N^{α}-(*tert*-butoxycarbonyl)-N^{τ}-(naphthalen-1-yl)-*L*-histidinate (3r)

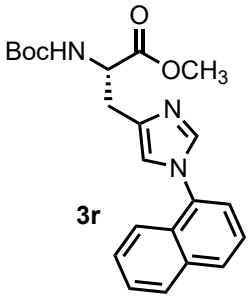

3r

The general procedure was followed starting from (*L*)-Boc–His–OMe **1a** (40 mg) and tri(naphthalen-1-yl)bismuthine **2r** (88 mg). The crude material was purified on silica gel (2% MeOH/CH_2Cl_2) to afford **3r** as a yellow oil (46 mg, 78%): $\mathbf{R_f}$ = 0.76 (5% MeOH/CH_2Cl_2); **^{1}H-NMR (300 MHz, $CDCl_3$)** δ 8.02 – 7.88 (m, 2H), 7.71 (s, 1H), 7.61 – 7.47 (m, 4H), 7.42 (d, *J* = 6.5 Hz, 1H), 7.04 (s, 1H), 6.00 (d, *J* = 7.8 Hz, 1H), 4.66 (s, 1H), 3.74 (s, 3H), 3.32 – 3.07 (m, 2H), 1.44 (s, 9H); **^{13}C-NMR (75 MHz, $CDCl_3$)** δ 172.6, 155.7, 134.3, 133.9, 129.5, 129.5, 128.4, 127.8, 127.1, 125.3, 123.7, 122.3, 79.8, 53.8, 52.4, 30.4, 28.5; **IR (ATR)/$\bar{\nu}$ (cm^{-1}):** 3413, 3345, 2981, 2950, 1741, 1706, 1599, 1488, 1435, 1365, 1161, 1055, 1022, 940, 864, 803, 773, 753, 644; **HRMS (ESI)** calcd. for $[C_{22}H_{25}N_3O_4 + H]^+$: 396.1918, found 396.1920.

Methyl N^{α}-((benzyloxy)carbonyl)-N^{τ}-(4-tolyl)-*L*-histidinate (3s)

In a sealed tube, *N*,*N*-diisopropylethylamine (22.5 µL, 0.13 mmol, 1.0 equiv) was added to the (*L*)-Cbz–His–OMe **1b** (40 mg, 0.13 mmol, 1.0 equiv), tri(4-tolyl)bismuthine **2a** (64 mg, 0.13 mmol, 1.0 equiv), copper(II) acetate (24 mg, 0.13 mmol, 1.0 equiv) and phenanthroline (24 mg, 0.13 mmol, 1.0 equiv) in CH_2Cl_2 (0.1 M). The mixture was purged with oxygen before stirred in an oil bath set at 40 °C for 16 hours under oxygen. The solvent was evaporated under

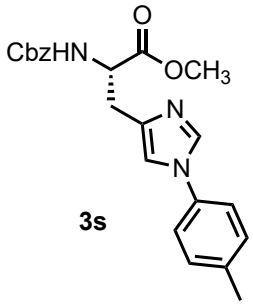

3s

reduce pressure and the crude material was purified on silica gel (2% MeOH/CH_2Cl_2) to afford **3s** as a yellow oil (45 mg, 87%): $\mathbf{R_f}$ = 0.26 (5% MeOH/CH_2Cl_2); **^{1}H-NMR (300 MHz, $CDCl_3$)** δ 7.72 (s, 1H), 7.39 – 7.29 (m, 5H), 7.27 – 7.14 (m, 4H), 7.07 – 6.91 (m, 1H), 6.31 (d, *J* = 6.7 Hz, 1H), 5.12 (d, *J* = 2.4 Hz, 2H), 4.67 (s, 1H), 3.72 (s, 3H), 3.29 – 3.00 (m, 2H), 2.38 (s, 3H); **^{13}C-NMR (150 MHz, $CDCl_3$)** δ 172.3, 156.2, 137.6, 136.6, 134.9, 130.5, 129.5, 128.5, 128.2, 128.1, 121.3, 116.2, 66.9, 54.0, 52.4, 30.2, 21.0; **IR (ATR)/$\bar{\nu}$ (cm^{-1}):** 3324, 3034, 2945, 1713, 1518, 1487, 1454, 1435, 1307, 1247, 1207, 1175, 1027, 969, 815, 739, 697; **HRMS (ESI)** calcd. for $[C_{22}H_{23}N_3O_4 + H]^+$: 394.1761, found 394.1771.

Methyl N$^{\alpha}$-(((9H-fluoren-9-yl)methoxy)carbonyl)-N$^{\tau}$-(4-tolyl)-*L*-histidinate (3t)

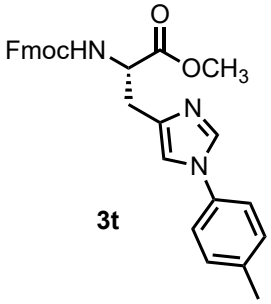

3t

In a sealed tube, *N*,*N*-diisopropylethylamine (17.5 µL, 0.10 mmol, 1.0 equiv) was added to the (*L*)-Fmoc–His–OMe **1c** (40 mg, 0.10 mmol, 1.0 equiv), tri(4-tolyl)bismuthine **2a** (49 mg, 0.10 mmol, 1.0 equiv), copper(II) acetate (19 mg, 0.10 mmol, 1.0 equiv) and phenanthroline (18 mg, 0.10 mmol, 1.0 equiv) in CH_2Cl_2 (0.1 M). The mixture was purged with oxygen before stirred in an oil bath set at 40 °C for 16 hours under oxygen. The solvent was evaporated under reduce pressure and the crude material was purified on silica gel (1% MeOH/CH_2Cl_2) to afford **3t** as an orange oil (25 mg, 51%): $\mathbf{R_f}$ = 0.35 (5% MeOH/CH_2Cl_2); **^{1}H-NMR (300 MHz, $CDCl_3$)** δ 10.89 (s(br), 1H), 8.55 (s, 1H), 7.72 (d, *J* = 7.5 Hz, 2H), 7.58 (t, *J* = 6.5 Hz, 2H), 7.43 – 7.16 (m, 8H), 6.66 – 6.51 (m, 1H), 4.66 (s, 1H), 4.45 – 4.24 (m, 2H), 4.16 (t, *J* = 7.0 Hz, 1H), 3.80 (s, 3H), 3.53 – 3.39 (m, 1H), 3.39 – 3.23 (m, 1H), 2.42 (s, 3H); **^{13}C-NMR (150 MHz, $CDCl_3$)** δ 171.0, 156.5, 143.9, 143.8, 141.4, 140.8, 133.1, 132.6, 131.1, 127.9, 127.2, 125.4, 122.0, 120.0, 118.5, 67.4, 53.7, 53.2, 47.1, 27.8, 21.2; **IR (ATR)/$\bar{\nu}$ (cm^{-1}):** 3297, 3137, 2950, 2919, 1669, 1541, 1513, 1437, 1177, 1130, 1079, 1045, 816, 797, 759, 740, 719; **HRMS (ESI)** calcd. for $[C_{29}H_{27}N_3O_4 + H]^+$: 482.2074, found 482.2086.

5. General procedure for the coupling between N-protected amino acid methyl ester and tri(4-tolyl)bismuthines (2a)

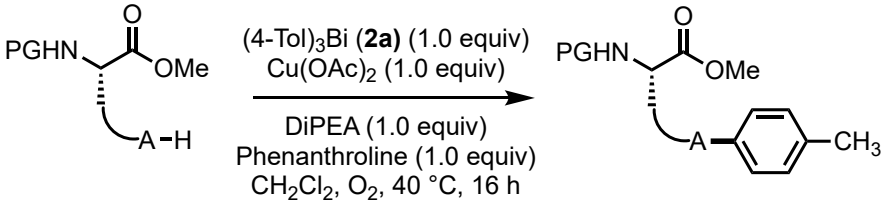

Manuscript, Figure 1: In a sealed tube, *N*,*N*-diisopropylethylamine (1.0 equiv) was added to the *N*-protected (*L*)-amino acid methyl ester (40 mg, 1.0 equiv), tri(4-tolyl)bismuthine **2a** (1.0 equiv), copper(II) acetate (1.0 equiv) and phenanthroline (1.0 equiv) in CH_2Cl_2 (0.1 M). Oxygen was bubbled in the reaction mixture before stirred in an oil bath set at 40 °C for 16 hours. The solvent was evaporated under reduce pressure and the residue was purified on silica gel chromatography using the corresponding eluent system to afford desired pure product.

Methyl (*S*)-2-((*tert*-butoxycarbonyl)amino)-3-(4-(*p*-tolyloxy)phenyl)propanoate (4')

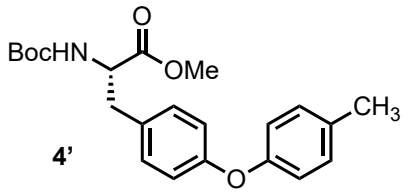

4'

The general procedure was followed starting from (*L*)-Boc–Tyr–OMe (40 mg, 0.14 mmol), tri(4-tolyl)bismuthine **2a** (65 mg, 0.14 mmol), *N*,*N*-diisopropylethylamine (23.0 µL, 0.14 mmol), copper(II) acetate (25 mg, 0.14 mmol) and phenanthroline (25 mg, 0.14 mmol). The crude material was purified on silica gel (2% MeOH/CH_2Cl_2) to afford **4'** as a colorless oil (38 mg, 73%). $\mathbf{R_f}$ = 0.53 (30% EtOAc/Hexane); This compound has been previously reported [ii] : **^{1}H-NMR (600 MHz, $CDCl_3$)** δ 7.13 (d, *J* = 8.3 Hz, 2H), 7.06 (d, *J* = 8.3 Hz, 2H), 6.91 (d, *J* = 2.4 Hz, 2H), 6.89 (d, *J* = 2.4 Hz, 2H), 5.03 (d, *J* = 7.9 Hz, 1H), 4.57 (X of ABX, *J* = 13.3, 6.1 Hz, 1H), 3.72 (s, 3H), 3.09 (A of ABX, *J* = 13.8, 5.5 Hz, 1H), 3.01 (B of ABX, *J* = 13.9, 6.1 Hz, 1H), 2.34 (s, 3H), 1.43 (s, 9H).

Methyl N^{α}-(*tert*-butoxycarbonyl)-1-(*p*-tolyl)-*L*-tryptophanate (5')

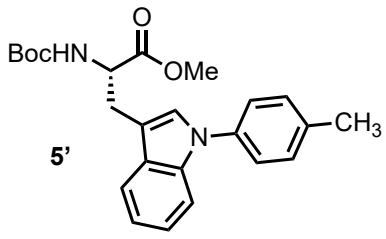

5'

The general procedure was followed starting from (*L*)-Boc–Trp–OMe (40 mg, 0.13 mmol), tri(4-tolyl)bismuthine **2a** (61 mg, 0.13 mmol), *N*,*N*-diisopropylethylamine (21.5 µL, 0.13 mmol), copper(II) acetate (23 mg, 0.13 mmol) and

[ii] Le Roch, A.; Hébert, M.; Gagnon, A. Eur. *J. Org. Chem.* **2020**, *33*, 5363–5367

phenanthroline (23 mg, 0.13 mmol). The crude material was purified on silica gel (2% MeOH/CH_2Cl_2) to afford **5'** as a white solid (6 mg, 12%). The compound contained impurities. **R_f** = 0.30 (EtOAc:Hexane 2:8); This compound has been previously reported[iii]: **^{1}H-NMR (300 MHz, $CDCl_3$)** δ 7.59 (d, *J* = 7.3 Hz, 1H), 7.49 (d, *J* = 7.5 Hz, 1H), 7.39 – 7.26 (m, 4H), 7.24 – 7.09 (m, 3H), 5.11 (d, *J* = 7.0 Hz, 1H), 4.74 – 4.65 (m, 1H), 3.71 (s, 3H), 3.41 – 3.25 (m, 2H), 2.43 (s, 3H), 1.43 (s, 9H).

Methyl *N*-(*tert*-butoxycarbonyl)-*S*-(*p*-tolyl)-*L*-cysteinate (6')

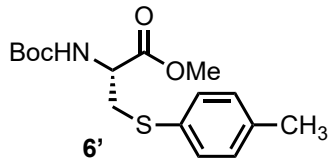

The general procedure was followed starting from (*L*)-Boc–Cys–OMe (40 mg, 0.17 mmol), tri(4-tolyl)bismuthine **2a** (82 mg, 0.17 mmol), *N*,*N*-diisopropylethylamine (29.0 µL, 0.17 mmol), copper(II) acetate (31 mg, 0.17 mmol) and phenanthroline (31 mg, 0.17 mmol). The crude material was purified on silica gel (2% MeOH/CH_2Cl_2) to afford **6'** as a yellow oil (11 mg, 19%). The compound contained impurities **R_f** = 0.30 (1% MeOH/CH_2Cl_2); This compound has been previously reported [ii] : **^{1}H-NMR (300 MHz, $CDCl_3$)** δ 7.31 (dt, *J* = 8.5, 2.2 Hz, 2H), 7.10 (d, *J* = 7.9 Hz, 2H), 5.45 – 5.19 (m, 1H), 4.60 – 4.45 (m, 1H), 3.54 (s, 3H), 3.32 (d, *J* = 4.7 Hz, 2H), 2.31 (s, 3H), 1.41 (s, 9H).

Methyl N^2-(*tert*-butoxycarbonyl)-N^6-(*p*-tolyl)-*L*-lysinate (8')

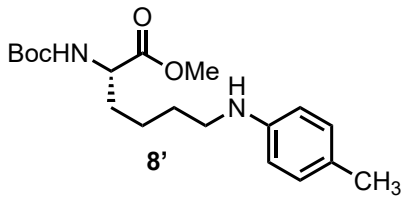

The general procedure was followed starting from (*L*)-Boc–Lys–OMe•HCl (40 mg, 0.14 mmol), tri(4-tolyl)bismuthine **2a** (65 mg, 0.14 mmol), *N*,*N*-diisopropylethylamine (23.0 µL, 0.14 mmol), copper(II) acetate (25 mg, 0.14 mmol) and phenanthroline (25 mg, 0.14 mmol). The crude material was purified on silica gel (1% MeOH/CH_2Cl_2) to afford **8'** as a yellow oil (31 mg, 66%). **R_f** = 0.74 (5% MeOH/CH_2Cl_2); This compound has been previously reported [iv] : **^{1}H-NMR (300 MHz, $CDCl_3$)** δ 6.98 (d, *J* = 8.0 Hz, 2H), 6.53 (dt, *J* = 9.1, 2.6 Hz, 2H), 5.05 (d, *J* = 7.9 Hz, 1H), 4.32 (dd, *J* = 12.4, 6.9 Hz, 1H), 3.73 (s, 3H), 3.09 (t, *J* = 6.9 Hz, 2H), 2.23 (s, 3H), 1.90 – 1.75 (m, 1H), 1.71 – 1.55 (m, 3H), 1.53 – 1.33 (m, 11H).

[iii] Le Roch, A.; Chan, H-C..; Gagnon, A. Eur. *J. Org. Chem.* **2020**, *36*, 5815–5819

[iv] Sun, H-B.; Gong, L.; Tian, Y-B.; Wu, J-G.; Zhang, X.; Liu, J.; Fu, Z.; Niu, D. *Angew. Chem. Int. Ed.* **2018**, *57*, 1–6

6. Procedures for the preparation of dipeptides

a. Procedure for synthesis of Boc–His–A.A.–OMe (12a–f and 12j–l)

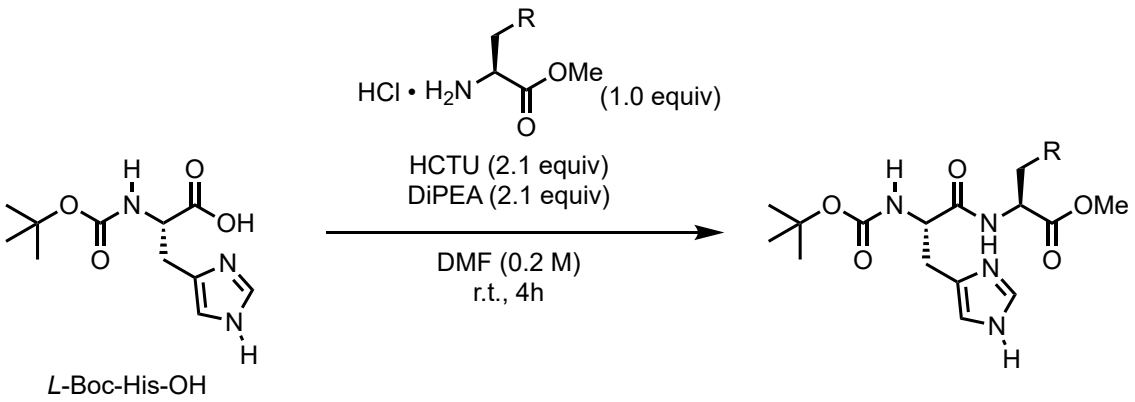

Manuscript, Scheme 3a): In a 50 mL flask, DIPEA (280 µL, 1.64 mmol, 2.1 equiv) was added to *L*–Boc–His–OH (200 mg, 783 µmol, 1.0 equiv), *L*–H-A.A.–OMe•HCl (783 µmol, 1.0 equiv) and HCTU (681 mg, 1.65 mmol, 2.1 equiv) in DMF (4 mL, 0.2 M). The mixture was stirred for 4h at room temperature before being extracted twice with dichloromethane. The combined organic phases were successively washed with sat. aq. NaHCO3 (2x20 mL), brine (2x20 mL), dried over Na_2SO_4, filtered and concentrated under reduce pressure. The resulting crude product was purified by column chromatography using the indicated eluent system to afford the desired pure product.

Methyl (*tert*-butoxycarbonyl)-*L*-histidyl-*L*-alaninate (12a)

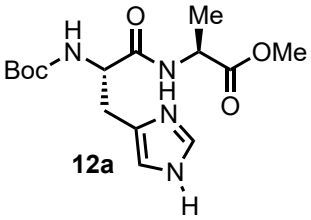

12a

The general procedure was followed starting from *L*–H-Ala–OMe•HCl (109 mg, 783 µmol). The crude material was purified on silica gel (10% MeOH/CH_2Cl_2) to afford **12a** as a white solid (109 mg, 41%). $\mathbf{R_f}$ = 0.28 (10% MeOH/DCM); **m.p.**= 94 – 96 °C; **^{1}H-NMR (600 MHz, $CDCl_3$)** δ 7.74 (s, 1H), 7.60 – 7.32 (m, 2H), 6.79 (s, 1H), 5.99 – 5.86 (d, *J* = 5.5 Hz, 1H), 4.51 – 4.35 (m, 2H), 3.68 (s, 3H), 3.09 – 2.98 (m, 2H), 1.38 (s, 9H), 1.31 (d, *J* = 7.2 Hz, 3H); **^{13}C-NMR (150 MHz, $CDCl_3$)** δ 173.5, 171.8, 155.8, 135.2, 131.6, 119.5, 80.2, 54.2, 52.6, 48.3, 29.7, 28.4, 17.7; **IR (ATR)/$\bar{\nu}$ (cm^{-1}):** 3288, 3195, 2959, 2919, 1753, 1705, 1683, 1662, 1540, 1494, 1361, 1254, 1196, 1154, 1019, 853, 761, 617; **HRMS (ESI)** calcd. for $[C_{15}H_{24}N_4O_5 + H]^+$: 341.1820, found 341.1817.

Methyl (*tert*-butoxycarbonyl)-*L*-histidyl-*L*-valinate (12b)

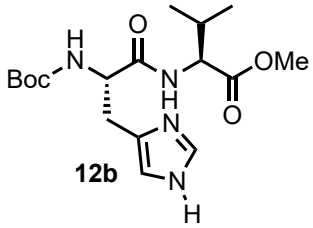

The general procedure was followed starting from *L*–H-Val–OMe•HCl (131 mg, 783 µmol). The crude material was purified on silica gel (10% MeOH/CH_2Cl_2) to afford **12b** as a white solid (225 mg, 78%). **R_f** = 0.32 (10% MeOH/DCM); **m.p.**= 82 – 84 °C; **^{1}H-NMR (300 MHz, $CDCl_3$)** δ 8.44 (s, 1H), 7.60 (s, 1H), 7.43 (d, *J* = 6.6 Hz, 1H), 6.85 (s, 1H), 5.94 (d, *J* = 5.9 Hz, 1H), 4.54 – 4.30 (m, 2H), 3.70 (s, 3H), 3.13 (A of ABX, *J* = 15.0, 4.4 Hz, 1H), 3.01 (B of ABX, *J* = 14.9, 6.3 Hz, 1H), 2.20 – 2.02 (m, 1H), 1.43 (s, 9H), 0.82 (dd, *J* = 6.8, 2.6 Hz, 6H); **^{13}C-NMR (75 MHz, $CDCl_3$)** δ 172.0, 155.8, 135.0, 132.7, 117.8, 80.0, 57.5, 54.5, 52.0, 30.8, 28.2, 18.8, 17.6; **IR (ATR)/$\bar{\nu}$ (cm^{-1}):** 3306, 2963, 1738, 1659, 1515, 1436, 1366, 1250, 1210, 1162, 1019, 843, 760; **HRMS (ESI)** calcd. for $[C_{17}H_{28}N_4O_5 + H]^+$: 369.2133, found 369.2131.

Methyl (*tert*-butoxycarbonyl)-*L*-histidyl-*L*-phenylalaninate (12c)

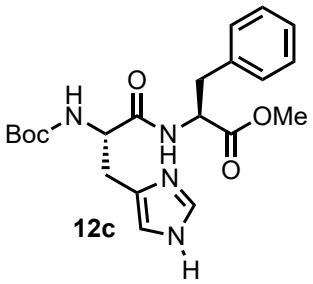

The general procedure was followed starting from *L*–H-Phe–OMe•HCl (169 mg, 783 µmol). The crude material was purified on silica gel (2% MeOH/CH_2Cl_2) to afford **12c** as a white solid (322 mg, 99%). **R_f** = 0.62 (10% MeOH/DCM); **m.p.**= 85 – 87 °C; **^{1}H-NMR (300 MHz, $CDCl_3$)** δ 10.35 (s, 1H), 7.53 (s, 2H), 7.24 – 7.11 (m, 3H), 6.98 (d, *J* = 6.4 Hz, 2H), 6.76 (s, 1H), 6.03 (d, *J* = 7.2 Hz, 1H), 4.72 (dd, *J* = 12.9, 6.3 Hz, 1H), 4.38 (s(br), 1H), 3.60 (s, 3H), 3.09 – 2.88 (m, 4H), 1.36 (s, 9H) ; **^{13}C-NMR (75 MHz, $CDCl_3$)** δ 171.8, 155.7, 135.9, 135.1, 132.5, 129.1, 128.5, 127.0, 118.1, 80.1, 54.4, 53.5, 52.3, 37.7, 29.2, 28.2; **IR (ATR)/$\bar{\nu}$ (cm^{-1}):** 3280, 2978, 1739, 1658, 1496, 1455, 1435, 1366, 1248, 1216, 1163, 1020, 843, 746, 700; **HRMS (ESI)** calcd. for $[C_{21}H_{28}N_4O_5 + H]^+$: 417.2133, found 417.2146.

Methyl (*tert*-butoxycarbonyl)-*L*-histidyl-*L*-prolinate (12d)

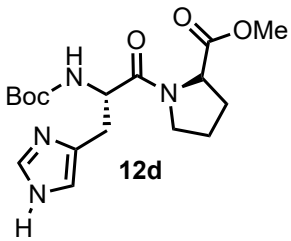

The general procedure was followed starting from *L*–H-Pro–OMe•HCl (101 mg, 783 µmol). The crude material was purified on silica gel (4% MeOH/CH_2Cl_2) to afford **12d** as a white solid (163 mg, 57%). **R_f** = 0.14 (5% MeOH/DCM); **m.p.**= 59 – 62 °C; **^{1}H-NMR (300 MHz, $CDCl_3$)** δ 8.53 (s(br), 1H), 7.68 (s, 1H), 6.94 (s, 1H), 5.43 (d, *J* = 7.8 Hz, 1H), 4.66 – 4.56 (m, 1H), 4.55 – 4.47 (m, 1H), 3.79 (s, 3H), 3.67 – 3.56 (m, 1H), 3.25 – 3.15 (m, 1H), 3.08 (d, *J* = 5.6 Hz, 2H), 2.32 – 2.17 (m, 1H), 2.02 – 1.88 (m, 3H), 1.41 (s, 9H) ; **^{13}C-**

NMR (150 MHz, $CDCl_3$) δ 173.4, 170.6, 155.3, 135.3, 128.1, 122.6, 79.9, 59.1, 52.7, 52.0, 47.1, 38.6, 29.0, 28.3, 25.0; **IR (ATR)/$\bar{\nu}$ (cm^{-1}):** 3275, 2977, 1739, 1704, 1635, 1506, 1436, 1365, 1248, 1161, 1046, 1019, 841, 751; **HRMS (ESI)** calcd. for $[C_{17}H_{26}N_4O_5 + H]^+$: 367.1976, found 367.1983.

Methyl (*tert*-butoxycarbonyl)-*L*-histidylglycinate (12e)

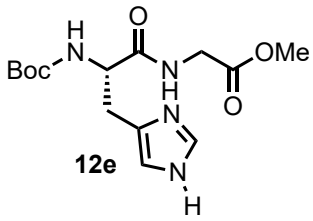

The general procedure was followed starting from *L*–H-Gly–OMe•HCl (99 mg, 0.78 mmol). The crude material was purified on silica gel (5% MeOH/CH_2Cl_2) to afford **12e** as a white solid (54 mg, 21%). **R_f** = 0.38 (10% MeOH/DCM); **m.p.**= 86 – 88 °C; **^{1}H-NMR (600 MHz, $CDCl_3$)** δ 9.31 (s(br), 1H), 7.88 (s(br), 1H), 7.51 (s, 1H), 6.80 (s, 1H), 5.91 (s, 1H), 4.43 (s, 1H), 4.03 – 3.90 (m, 2H), 3.69 (s, 3H), 3.16 – 3.06 (m, 1H), 3.06 – 2.99 (m, 1H), 1.38 (s, 9H); ***presence of conformers*** **^{13}C-NMR (151 MHz, $CDCl_3$)** δ 172.6, 170.6, 155.8, 135.4, 131.4, 119.8, 80.3, 54.2, 53.3, 52.4, 41.3, 38.7, 29.4, 28.4, 18.3; **IR (ATR)/$\bar{\nu}$ (cm^{-1}):** 3276, 2920, 2850, 1747, 1674, 1520, 1436, 1366, 1248, 1211, 1162, 1022; **HRMS (ESI)** calcd. for $[C_{14}H_{22}N_4O_5 + H]^+$: 327.1663, found 327.1680.

Methyl (*tert*-butoxycarbonyl)-*L*-histidyl-*L*-methioninate (12f)

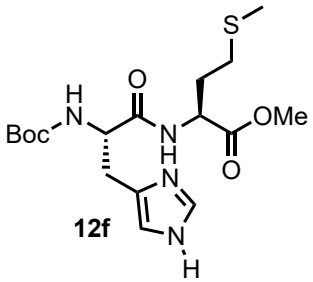

The general procedure was followed starting from *L*–H-Met–OMe•HCl (156 mg, 783 µmol). The crude material was purified on silica gel (10% MeOH/CH_2Cl_2) to afford **12f** as a white solid (228 mg, 73%). **R_f** = 0.23 (10% MeOH/DCM); **m.p.**= 62 – 64 °C; **^{1}H-NMR (300 MHz, $CDCl_3$)** δ 8.06 (s, 1H), 7.69 (d, *J* = 6.6 Hz, 1H), 7.51 (s, 1H), 6.75 (s, 1H), 6.06 (d, *J* = 7.5 Hz, 1H), 4.59 – 4.48 (m, 1H), 4.40 – 4.28 (m, 1H), 3.60 (s, 3H), 2.97 (d, *J* = 5.1 Hz, 2H), 2.30 (t, *J* = 7.6 Hz, 2H), 2.07 – 1.95 (m, 1H), 1.93 (s, 3H), 1.91 – 1.76 (m, 1H), 1.31 (s, 9H); ***presence of conformers*** **^{13}C-NMR (150 MHz, $CDCl_3$)** δ 172.3, 172.0, 155.7, 135.0, 131.9, 118.5, 80.2, 54.2, 52.6, 51.6, 31.1, 29.8, 29.1, 28.3, 15.2; **IR (ATR)/$\bar{\nu}$ (cm^{-1}):** 3288, 2921, 2852, 1739, 1661, 1506, 1436, 1366, 1273, 1348, 1162, 1019, 841, 778; **HRMS (ESI)** calcd. for $[C_{17}H_{28}N_4O_5S + H]^+$: 401.1853, found 401.1869.

Dimethyl N^{α}-(*tert*-butoxycarbonyl)-*L*-histidyl-*L*-glutamate (12g)

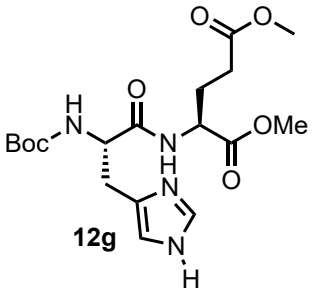

The procedure is described below, see section **6c** for complete characterization of **12g**.

Methyl N^{α}-(*tert*-butoxycarbonyl)-*L*-histidyl-*L*-allothreoninate (12h)

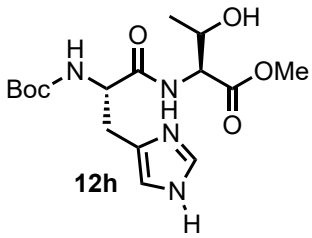

The procedure is described below, see section **6c** for complete characterization of **12h**.

Methyl N^{α}-(*tert*-butoxycarbonyl)-*L*-histidyl-*L*-serinate (12i)

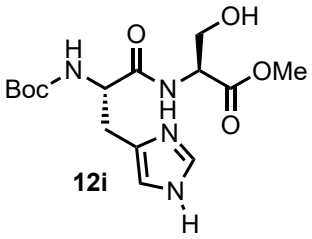

The procedure is described below, see section **6c** for complete characterization of **12i**.

Methyl N^{6}-(((9*H*-fluoren-9-yl)methoxy)carbonyl)-N^{2}-((*tert*-butoxycarbonyl)-*L*-histidyl)-*L*-lysinate (12j)

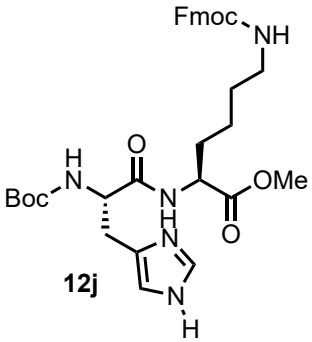

The general procedure was followed starting from *L*–H-Lys(Fmoc)–OMe•HCl (328 mg, 783 µmol). The crude material was purified on silica gel (3% MeOH/CH_2Cl_2) to afford **12j** as a white solid (454 mg, 94%). **R_f** = 0.46 (10% MeOH/DCM); **m.p.**= 76 – 78 °C; **^{1}H-NMR (600 MHz, $CDCl_3$)** δ 10.35 (s(br), 1H), 7.71 (d, *J* = 7.7 Hz, 3H), 7.55 (d, *J* = 7.4 Hz, 2H), 7.35 (t, *J* = 7.5 Hz, 2H), 7.29 – 7.22 (m, 3H), 6.81 (s, 1H), 6.41 (s(br), 1H), 5.53 (t, *J* = 5.8 Hz, 1H), 4.46 (s(br), 2H), 4.35 (d, *J* = 7.0 Hz, 2H), 4.16 (t, *J* = 7.0 Hz, 1H), 3.64 (s, 3H), 3.19 – 3.11 (m, 1H), 3.08 – 2.95 (m, 3H), 1.78 – 1.67 (m, 1H), 1.60 – 1.51 (m, 1H), 1.40 (s, 9H), 1.37 – 1.29 (m, 3H), 1.03 – 0.89 (m, 1H); **^{13}C-NMR (150 MHz, $CDCl_3$)** δ 172.5, 171.5, 165.8, 157.1, 155.7, 143.9, 143.9, 141.3, 134.9, 127.7, 127.1, 125.1, 120.0, 80.1, 66.7, 54.5, 52.4, 52.2, 47.2, 38.6, 31.5, 29.7, 29.1, 28.3, 21.9; **IR (ATR)/$\bar{\nu}$ (cm^{-1}):** 3408, 3288,

2936, 1694, 1515, 1449, 1366, 1248, 1161, 1021, 841, 760, 740; **HRMS (ESI)** calcd. for $[C_{33}H_{41}N_5O_7 + H]^+$: 620.3079, found 620.3097.

Methyl (*tert*-butoxycarbonyl)-*L*-histidyl-*L*-tryptophanate (12k)

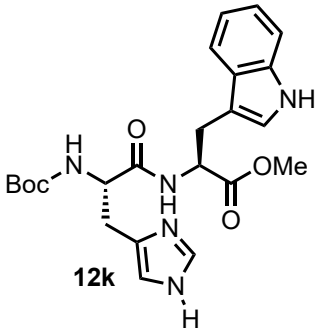

The general procedure was followed starting from *L*–H-Trp–OMe•HCl (200 mg, 783 µmol). The crude material was purified on silica gel (4% MeOH/CH_2Cl_2) to afford **12k** as a white solid (249 mg, 70%). **R_f** = 0.33 (10% MeOH/DCM); **m.p.**= 97 – 99 °C; **^{1}H-NMR (600 MHz, $CDCl_3$)** δ 10.20 (s, 1H), 9.40 (s, 1H), 7.44 (s, 1H), 7.41 (d, *J* = 7.1 Hz, 1H), 7.33 (s, 1H), 7.28 (d, *J* = 8.0 Hz, 1H), 7.10 (t, *J* = 7.5 Hz, 1H), 7.03 (t, *J* = 7.4 Hz, 1H), 6.78 (s, 1H), 6.67 (s, 1H), 6.20 (d, *J* = 5.6 Hz, 1H), 4.79 (s, 1H), 4.45 (s, 1H), 3.55 (s, 3H), 3.20 (s, 2H), 2.99 (s, 2H), 1.36 (s, 9H); **^{13}C-NMR (150 MHz, $CDCl_3$)** δ 172.3, 172.0, 155.8, 136.3, 135.1, 132.4, 127.3, 123.5, 121.8, 119.2, 118.1, 117.9, 111.6, 108.8, 80.3, 54.7, 53.1, 52.4, 29.2, 28.2, 27.4; **IR (ATR)/$\bar{\nu}$ (cm^{-1}):** 3289, 2972, 1660, 1506, 1456, 1435, 1366, 1245, 1161, 1010, 845, 741; **HRMS (ESI)** calcd. for $[C_{23}H_{29}N_5O_5 + H]^+$: 456.2242, found 456.2243.

Methyl (*tert*-butoxycarbonyl)-*L*-histidyl-*L*-tyrosinate (12l)

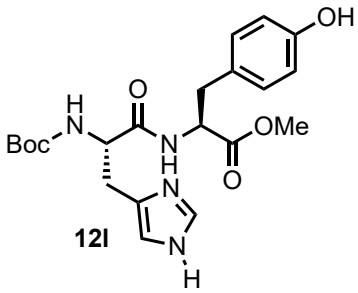

The general procedure was followed starting from *L*–H-Tyr–OMe•HCl (182 mg, 783 µmol). The crude material was purified on silica gel (2% MeOH/CH_2Cl_2) to afford **12l** as a white solid (276 mg, 81%). This compound has been previously reported.[ii] **R_f** = 0.24 (10% MeOH/DCM); **m.p.**= 93 – 95 °C; **^{1}H-NMR (300 MHz, $CDCl_3$)** δ 8.25 (s(br), 1H), 7.47 (s, 1H), 7.24 – 7.12 (m, 1H), 6.77 (d, *J* = 8.4 Hz, 2H), 6.73 – 6.57 (m, 3H), 5.96 (s(br), 1H), 4.81 – 4.63 (m, 1H), 4.38 (s(br), 1H), 3.67 (s, 3H), 3.07 – 2.82 (m, 4H), 1.38 (s, 9H); **IR (ATR)/$\bar{\nu}$ (cm^{-1}):** 3284, 2972, 1661, 1515, 1437, 1366, 1248, 1162, 1020, 828, 753; **HRMS (ESI)** calcd. for $[C_{21}H_{28}N_4O_6 + H]^+$: 433.2082, found 433.2094.

[ii] Le Roch, A.; Hébert, M.; Gagnon, A. Eur. *J. Org. Chem.* **2020**, *33*, 5363–5367

b. Procedure for synthesis of intermediate Boc–His(Trt)–Glu(OMe)–OMe (12g') ; Boc–His(Trt)–Thr–OMe (12h') and Boc–His(Trt)–Ser–OMe (12i')

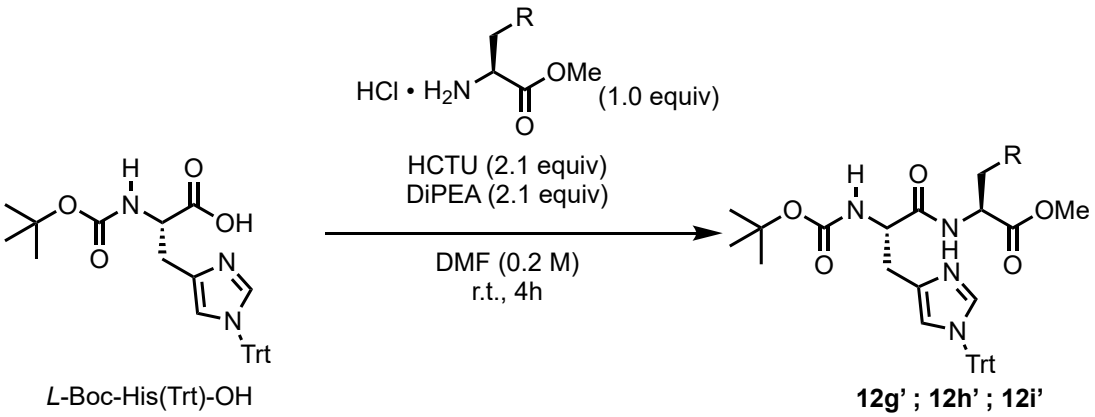

In a 50 mL flask, DIPEA (215 µL, 1.27 mmol, 2.1 equiv) was added to *L*–Boc–His(Trt)–OH (300 mg, 603 µmol, 1.0 equiv), *L*–H-A.A.–OMe•HCl (603 µmol, 1.0 equiv) and HCTU (524 mg, 1.27 mmol, 2.1 equiv) in DMF (3 mL, 0.2 M). The mixture was stirred for 4h at room temperature before being extracted twice with dichloromethane. The combined organic phases were successively washed with sat. aq. NaHCO3 (2x20 mL), brine (2x20 mL), dried over Na_2SO_4, filtered and concentrated under reduce pressure. The resulting crude product was purified by column chromatography using the indicated eluent system to afford the desired pure product (**12g'** ; **12h' and 12i'**).

Dimethyl N^{α}-(*tert*-butoxycarbonyl)-N^{τ}-trityl-*L*-histidyl-*L*-glutamate (12g')

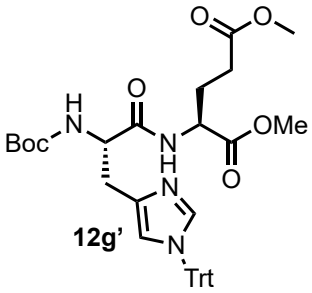

In a 50 mL flask, DIPEA (145 µL, 844 µmol, 2.1 equiv) was added to *L*–Boc–His(Trt)–OH (200 mg, 402 µmol, 1.0 equiv), *L*–Glu(OMe)–OMe•HCl (85 mg, 0.40 mmol, 1.0 equiv) and HCTU (349 mg, 844 µmol, 2.1 equiv) in DMF (2 mL, 0.2 M). The crude material was purified on silica gel (2% MeOH/CH_2Cl_2) to afford **12g'** as a white solid (207 mg, 79%). **R_f** = 0.33 (5% MeOH/DCM); **m.p.**= 68 – 70 °C; **^{1}H-NMR (300 MHz, $CDCl_3$)** δ 7.58 (d, *J* = 6.6 Hz, 1H), 7.34 (d, *J* = 1.2 Hz, 1H), 7.31 – 7.22 (m, 9H), 7.10 – 7.01 (m, 6H), 6.62 (s, 1H), 6.39 – 6.26 (m, 1H), 4.57 – 4.44 (m, 1H), 4.44 – 4.33 (m, 1H), 3.60 (s, 3H), 3.52 (s, 3H), 3.01 (A of ABX, *J* = 14.9, 4.6 Hz, 1H), 2.89 (B of ABX, *J* = 14.8, 6.1 Hz, 1H), 2.37 – 2.20 (m, 2H), 2.20 – 2.03 (m, 1H), 1.95 – 1.80 (m, 1H), 1.38 (s, 9H); **^{13}C-NMR**

(75 MHz, $CDCl_3$) δ 172.9, 171.8, 171.7, 155.6, 142.2, 138.4, 136.6, 129.7, 128.0, 128.0, 119.5, 79.6, 75.3, 54.4, 52.3, 51.6, 51.5, 30.0, 29.8, 28.3, 27.3; **IR (ATR)/$\bar{\nu}$ (cm^{-1}):** 3221, 2945, 1737, 1712, 1660, 1493, 1445, 1365, 1242, 1204, 1164, 1131, 1038, 1016, 1001, 871, 841, 748, 701, 659, 638; **HRMS (ESI)** calcd. for $[C_{37}H_{42}N_4O_7 + H]^+$: 655.3126, found 655.3128.

Methyl *N*$^{\alpha}$-(*tert*-butoxycarbonyl)-*N*$^{\tau}$-trityl-*L*-histidyl-*L*-allothreoninate (12h')

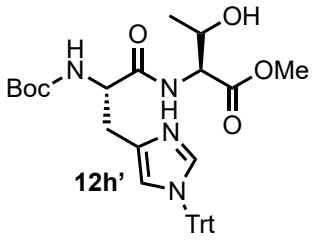

The general procedure was followed starting from *L*–H-Thr–OMe•HCl (102 mg, 603 µmol). The crude material was purified on silica gel (5% MeOH/CH_2Cl_2) to afford **12h'** as a white solid (225 mg, 61%). **R_f** = 0.55 (5% MeOH/DCM); **m.p.**= 105 – 107 °C; **^{1}H-NMR (300 MHz, $CDCl_3$)** δ 7.46 – 7.37 (m, 2H), 7.37 – 7.28 (m, 9H), 7.15 – 7.05 (m, 6H), 6.66 (d, *J* = 1.0 Hz, 1H), 5.83 (d, *J* = 5.5 Hz, 1H), 4.68 – 4.34 (m, 3H), 4.30 – 4.13 (m, 1H), 3.63 (s, 3H), 3.22 – 2.91 (m, 2H), 1.41 (s, 9H), 1.16 (d, *J* = 6.4 Hz, 3H) ; **^{13}C-NMR (75 MHz, $CDCl_3$)** δ 172.3, 171.3, 155.6, 142.2, 138.8, 136.2, 129.8, 128.3, 128.2, 120.2, 80.0, 75.6, 68.4, 58.2, 55.3, 52.4, 30.7, 28.4, 20.2 ; **IR (ATR)/$\bar{\nu}$ (cm^{-1}):** 3288, 2959, 1744, 1674, 1493, 1445, 1366, 1159, 1019, 1101, 841, 748, 701, 660, 638; **HRMS (ESI)** calcd. for $[C_{35}H_{40}N_4O_6 + H]^+$: 613.3021, found 613.3034.

Methyl *N*$^{\alpha}$-(*tert*-butoxycarbonyl)-*N*$^{\tau}$-trityl-*L*-histidyl-*L*-serinate (12i')

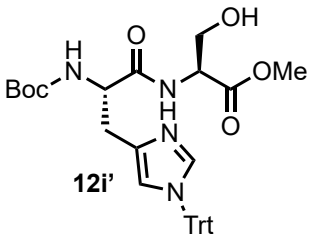

The general procedure was followed starting from *L*–H-Ser–OMe•HCl (94 mg, 0.60 mmol). The crude material was purified on silica gel (5% MeOH/CH_2Cl_2) to afford **12i'** as a white solid (221 mg, 61%). **R_f** = 0.47 (5% MeOH/DCM); **m.p.**= 93 – 95 °C; **^{1}H-NMR (300 MHz, $CDCl_3$)** δ 7.44 (s, 1H), 7.37 – 7.29 (m, 10H), 7.15 – 7.05 (m, 6H), 6.66 (s, 1H), 5.28 (s, 1H), 4.70 – 4.30 (m, 3H), 4.17 (A of ABX, *J* = 11.7, 3.4 Hz, 1H), 3.83 (B of ABX, *J* = 11.7, 3.7 Hz, 1H), 3.74 (s, 3H), 3.29 (A' of A'B'X', *J* = 15.0, 3.4 Hz, 1H), 2.92 (B' of A'B'X', *J* = 15.0, 6.3 Hz, 1H), 1.44 (s, 9H); **^{13}C-NMR (75 MHz, $CDCl_3$)** δ 171.7, 171.0, 155.4, 142.0, 139.2, 135.4, 129.8, 128.4, 128.3, 121.1, 80.4, 75.9, 61.6, 55.6, 53.6, 52.7, 30.2, 28.4; **IR (ATR)/$\bar{\nu}$ (cm^{-1}):** 3275, 2963, 2928, 1743, 1674, 1493, 1445, 1365, 1238, 1207, 1162, 1131, 1020, 1001, 841, 747, 700, 660, 638; **HRMS (ESI)** calcd. for $[C_{34}H_{38}N_4O_6 + H]^+$: 599.2864, found 599.2875.

c. Procedure for synthesis of Boc–His–Glu(OMe)–OMe (12g); Boc–His–Thr–OMe (12h) and Boc–His–Ser–OMe (12i)

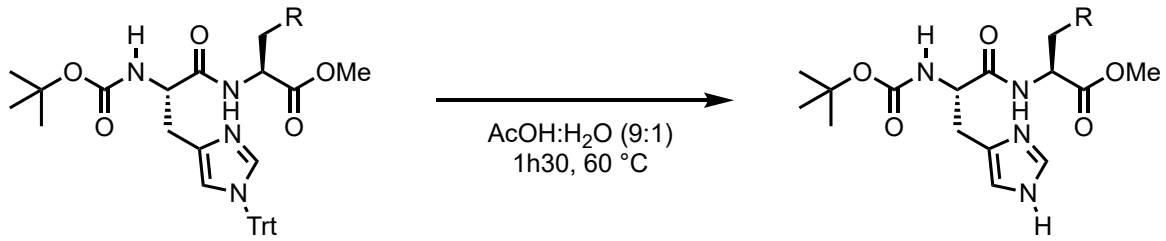

12g' ; 12h' ; 12i' **12g ; 12h ; 12i**

In a flask, *L*–Boc–His(Trt)–A.A–OMe in AcOH:H_2O (9:1, 0.35 M) was stirred for 1h30 at 60 °C. After cooling down at room temperature, the solvent was co-evaporated with cyclohexane under reduce pressure. The resulting crude product was purified by column chromatography using the indicated eluent system to afford the desired pure product (**12g** ; **12h and 12i**).

Dimethyl N^{α}-(*tert*-butoxycarbonyl)-*L*-histidyl-*L*-glutamate (12g)

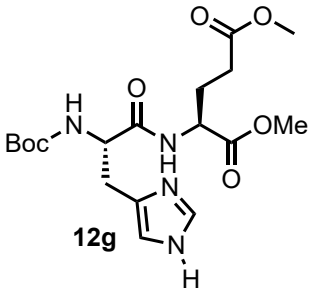

The general procedure was followed starting from *L*–Boc–His–Glu(OMe)–OMe **12g'** (130 mg, 200 µmol). The crude material was purified on silica gel (7% MeOH/CH_2Cl_2) to afford **12g** as a white solid (64 mg, 78%). **R_f** = 0.28 (10% MeOH/DCM); **m.p.**= 47 – 49 °C; **^{1}H-NMR (600 MHz, $CDCl_3$)** δ 10.50 (s, 1H), 7.67 (s(br), 1H), 7.63 (s, 1H), 6.82 (s, 1H), 6,00 (d, *J* = 5.6 Hz, 1H), 4.53 – 4.46 (m, 1H), 4.40 (s(br), 1H), 3.66 (s, 3H), 3.60 (s, 3H), 3.04 (s, 2H), 2.30 – 2.19 (m, 2H), 2.16 – 2.08 (m, 1H), 1.95 – 1.85 (m, 1H), 1.37 (s, 9H); **^{13}C-NMR (150 MHz, $CDCl_3$)** δ 173.2, 172.1, 172.0, 155.7, 135.1, 132.0, 118.5, 80.2, 54.4, 52.6, 51.8, 51.8, 29.8, 29.2, 28.3, 26.9; **IR (ATR)/$\bar{\nu}$ (cm^{-1}):** 3300, 2955, 1733, 1666, 1515, 1436, 1366, 1249, 1208, 1162, 1018, 985, 844, 755, 616; **HRMS (ESI)** calcd. for $[C_{18}H_{28}N_4O_7 + H]^+$: 413.2031, found 413.2048.

Methyl N^{α}-(*tert*-butoxycarbonyl)-*L*-histidyl-*L*-allothreoninate (12h)

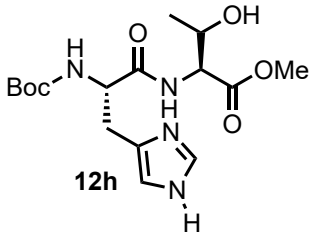

The general procedure was followed starting from *L*–Boc–His–Thr–OMe **12h'** (183 mg, 300 µmol). The crude material was purified on silica gel (7% MeOH/CH_2Cl_2) to afford **12h** as a white solid (89 mg, 81%). **R_f** = 0.19 (5% MeOH/DCM); **m.p.**= 90 – 92 °C; **^{1}H-NMR (300 MHz, $CDCl_3$)** δ 8.65 (s(br), 2H), 7.68 – 7.48 (m, 2H), 6.84 (s, 1H), 5.93 (d, *J* = 7.2 Hz, 1H), 4.56 – 4.37 (m, 2H), 4.32 – 4.19 (m, 1H), 3.63 (s, 3H), 3.04 (s(br), 2H), 1.36 (s, 9H), 1.14 (d, *J* = 6.1 Hz, 3H); **^{13}C-NMR (75 MHz, $CDCl_3$)** δ 172.6, 171.5, 155.7, 135.3, 131.6, 118.9, 80.2, 67.8, 58.4, 54.4, 52.5, 29.6, 28.3, 20.0; **IR (ATR)/$\bar{\nu}$ (cm^{-1}):** 3270, 2979, 1661, 1515, 1435, 1366, 1250, 1161, 1084, 1018, 846, 743; **HRMS (ESI)** calcd. for $[C_{16}H_{26}N_4O_6 + H]^+$: 371.1925, found 371.1927.

Methyl N^{α}-(*tert*-butoxycarbonyl)-*L*-histidyl-*L*-serinate (12i)

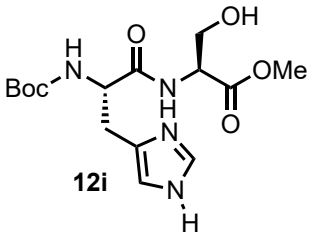

The general procedure was followed starting from *L*–Boc–His–Ser–OMe **12i'** (195 mg, 326 µmol). The crude material was purified on silica gel (7% MeOH/CH_2Cl_2) to afford **12i** as a white solid (86 mg, 74%). **m.p.**= 90 – 92 °C; **^{1}H-NMR (300 MHz, $CDCl_3$)** δ 8.16 (s(br), 2H), 7.72 (s(br), 1H), 7.57 (s, 1H), 6.83 (s, 1H), 5.88 – 5.75 (m, 1H), 4.57 (s(br), 1H), 4.47 – 4.30 (m, 1H), 3.90 (s(br), 2H), 3.67 (s, 3H), 3.12 – 2.95 (m, 2H), 1.36 (s, 9H); **^{13}C-NMR (75 MHz, $CDCl_3$)** δ 172.3, 171.1, 155.7, 135.5, 131.9, 118.5, 80.4, 62.0, 55.2, 54.4, 52.7, 29.7, 28.3; **IR (ATR)/$\bar{\nu}$ (cm^{-1}):** 3279, 2979, 1740, 1662, 1509, 1366, 1245, 1161, 1051, 1020, 847, 758; **HRMS (ESI)** calcd. for $[C_{15}H_{24}N_4O_6 + H]^+$: 357.1769, found 357.1769.

d. Procedure for synthesis Boc–Ala–His–OMe (14)

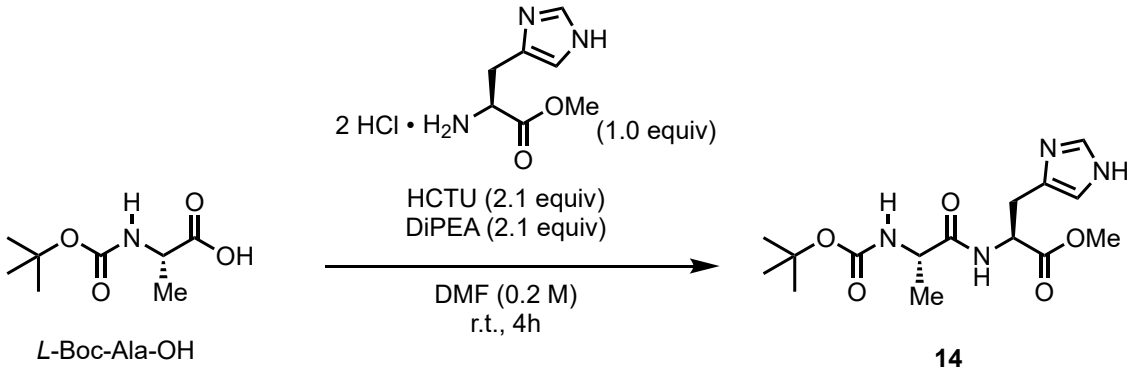

Methyl (*tert*-butoxycarbonyl)-*L*-alanyl-*L*-histidinate (14)

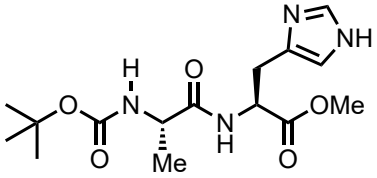

14

Manuscript, Scheme 3b) : In a 50 mL flask, DIPEA (190 µL, 1.11 mmol, 2.1 equiv) was added to *L*–Boc–Ala–OH (100 mg, 529 µmol, 1.0 equiv), *L*–H–His–OMe•2HCl (128 mg, 529 µmol, 1.0 equiv) and HCTU (459 mg, 1.11 mmol, 2.1 equiv) in DMF (2.6 mL, 0.2 M). The mixture was stirred for 4h at room temperature before being extracted twice with dichloromethane. The combined organic phases were successively washed with sat. aq. NaHCO3 (2x20 mL), brine (2x20 mL), dried over Na_2SO_4, filtered and concentrated under reduce pressure. The resulting crude product was purified on silica gel (5% MeOH/CH2Cl2) to afford **14** as a white solid (97mg, 54%). **Rf** = 0.26 (10% MeOH/DCM); **m.p.=** 145 – 147 °C; **^{1}H-NMR (300 MHz, $CDCl_3$)** δ 8.44 (s(br), 1H), 7.59 (d, *J* = 6.7 Hz, 1H), 7.50 (s, 1H), 6.74 (s, 1H), 5.59 (d, *J* = 6.4 Hz, 1H), 4.80 – 4.67 (m, 1H), 4.22 – 4.02 (m, 1H), 3.64 (s, 3H), 3.17 – 3.03 (m, 2H), 1.38 (s, 9H), 1.30 (d, *J* = 7.0 Hz, 3H); **^{13}C-NMR (75 MHz, $CDCl_3$)** δ 173.1, 171.5, 155.9, 135.4, 129.0, 119.3, 80.2, 52.8, 52.5, 50.5, 29.7, 28.3, 18.2; **IR (ATR)/$\bar{\nu}$ (cm^{-1}):** 3381, 3248, 2972, 1728, 1694, 1645, 1553, 1505, 1435, 1337, 1291, 1231, 1162, 1067, 1005, 947, 758, 620; **HRMS (ESI)** calcd. for $[C_{15}H_{24}N_4O_5 + H]^+$: 341.1820, found 341.1818.

e. Procedure for synthesis Boc–Ala–His(trt)–OMe (17)

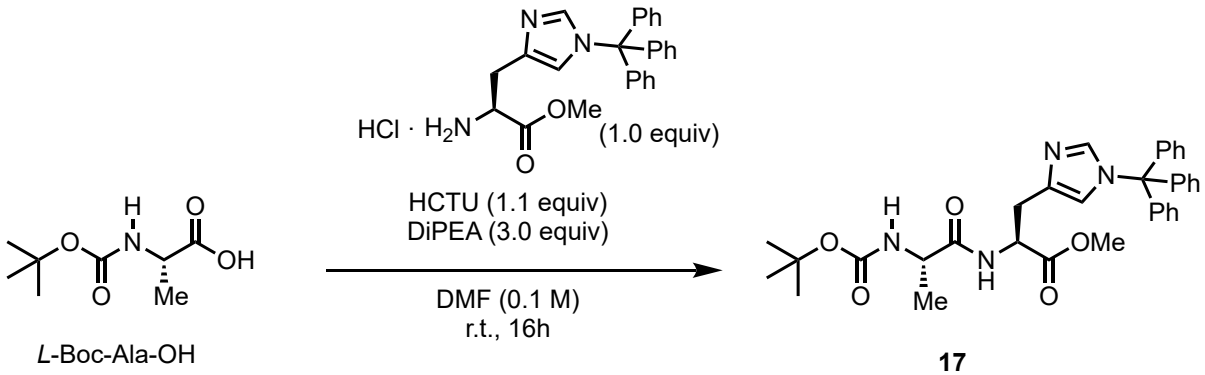

L-Boc-Ala-OH

17

Methyl N^{α}-((*tert*-butoxycarbonyl)-*L*-alanyl)-N^{τ}-trityl-*L*-histidinate (17)

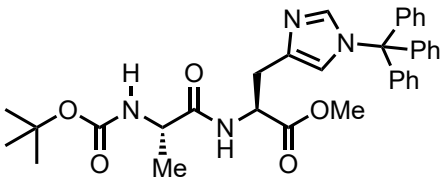

17

Manuscript, Scheme 4: In a 50 mL flask, DIPEA (570 µL, 3.35 mmol, 3.0 equiv) was added to *L*–Boc–Ala–OH (211 mg, 1.12 mmol, 1.0 equiv), *L*–H–His(trt)–OMe•HCl (500 mg, 1.12 mmol, 1.0 equiv) and HCTU (508 mg, 1.23 mmol, 1.1 equiv) in DMF (11 mL, 0.1 M). The mixture was stirred for 16h at room temperature before being extracted twice with ethyl acetate. The combined organic phases were successively washed with sat. aq. $NaHCO_3$ (2x30 mL), brine (2x30 mL), dried over Na_2SO_4, filtered and concentrated under reduce pressure. The resulting crude product was purified on silica gel (30% EtOAc/Hexane) to afford **17** as a white solid (606 mg, 93%). **R_f** = 0.42 (5% MeOH/DCM); **m.p.=** 74 – 76 °C; **^{1}H-NMR (300 MHz, $CDCl_3$)** δ 7.60 (d, *J* = 5.2, 1H), 7.37 (d, *J* = 1.1 Hz, 1H), 7.35 – 7.27 (m, 9H), 7.15 – 6.98 (m, 6H), 6.54 (s, 1H), 5.33 (s, 1H), 4.77 (dt, *J* = 8.0, 4.7 Hz, 1H), 4.29 – 4.13 (m, 1H), 3.58 (s, 3H), 3.09 – 2.97 (m, 2H), 1.39 (s, 9H), 1.34 (d, *J* = 7.0 Hz, 3H); **^{13}C-NMR (75 MHz, $CDCl_3$)** δ 172.4, 171.3, 155.0, 142.1, 138.5, 136.2, 129.6, 128.0, 119.5, 79.3, 75.2, 52.3, 52.0, 49.9, 29.6, 28.2, 18.9; **IR (ATR)/$\bar{\nu}$ (cm^{-1}):** 3284, 2977, 1744, 1711, 1673, 1492, 1445, 1365, 1243, 1163, 1133, 1033, 1001, 870, 848, 748, 700, 660, 638; **HRMS (ESI)** calcd. for $[C_{34}H_{38}N_4O_5 + H]^+$: 583.2915, found 583.2943.

7. Procedure for the preparation of aryl dipeptides

a. General procedure for synthesis of Boc–His(4-tolyl)–A.A.–OMe (13a–l)

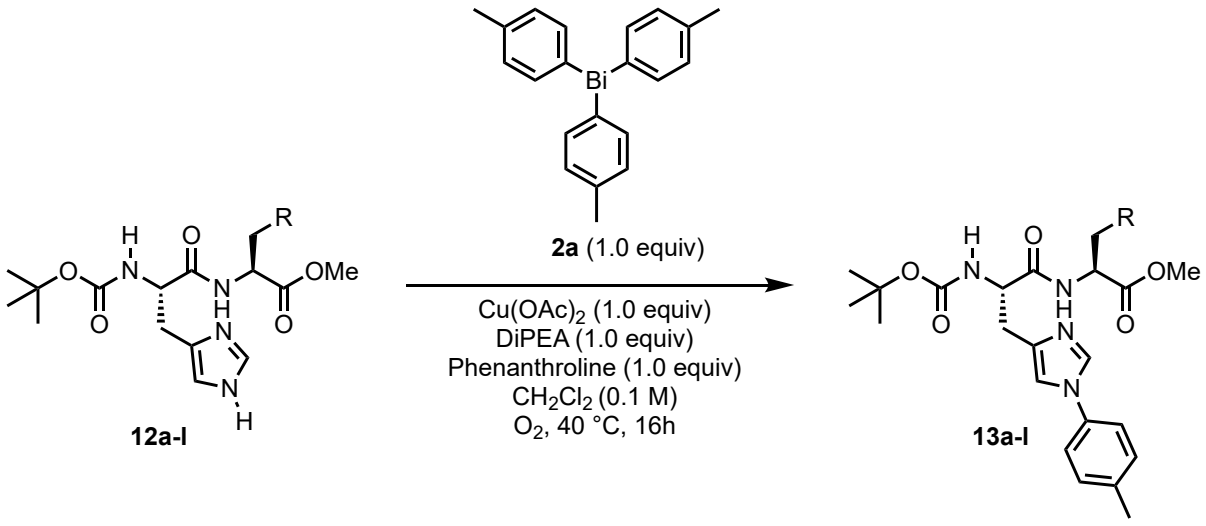

12a-l **13a-l**

Manuscript, Scheme 3a : In a sealed tube, *N*,*N*-diisopropylethylamine (20.5 µL, 0.12 mmol,

1.0 equiv) was added to the *N*-protected *L*-histidine *L*-amio acid methyl ester **12a–l** (0.12 mmol, 1.0 equiv), tri(4-tolyl)bismuthine **2a** (58 mg, 0.12 mmol, 1.0 equiv), copper(II) acetate (22 mg, 0.12 mmol, 1.0 equiv) and phenanthroline (22 mg, 0.12 mmol, 1.0 equiv) in CH_2Cl_2 (0.1 M). Oxygen was bubbled in the reaction mixture before stirred in an oil bath set at 40 °C for 16 hours. The solvent was evaporated under reduce pressure and the residue was purified on silica gel chromatography using the corresponding eluent system to afford desired pure product **13a**–**l**.

Methyl N^{α}-(*tert*-butoxycarbonyl)-N^{τ}-(*p*-tolyl)-*L*-histidyl-*L*-alaninate (13a)

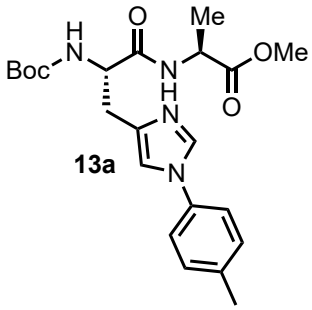

The general procedure was followed starting from Boc–(*L*)His–(*L*)Ala–OMe **12a** (41 mg, 0.12 mmol). The crude material was purified on silica gel (2% MeOH/CH_2Cl_2) to afford **13a** as a white solid (40 mg, 77%). $\mathbf{R_f}$ = 0.26 (5% MeOH/CH_2Cl_2) ; **m.p.**= 62 – 64 °C; **^{1}H-NMR (600 MHz, $CDCl_3$)** δ 7.80 (s, 1H), 7.51 (s(br), 1H), 7.24 – 7.19 (m, 4H), 7.08 (s, 1H), 6.21 (s, 1H), 4.55 – 4.43 (m, 2H), 3.66 (s, 3H), 3.19 – 3.10 (m, 1H), 3.01 (dd, *J* = 14.4, 4.9 Hz, 1H), 2.37 (s, 3H), 1.42 (s, 9H), 1.26 (d, *J* = 7.1 Hz, 3H); **^{13}C-NMR (150 MHz, $CDCl_3$)** δ 173.1, 171.3, 155.8, 138.6, 137.7, 134.9, 134.7, 130.5, 121.2, 116.5, 79.9, 54.5, 52.4, 48.1, 29.8, 28.4, 21.0, 18.2; **IR (ATR)/$\bar{\nu}$ (cm^{-1}):** 3310, 2922, 1744, 1683, 1653, 1520, 1453, 1366, 1244, 1207, 1163, 1149, 816; **HRMS (ESI)** calcd. for $[C_{22}H_{30}N_4O_5 + H]^+$: 431.2289, found 431.2308.

Methyl N^{α}-(*tert*-butoxycarbonyl)-N^{τ}-(*p*-tolyl)-*L*-histidyl-*L*-valinate (13b)

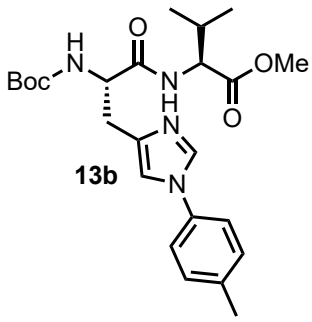

The general procedure was followed starting from Boc–(*L*)His–(*L*)Val–OMe **12b** (40 mg, 0.11 mmol), tri(4-tolyl)bismuthine **2a** (52 mg, 0.11 mmol), *N*,*N*-diisopropylethylamine (18.5 µL, 0.11 mmol), copper(II) acetate (20 mg, 0.11 mmol) and phenanthroline (20 mg, 0.11 mmol). The crude material was purified on silica gel (2% MeOH/CH_2Cl_2) to afford **13b** as a white solid (45 mg, 91%). $\mathbf{R_f}$ = 0.38 (5% MeOH/CH_2Cl_2); **m.p.**= 55 – 57 °C; **^{1}H-NMR (300 MHz, $CDCl_3$)** δ 7.75 (s, 1H), 7.35 (s(br), 1H), 7.25 – 7.14 (m, 4H), 7.06 (s, 1H), 6.47 (d, *J* = 4.2 Hz, 1H), 4.48 (s(br), 1H), 4.45 – 4.35 (m, 1H),

3.64 (s, 3H), 3.26 – 3.11 (m, 1H), 3.06 – 2.91 (m, 1H), 2.36 (s, 3H), 2.10 – 1.94 (m, 1H), 1.44 (s, 9H), 0.73 (d, *J* = 6.6 Hz, 6H); **^{13}C-NMR (75 MHz, $CDCl_3$)** δ 171.0, 170.6, 154.8, 137.9, 136.6, 133.9, 133.7, 129.5, 120.2, 115.6, 79.0, 56.3, 51.1, 30.2, 28.8, 27.4, 20.0, 17.8, 16.6; **IR (ATR)/$\bar{\nu}$ (cm^{-1}):** 3297, 2963, 2923, 1739, 1667, 1519, 1487, 1435, 1366, 1248, 1205, 1163, 1019, 845, 816, 624; **HRMS (ESI)** calcd. for $[C_{24}H_{34}N_4O_5 + H]^+$: 459.2602, found 459.2611.

Methyl *N*$^{\alpha}$-(*tert*-butoxycarbonyl)-*N*$^{\tau}$-(*p*-tolyl)-*L*-histidyl-*L*-phenylalaninate (13c)

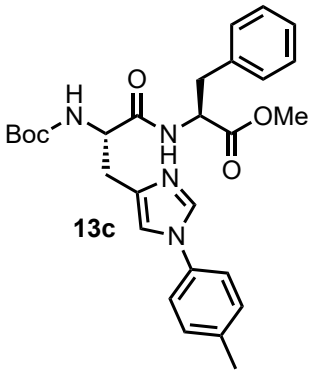

The general procedure was followed starting from Boc–(*L*)His–(*L*)Phe–OMe **12c** (50 mg, 0.12 mmol). The crude material was purified on silica gel (2% MeOH/CH_2Cl_2) to afford **13c** as a yellow solid (54 mg, 89%); **R_f** = 0.44 (5% MeOH/CH_2Cl_2) ; **m.p.**= 66 – 68 °C; **^{1}H-NMR (600 MHz, $CDCl_3$)** δ 7.88 (s, 1H), 7.60 (s, 1H), 7.31 (s, 1H), 7.26 – 7.17 (m, 5H), 7.14 (s(br), 1H), 7.06 – 7.00 (m, 2H), 6.28 (s, 1H), 4.82 (s, 1H), 4.66 – 4.37 (m, 2H), 3.65 (s, 3H), 3.18 (s(br), 1H), 3.13 – 3.00 (m, 3H), 2.41 (s, 3H), 1.44 (s, 9H); **^{13}C-NMR (150 MHz, $CDCl_3$)** δ 171.6, 171.4, 155.7, 138.4, 137.8, 136.1, 134.7, 134.6, 130.5, 129.3, 128.5, 126.9, 121.3, 116.5, 79.9, 54.5, 53.5, 52.1, 38.0, 29.7, 28.3, 21.0; **IR (ATR)/$\bar{\nu}$ (cm^{-1}):** 3288, 2922, 1741, 1682, 1647, 1520, 1495, 1455, 1365, 1247, 1214, 1165, 1047, 1020, 816, 670; **HRMS (ESI)** calcd. for $[C_{28}H_{34}N_4O_5 + H]^+$: 507.2602, found 507.2611.

Methyl *N*$^{\alpha}$-(*tert*-butoxycarbonyl)-*N*$^{\tau}$-(*p*-tolyl)-*L*-histidyl-*L*-prolinate (13d)

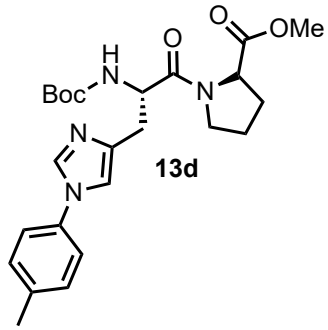

The general procedure was followed starting from Boc–(*L*)His–(*L*)Pro–OMe **12d** (44 mg, 0.12 mmol). The crude material was purified on silica gel (2% MeOH/CH_2Cl_2) to afford **13d** as a yellow solid (53 mg, 97%). **R_f** = 0.37 (5% MeOH/CH_2Cl_2); **m.p.**= 68 – 70 °C; ***presence of conformers :*** **^{1}H-NMR (600 MHz, $CDCl_3$)** δ 7.85 (s, 1H), 7.31 – 7.26 (m, 2H), 7.24 – 7.18 (m, 3H), 5.60 – 5.44 (m, 1H), 4.80 – 4.67 (m, 1H), 4.48 (d, *J* = 4.6 Hz, 1H), 3.78 – 3.70 (m, 1H), 3.65 (s, 3H), 3.58 – 3.51 (m, 1H), 3.14 – 3.03 (m, 1H), 2.99 – 2.87 (m, 1H), 2.35 (s, 3H), 2.20 – 2.10 (m, 1H), 1.93 (s, 3H), 1.35 (s, 9H); **^{13}C-NMR (150 MHz, $CDCl_3$)** δ 172.6, 170.8, 155.5, 137.4, 134.9, 130.5, 130.4, 126.9, 121.1, 117.0, 79.6, 58.9, 54.3, 52.2, 47.0, 42.5, 29.1, 28.3, 25.0, 21.0; **IR (ATR)/$\bar{\nu}$ (cm^{-1}):** 3275, 2968,

1741, 1704, 1643, 1520, 1488, 1435, 1365, 1163, 1018, 843, 817; **HRMS (ESI)** calcd. for $[C_{24}H_{32}N_4O_5 + H]^+$: 457.2446, found 457.2467.

Methyl N^{α}-(*tert*-butoxycarbonyl)-N^{τ}-(*p*-tolyl)-*L*-histidylglycinate (13e)

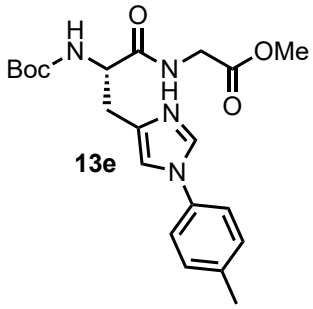

The general procedure was followed starting from Boc–(*L*)His–Gly–OMe **12e** (39 mg, 0.12 mmol). The crude material was purified on silica gel (2% MeOH/CH_2Cl_2) to afford **13e** as a white solid (27 mg, 54%). **R_f** = 0.23 (5% MeOH/CH_2Cl_2); **m.p.**= 52 – 54 °C; **^{1}H-NMR (600 MHz, $CDCl_3$)** δ 7.79 (s(br), 1H), 7.54 (s(br), 1H), 7.24 (s, 4H), 7.10 (s(br), 1H), 6.27 (s, 1H), 4.52 (s(br), 1H), 4.07 – 3.92 (m, 2H), 3.67 (s, 3H), 3.19 (s(br), 1H), 3.04 (s(br), 1H), 2.38 (s, 3H), 1.44 (s, 9H); **^{13}C-NMR (150 MHz, $CDCl_3$)** δ 172.2, 170.2, 155.9, 137.6, 134.9, 130.5, 121.4, 116.5, 80.1, 54.6, 52.3, 41.3, 29.8, 28.5, 21.1; **IR (ATR)/$\bar{\nu}$ (cm^{-1}):** 3292, 2972, 2923, 1748, 1668, 1519, 1487, 1365, 1246, 1204, 1163, 1020, 815; **HRMS (ESI)** calcd. for $[C_{21}H_{28}N_4O_5 + H]^+$: 417.2133, found 417.2120.

Methyl N^{α}-(*tert*-butoxycarbonyl)-N^{τ}-(*p*-tolyl)-*L*-histidyl-*L*-methioninate (13f)

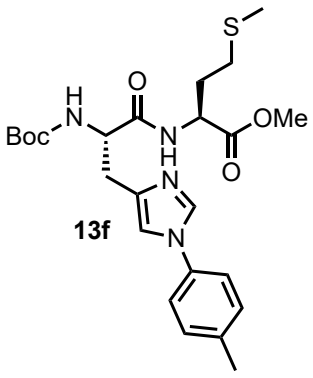

The general procedure was followed starting from Boc–(*L*)His–(*L*)Met–OMe **12f** (48 mg, 0.12 mmol). The crude material was purified on silica gel (2% MeOH/CH_2Cl_2) to afford **13f** as a white solid (30 mg, 51%). **R_f** = 0.38 (5% MeOH/CH_2Cl_2); **m.p.**= 53 – 55 °C ; **^{1}H-NMR (300 MHz, $CDCl_3$)** δ 7.81 (s, 1H), 7.53 (s(br), 1H), 7.24 (s, 4H), 7.09 (s, 1H), 6.36 (s(br), 1H), 4.66 – 4.57 (m, 1H), 4.49 (s(br), 1H), 3.67 (s, 3H), 3.24 – 3.16 (m, 1H), 3.00 (dd, *J* = 14.4, 5.2 Hz, 1H), 2.38 (s, 3H), 2.34 – 2.23 (m, 2H), 2.11 – 2.01 (m, 1H), 1.96 (s, 3H), 1.93 – 1.83 (m, 1H), 1.45 (s, 9H); **^{13}C-NMR (150 MHz, $CDCl_3$)** δ 172.1, 171.6, 155.8, 138.6, 137.8, 134.9, 134.7, 130.5, 121.3, 116.6, 80.1, 54.6, 52.5, 51.6, 31.7, 29.8, 29.7, 28.4, 21.1, 15.4; **IR (ATR)/$\bar{\nu}$ (cm^{-1}):** 3296, 2920, 1740, 1667, 1520, 1367, 1164, 1023, 847, 817; **HRMS (ESI)** calcd. for $[C_{24}H_{34}N_4O_5S + H]^+$: 491.2323, found 491.2341.

Dimethyl N^{α}-(*tert*-butoxycarbonyl)-N^{τ}-(*p*-tolyl)-*L*-histidyl-*L*-glutamate (13g)

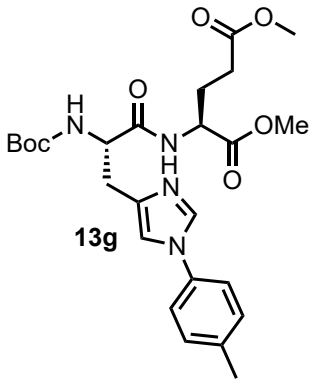

The general procedure was followed starting from Boc–(*L*)His–(*L*)Glu(OMe)–Ome **12g** (64 mg, 0.16 mmol), tri(4-tolyl)bismuthine **2a** (75 mg, 0.16 mmol), *N*,*N*-diisopropylethylamine (26.5 µL, 0.16 mmol), copper(II) acetate (28 mg, 0.16 mmol) and phenanthroline (28 mg, 0.16 mmol). The crude material was purified on silica gel (2% MeOH/CH_2Cl_2) to afford **13g** as a white solid (24 mg, 31%). $\mathbf{R_f}$ = 0.57 (10% MeOH/CH_2Cl_2); **m.p.**= 46 – 48 °C; **^{1}H-NMR (300 MHz, $CDCl_3$)** δ 7.84 (s, 1H), 7.46 (s(br), 1H), 7.24 (s, 4H), 7.10 (s, 1H), 6.33 (s(br), 1H), 4.60 – 4.43 (m, 2H), 3.67 (s, 3H), 3.53 (s, 3H), 3.25 – 3.11 (m, 1H), 3.06 – 2.95 (m, 1H), 2.38 (s, 3H), 2.24 – 2.04 (m, 3H), 1.96 – 1.80 (m, 1H), 1.44 (s, 9H); **^{13}C-NMR (150 MHz, $CDCl_3$)** δ 177.9, 173.1, 172.0, 171.7, 155.8, 138.0, 134.8, 134.6, 130.6, 121.4, 116.8, 80.1, 54.6, 52.5, 51.7, 51.7, 29.8, 29.8, 28.4, 27.4, 21.1; **IR (ATR)/$\bar{\nu}$ (cm^{-1}):** 3333, 2953, 1708, 1520, 1437, 1367, 1249, 1207, 1166, 1022, 848, 819; **HRMS (ESI)** calcd. for $[C_{25}H_{34}N_4O_7 + H]^+$: 503.2500, found 503.2511.

Methyl N^{α}-(*tert*-butoxycarbonyl)-N^{τ}-(*p*-tolyl)-*L*-histidyl-*L*-allothreoninate (13h)

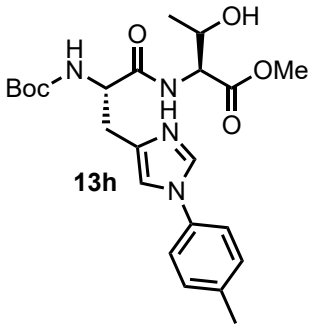

The general procedure was followed starting from Boc–(*L*)His–(*L*)Thr–OMe **12h** (44 mg, 0.12 mmol). The crude material was purified on silica gel (2% MeOH/CH_2Cl_2) to afford **13h** as a white solid (17 mg, 31%). $\mathbf{R_f}$ = 0.35 (5% MeOH/CH_2Cl_2); **m.p.**= 82 – 84 °C ; **^{1}H-NMR (300 MHz, $CDCl_3$)** δ 7.82 (s, 1H), 7.51 – 7.37 (m, 1H), 7.24 (s, 4H), 7.10 (s, 1H), 6.05 (s(br), 1H), 4.64 – 4.46 (m, 2H), 4.28 – 4.15 (m, 1H), 3.69 (s, 3H), 3.21 (A of ABX, *J* = 14.7, 5.0 Hz, 1H), 3.04 (B of ABX, *J* = 14.8, 5.9 Hz, 1H), 2.38 (s, 3H), 1.43 (s, 9H), 1.09 (d, *J* = 6.4 Hz, 3H); **^{13}C-NMR (75 MHz, $CDCl_3$)** δ 172.2, 171.2, 155.7, 137.9, 135.3, 135.2, 134.6, 130.5, 121.3, 117.0, 80.2, 68.5, 58.0, 54.6, 52.5, 30.5, 28.4, 21.1, 19.9; **IR (ATR)/$\bar{\nu}$ (cm^{-1}):** 3301, 2972, 2919, 1689, 1646, 1520, 1435, 1366, 1252, 1164, 1015, 845, 814, 747; **HRMS (ESI)** calcd. for $[C_{23}H_{32}N_4O_6 + H]^+$: 461.2395, found 461.2416.

Methyl N^{α}-(*tert*-butoxycarbonyl)-N^{τ}-(*p*-tolyl)-*L*-histidyl-*L*-serinate (13i)

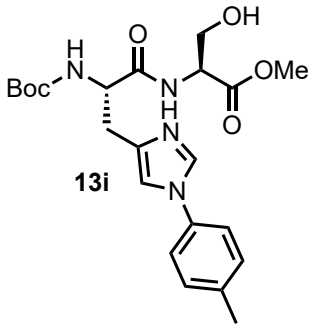

The general procedure was followed starting from Boc–(*L*)His–(*L*)Ser–OMe **12i** (43 mg, 0.12 mmol). The crude material was purified on silica gel (2% MeOH/CH_2Cl_2) to afford **13i** as a white solid (15 mg, 28%). $\mathbf{R_f}$ = 0.26 (10% MeOH/CH_2Cl_2); **m.p.**= 65 – 67 °C ; **^{1}H-NMR (300 MHz, $CDCl_3$)** δ 7.88 (s, 1H), 7.47 (s, 1H), 7.25 (s, 4H), 7.13 (s, 1H), 5.59 (s, 1H), 4.66 – 4.42 (m, 2H), 4.13 (A of ABX, *J* = 11.7, 3.3 Hz, 1H), 3.85 (B of ABX, *J* = 11.6, 3.8 Hz, 1H), 3.75 (s, 3H), 3.43 – 3.28 (m, 1H), 3.01 (dd, *J* = 14.5, 5.7 Hz, 1H), 2.39 (s, 3H), 1.44 (s, 9H); **^{13}C-NMR (150 MHz, $CDCl_3$)** δ 171.6, 170.9, 155.5, 138.1, 137.0, 135.6, 134.5, 130.6, 121.5, 117.6, 80.4, 62.0, 55.6, 54.0, 52.6, 29.8, 28.4, 21.1; **IR (ATR)/$\bar{\nu}$ (cm^{-1}):** 3297, 2932, 1741, 1667, 1520, 1367, 1247, 1164, 1073, 1023, 817; **HRMS (ESI)** calcd. for $[C_{22}H_{30}N_4O_6 + H]^+$: 447.2238, found 447.2246.

Methyl N^6-(((9*H*-fluoren-9-yl)methoxy)carbonyl)-N^2-(N^{α}-(*tert*-butoxycarbonyl)-N^{τ}-(*p*-tolyl)-*L*-histidyl)-*L*-lysinate (13j)

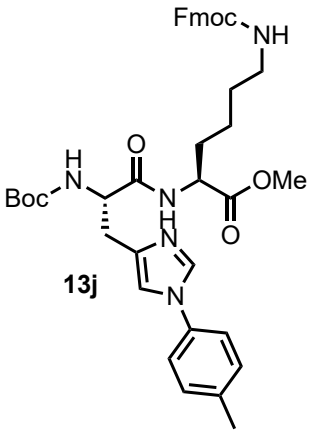

The general procedure was followed starting from Boc–(*L*)His–(*L*)Lys(Fmoc)–OMe **12j** (60 mg, 0.97 mmol), tri(4-tolyl)bismuthine **2a** (47 mg, 0.97 mmol), *N*,*N*-diisopropylethylamine (16.5 µL, 0.97 mmol), copper(II) acetate (18 mg, 0.97 mmol) and phenanthroline (18 mg, 0.97 mmol). The crude material was purified on silica gel (% MeOH/CH_2Cl_2) to afford **13j** as a white solid (32 mg, 47%). $\mathbf{R_f}$ = 0.24 (5% MeOH/CH_2Cl_2); **^{1}H-NMR (300 MHz, $CDCl_3$)** δ 8.35 (s, 1H), 8.25 – 8.13 (m, 1H), 7.75 (d, *J* = 7.4 Hz, 2H), 7.61 (d, *J* = 7.1 Hz, 2H), 7.45 – 7.25 (m, 8H), 7.17 (s, 1H), 6.05 – 5.89 (m, 1H), 5.23 – 5.08 (m, 1H), 4.73 (s, 1H), 4.49 – 4.39 (m, 1H), 4.35 (d, *J* = 7.1 Hz, 2H), 4.21 (t, *J* = 6.8 Hz, 1H), 3.68 (s, 3H), 3.59 – 3.44 (m, 1H), 3.29 – 3.14 (m, 2H), 3.07 – 2.91 (m, 1H), 2.43 (s, 3H), 1.94 – 1.71 (m, 2H), 1.63 – 1.37 (m, 4H), 1.32 (s, 9H); **IR (ATR)/$\bar{\nu}$ (cm^{-1}):** 3321, 2922, 2852, 1720, 1688, 1650, 1520, 1450, 1256, 1167, 1019, 814, 758, 730; **HRMS (ESI)** calcd. for $[C_{40}H_{47}N_5O_7 + H]^+$: 710.3548, found 710.3569.

Methyl N^{α}-(*tert*-butoxycarbonyl)-N^{τ}-(*p*-tolyl)-*L*-histidyl-*L*-tryptophanate (13k)

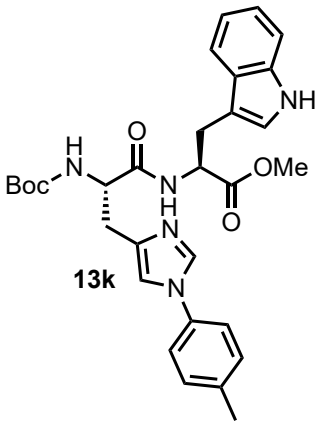

The general procedure was followed starting from Boc–(*L*)His–(*L*)Trp–OMe **12k** (55 mg, 0.12 mmol). The crude material was purified on silica gel (2% MeOH/CH_2Cl_2) to afford **13k** as a white solid (45 mg, 68%). **R_f** = 0.24 (5% MeOH/CH_2Cl_2); **m.p.**= 96 – 98 °C; **^{1}H-NMR (300 MHz, $CDCl_3$)** δ 8.18 (s, 1H), 7.61 (s, 1H), 7.45 (d, *J* = 7.8 Hz, 2H), 7.29 (d, *J* = 8.0 Hz, 1H), 7.23 – 7,15 (m, 2H), 7.15 – 7.08 (m, 3H), 7.08 – 7.02 (m, 2H), 6.95 (s, 1H), 6.12 (s(br), 1H), 4.84 (dd, *J* = 12.7, 5.7 Hz, 1H), 4.52 (s(br), 1H), 3.57 (s, 3H), 3.27 (dd, *J* = 14.7, 5.5 Hz, 1H), 3.16 (dd, *J* = 14.7, 5.0 Hz, 2H), 3.01 (dd, *J* = 14.5, 5.9 Hz, 1H), 2.37 (s, 3H), 1.39 (s, 9H); **^{13}C-NMR (150 MHz, $CDCl_3$)** δ 172.1, 171.5, 155.8, 139.0, 137.7, 136.2, 134.7, 130.5, 127.2, 123.1, 122.2, 121.3, 119.7, 118.8, 116.5, 111.3, 80.0, 54.8, 53.0, 52.3, 30.6, 28.4, 27.9, 21.1; **IR (ATR)/$\bar{\nu}$ (cm^{-1}):** 3299, 2928, 1663, 1519, 1437, 1367, 1249, 1163, 1022, 846, 743; **HRMS (ESI)** calcd. for $[C_{30}H_{35}N_5O_5 + H]^+$: 546.2711, found 546.2709.

Methyl (*S*)-2-((*S*)-2-((*tert*-butoxycarbonyl)amino)-3-(1-(*p*-tolyl)-1*H*-imidazol-4-yl)propanamido)-3-(4-(*p*-tolyloxy)phenyl)propanoate (13l)

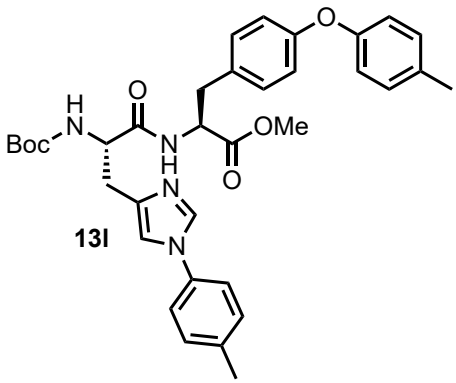

The general procedure was followed starting from Boc–(*L*)His–(*L*)Tyr–OMe **12l** (52 mg, 0.12 mmol). The crude material was purified on silica gel (2% MeOH/CH_2Cl_2) to afford **13l** as a yellow solid (24 mg, 33%). **R_f** = 0.33 (5% MeOH/CH_2Cl_2); **m.p.**= 60 – 62 °C; **^{1}H-NMR (600 MHz, $CDCl_3$)** δ 7.64 (s(br), 1H), 7.45 (s(br), 1H), 7.14 – 7.06 (m, 4H), 7.01 (d, *J* = 8.2 Hz, 3H), 6.82 (s(br), 2H), 6.76 (d, *J* = 8.4 Hz, 2H), 6.70 (d, *J* = 7.4 Hz, 2H), 6.20 (s(br), 1H), 4.67 (s(br), 1H), 4.39 (s(br), 1H), 3.53 (s, 3H), 3.07 (s(br), 1H), 2.90 (s(br), 3H), 2.27 (s, 3H), 2.22 (s, 3H), 1.33 (s, 9H); **^{13}C-NMR (150 MHz, $CDCl_3$)** δ 171.7, 156.9, 155.8, 154.7, 137.7, 134.8, 133.0, 130.5, 130.3, 121.3, 119.2, 119.2, 118.4, 116.4, 80.0, 53.7, 52.3, 38.7, 37.4, 28.4, 21.1, 20.8, 14.2; **IR (ATR)/$\bar{\nu}$ (cm^{-1}):** 3279, 2977, 1741, 1705, 1640, 1500, 1436, 1365, 1238, 1163, 1045, 1017, 843, 750; **HRMS (ESI)** calcd. for $[C_{35}H_{40}N_4O_6 + H]^+$: 613.3021, found 613.3037.

b. Procedure for synthesis of Boc–Ala–His(4-tolyl)–OMe (15) and Boc-N(4-tolyl)-Ala–His(4-tolyl)–OMe (16)

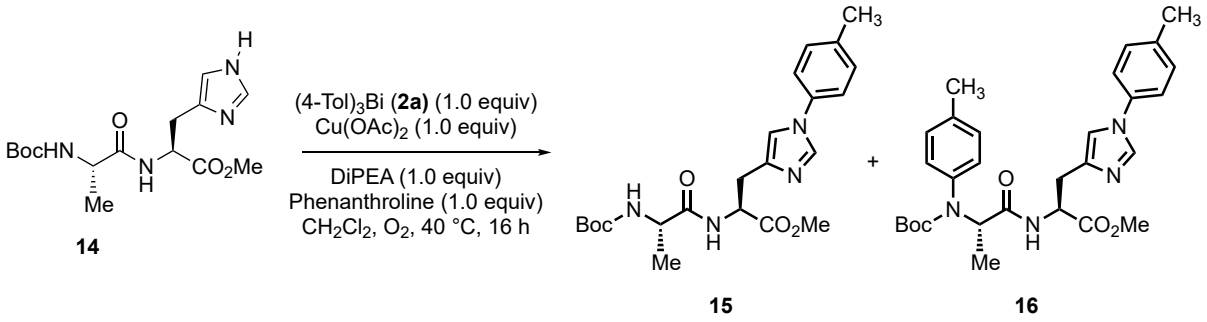

Manuscript, Scheme 3b): In a sealed tube, *N*,*N*-diisopropylethylamine (25.0 µL, 0.15 mmol, 1.0 equiv) was added to the methyl (*tert*-butoxycarbonyl)-*L*-alanyl-*L*-histidinate **14** (50 mg, 0.15 mmol, 1.0 equiv), tri(4-tolyl)bismuthine **2a** (71 mg, 0.15 mmol, 1.0 equiv), copper(II) acetate (27 mg, 0.15 mmol, 1.0 equiv) and phenanthroline (27 mg, 0,15 mmol, 1.0 equiv) in CH_2Cl_2 (1.50 mL, 0.1 M). Oxygen was bubbled in the reaction mixture before stirred in an oil bath set at 40 °C for 16 hours. The solvent was evaporated under reduce pressure and the residue was purified on silica gel chromatography using 2% MeOH/CH_2Cl_2 to afford **15** and **16** reported below.

Methyl N^{α}-((*tert*-butoxycarbonyl)-*L*-alanyl)-N^{τ}-(*p*-tolyl)-*L*-histidinate (15)

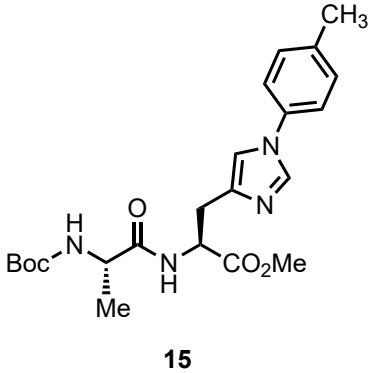

15

Yellow solid (30 mg, 47%). **R_f** = 0.54 (10% MeOH/CH_2Cl_2); **m.p.**= 54 – 56 °C; **^{1}H-NMR (300 MHz, $CDCl_3$)** δ 7.74 (s, 1H), 7.52 (s(br), 1H), 7.24 (s, 4H), 7.08 (s, 1H), 5.26 (s, 1H), 4.90 – 4.76 (m, 1H), 4.30 – 4.14 (m, 1H), 3.70 (s, 3H), 3.25 – 3.04 (m, 2H), 2.38 (s, 3H), 1.41 (s, 9H), 1.37 (d, *J* = 7.0 Hz, 3H); ***presence of conformers***: **^{13}C-NMR (150 MHz, $CDCl_3$)** δ 172.8, 171.7, 155.5, 137.8, 135.2, 134.7, 130.5, 121.4, 116.6, 79.9, 55.3, 52.5, 52.4, 50.3, 43.3, 29.6, 28.4, 21.1, 18.9, 12.5; **IR (ATR)/$\bar{\nu}$ (cm^{-1}):** 3292, 2977, 2923, 1742, 1668, 1519, 1489, 1439, 1365, 1247, 1213, 1163, 1068, 1020, 842, 817, 754; **HRMS (ESI)** calcd. for $[C_{22}H_{30}N_4O_5 + H]^+$: 431.2289, found 431.2290.

Methyl N^{α}-(*N*-(tert-butoxycarbonyl)-*N*-(*p*-tolyl)-*L*-alanyl)-N^{τ}-(*p*-tolyl)-*L*-histidinate (16)

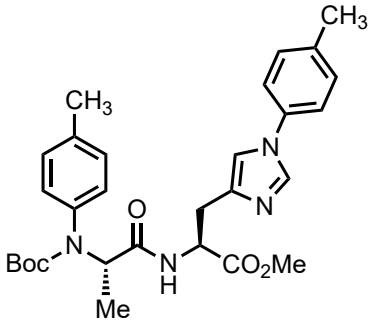

16

Yellow solid (13 mg, 17%). $\mathbf{R_f}$ = 0.62 (10% MeOH/CH_2Cl_2); **m.p.**= 60 – 62 °C; **^{1}H-NMR (300 MHz, $CDCl_3$)** δ 7.85 (s(br), 1H), 7.73 (s, 1H), 7.25 – 7.14 (m, 4H), 7.14 – 7.00 (m, 5H), 4.89 – 4.78 (m, 1H), 4.72 – 4.61 (m, 1H), 3.74 (s, 3H), 3.21 – 3.14 (m, 2H), 2.38 (s, 3H), 2.29 (s, 3H), 1.33 (s, 9H), 1.28 (d, *J* = 7.2 Hz, 3H); **IR (ATR)/$\bar{\nu}$ (cm^{-1}):** 3346, 2977, 2923, 1743, 1681, 1515, 1367, 1251, 1210, 1162, 1022, 843; **HRMS (ESI)** calcd. for [$C_{29}H_{36}N_4O_5$ + H]$^+$: 521.2759, found 521.2781.

c. General procedure for synthesis of Boc–*N*(Aryl)–Ala–His(trt)–OMe (18a–c)

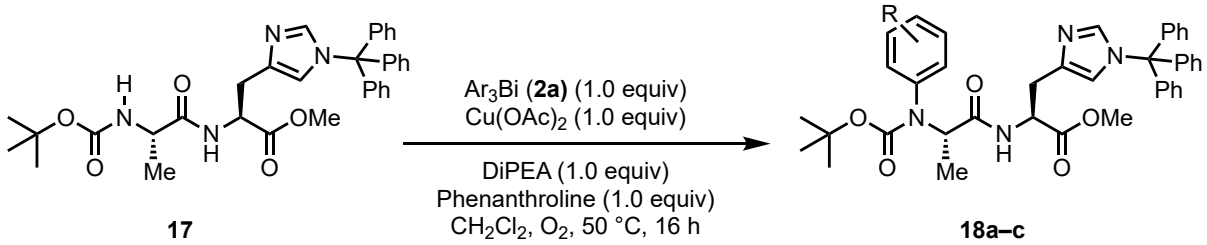

17 **18a–c**

Manuscript, Scheme 4: In a sealed tube, *N*,*N*-diisopropylethylamine (17.5 µL, 0.10 mmol, 1.0 equiv) was added to the methyl N^{α}-((*tert*-butoxycarbonyl)-*L*-alanyl)-N^{τ}-trityl-*L*-histidinate **17** (60 mg, 0.10 mmol, 1.0 equiv), triarylbismuthine (0.10 mmol, 1.0 equiv), copper(II) acetate (19 mg, 0.10 mmol, 1.0 equiv) and phenanthroline (19 mg, 0.10 mmol, 1.0 equiv) in CH_2Cl_2 (1.00 mL, 0.1 M). Oxygen was bubbled in the reaction mixture before stirred in an oil bath set at 50 °C for 16 hours. The solvent was evaporated under reduce pressure and the residue was purified on silica gel chromatography using the corresponding eluent system to afford the desired pure product **18a–c**.

Methyl N^{α}-(*N*-(*tert*-butoxycarbonyl)-*N*-(*p*-tolyl)-*L*-alanyl)-N^{τ}-trityl-*L*-histidinate (18a)

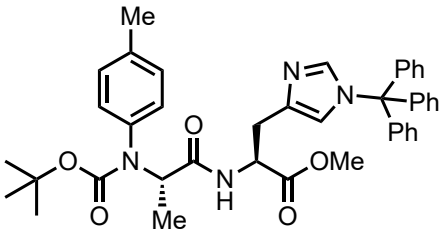

18a

The general procedure was followed starting from tri(4-tolyl)bismuthine **2a** (50 mg, 0.10 mmol). The crude material was purified on silica gel (2% MeOH/CH_2Cl_2) to afford **18a** as a white solid (58 mg, 84%). $\mathbf{R_f}$ = 0.47 (5% MeOH/CH_2Cl_2); **m.p.**= 64 – 66 °C; **^{1}H-NMR (300 MHz, $CDCl_3$)** δ 8.07 (s, 1H), 7.38 – 7.28 (m, 10H), 7.17 (d, *J* = 8.1 Hz, 2H), 7.12 – 7.00 (m, 8H), 6.58 (s, 1H), 4.85 – 4.75 (m, 1H), 4.67 – 4.57 (m, 1H), 3.60 (s, 3H), 3.12 (A of ABX, *J* = 14.6, 5.1 Hz, 1H), 3.00 (B of ABX, *J* = 14.6, 4.8 Hz, 1H), 2.29 (s, 3H), 1.36 (s, 9H), 1.30 (d, *J* = 7.1 Hz, 3H) ; **^{13}C-NMR (150 MHz, $CDCl_3$)** δ 172.3, 171.9, 154.9, 142.3, 138.7, 137.9, 136.4, 129.8, 129.3, 128.4, 128.1, 119.6, 80.8, 75.4, 52.9, 52.1, 38.7, 29.8, 28.4, 21.1, 15.8; **IR (ATR)/$\bar{\nu}$ (cm^{-1}):** 3288, 2972, 2928, 1746, 1687, 1514, 1494, 1445, 1366, 1323, 1159, 1132, 748, 701, 660, 637; **HRMS (ESI)** calcd. for $[C_{41}H_{44}N_4O_5 + H]^+$: 673.3385, found 673.3418.

Methyl N^{α}-(*N*-(*tert*-butoxycarbonyl)-*N*-(4-methoxyphenyl)-*L*-alanyl)-N^{τ}-trityl-*L*-histidinate (18b)

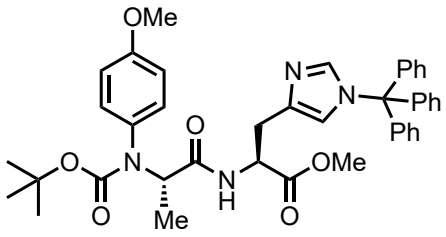

18b

The general procedure was followed starting from tri(4-methoxyphenyl)bismuthine (55 mg, 0.10 mmol). The crude material was purified on silica gel (2% MeOH/CH_2Cl_2) to afford **18b** as a white solid (55 mg, 78%). $\mathbf{R_f}$ = 0.47 (5% MeOH/CH_2Cl_2); **m.p.**= 61 – 63 °C; **^{1}H-NMR (600 MHz, $CDCl_3$)** δ 8.01 (s(br), 1H), 7.36 (s, 1H), 7.33 – 7.27 (m, 9H), 7.21 (s(br), 2H), 7.12 – 7.04 (m, 6H), 6.77 (d, *J* = 8.8 Hz, 2H), 6.59 (s, 1H), 4.82 – 4.77 (m, 1H), 4.65 (s(br), 1H), 3.75 (s, 3H), 3.60 (s, 3H), 3.12 (A of ABX, *J* = 14.6, 5.2 Hz, 1H), 3.00 (B of ABX, *J* = 14.6, 4.6 Hz, 1H), 1.35 (s, 9H), 1.29 – 1.23 (m, 3H); **^{13}C-NMR (150 MHz, $CDCl_3$)** δ 172.4, 171.9, 158.3, 155.3, 142.4, 138.7, 136.5, 133.3, 130.0, 129.9, 128.2, 119.7, 113.9, 80.7, 75.5, 55.5, 52.9, 52.2, 38.7, 29.8, 28.4, 15.9; **IR (ATR)/$\bar{\nu}$ (cm^{-1}):** 3275, 3048, 2919, 1722, 1667, 1493, 1445, 1238, 1207, 1034, 741, 700, 660; **HRMS (ESI)** calcd. for $[C_{41}H_{44}N_4O_6 + H]^+$: 689.3334, found 689.3347.

Methyl N^{α}-(*N*-(*tert*-butoxycarbonyl)-*N*-(4-fluorophenyl)-*L*-alanyl)-N^{τ}-trityl-*L*-histidinate (18c)

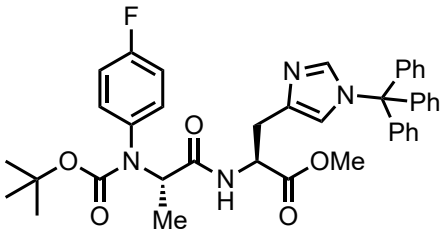

18c

The general procedure was followed starting from tri(4-fluorophenyl)bismuthine (51 mg, 0.10 mmol). The crude material was purified on silica gel (2% MeOH/CH_2Cl_2) to afford **18c** as a colorless oil (57 mg, 82%). $\mathbf{R_f}$ = 0.34 (5% MeOH/CH_2Cl_2); **^{1}H-NMR (600 MHz, $CDCl_3$)** δ 8.07 (s(br), 1H), 7.37 – 7.28 (m, 12H), 7.13 – 7.04 (m, 6H), 6.93 (t, *J* = 8.6 Hz, 2H), 6.58 (s, 1H), 4.80 (X of ABX, *J* = 12.0, 5.0 Hz, 1H), 4.66 (s(br), 1H), 3.59 (s, 3H), 3.11 (A of ABX, *J* = 14.7, 5.1 Hz, 1H), 2.99 (B of ABX, *J* = 14.6, 4.4 Hz, 1H), 1.35 (s, 9H), 1.28 (d, *J* = 6.1 Hz, 3H); **^{13}C-NMR (150 MHz, $CDCl_3$)** δ 172.1, 171.8, 161.4 (d, *J* = 244.5 Hz), 154.91, 142.33, 138.72, 136.53, 130.7 (d, *J* = 8,31 Hz), 129.85, 128.21, 128.18, 119.67, 115.4 (d, *J* = 22.3 Hz), 81.05, 75.47, 52.92, 52.16, 38.72, 29.72, 28.35, 15.94; **IR (ATR)/$\bar{\nu}$ (cm^{-1}):** 3319, 2980, 2930, 1747, 1689, 1508, 1445, 1367, 1319, 1215, 1153, 1132, 846, 828, 747, 700, 661, 638; **HRMS (ESI)** calcd. for $[C_{40}H_{41}FN_4O_5 + H]^+$: 677.3134, found 677.3133.

8. Procedure for the preparation of tripeptides

a. General procedure for synthesis of Boc–A.A$_1$–A.A$_2$–His(Trt)–OMe (19)

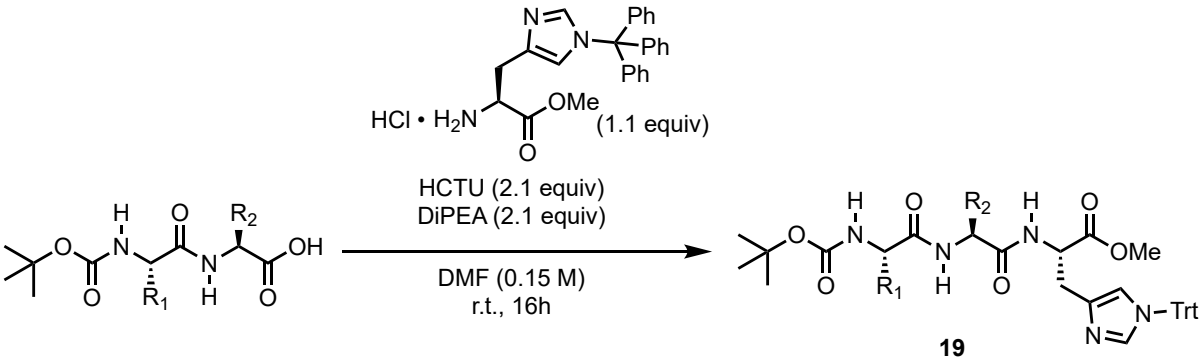

19

Manuscript, Scheme 5a): In a 50 mL flask, DIPEA (186 µL, 1.09 mmol, 2.1 equiv) was added to Boc–A.A$_1$–A.A$_2$–OH (150 mg, 520 µmol, 1.0 equiv), *L*–H-His(Trt)–OMe•HCl (256 mg, 572 µmol, 1.1 equiv) and HCTU (452 mg, 1.09 mmol, 2.1 equiv) in DMF (3.5 mL, 0.15 M). The mixture was stirred for 16h at room temperature before being extracted twice with dichloromethane. The combined organic phases were successively washed with sat. aq. NaHCO3 (2x20 mL), brine (2x20 mL), dried over Na_2SO_4, filtered and concentrated under reduce pressure. The

resulting crude product was purified by column chromatography using the indicated eluent system to afford the desired pure product (**19a-b**).

Methyl N^{α}-(*tert*-butoxycarbonyl)-*L*-alanyl-*L*-valyl-N^{τ}-trityl-*L*-histidinate (19a)

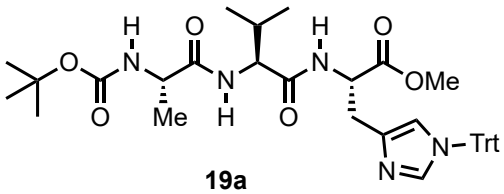

19a

The general procedure was followed. The crude material was purified on silica gel (1% MeOH/CH_2Cl_2) to afford **19a** as a white solid (259 mg, 73%): $\mathbf{R_f}$ = 0.34 (5% MeOH/CH_2Cl_2); **m.p.**: 87 – 89 °C; **^{1}H-NMR (300 MHz, $CDCl_3$)** δ 7.82 (d, *J* = 7.4 Hz, 1H), 7.43 (s, 1H), 7.35 – 7.25 (m, 9H), 7.15 – 7.09 (m, 1H), 7.09 – 7.01 (m, 6H), 6.58 (s, 1H), 5.44 (s, 1H), 4.79 – 4.63 (m, 1H), 4.31 (dd, *J* = 8.2, 5.7 Hz, 1H), 4.23 – 4.09 (m, 1H), 3.53 (s, 3H), 3.01 (A of ABX, *J* = 14.6, 5.1 Hz, 1H), 2.94 (B of ABX, *J* = 14.9, 5.0 Hz, 1H), 2.20 – 2.05 (m, 1H), 1.38 (s, 9H), 1.26 (d, *J* = 7.0 Hz, 3H), 0.90 (t, *J* = 6.1 Hz, 6H); ***presence of conformers*** **^{13}C-NMR (75 MHz, $CDCl_3$)** δ 172.9, 171.1, 170.8, 155.5, 141.8, 138.3, 135.5, 129.6, 128.1, 128.1, 119.7, 79.8, 75.6, 58.2, 55.4, 52.5, 52.0, 50.0, 43.4, 38.5, 31.1, 29.1, 28.2, 18.8, 17.9, 17.6, 12.7; **IR (ATR)/$\bar{\nu}$ (cm^{-1}):** 3292, 2972, 1650, 1493, 1445, 1162, 838, 748, 701, 660; **HRMS (ESI)** calcd. for $[C_{39}H_{47}N_5O_6 + H]^+$: 682.3599, found 682.3609.

Methyl N^{α}-(*tert*-butoxycarbonyl)-*L*-valyl-*L*-alanyl-N^{τ}-trityl-*L*-histidinate (19b)

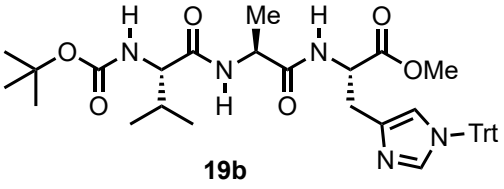

19b

The general procedure was followed. The crude material was purified on silica gel (2% MeOH/CH_2Cl_2) to afford **19b** as a white solid (248 mg, 70%): $\mathbf{R_f}$ = 0.36 (5% MeOH/CH_2Cl_2); **m.p.**: 92 – 94 °C; **^{1}H-NMR (300 MHz, $CDCl_3$)** δ 7.70 (d, *J* = 7.8 Hz, 1H), 7.45 (s, 1H), 7.34 – 7.27 (m, 9H), 7.13 – 7.00 (m, 7H), 6.56 (d, *J* = 1.0 Hz, 1H), 5.25 (d, *J* = 8.9 Hz, 1H), 4.80 – 4.70 (m, 1H), 4.48 (p, *J* = 6.9 Hz, 1H), 4.01 – 3.91 (m, 1H), 3.55 (s, 3H), 3.04 (A of ABX, *J* = 14.9, 5.1 Hz, 1H), 2.94 (B of ABX, *J* = 10.2, 5.6 Hz, 1H), 2.14 – 1.99 (m, 1H), 1.39 (s, 9H), 1.36 (d, *J* = 7.1 Hz, 3H), 0.85 (dd, *J* = 13.5, 6.8 Hz, 6H); ***presence of conformers*** **^{13}C-NMR (75 MHz, $CDCl_3$)** δ 172.0, 171.4, 171.2, 155.9, 141.9, 138.4, 135.6, 129.7, 128.2, 128.2, 119.9, 79.7, 75.7, 59.6, 55.6, 52.6, 52.2, 49.0, 43.6, 38.6, 31.2, 29.2, 28.3, 19.3, 18.6, 17.5, 12.8; **IR (ATR)/$\bar{\nu}$ (cm^{-1}):** 3275, 2972, 1745, 1651, 1493, 1445, 1366, 1160, 1132, 838, 748, 701, 660; **HRMS (ESI)** calcd. for $[C_{39}H_{47}N_5O_6 + H]^+$: 682.3599, found 682.3606.

b. Procedure for synthesis of Boc–Ala–His(Trt)–Val–OMe (21)

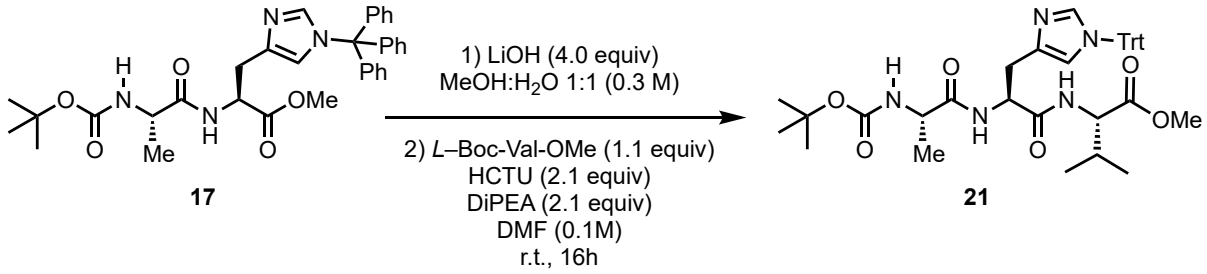

17 21

Methyl N^{α}-((*tert*-butoxycarbonyl)-*L*-alanyl)-N^{τ}-trityl-*L*-histidyl-*L*-valinate (21)

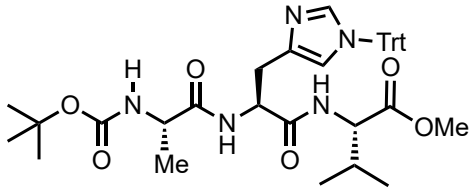

21

Manuscript, Scheme 5b): In a 25 mL flask, lithium hydroxide (26 mg, 1.1 mmol, 4.0 equiv) was added to a solution of methyl N^{α}-((*tert*-butoxycarbonyl)-*L*-alanyl)-N^{τ}-trityl-*L*-histidinate (**17**) (160 mg, 281 µmol, 1.0 equiv) in methanol:water 1:1 (1 mL). The mixture was stirred for 16h at room temperature before concentrated to water under reduce pressure. The residue was lyophilized to obtain Boc–Ala–His(Trt)–$O^{-}Li^{+}$ as white solid, used without further purification. In a 50 mL flask, DIPEA (100 µL, 590 µmol, 2.1 equiv) was added to Boc–Ala–His(Trt)–$O^{-}Li^{+}$, *L*–H-Val–OMe•HCl (52 mg, 0.31 mmol, 1.1 equiv) and HCTU (244 mg, 590 µmol, 2.1 equiv) in DMF (2.8 mL, 0.1 M). The mixture was stirred for 16h at room temperature before being extracted twice with dichloromethane. The combined organic phases were successively washed with sat. aq. NaHCO3 (2x20 mL), brine (2x20 mL), dried over Na_2SO_4, filtered and concentrated under reduce pressure. The resulting crude product was purified by column chromatography (2% MeOH/CH_2Cl_2) to afford **21** as a white solid (89 mg, 46%): $\mathbf{R_f}$ = 0.42 (5% MeOH/CH_2Cl_2); **m.p.**: 79 – 81 °C; **^{1}H-NMR (300 MHz, $CDCl_3$)** δ 8.46 (d, *J* = 6.1 Hz, 1H), 7.52 (d, *J* = 8.2 Hz, 1H), 7.38 – 7.27 (m, 10H), 7.13 – 7.00 (m, 6H), 6.66 (s, 1H), 5.22 (d, *J* = 6.6 Hz, 1H), 4.78 – 4.65 (m, 1H), 4.39 (dd, *J* = 8.4, 5.3 Hz, 1H), 4.24 – 4.12 (m, 1H), 3.64 (s, 3H), 3.11 (A of ABX, *J* = 15.1, 4.3 Hz, 1H), 2.89 (B of ABX, *J* = 15.1, 5.9 Hz, 1H), 2.14 – 2.01 (m, 1H), 1.38 (d, *J* = 7.2 Hz, 3H), 1.35 (s, 9H), 0.80 (d, *J* = 6.8 Hz, 6H); **^{13}C-NMR (75 MHz, $CDCl_3$)** δ ^{13}C NMR (75 MHz, $CDCl_3$) δ 172.8, 171.9, 171.0, 155.4, 142.2, 138.2, 136.9, 129.8, 128.2, 128.1, 119.7, 79.8, 75.5, 57.6, 53.3, 52.0, 50.7, 30.9, 29.3, 28.4, 19.1, 18.0; **IR (ATR)/$\bar{\nu}$ (cm^{-1}):** 3275, 2970, 1740, 1659, 1493, 1445, 1366, 1245, 1205, 1159, 1001, 841, 748, 701, 659, 638; **HRMS (ESI)** calcd. for $[C_{39}H_{47}N_5O_6 + H]^+$: 682.3599, found 682.3594.

c. Procedure for synthesis of Boc–Ala–Phe–Val–OMe (23)

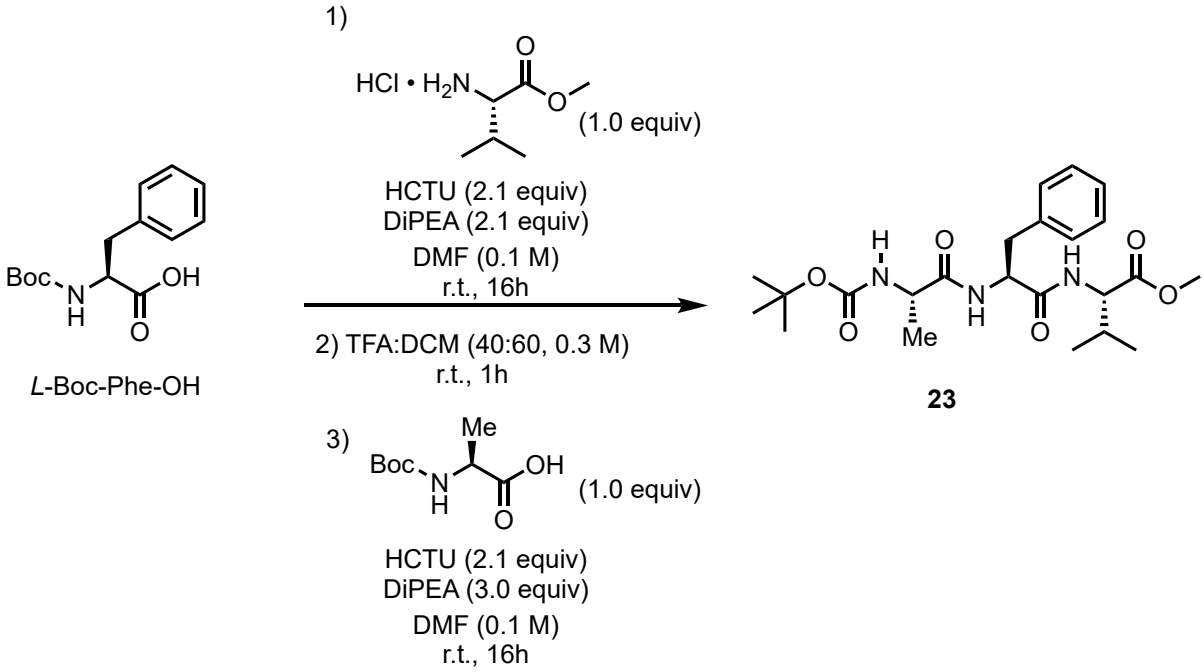

Methyl (*tert*-butoxycarbonyl)-*L*-alanyl-*L*-phenylalanyl-*L*-valinate (23)

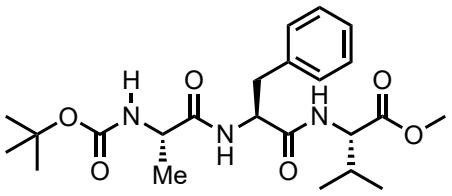

Manuscript, Scheme 5c): In a 50 mL flask, DIPEA (270 µL, 1.58 mmol, 2.1 equiv) was added to *L*-Boc–Phe–OH (200 mg, 754 µmol, 1.0 equiv), H-Val–OMe•HCl (126 mg, 754 µmol, 1.0 equiv), and HCTU (655 mg, 1.58 mmol, 2.1 equiv) in DMF (7.5 mL, 0.1 M). The mixture was stirred for 16h at room temperature before concentrated under reduce pressure. The residue was diluted in dichloromethane and successively washed with sat. aq. NaHCO3 (2x20 mL), brine (2x20 mL), dried over Na_2SO_4, filtered before concentrated under reduce pressure. The thick yellow oil residue was diluted in TFA:CH_2Cl_2 (40:60 ; 0.3 M) and stirred at room temperature for 1h. The trifluoroacetic acid was completely removed by several co-evaporation with dichloromethane under reduce pressure. To the residue was added Boc–Ala–OH (143 mg, 754 µmol, 1.0 equiv) and HCTU (655 mg, 1.58 mmol, 2.1 equiv) in DMF (7.5 mL, 0.1 M) followed by DIPEA (385 µL, 2.26 mmol, 3.0 equiv). The mixture was stirred for 16h at room temperature before concentrated under reduce pressure. The residue was diluted in dichloromethane and successively washed with sat. aq. NaHCO3 (2x20 mL), brine (2x20 mL), dried over Na_2SO_4, filtered before concentrated under reduce pressure. The resulting crude product was purified by column chromatography (3% MeOH/CH_2Cl_2) to afford **23** as a thick yellow oil (312 mg, 92%):

R_f = 0.41 (10% MeOH/CH_2Cl_2); **^{1}H-NMR (300 MHz, $CDCl_3$)** δ 7.31 – 7.14 (m, 4H), 6.87 (d, *J* = 7.9 Hz, 1H), 6.60 (d, *J* = 7.5 Hz, 1H), 5.07 (d, *J* = 7.2 Hz, 1H), 4.71 (q, *J* = 7.2 Hz, 1H), 4.41 (dd, *J* = 8.6, 5.3 Hz, 1H), 4.21 – 4.07 (m, 1H), 3.67 (s, 3H), 3.06 (d, *J* = 7.2 Hz, 2H), 2.12 – 1.99 (m, 2H), 1.40 (s, 9H), 1.28 (d, *J* = 7.1 Hz, 3H), 0.82 (dd, *J* = 10.3, 6.9 Hz, 6H); **^{13}C-NMR (75 MHz, $CDCl_3$)** δ 173.0, 171.8, 170.9, 155.4, 136.5, 129.3, 128.4, 126.8, 79.8, 57.4, 54.3, 52.0, 50.4, 38.6, 31.1, 28.3, 18.8, 17.8; **IR (ATR)/$\bar{\nu}$ (cm^{-1}):** 3287, 2969, 1741, 1712, 1646, 1499, 1454, 1366, 1246, 1206, 1164, 1049, 1023, 742, 698; **HRMS (ESI)** calcd. for $[C_{23}H_{35}N_3O_6 + H]^+$: 450.2599, found 450.2610.

9. Procedure for the preparation of aryl tripeptides

a. Procedure for synthesis of Boc–*N*(Tolyl)–Ala–His(trt)–Val–OMe (22)

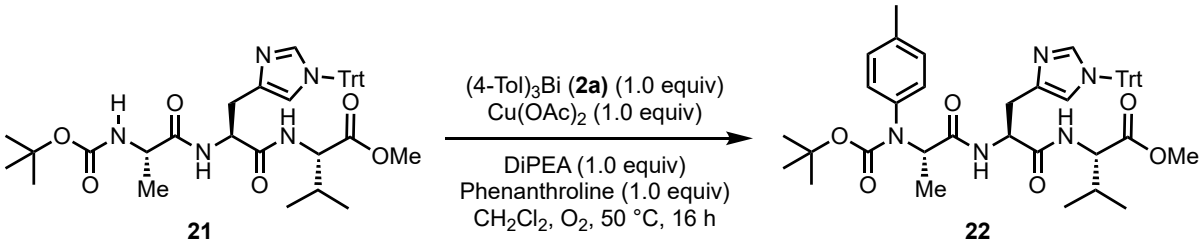

Manuscript, Scheme 5b: In a sealed tube, *N*,*N*-diisopropylethylamine (25.0 µL, 0.15 mmol, 1.0 equiv) was added to methyl Nα-((tert-butoxycarbonyl)-L-alanyl)-Nτ-trityl-L-histidyl-L-valinate **21** (100 mg, 0.15 mmol, 1.0 equiv), tri(4-tolyl)bismuthine **2a** (71 mg, 0.15 mmol, 1.0 equiv), copper(II) acetate (27 mg, 0.15 mmol, 1.0 equiv) and phenanthroline (27 mg, 0.15 µmol, 1.0 equiv) in CH_2Cl_2 (0.1 M). The raction mixture was purged with oxygen before stirred in an oil bath set at 50 °C for 16 hours. The solvent was evaporated under reduce pressure and the residue was purified on silica gel chromatography (2% MeOH/CH_2Cl_2) to afford **22** as a white solid (94 mg, 83%): **R_f** = 0.46 (5% MeOH/CH_2Cl_2); **m.p.**: 134 – 136 °C; **^{1}H-NMR (300 MHz, $CDCl_3$)** δ 8.35 (d, *J* = 7.2 Hz, 1H), 8.08 (s, 1H), 7.74 (d, *J* = 5.9 Hz, 1H), 7.41 – 7.31 (m, 10H), 7.10 (dd, *J* = 5.9, 1.7 Hz, 8H), 7.04 (d, *J* = 8.2 Hz, 1H), 6.87 (s, 1H), 5.27 – 5.11 (m, 1H), 4.50 – 4.29 (m, 2H), 3.67 (s, 3H), 3.54 (d, *J* = 15.1 Hz, 1H), 2.96 – 2.81 (m, 1H), 2.27 (s, 3H), 2.26 – 2.20 (m, 1H), 1.31 (d, *J* = 6.6 Hz, 3H), 1.22 (s, 9H), 1.02 (dd, *J* = 15.7, 6.8 Hz, 6H); **^{13}C-NMR (75 MHz, $CDCl_3$)** δ 172.1, 172.0, 170.7, 154.4, 140.0, 138.5, 136.6, 134.3, 132.2, 129.8, 129.4, 129.2, 128.9, 128.1, 120.9, 80.6, 78.7, 58.7, 52.8, 52.0, 30.6, 30.2, 28.3, 21.1, 19.3, 18.5, 15.7; **IR (ATR)/$\bar{\nu}$ (cm^{-1}):** 3155, 2970, 1740, 1668, 1514, 1495, 1447, 1367, 1155, 1129, 1019, 1001, 839, 747, 701, 662, 640; **HRMS (ESI)** calcd. for $[C_{46}H_{53}N_5O_6 + H]^+$: 772.4069, found 772.4058.

b. Procedure for synthesis of Boc–*N*(Tolyl)–Ala–His–Val–OMe (25)

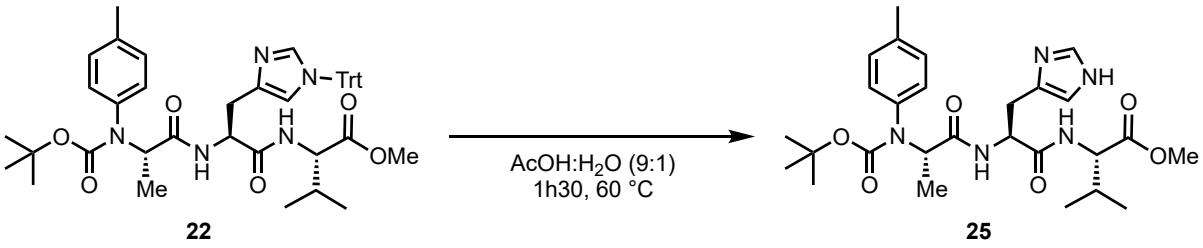

22 **25**

Manuscript, Scheme 7: In a flask, Boc–*N*(Tolyl)–Ala–His(trt)–Val–OMe **22** (50 mg, 0.65 mmol) in AcOH:H_2O (9:1, 0.35 M) was stirred for 1h30 at 60 °C. After cooling down at room temperature, the solvent was co-evaporated with cyclohexane under reduce pressure. The white solid residue was purified on silica gel chromatography (5% MeOH/CH_2Cl_2) to afford **25** as a white solid (35 mg, 99%): $\mathbf{R_f}$ = 0.46 (6% MeOH/CH_2Cl_2); **m.p.**: 154 – 157 °C; **^{1}H-NMR (600 MHz, $CDCl_3$)** δ 7.86 (s(br), 1H), 7.62 (s(br), 1H), 7.56 (s, 1H), 7.14 – 7.08 (m, 4H), 6.83 (s, 1H), 4.80 – 4.75 (m, 1H), 4.57 – 4.51 (m, 1H), 4.39 (dd, *J* = 8.3, 5.2 Hz, 1H), 3.71 (s, 3H), 3.16 (dd, *J* = 15.1, 4.7 Hz, 1H), 3.09 (dd, *J* = 15.2, 5.9 Hz, 1H), 2.33 (s, 3H), 2.18 – 2.11 (m, 1H), 1.36 (s, 9H), 1.30 (d, *J* = 6.9 Hz, 3H), 0.86 (dd, *J* = 6.8, 3.5 Hz, 6H); **^{13}C-NMR (150 MHz, $CDCl_3$)** δ 172.5, 172.2, 171.3, 155.2, 137.6, 136.8, 134.9, 129.4, 128.2, 81.1, 64.2, 57.8, 53.1, 52.2, 30.6, 28.8, 28.3, 28.2, 21.1, 19.0, 17.8, 15.5; **IR (ATR)/$\bar{\nu}$ (cm^{-1}):** 3287, 2971, 1741, 1661, 1514, 1455, 1391, 1367, 1323, 1255, 1158, 1107, 1019, 855, 832, 755, 622; **HRMS (ESI)** calcd. for $[C_{27}H_{39}N_5O_6 + H]^+$: 530.2973, found 530.2976.

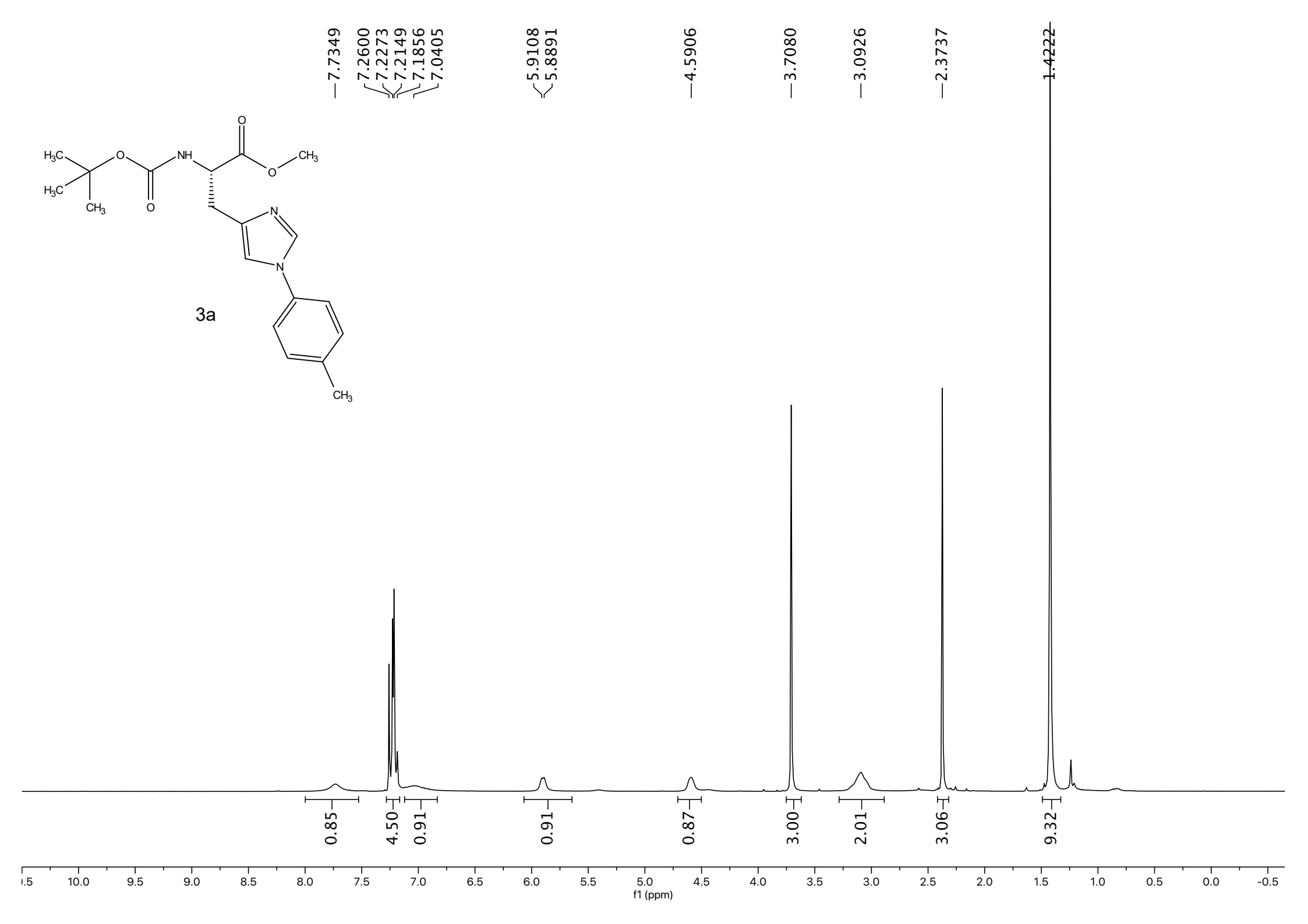
7.7349
7.2600
7.2273
7.2149
7.1856
7.0405
5.9108
5.8891
4.5906
3.7080
3.0926
2.3737
1.4222
3a
0.85
4.50
0.91
0.91
0.87
3.00
2.01
3.06
9.32
f1 (ppm)

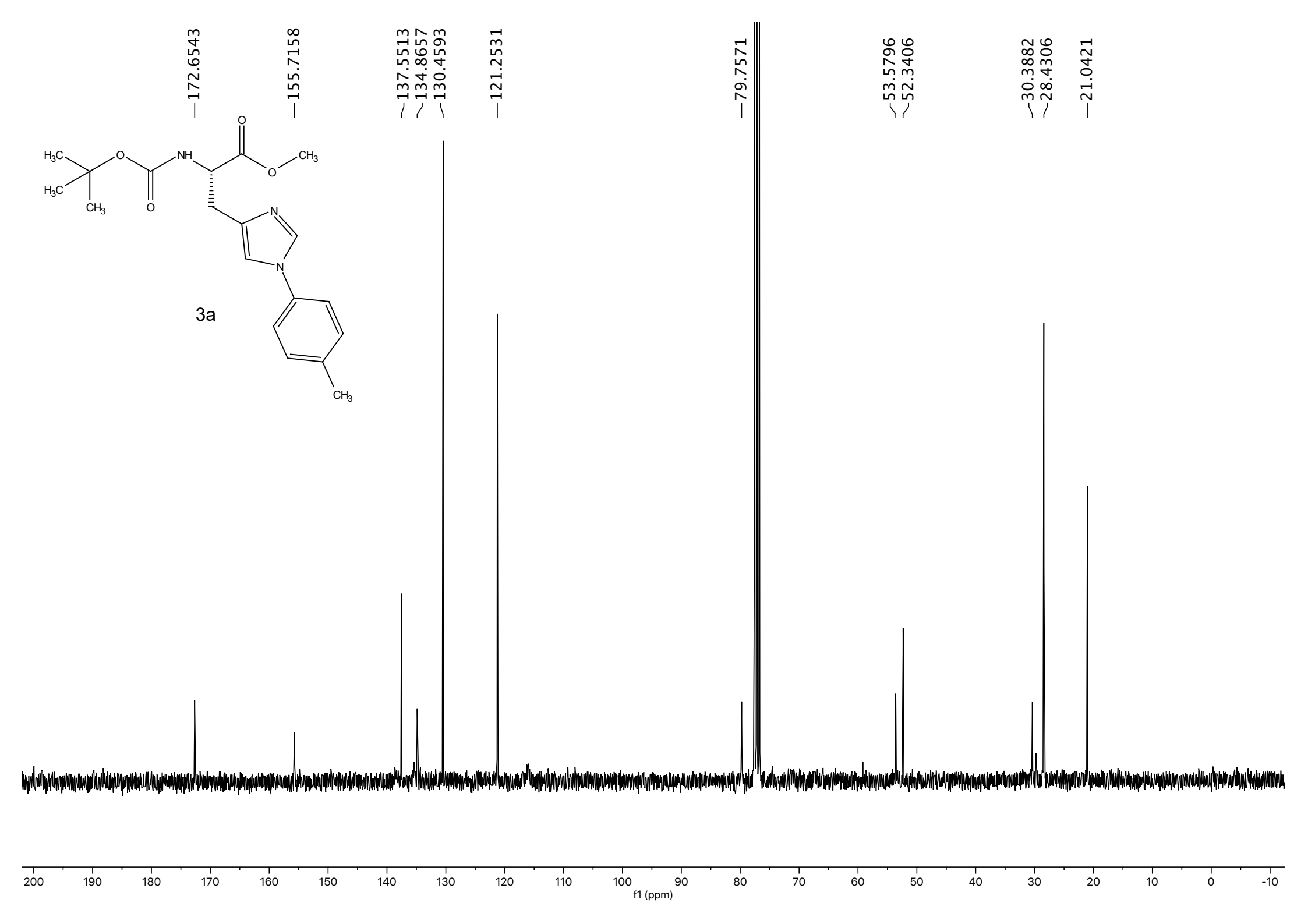
172.6543
155.7158
137.5513
134.8657
130.4593
121.2531
79.7571
53.5796
52.3406
30.3882
28.4306
21.0421
3a
200
190
180
170
160
150
140
130
120
110
100
90
80
70
60
50
40
30
20
10
0
-10
f1 (ppm)

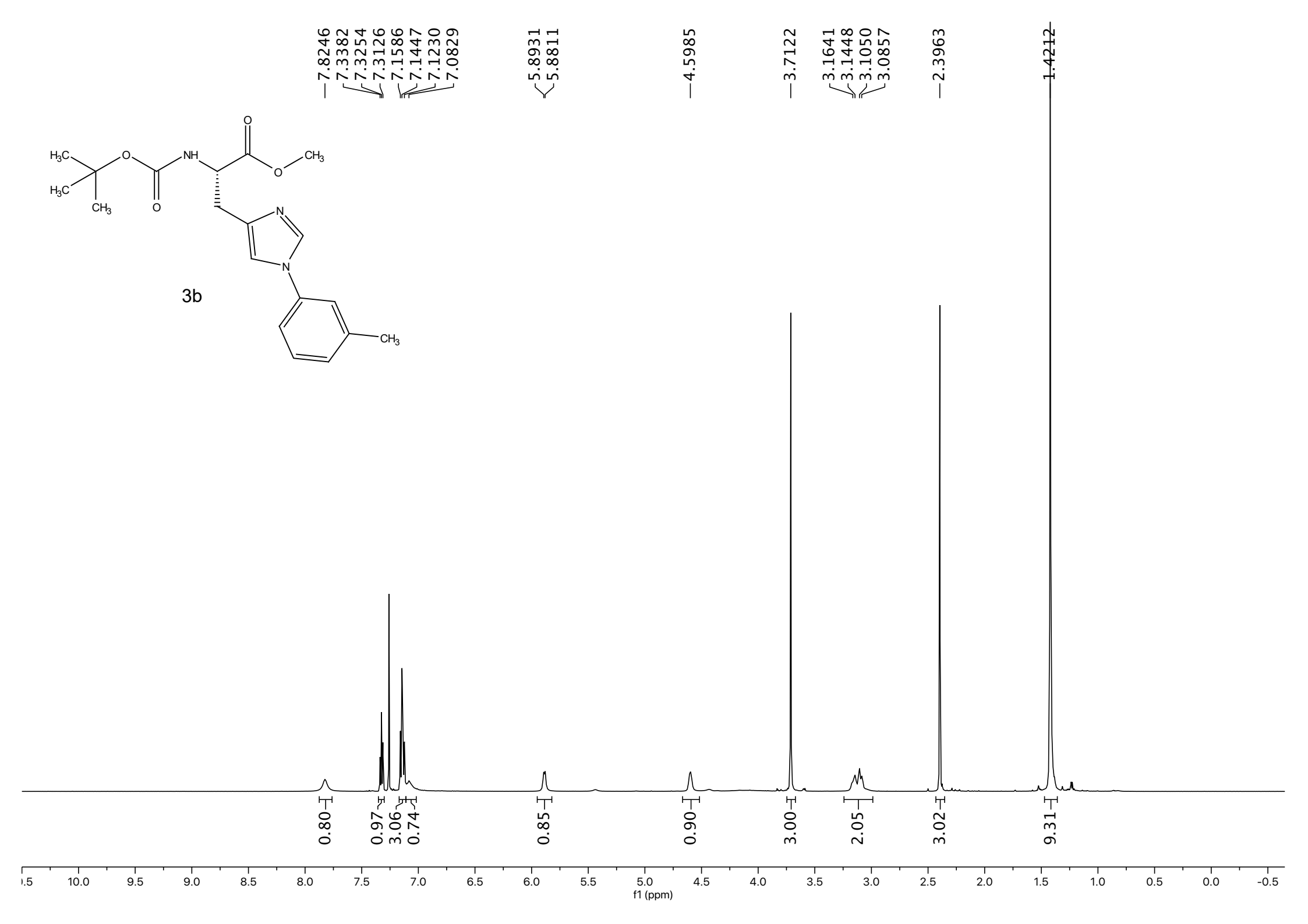
7.8246
7.3382
7.3254
7.3126
7.1586
7.1447
7.1230
7.0829
5.8931
5.8811
4.5985
3.7122
3.1641
3.1448
3.1050
3.0857
2.3963
1.4212
3b
0.80
0.97
3.06
0.74
0.85
0.90
3.00
2.05
3.02
9.31
f1 (ppm)

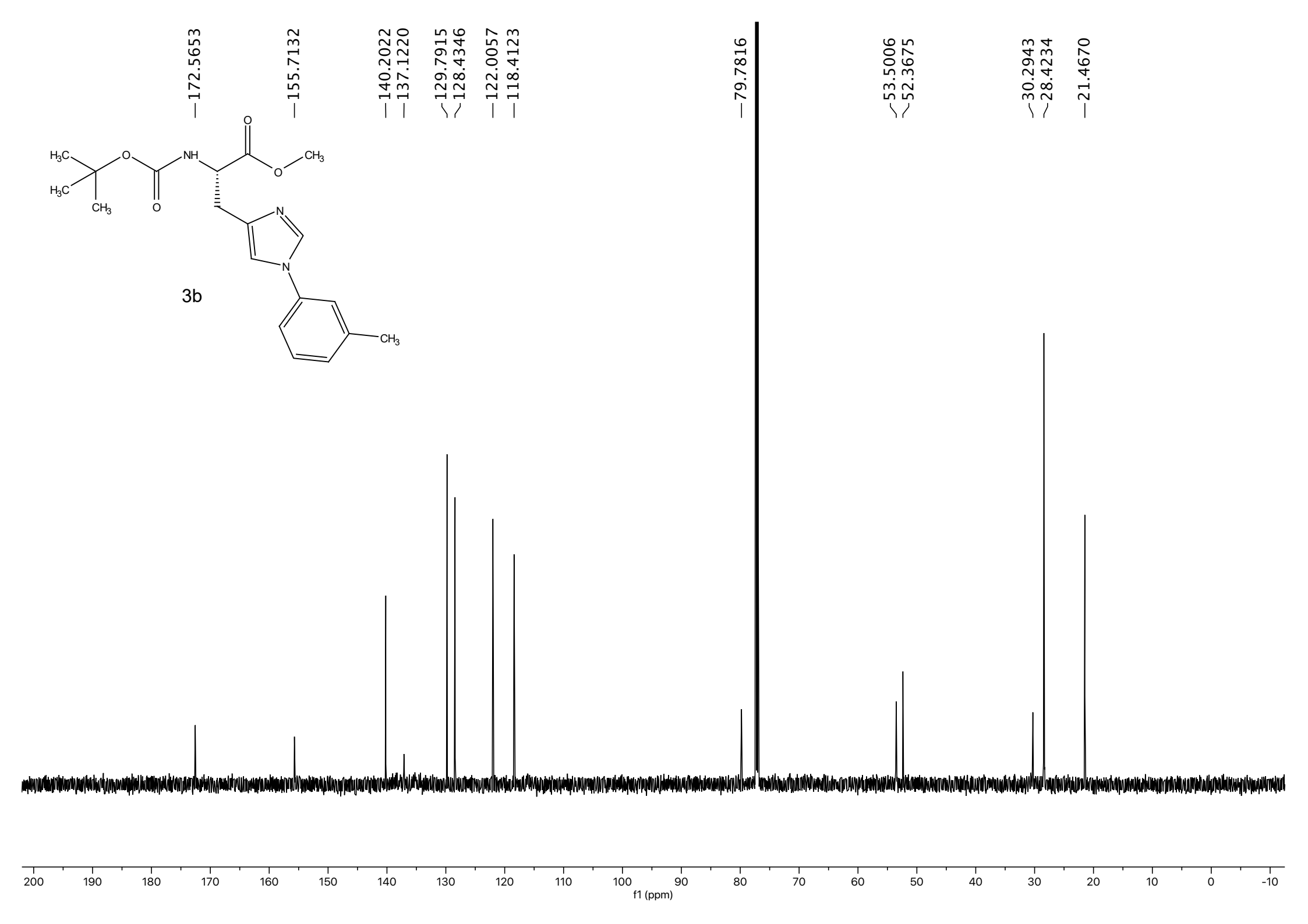
172.5653
155.7132
140.2022
137.1220
129.7915
128.4346
122.0057
118.4123
79.7816
53.5006
52.3675
30.2943
28.4234
21.4670
3b
f1 (ppm)

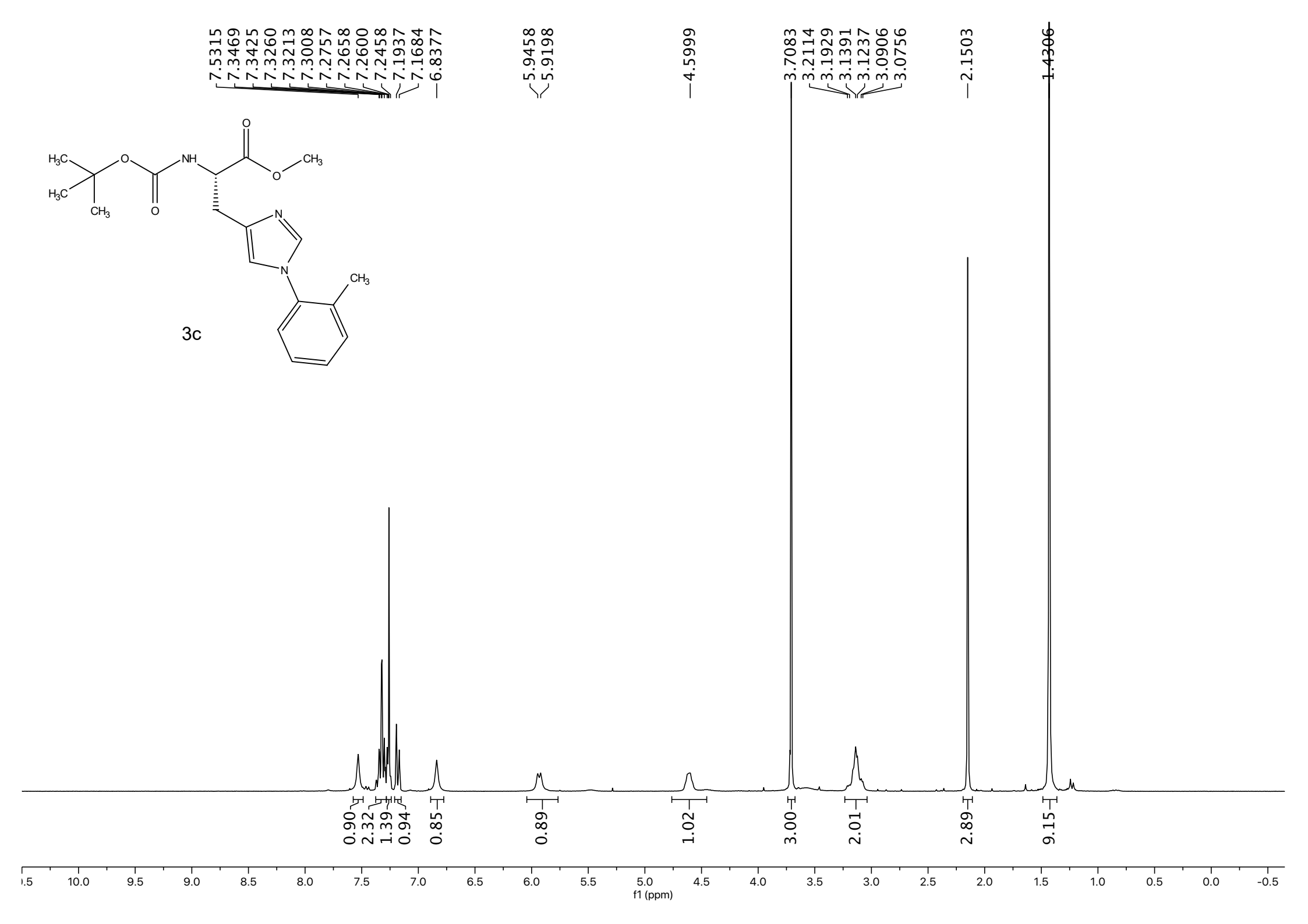
7.5315
7.3469
7.3425
7.3260
7.3213
7.3008
7.2757
7.2658
7.2600
7.2458
7.1937
7.1684
6.8377
5.9458
5.9198
4.5999
3.7083
3.2114
3.1929
3.1391
3.1237
3.0906
3.0756
2.1503
1.4306
0.90
2.32
1.39
0.94
0.85
0.89
1.02
3.00
2.01
2.89
9.15
f1 (ppm)
3c

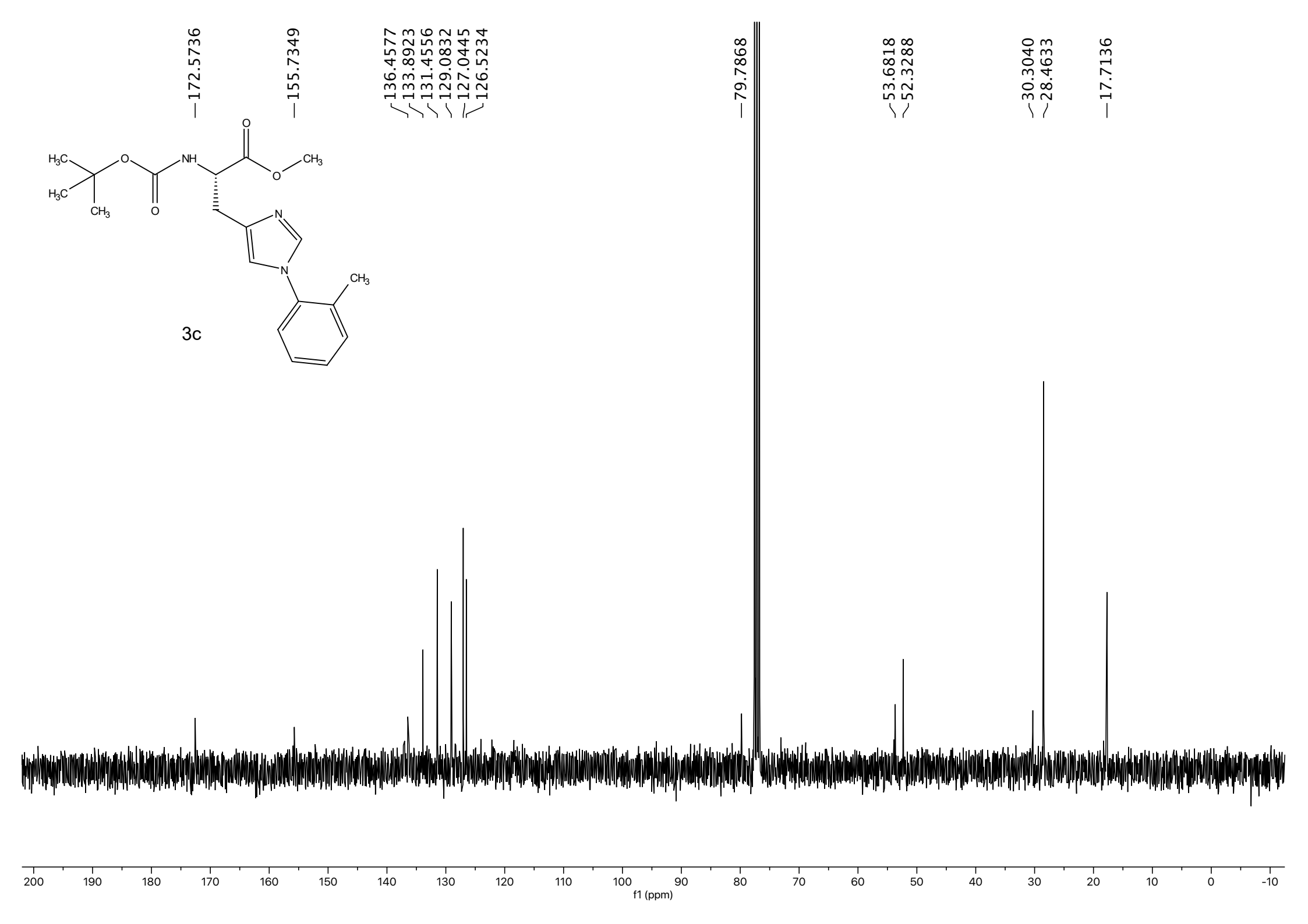
172.5736
155.7349
136.4577
133.8923
131.4556
129.0832
127.0445
126.5234
79.7868
53.6818
52.3288
30.3040
28.4633
17.7136
3c
f1 (ppm)

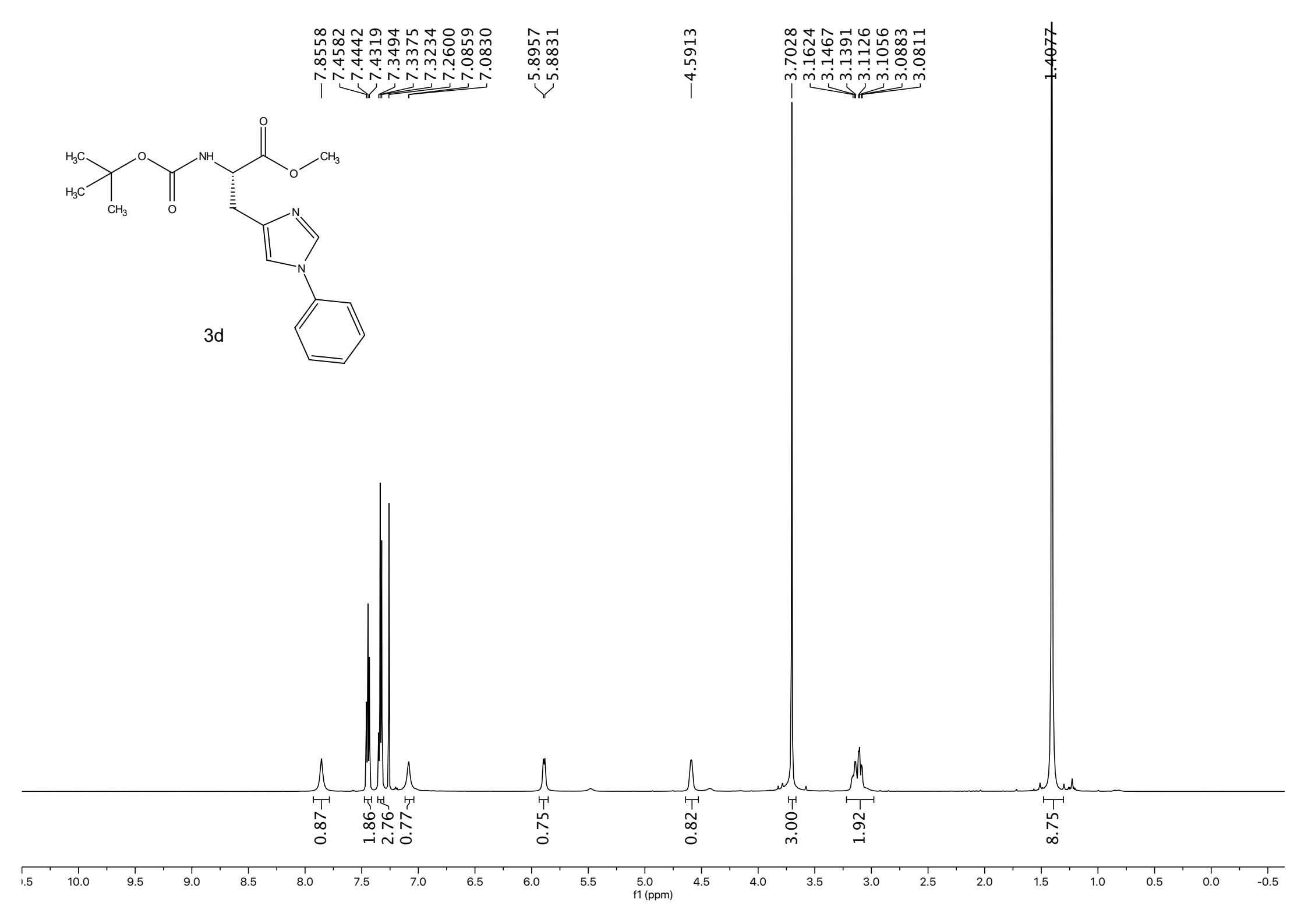
7.8558
7.4582
7.4442
7.4319
7.3494
7.3375
7.3234
7.2600
7.0859
7.0830
5.8957
5.8831
4.5913
3.7028
3.1624
3.1467
3.1391
3.1126
3.1056
3.0883
3.0811
1.4077
0.87
1.86
2.76
0.77
0.75
0.82
3.00
1.92
8.75
f1 (ppm)

3d

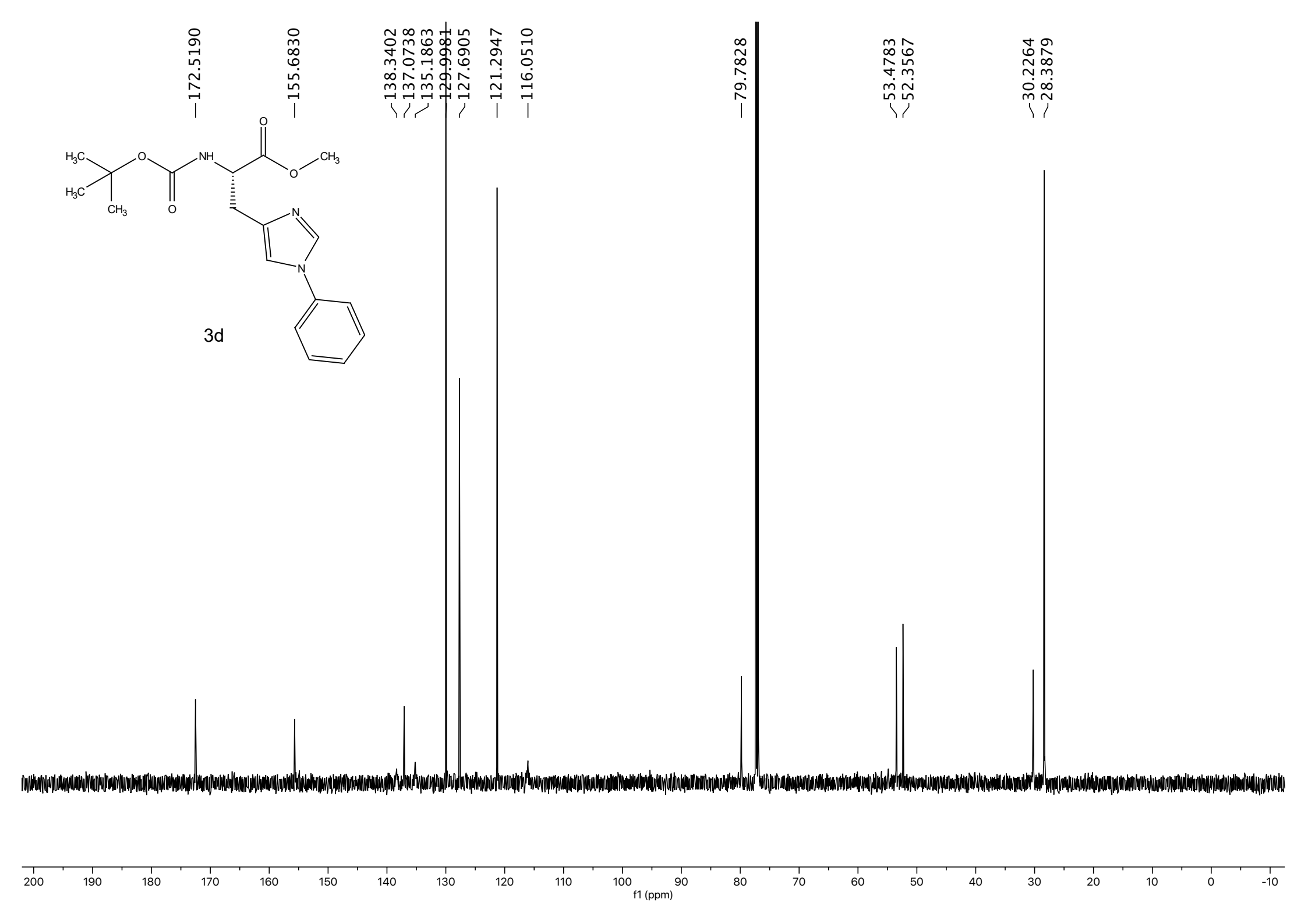
172.5190
155.6830
138.3402
137.0738
135.1863
129.9981
127.6905
121.2947
116.0510
79.7828
53.4783
52.3567
30.2264
28.3879
3d
f1 (ppm)

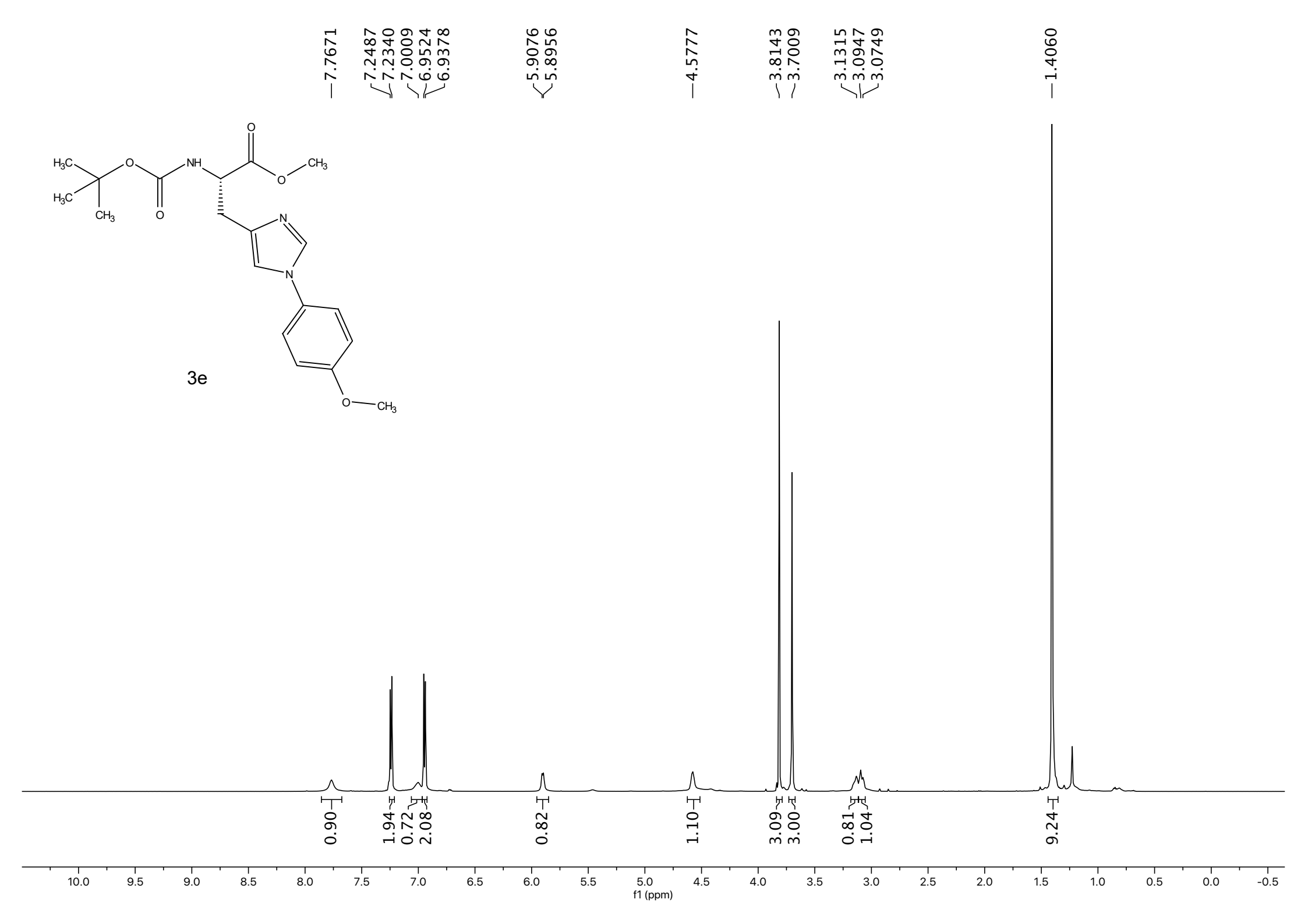
7.7671
7.2487
7.2340
7.0009
6.9524
6.9378
5.9076
5.8956
4.5777
3.8143
3.7009
3.1315
3.0947
3.0749
1.4060
3e
0.90
1.94
0.72
2.08
0.82
1.10
3.09
3.00
0.81
1.04
9.24
f1 (ppm)

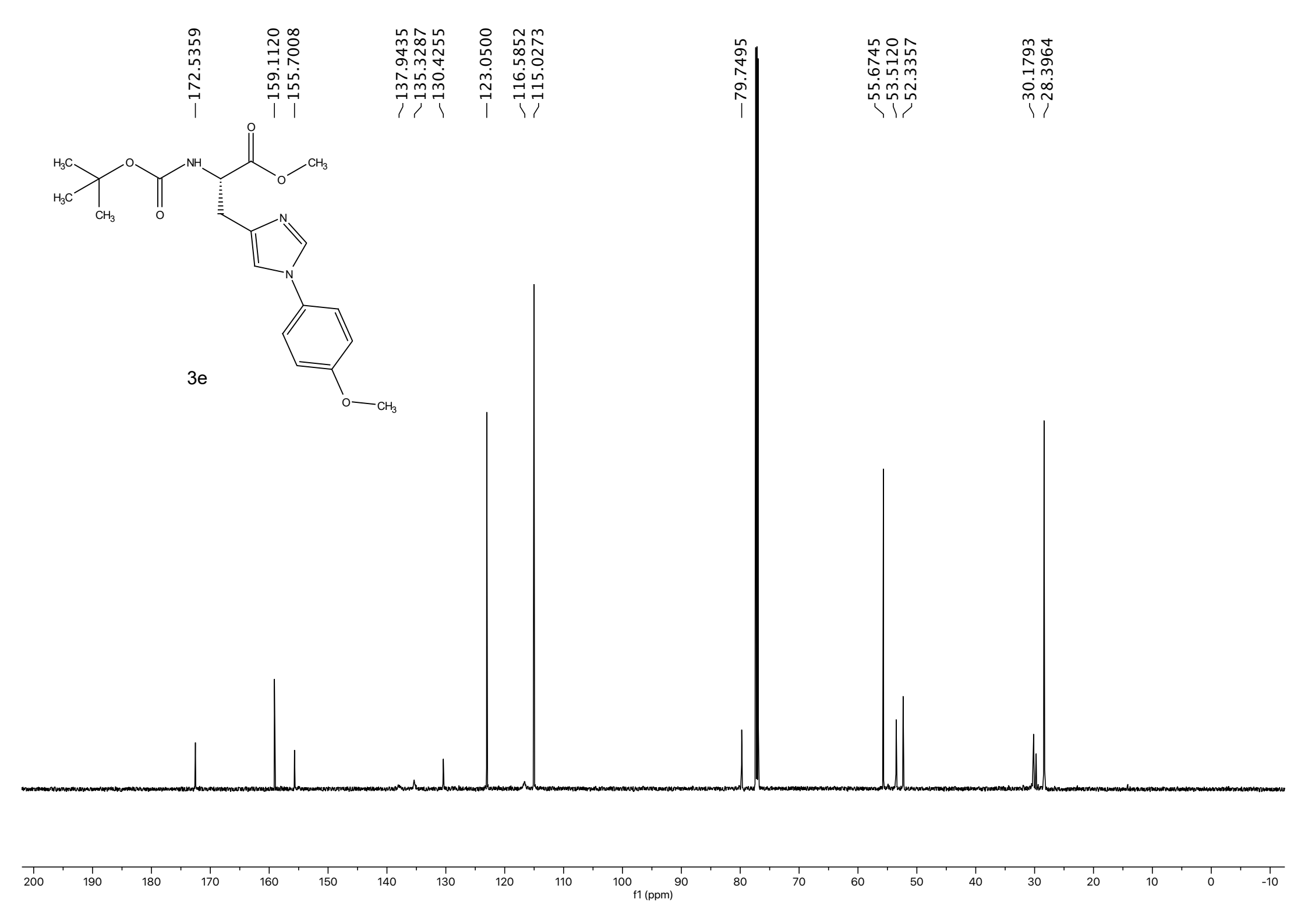
172.5359
159.1120
155.7008
137.9435
135.3287
130.4255
123.0500
116.5852
115.0273
79.7495
55.6745
53.5120
52.3357
30.1793
28.3964
3e
f1 (ppm)

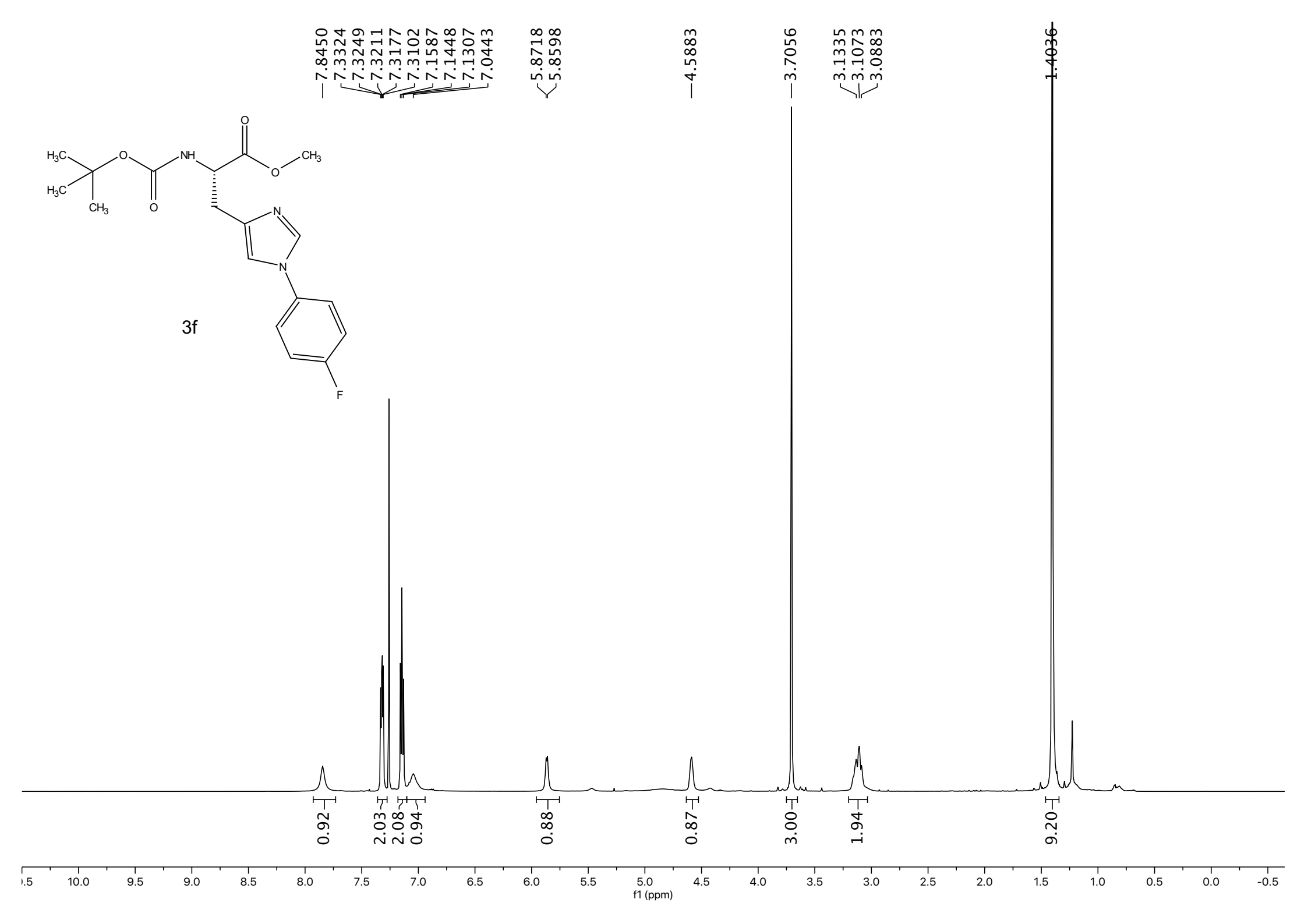
7.8450
7.3324
7.3249
7.3211
7.3177
7.3102
7.1587
7.1448
7.1307
7.0443
5.8718
5.8598
4.5883
3.7056
3.1335
3.1073
3.0883
1.4036
3f
0.92
2.03
2.08
0.94
0.88
0.87
3.00
1.94
9.20
f1 (ppm)

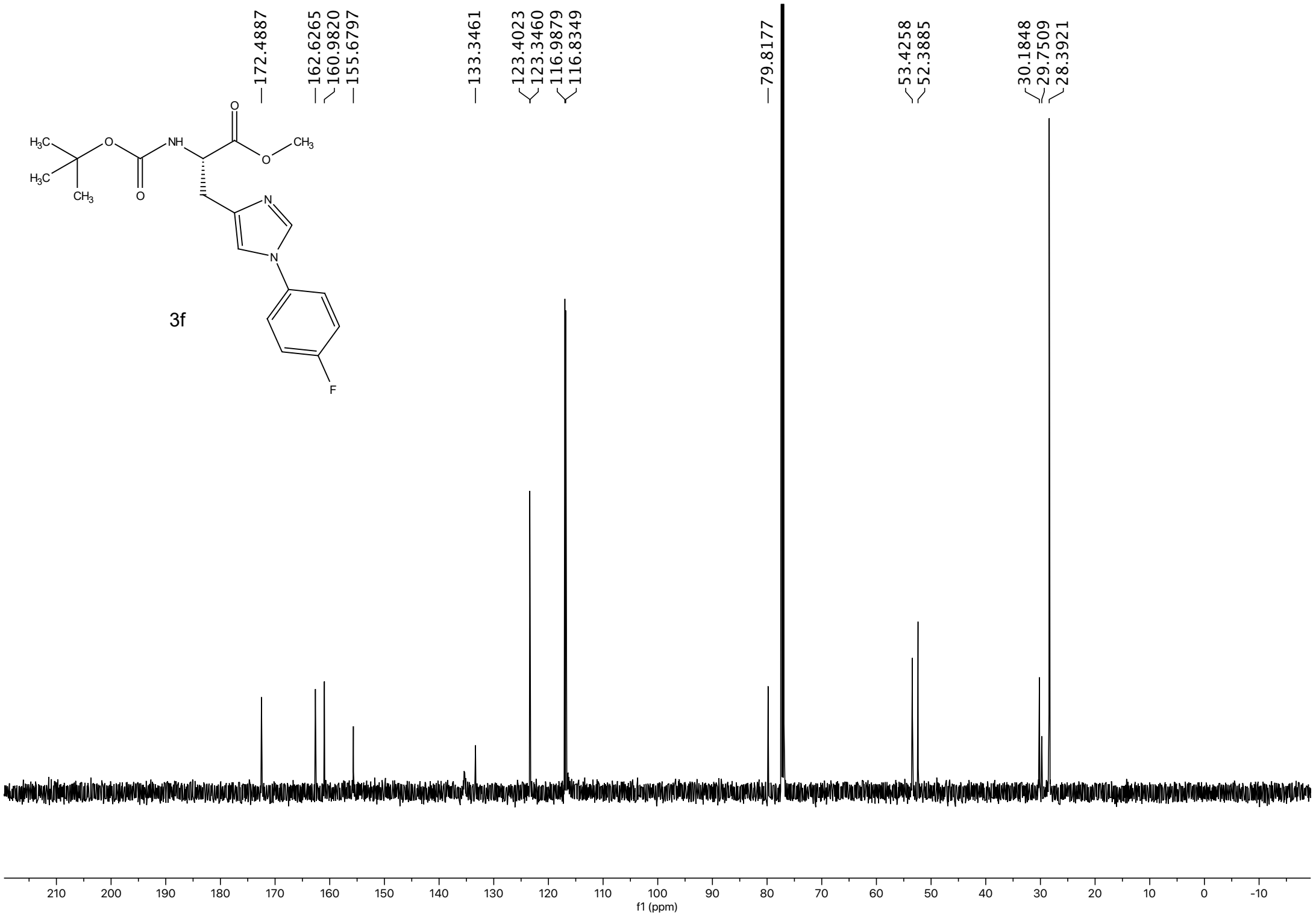
172.4887
162.6265
160.9820
155.6797
133.3461
123.4023
123.3460
116.9879
116.8349
79.8177
53.4258
52.3885
30.1848
29.7509
28.3921
3f
f1 (ppm)

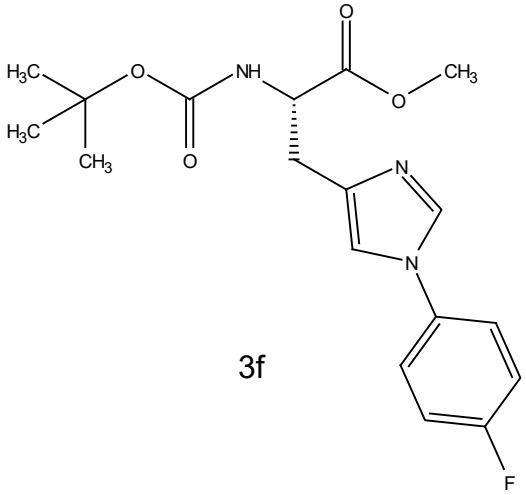
H3C
O
NH
O
CH3
H3C
CH3
O
O
N
N
F

3f

-113.6453
10
0
-10
-20
-30
-40
-50
-60
-70
-80
-90
-100
-110
-120
-130
-140
-150
-160
-170
-180
-190
-200
-210
f1 (ppm)

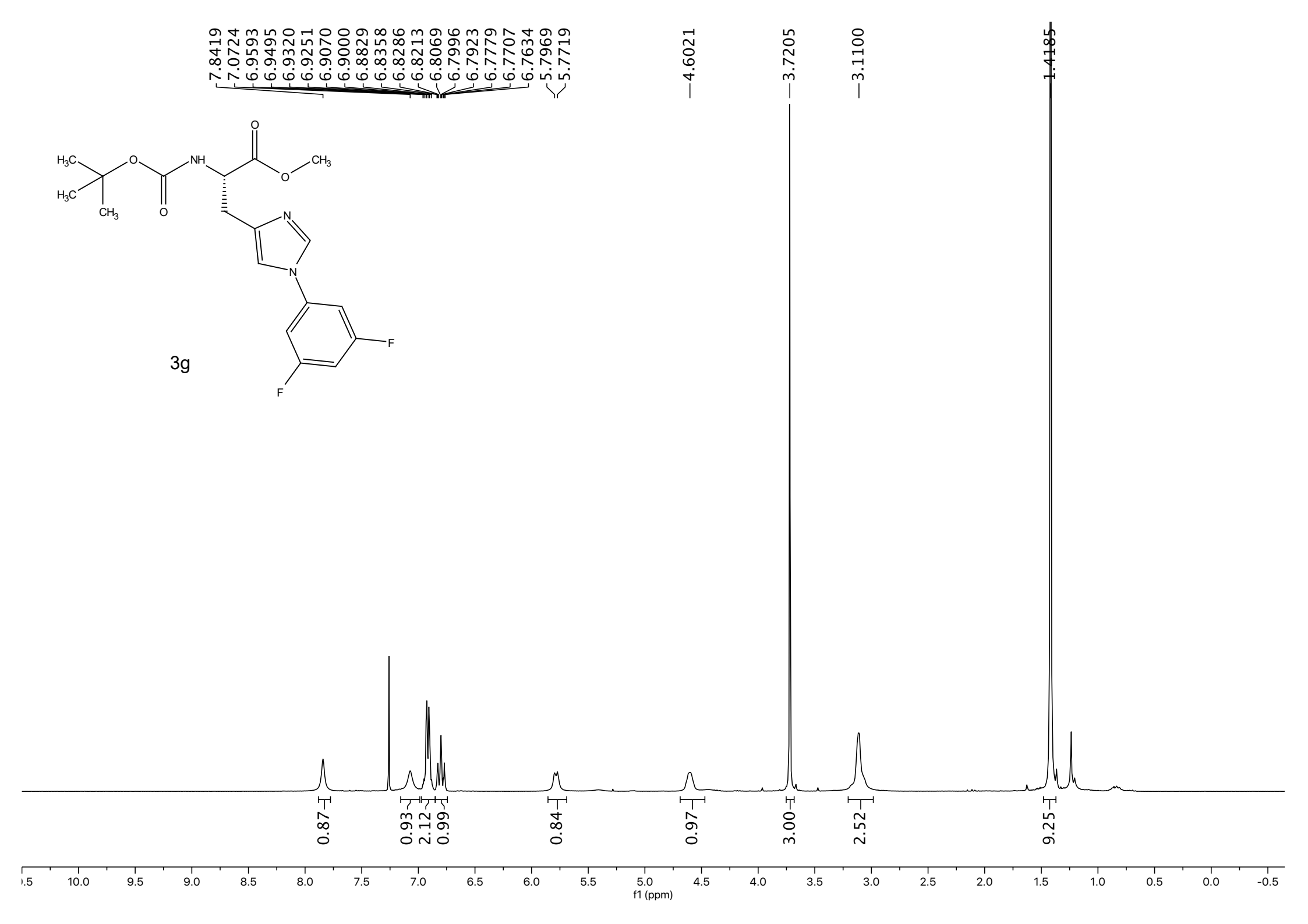
7.8419
7.0724
6.9593
6.9495
6.9320
6.9251
6.9070
6.9000
6.8829
6.8358
6.8286
6.8213
6.8069
6.7996
6.7923
6.7779
6.7707
6.7634
5.7969
5.7719
4.6021
3.7205
3.1100
1.4185
0.87
0.93
2.12
0.99
0.84
0.97
3.00
2.52
9.25
f1 (ppm)
3g

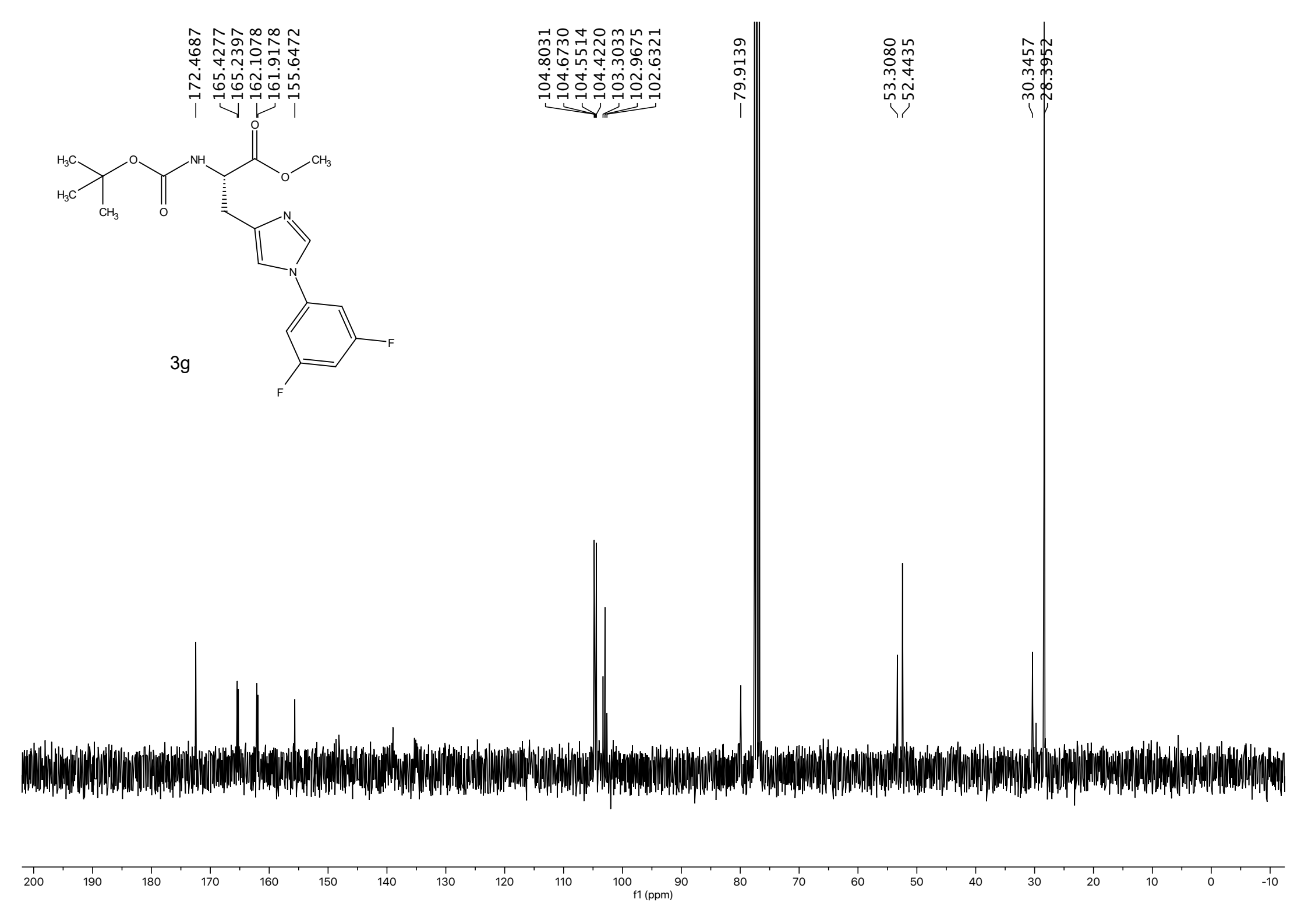
172.4687
165.4277
165.2397
162.1078
161.9178
155.6472
104.8031
104.6730
104.5514
104.4220
103.3033
102.9675
102.6321
79.9139
53.3080
52.4435
30.3457
28.3952
3g
f1 (ppm)

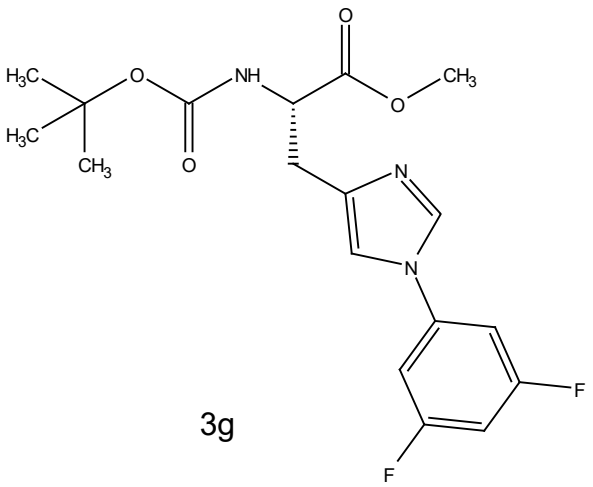
H3C
O
NH
O
CH3
H3C
CH3
O
O
N
N
F
F

3g

-106.2532
10
0
-10
-20
-30
-40
-50
-60
-70
-80
-90
-100
-110
-120
-130
-140
-150
-160
-170
-180
-190
-200
-210
f1 (ppm)

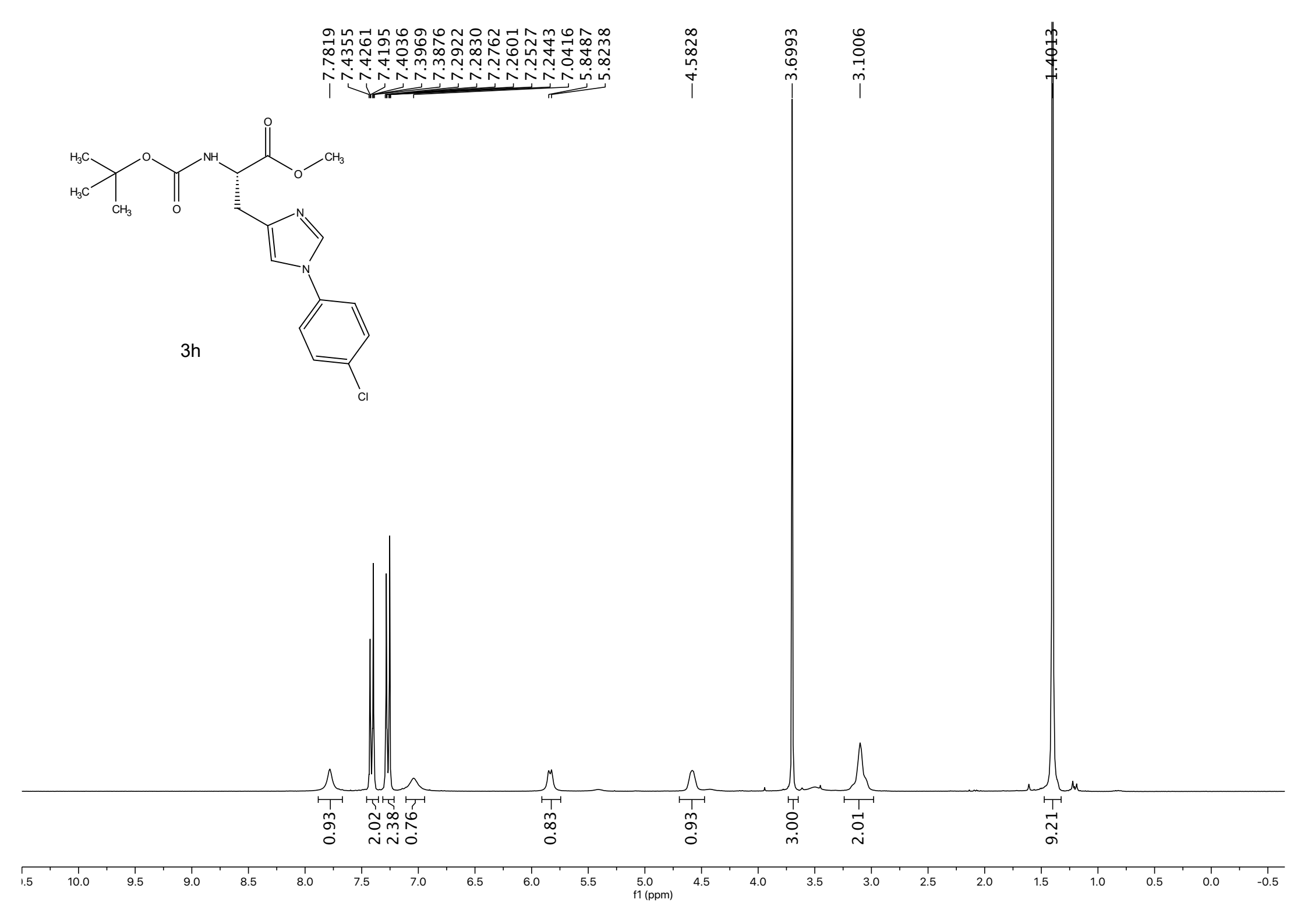
7.7819
7.4355
7.4261
7.4195
7.4036
7.3969
7.3876
7.2922
7.2830
7.2762
7.2601
7.2527
7.2443
7.0416
5.8487
5.8238
4.5828
3.6993
3.1006
1.4013
3h
0.93
2.02
2.38
0.76
0.83
0.93
3.00
2.01
9.21
f1 (ppm)

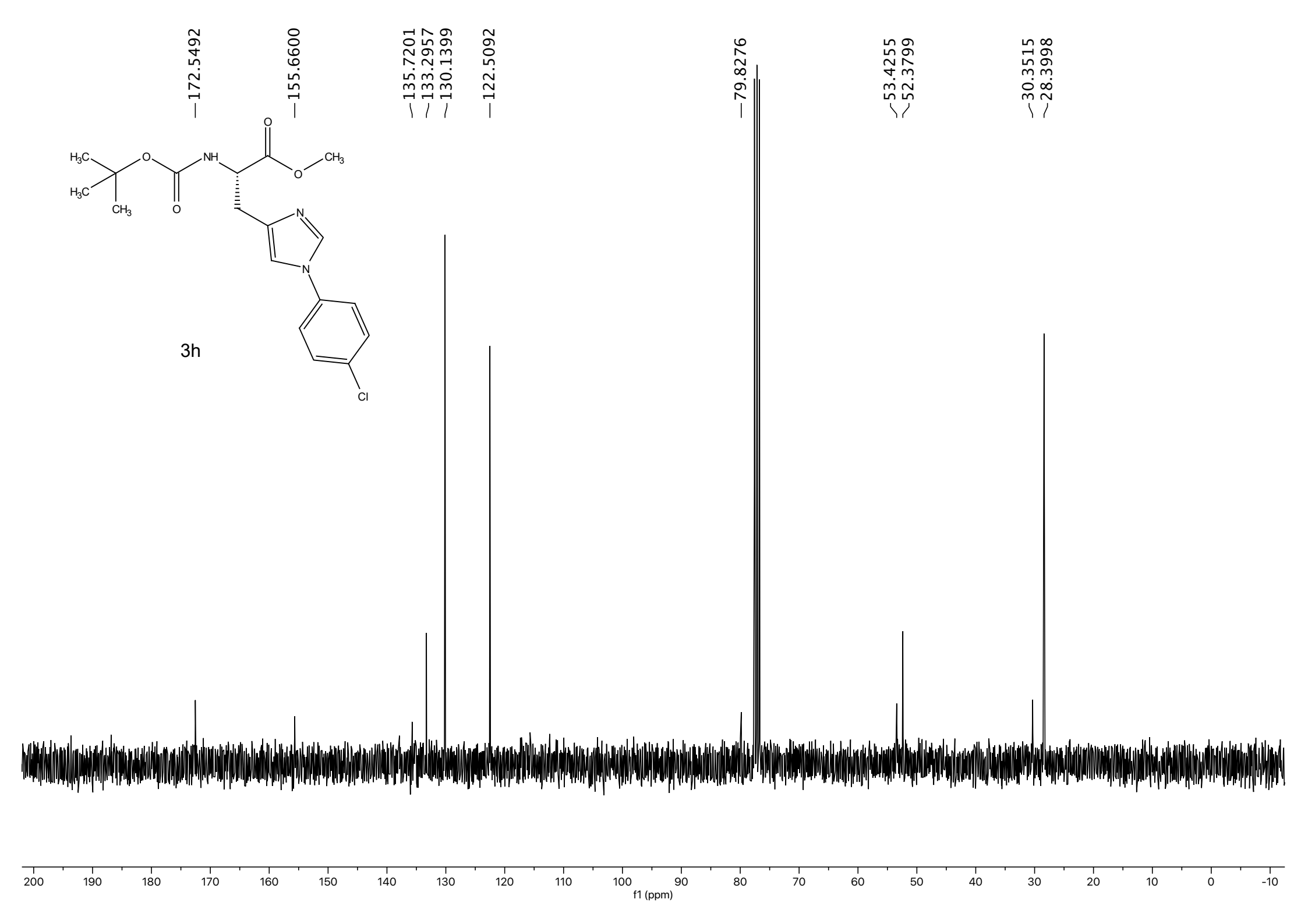
172.5492
155.6600
135.7201
133.2957
130.1399
122.5092
79.8276
53.4255
52.3799
30.3515
28.3998
3h
f1 (ppm)

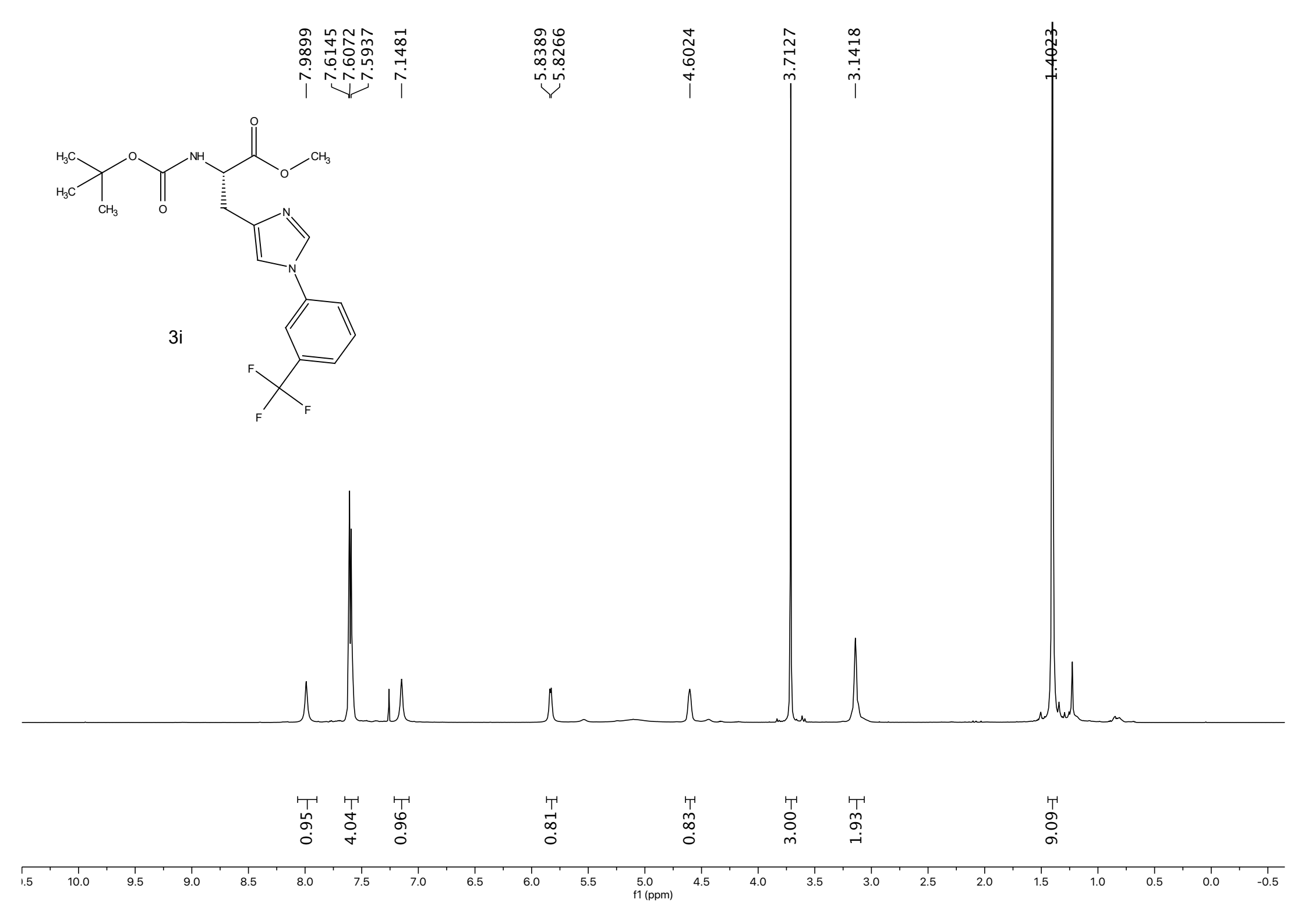
7.9899
7.6145
7.6072
7.5937
7.1481
5.8389
5.8266
4.6024
3.7127
3.1418
1.4023
3i
0.95
4.04
0.96
0.81
0.83
3.00
1.93
9.09
f1 (ppm)

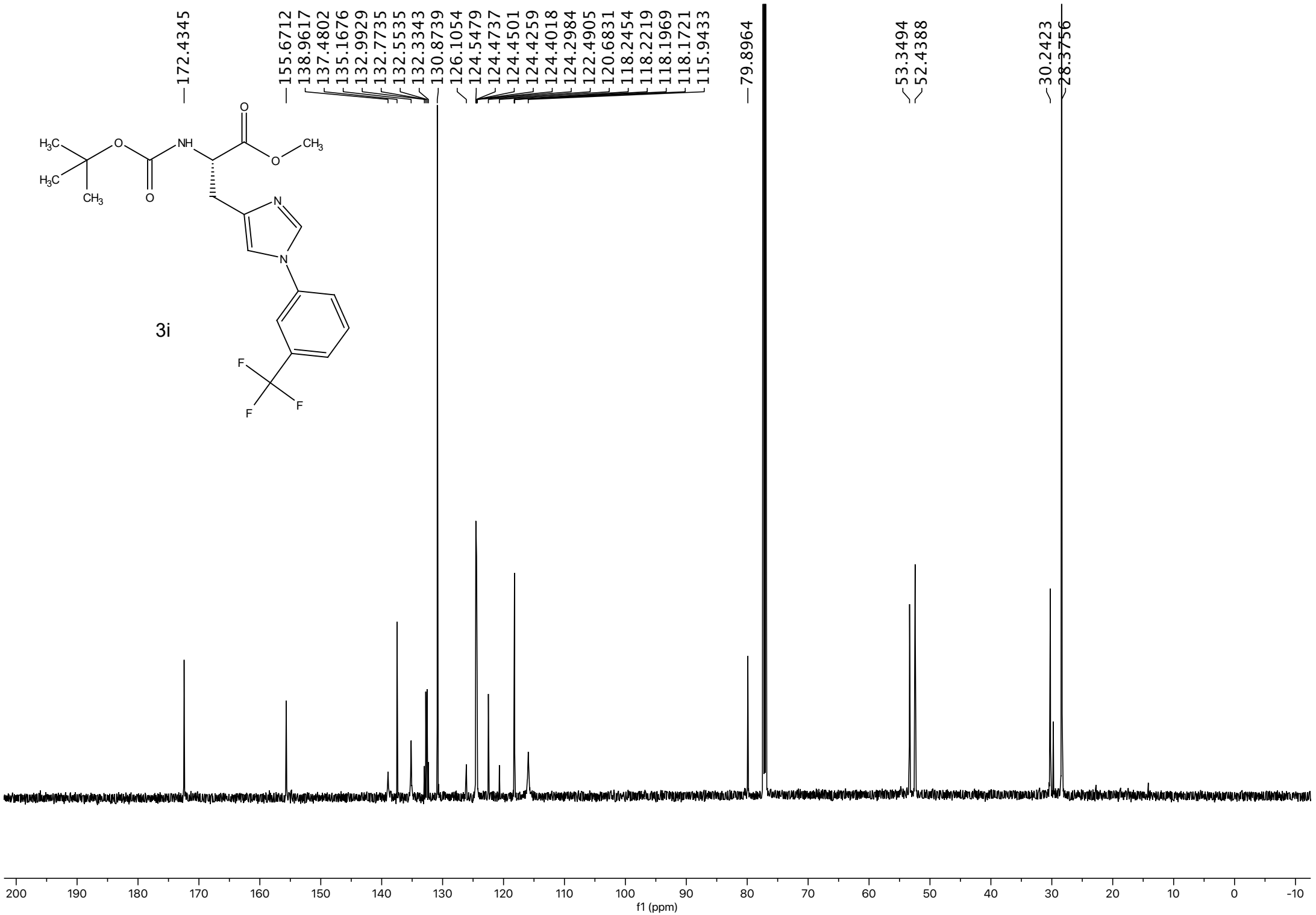
172.4345
155.6712
138.9617
137.4802
135.1676
132.9929
132.7735
132.5535
132.3343
130.8739
126.1054
124.5479
124.4737
124.4501
124.4259
124.4018
124.2984
122.4905
120.6831
118.2454
118.2219
118.1969
118.1721
115.9433
79.8964
53.3494
52.4388
30.2423
28.3756
3i
f1 (ppm)

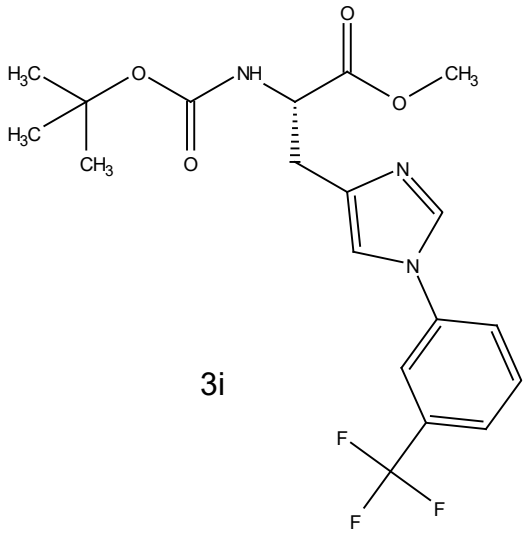
H3C
O
NH
O
CH3
H3C
CH3
O
O
N
N
F
F
F

3i

-62.8760
10
0
-10
-20
-30
-40
-50
-60
-70
-80
-90
-100
-110
-120
-130
-140
-150
-160
-170
-180
-190
-200
-210
f1 (ppm)

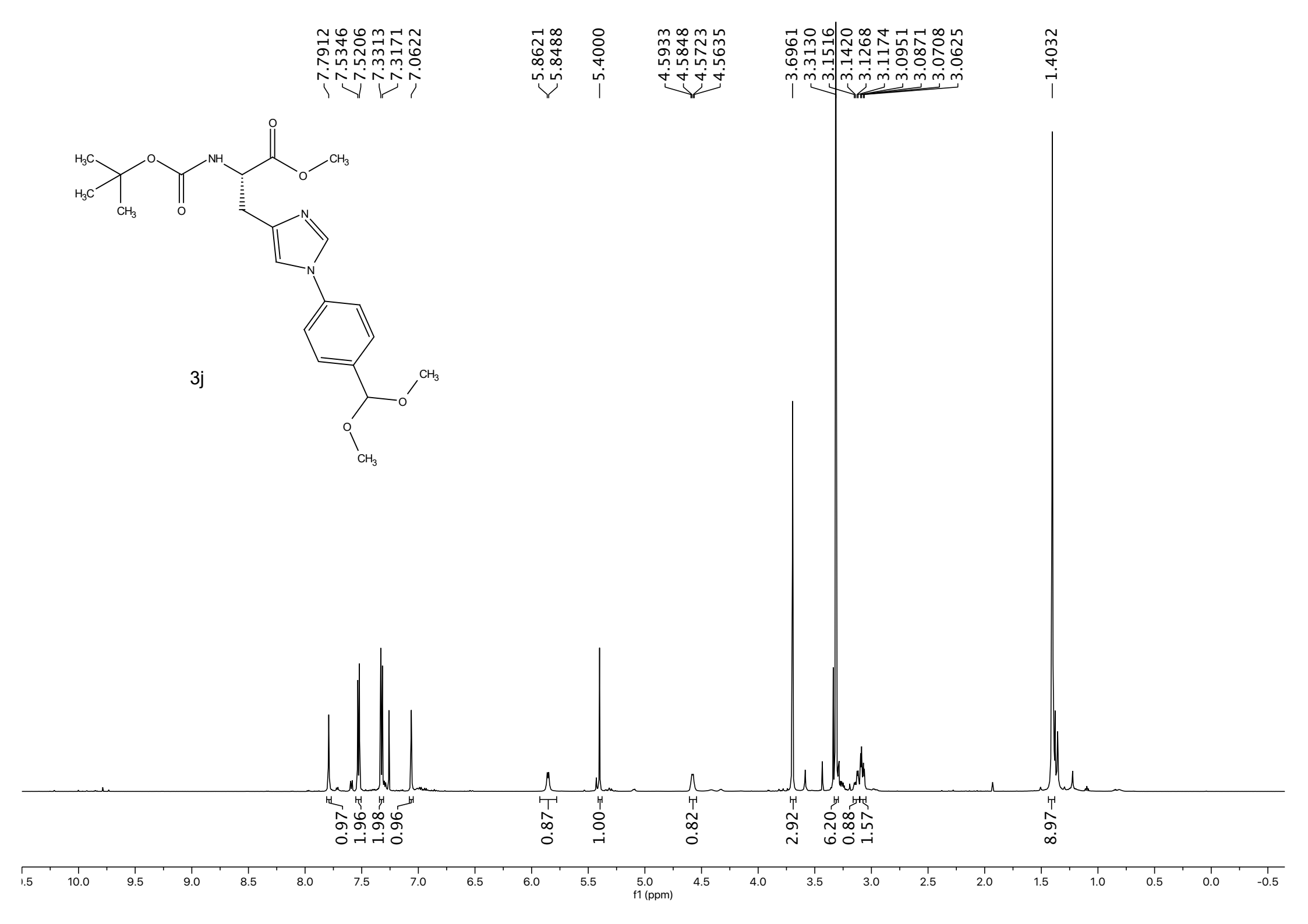
7.7912
7.5346
7.5206
7.3313
7.3171
7.0622
5.8621
5.8488
5.4000
4.5933
4.5848
4.5723
4.5635
3.6961
3.3130
3.1516
3.1420
3.1268
3.1174
3.0951
3.0871
3.0708
3.0625
1.4032
3j
0.97
1.96
1.98
0.96
0.87
1.00
0.82
2.92
6.20
0.88
1.57
8.97
f1 (ppm)

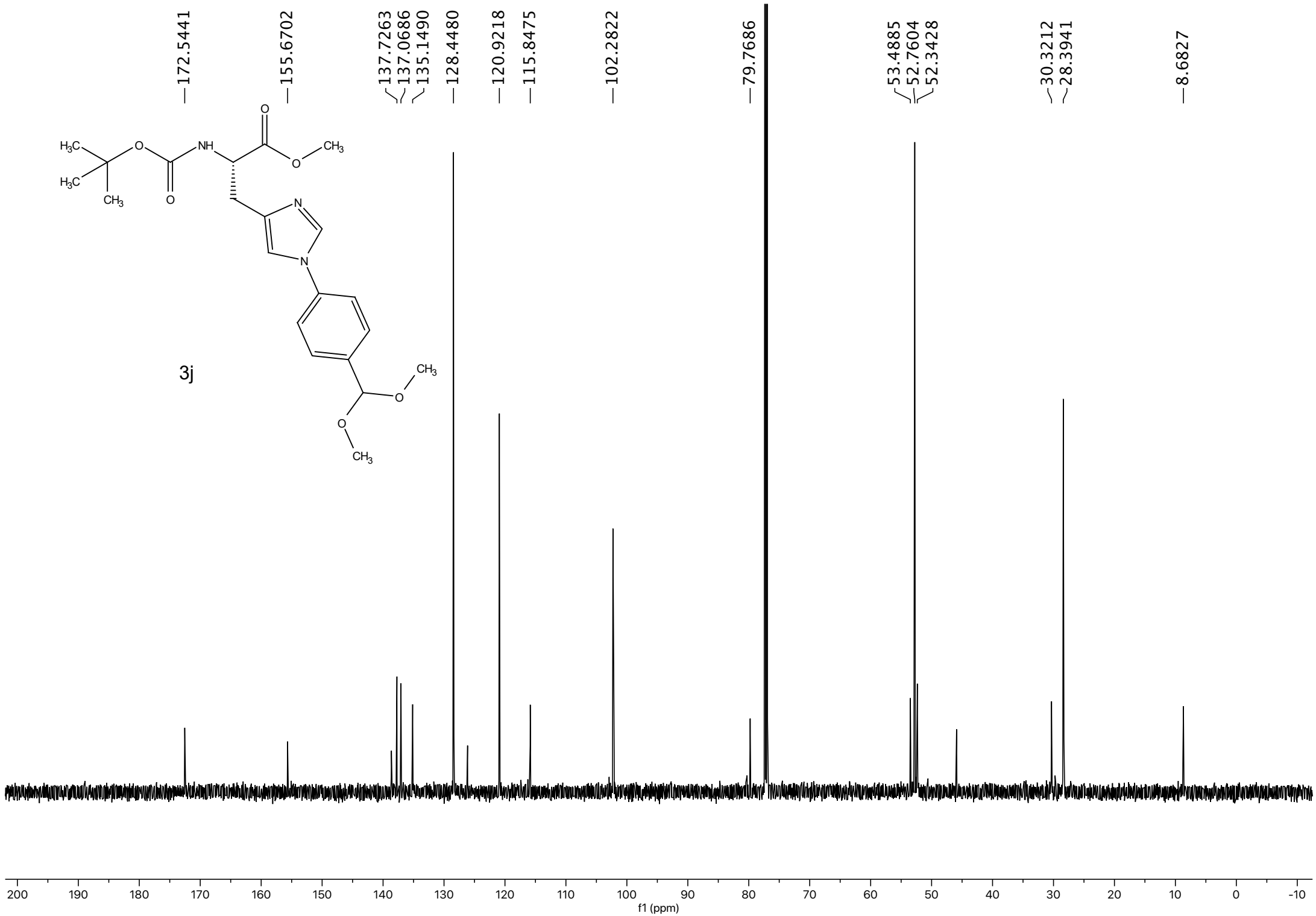
172.5441
155.6702
137.7263
137.0686
135.1490
128.4480
120.9218
115.8475
102.2822
79.7686
53.4885
52.7604
52.3428
30.3212
28.3941
8.6827
3j
f1 (ppm)

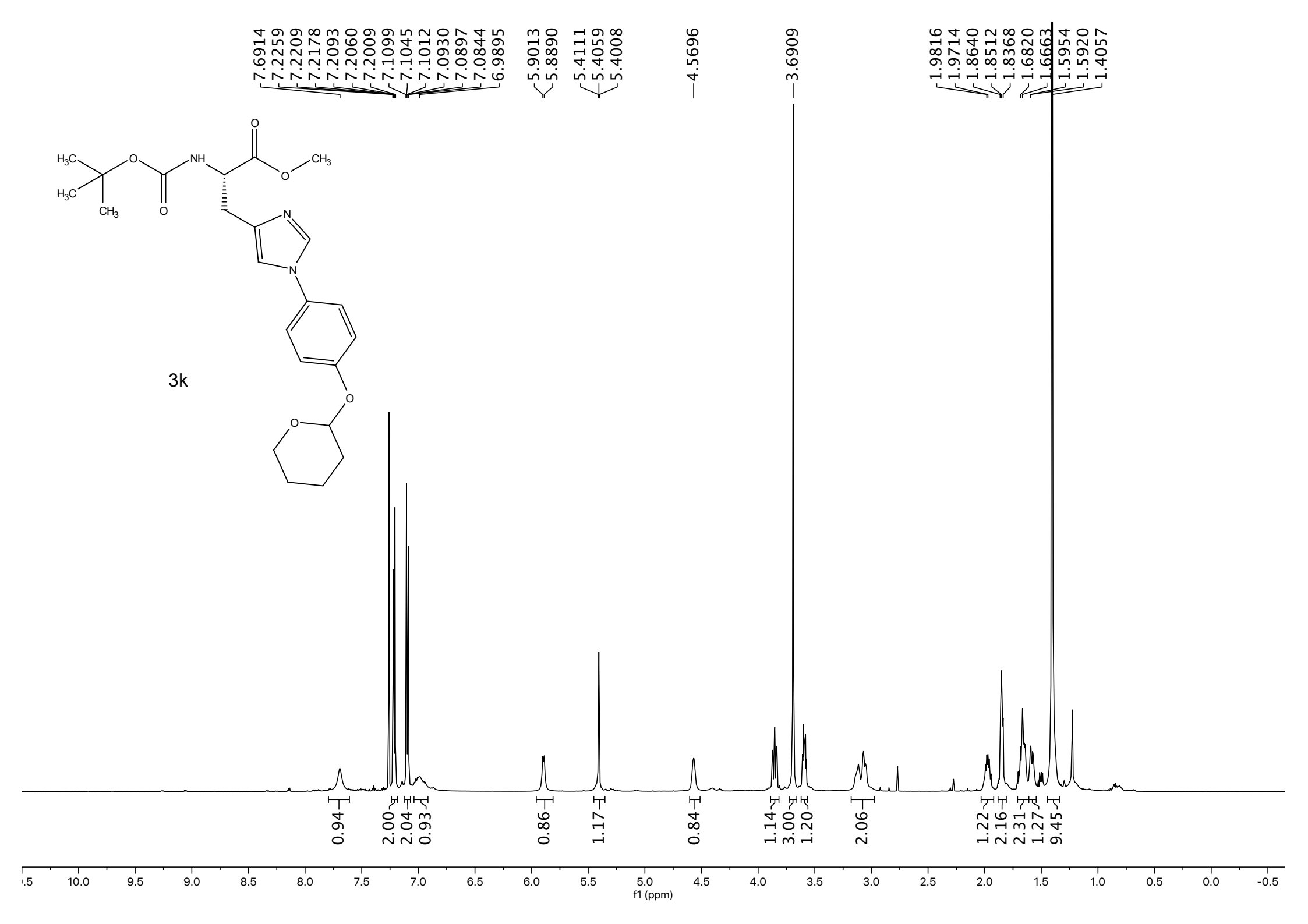
7.6914
7.2259
7.2209
7.2178
7.2093
7.2060
7.2009
7.1099
7.1045
7.1012
7.0930
7.0897
7.0844
6.9895
5.9013
5.8890
5.4111
5.4059
5.4008
4.5696
3.6909
1.9816
1.9714
1.8640
1.8512
1.8368
1.6820
1.6663
1.5954
1.5920
1.4057
3k
0.94
2.00
2.04
0.93
0.86
1.17
0.84
1.14
3.00
1.20
2.06
1.22
2.16
2.31
1.27
9.45
f1 (ppm)

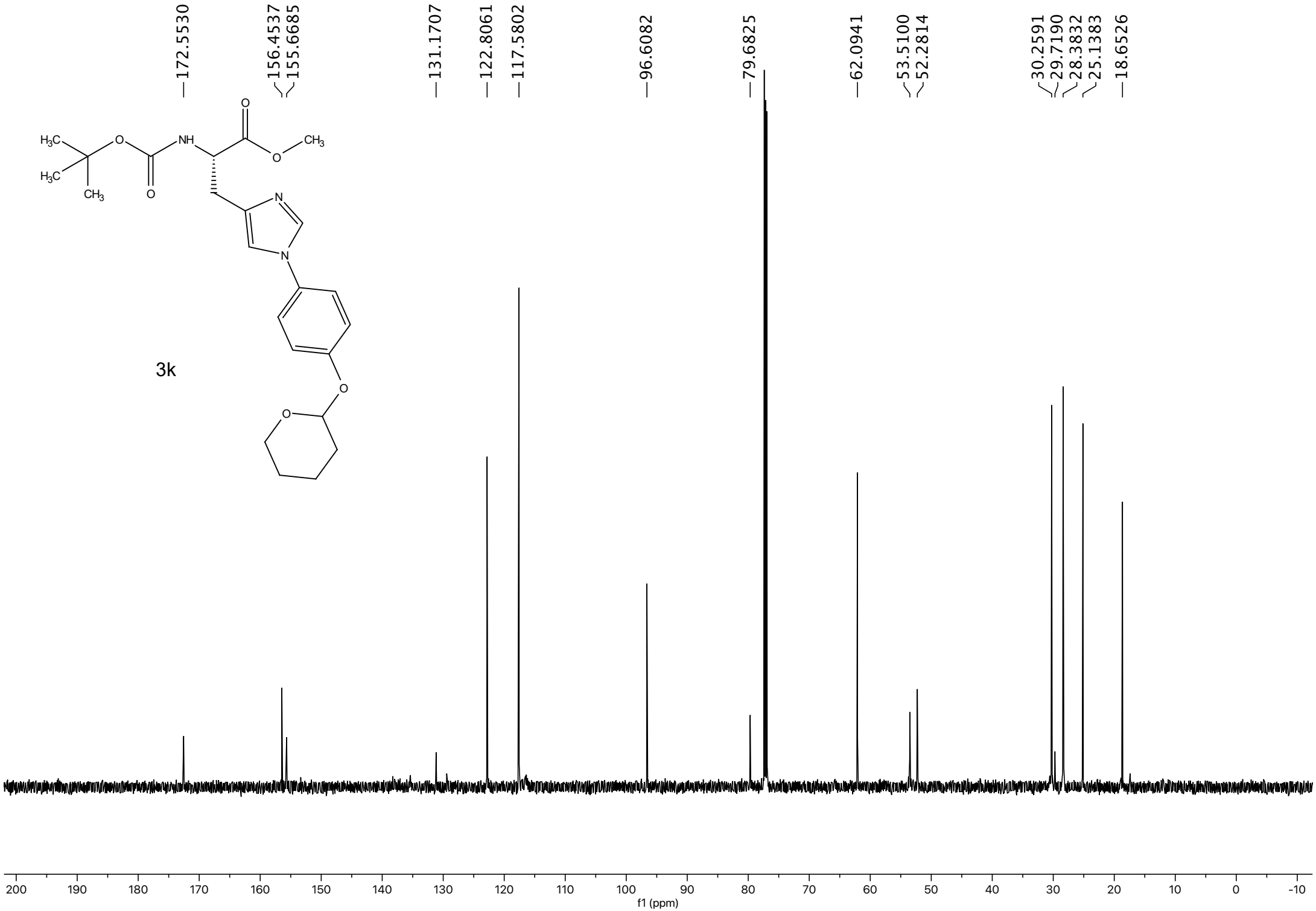
172.5530
156.4537
155.6685
131.1707
122.8061
117.5802
96.6082
79.6825
62.0941
53.5100
52.2814
30.2591
29.7190
28.3832
25.1383
18.6526
3k
f1 (ppm)

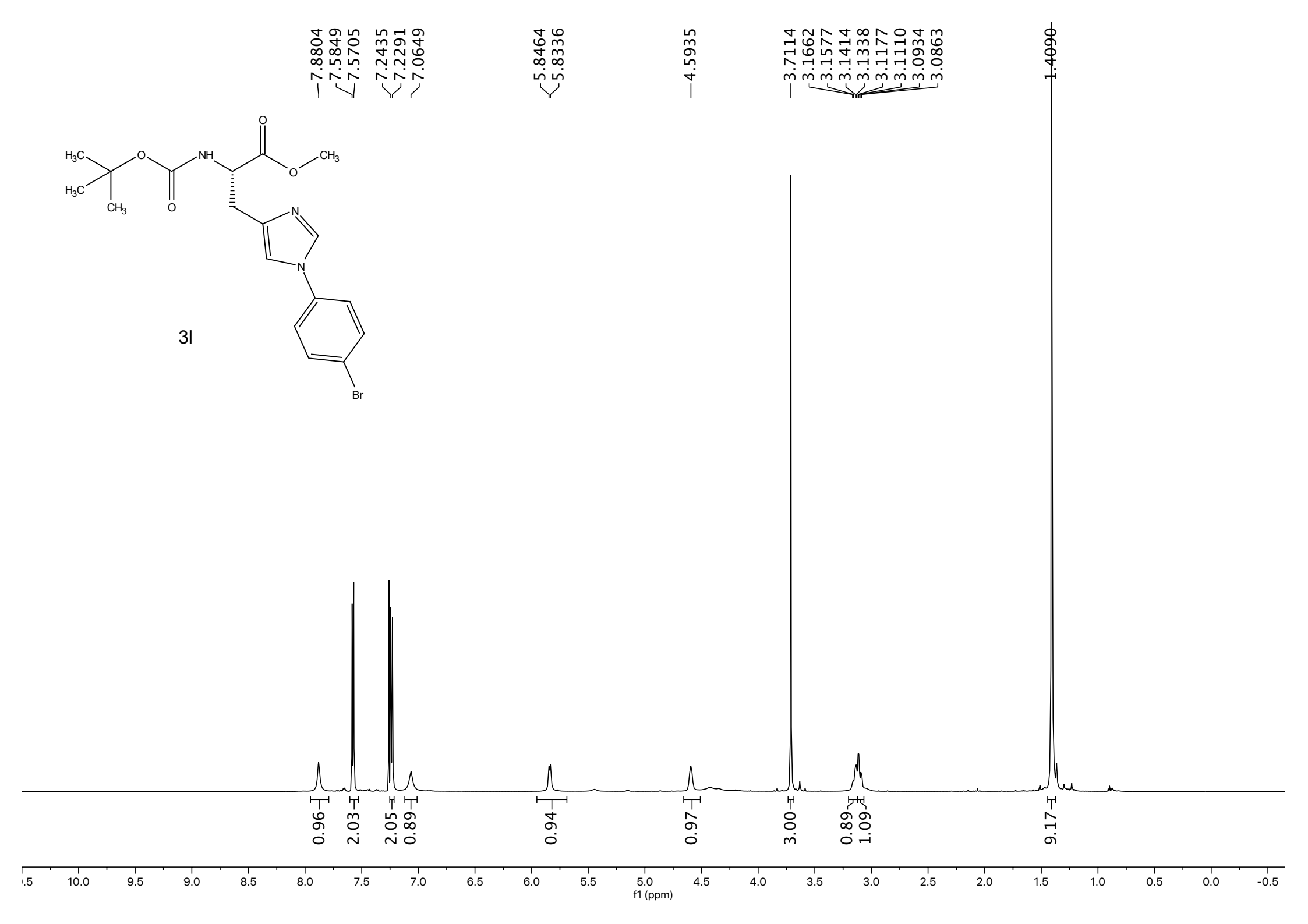
7.8804
7.5849
7.5705
7.2435
7.2291
7.0649
5.8464
5.8336
4.5935
3.7114
3.1662
3.1577
3.1414
3.1338
3.1177
3.1110
3.0934
3.0863
1.4090
3l
Br
0.96
2.03
2.05
0.89
0.94
0.97
3.00
0.89
1.09
9.17
f1 (ppm)

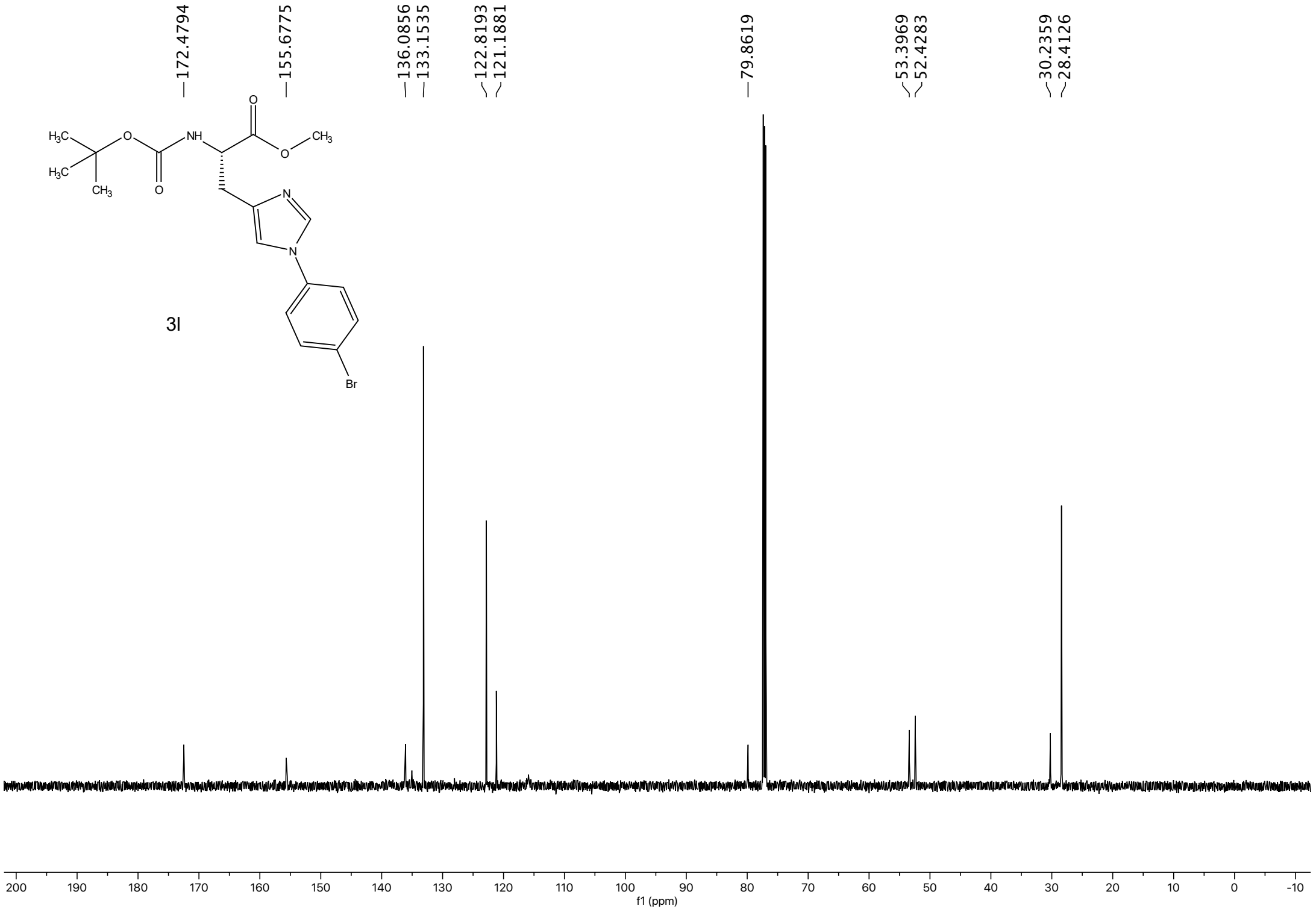
172.4794
155.6775
136.0856
133.1535
122.8193
121.1881
79.8619
53.3969
52.4283
30.2359
28.4126
3l
Br
f1 (ppm)

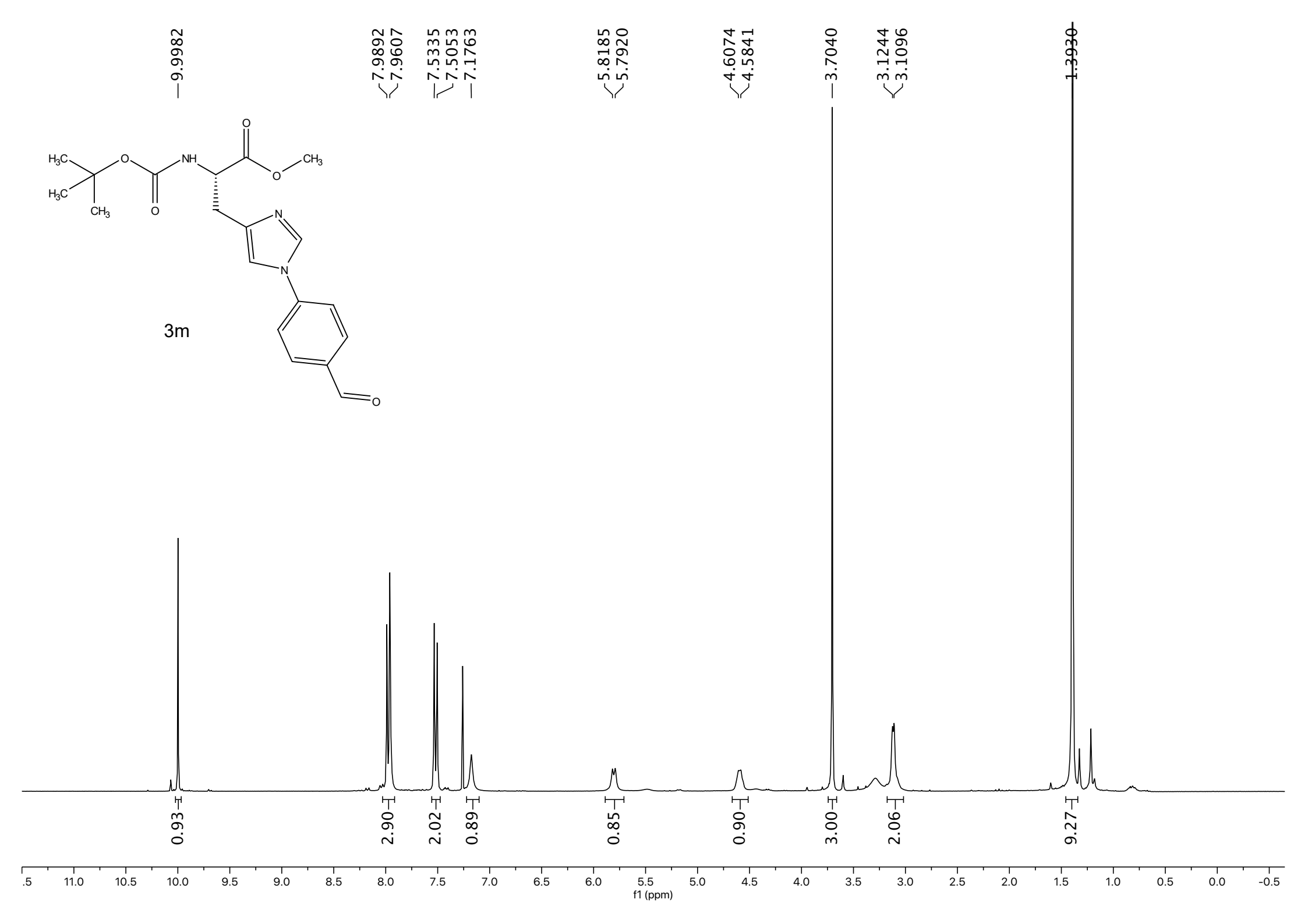
9.9982
7.9892
7.9607
7.5335
7.5053
7.1763
5.8185
5.7920
4.6074
4.5841
3.7040
3.1244
3.1096
1.3930
3m
0.93
2.90
2.02
0.89
0.85
0.90
3.00
2.06
9.27
f1 (ppm)

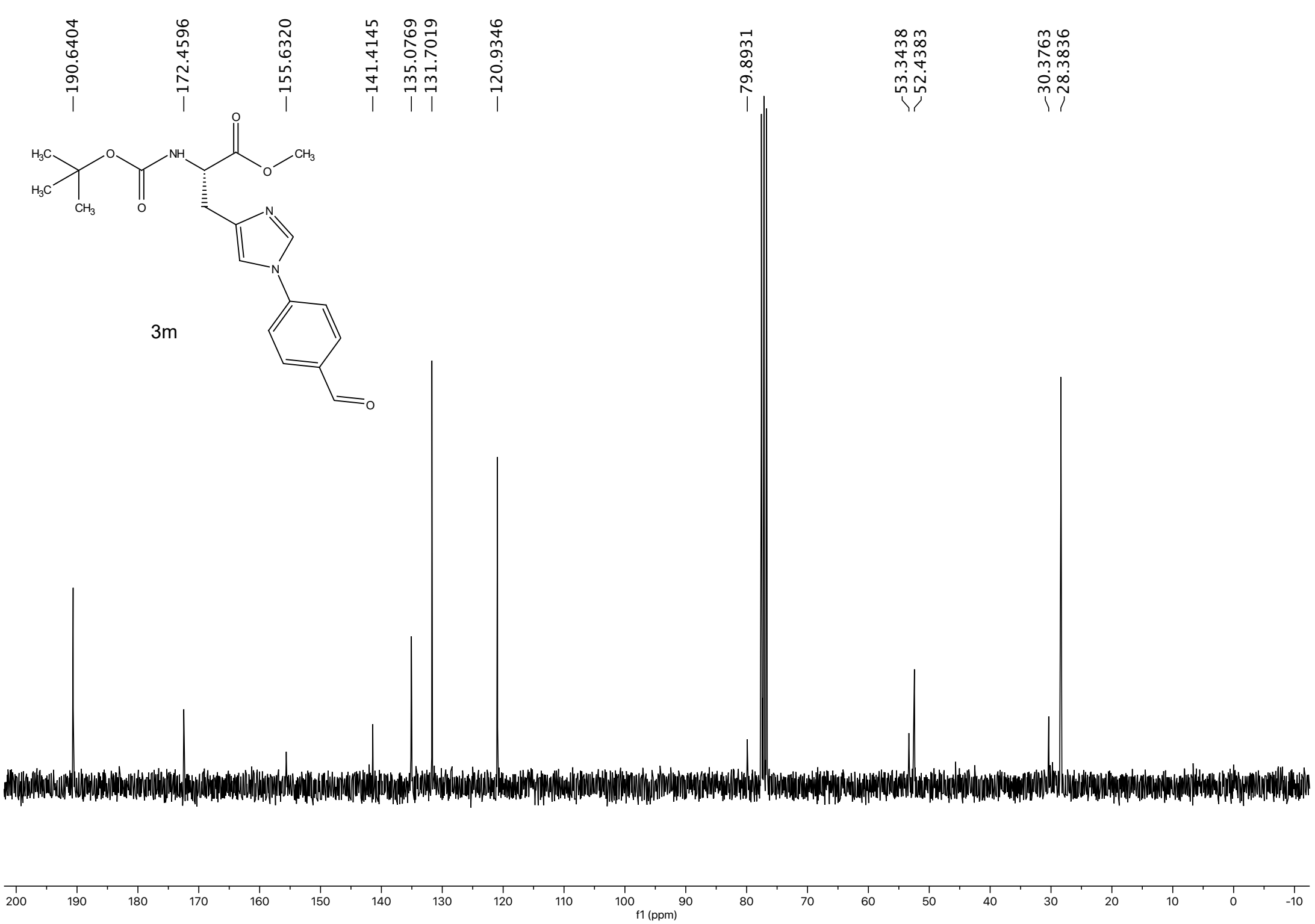
190.6404
172.4596
155.6320
141.4145
135.0769
131.7019
120.9346
79.8931
53.3438
52.4383
30.3763
28.3836
3m
200
190
180
170
160
150
140
130
120
110
100
90
80
70
60
50
40
30
20
10
0
-10
f1 (ppm)

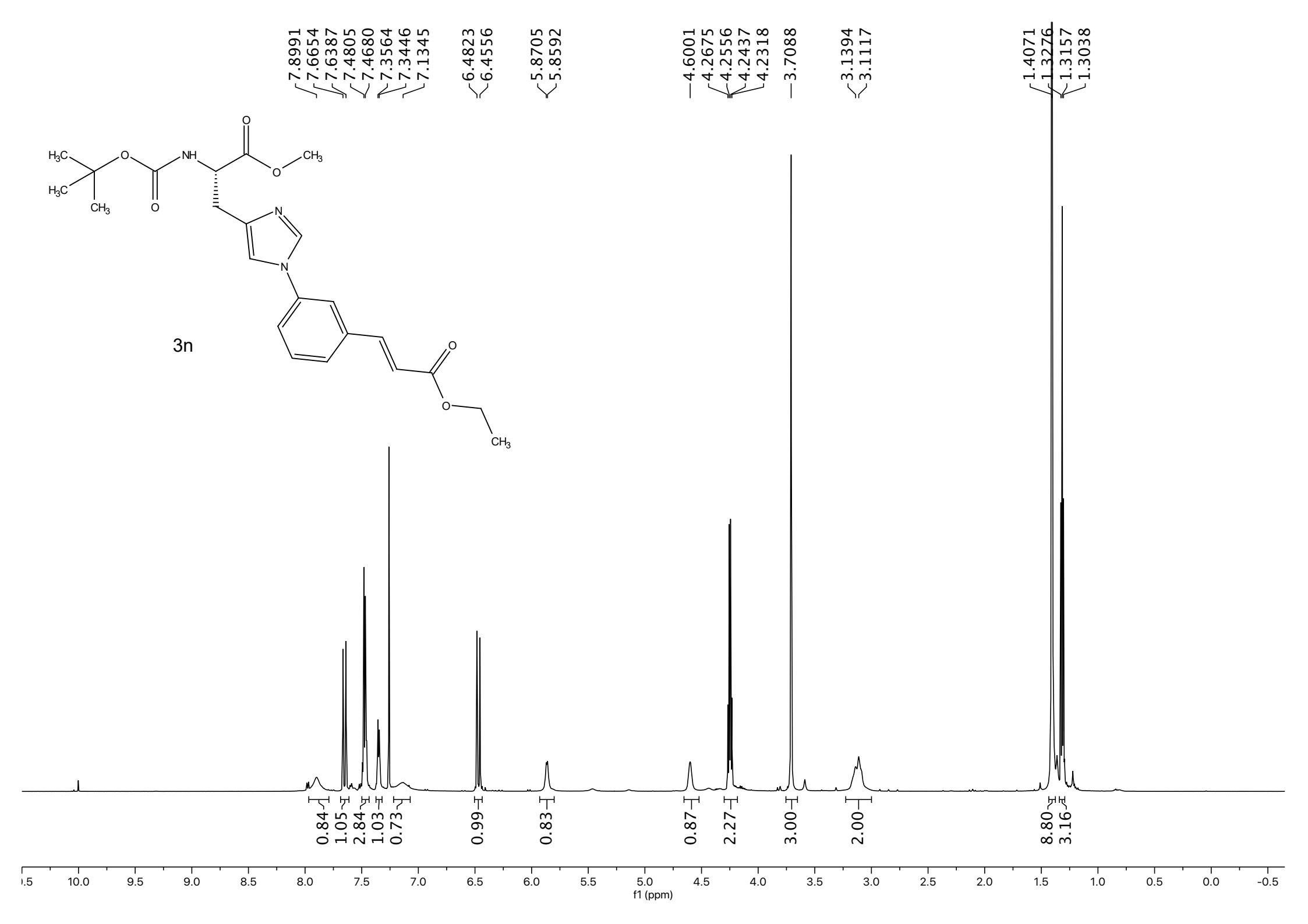
7.8991
7.6654
7.6387
7.4805
7.4680
7.3564
7.3446
7.1345
6.4823
6.4556
5.8705
5.8592
4.6001
4.2675
4.2556
4.2437
4.2318
3.7088
3.1394
3.1117
1.4071
1.3276
1.3157
1.3038
3n
0.84
1.05
2.84
1.03
0.73
0.99
0.83
0.87
2.27
3.00
2.00
8.80
3.16
f1 (ppm)

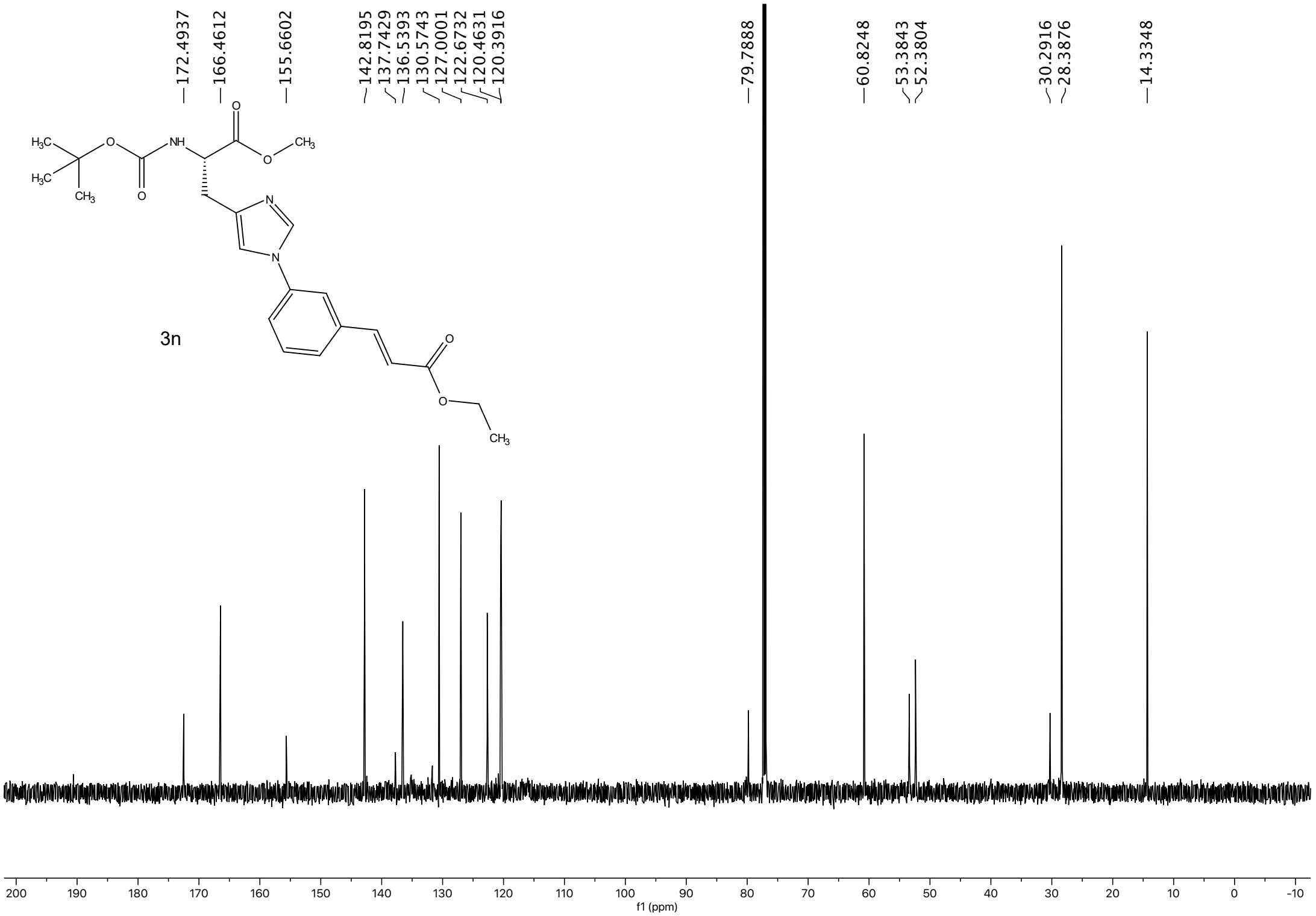
172.4937
166.4612
155.6602
142.8195
137.7429
136.5393
130.5743
127.0001
122.6732
120.4631
120.3916
79.7888
60.8248
53.3843
52.3804
30.2916
28.3876
14.3348
3n
f1 (ppm)

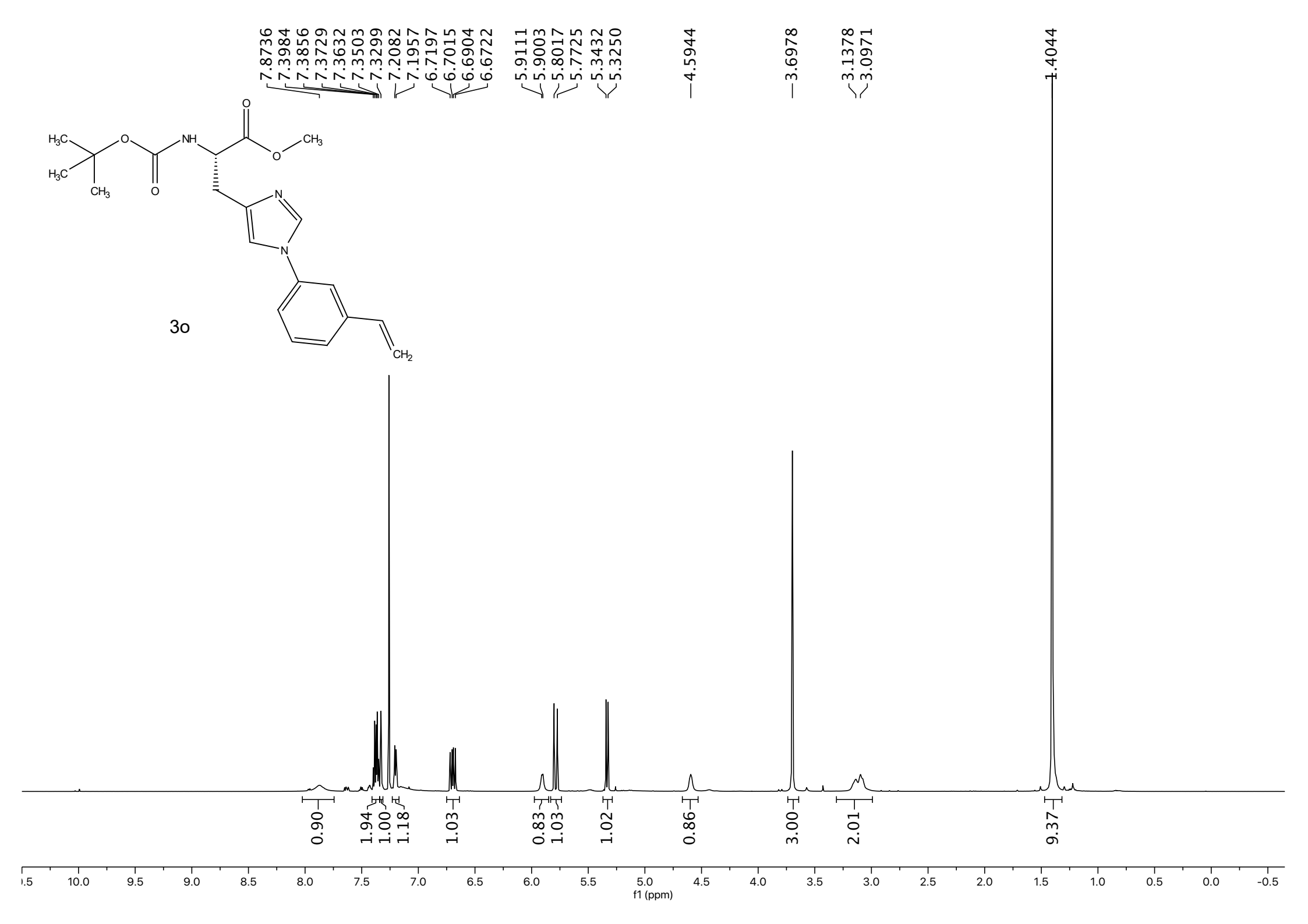
7.8736
7.3984
7.3856
7.3729
7.3632
7.3503
7.3299
7.2082
7.1957
6.7197
6.7015
6.6904
6.6722
5.9111
5.9003
5.8017
5.7725
5.3432
5.3250
4.5944
3.6978
3.1378
3.0971
1.4044
3o
0.90
1.94
1.00
1.18
1.03
0.83
1.03
1.02
0.86
3.00
2.01
9.37
f1 (ppm)

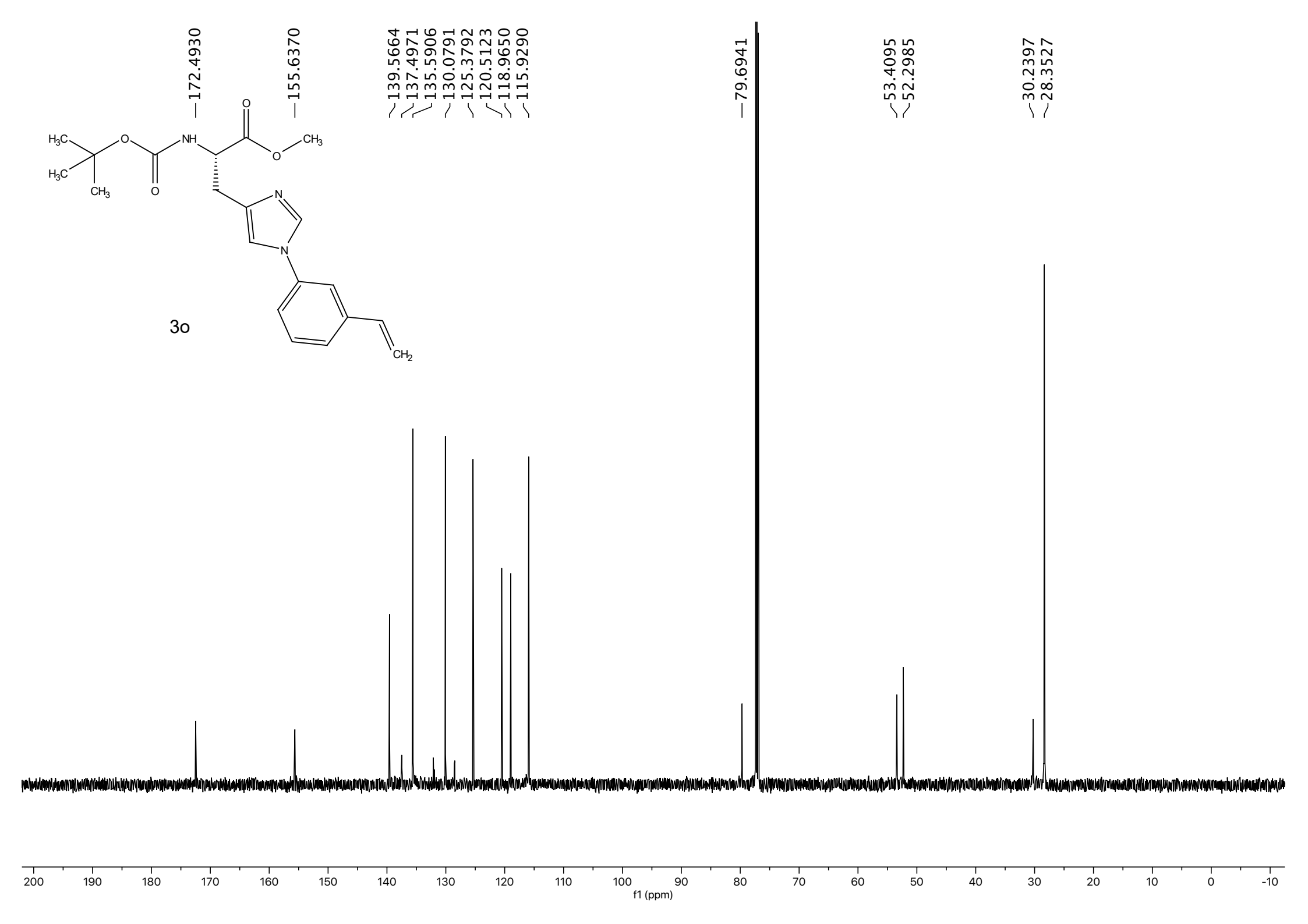
172.4930
155.6370
139.5664
137.4971
135.5906
130.0791
125.3792
120.5123
118.9650
115.9290
79.6941
53.4095
52.2985
30.2397
28.3527
3o
f1 (ppm)

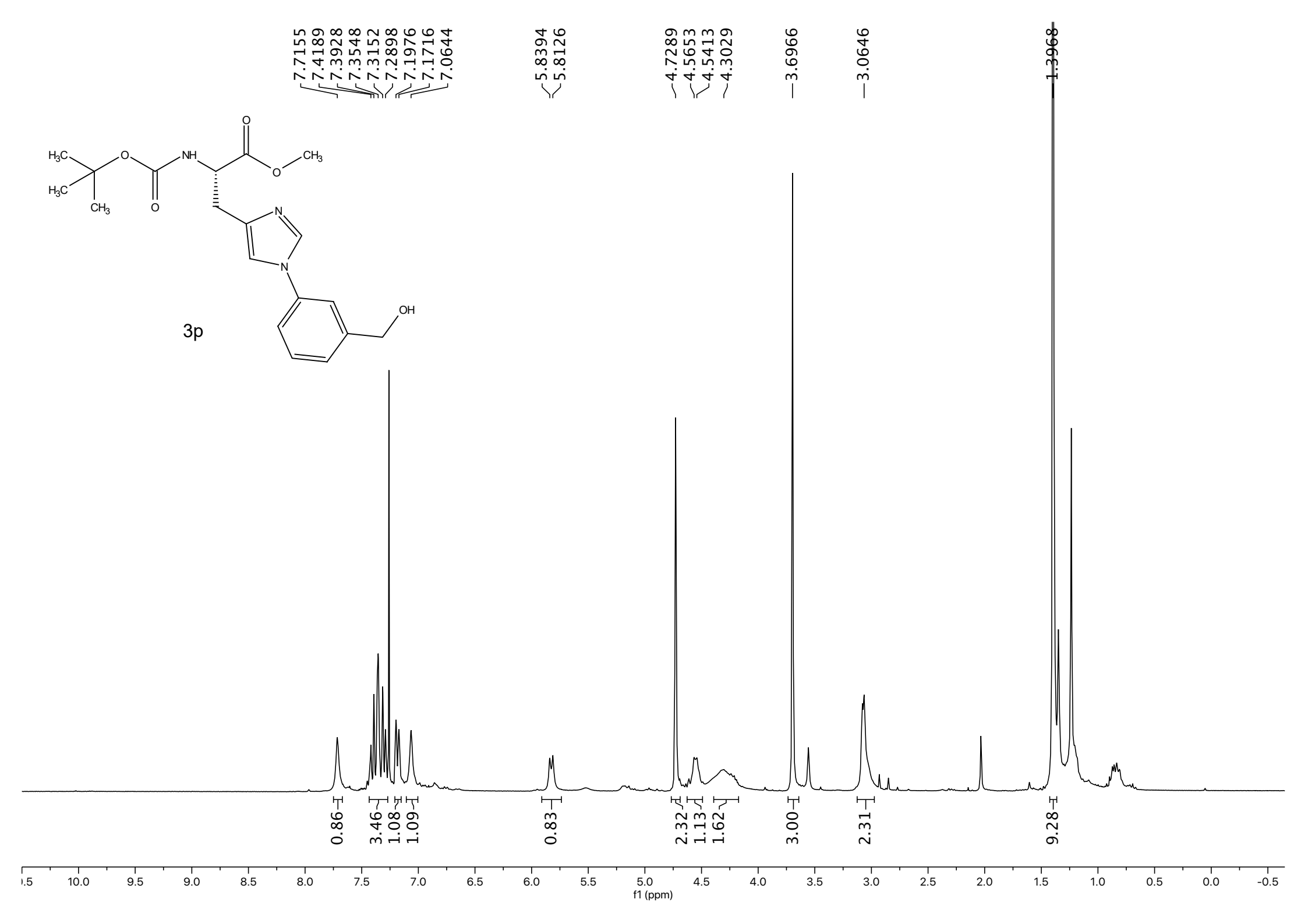
7.7155
7.4189
7.3928
7.3548
7.3152
7.2898
7.1976
7.1716
7.0644
5.8394
5.8126
4.7289
4.5653
4.5413
4.3029
3.6966
3.0646
1.3968
3p
0.86
3.46
1.08
1.09
0.83
2.32
1.13
1.62
3.00
2.31
9.28
f1 (ppm)

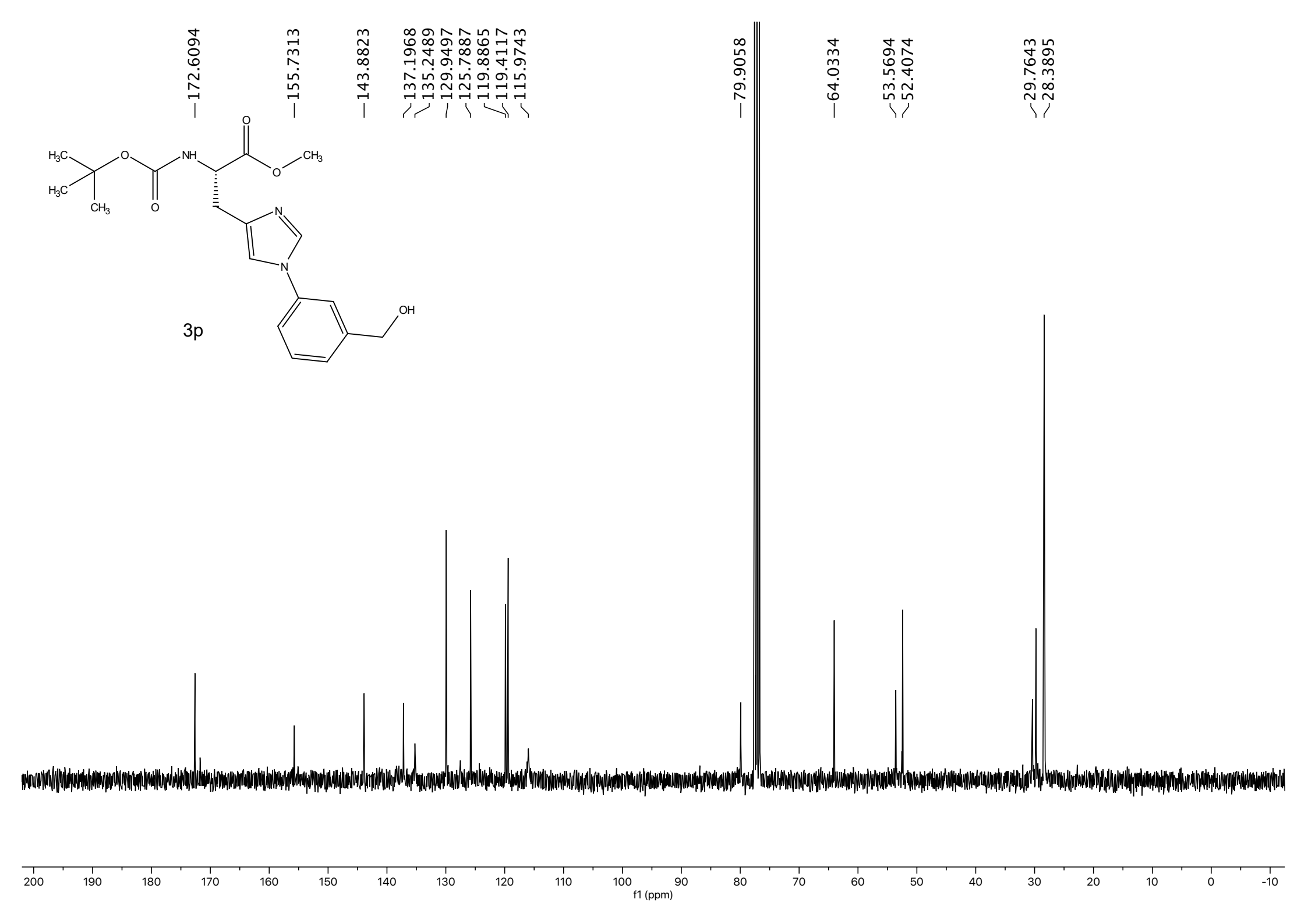
172.6094
155.7313
143.8823
137.1968
135.2489
129.9497
125.7887
119.8865
119.4117
115.9743
79.9058
64.0334
53.5694
52.4074
29.7643
28.3895
3p
f1 (ppm)

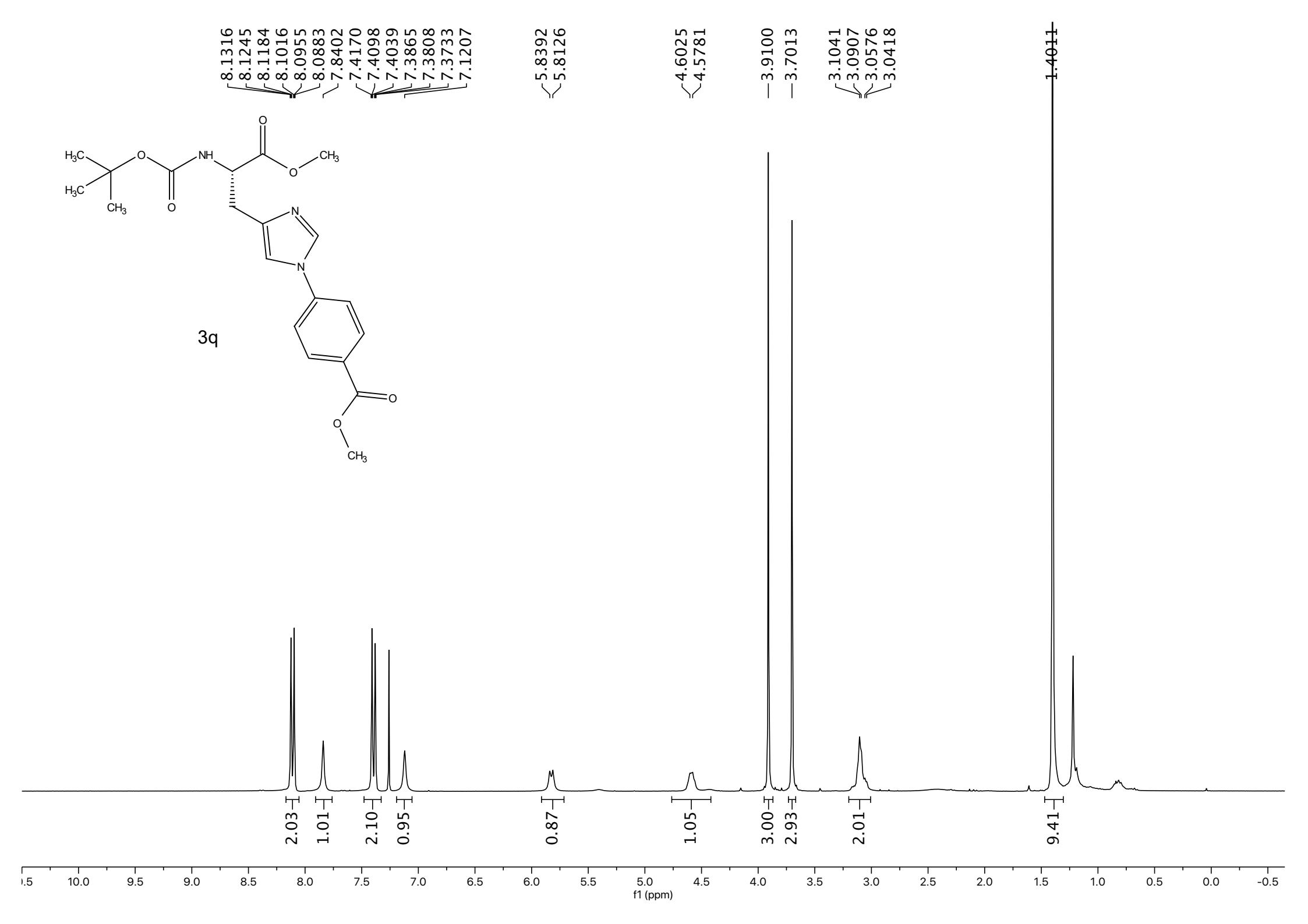
8.1316
8.1245
8.1184
8.1016
8.0955
8.0883
7.8402
7.4170
7.4098
7.4039
7.3865
7.3808
7.3733
7.1207
5.8392
5.8126
4.6025
4.5781
3.9100
3.7013
3.1041
3.0907
3.0576
3.0418
1.4011
3q
2.03
1.01
2.10
0.95
0.87
1.05
3.00
2.93
2.01
9.41
f1 (ppm)

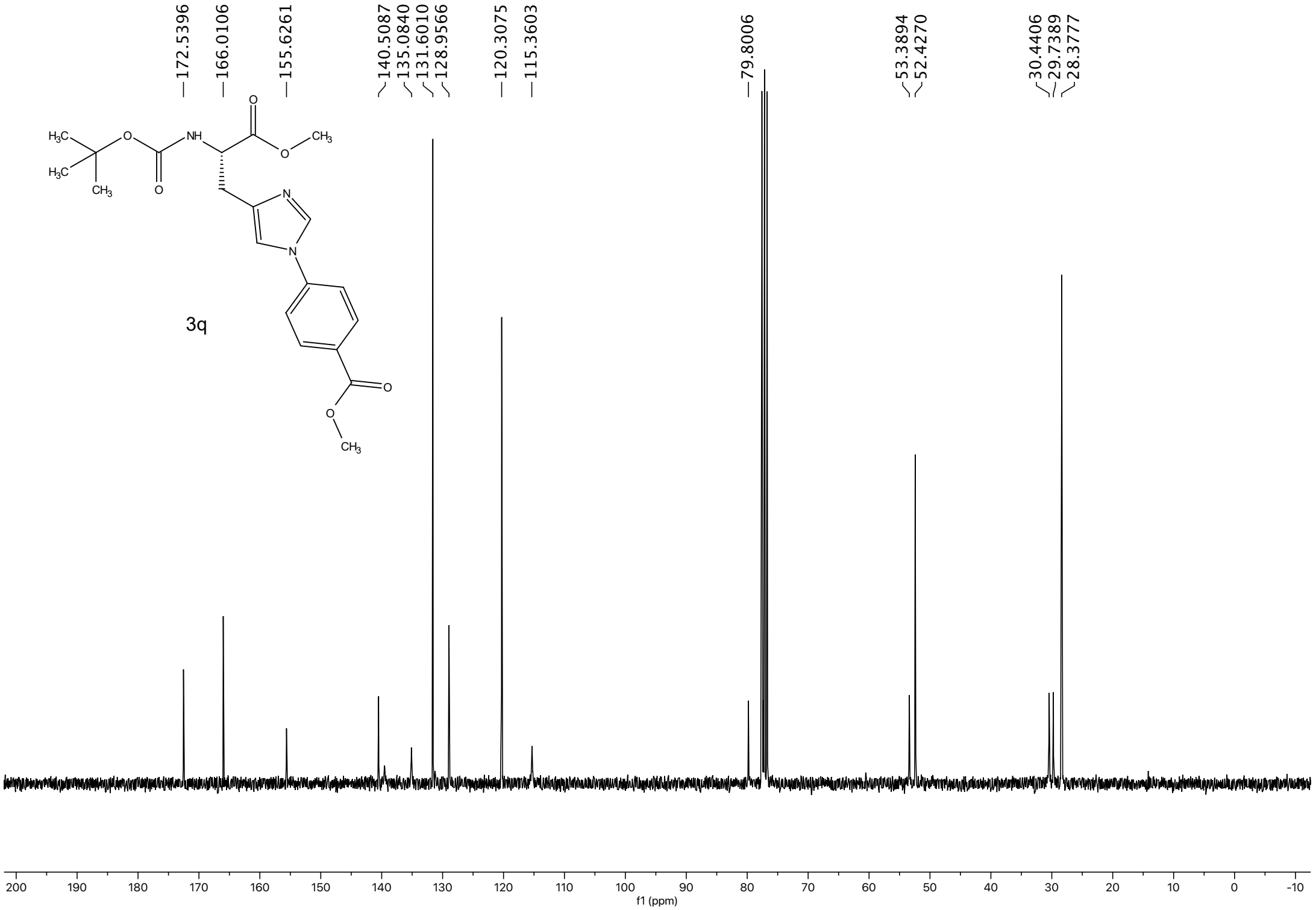
172.5396
166.0106
155.6261
140.5087
135.0840
131.6010
128.9566
120.3075
115.3603
79.8006
53.3894
52.4270
30.4406
29.7389
28.3777
3q
f1 (ppm)

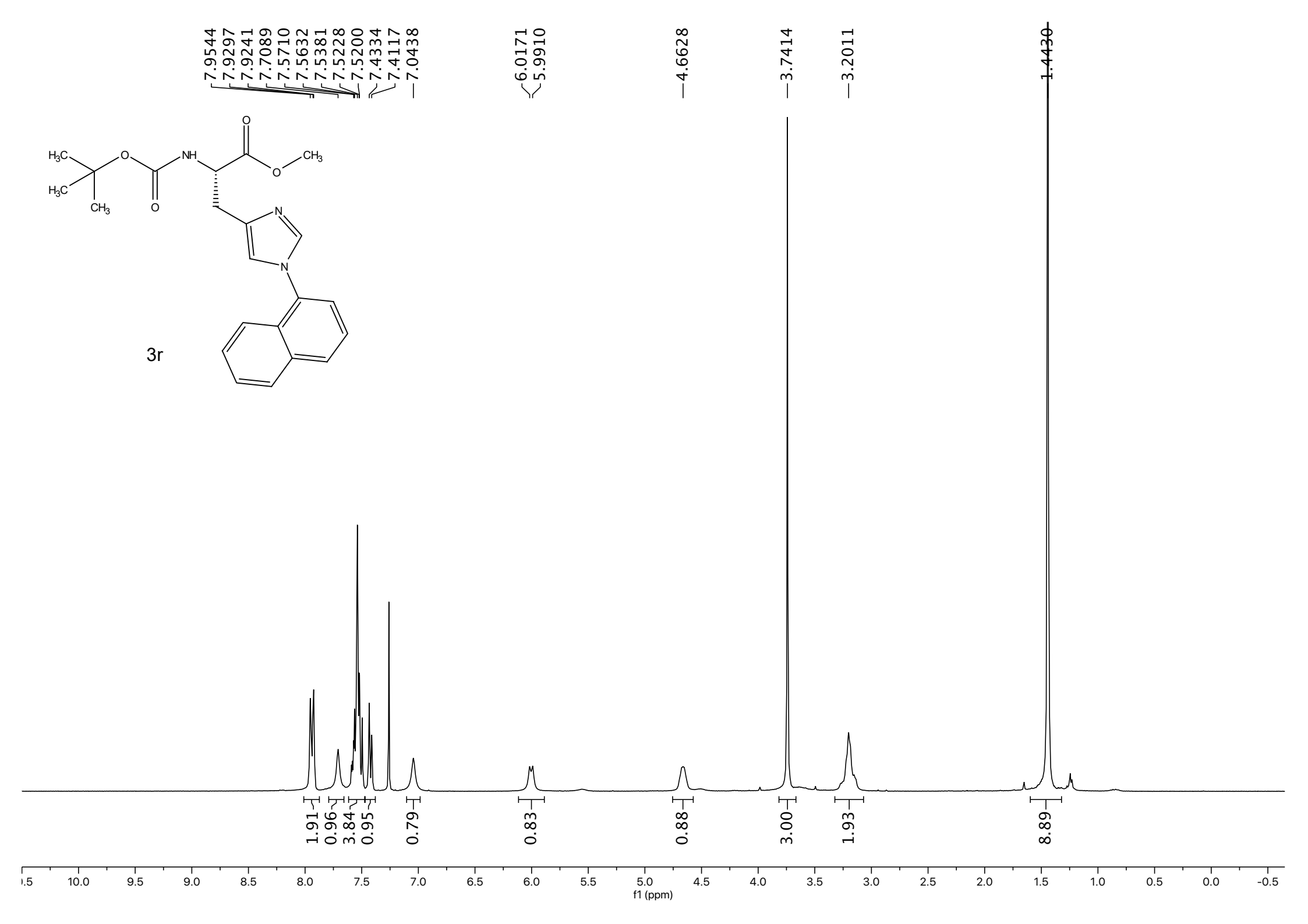
7.9544
7.9297
7.9241
7.7089
7.5710
7.5632
7.5381
7.5228
7.5200
7.4334
7.4117
7.0438
6.0171
5.9910
4.6628
3.7414
3.2011
1.4430
3r
1.91
0.96
3.84
0.95
0.79
0.83
0.88
3.00
1.93
8.89
f1 (ppm)

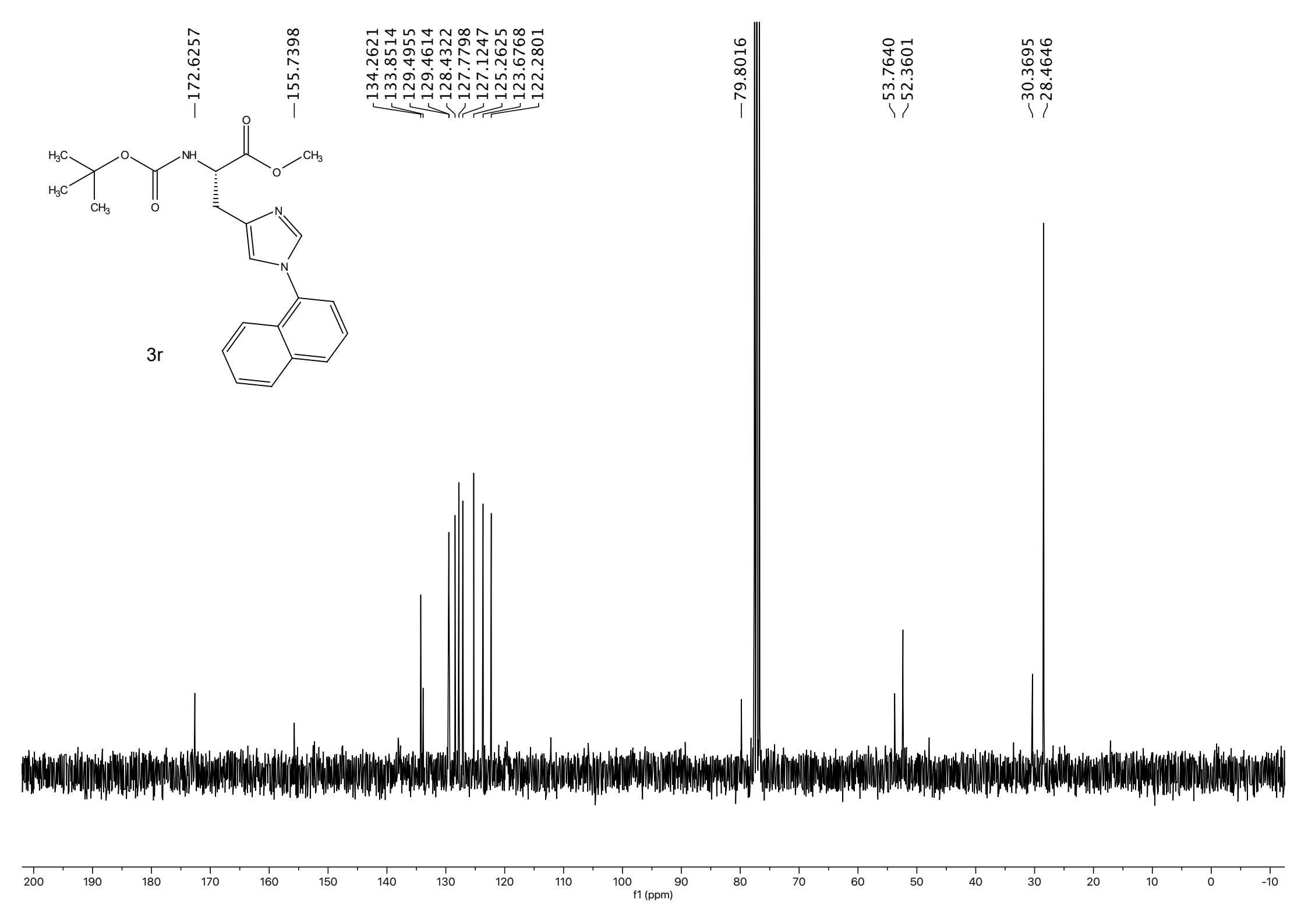
172.6257
155.7398
134.2621
133.8514
129.4955
129.4614
128.4322
127.7798
127.1247
125.2625
123.6768
122.2801
79.8016
53.7640
52.3601
30.3695
28.4646
3r
200
190
180
170
160
150
140
130
120
110
100
90
80
70
60
50
40
30
20
10
0
-10
f1 (ppm)

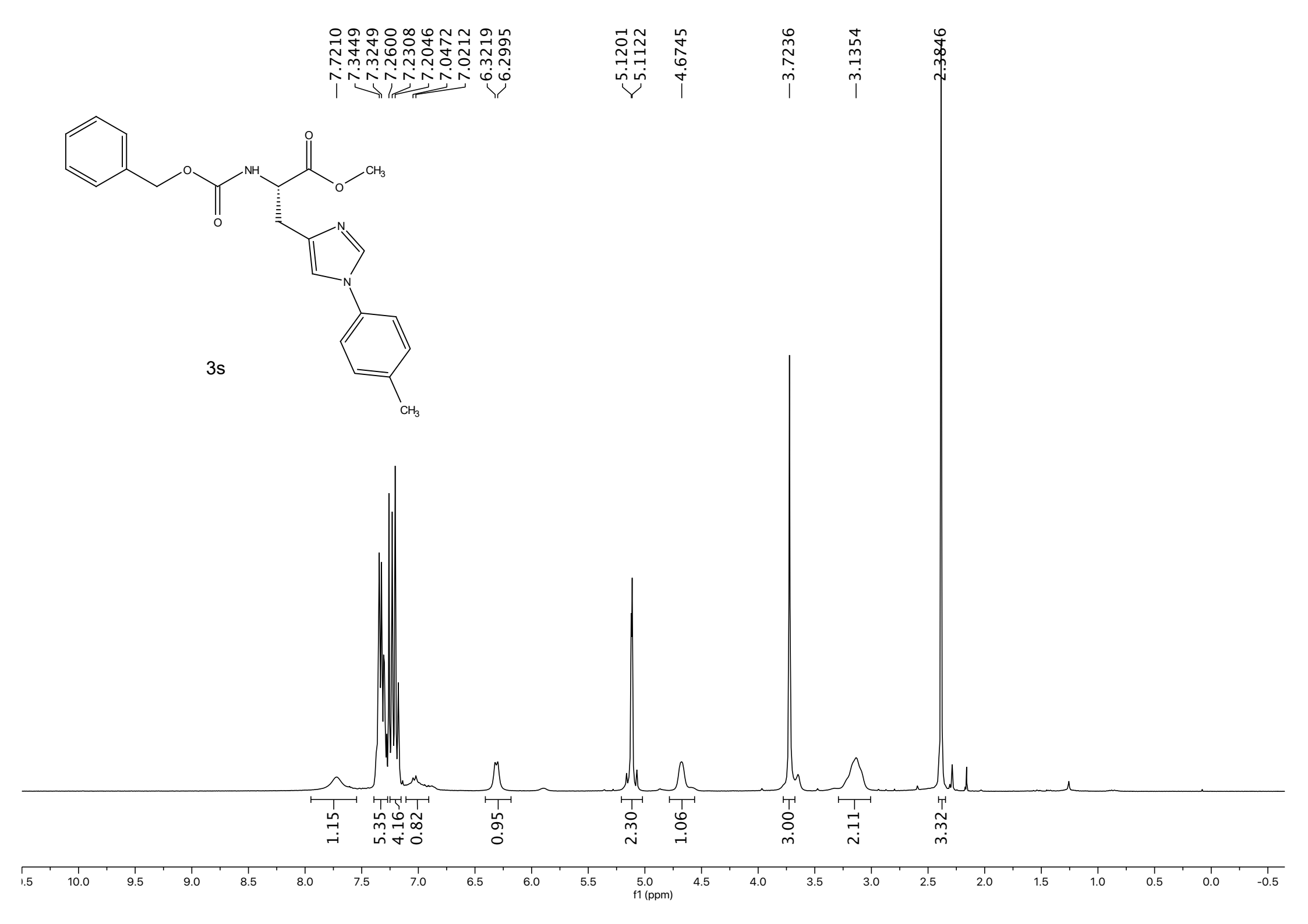
7.7210
7.3449
7.3249
7.2600
7.2308
7.2046
7.0472
7.0212
6.3219
6.2995
5.1201
5.1122
4.6745
3.7236
3.1354
2.3846
O
NH
O
O
O
CH3
N
N
CH3
3s
1.15
5.35
4.16
0.82
0.95
2.30
1.06
3.00
2.11
3.32
f1 (ppm)

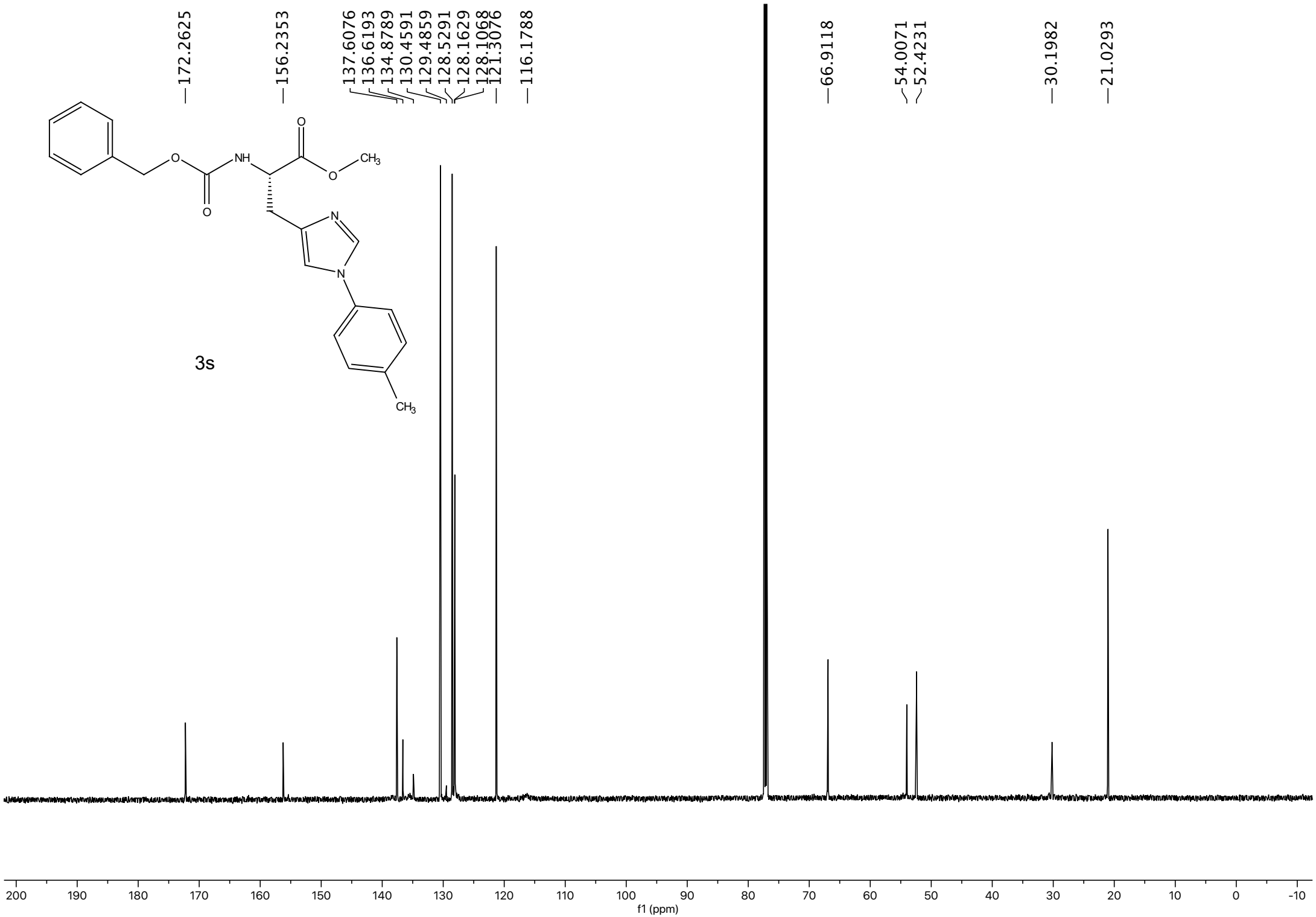
172.2625
156.2353
137.6076
136.6193
134.8789
130.4591
129.4859
128.5291
128.1629
128.1068
121.3076
116.1788
66.9118
54.0071
52.4231
30.1982
21.0293
O
NH
O
O
O
CH3
N
N
CH3
3s
200
190
180
170
160
150
140
130
120
110
100
90
80
70
60
50
40
30
20
10
0
-10
f1 (ppm)

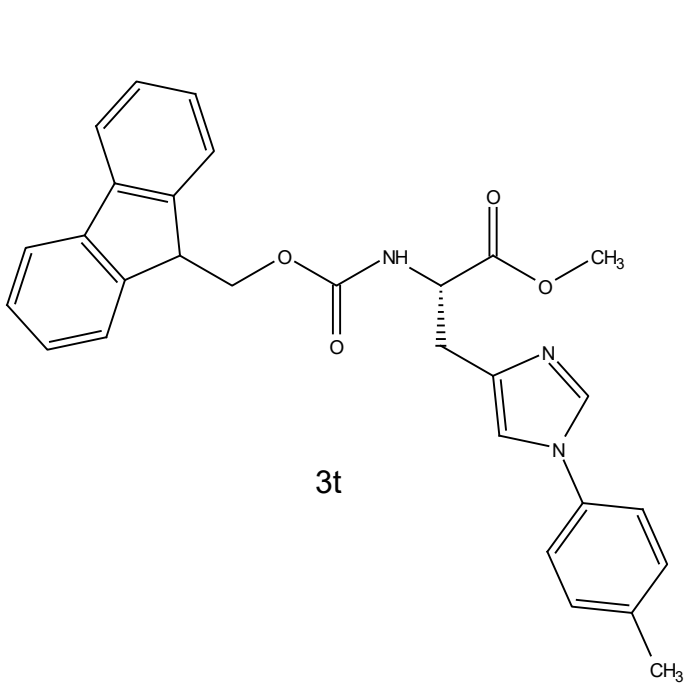
O
NH
O
O
CH3
O
N
N
CH3

3t

1.37
0.80
1.73
1.92
8.70
0.96
0.93
1.74
0.94
2.88
0.83
0.99
3.00
11.5
11.0
10.5
10.0
9.5
9.0
8.5
8.0
7.5
7.0
6.5
6.0
5.5
5.0
4.5
4.0
3.5
3.0
2.5
2.0
1.5
1.0
0.5
0.0
-0.5
f1 (ppm)

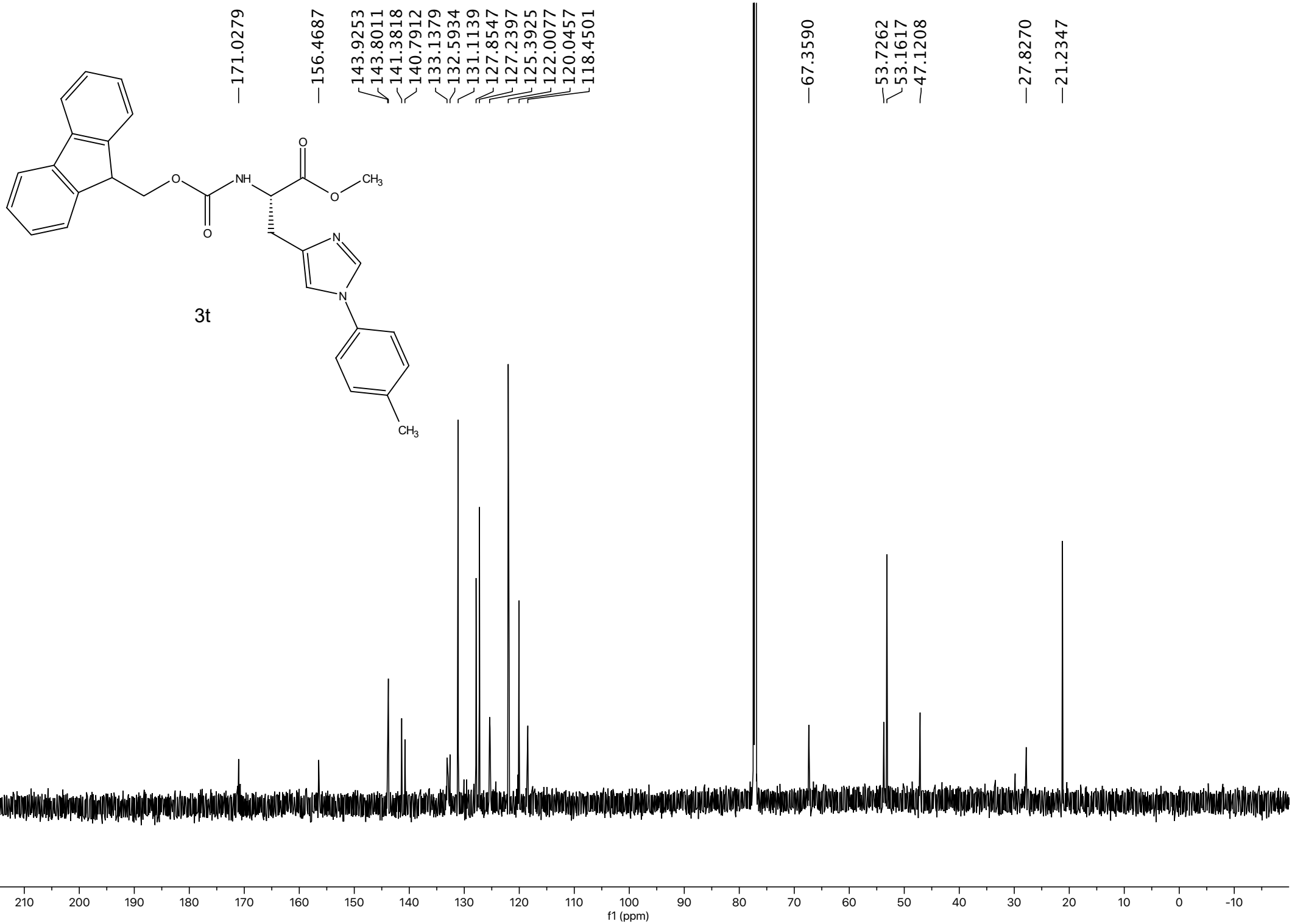
171.0279
156.4687
143.9253
143.8011
141.3818
140.7912
133.1379
132.5934
131.1139
127.8547
127.2397
125.3925
122.0077
120.0457
118.4501
67.3590
53.7262
53.1617
47.1208
27.8270
21.2347
O
NH
O
O
CH3
O
N
N
CH3
3t
f1 (ppm)

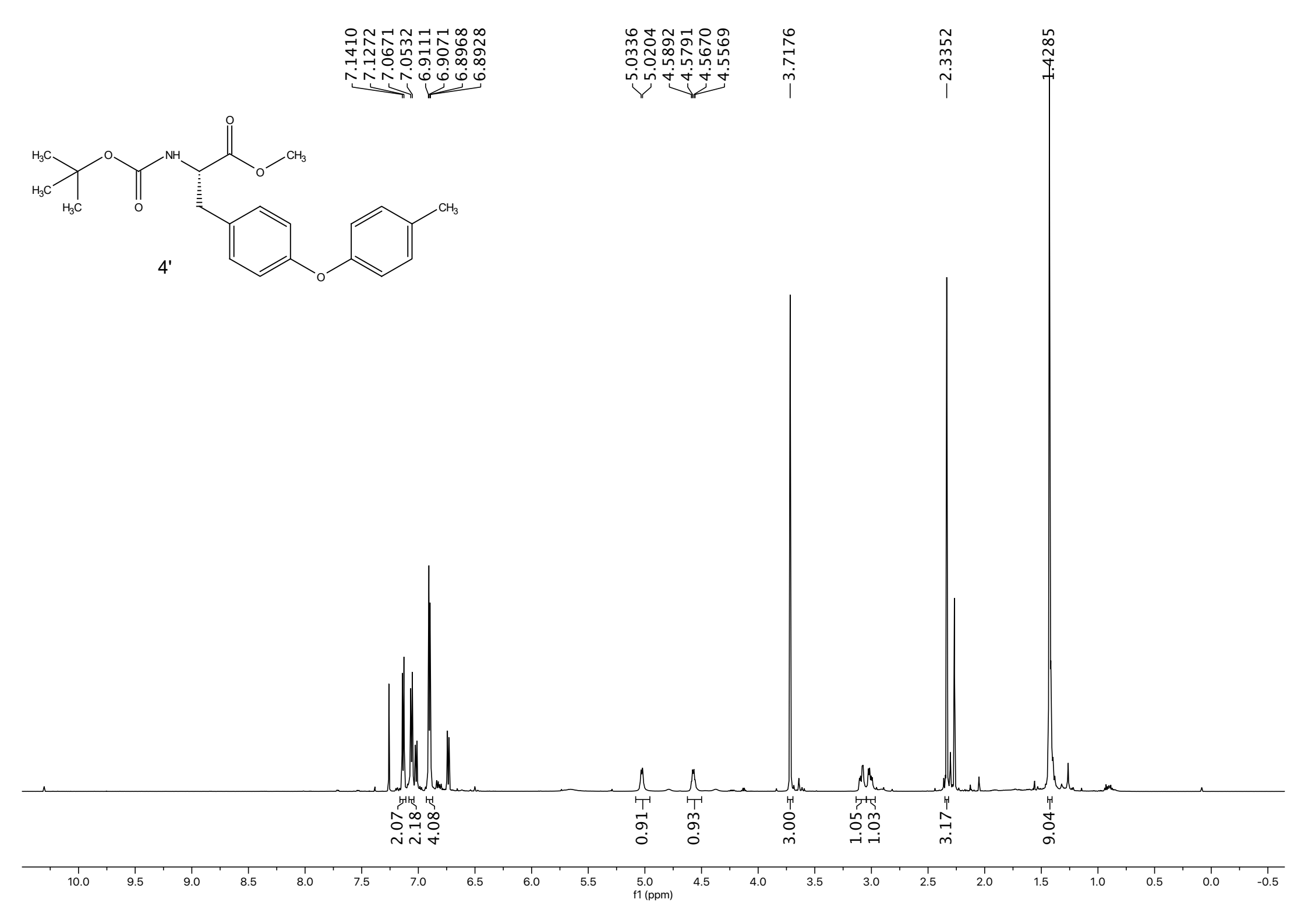
7.1410
7.1272
7.0671
7.0532
6.9111
6.9071
6.8968
6.8928
5.0336
5.0204
4.5892
4.5791
4.5670
4.5569
3.7176
2.3352
1.4285
4'
2.07
2.18
4.08
0.91
0.93
3.00
1.05
1.03
3.17
9.04
f1 (ppm)

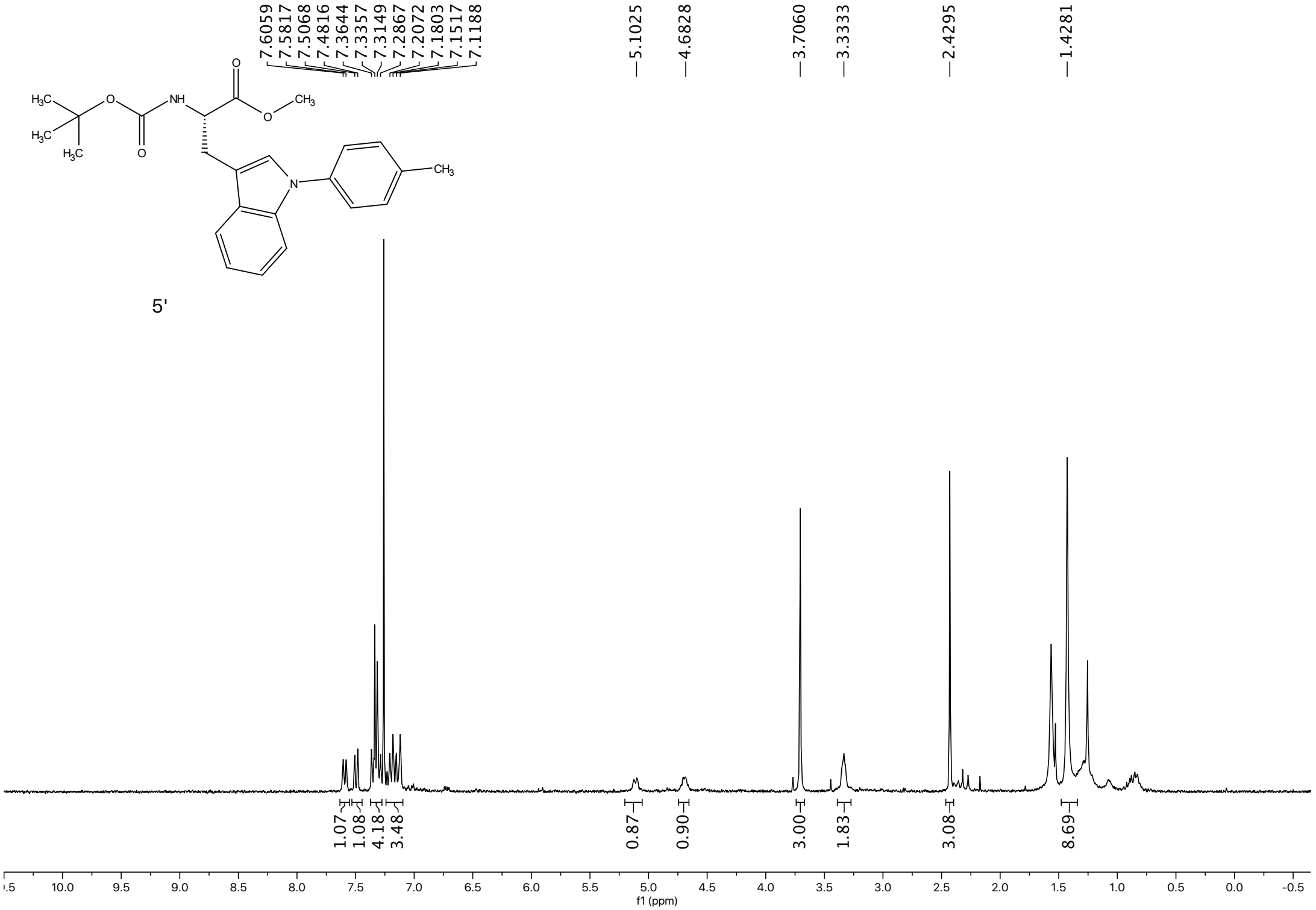
7.6059
7.5817
7.5068
7.4816
7.3644
7.3357
7.3149
7.2867
7.2072
7.1803
7.1517
7.1188
5.1025
4.6828
3.7060
3.3333
2.4295
1.4281
1.07
1.08
4.18
3.48
0.87
0.90
3.00
1.83
3.08
8.69
f1 (ppm)

5'

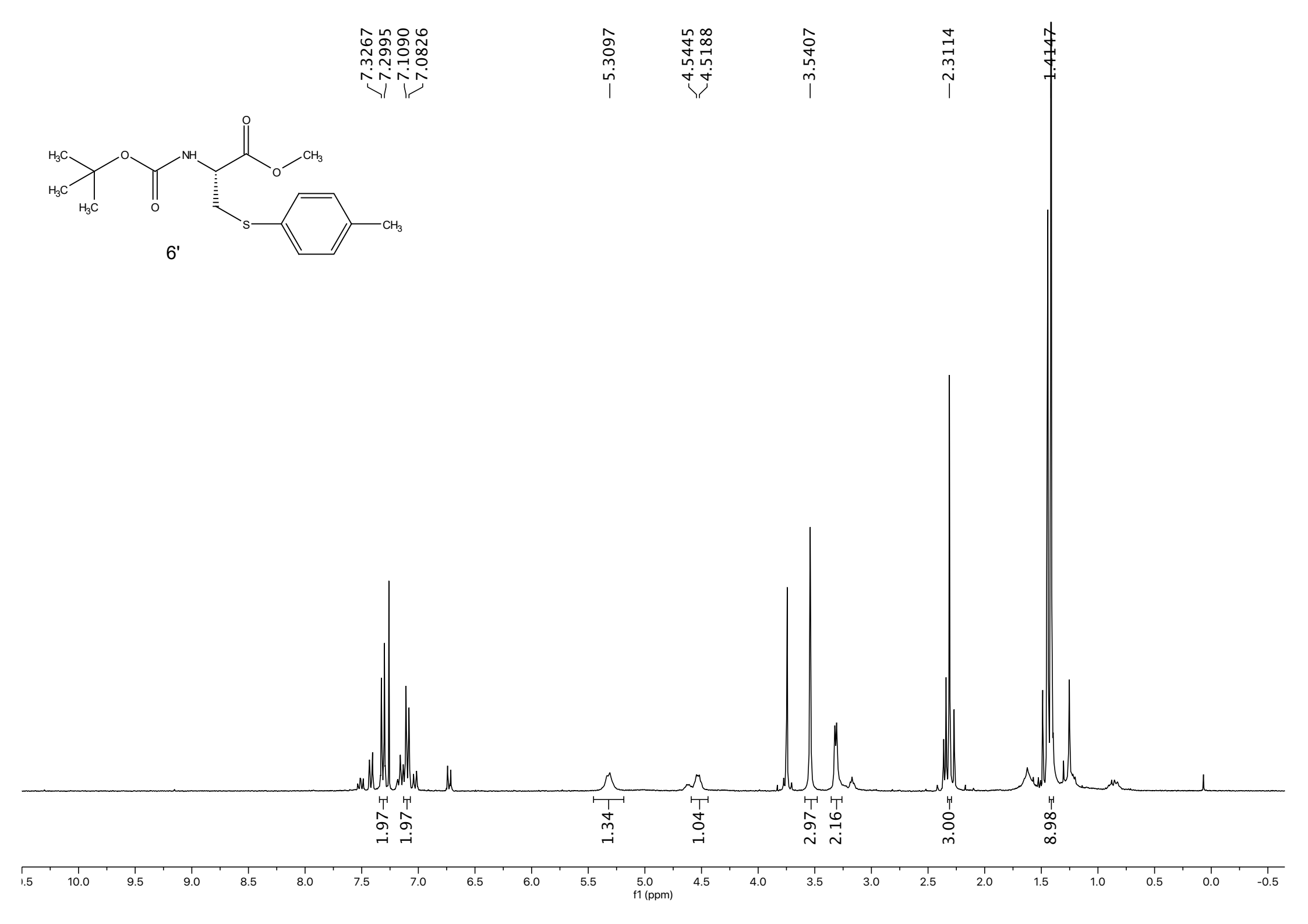
7.3267
7.2995
7.1090
7.0826
5.3097
4.5445
4.5188
3.5407
2.3114
1.4147
1.97
1.97
1.34
1.04
2.97
2.16
3.00
8.98
f1 (ppm)

6'

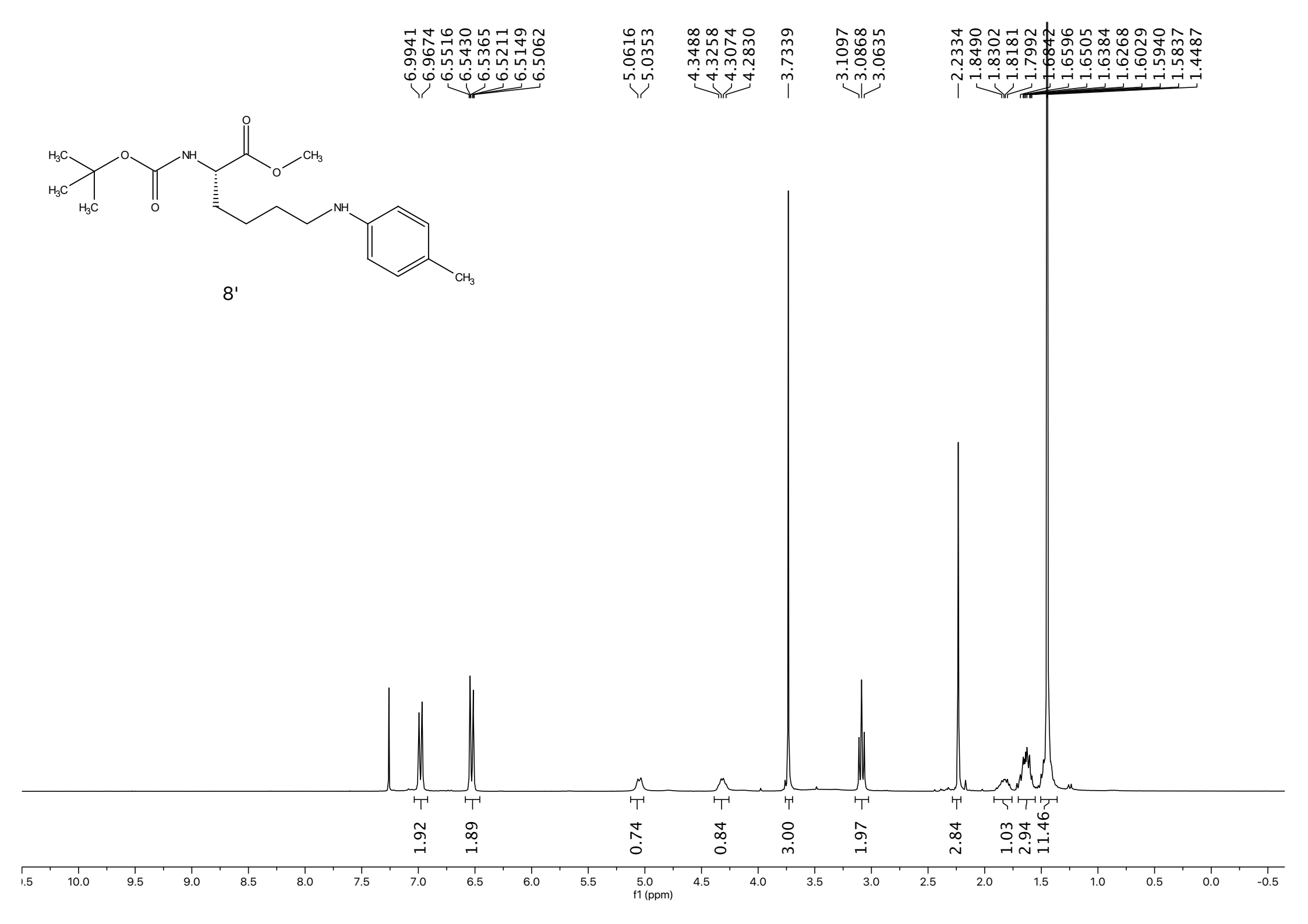
6.9941
6.9674
6.5516
6.5430
6.5365
6.5211
6.5149
6.5062
5.0616
5.0353
4.3488
4.3258
4.3074
4.2830
3.7339
3.1097
3.0868
3.0635
2.2334
1.8490
1.8302
1.8181
1.7992
1.6842
1.6596
1.6505
1.6384
1.6268
1.6029
1.5940
1.5837
1.4487
1.92
1.89
0.74
0.84
3.00
1.97
2.84
1.03
2.94
11.46
f1 (ppm)

8'

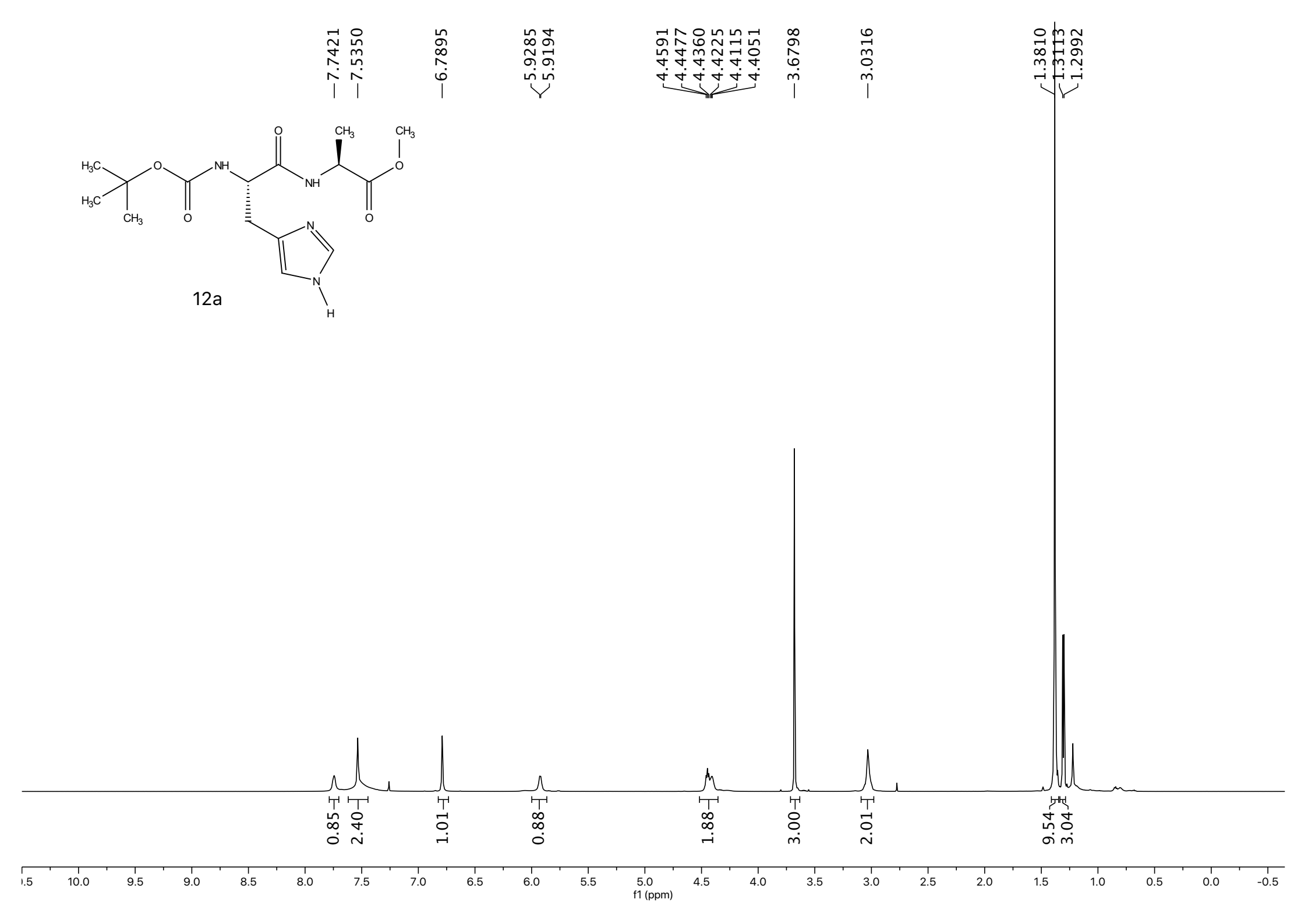
7.7421
7.5350
6.7895
5.9285
5.9194
4.4591
4.4477
4.4360
4.4225
4.4115
4.4051
3.6798
3.0316
1.3810
1.3113
1.2992
12a
0.85
2.40
1.01
0.88
1.88
3.00
2.01
9.54
3.04
f1 (ppm)

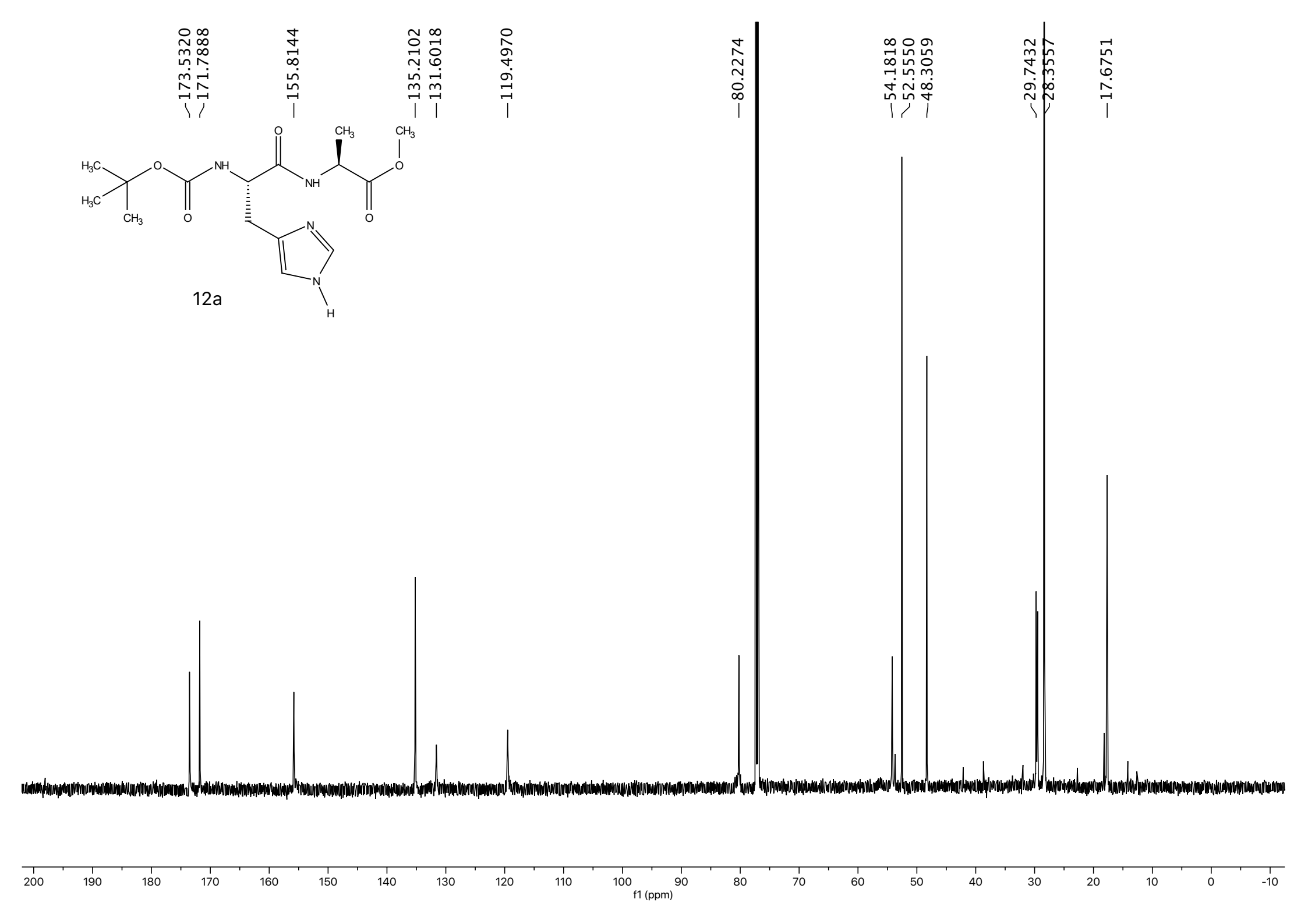
173.5320
171.7888
155.8144
135.2102
131.6018
119.4970
80.2274
54.1818
52.5550
48.3059
29.7432
28.3557
17.6751
12a
200
190
180
170
160
150
140
130
120
110
100
90
80
70
60
50
40
30
20
10
0
-10
f1 (ppm)

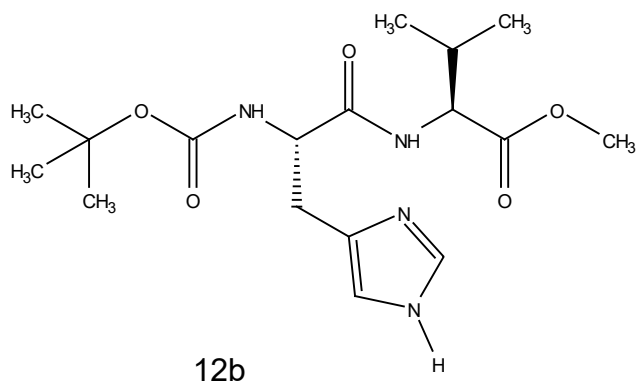

12b

8.4447
7.6001
7.4401
7.4181
6.8506
5.9490
5.9294
4.4275
4.4107
4.3997
4.3828
3.1619
3.1474
3.1122
3.0974
3.0416
3.0206
2.9921
2.9711
2.1589
2.1346
2.1121
2.0940
2.0717
2.0490
1.4295
0.8405
0.8321
0.8179
0.8093

1.36
1.01
0.82
1.02
0.92
2.04
3.00
1.04
1.06
1.03
9.26
5.96

f1 (ppm)

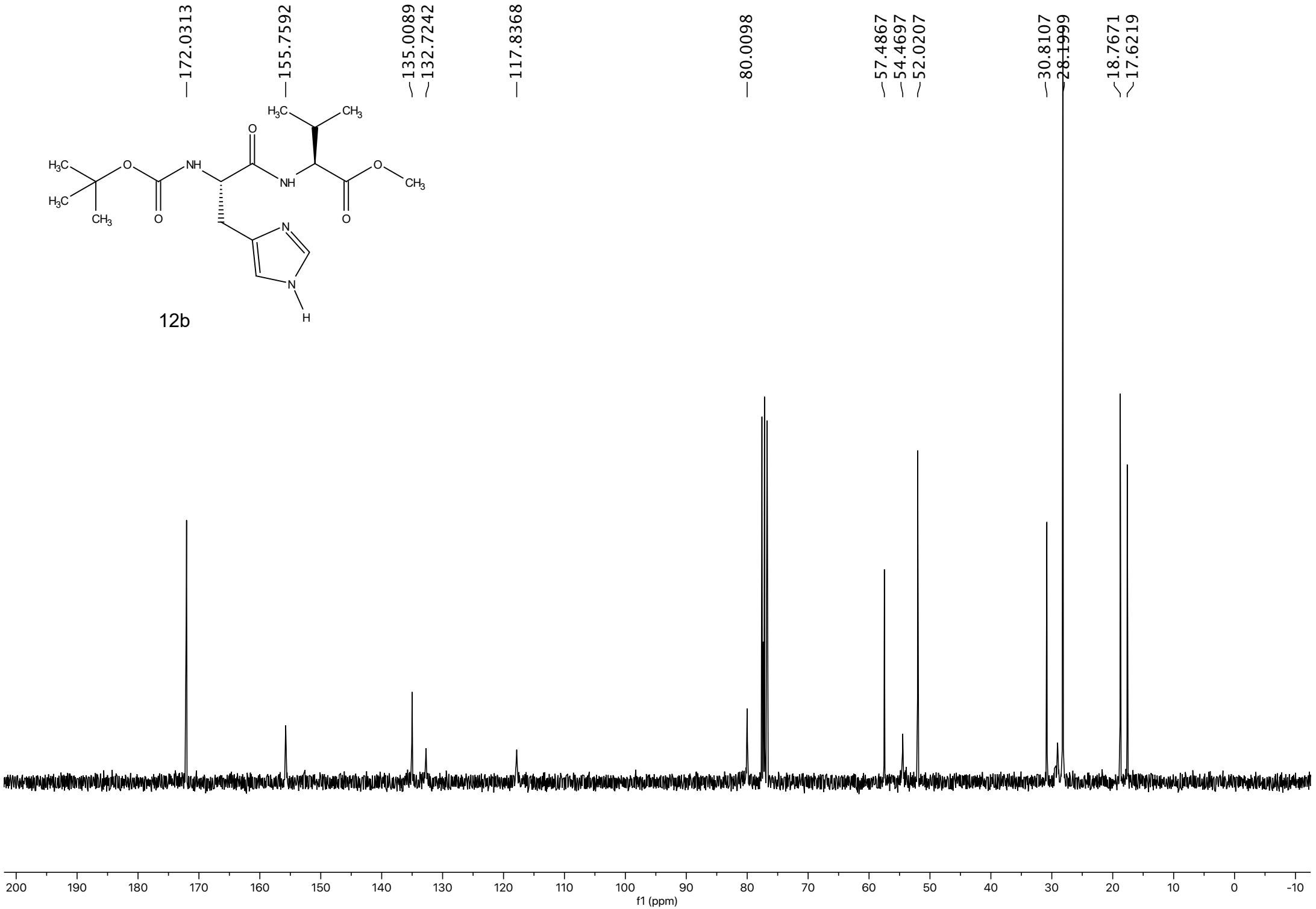
172.0313
155.7592
135.0089
132.7242
117.8368
80.0098
57.4867
54.4697
52.0207
30.8107
28.1999
18.7671
17.6219
12b
f1 (ppm)

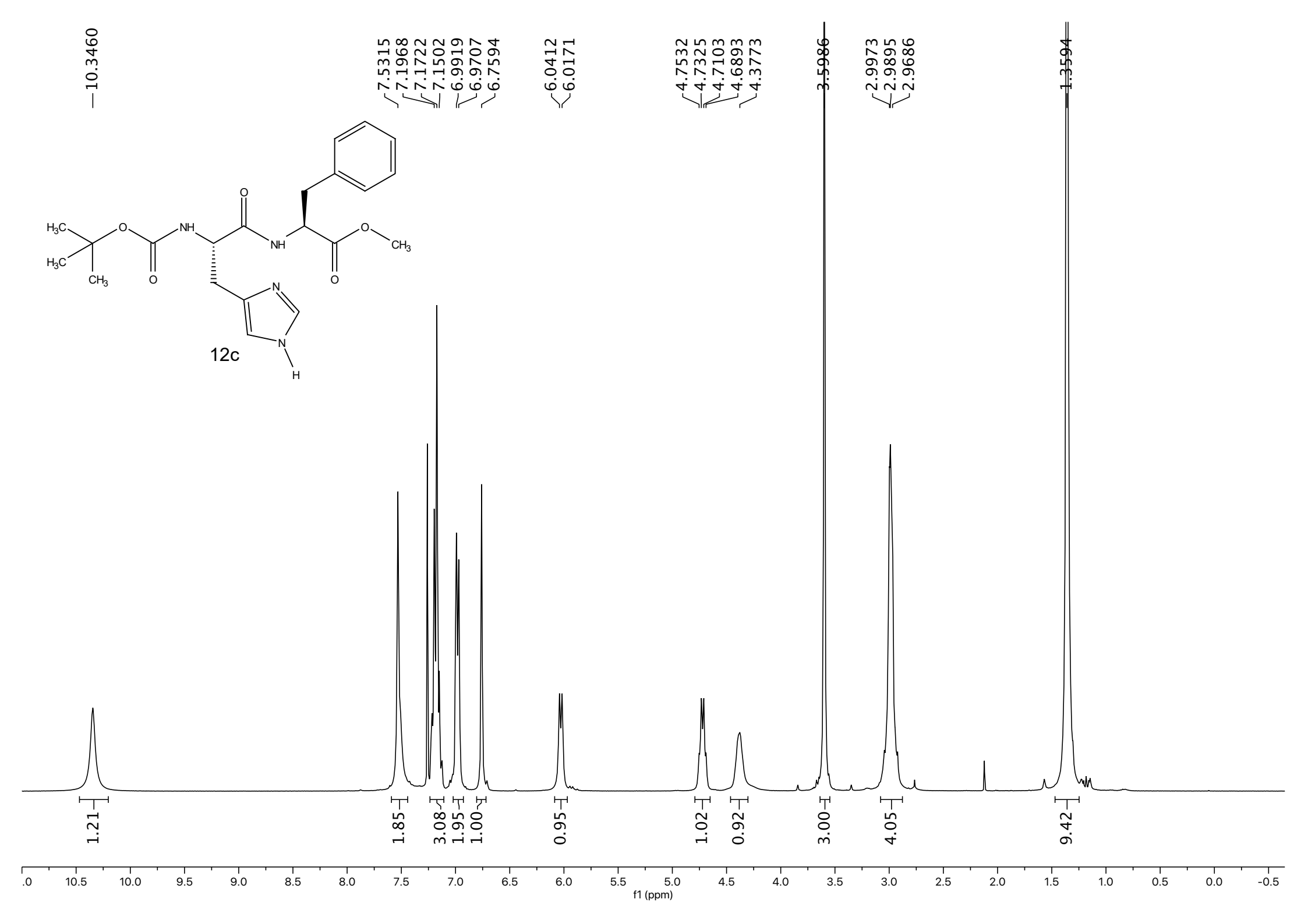
10.3460
7.5315
7.1968
7.1722
7.1502
6.9919
6.9707
6.7594
6.0412
6.0171
4.7532
4.7325
4.7103
4.6893
4.3773
3.5986
2.9973
2.9895
2.9686
1.3594
12c
1.21
1.85
3.08
1.95
1.00
0.95
1.02
0.92
3.00
4.05
9.42
f1 (ppm)

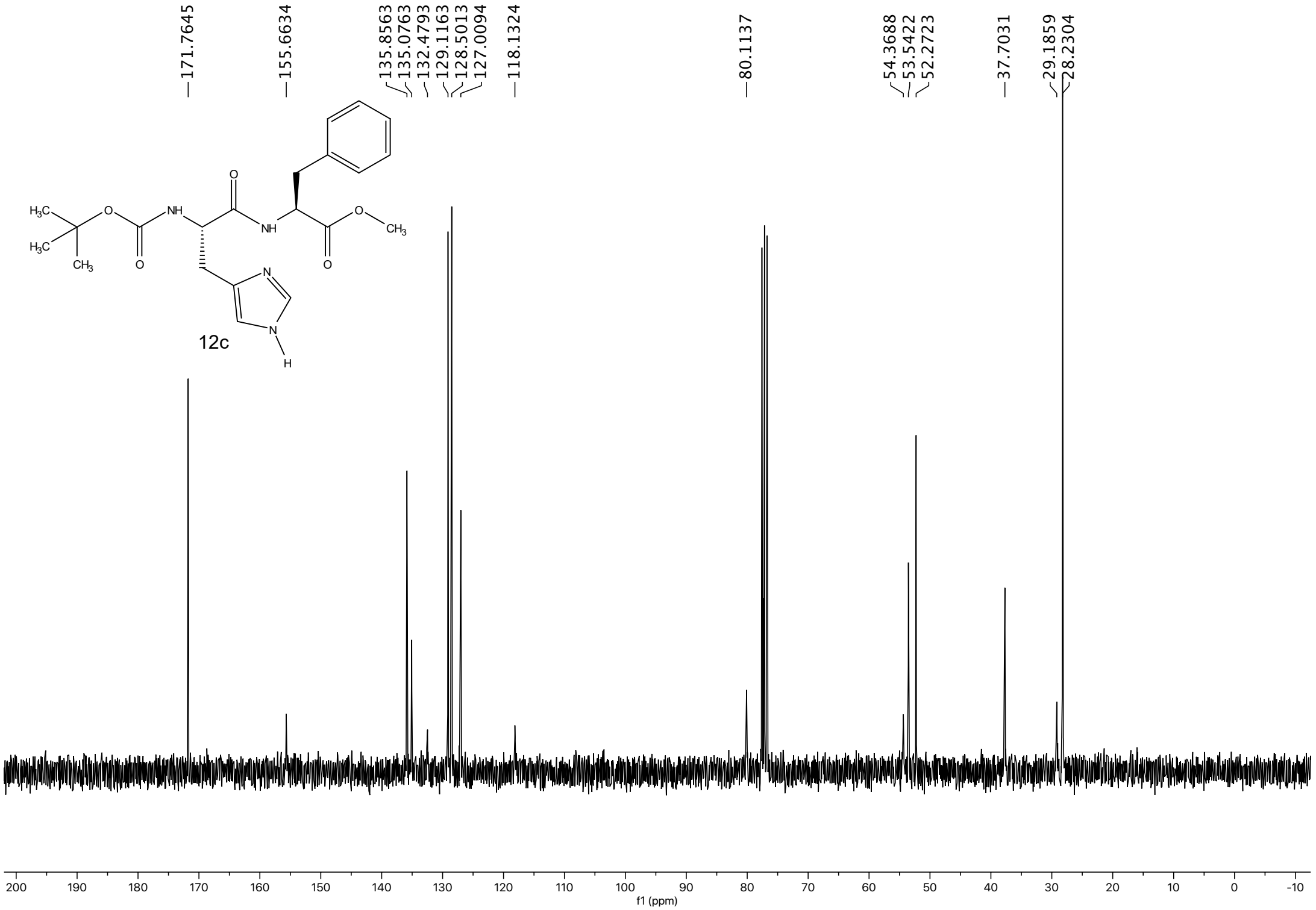
171.7645
155.6634
135.8563
135.0763
132.4793
129.1163
128.5013
127.0094
118.1324
80.1137
54.3688
53.5422
52.2723
37.7031
29.1859
28.2304
12c
f1 (ppm)

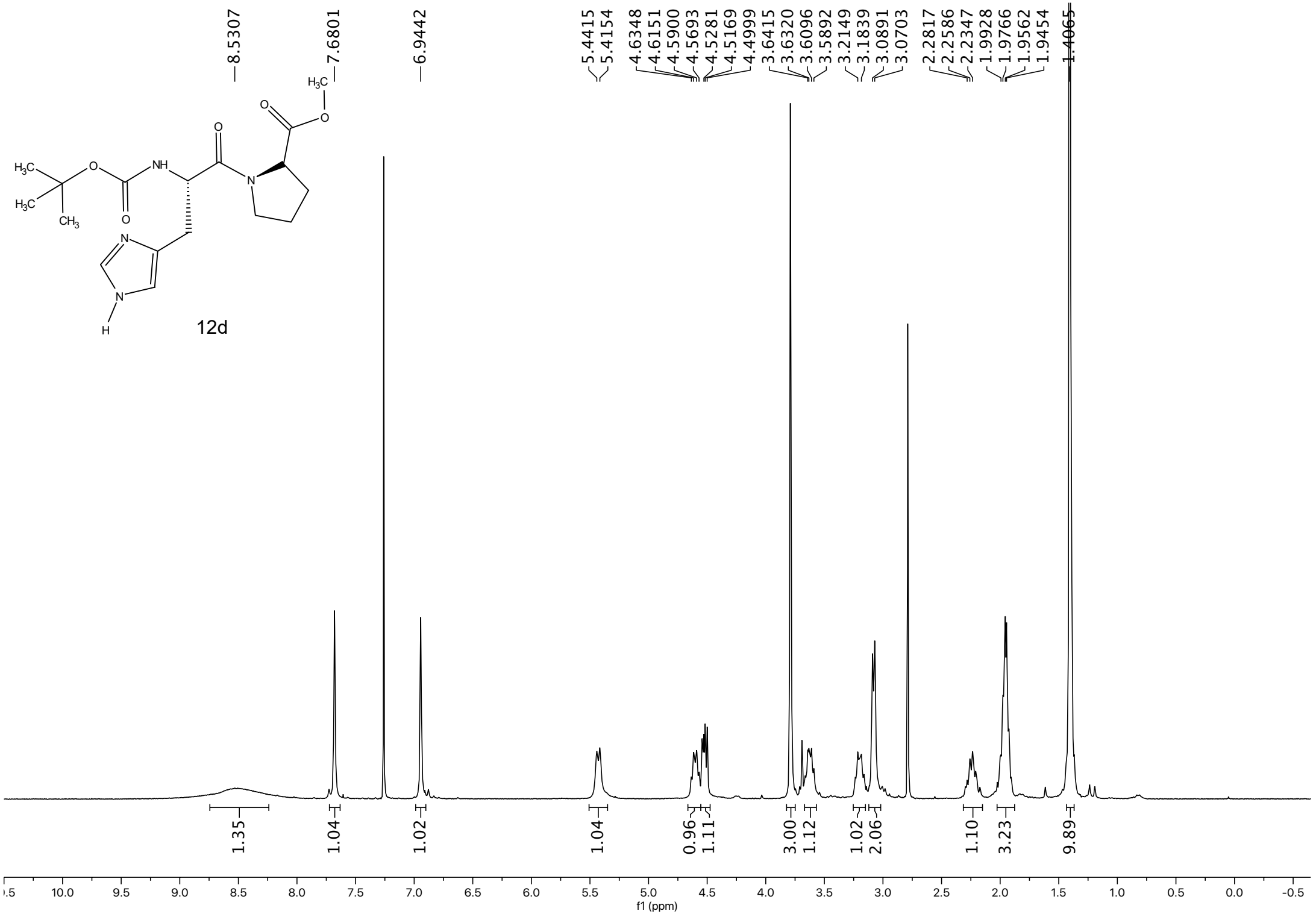
8.5307
7.6801
6.9442
5.4415
5.4154
4.6348
4.6151
4.5900
4.5693
4.5281
4.5169
4.4999
3.6415
3.6320
3.6096
3.5892
3.2149
3.1839
3.0891
3.0703
2.2817
2.2586
2.2347
1.9928
1.9766
1.9562
1.9454
1.4065
1.35
1.04
1.02
1.04
0.96
1.11
3.00
1.12
1.02
2.06
1.10
3.23
9.89
f1 (ppm)

12d

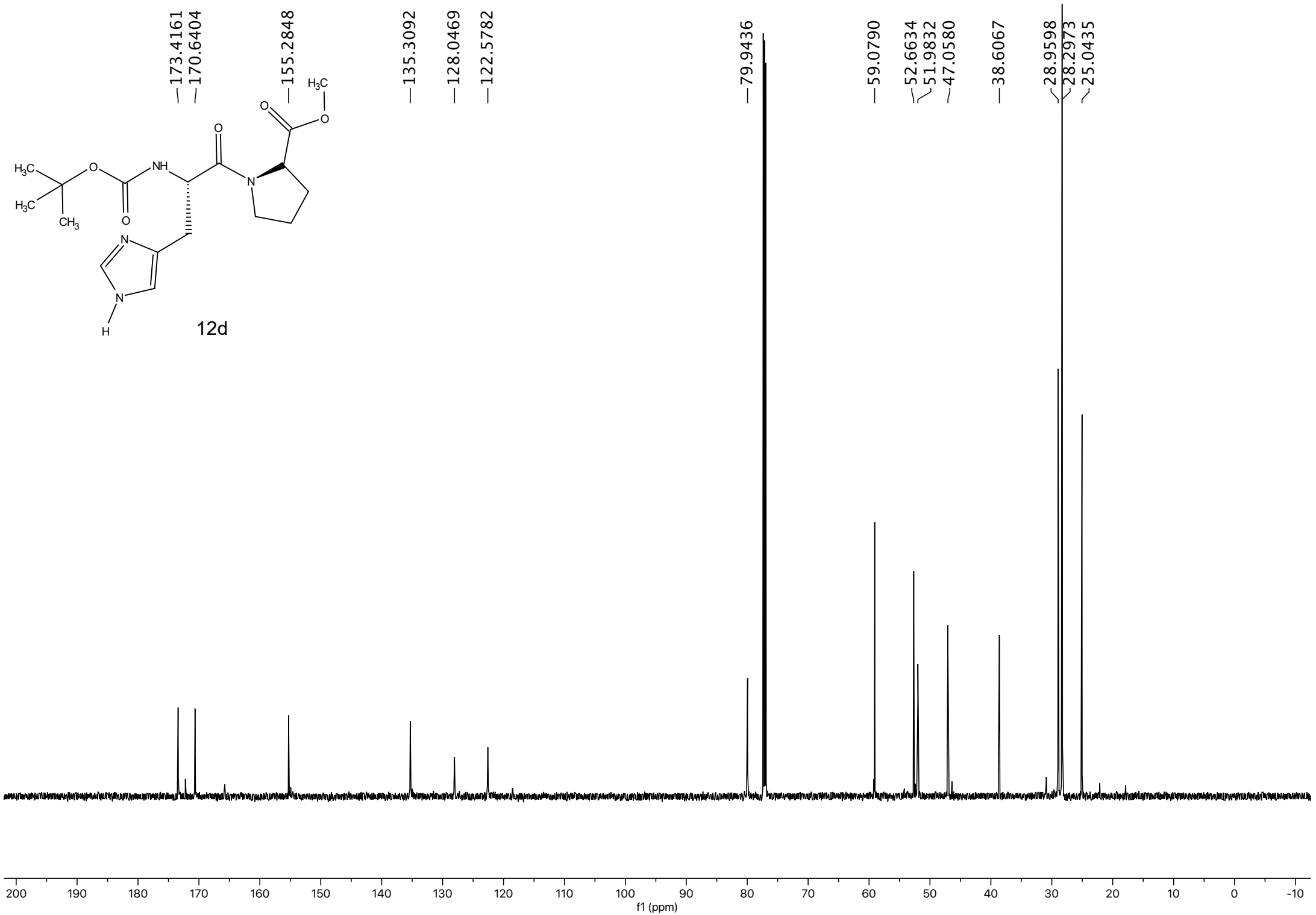
173.4161
170.6404
155.2848
135.3092
128.0469
122.5782
79.9436
59.0790
52.6634
51.9832
47.0580
38.6067
28.9598
28.2973
25.0435
12d
200
190
180
170
160
150
140
130
120
110
100
90
80
70
60
50
40
30
20
10
0
-10
f1 (ppm)

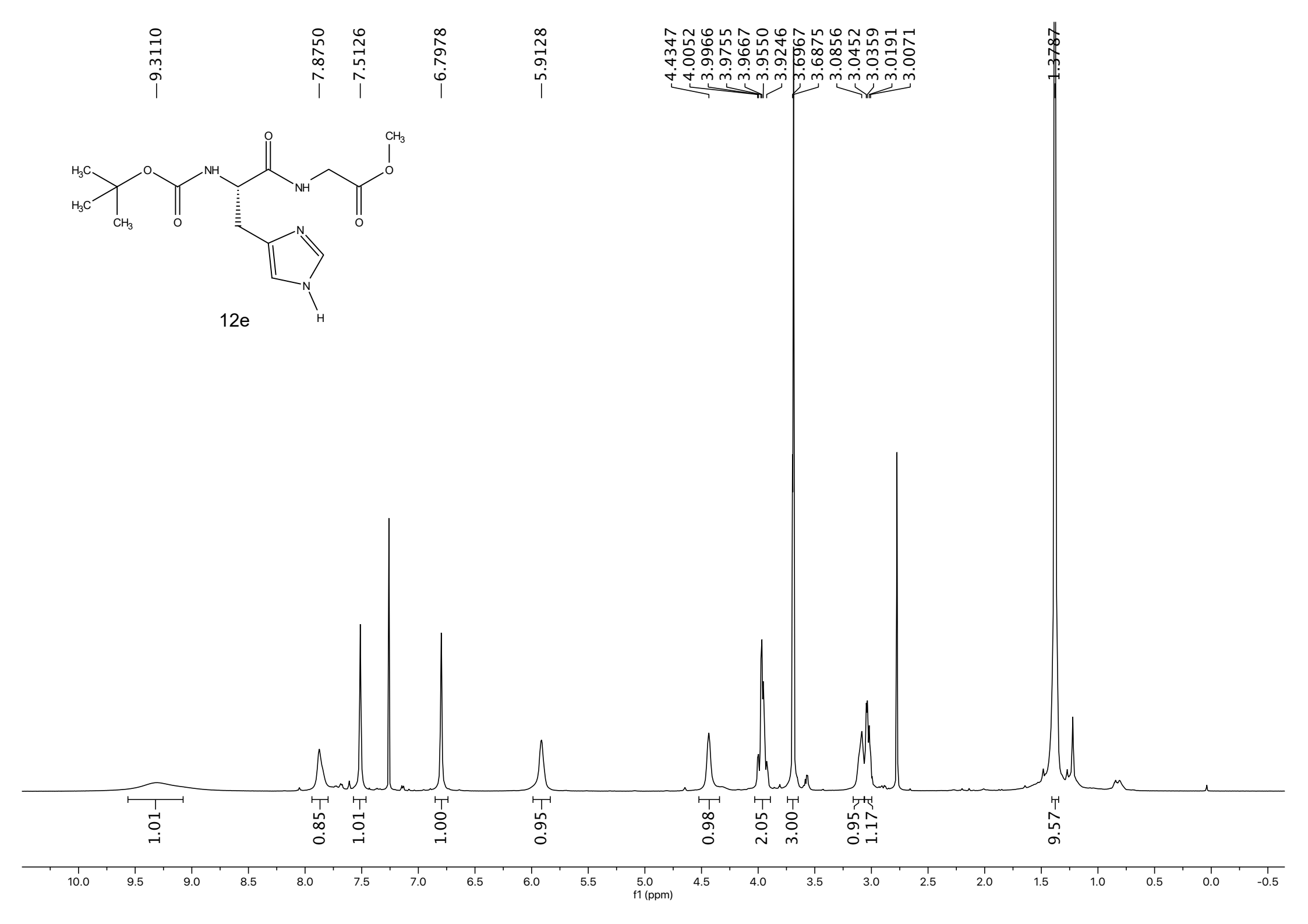
9.3110
7.8750
7.5126
6.7978
5.9128
4.4347
4.0052
3.9966
3.9755
3.9667
3.9550
3.9246
3.6967
3.6875
3.0856
3.0452
3.0359
3.0191
3.0071
1.3787
12e
1.01
0.85
1.01
1.00
0.95
0.98
2.05
3.00
0.95
1.17
9.57
f1 (ppm)

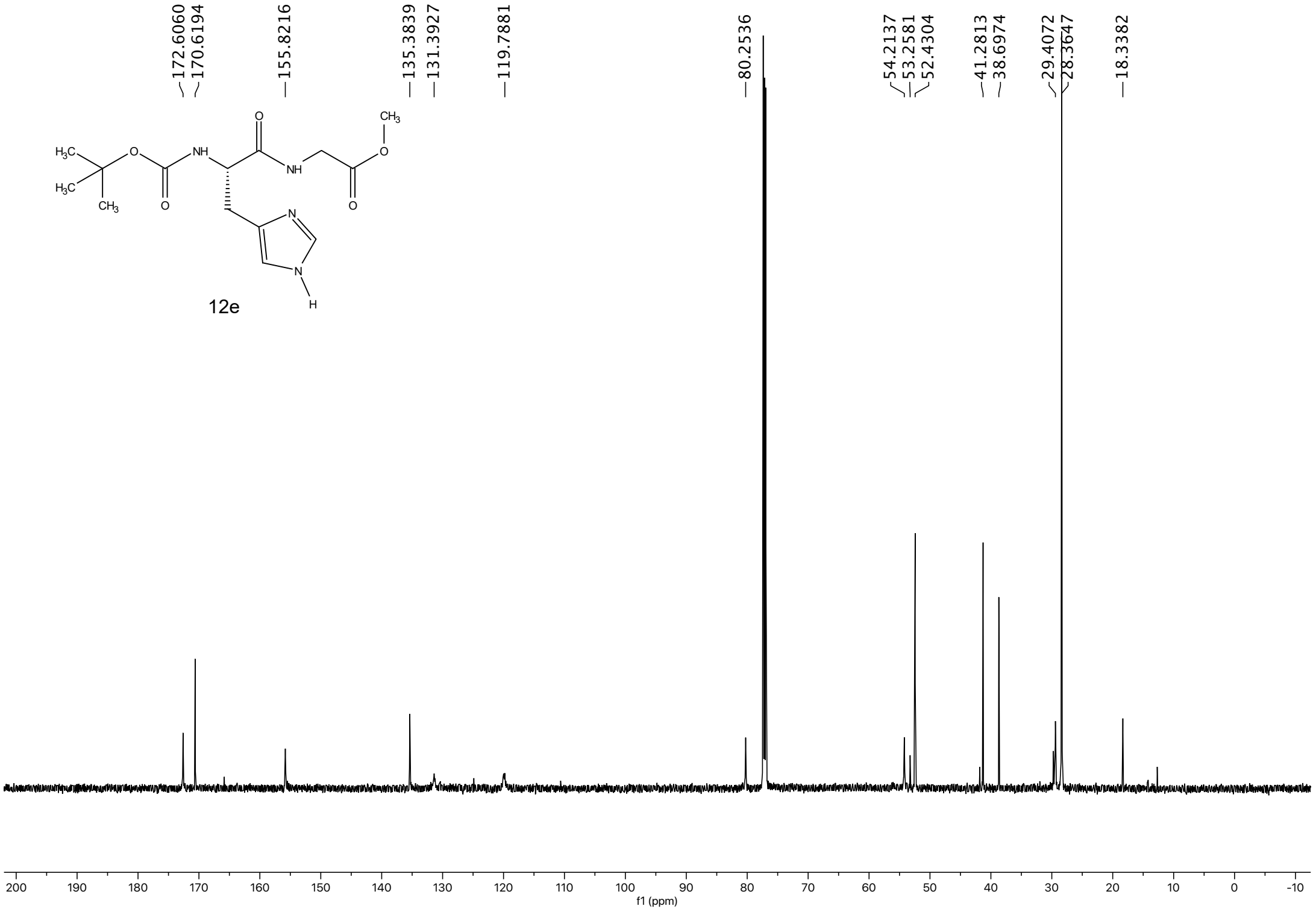
172.6060
170.6194
155.8216
135.3839
131.3927
119.7881
80.2536
54.2137
53.2581
52.4304
41.2813
38.6974
29.4072
28.3647
18.3382
12e
f1 (ppm)

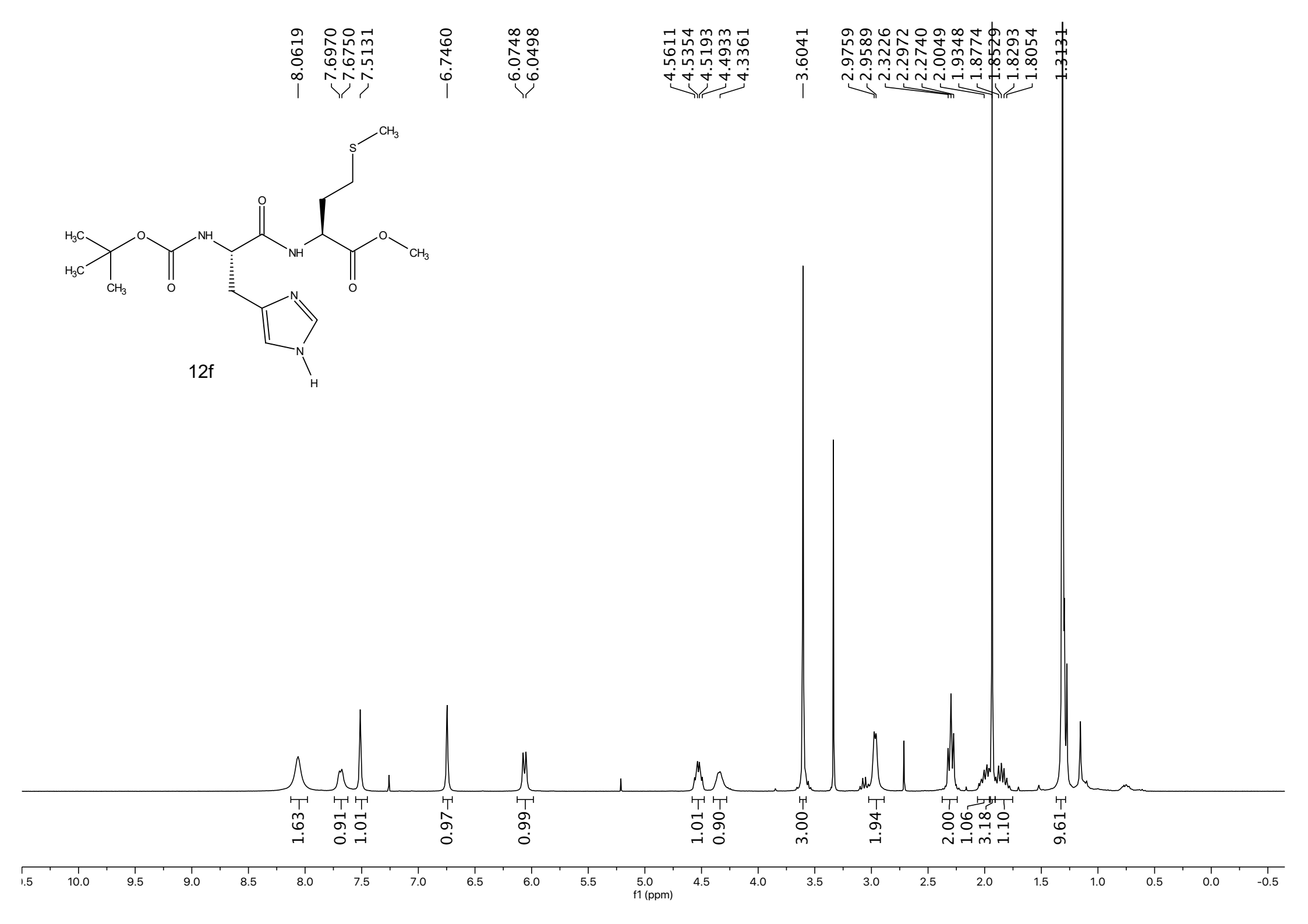
8.0619
7.6970
7.6750
7.5131
6.7460
6.0748
6.0498
4.5611
4.5354
4.5193
4.4933
4.3361
3.6041
2.9759
2.9589
2.3226
2.2972
2.2740
2.0049
1.9348
1.8774
1.8529
1.8293
1.8054
1.3131
12f
1.63
0.91
1.01
0.97
0.99
1.01
0.90
3.00
1.94
2.00
1.06
3.18
1.10
9.61
f1 (ppm)

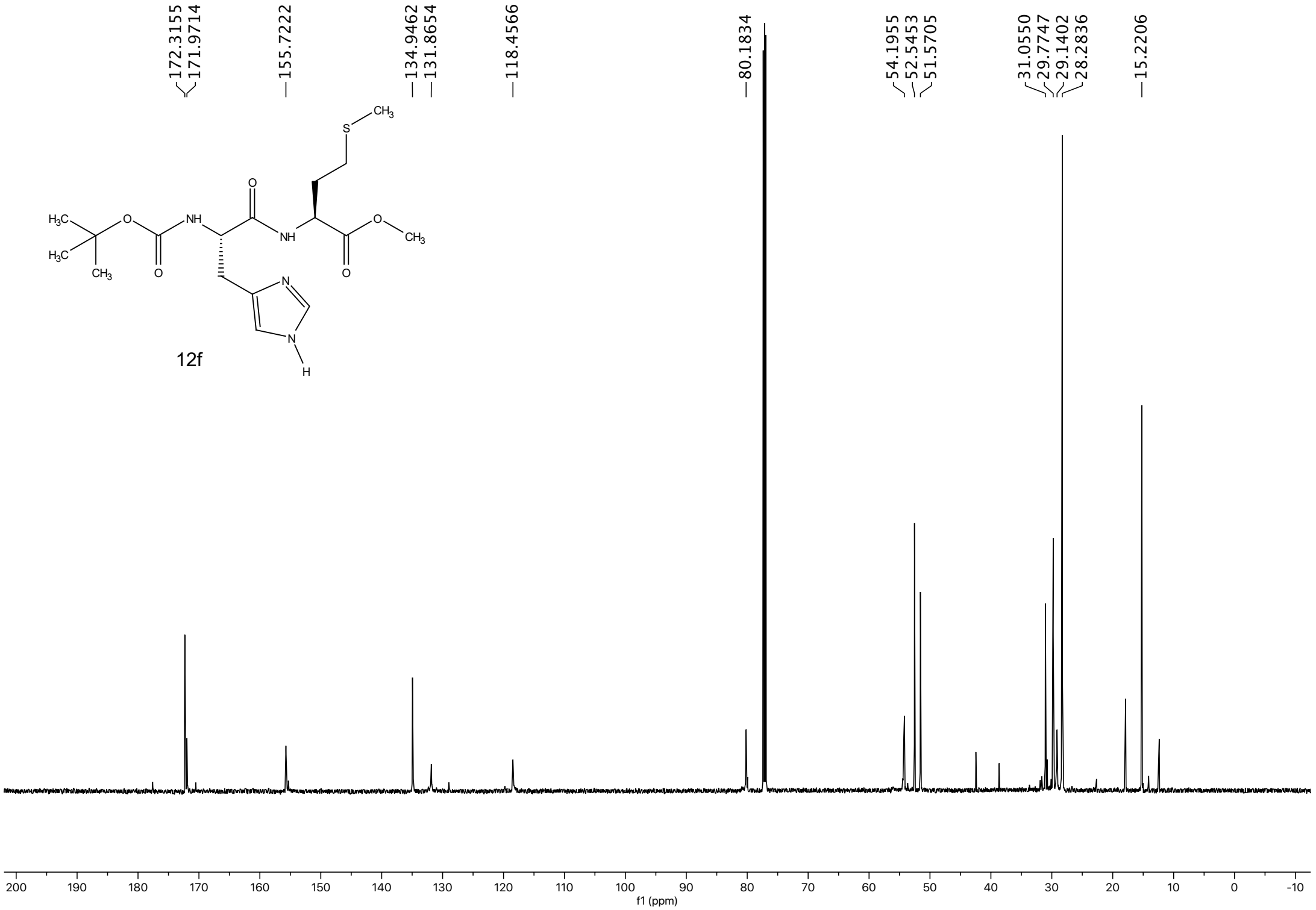
172.3155
171.9714
155.7222
134.9462
131.8654
118.4566
80.1834
54.1955
52.5453
51.5705
31.0550
29.7747
29.1402
28.2836
15.2206
12f
f1 (ppm)

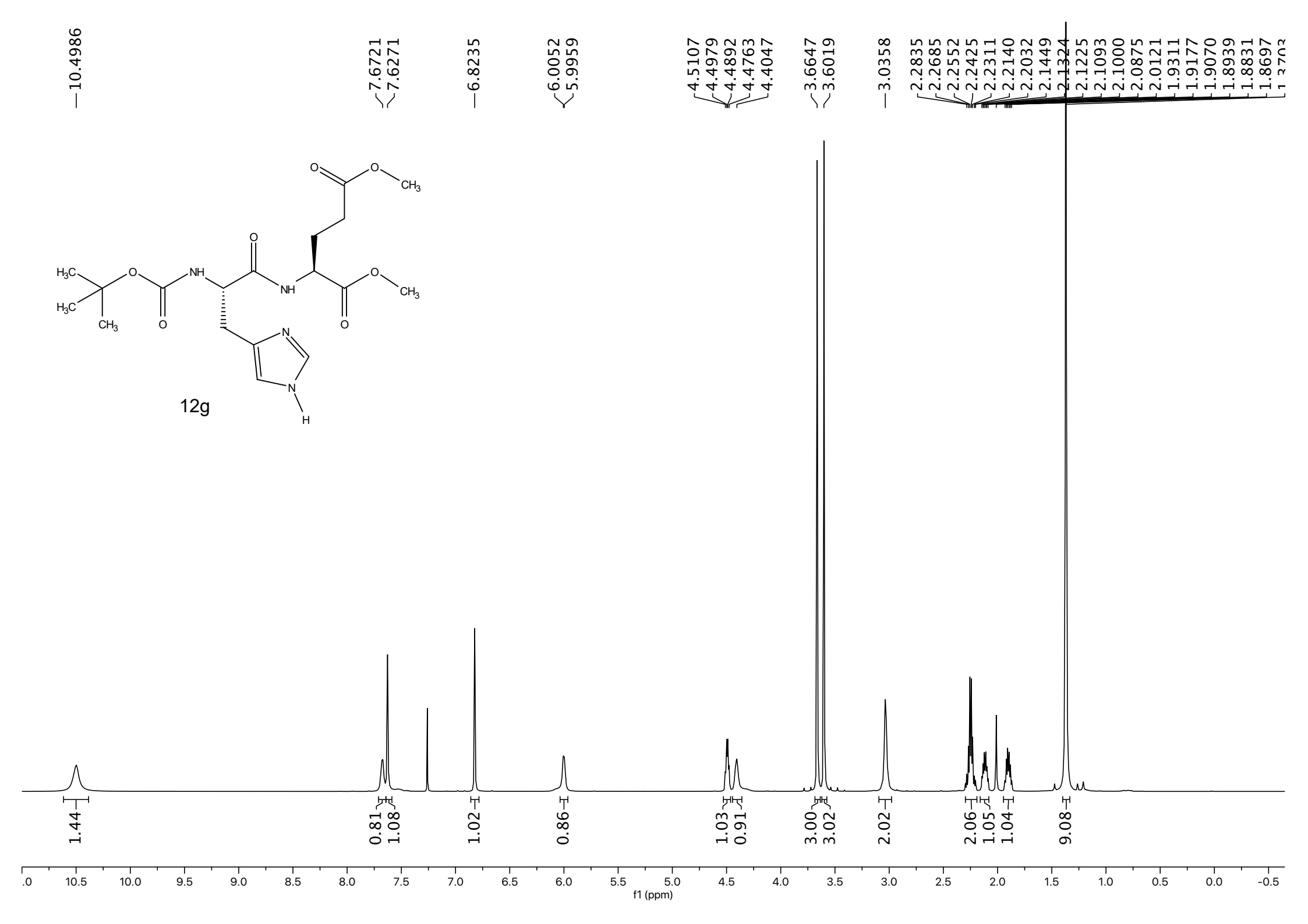
10.4986
7.6721
7.6271
6.8235
6.0052
5.9959
4.5107
4.4979
4.4892
4.4763
4.4047
3.6647
3.6019
3.0358
2.2835
2.2685
2.2552
2.2425
2.2311
2.2140
2.2032
2.1449
2.1324
2.1225
2.1093
2.1000
2.0875
2.0121
1.9311
1.9177
1.9070
1.8939
1.8831
1.8697
12g
1.44
0.81
1.08
1.02
0.86
1.03
0.91
3.00
3.02
2.02
2.06
1.05
1.04
9.08
f1 (ppm)

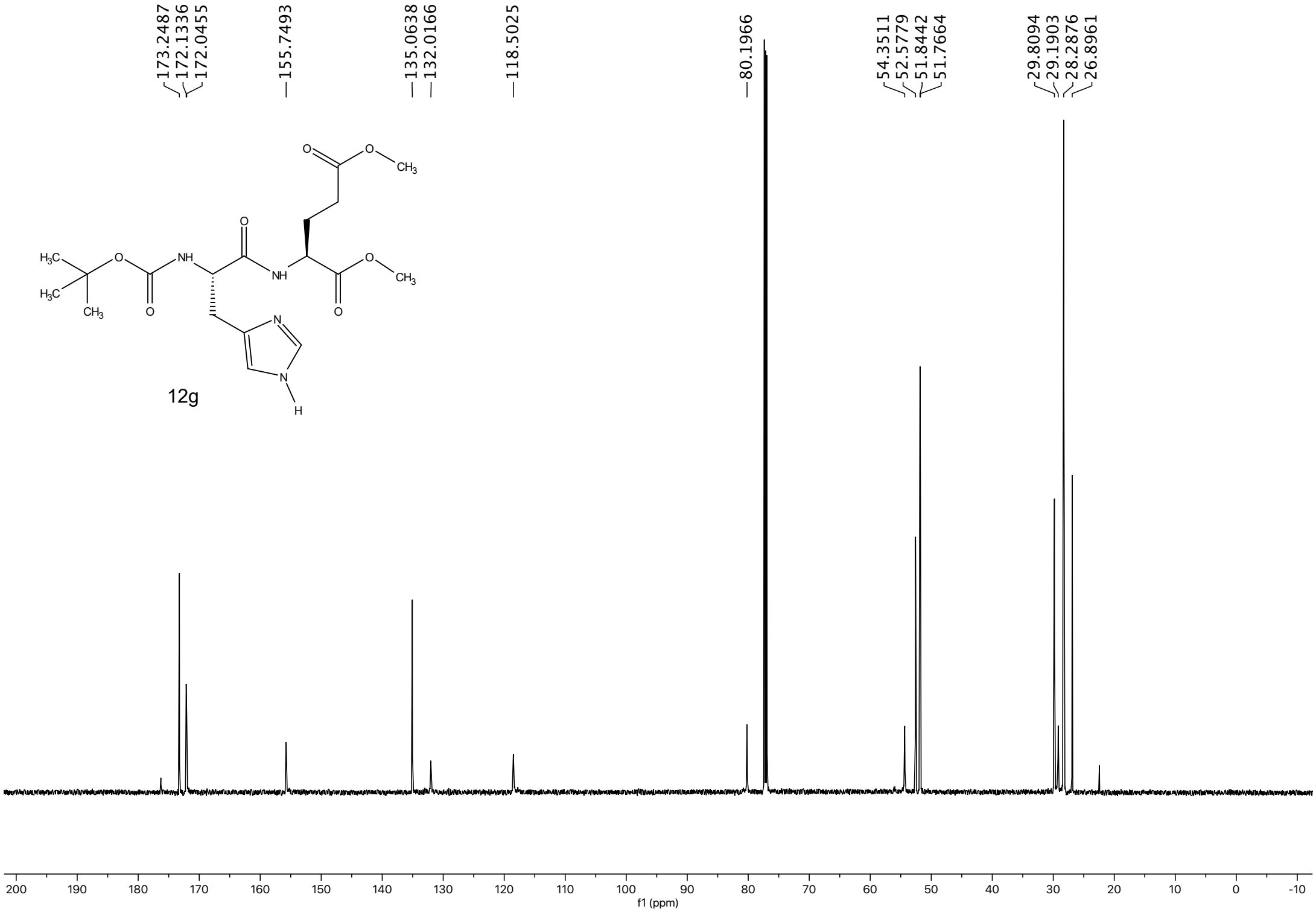
173.2487
172.1336
172.0455
155.7493
135.0638
132.0166
118.5025
80.1966
54.3511
52.5779
51.8442
51.7664
29.8094
29.1903
28.2876
26.8961
12g
f1 (ppm)

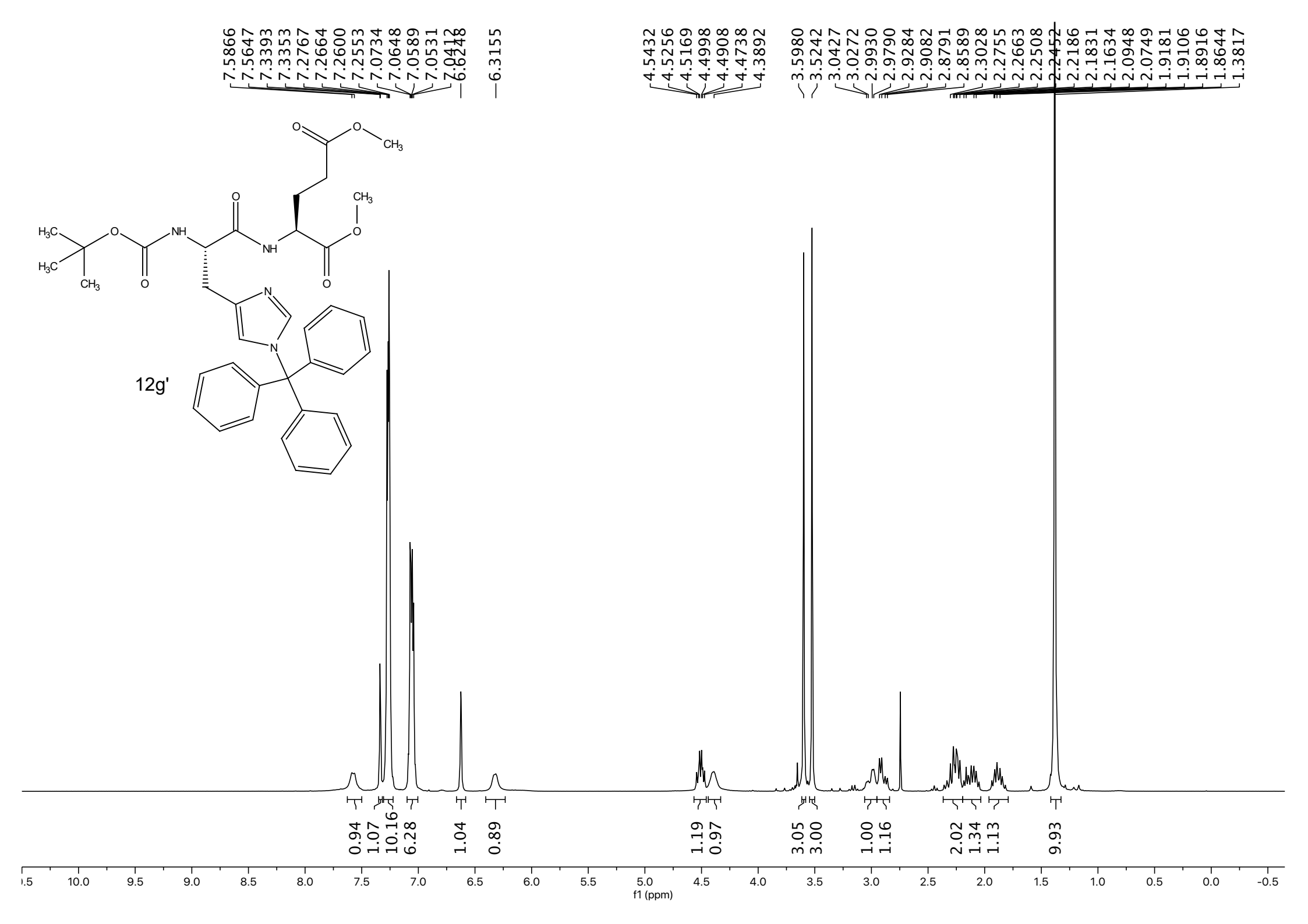
7.5866
7.5647
7.3393
7.3353
7.2767
7.2664
7.2600
7.2553
7.0734
7.0648
7.0589
7.0531
7.0412
6.8248
6.3155
4.5432
4.5256
4.5169
4.4998
4.4908
4.4738
4.3892
3.5980
3.5242
3.0427
3.0272
2.9930
2.9790
2.9284
2.9082
2.8791
2.8589
2.3028
2.2755
2.2663
2.2508
2.2452
2.2186
2.1831
2.1634
2.0948
2.0749
1.9181
1.9106
1.8916
1.8644
1.3817
12g'
0.94
1.07
10.16
6.28
1.04
0.89
1.19
0.97
3.05
3.00
1.00
1.16
2.02
1.34
1.13
9.93
f1 (ppm)

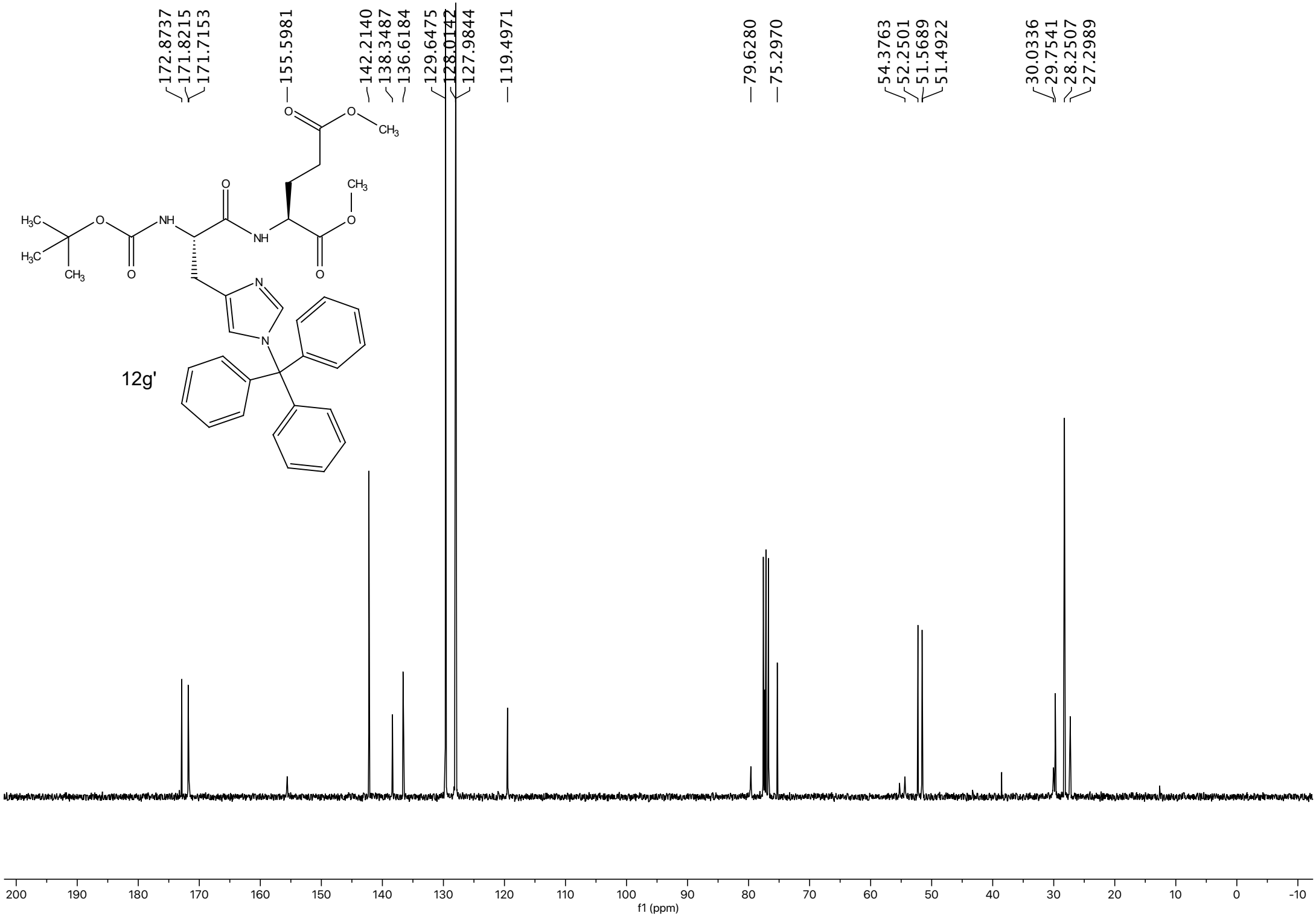
172.8737
171.8215
171.7153
155.5981
142.2140
138.3487
136.6184
129.6475
128.0142
127.9844
119.4971
79.6280
75.2970
54.3763
52.2501
51.5689
51.4922
30.0336
29.7541
28.2507
27.2989
12g'
f1 (ppm)

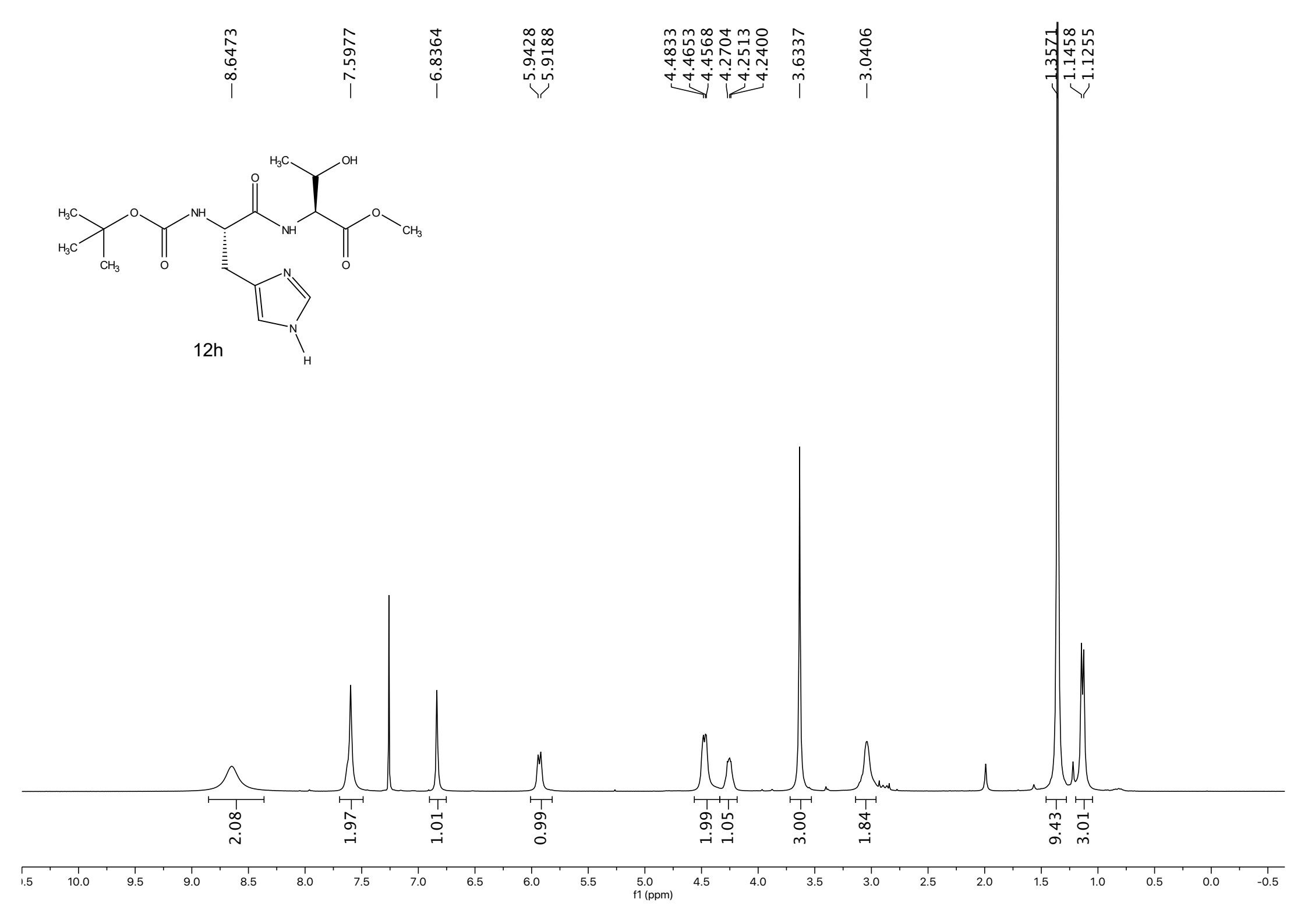
8.6473
7.5977
6.8364
5.9428
5.9188
4.4833
4.4653
4.4568
4.2704
4.2513
4.2400
3.6337
3.0406
1.3571
1.1458
1.1255
12h
2.08
1.97
1.01
0.99
1.99
1.05
3.00
1.84
9.43
3.01
f1 (ppm)

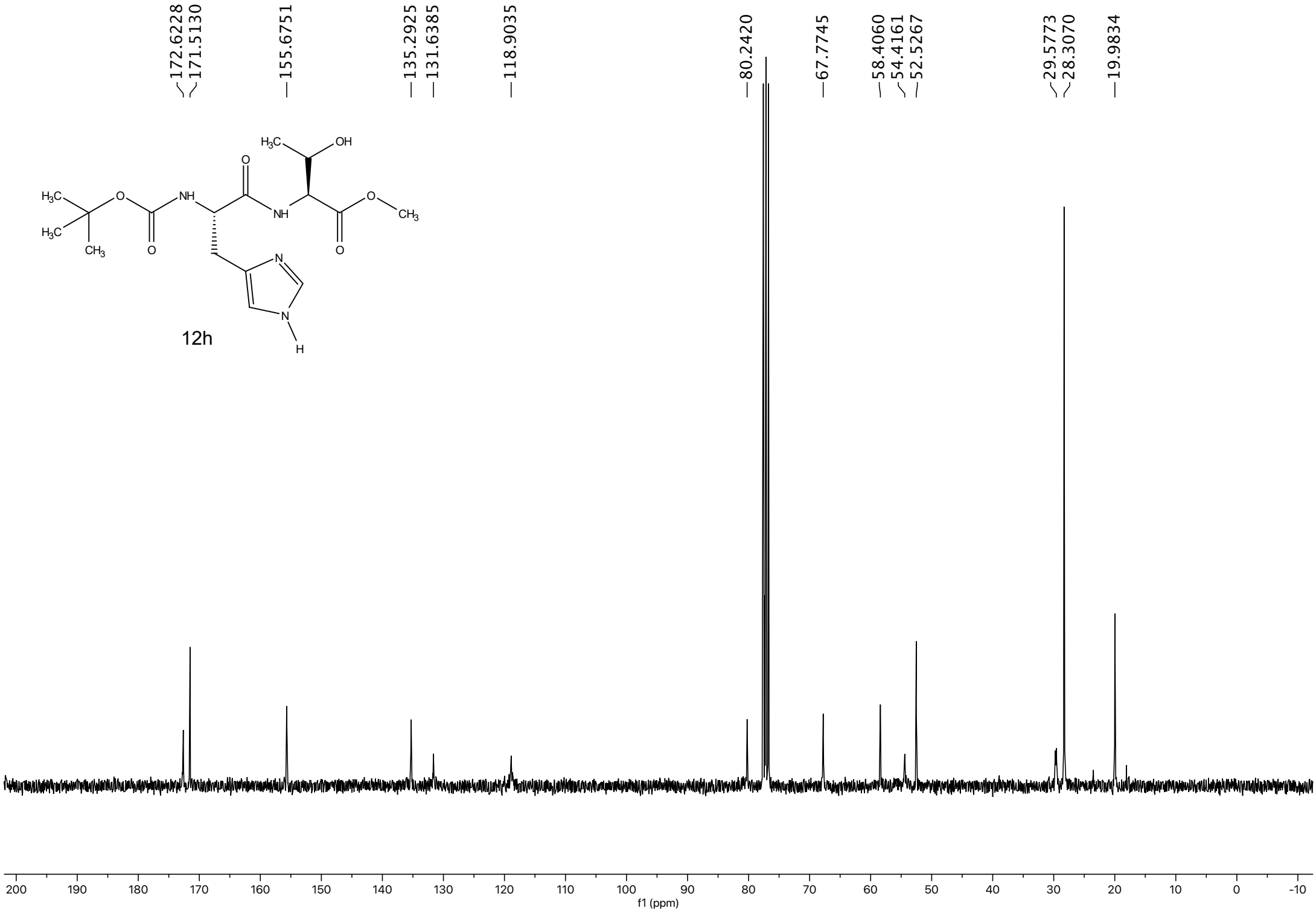
172.6228
171.5130
155.6751
135.2925
131.6385
118.9035
80.2420
67.7745
58.4060
54.4161
52.5267
29.5773
28.3070
19.9834
12h
f1 (ppm)

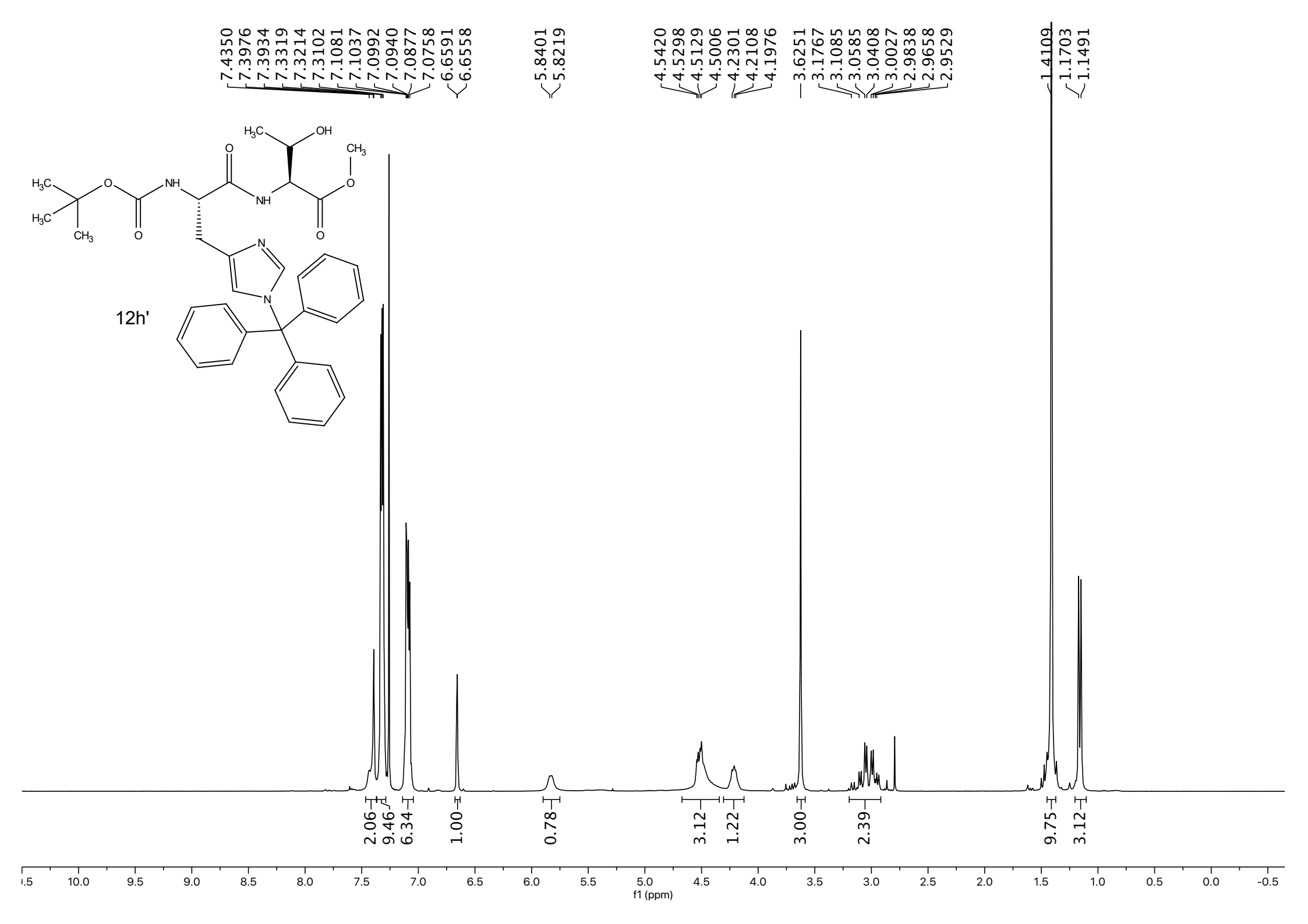
7.4350
7.3976
7.3934
7.3319
7.3214
7.3102
7.1081
7.1037
7.0992
7.0940
7.0877
7.0758
6.6591
6.6558
5.8401
5.8219
4.5420
4.5298
4.5129
4.5006
4.2301
4.2108
4.1976
3.6251
3.1767
3.1085
3.0585
3.0408
3.0027
2.9838
2.9658
2.9529
1.4109
1.1703
1.1491
12h'
2.06
9.46
6.34
1.00
0.78
3.12
1.22
3.00
2.39
9.75
3.12
f1 (ppm)

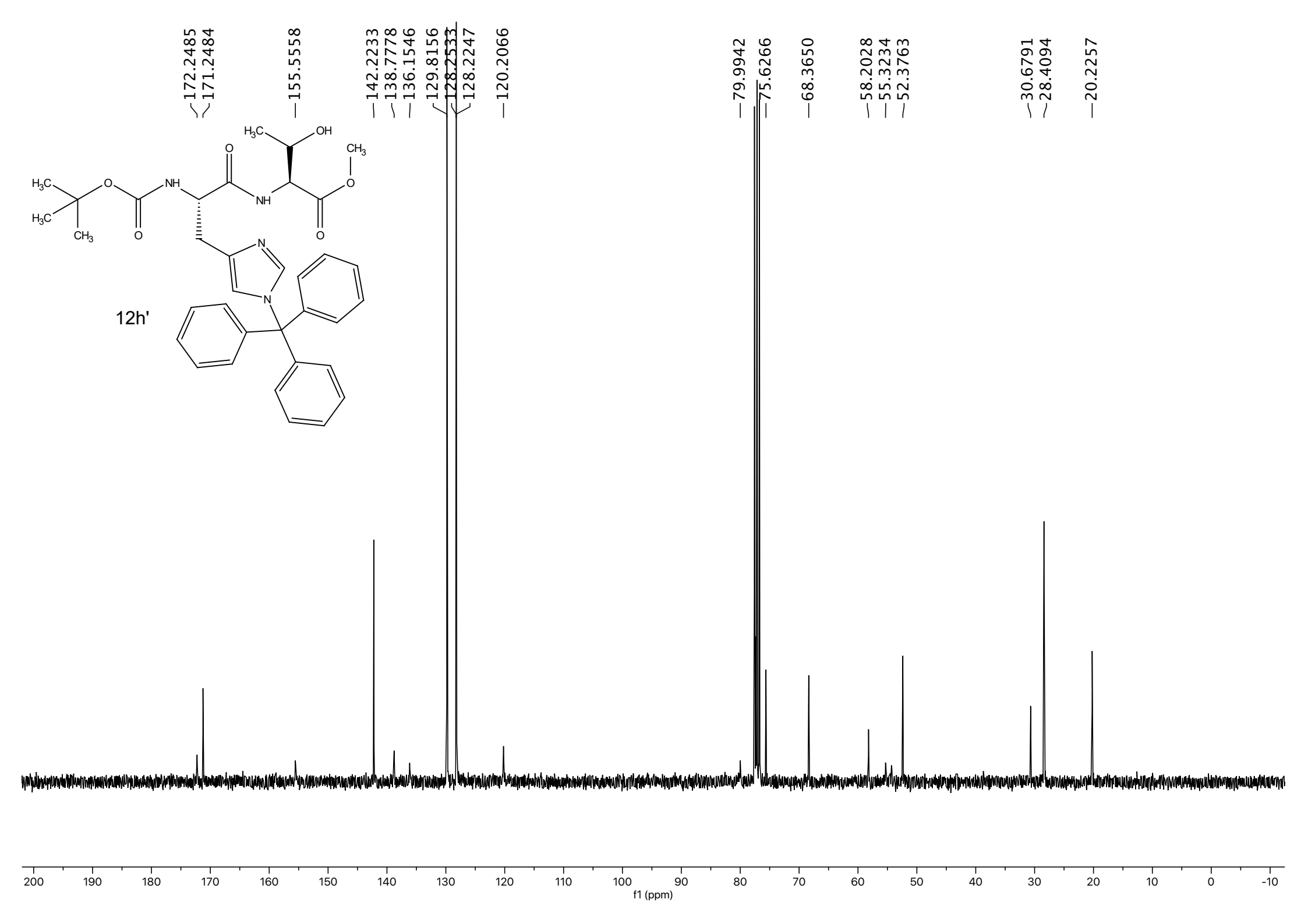
172.2485
171.2484
155.5558
142.2233
138.7778
136.1546
129.8156
128.2533
128.2247
120.2066
79.9942
75.6266
68.3650
58.2028
55.3234
52.3763
30.6791
28.4094
20.2257
12h'
200
190
180
170
160
150
140
130
120
110
100
90
80
70
60
50
40
30
20
10
0
-10
f1 (ppm)

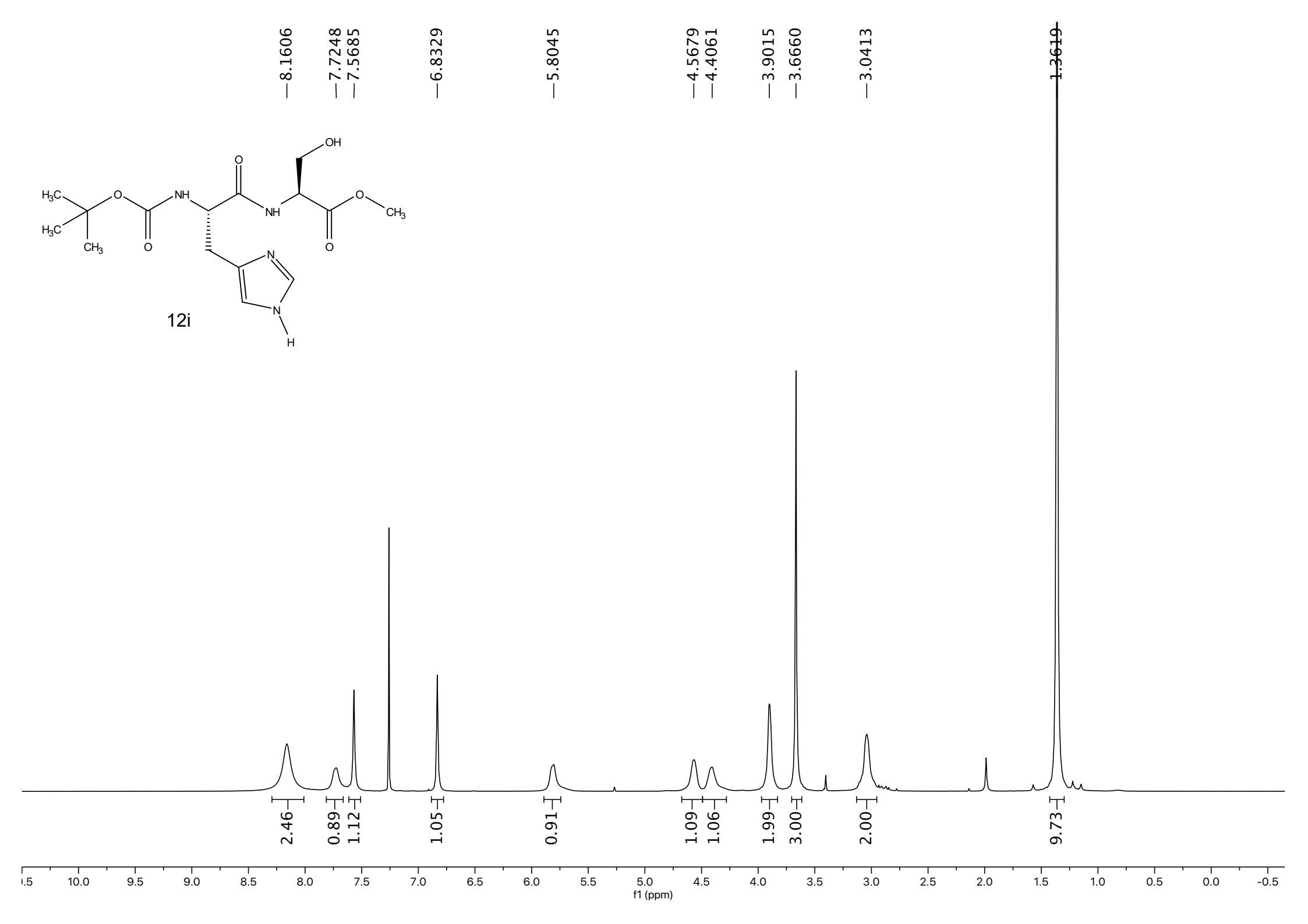
8.1606
7.7248
7.5685
6.8329
5.8045
4.5679
4.4061
3.9015
3.6660
3.0413
1.3619
OH
O
NH
NH
O
O
O
O
CH3
H3C
H3C
CH3
N
N
H
12i
2.46
0.89
1.12
1.05
0.91
1.09
1.06
1.99
3.00
2.00
9.73
10.0
9.5
9.0
8.5
8.0
7.5
7.0
6.5
6.0
5.5
5.0
4.5
4.0
3.5
3.0
2.5
2.0
1.5
1.0
0.5
0.0
-0.5
f1 (ppm)

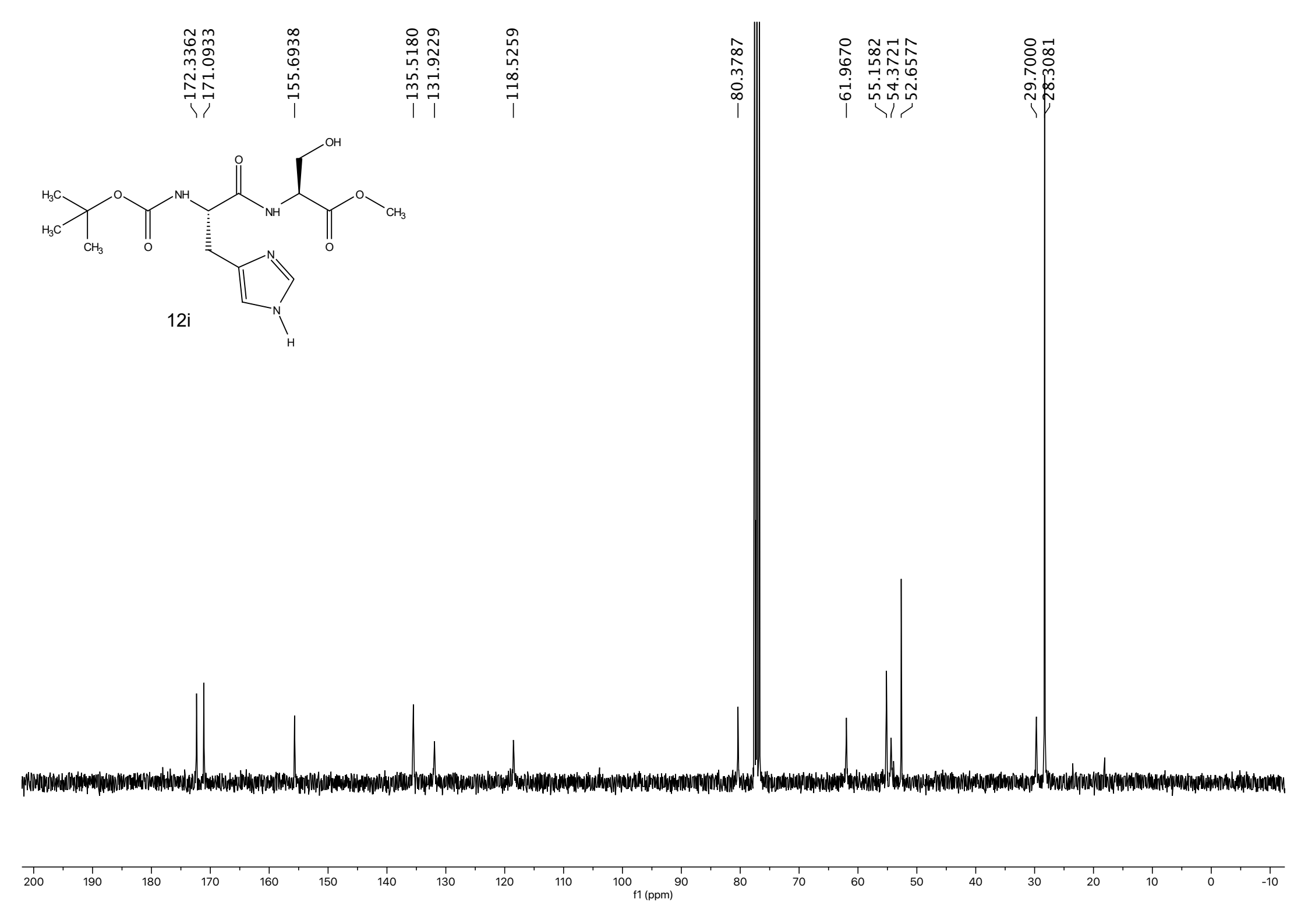
172.3362
171.0933
155.6938
135.5180
131.9229
118.5259
80.3787
61.9670
55.1582
54.3721
52.6577
29.7000
28.3081
OH
O
NH
NH
O
O
O
O
CH3
H3C
H3C
CH3
N
N
H
12i
200
190
180
170
160
150
140
130
120
110
100
90
80
70
60
50
40
30
20
10
0
-10
f1 (ppm)

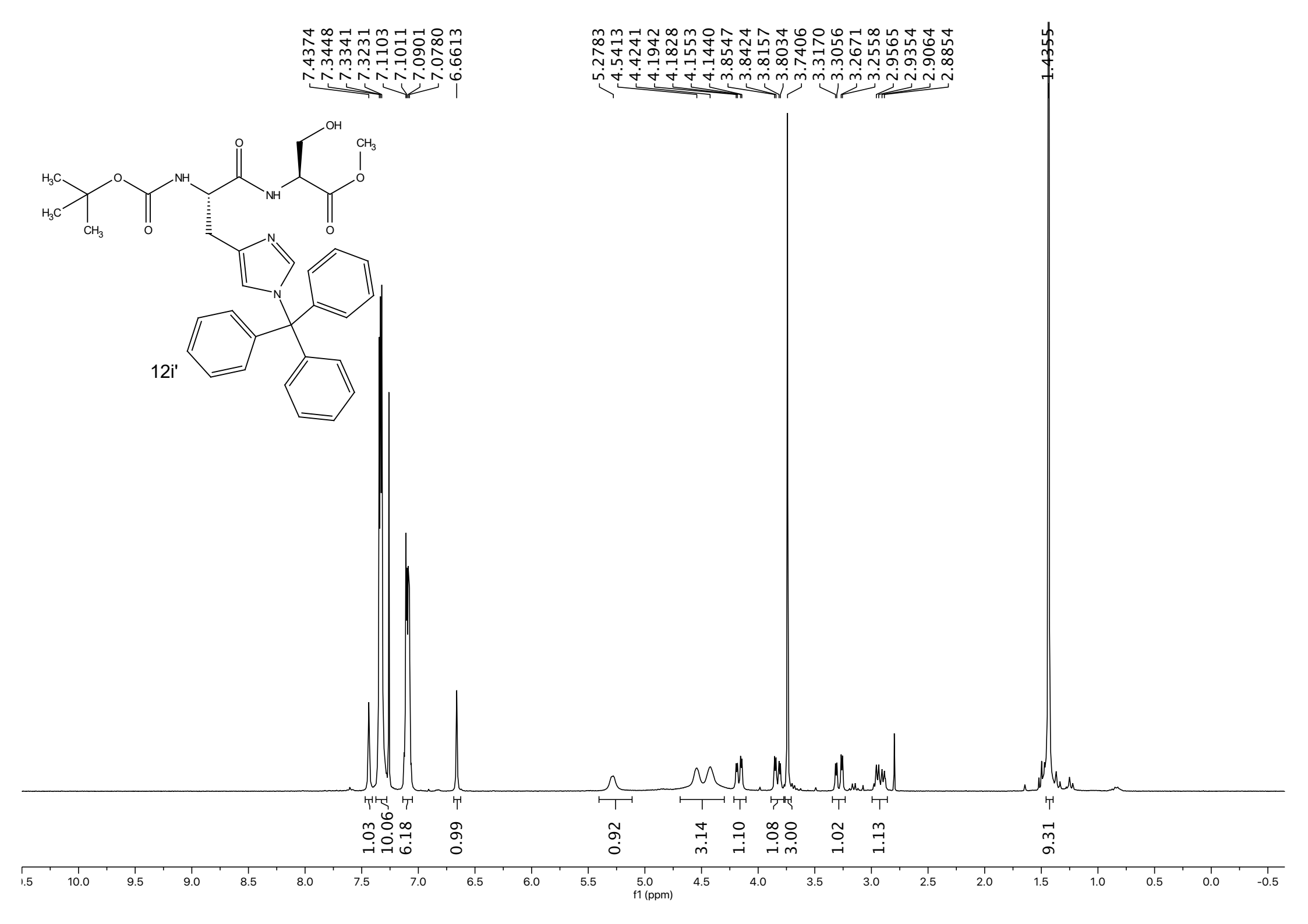
7.4374
7.3448
7.3341
7.3231
7.1103
7.1011
7.0901
7.0780
6.6613
5.2783
4.5413
4.4241
4.1942
4.1828
4.1553
4.1440
3.8547
3.8424
3.8157
3.8034
3.7406
3.3170
3.3056
3.2671
3.2558
2.9565
2.9354
2.9064
2.8854
1.4355
12i'
1.03
10.06
6.18
0.99
0.92
3.14
1.10
1.08
3.00
1.02
1.13
9.31
f1 (ppm)

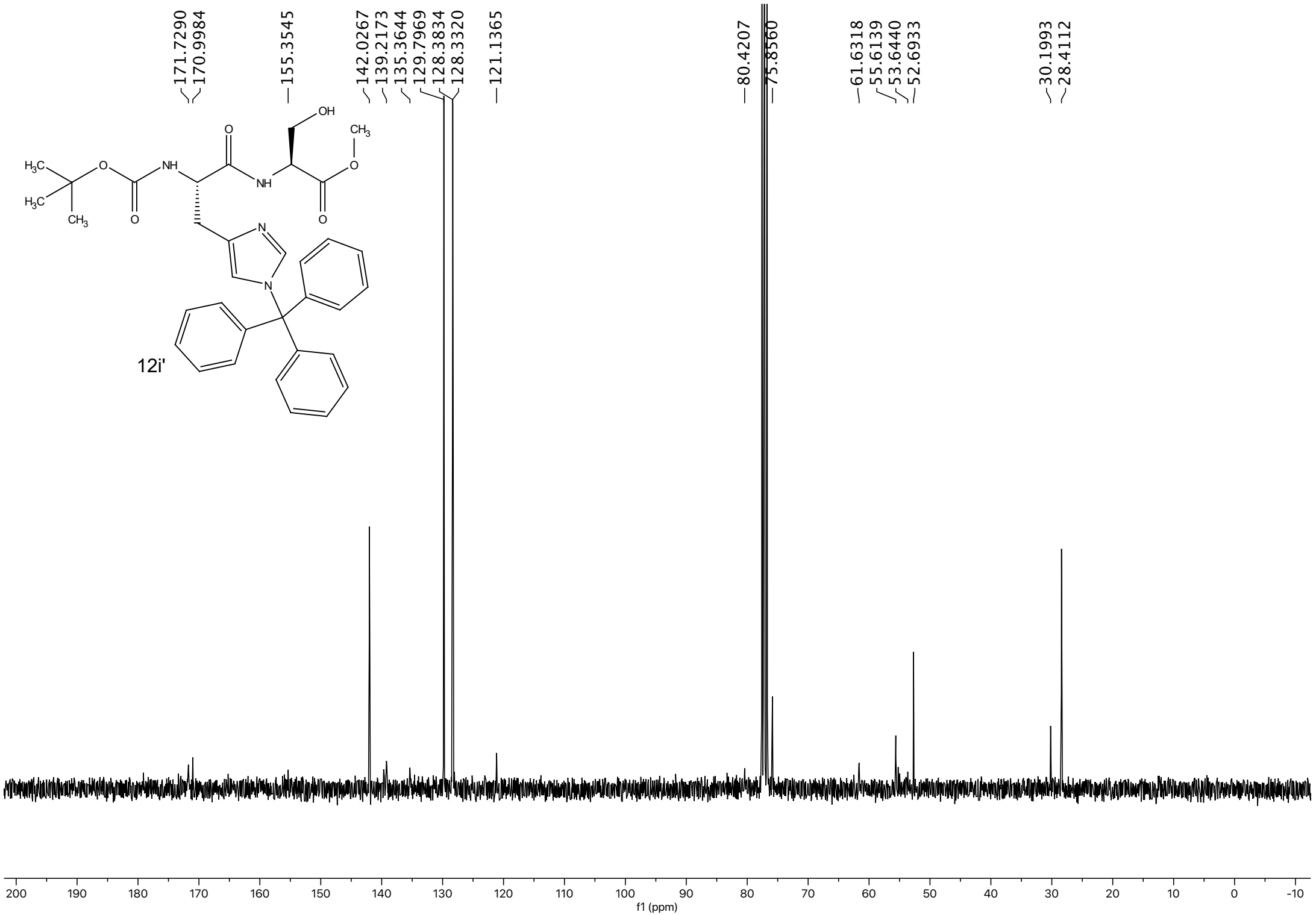
171.7290
170.9984
155.3545
142.0267
139.2173
135.3644
129.7969
128.3834
128.3320
121.1365
80.4207
75.8560
61.6318
55.6139
53.6440
52.6933
30.1993
28.4112
12i'
200
190
180
170
160
150
140
130
120
110
100
90
80
70
60
50
40
30
20
10
0
-10
f1 (ppm)

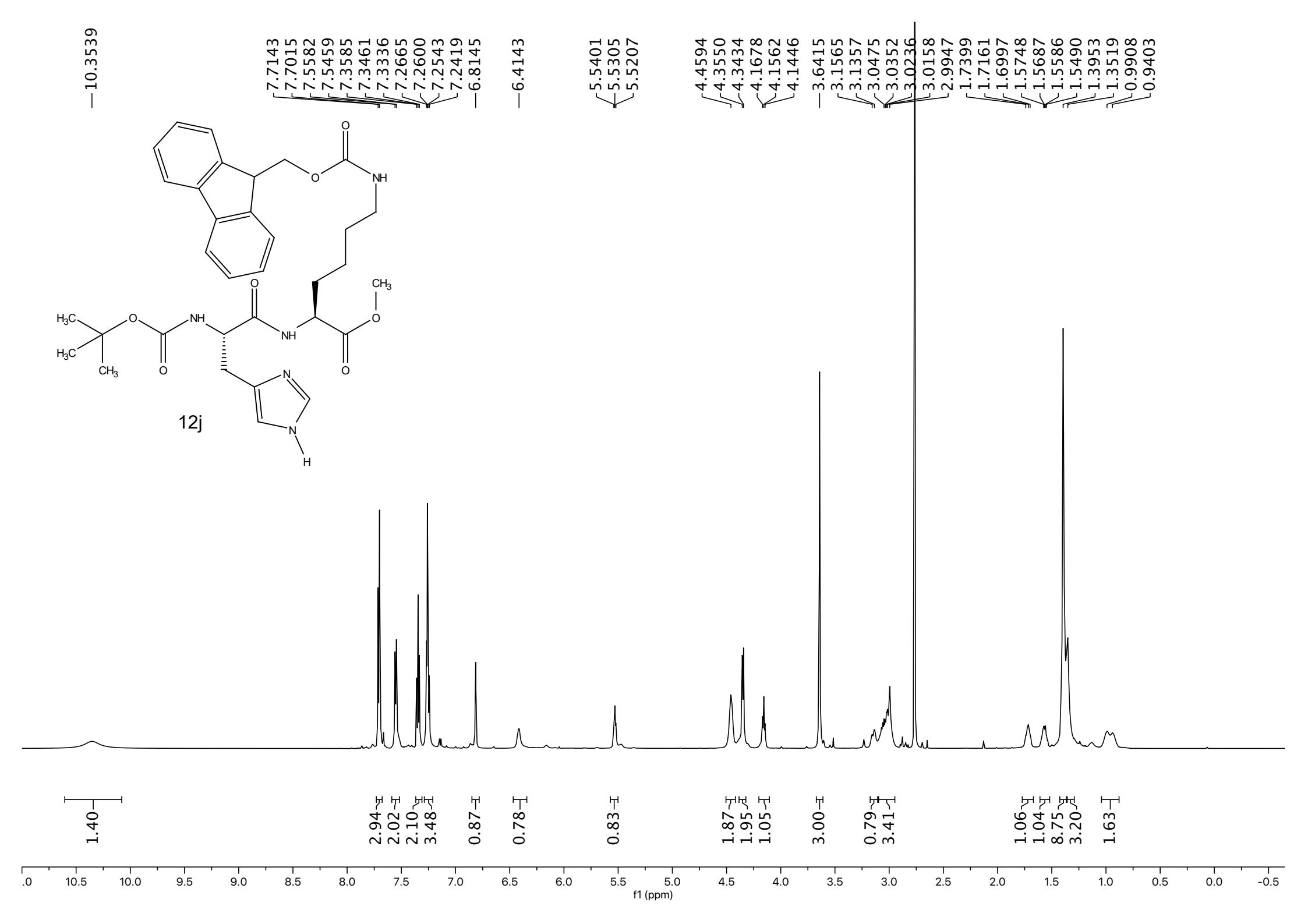
10.3539
7.7143
7.7015
7.5582
7.5459
7.3585
7.3461
7.3336
7.2665
7.2600
7.2543
7.2419
6.8145
6.4143
5.5401
5.5305
5.5207
4.4594
4.3550
4.3434
4.1678
4.1562
4.1446
3.6415
3.1565
3.1357
3.0475
3.0352
3.0236
3.0158
2.9947
1.7399
1.7161
1.6997
1.5748
1.5687
1.5586
1.5490
1.3953
1.3519
0.9908
0.9403
12j
1.40
2.94
2.02
2.10
3.48
0.87
0.78
0.83
1.87
1.95
1.05
3.00
0.79
3.41
1.06
1.04
8.75
3.20
1.63
f1 (ppm)

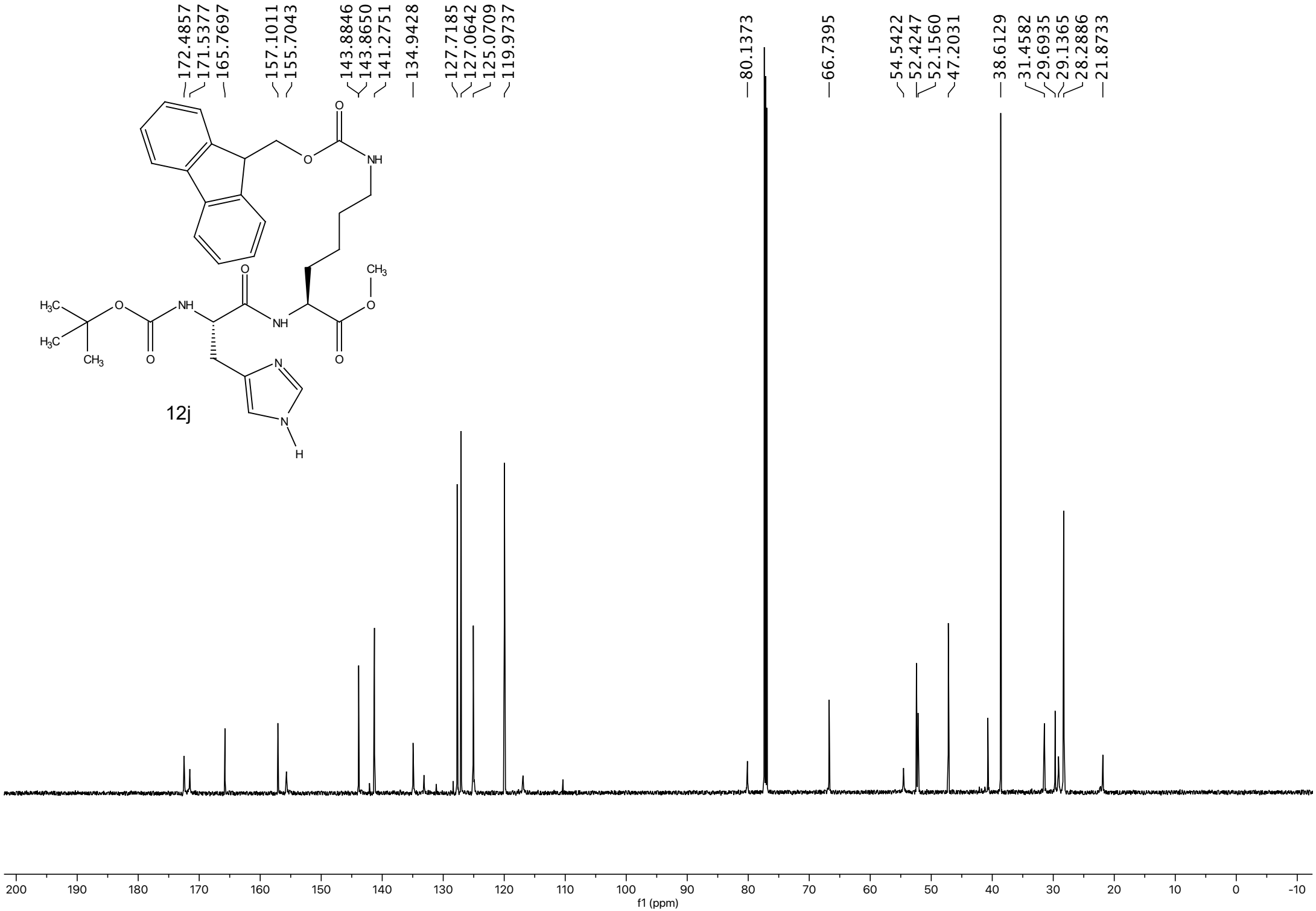
172.4857
171.5377
165.7697
157.1011
155.7043
143.8846
143.8650
141.2751
134.9428
127.7185
127.0642
125.0709
119.9737
80.1373
66.7395
54.5422
52.4247
52.1560
47.2031
38.6129
31.4582
29.6935
29.1365
28.2886
21.8733
12j
f1 (ppm)

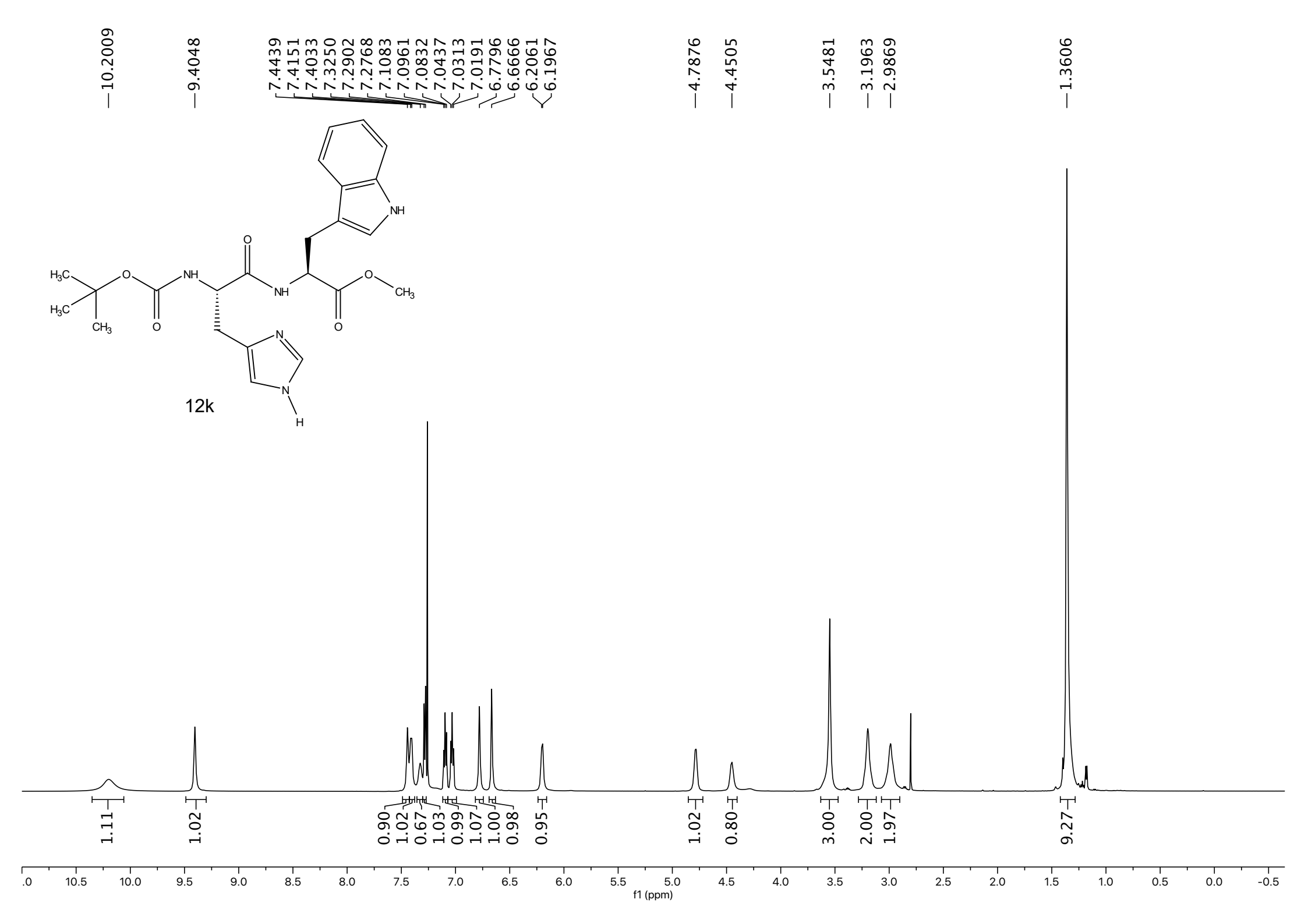
10.2009
9.4048
7.4439
7.4151
7.4033
7.3250
7.2902
7.2768
7.1083
7.0961
7.0832
7.0437
7.0313
7.0191
6.7796
6.6666
6.2061
6.1967
4.7876
4.4505
3.5481
3.1963
2.9869
1.3606
12k
1.11
1.02
0.90
1.02
0.67
1.03
0.99
1.07
1.00
0.98
0.95
1.02
0.80
3.00
2.00
1.97
9.27
f1 (ppm)

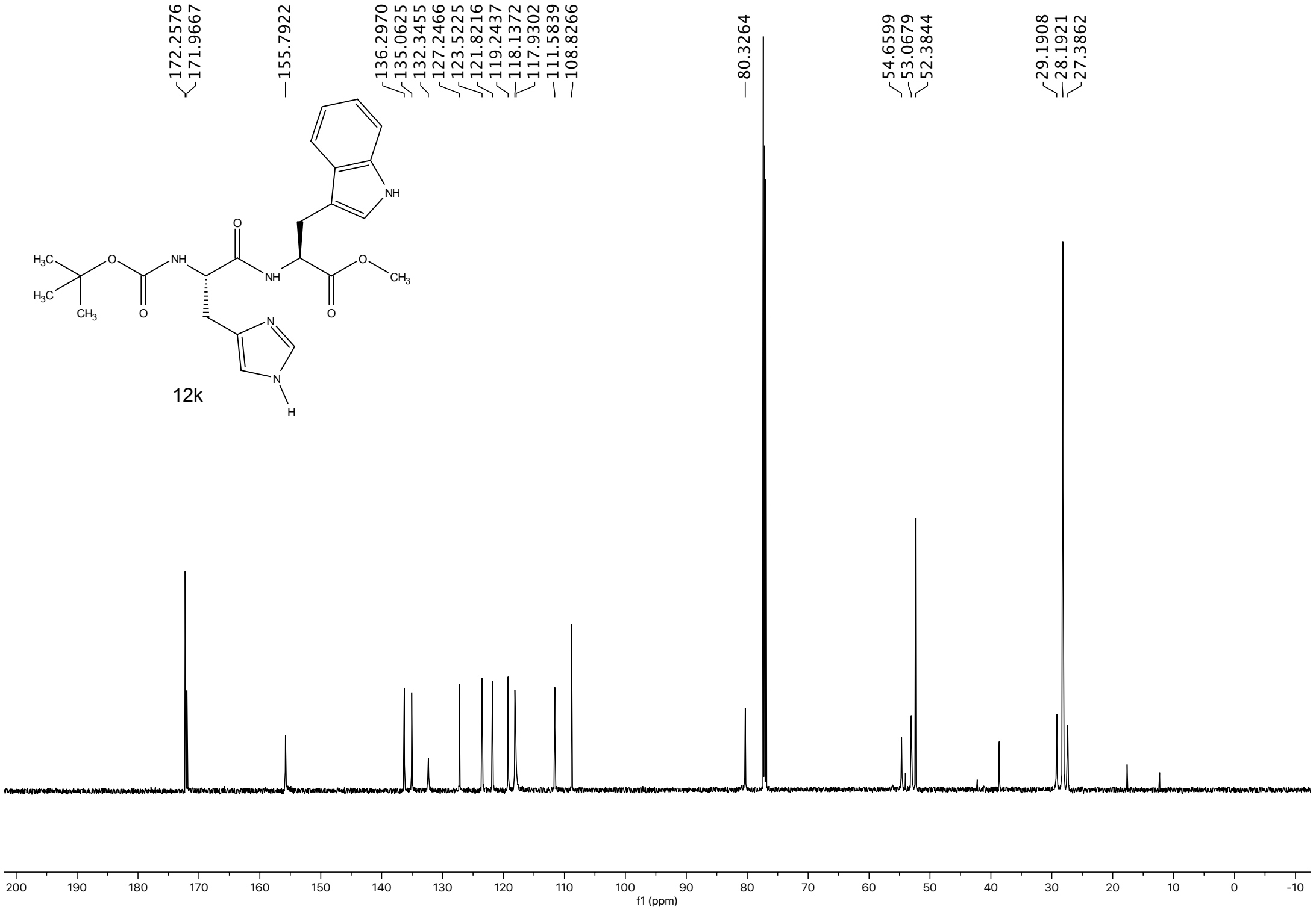
172.2576
171.9667
155.7922
136.2970
135.0625
132.3455
127.2466
123.5225
121.8216
119.2437
118.1372
117.9302
111.5839
108.8266
80.3264
54.6599
53.0679
52.3844
29.1908
28.1921
27.3862
12k
f1 (ppm)

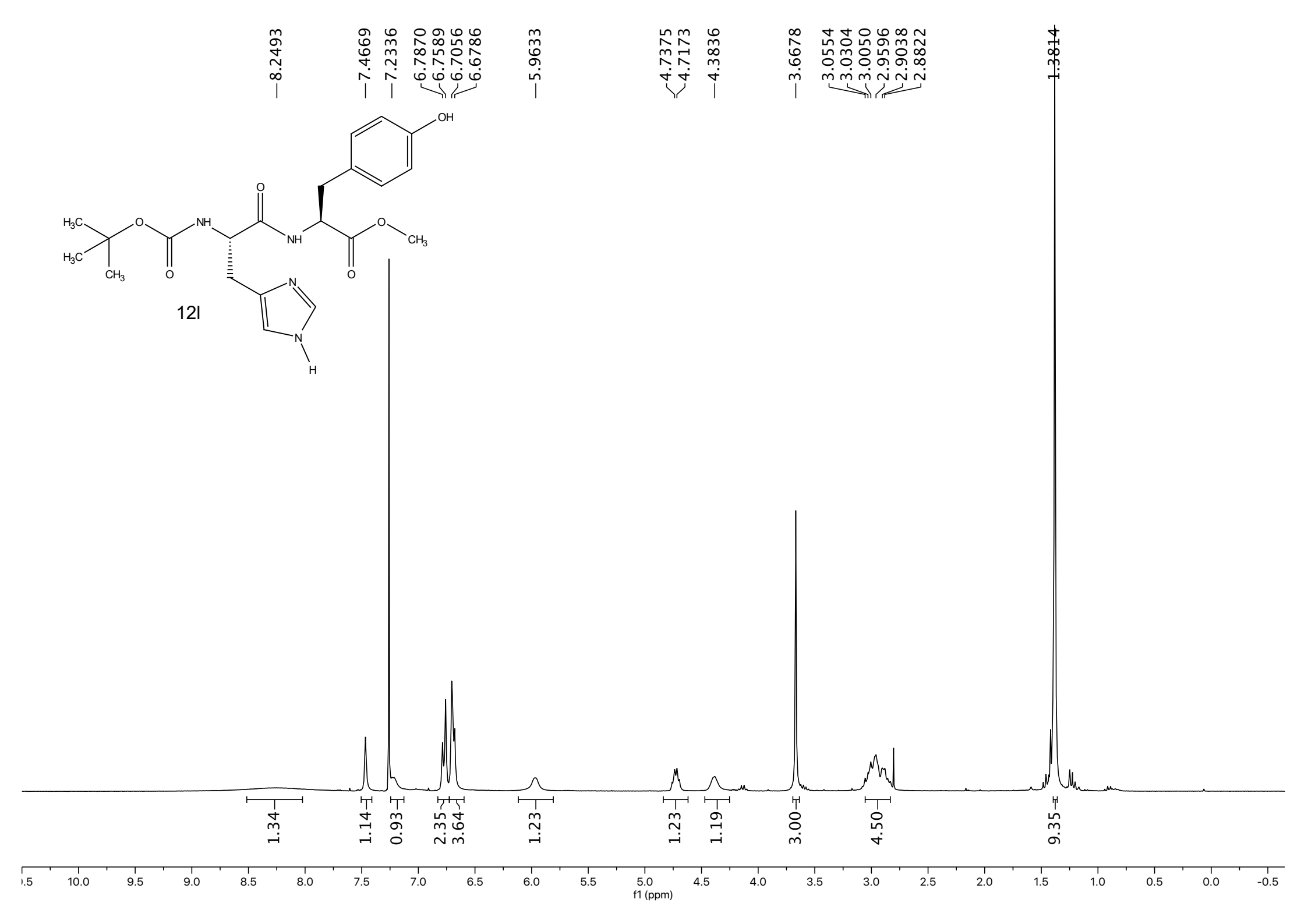
8.2493
7.4669
7.2336
6.7870
6.7589
6.7056
6.6786
5.9633
4.7375
4.7173
4.3836
3.6678
3.0554
3.0304
3.0050
2.9596
2.9038
2.8822
1.3814
12l
1.34
1.14
0.93
2.35
3.64
1.23
1.23
1.19
3.00
4.50
9.35
f1 (ppm)

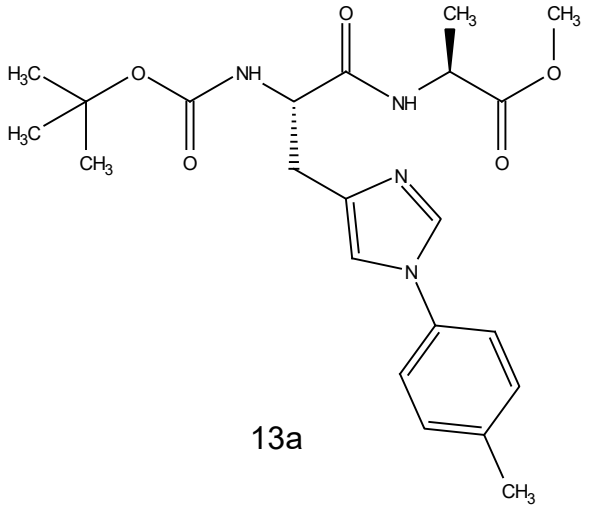
13a

7.7969
7.5092
7.2363
7.2243
7.2163
7.2020
7.0751
6.2116
4.5041
4.4931
4.4819
3.6590
3.1429
3.0293
3.0211
3.0054
2.9970
2.3667
1.4236
1.2678
1.2560
0.99
0.78
3.86
0.94
0.83
1.84
3.00
0.91
1.05
2.91
9.27
3.40
f1 (ppm)

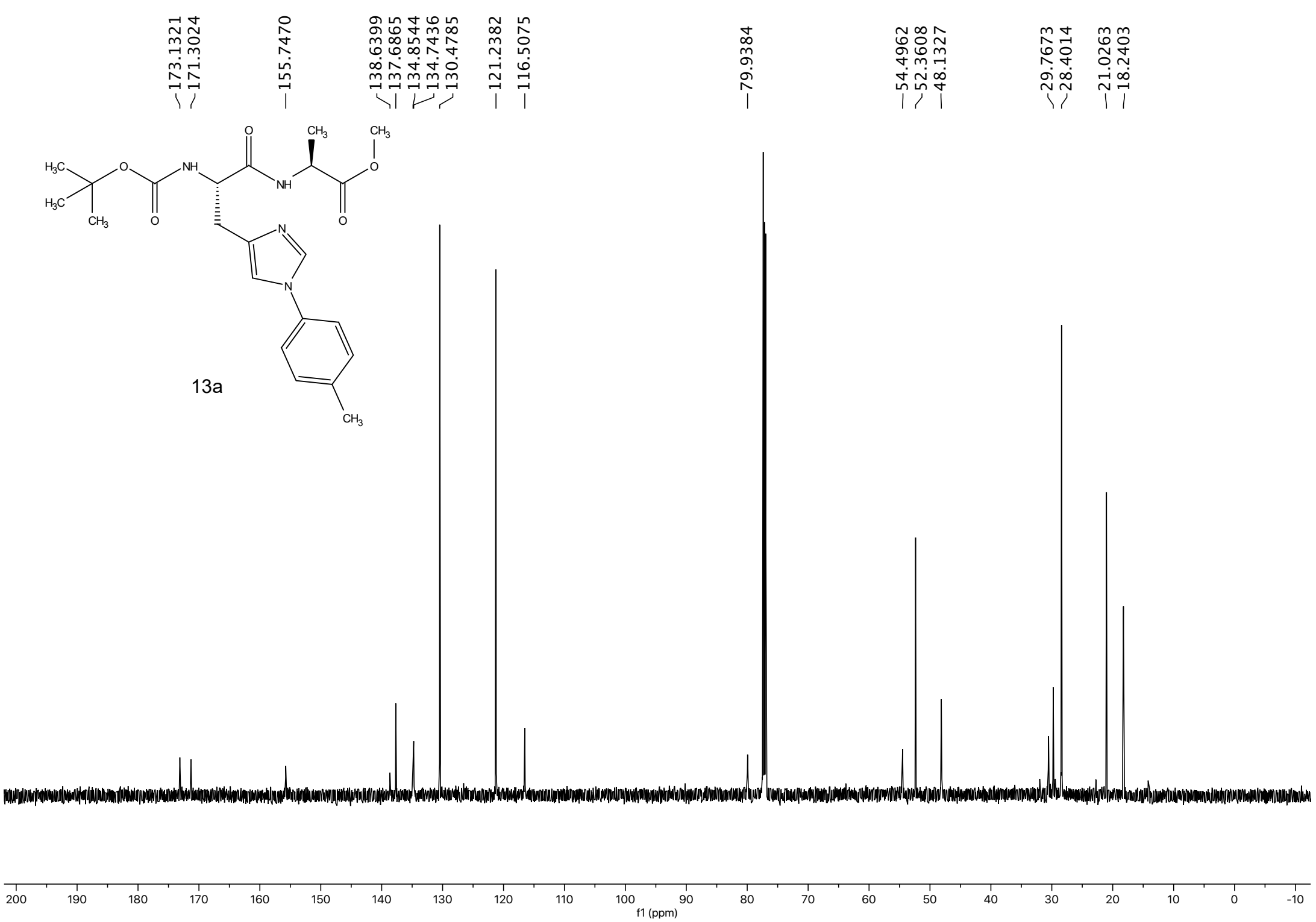
173.1321
171.3024
155.7470
138.6399
137.6865
134.8544
134.7436
130.4785
121.2382
116.5075
79.9384
54.4962
52.3608
48.1327
29.7673
28.4014
21.0263
18.2403
13a
f1 (ppm)

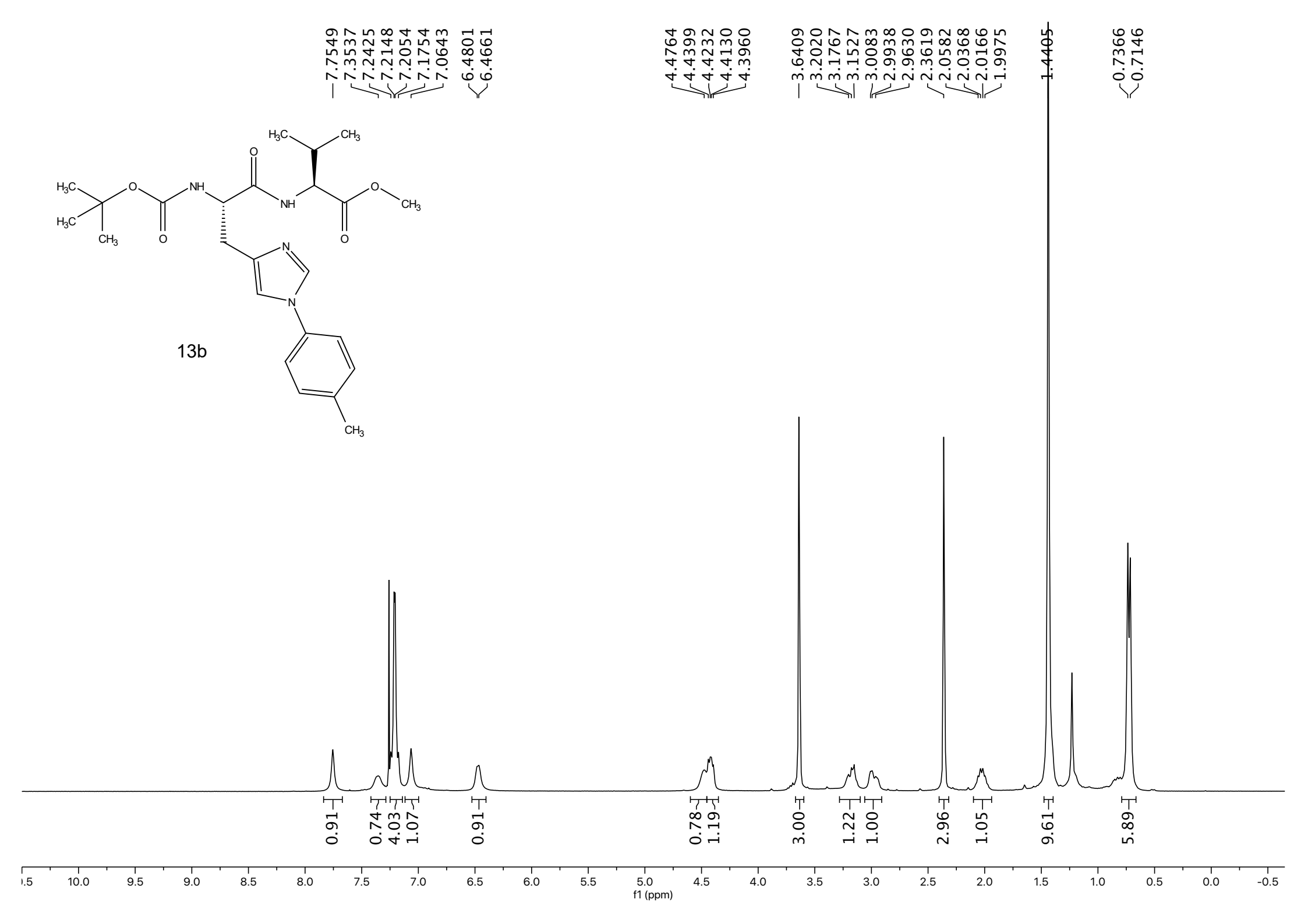
7.7549
7.3537
7.2425
7.2148
7.2054
7.1754
7.0643
6.4801
6.4661
4.4764
4.4399
4.4232
4.4130
4.3960
3.6409
3.2020
3.1767
3.1527
3.0083
2.9938
2.9630
2.3619
2.0582
2.0368
2.0166
1.9975
1.4405
0.7366
0.7146
13b
0.91
0.74
4.03
1.07
0.91
0.78
1.19
3.00
1.22
1.00
2.96
1.05
9.61
5.89
f1 (ppm)

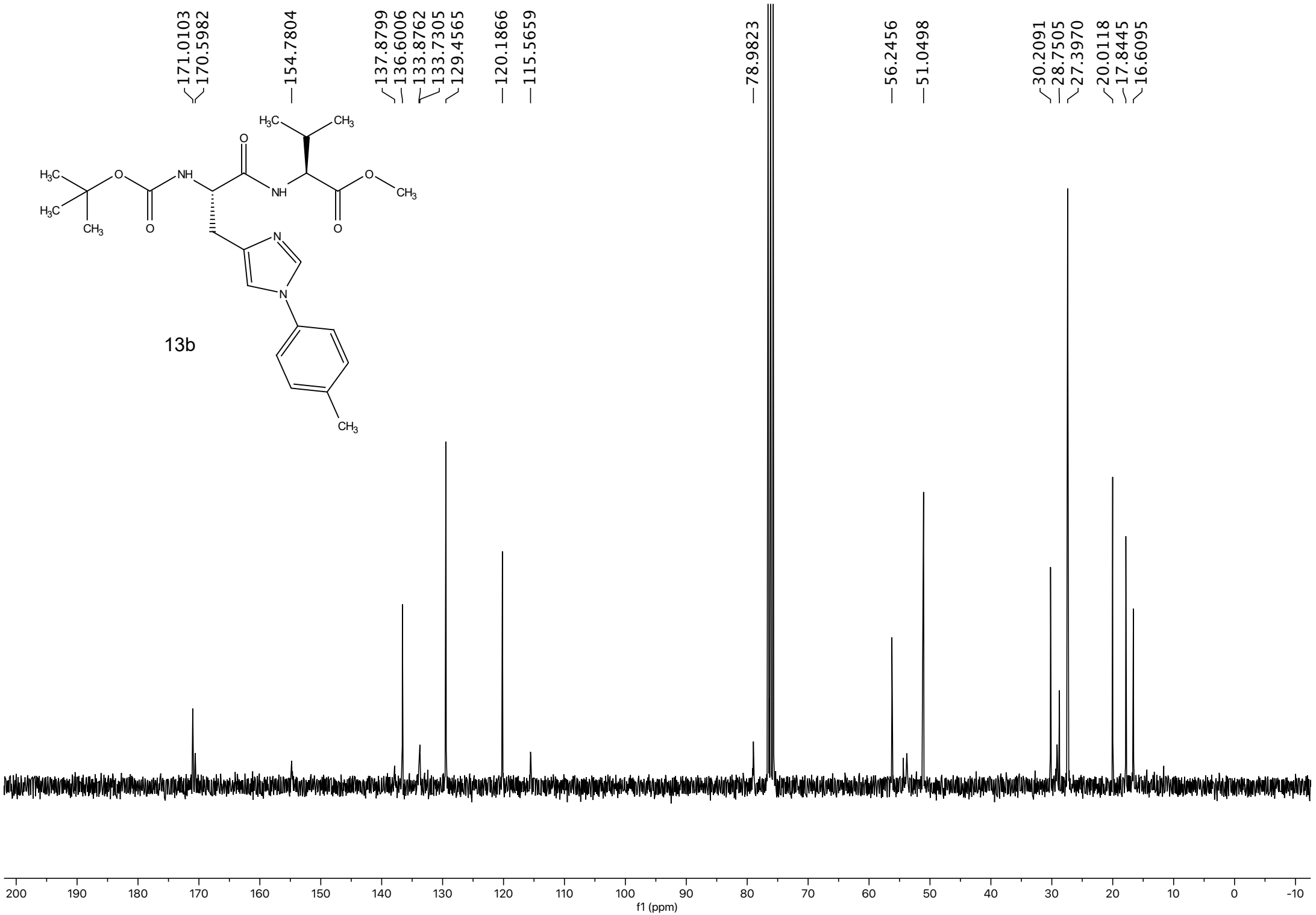
171.0103
170.5982
154.7804
137.8799
136.6006
133.8762
133.7305
129.4565
120.1866
115.5659
78.9823
56.2456
51.0498
30.2091
28.7505
27.3970
20.0118
17.8445
16.6095
13b
f1 (ppm)

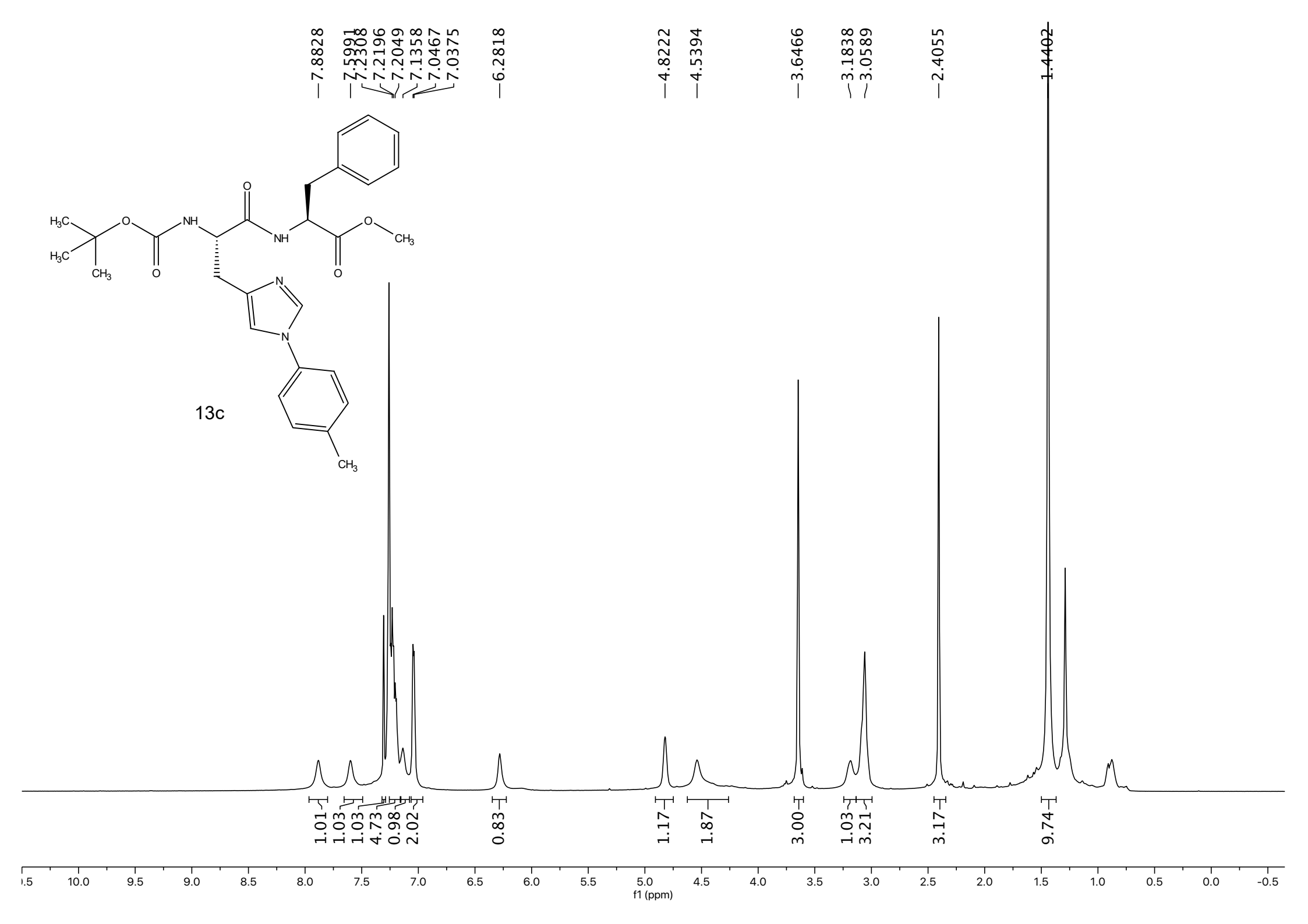
7.8828
7.5991
7.5808
7.2196
7.2049
7.1358
7.0467
7.0375
6.2818
4.8222
4.5394
3.6466
3.1838
3.0589
2.4055
1.4402
13c
1.01
1.03
1.03
4.73
0.98
2.02
0.83
1.17
1.87
3.00
1.03
3.21
3.17
9.74
f1 (ppm)

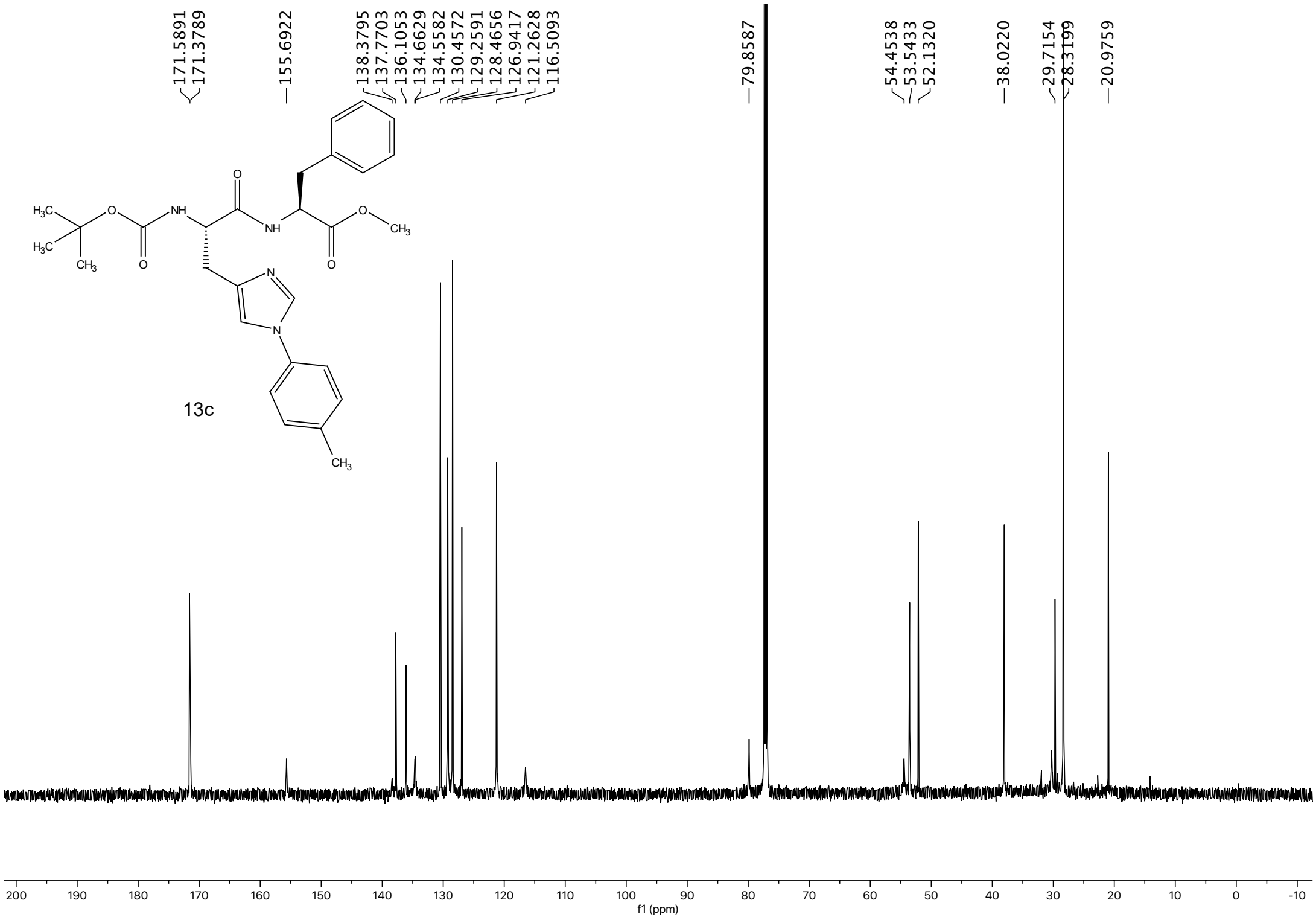
171.5891
171.3789
155.6922
138.3795
137.7703
136.1053
134.6629
134.5582
130.4572
129.2591
128.4656
126.9417
121.2628
116.5093
79.8587
54.4538
53.5433
52.1320
38.0220
29.7154
28.3199
20.9759
13c
f1 (ppm)

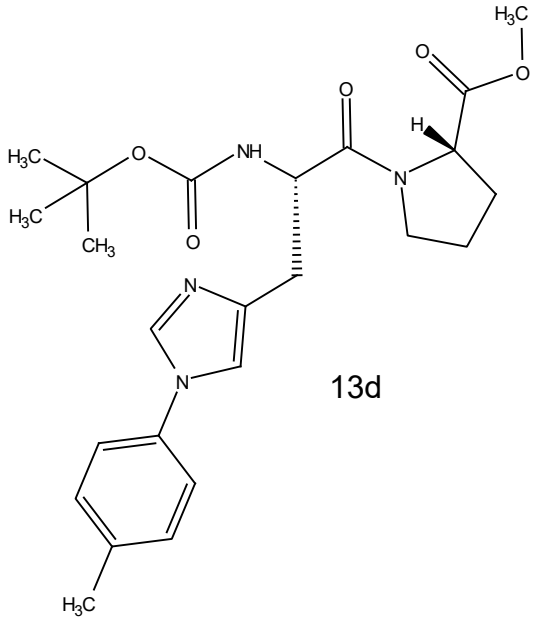
H3C
O
O
O
H
NH
N
H3C
H3C
CH3
O
N
N
H3C

13d

7.8485
7.2894
7.2755
7.2212
7.2076
5.5133
5.5037
4.7468
4.7369
4.4876
4.4800
3.7259
3.6498
3.5509
3.1159
3.1034
3.0910
3.0634
2.9498
2.9403
2.9244
2.3505
2.1633
2.1553
2.1423
1.9341
1.3476
0.98
1.99
2.86
0.85
0.86
1.01
0.97
3.00
0.83
1.04
1.12
2.81
1.06
2.88
8.68
f1 (ppm)

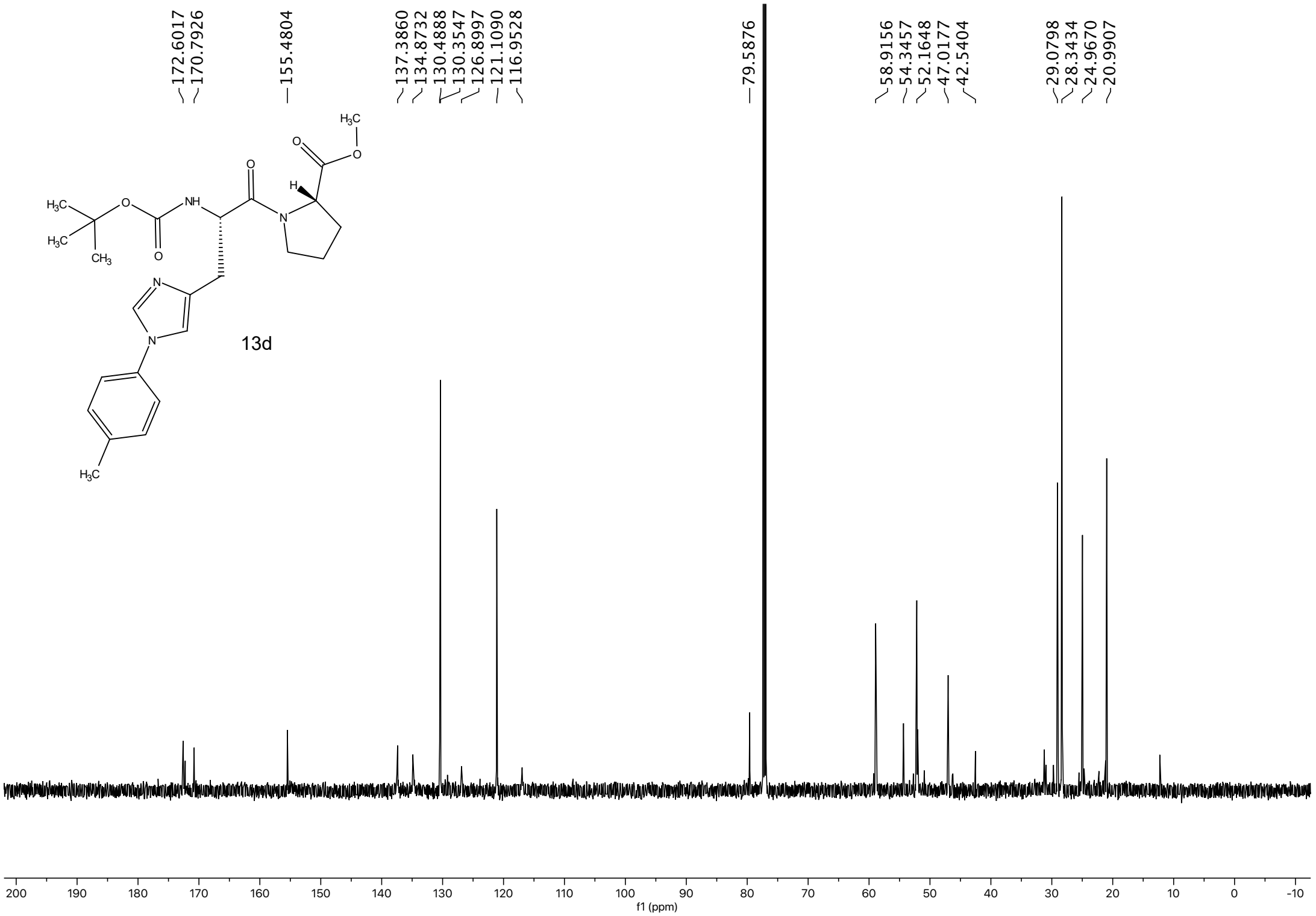
172.6017
170.7926
155.4804
137.3860
134.8732
130.4888
130.3547
126.8997
121.1090
116.9528
79.5876
58.9156
54.3457
52.1648
47.0177
42.5404
29.0798
28.3434
24.9670
20.9907
13d
f1 (ppm)

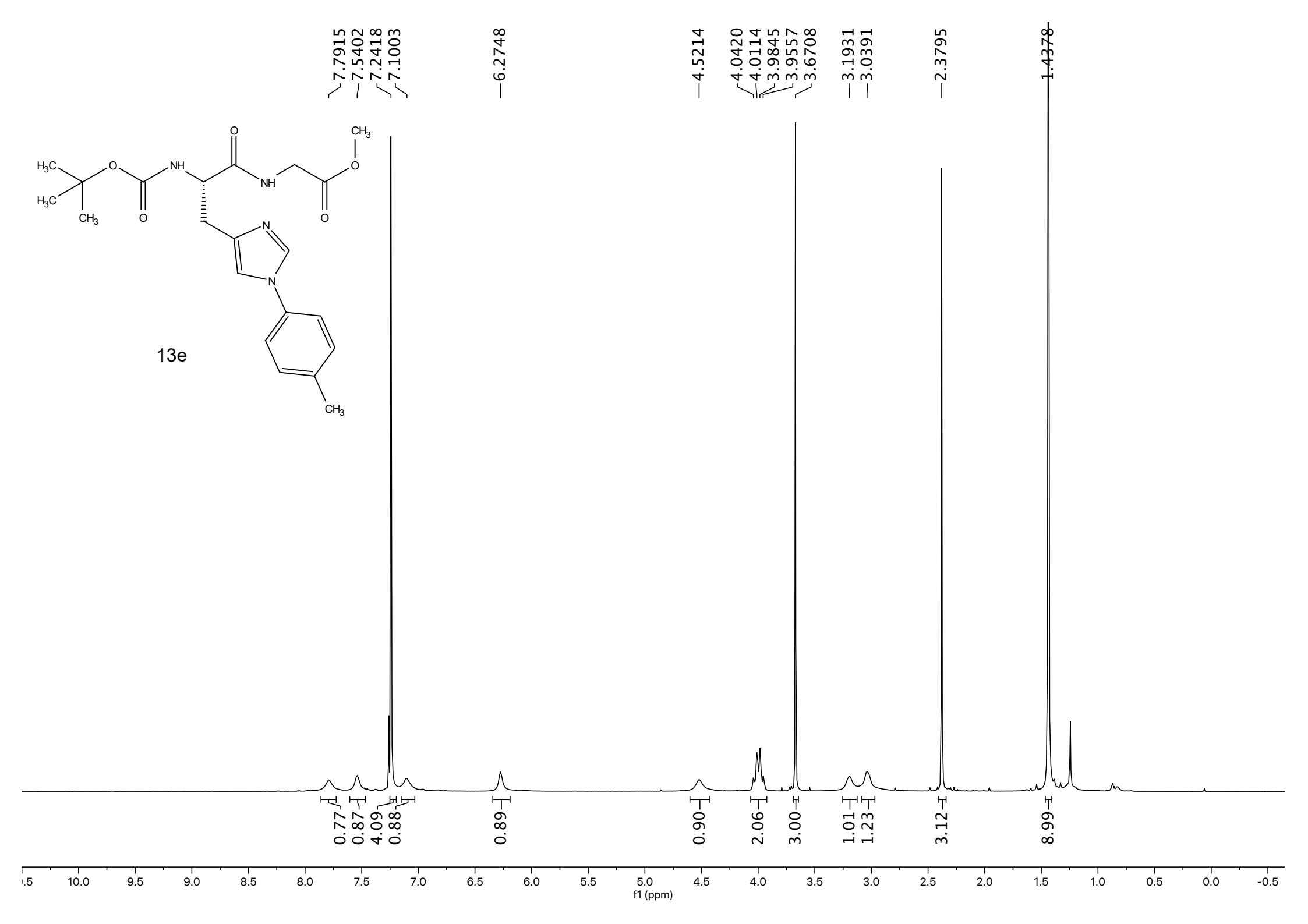
7.7915
7.5402
7.2418
7.1003
6.2748
4.5214
4.0420
4.0114
3.9845
3.9557
3.6708
3.1931
3.0391
2.3795
1.4378
13e
0.77
0.87
4.09
0.88
0.89
0.90
2.06
3.00
1.01
1.23
3.12
8.99
f1 (ppm)

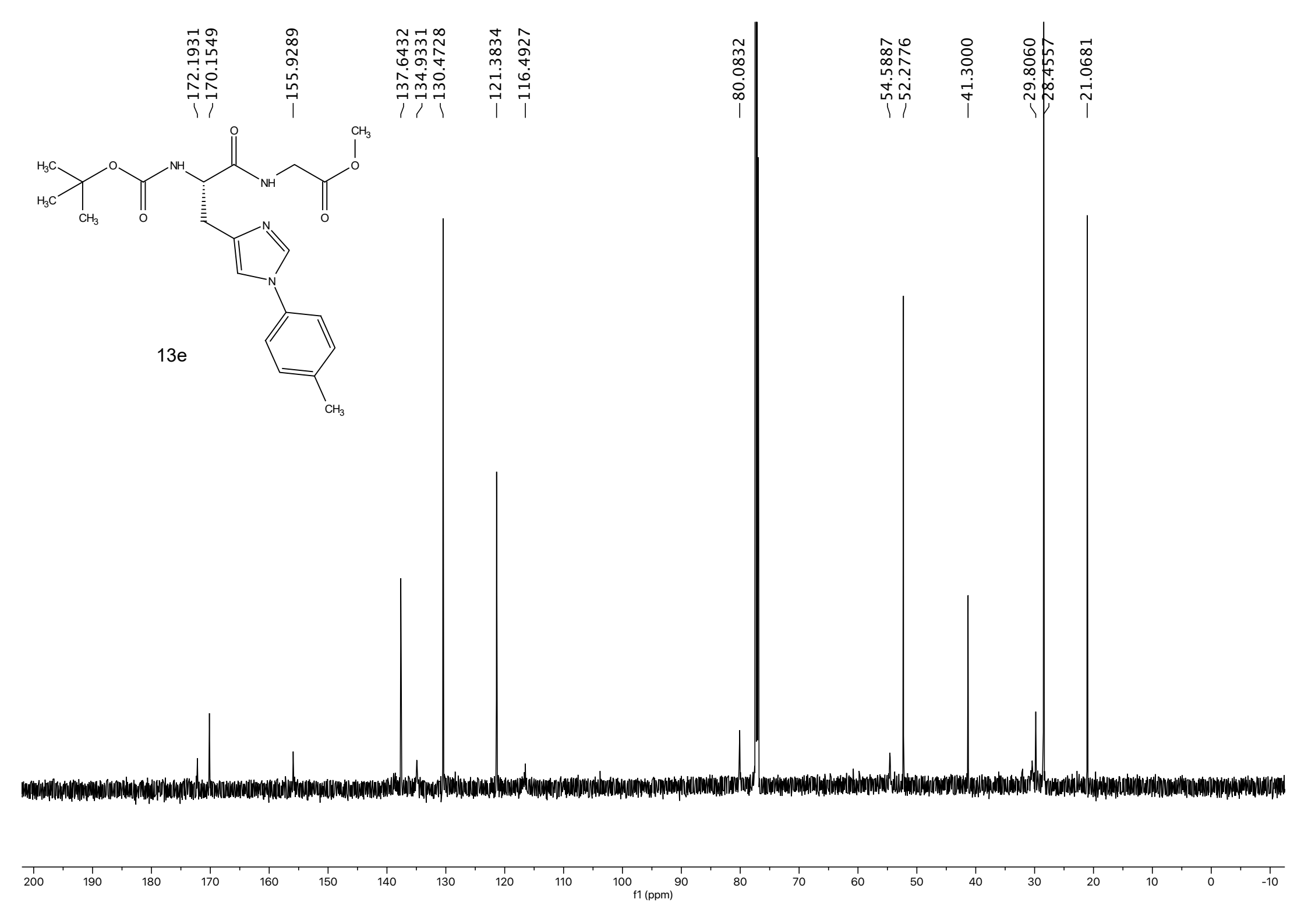
172.1931
170.1549
155.9289
137.6432
134.9331
130.4728
121.3834
116.4927
80.0832
54.5887
52.2776
41.3000
29.8060
28.4557
21.0681
13e
f1 (ppm)

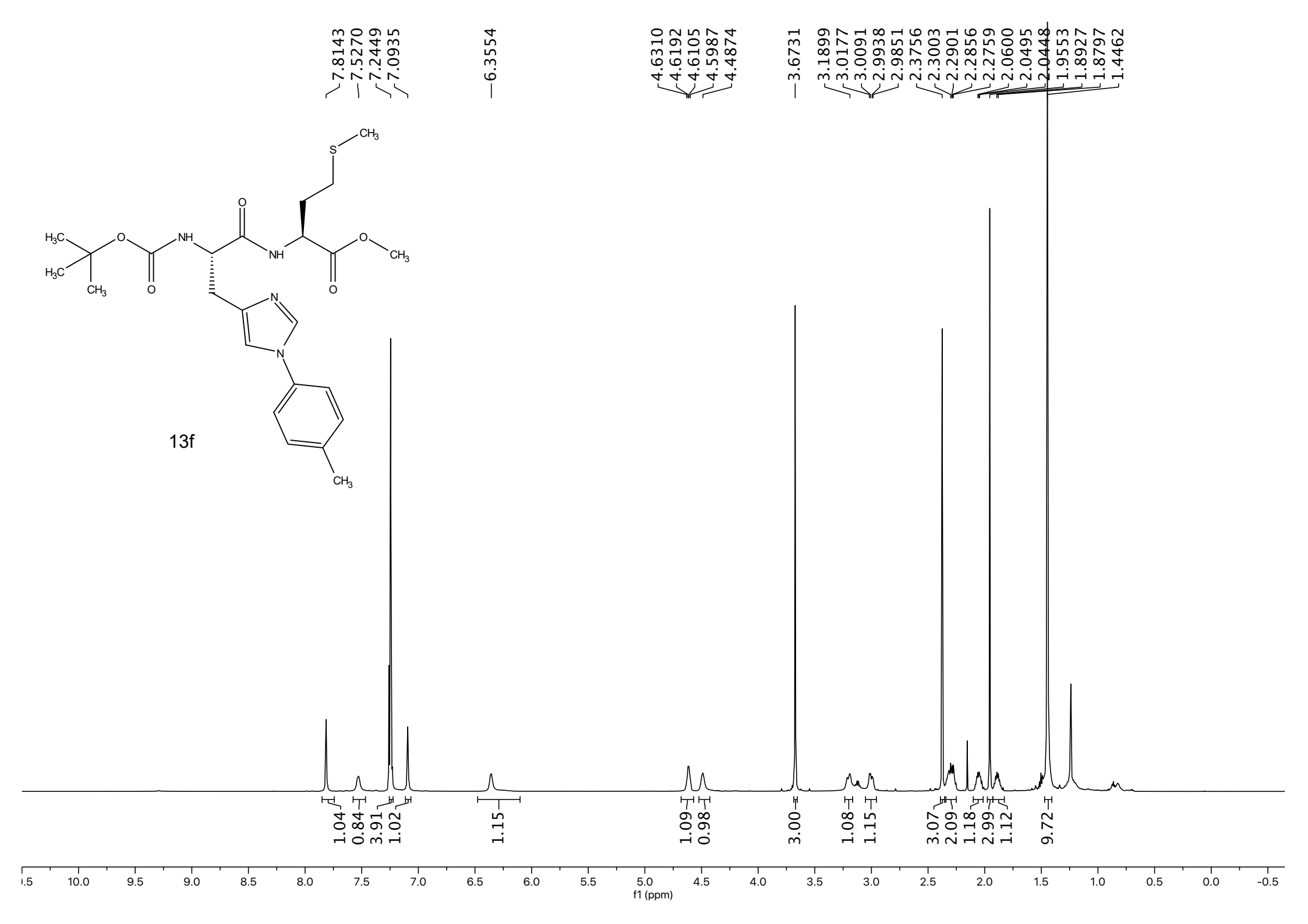
7.8143
7.5270
7.2449
7.0935
6.3554
4.6310
4.6192
4.6105
4.5987
4.4874
3.6731
3.1899
3.0177
3.0091
2.9938
2.9851
2.3756
2.3003
2.2901
2.2856
2.2759
2.0600
2.0495
2.0448
1.9553
1.8927
1.8797
1.4462
13f
1.04
0.84
3.91
1.02
1.15
1.09
0.98
3.00
1.08
1.15
3.07
2.09
1.18
2.99
1.12
9.72
f1 (ppm)

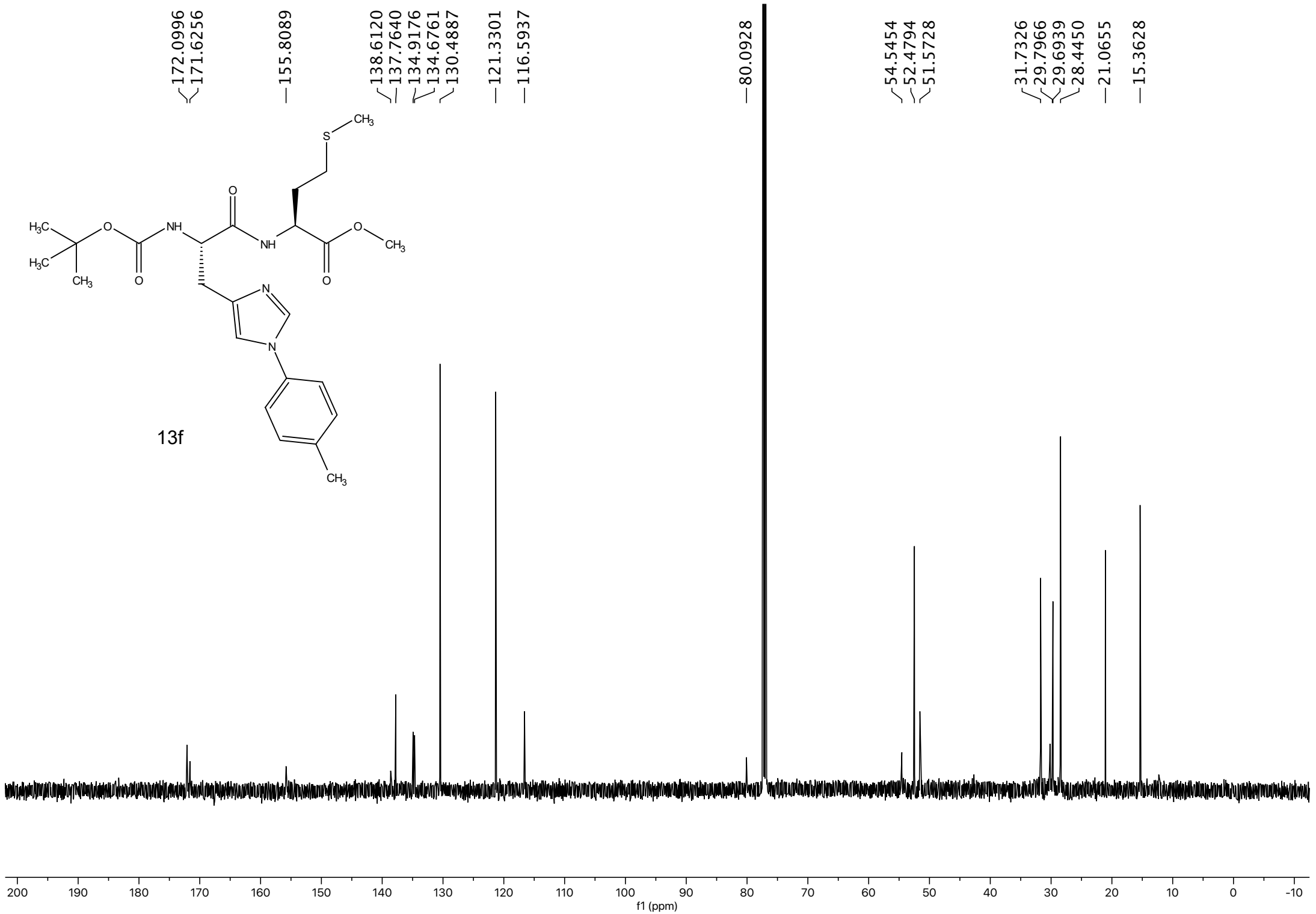
172.0996
171.6256
155.8089
138.6120
137.7640
134.9176
134.6761
130.4887
121.3301
116.5937
80.0928
54.5454
52.4794
51.5728
31.7326
29.7966
29.6939
28.4450
21.0655
15.3628
13f
f1 (ppm)

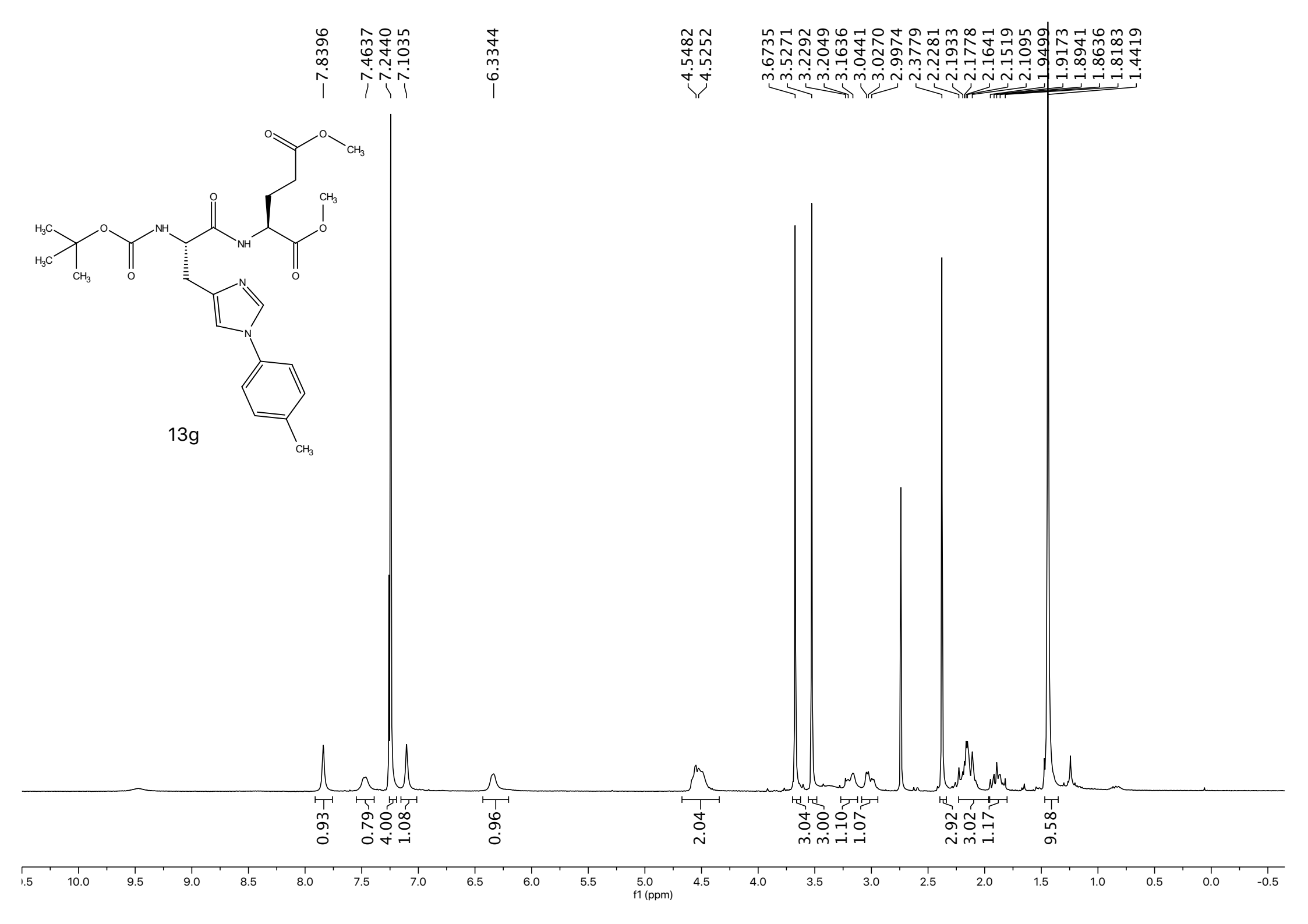
7.8396
7.4637
7.2440
7.1035
6.3344
4.5482
4.5252
3.6735
3.5271
3.2292
3.2049
3.1636
3.0441
3.0270
2.9974
2.3779
2.2281
2.1933
2.1778
2.1641
2.1519
2.1095
1.9499
1.9173
1.8941
1.8636
1.8183
1.4419
0.93
0.79
4.00
1.08
0.96
2.04
3.04
3.00
1.10
1.07
2.92
3.02
1.17
9.58
f1 (ppm)
13g

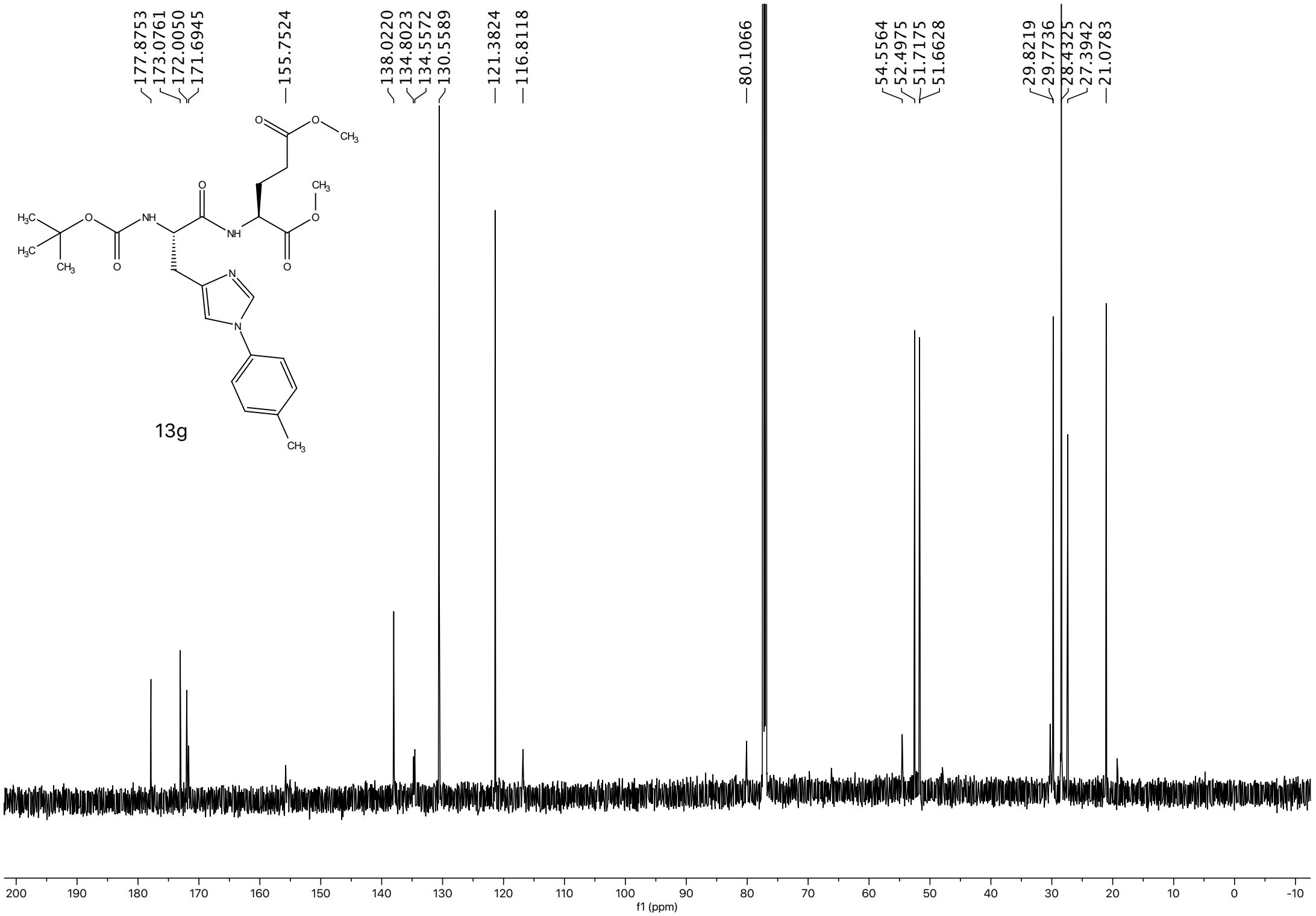
177.8753
173.0761
172.0050
171.6945
155.7524
138.0220
134.8023
134.5572
130.5589
121.3824
116.8118
80.1066
54.5564
52.4975
51.7175
51.6628
29.8219
29.7736
28.4325
27.3942
21.0783
13g
f1 (ppm)

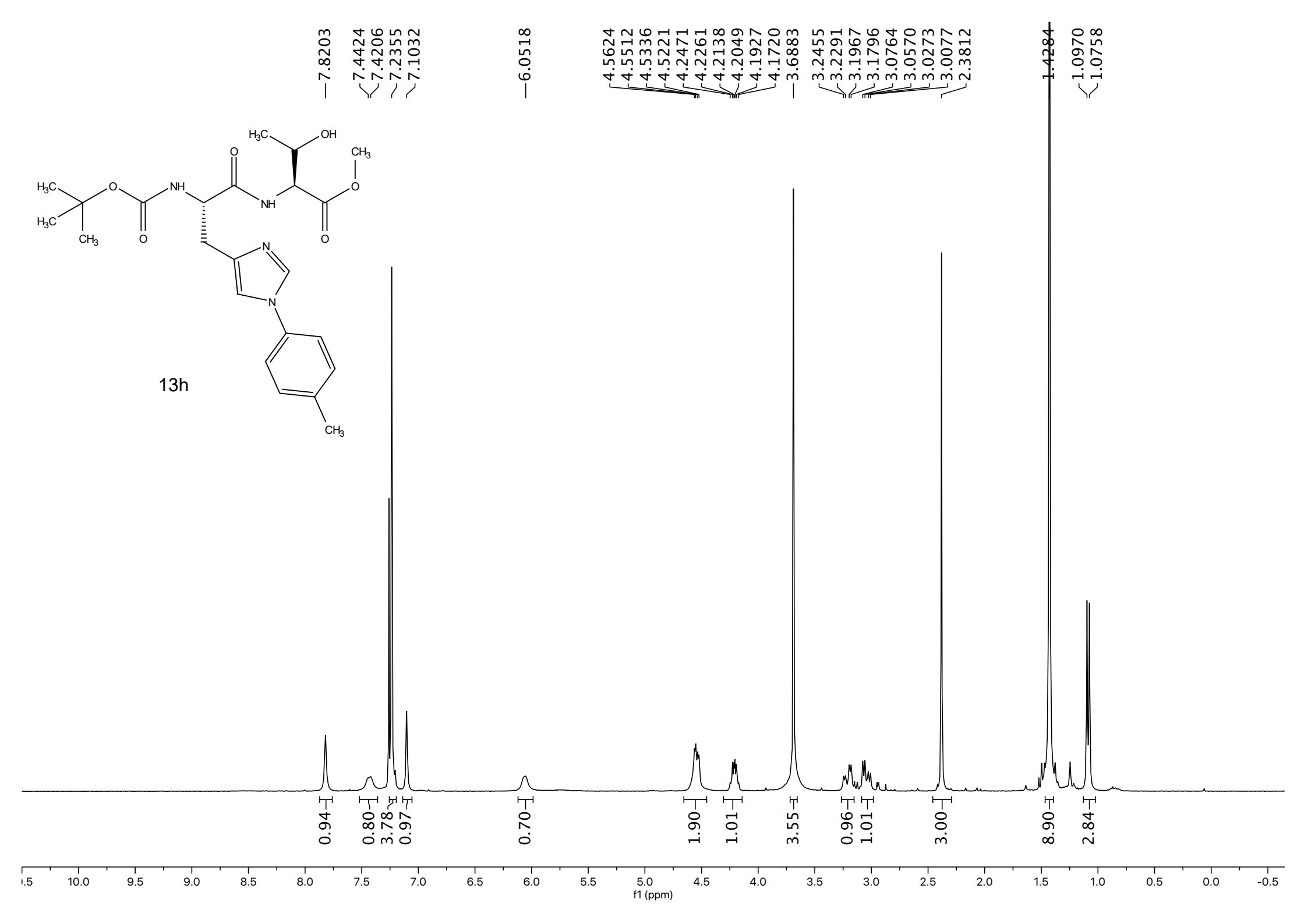
7.8203
7.4424
7.4206
7.2355
7.1032
6.0518
4.5624
4.5512
4.5336
4.5221
4.2471
4.2261
4.2138
4.2049
4.1927
4.1720
3.6883
3.2455
3.2291
3.1967
3.1796
3.0764
3.0570
3.0273
3.0077
2.3812
1.4284
1.0970
1.0758
13h
0.94
0.80
3.78
0.97
0.70
1.90
1.01
3.55
0.96
1.01
3.00
8.90
2.84
f1 (ppm)

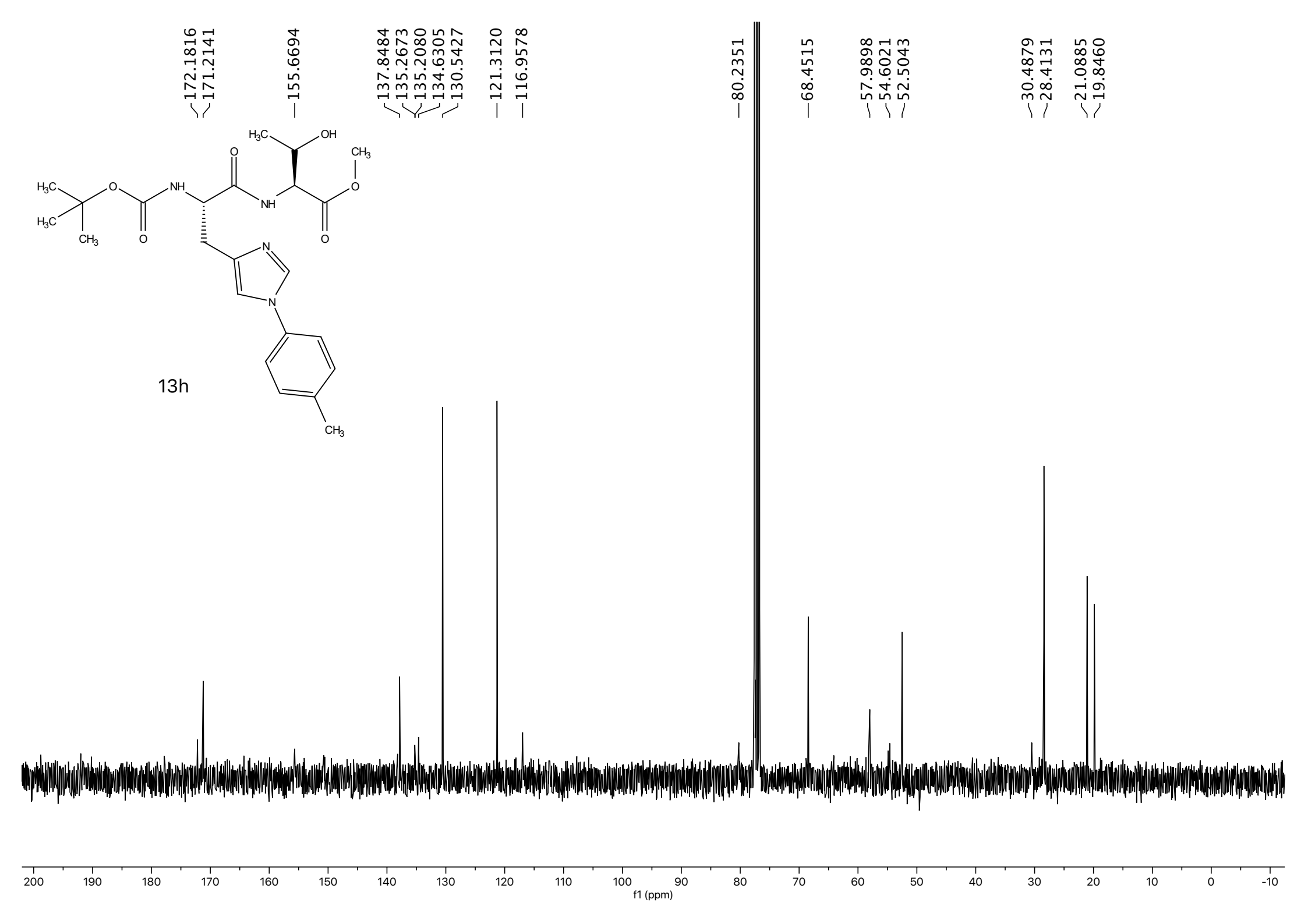
172.1816
171.2141
155.6694
137.8484
135.2673
135.2080
134.6305
130.5427
121.3120
116.9578
80.2351
68.4515
57.9898
54.6021
52.5043
30.4879
28.4131
21.0885
19.8460
13h
f1 (ppm)

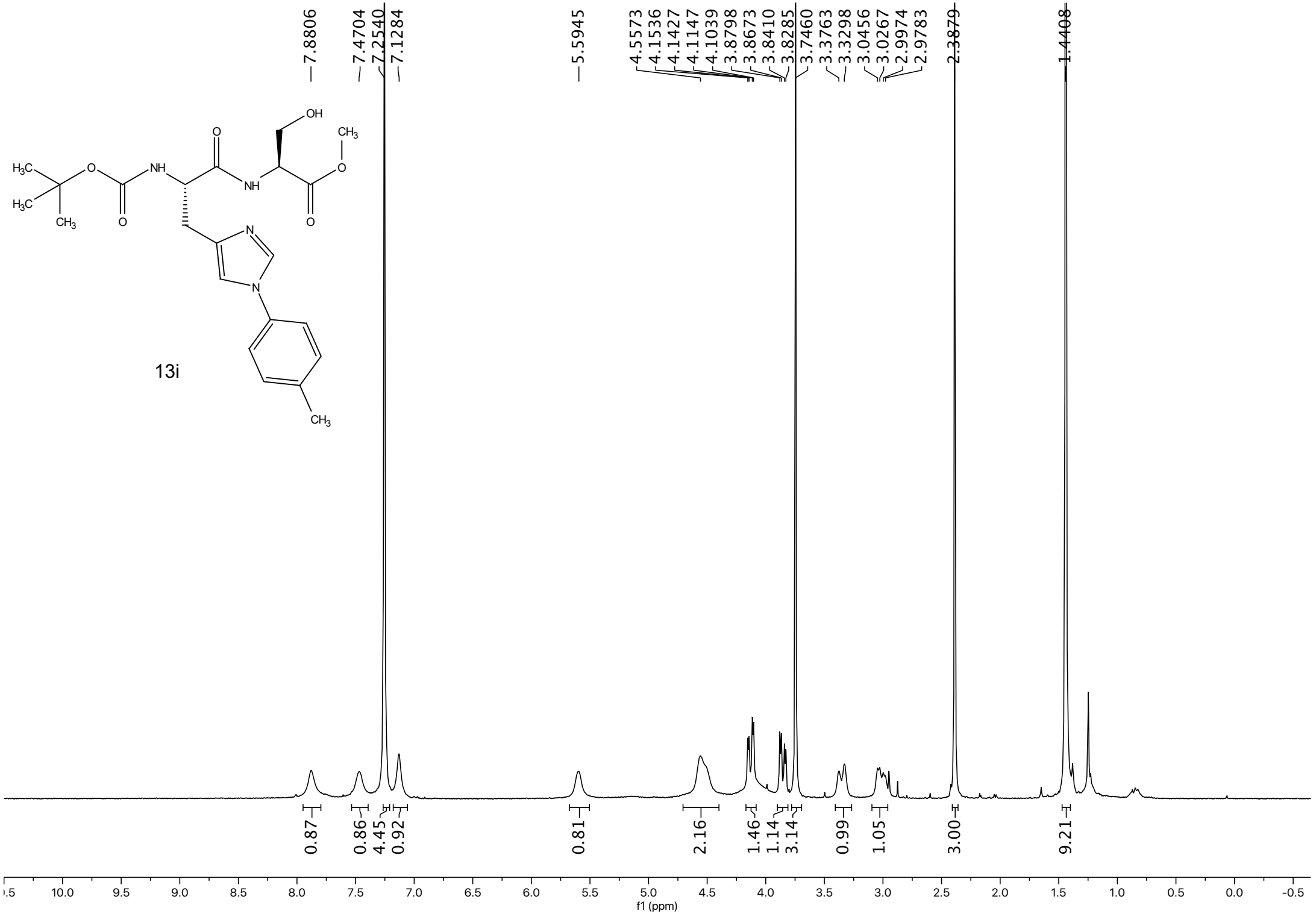
7.8806
7.4704
7.2540
7.1284
5.5945
4.5573
4.1536
4.1427
4.1147
4.1039
3.8798
3.8673
3.8410
3.8285
3.7460
3.3763
3.3298
3.0456
3.0267
2.9974
2.9783
2.3879
1.4408
13i
0.87
0.86
4.45
0.92
0.81
2.16
1.46
1.14
3.14
0.99
1.05
3.00
9.21
f1 (ppm)

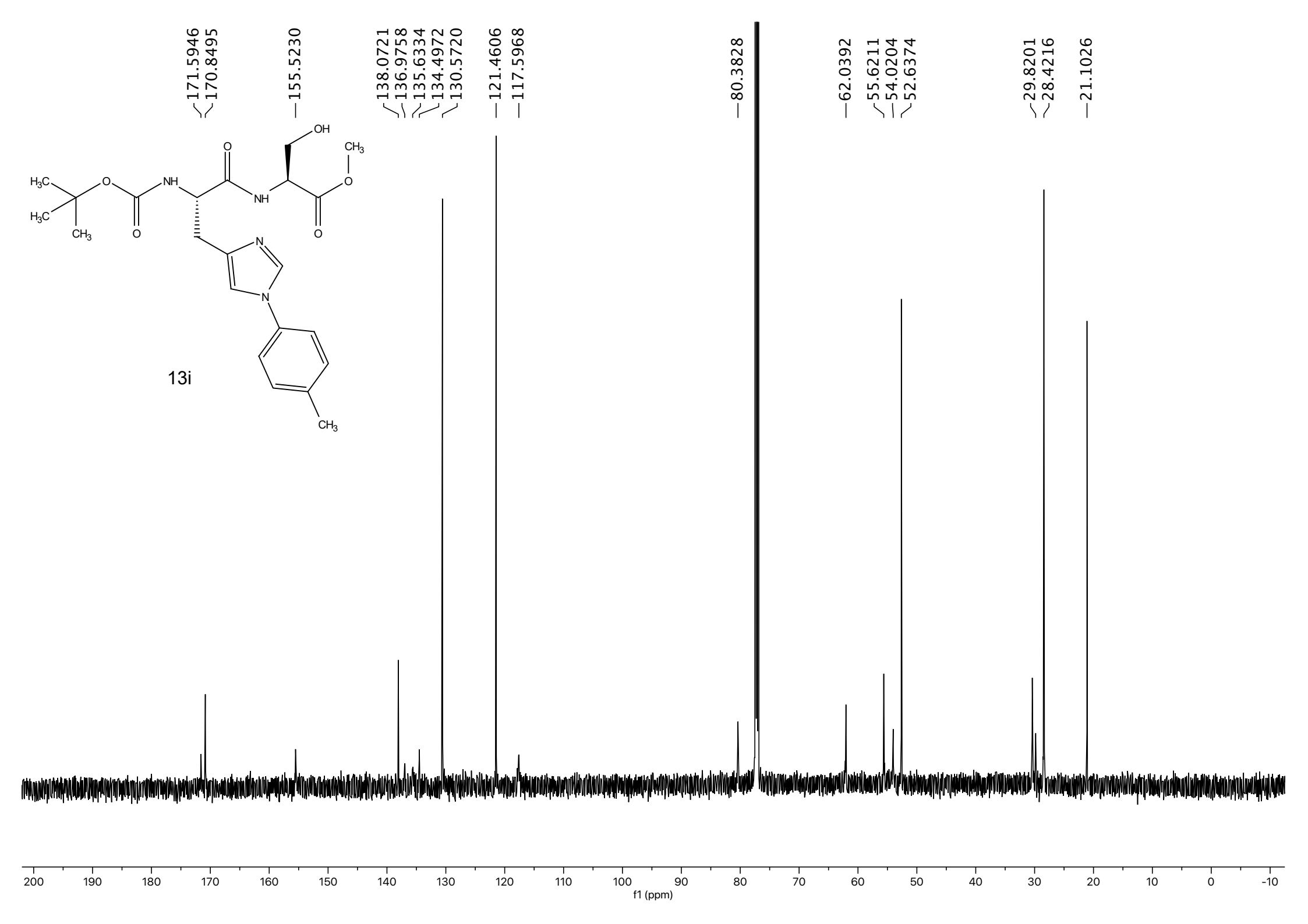
171.5946
170.8495
155.5230
138.0721
136.9758
135.6334
134.4972
130.5720
121.4606
117.5968
80.3828
62.0392
55.6211
54.0204
52.6374
29.8201
28.4216
21.1026
13i
f1 (ppm)

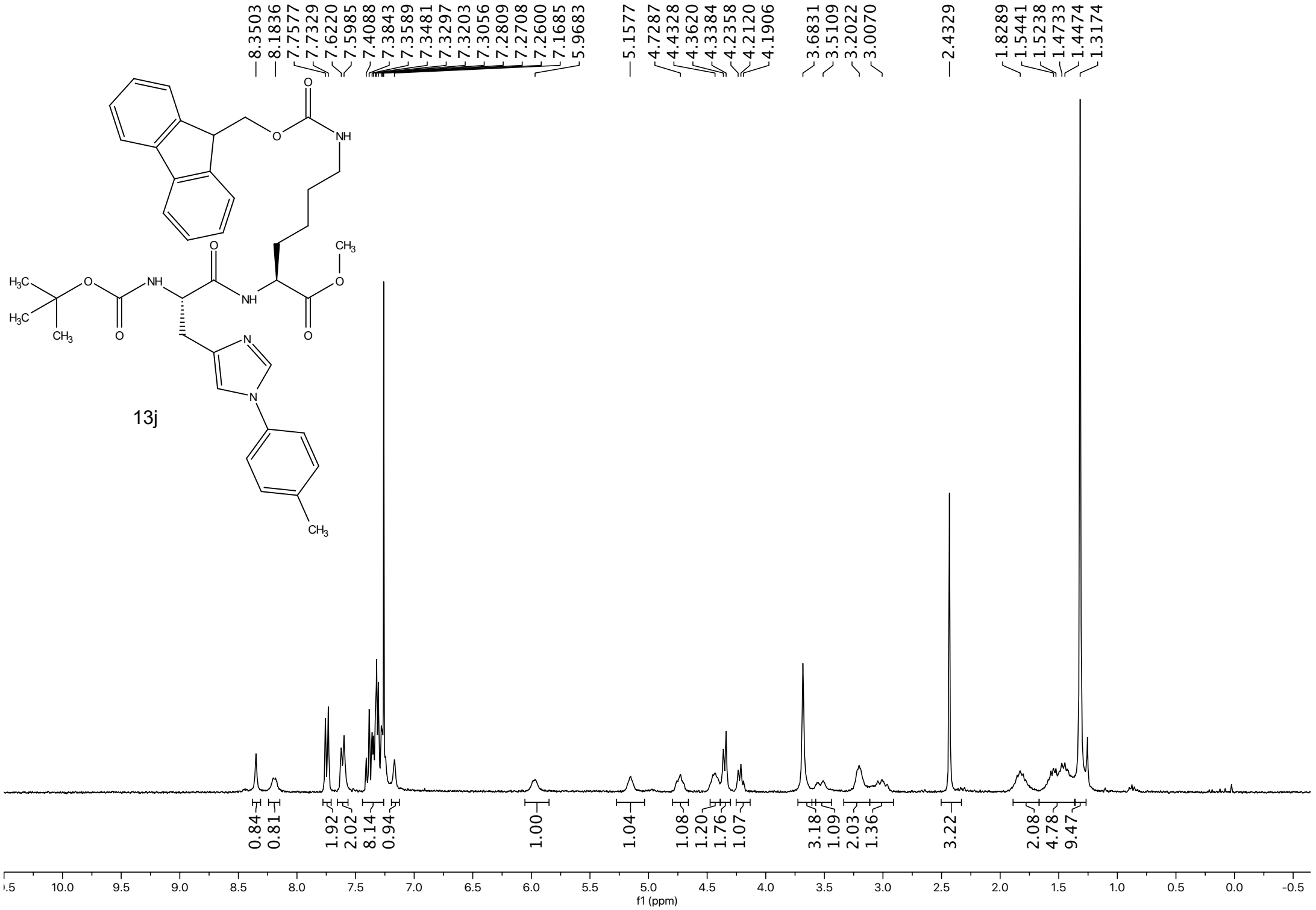
8.3503
8.1836
7.7577
7.7329
7.6220
7.5985
7.4088
7.3843
7.3589
7.3481
7.3297
7.3203
7.3056
7.2809
7.2708
7.2600
7.1685
5.9683
5.1577
4.7287
4.4328
4.3620
4.3384
4.2358
4.2120
4.1906
3.6831
3.5109
3.2022
3.0070
2.4329
1.8289
1.5441
1.5238
1.4733
1.4474
1.3174
13j
0.84
0.81
1.92
2.02
8.14
0.94
1.00
1.04
1.08
1.20
1.76
1.07
3.18
1.09
2.03
1.36
3.22
2.08
4.78
9.47
f1 (ppm)

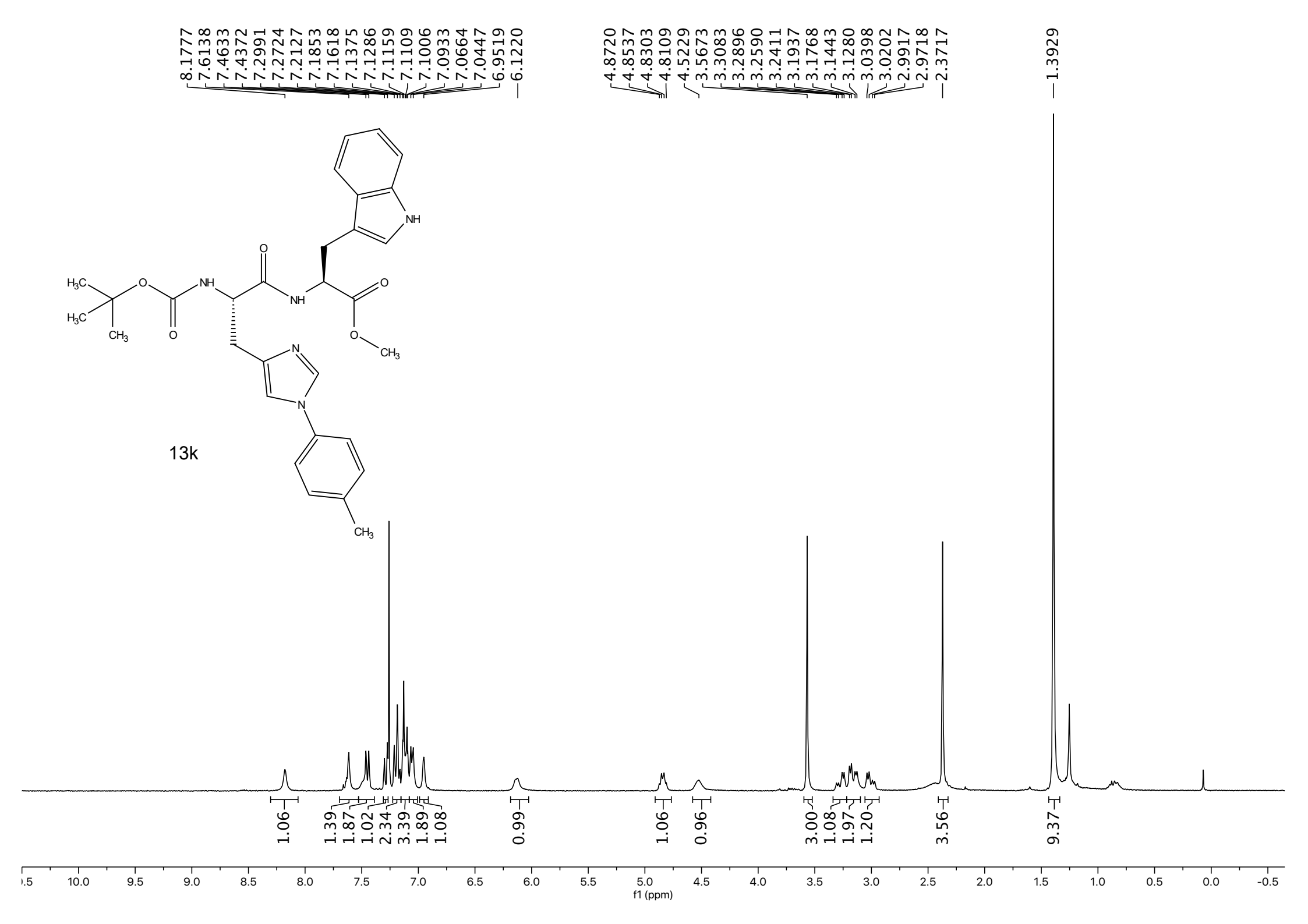
8.1777
7.6138
7.4633
7.4372
7.2991
7.2724
7.2127
7.1853
7.1618
7.1375
7.1286
7.1159
7.1109
7.1006
7.0933
7.0664
7.0447
6.9519
6.1220
4.8720
4.8537
4.8303
4.8109
4.5229
3.5673
3.3083
3.2896
3.2590
3.2411
3.1937
3.1768
3.1443
3.1280
3.0398
3.0202
2.9917
2.9718
2.3717
1.3929
13k
1.06
1.39
1.87
1.02
2.34
3.39
1.89
1.08
0.99
1.06
0.96
3.00
1.08
1.97
1.20
3.56
9.37
f1 (ppm)

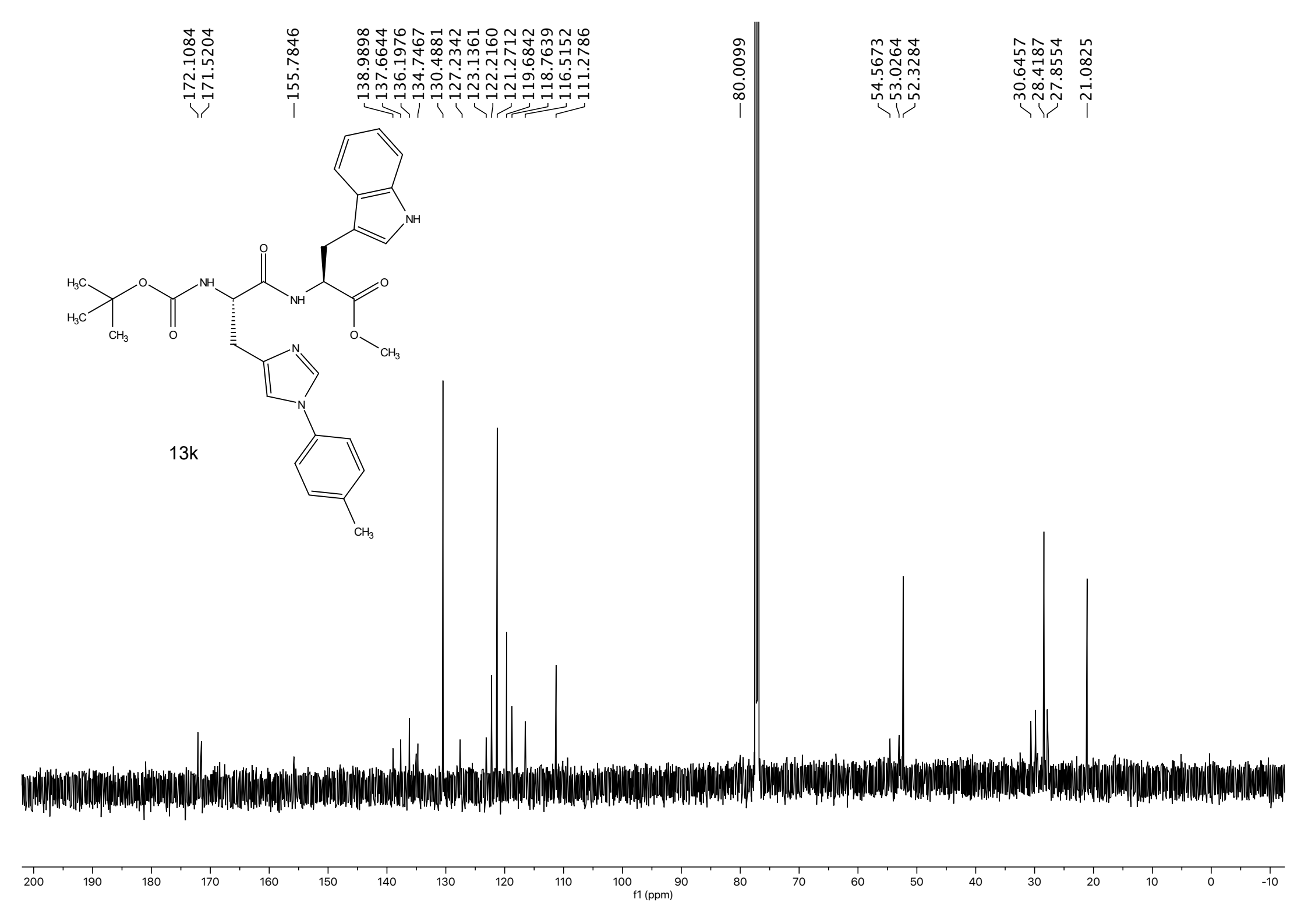
172.1084
171.5204
155.7846
138.9898
137.6644
136.1976
134.7467
130.4881
127.2342
123.1361
122.2160
121.2712
119.6842
118.7639
116.5152
111.2786
80.0099
54.5673
53.0264
52.3284
30.6457
28.4187
27.8554
21.0825
13k
f1 (ppm)

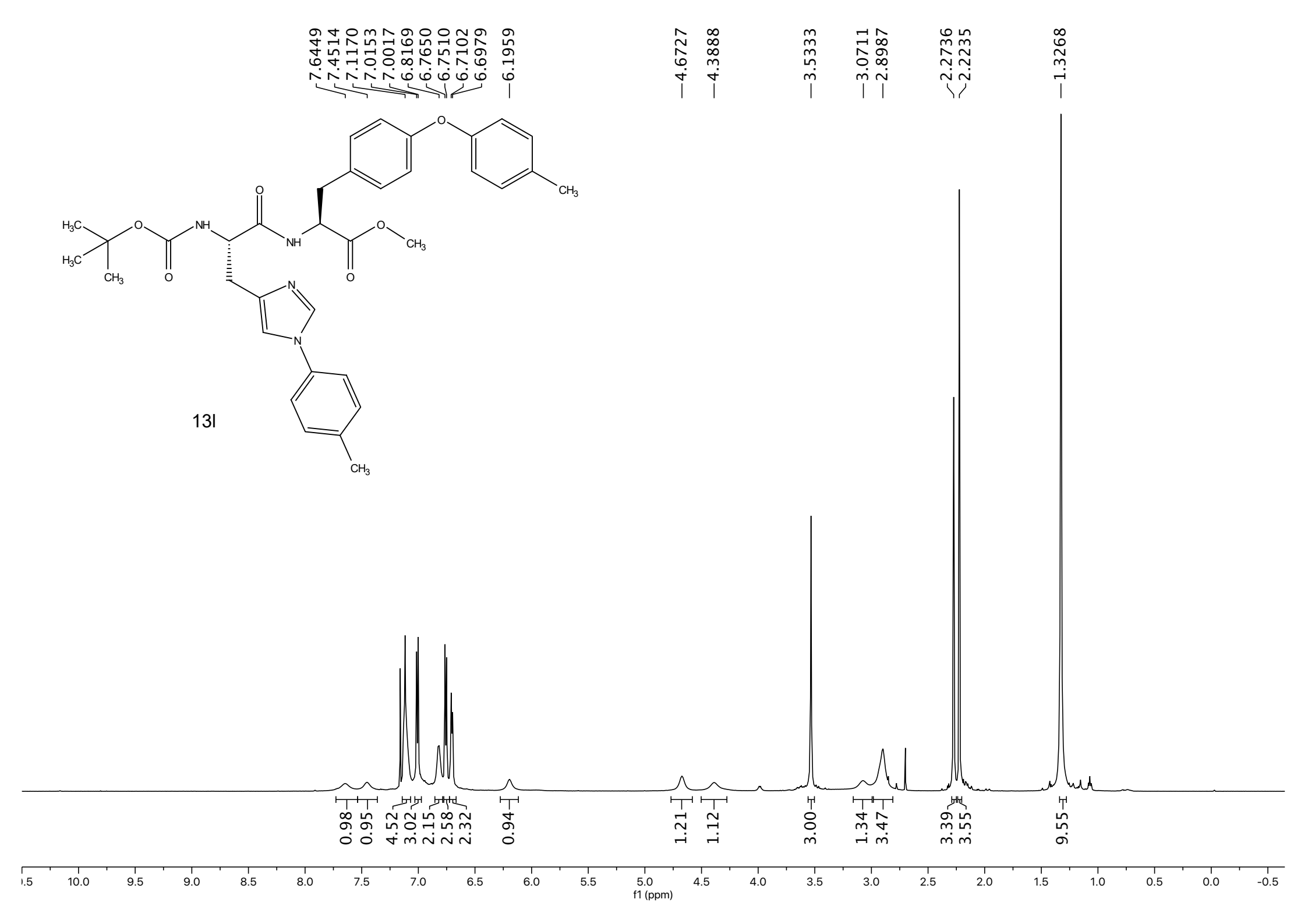
7.6449
7.4514
7.1170
7.0153
7.0017
6.8169
6.7650
6.7510
6.7102
6.6979
6.1959
4.6727
4.3888
3.5333
3.0711
2.8987
2.2736
2.2235
1.3268
13l
0.98
0.95
4.52
3.02
2.15
2.58
2.32
0.94
1.21
1.12
3.00
1.34
3.47
3.39
3.55
9.55
f1 (ppm)

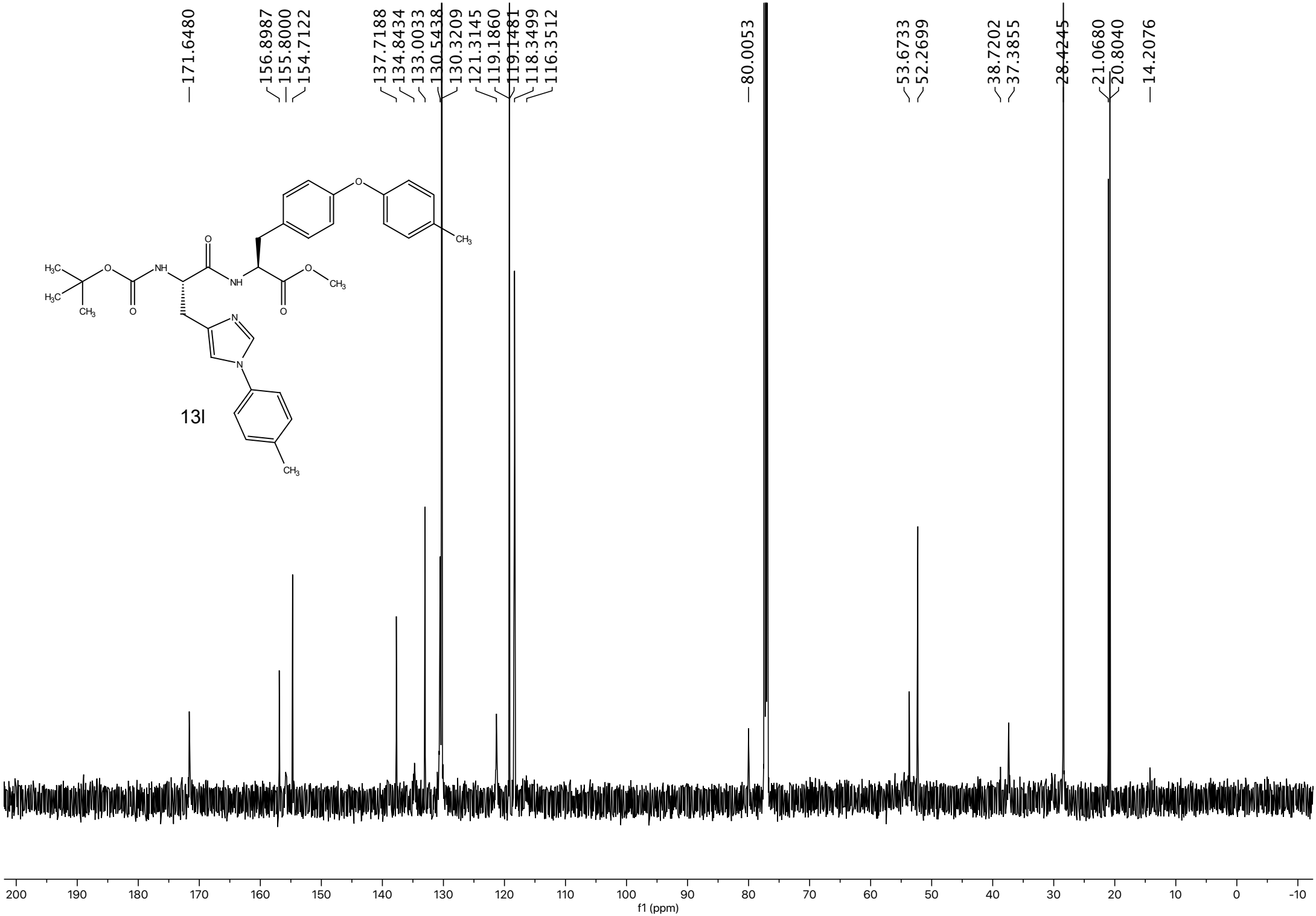
171.6480
156.8987
155.8000
154.7122
137.7188
134.8434
133.0033
130.5438
130.3209
121.3145
119.1860
119.1481
118.3499
116.3512
80.0053
53.6733
52.2699
38.7202
37.3855
28.4245
21.0680
20.8040
14.2076
13l
f1 (ppm)

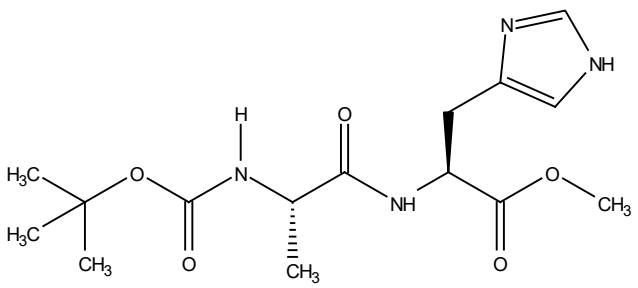
H
O
N
NH
N
NH
H3C
O
O
CH3
H3C
CH3
O
CH3
O

14

8.4429
7.5862
7.5640
7.5007
6.7445
5.5959
5.5745
4.7667
4.7495
4.7245
4.7072
4.1378
4.1162
3.6368
3.1010
3.0862
1.3768
1.3069
1.2835
1.45
0.86
1.14
1.04
1.00
0.99
1.04
3.00
1.94
9.39
3.00
f1 (ppm)

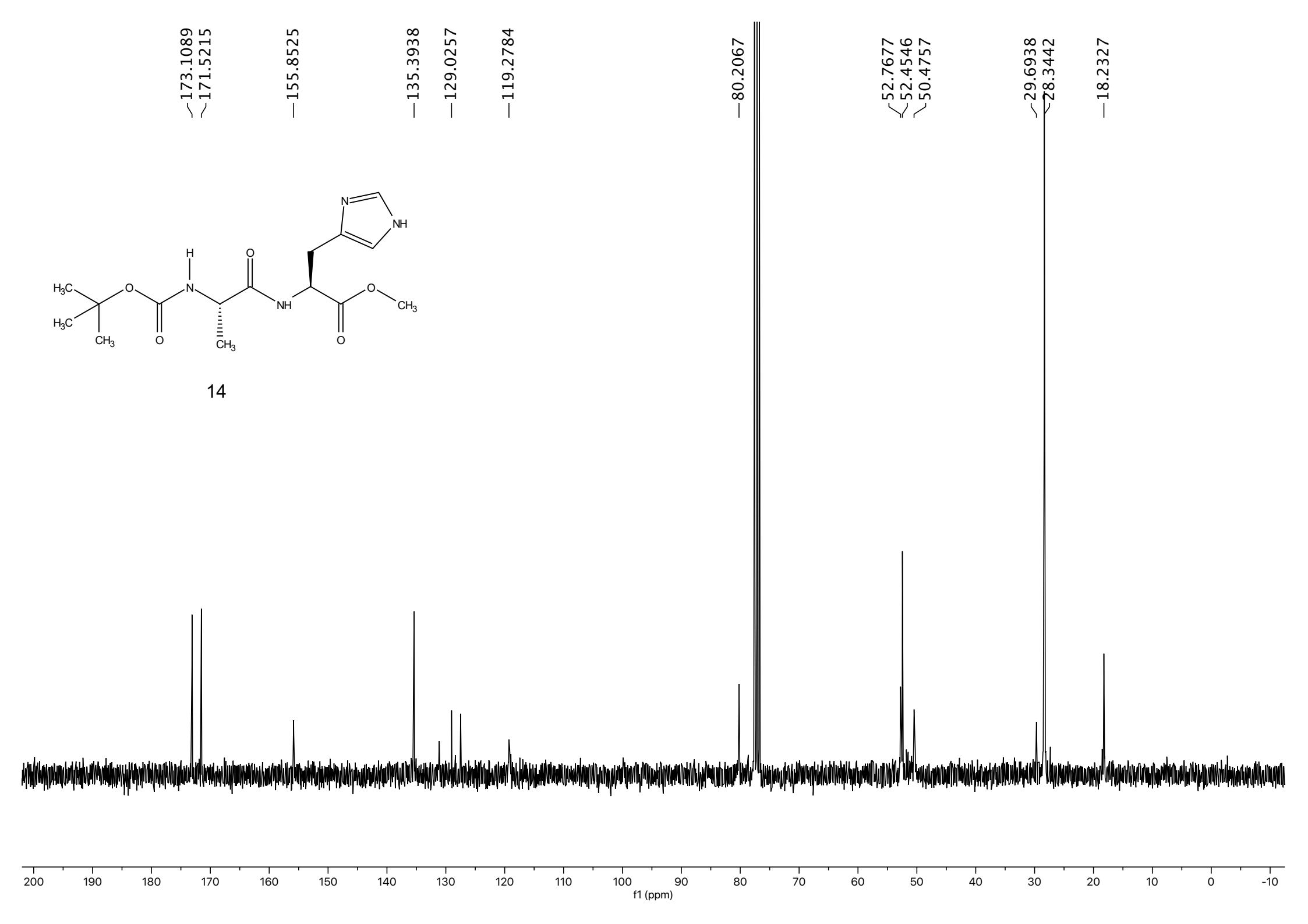
173.1089
171.5215
155.8525
135.3938
129.0257
119.2784
80.2067
52.7677
52.4546
50.4757
29.6938
28.3442
18.2327
14
f1 (ppm)

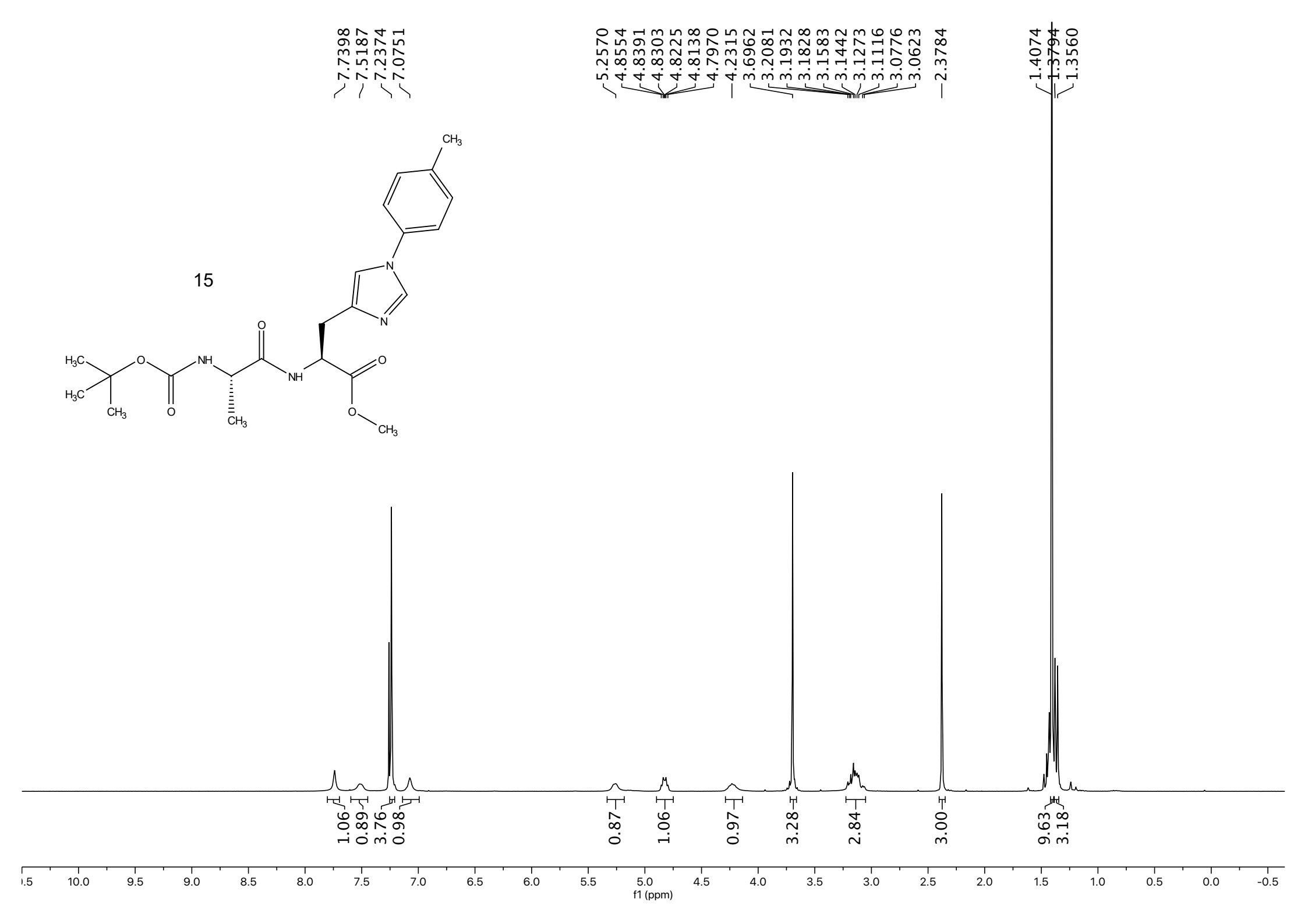
7.7398
7.5187
7.2374
7.0751
5.2570
4.8554
4.8391
4.8303
4.8225
4.8138
4.7970
4.2315
3.6962
3.2081
3.1932
3.1828
3.1583
3.1442
3.1273
3.1116
3.0776
3.0623
2.3784
1.4074
1.3794
1.3560
15
1.06
0.89
3.76
0.98
0.87
1.06
0.97
3.28
2.84
3.00
9.63
3.18
f1 (ppm)

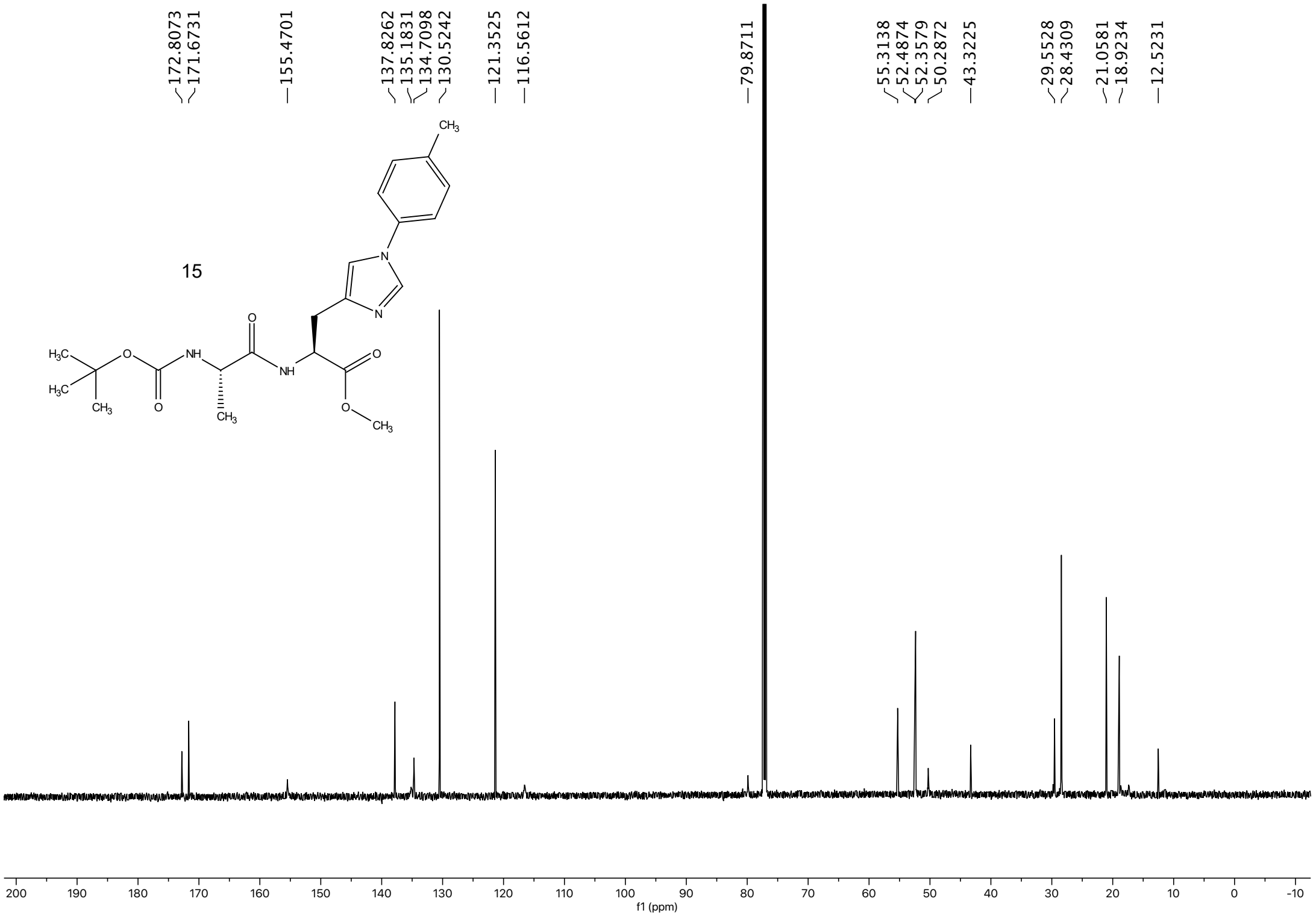
172.8073
171.6731
155.4701
137.8262
135.1831
134.7098
130.5242
121.3525
116.5612
79.8711
55.3138
52.4874
52.3579
50.2872
43.3225
29.5528
28.4309
21.0581
18.9234
12.5231
15
CH3
N
N
O
NH
NH
O
O
O
O
H3C
H3C
CH3
CH3
CH3
200
190
180
170
160
150
140
130
120
110
100
90
80
70
60
50
40
30
20
10
0
-10
f1 (ppm)

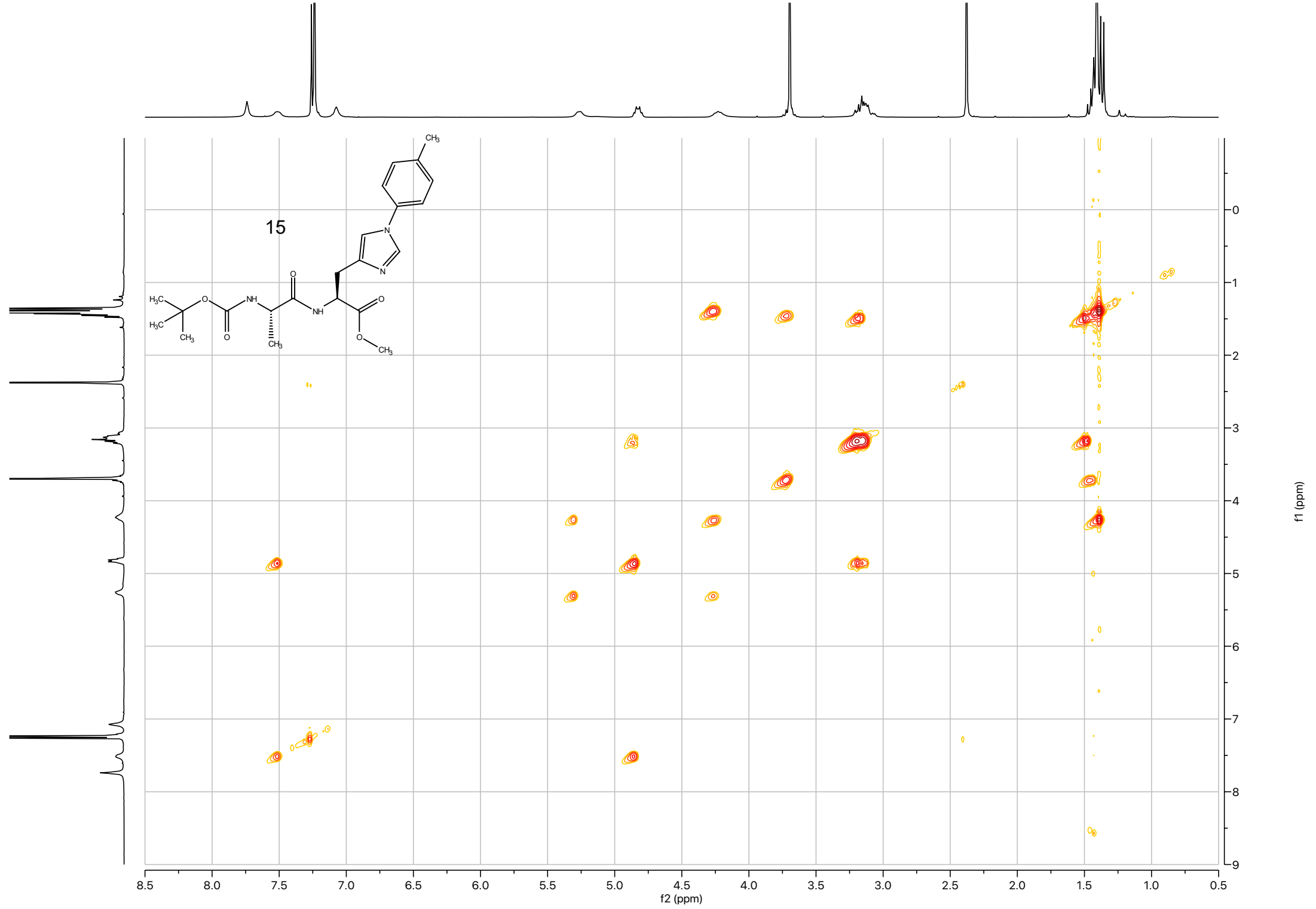
15
f2 (ppm)
f1 (ppm)

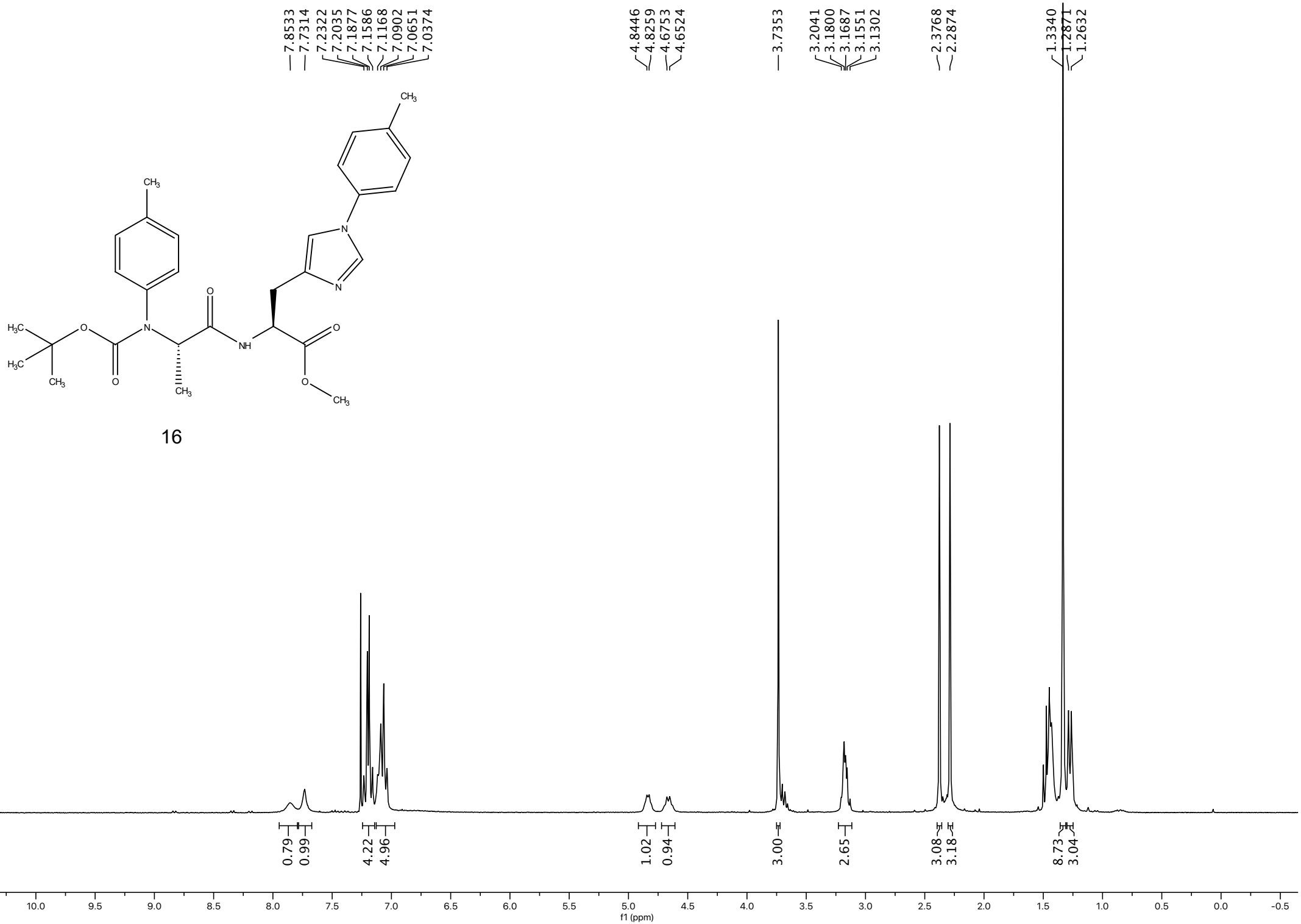
7.8533
7.7314
7.2322
7.2035
7.1877
7.1586
7.1168
7.0902
7.0651
7.0374
4.8446
4.8259
4.6753
4.6524
3.7353
3.2041
3.1800
3.1687
3.1551
3.1302
2.3768
2.2874
1.3340
1.2871
1.2632
0.79
0.99
4.22
4.96
1.02
0.94
3.00
2.65
3.08
3.18
8.73
3.04
f1 (ppm)

16

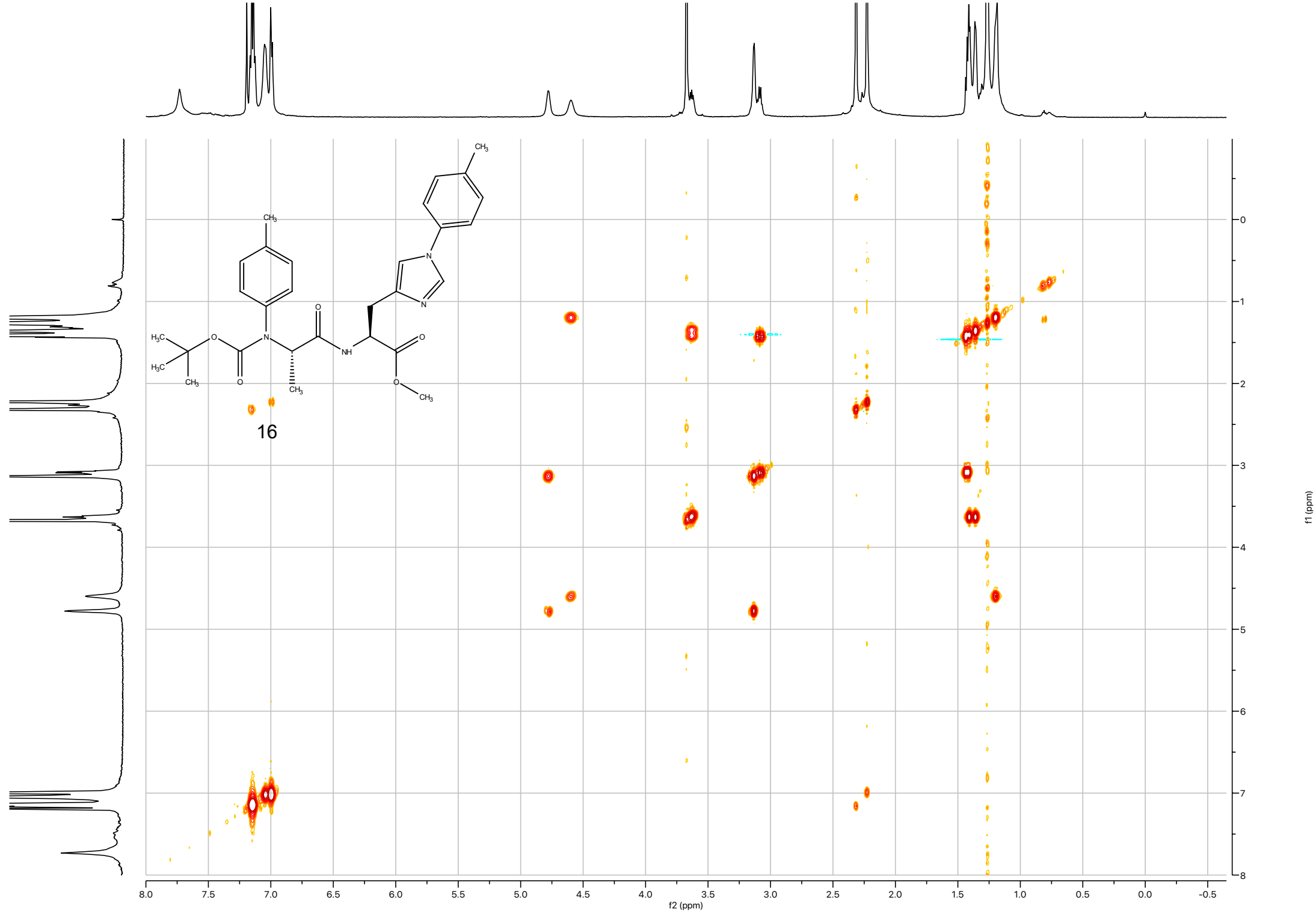
16
f2 (ppm)
f1 (ppm)

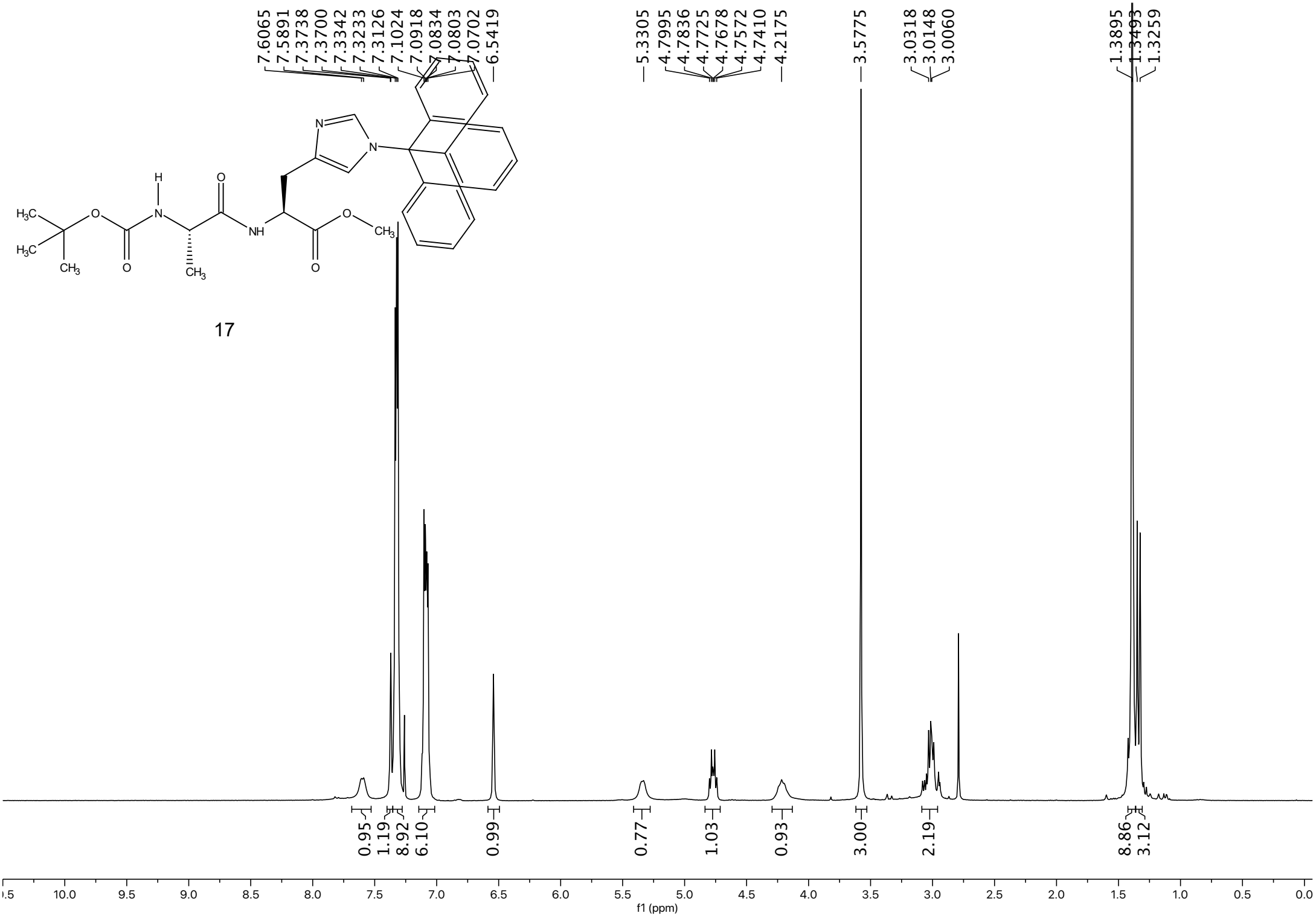
7.6065
7.5891
7.3738
7.3700
7.3342
7.3233
7.3126
7.1024
7.0918
7.0834
7.0803
7.0702
6.5419
5.3305
4.7995
4.7836
4.7725
4.7678
4.7572
4.7410
4.2175
3.5775
3.0318
3.0148
3.0060
1.3895
1.3493
1.3259
0.95
1.19
8.92
6.10
0.99
0.77
1.03
0.93
3.00
2.19
8.86
3.12
f1 (ppm)

17

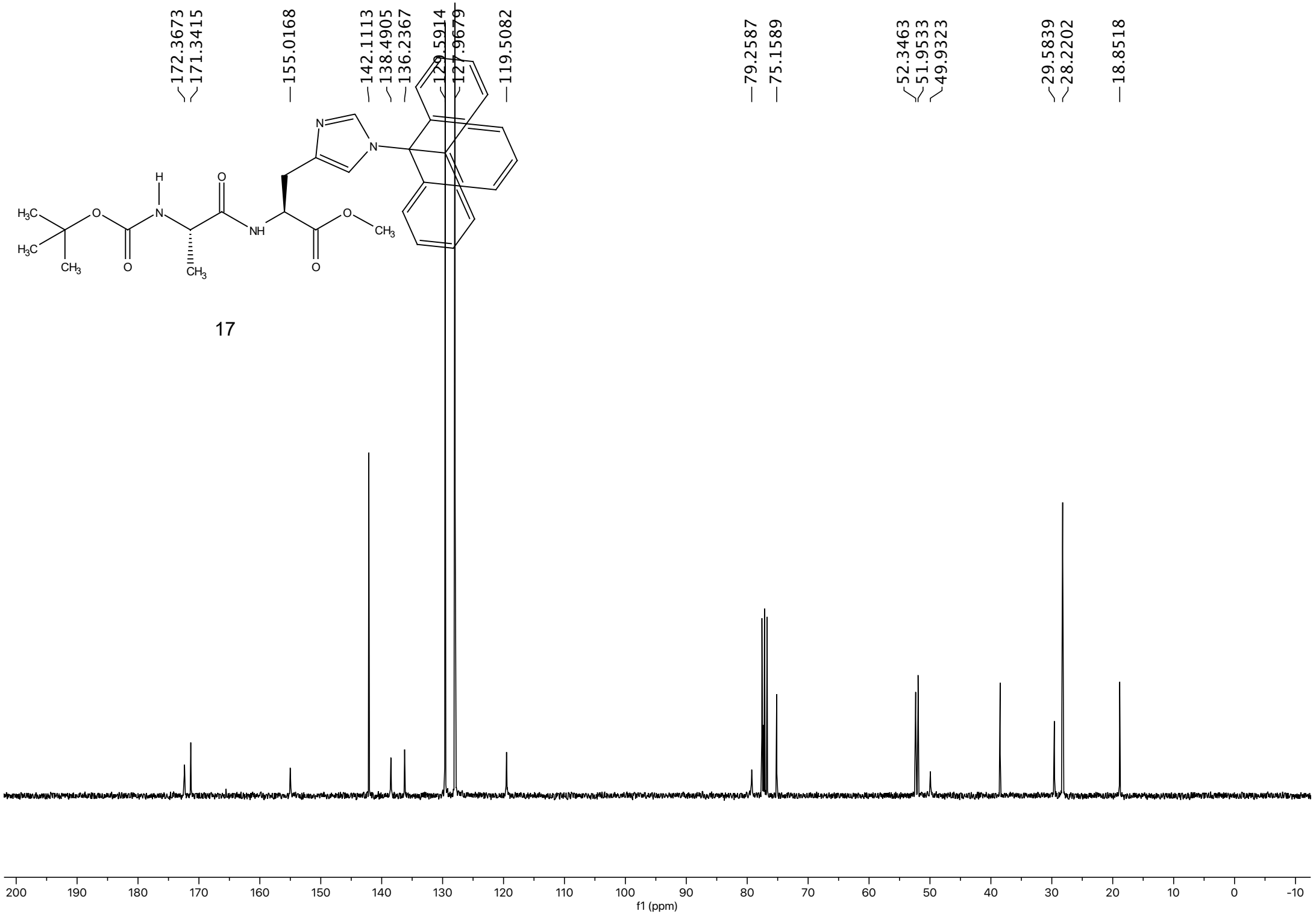
172.3673
171.3415
155.0168
142.1113
138.4905
136.2367
129.5914
127.9679
119.5082
79.2587
75.1589
52.3463
51.9533
49.9323
29.5839
28.2202
18.8518
17
f1 (ppm)

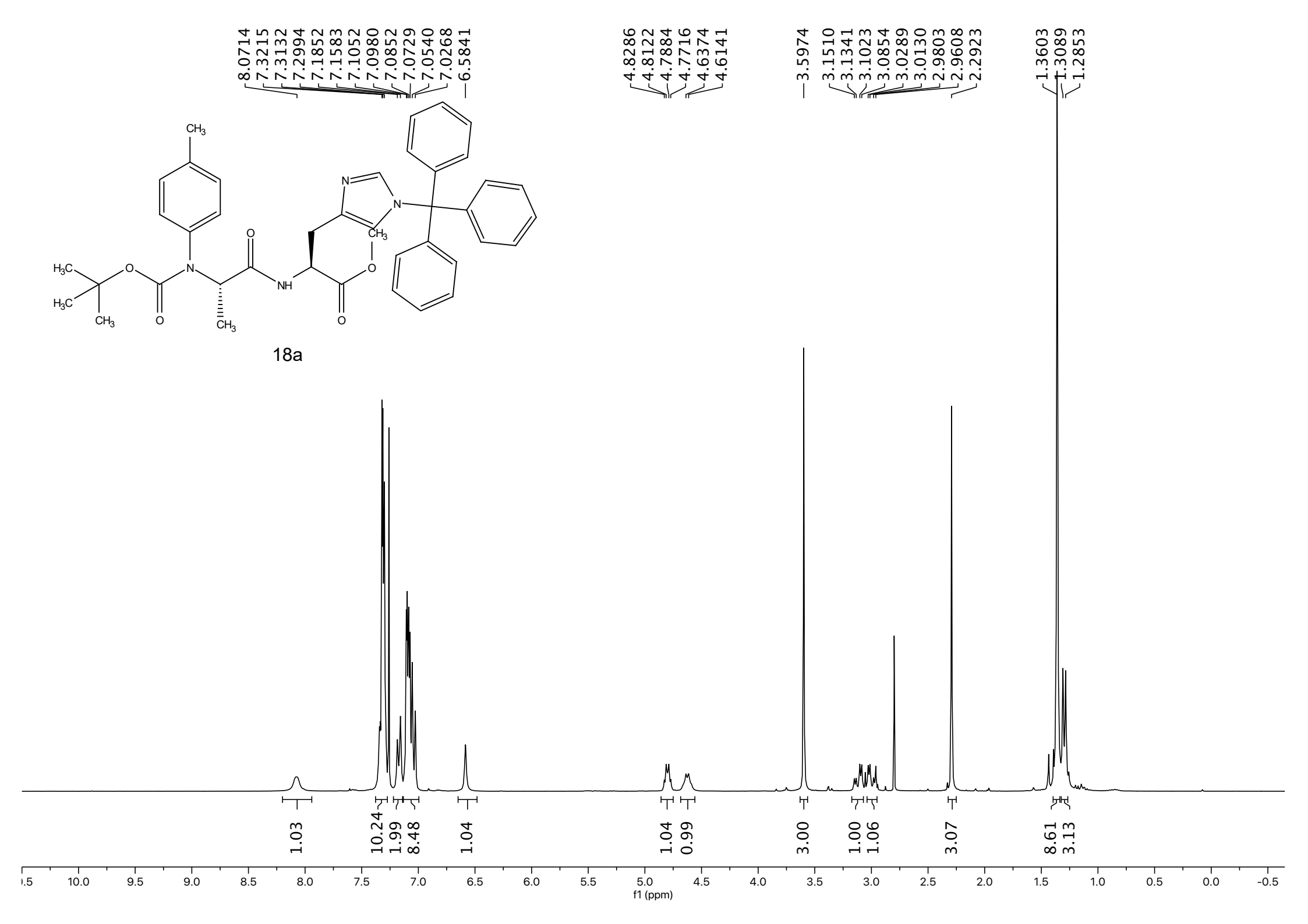
8.0714
7.3215
7.3132
7.2994
7.1852
7.1583
7.1052
7.0980
7.0852
7.0729
7.0540
7.0268
6.5841
4.8286
4.8122
4.7884
4.7716
4.6374
4.6141
3.5974
3.1510
3.1341
3.1023
3.0854
3.0289
3.0130
2.9803
2.9608
2.2923
1.3603
1.3089
1.2853
18a
1.03
10.24
1.99
8.48
1.04
1.04
0.99
3.00
1.00
1.06
3.07
8.61
3.13
f1 (ppm)

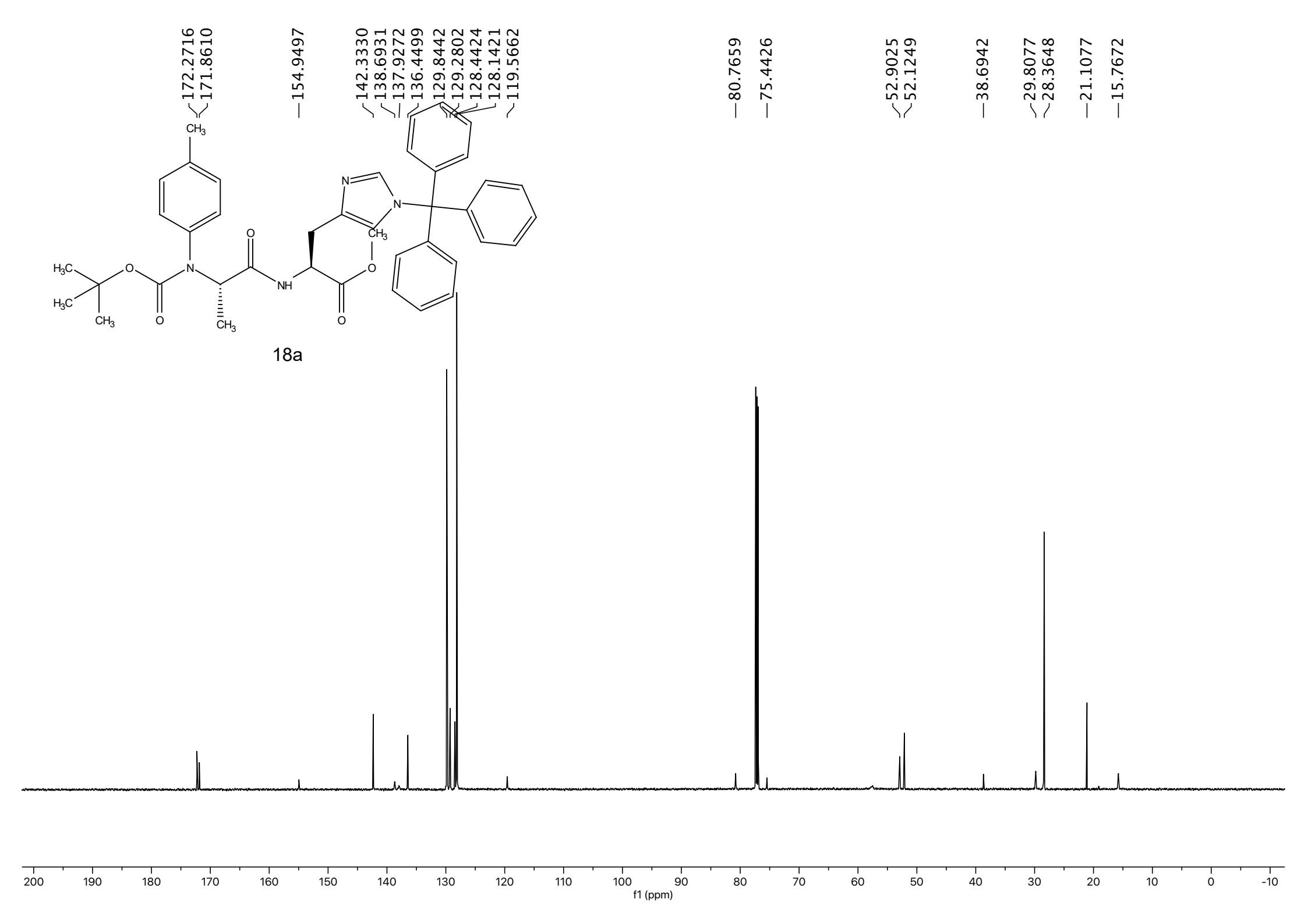
172.2716
171.8610
154.9497
142.3330
138.6931
137.9272
136.4499
129.8442
129.2802
128.4424
128.1421
119.5662
80.7659
75.4426
52.9025
52.1249
38.6942
29.8077
28.3648
21.1077
15.7672
18a
f1 (ppm)

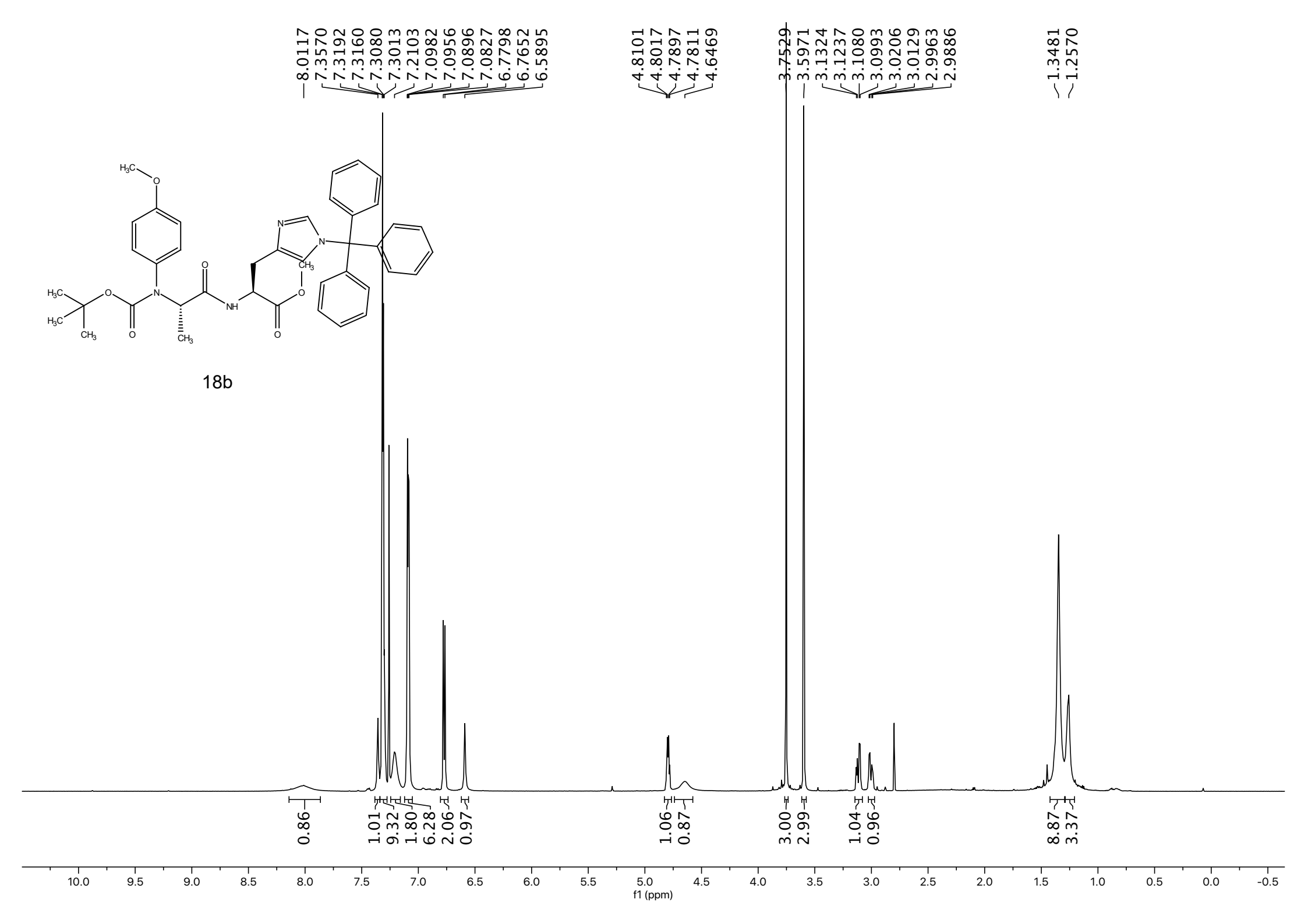
8.0117
7.3570
7.3192
7.3160
7.3080
7.3013
7.2103
7.0982
7.0956
7.0896
7.0827
6.7798
6.7652
6.5895
4.8101
4.8017
4.7897
4.7811
4.6469
3.7529
3.5971
3.1324
3.1237
3.1080
3.0993
3.0206
3.0129
2.9963
2.9886
1.3481
1.2570
0.86
1.01
9.32
1.80
6.28
2.06
0.97
1.06
0.87
3.00
2.99
1.04
0.96
8.87
3.37
10.0
9.5
9.0
8.5
8.0
7.5
7.0
6.5
6.0
5.5
5.0
4.5
4.0
3.5
3.0
2.5
2.0
1.5
1.0
0.5
0.0
-0.5
f1 (ppm)

18b

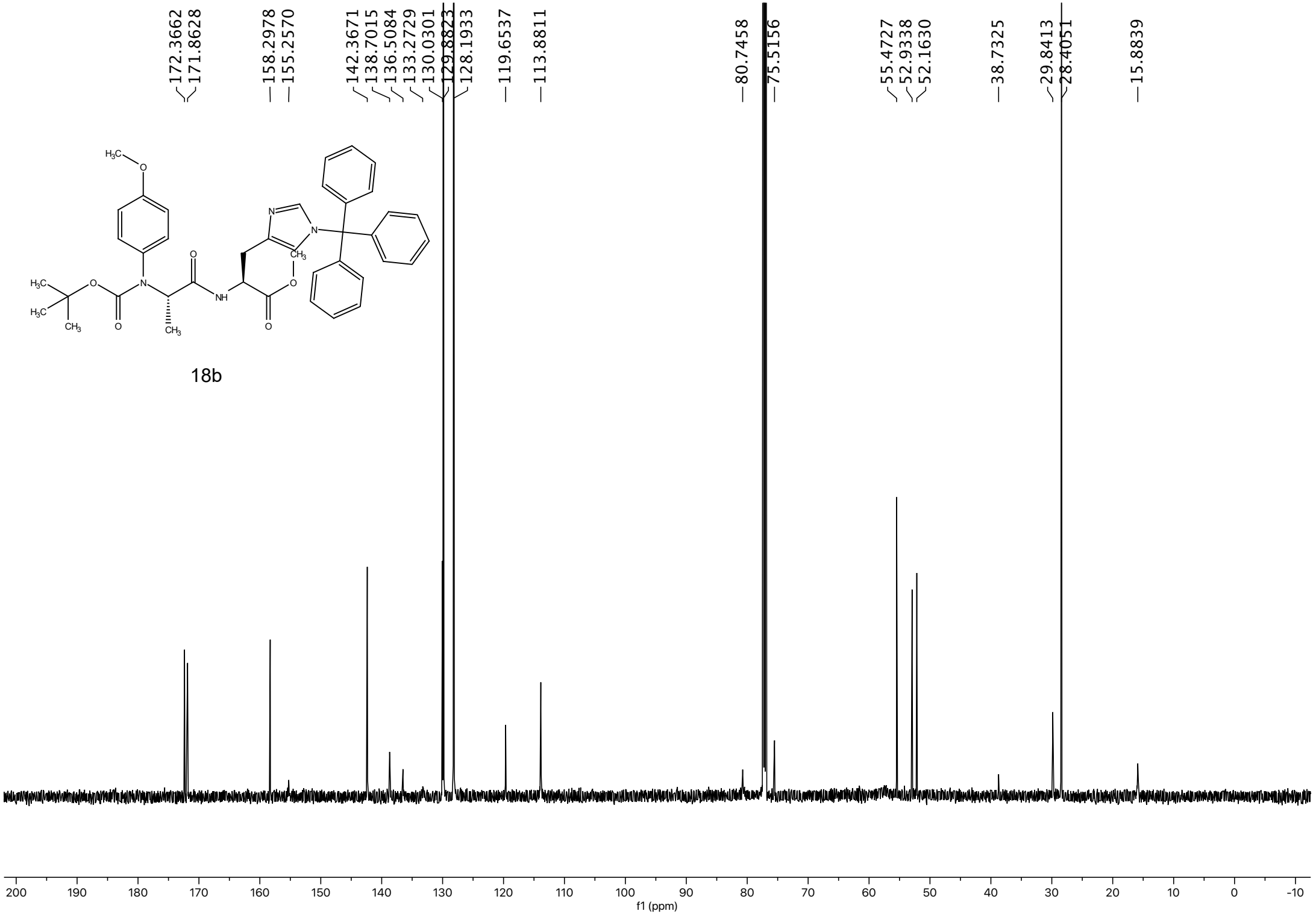
172.3662
171.8628
158.2978
155.2570
142.3671
138.7015
136.5084
133.2729
130.0301
129.8823
128.1933
119.6537
113.8811
80.7458
75.5156
55.4727
52.9338
52.1630
38.7325
29.8413
28.4051
15.8839
18b
f1 (ppm)

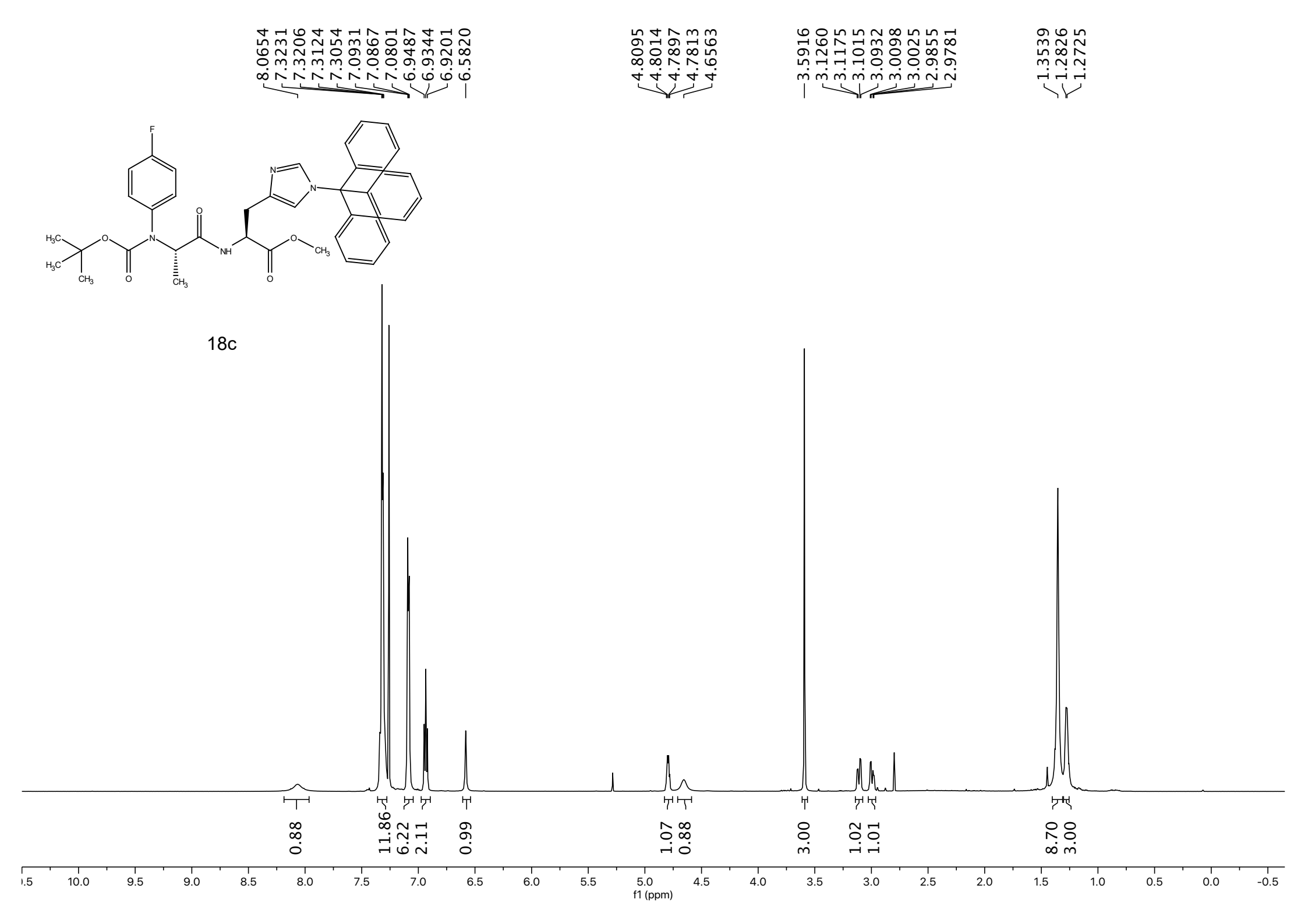
8.0654
7.3231
7.3206
7.3124
7.3054
7.0931
7.0867
7.0801
6.9487
6.9344
6.9201
6.5820
4.8095
4.8014
4.7897
4.7813
4.6563
3.5916
3.1260
3.1175
3.1015
3.0932
3.0098
3.0025
2.9855
2.9781
1.3539
1.2826
1.2725
18c
0.88
11.86
6.22
2.11
0.99
1.07
0.88
3.00
1.02
1.01
8.70
3.00
f1 (ppm)

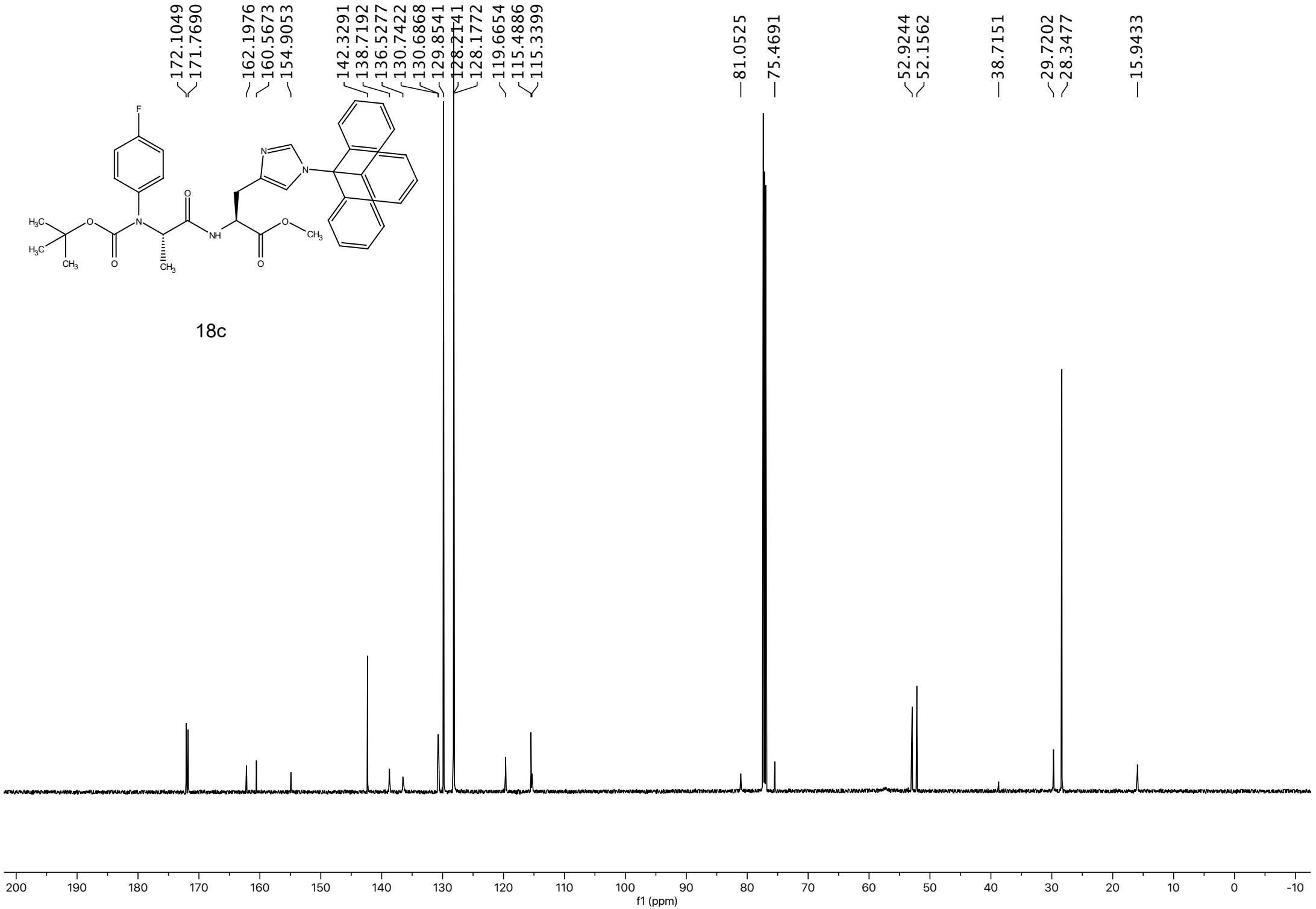
172.1049
171.7690
162.1976
160.5673
154.9053
142.3291
138.7192
136.5277
130.7422
130.6868
129.8541
128.2141
128.1772
119.6654
115.4886
115.3399
81.0525
75.4691
52.9244
52.1562
38.7151
29.7202
28.3477
15.9433
F
N
N
O
O
NH
O
O
O
CH3
H3C
H3C
CH3
CH3
18c
200
190
180
170
160
150
140
130
120
110
100
90
80
70
60
50
40
30
20
10
0
-10
f1 (ppm)

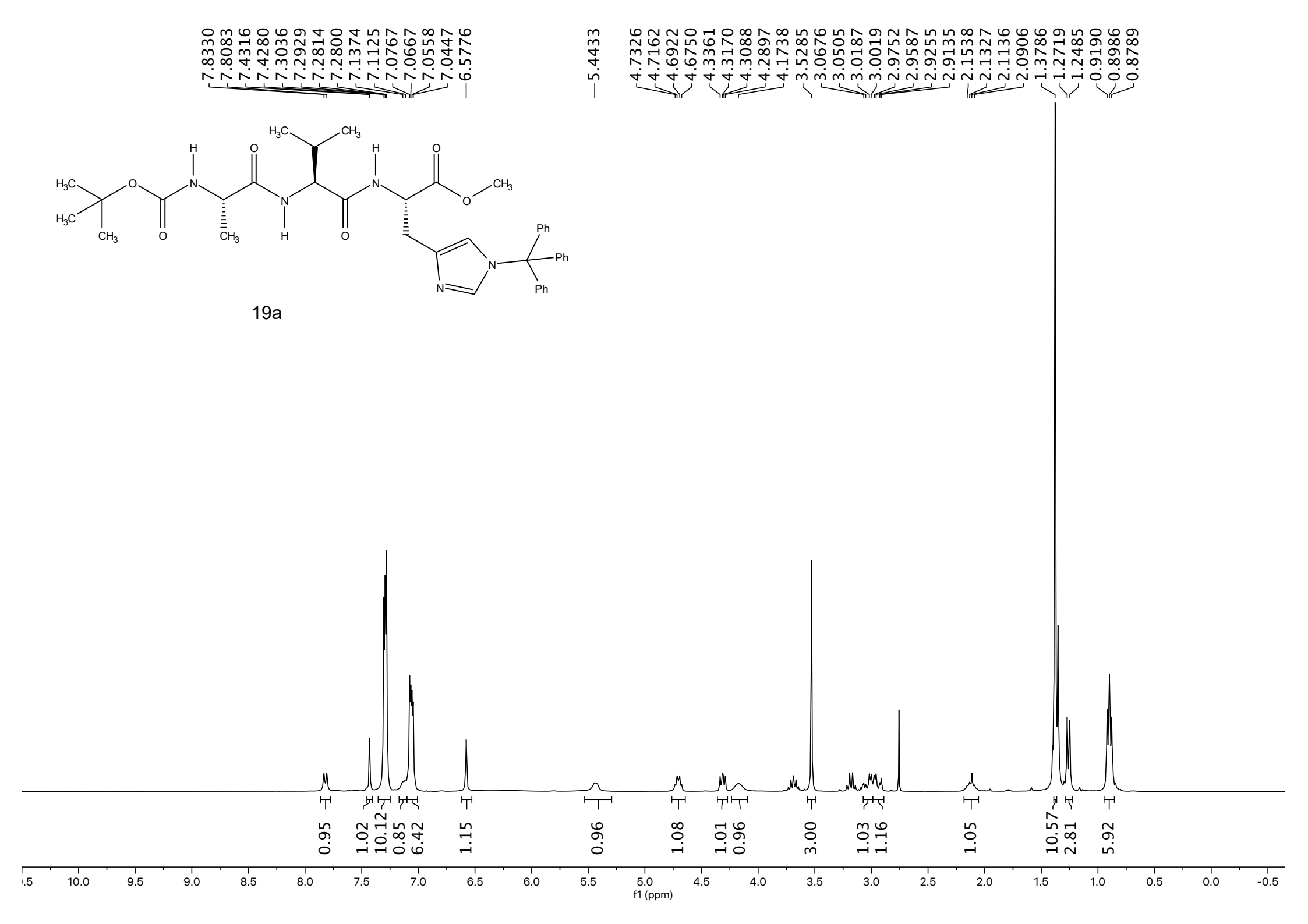
7.8330
7.8083
7.4316
7.4280
7.3036
7.2929
7.2814
7.2800
7.1374
7.1125
7.0767
7.0667
7.0558
7.0447
6.5776
5.4433
4.7326
4.7162
4.6922
4.6750
4.3361
4.3170
4.3088
4.2897
4.1738
3.5285
3.0676
3.0505
3.0187
3.0019
2.9752
2.9587
2.9255
2.9135
2.1538
2.1327
2.1136
2.0906
1.3786
1.2719
1.2485
0.9190
0.8986
0.8789
0.95
1.02
10.12
0.85
6.42
1.15
0.96
1.08
1.01
0.96
3.00
1.03
1.16
1.05
10.57
2.81
5.92
f1 (ppm)

19a

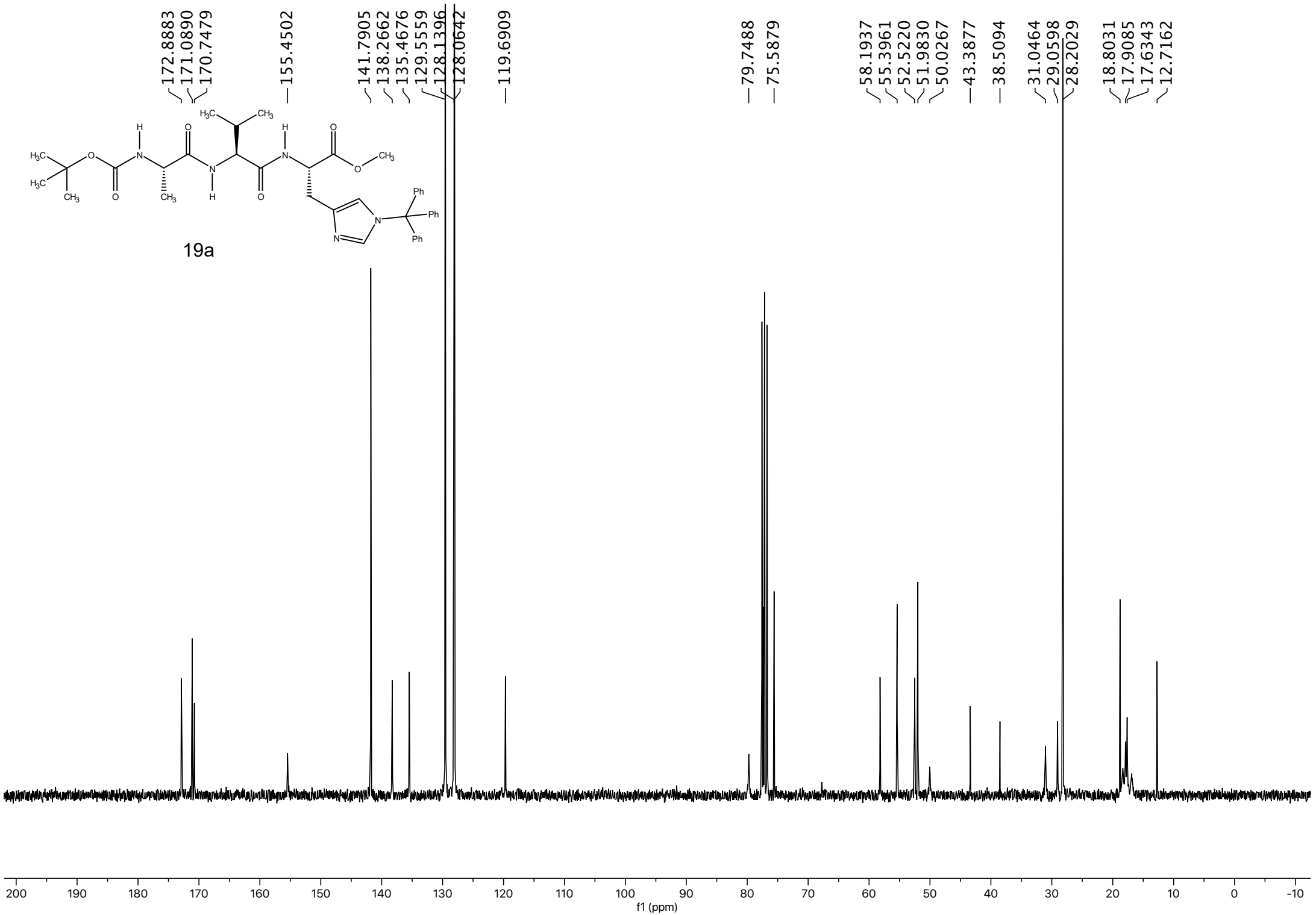
172.8883
171.0890
170.7479
155.4502
141.7905
138.2662
135.4676
129.5559
128.1396
128.0642
119.6909
79.7488
75.5879
58.1937
55.3961
52.5220
51.9830
50.0267
43.3877
38.5094
31.0464
29.0598
28.2029
18.8031
17.9085
17.6343
12.7162
19a
200
190
180
170
160
150
140
130
120
110
100
90
80
70
60
50
40
30
20
10
0
-10
f1 (ppm)

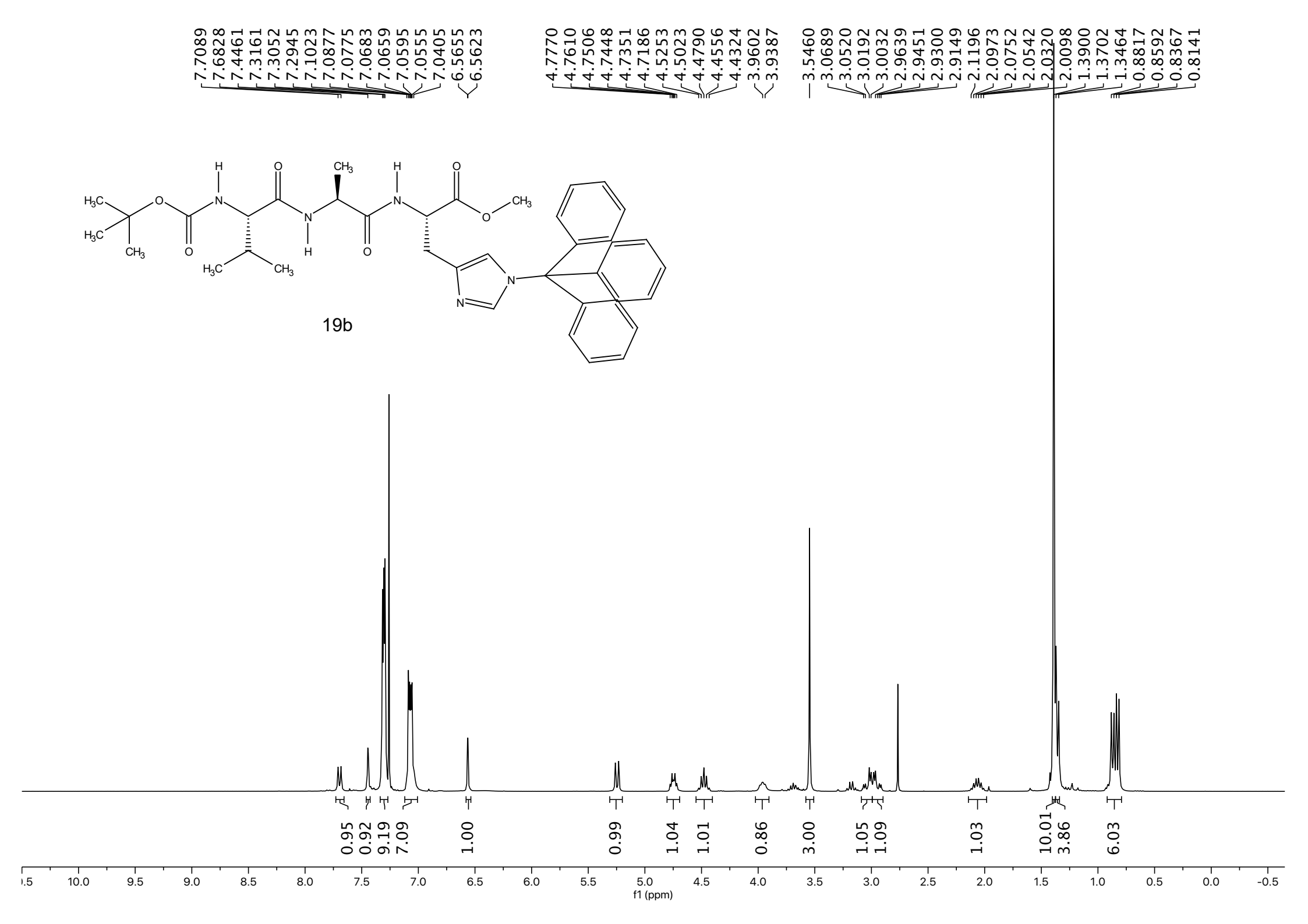
7.7089
7.6828
7.4461
7.3161
7.3052
7.2945
7.1023
7.0877
7.0775
7.0683
7.0659
7.0595
7.0555
7.0405
6.5655
6.5623
4.7770
4.7610
4.7506
4.7448
4.7351
4.7186
4.5253
4.5023
4.4790
4.4556
4.4324
3.9602
3.9387
3.5460
3.0689
3.0520
3.0192
3.0032
2.9639
2.9451
2.9300
2.9149
2.1196
2.0973
2.0752
2.0542
2.0320
2.0098
1.3900
1.3702
1.3464
0.8817
0.8592
0.8367
0.8141
19b
0.95
0.92
9.19
7.09
1.00
0.99
1.04
1.01
0.86
3.00
1.05
1.09
1.03
10.01
3.86
6.03
f1 (ppm)

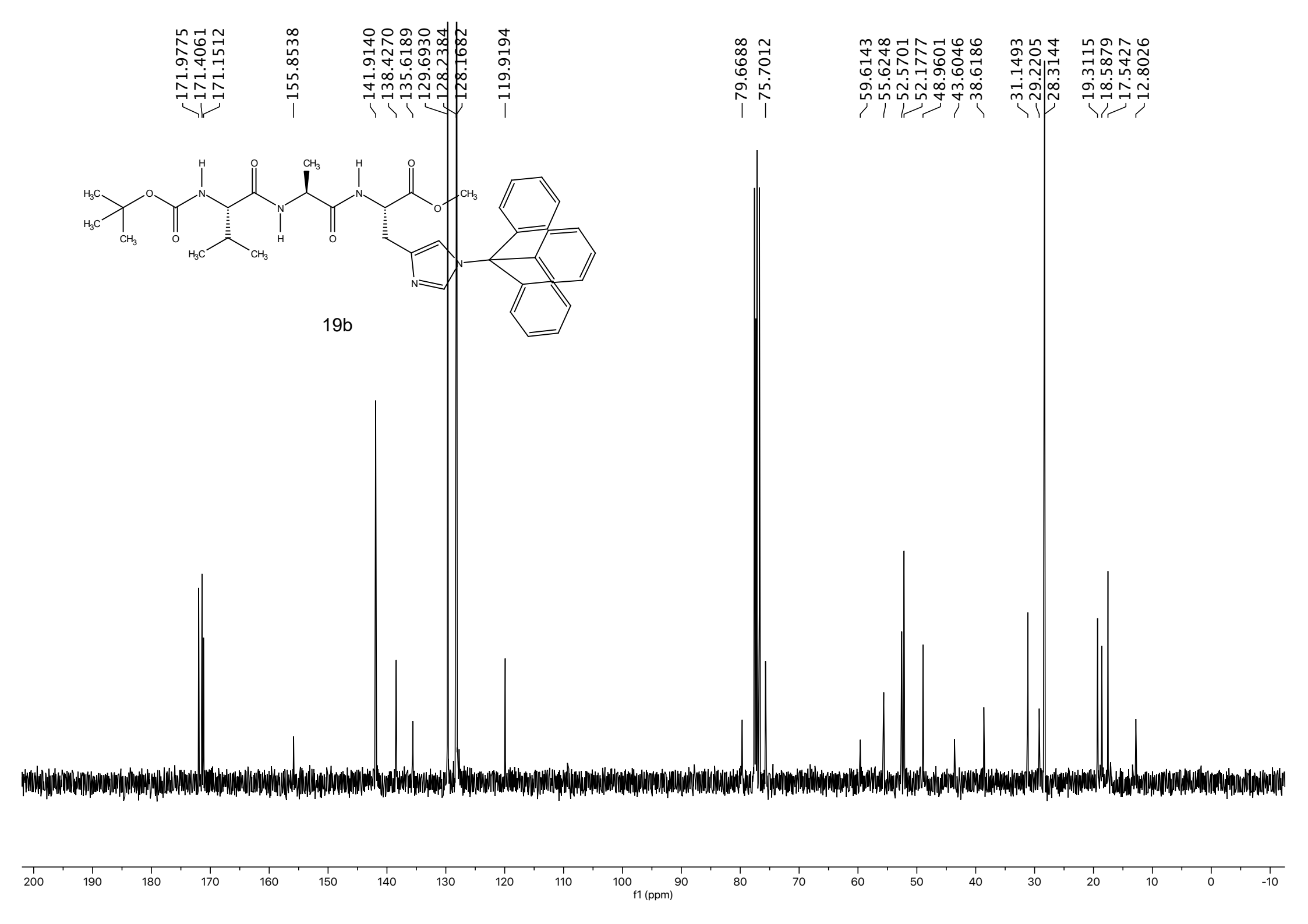
171.9775
171.4061
171.1512
155.8538
141.9140
138.4270
135.6189
129.6930
128.2384
128.1682
119.9194
79.6688
75.7012
59.6143
55.6248
52.5701
52.1777
48.9601
43.6046
38.6186
31.1493
29.2205
28.3144
19.3115
18.5879
17.5427
12.8026
19b
200
190
180
170
160
150
140
130
120
110
100
90
80
70
60
50
40
30
20
10
0
-10
f1 (ppm)

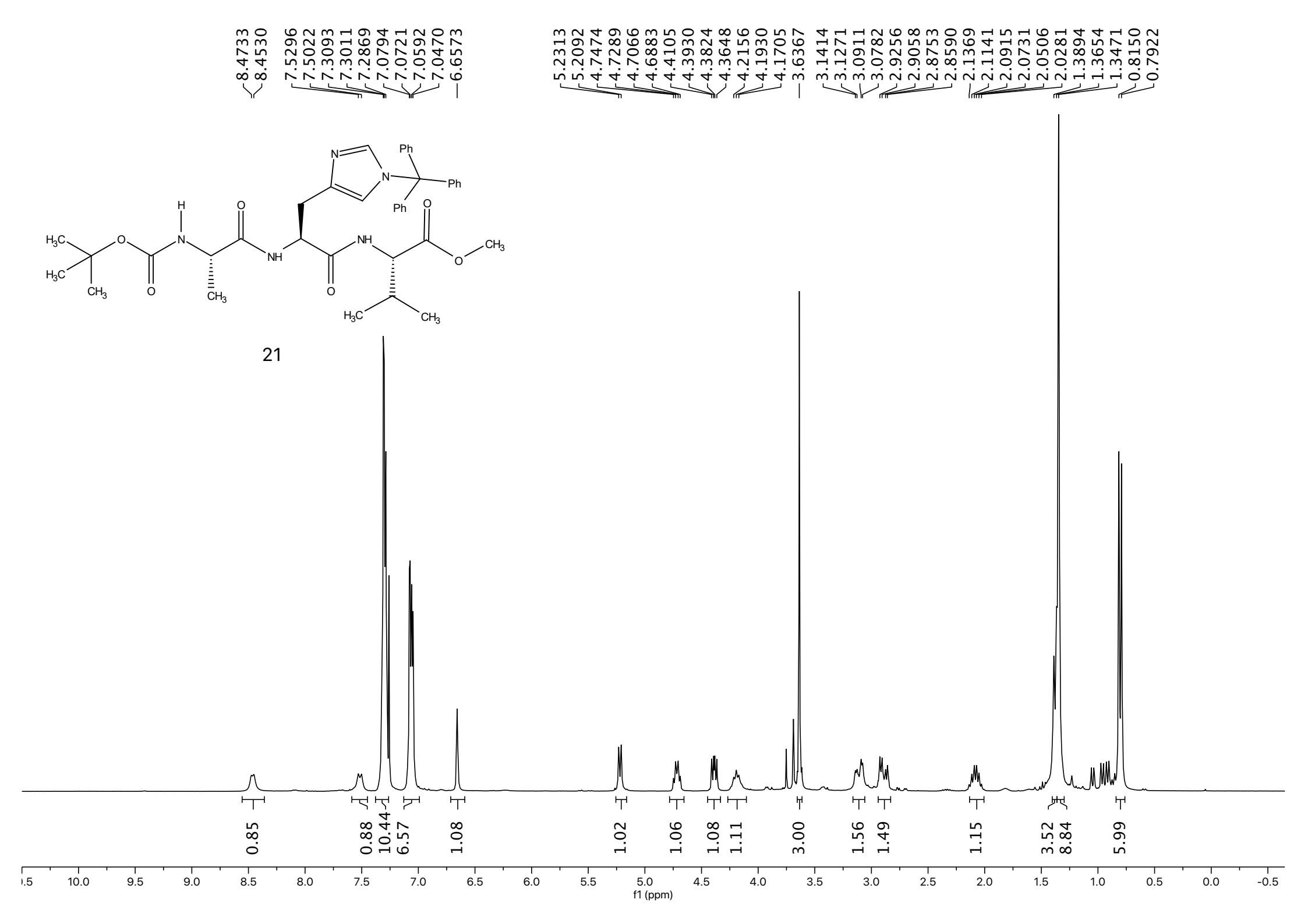
8.4733
8.4530
7.5296
7.5022
7.3093
7.3011
7.2869
7.0794
7.0721
7.0592
7.0470
6.6573
5.2313
5.2092
4.7474
4.7289
4.7066
4.6883
4.4105
4.3930
4.3824
4.3648
4.2156
4.1930
4.1705
3.6367
3.1414
3.1271
3.0911
3.0782
2.9256
2.9058
2.8753
2.8590
2.1369
2.1141
2.0915
2.0731
2.0506
2.0281
1.3894
1.3654
1.3471
0.8150
0.7922
Ph
Ph
Ph
N
N
H
O
O
NH
NH
O
O
O
O
CH3
H3C
H3C
CH3
CH3
H3C
CH3
21
0.85
0.88
10.44
6.57
1.08
1.02
1.06
1.08
1.11
3.00
1.56
1.49
1.15
3.52
8.84
5.99
f1 (ppm)

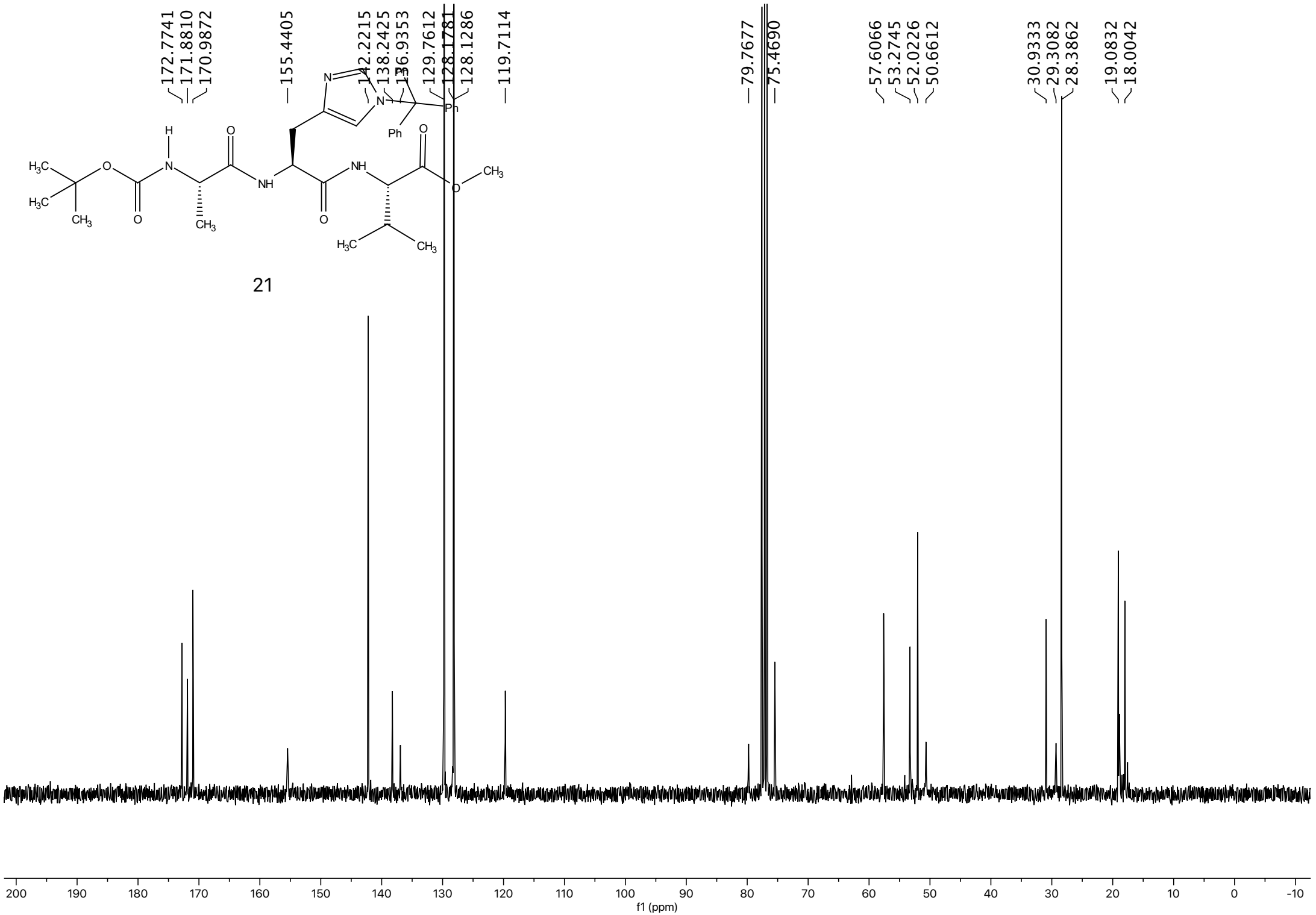
172.7741
171.8810
170.9872
155.4405
142.2215
138.2425
136.9353
129.7612
128.1781
128.1286
119.7114
79.7677
75.4690
57.6066
53.2745
52.0226
50.6612
30.9333
29.3082
28.3862
19.0832
18.0042
21
f1 (ppm)

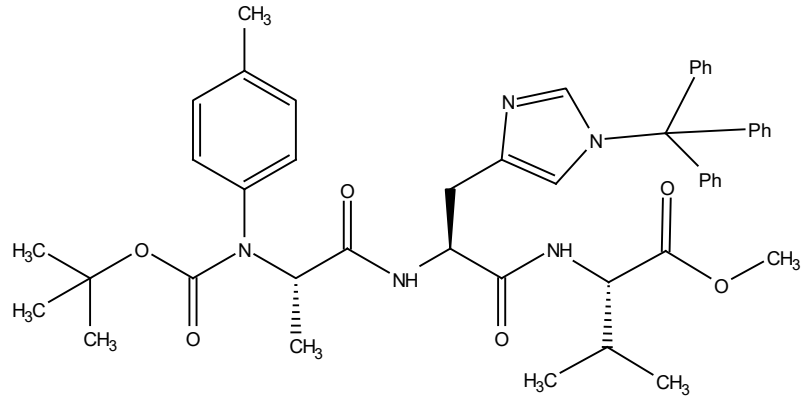

22

f1 (ppm)

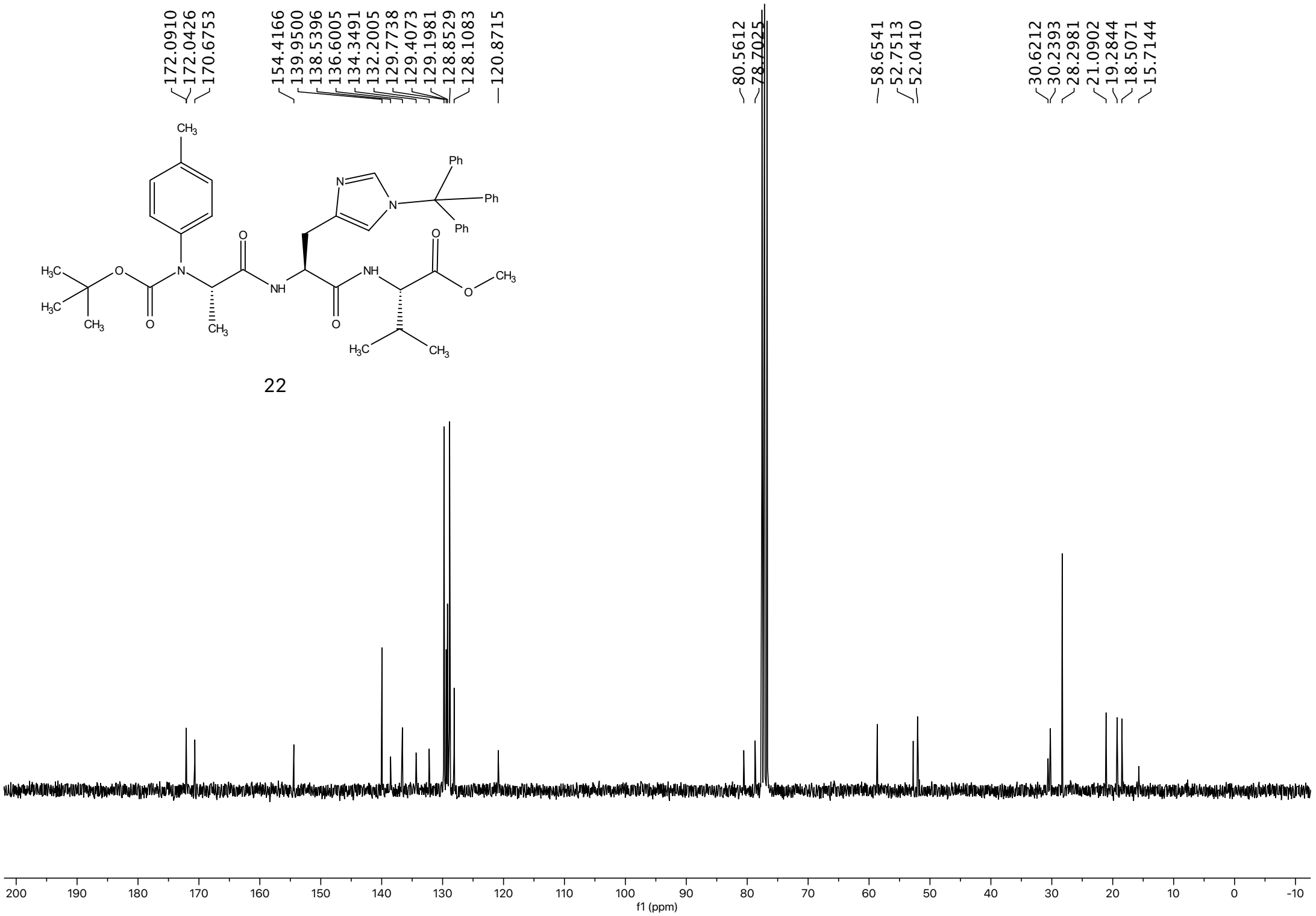
172.0910
172.0426
170.6753
154.4166
139.9500
138.5396
136.6005
134.3491
132.2005
129.7738
129.4073
129.1981
128.8529
128.1083
120.8715
80.5612
78.7025
58.6541
52.7513
52.0410
30.6212
30.2393
28.2981
21.0902
19.2844
18.5071
15.7144
22
f1 (ppm)

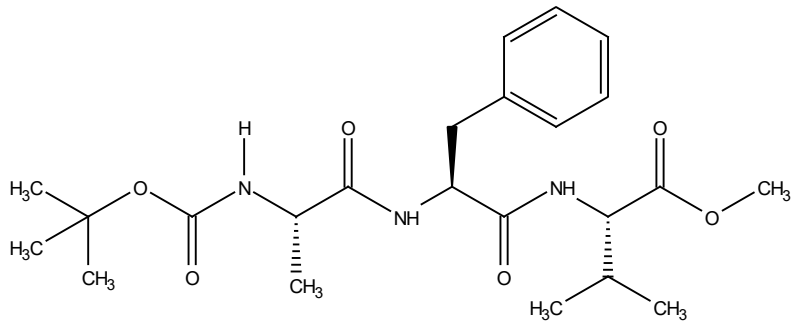

23

7.2600
7.2311
7.1919
7.1858
6.8787
6.8525
6.6084
6.5833
5.0852
5.0613
4.7429
4.7195
4.6940
4.6708
4.4362
4.4187
4.4075
4.3900
4.1679
4.1491
4.1281
3.6698
3.0704
3.0465
2.0972
2.0744
2.0562
2.0516
2.0340
1.4002
1.2897
1.2660
0.8495
0.8266
0.8153
0.7924
5.56
0.99
0.86
1.07
1.05
1.04
0.97
3.00
2.01
1.78
9.43
3.16
6.12
f1 (ppm)

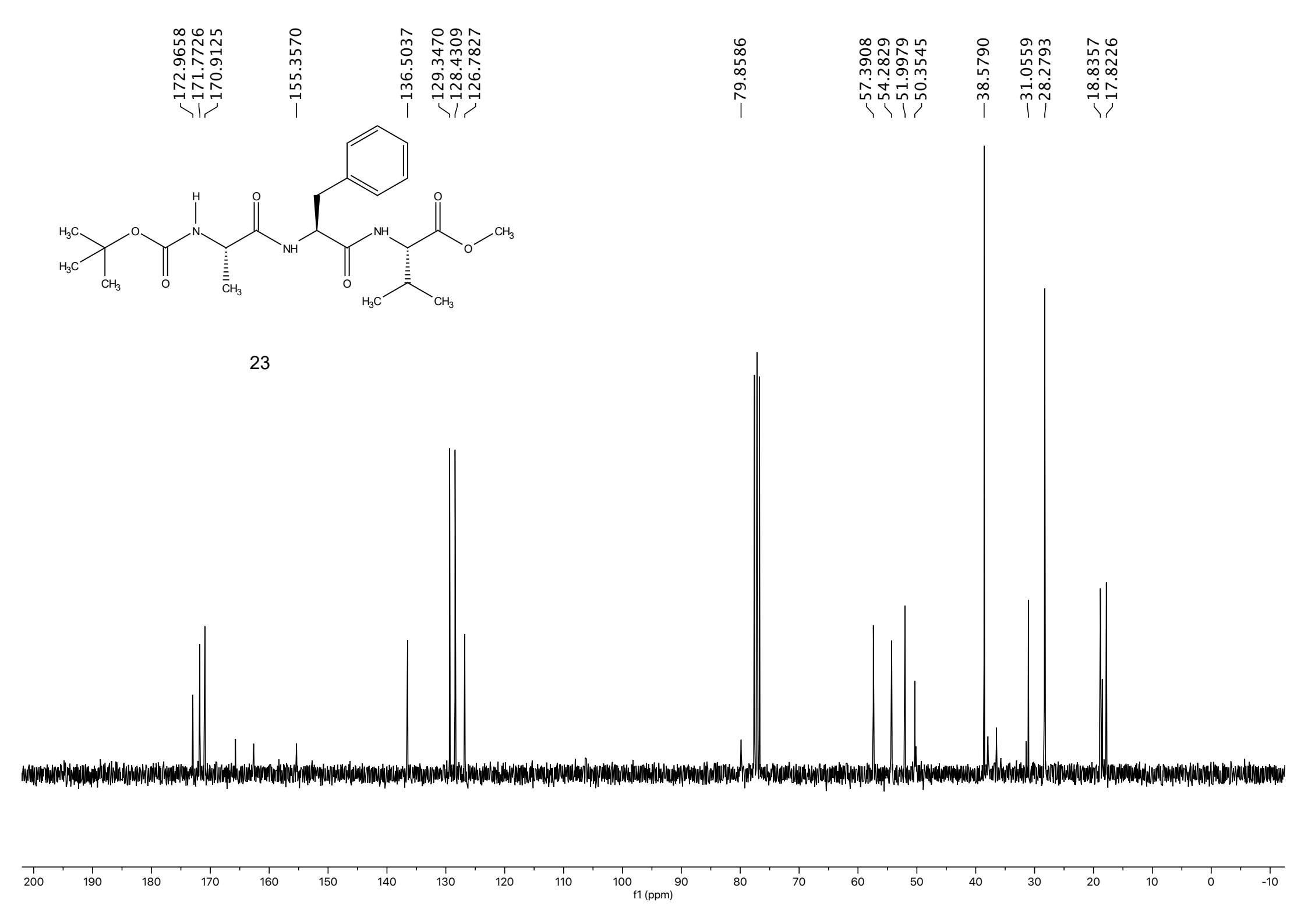
172.9658
171.7726
170.9125
155.3570
136.5037
129.3470
128.4309
126.7827
79.8586
57.3908
54.2829
51.9979
50.3545
38.5790
31.0559
28.2793
18.8357
17.8226
23
200
190
180
170
160
150
140
130
120
110
100
90
80
70
60
50
40
30
20
10
0
-10
f1 (ppm)

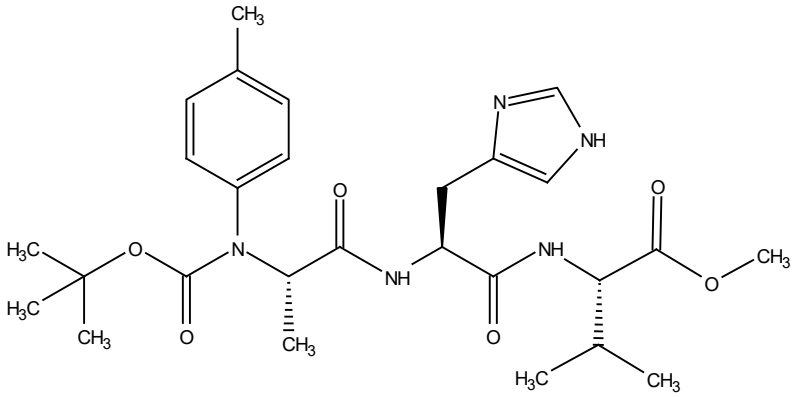

25

7.8628
7.6177
7.5564
7.1347
7.1289
7.1232
7.1084
7.0934
6.8323
4.7880
4.7783
4.7680
4.7581
4.5536
4.5416
4.5296
4.5176
4.4046
4.3959
4.3908
4.3821
3.7081
3.1751
3.1672
3.1500
3.1421
3.1111
3.1012
3.0858
3.0759
2.3284
2.1648
2.1557
2.1530
2.1442
2.1414
2.1322
1.3602
1.3048
1.2933
0.8643
0.8585
0.8529
0.8470
1.00
1.06
1.32
5.17
1.26
1.23
1.25
1.26
3.66
1.26
1.26
3.55
1.32
11.40
4.67
7.85
f1 (ppm)

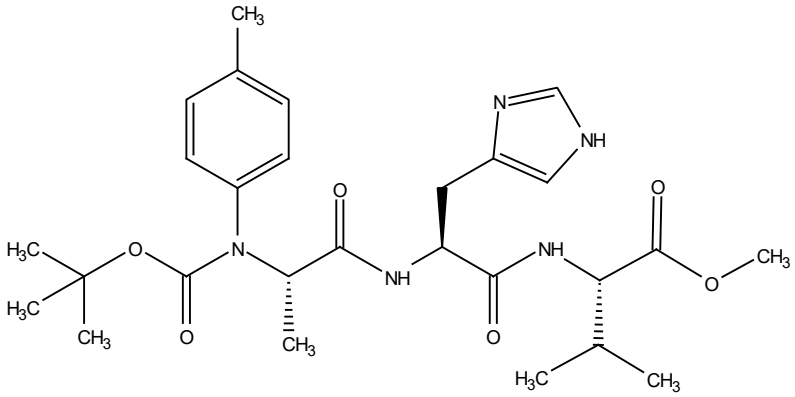

25

172.4878
172.1494
171.2791
155.1908
137.6359
136.8299
134.8755
129.3617
128.2370
81.1313
64.1848
57.8344
53.1254
52.1469
30.6353
28.7529
28.2687
28.1459
21.0496
18.9858
17.8408
15.5390
200
190
180
170
160
150
140
130
120
110
100
90
80
70
60
50
40
30
20
10
0
-10
f1 (ppm)

Annexe B

Informations supplémentaires

On the Copper-Promoted Backbone Arylation of the Histidine-Containing Peptides using Triarylbismuthines

SUPPORTING INFORMATION

On the Copper-Promoted Arylation of the Backbone of Histidine-Containing Peptides using Triarylbismuthines

Hwai-Chien Chan, Alexandre Gagnon*

Département de chimie
Université du Québec à Montréal
C.P. 8888, Succ. Centre-Ville, Montréal, Québec, Canada, H3C 3P8
gagnon.alexandre@uqam.ca

Table of contents

1. General information

Unless otherwise indicated, all reactions were run under ambient atmosphere in non-flame dried glassware. For reactions performed under oxygen, 99.6% extra dry oxygen was used. Unless otherwise stated, commercial reagents were used without further purification. Anhydrous solvents were obtained using a MBRAUN (model MB-SPS 800) encapsulated solvent purification system. The evolution of reactions was monitored by analytical thin-layer chromatography using silica gel 60 F254 precoated plates. Flash chromatography was performed employing 220 mesh silica (Silicycle) using the indicated solvent system according to standard techniques. Nuclear magnetic resonance spectra ^{1}H were recorded on a BrukerAvance-III 300MHz spectrometer or a BrukerAvance-III 600MHz and ^{13}C were recorded on a BrukerAvance-III 75MHz spectrometer or a BrukerAvance-III 150MHz. Chemical shifts for ^{1}H-NMR spectra are recorded in parts per million from tetramethylsilane with the solvent resonance as the internal standard (chloroform, δ 7.26 ppm). Data are reported as follows: chemical shift, multiplicity (s = singlet, d = doublet, t = triplet, q = quartet, p = quintuplet, m = multiplet, dd = doublet of doublet, dt = doublet of triplet, dq = doublet of quartet, tt = triplet of triplet, td = triplet of doublet, s(br) = broad singlet), coupling constant *J* in Hz and integration. Chemical shifts for ^{13}C-NMR spectra are recorded in parts per million from tetramethylsilane using the central peak of deuterochloroform (77.16 ppm) as the internal standard. All ^{13}C-NMR spectra were obtained with complete proton decoupling. IR spectra were recorded on a Thermo Scientific Nicolet 6700 Smart ITR from thin films and are reported in reciprocal centimeters (cm^{-1}). Melting points were measured using Büchi M560 melting point apparatus in open capillaries.

2. Triarylbismuthines (2) used in this work

The organobismuthines used in this publication are illustrated in **Figure S1.** The procedures for synthesis of these organobismuthines can be found in the following references: [a] Hébert, M.; Petiot, P.; Benoit, E.; Dansereau, J.; Ahmad, T.; Le Roch, A.; Ottenwaelder, X.; A. Gagnon, *Eur. J. Org. Chem.*, **2016**, *81*, 5401; [b] Petiot, P.; A. Gagnon, *Eur. J. Org. Chem.*, **2013**, 5282; [c] X. Marset, J. Torregrosa-Crespo, R. M. Martínez-Espinosa, G. Guillena, D. J. Ramón, *Green Chem.*, **2019**, *21*, 4127; [d] R. Ding, C.-S. Ge, Y.- J. Chen, D. Wanga, C.-J. Li, *Tetrahedron Lett.*, **2002**, *43*, 7789.

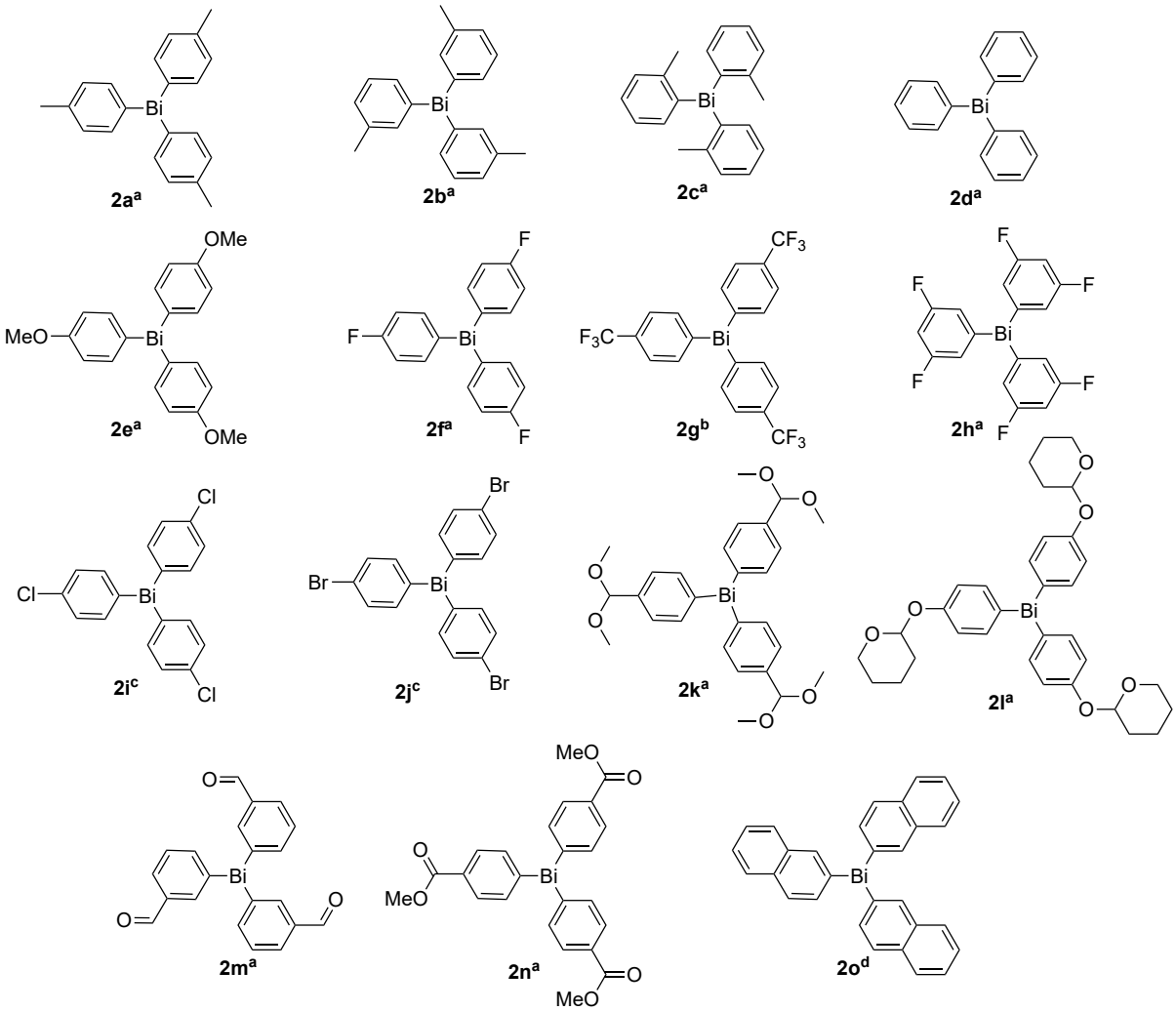

Figure S1. Functionalized organobismuthines used in this publication

3. General procedures for peptides synthesis

a. Synthesis of dipeptides Boc–A.A.–His(Trt)–OMe (1)

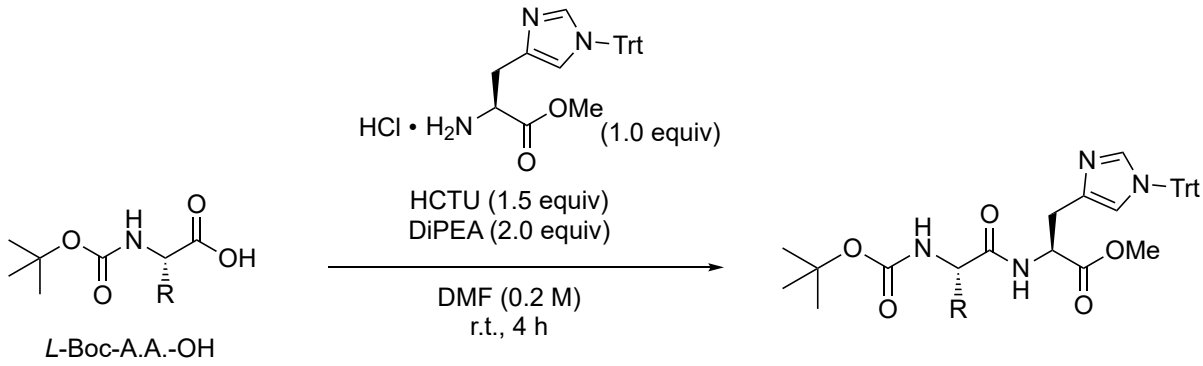

Manuscript, Scheme 2.: In a 50 mL flask, DIPEA (155 µL, 893 mmol, 2.0 equiv) was added to *L*–H–His(Trt)–OMe•HCl (200 mg, 446 µmol, 1.0 equiv), *L*–Boc–A.A.–OH (446 µmol, 1.0 equiv) and HCTU (277 mg, 670 mmol, 1.5 equiv) in DMF (2 mL, 0.2 M). The mixture was stirred for 4h at room temperature before being extracted twice with dichloromethane. The combined organic phases were successively washed with sat. aq. $NaHCO_3$ (2x20 mL), brine (2x20 mL), dried over Na_2SO_4, filtered and concentrated under reduce pressure. The resulting crude product was purified by column chromatography using the indicated eluent system to afford the desired pure product.

Methyl N^{α}-((*tert*-butoxycarbonyl)-*L*-alanyl)-N^{τ}-trityl-*L*-histidinate (1a)

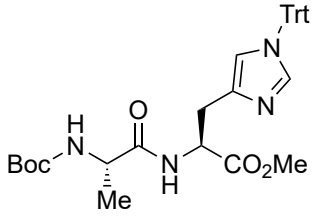

1a

The general procedure was followed starting from *L*–Boc–Ala–OH (85 mg, 449 µmol). The resulting crude product was purified on silica gel (Hexane–EtOAc, gradient from 80:20 to 30:70) to afford **1a** as a white solid (250 mg, 96%). **Mp** 74 – 76 °C; $\mathbf{R_f}$ = 0.42 (DCM–MeOH, 95:5).

IR (ATR)/$\bar{\nu}$: 3284, 2977, 1744, 1711, 1673, 1492, 1445, 1365, 1243, 1163, 1133, 1033, 1001, 870, 848, 748, 700, 660, 638 cm^{-1}.

^{1}H-NMR (300 MHz, $CDCl_3$) δ 7.60 (d, *J* = 5.2, 1H), 7.37 (d, *J* = 1.1 Hz, 1H), 7.35 – 7.27 (m, 9H), 7.15 – 6.98 (m, 6H), 6.54 (s, 1H), 5.33 (s, 1H), 4.77 (dt, *J* = 8.0, 4.7 Hz, 1H), 4.29 – 4.13 (m, 1H), 3.58 (s, 3H), 3.09 – 2.97 (m, 2H), 1.39 (s, 9H), 1.34 (d, *J* = 7.0 Hz, 3H).

^{13}C-NMR (75 MHz, $CDCl_3$) δ 172.4, 171.3, 155.0, 142.1, 138.5, 136.2, 129.6, 128.0, 119.5, 79.3, 75.2, 52.3, 52.0, 49.9, 29.6, 28.2, 18.9.

HRMS–ESI: *m/z* $[M + H]^+$ calcd. for $C_{34}H_{38}N_4O_5$: 583.2915; found 583.2943.

Methyl N^{α}-((*tert*-butoxycarbonyl)-*L*-leucyl)-N^{τ}-trityl-*L*-histidinate (1b)

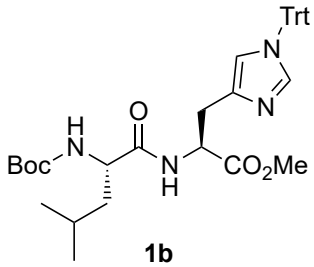

1b

The general procedure was followed starting from *L*–Boc–Leu–OH (103 mg, 446 µmol). The resulting crude product was purified on silica gel (DCM–MeOH, gradient from 100:0 to 98:2) to afford **1b** as a white solid (192 mg, 69%). **Mp** 67 – 69 °C; $\mathbf{R_f}$ = 0.33 (DCM–MeOH, 95:5).

IR (ATR)/$\bar{\nu}$: 3292, 2954, 1745, 1711, 1669, 1493, 1445, 1365, 1245, 1164, 1132, 1036, 1001, 871, 823, 748, 700, 660, 638 cm^{-1}.

^{1}H-NMR (300 MHz, $CDCl_3$) δ 7.69 (d, *J* = 6.8 Hz, 1H), 7.37 – 7.27 (m, 10H), 7.13 – 7.03 (m, 6H), 6.54 (s, 1H), 5.09 (d, *J* = 7.9 Hz, 1H), 4.74 (dt, *J* = 7.7, 4.8 Hz, 1H), 4.26 – 4.09 (m, 1H), 3.56 (s, 3H), 3.04 (dd, *J* = 14.6, 4.9 Hz, 1H), 2.95 (dd, *J* = 14.6, 4.7 Hz, 1H), 1.79 – 1.58 (m, 2H), 1.43 – 1.39 (m, 1H), 1.37 (s, 9H), 0.89 (dd, *J* = 6.2, 3.5 Hz, 6H).

^{13}C-NMR (75 MHz, $CDCl_3$) δ 172.3, 171.4, 165.7, 155.3, 142.2, 138.6, 136.3, 129.7, 128.1, 119.6, 79.4, 75.2, 53.0, 52.5, 52.0, 42.1, 29.6, 28.3, 24.6, 22.9.

HRMS–ESI: *m/z* $[M + H]^+$ calcd. for $C_{37}H_{44}N_4O_5$: 625.3385; found 625.3396.

Methyl N^{α}-((*tert*-butoxycarbonyl)-*L*-phenylalanyl)-N^{τ}-trityl-*L*-histidinate (1c)

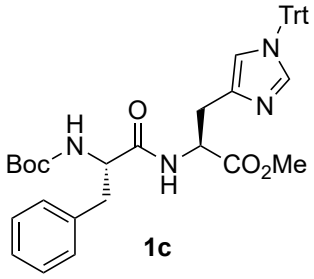

1c

The general procedure was followed starting from *L*–Boc–Phe–OH (118 mg, 446 µmol). The resulting crude product was purified on silica gel (Hexane–EtOAc, gradient from 80:20 to 30:70) to afford **1c** as a white solid (147 mg, 50%). **Mp** 76 – 78 °C; $\mathbf{R_f}$ = 0.68 (Hexane–EtOAc, 20:80).

IR (ATR)/$\bar{\nu}$: 3289, 2976, 1743, 1711, 1673, 1492, 1444, 1390, 1365, 1244, 1163, 1132, 1022, 1001, 870, 748, 699, 659, 638 cm^{-1}.

^{1}H-NMR (300 MHz, $CDCl_3$) δ 7.62 – 7.50 (m, 1H), 7.37 – 7.28 (m, 10H), 7.21 (d, *J* = 4.4 Hz, 4H), 7.14 – 7.02 (m, 7H), 6.49 (s, 1H), 5.27 (d, *J* = 7.3 Hz, 1H), 4.77 (dt, *J* = 7.8, 4.7 Hz, 1H), 4.55 – 4.36 (m, 1H), 3.58 (s, 3H), 3.14 (dd, *J* = 13.9, 5.9 Hz, 1H), 3.08 – 2.87 (m, 3H), 1.34 (s, 9H).

^{13}C-NMR (75 MHz, $CDCl_3$) δ 171.3, 171.1, 155.2, 142.2, 138.6, 136.9, 136.2, 129.7, 129.5, 128.4, 128.1, 128.1, 126.6, 119.6, 79.6, 75.3, 55.5, 52.6, 52.1, 38.6, 29.9, 28.3.

HRMS–ESI: *m/z* $[M + H]^+$ calcd. for $C_{40}H_{42}N_4O_5$: 659.3228; found 659.3234.

Methyl N^{α}-((*tert*-butoxycarbonyl)glycyl)-N^{τ}-trityl-*L*-histidinate (1d)

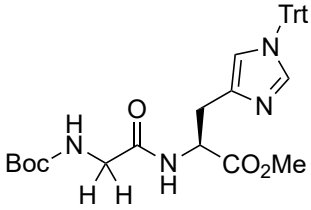

1d

The general procedure was followed starting from Boc–Gly–OH (78 mg, 446 µmol). The resulting crude product was purified on silica gel (Hexane–EtOAc, gradient from 80:20 to 30:70) to afford **1d** as a white solid (165 mg, 61%). **Mp** 80 – 82 °C; $\mathbf{R_f}$ = 0.43 (DCM–MeOH, 95:5).

IR (ATR)/$\bar{\nu}$: 3288, 2978, 2923, 1668, 1494, 1445, 1367, 1279, 1244, 1158, 1035, 1001, 942, 838, 748, 701, 660 cm^{-1}.

^{1}H-NMR (600 MHz, $CDCl_3$) δ 7.75 – 7.70 (m, 1H), 7.36 (s, 1H), 7.35 – 7.29 (m, 9H), 7.12 – 7.06 (m, 6H), 6.53 (s, 1H), 5.30 (s, 1H), 4.82 – 4.76 (m, 1H), 3.84 – 3.80 (m, 2H), 3.58 (s, 3H), 3.04 (dd, *J* = 14.7, 5.0 Hz, 1H), 3.00 – 2.93 (m, 1H), 1.39 (s, 9H).

^{13}C-NMR (150 MHz, $CDCl_3$) δ 171.7, 169.4, 156.0, 142.3, 138.8, 136.4, 129.8, 128.2, 128.2, 119.8, 79.9, 75.5, 52.6, 52.3, 44.2, 29.7, 28.4.

HRMS–ESI: *m/z* $[M + H]^+$ calcd. for $C_{33}H_{36}N_4O_5$: 569.2759; found 569.2764.

Methyl N^{α}-((*tert*-butoxycarbonyl)-*L*-methionyl)-N^{τ}-trityl-*L*-histidinate (1e)

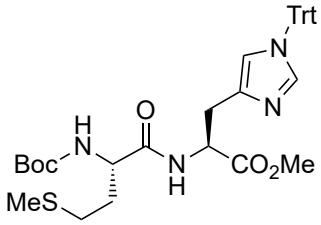

1e

The general procedure was followed starting from *L*–Boc–Met–OH (111 mg, 446 µmol). The resulting crude product was purified on silica gel (Hexane–EtOAc, gradient from 100:0 to 50:50) to afford **1e** as a white solid (169 mg, 59%). **Mp** 55 – 57 °C; $\mathbf{R_f}$ = 0.49 (DCM–MeOH, 95:5).

IR (ATR)/$\bar{\nu}$: 3288, 2920, 1745, 1711, 1673, 1492, 1444, 1365, 1239, 1164, 1132, 1024, 1001, 908, 869, 748, 700, 660, 637 cm^{-1}.

^{1}H-NMR (300 MHz, $CDCl_3$) δ 7.79 (d, *J* = 7.7 Hz, 1H), 7.34 (s, 1H), 7.32 – 7.22 (m, 9H), 7.12 – 6.99 (m, 6H), 6.51 (s, 1H), 5.48 (d, *J* = 8.1 Hz, 1H), 4.72 (dt, *J* = 7.7, 4.8 Hz, 1H), 4.36 – 4.27 (m, 1H), 3.53 (s, 3H), 3.09 – 2.86 (m, 2H), 2.52 (t, *J* = 7.5 Hz, 2H), 2.15 – 2.01 (m, 1H), 1.99 (s, 3H), 1.96 – 1.78 (m, 1H), 1.36 (s, 9H).

^{13}C-NMR (75 MHz, $CDCl_3$) δ 171.3, 171.2, 165.7, 155.3, 142.2, 138.7, 136.2, 129.7, 128.1, 119.6, 79.5, 75.4, 53.4, 52.6, 52.1, 32.6, 29.7, 29.5, 28.4, 15.2.

HRMS–ESI: *m/z* $[M + H]^+$ calcd. for $C_{36}H_{42}N_4O_5S$: 643.2949; found 643.2963.

Methyl N^{α}-((*tert*-butoxycarbonyl)-*L*-valyl)-N^{τ}-trityl-*L*-histidinate (1f)

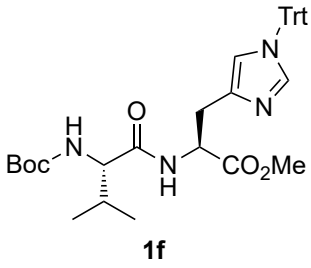

1f

The general procedure was followed starting from *L*–Boc–Val–OH (97 mg, 446 µmol). The resulting crude product was purified on silica gel (Hexane–EtOAc, gradient from 80:20 to 30:70) to afford **1f** as a white solid (160 mg, 59%). **Mp** 61 – 63 °C; $\mathbf{R_f}$ = 0.25 (Hexane–EtOAc, 50:50).

IR (ATR)/$\bar{\nu}$: 3303, 2964, 1745, 1712, 1673, 1492, 1445, 1365, 1238, 1160, 1133, 1088, 1037, 1001, 909, 871, 841, 748, 700, 660, 637 cm^{-1}.

^{1}H-NMR (300 MHz, $CDCl_3$) δ 7.66 (d, *J* = 7.6 Hz, 1H), 7.36 (d, *J* = 1.4 Hz, 1H), 7.34 – 7.27 (m, 9H), 7.13 – 7.01 (m, 6H), 6.54 (s, 1H), 5.30 (d, *J* = 8.8 Hz, 1H), 4.75 (dt, *J* = 7.6, 4.9 Hz, 1H), 4.12 – 4.00 (m, 1H), 3.55 (s, 3H), 3.04 (dd, *J* = 14.7, 5.2 Hz, 1H), 2.93 (dd, *J* = 14.4, 5.0 Hz, 1H), 2.12 (h, *J* = 6.4 Hz, 1H), 1.38 (s, 9H), 0.90 (dd, *J* = 22.7, 6.8 Hz, 6H).

^{13}C-NMR (75 MHz, $CDCl_3$) δ 171.5, 171.4, 155.8, 142.2, 138.7, 136.3, 129.8, 128.2, 128.1, 119.7, 79.5, 75.4, 59.4, 52.6, 52.1, 31.5, 29.6, 28.4, 19.0.

HRMS–ESI: *m/z* $[M + H]^+$ calcd. for $C_{36}H_{42}N_4O_5$: 611.3228; found 611.3244.

Methyl N^{α}-(N^6-(((9*H*-fluoren-9-yl)methoxy)carbonyl)-N^2-(*tert*-butoxycarbonyl)-*L*-lysyl)-N^{τ}-trityl-*L*-histidinate (1g)

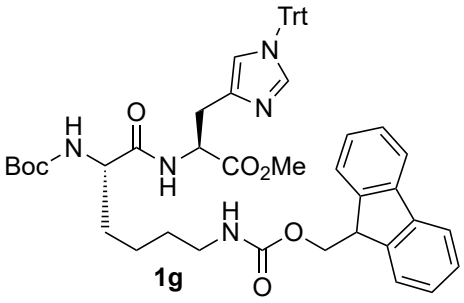

1g

The general procedure was followed starting from *L*–Boc–Lys(Fmoc)–OH (209 mg, 446 µmol). The resulting crude product was purified on silica gel (DCM–MeOH, gradient from 100:0 to 98:2) to afford **1g** as a white solid (224 mg, 58%). **Mp** 86 – 88 °C; $\mathbf{R_f}$ = 0.36 (DCM–MeOH, 95:5).

IR (ATR)/$\bar{\nu}$: 3296, 2931, 1709, 1494, 1446, 1365, 1243, 1163, 1134, 1088, 1023, 1001, 842, 742, 701, 660, 637 cm^{-1}.

^{1}H-NMR (300 MHz, $CDCl_3$) δ 7.81 (d, *J* = 7.7 Hz, 1H), 7.76 (d, *J* = 7.5 Hz, 2H), 7.58 (d, *J* = 7.3 Hz, 2H), 7.38 (t, *J* = 7.1 Hz, 3H), 7.35 – 7.28 (m, 11H), 7.16 – 7.02 (m, 6H), 6.55 (s, 1H), 5.36 (d, *J* = 7.8 Hz, 1H), 5.32 – 5.22 (m, 1H), 4.79 (dt, *J* = 7.7, 4.7 Hz, 1H), 4.44 – 4.30 (m, 2H), 4.28 – 4.13 (m, 2H), 3.56 (s, 3H), 3.27 – 2.92 (m, 4H), 2.02 – 1.77 (m, 1H), 1.75 – 1.47 (m, 5H), 1.41 (s, 9H).

^{13}C-NMR (75 MHz, $CDCl_3$) δ 171.8, 171.6, 156.6, 155.5, 144.1, 142.3, 141.4, 138.8, 136.4, 129.8, 128.2, 128.2, 127.7, 127.1, 125.2, 120.0, 119.7, 79.7, 75.4, 66.6, 54.1, 52.6, 52.3, 47.4, 40.6, 32.8, 29.5, 29.3, 28.4, 22.0.

HRMS–ESI: *m/z* $[M + H]^+$ calcd. for $C_{52}H_{55}N_5O_7$: 862.4174; found 862.4177.

Methyl N^{α}-((*tert*-butoxycarbonyl)-*L*-seryl)-N^{τ}-trityl-*L*-histidinate (1h)

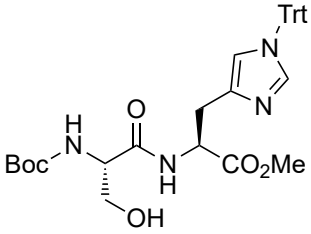

1h

The general procedure was followed starting from *L*–Boc–Ser–OH (92 mg, 446 µmol). The resulting crude product was purified on silica gel (Hexane–EtOAc, gradient from 80:20 to 20:80) to afford **1h** as a white solid (76 mg, 28%). **Mp** 86 – 88 °C; $\mathbf{R_f}$ = 0.21 (Hexane–EtOAc, 30:70).

IR (ATR)/$\bar{\nu}$: 3300, 2933, 1713, 1667, 1492, 1445, 1390, 1365, 1240, 1159, 1133, 1086, 1056, 1034, 1002, 840, 748, 701, 660, 638 cm^{-1}.

^{1}H-NMR (600 MHz, $CDCl_3$) δ 7.36 (s, 1H), 7.35 – 7.29 (m, 9H), 7.26 – 7.20 (m, 1H), 7.10 – 7.03 (m, 6H), 6.50 (s, 1H), 5.76 (s, 1H), 4.77 (s, 1H), 4.12 – 4.06 (m, 2H), 3.66 (dd, *J* = 12.0, 4.7 Hz, 1H), 3.56 (s, 3H), 3.29 – 3.23 (m, 1H), 2.84 (dd, *J* = 14.6, 5.9 Hz, 1H), 1.42 (s, 9H).

^{13}C-NMR (150 MHz, $CDCl_3$) δ 171.4, 171.2, 155.5, 142.1, 138.8, 135.9, 129.8, 128.3, 128.2, 120.0, 80.1, 75.6, 63.0, 57.3, 53.3, 52.4, 29.2, 28.4.

Methyl N^{α}-((*tert*-butoxycarbonyl)-*L*-threonyl)-N^{τ}-trityl-*L*-histidinate (1i)

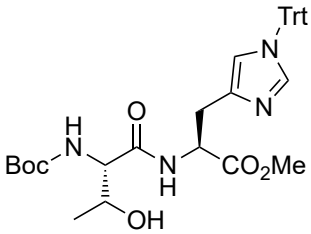

1i

The general procedure was followed starting from *L*–Boc–Thr–OH (98 mg, 446 µmol). The resulting crude product was purified on silica gel (Hexane–EtOAc, gradient from 80:20 to 20:80) to afford **1i** as a white solid (152 mg, 56%). **Mp** 68 – 70 °C; $\mathbf{R_f}$ = 0.14 (Hexane–EtOAc, 30:70).

IR (ATR)/$\bar{\nu}$: 3312, 2975, 2931, 1742, 1712, 1672, 1491, 1445, 1366, 1240, 1160, 1133, 1088, 1063, 1036, 1000, 871, 841, 748, 701, 661, 638 cm^{-1}.

^{1}H-NMR (600 MHz, $CDCl_3$) δ 7.26 (s, 1H), 7.23 – 7.19 (m, 9H), 7.02 (d, *J* = 7.1 Hz, 1H), 6.99 – 6.93 (m, 6H), 6.36 (s, 1H), 5.47 (d, *J* = 7.3 Hz, 1H), 4.65 (s, 1H), 4.29 (d, *J* = 6.6 Hz, 1H), 3.87 (d, *J* = 7.3 Hz, 1H), 3.44 (s, 3H), 3.27 (d, *J* = 13.9 Hz, 1H), 2.72 (dd, *J* = 14.5, 4.9 Hz, 1H), 1.34 (s, 9H), 1.12 (d, *J* = 6.4 Hz, 3H)./1

^{13}C-NMR (150 MHz, $CDCl_3$) δ 171.4, 171.3, 156.0, 142.1, 138.8, 135.9, 130.0, 128.2, 120.0, 80.0, 75.5, 67.3, 61.0, 53.4, 52.3, 28.9, 28.4, 20.0.

HRMS–ESI: *m/z* $[M + H]^+$ calcd. for $C_{35}H_{40}N_4O_6$: 613.3021; found 613.3025.

b. Synthesis of tripeptides Boc–Ala–His(Trt)–A.A–OMe (4a–f)

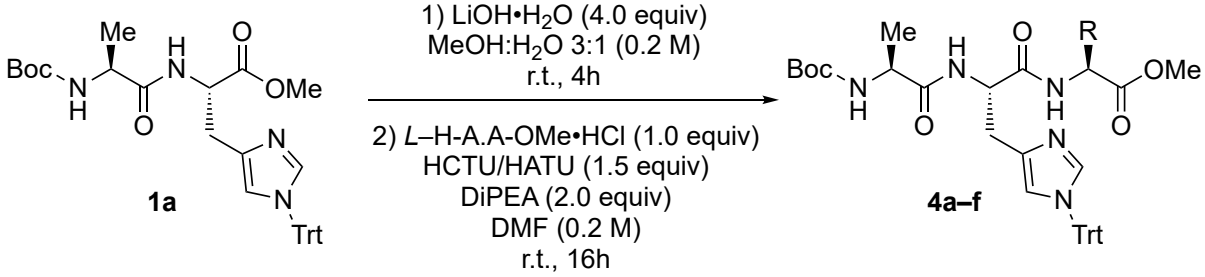

Manuscript, Scheme 4.: In a 50 mL flask, lithium hydroxide monohydrate (288 mg, 6.86 mmol, 4.0 equiv) was added to a solution of methyl N^{α}-((*tert*-butoxycarbonyl)-*L*-alanyl)-N^{τ}-trityl-*L*-histidinate (**1a**) (1g, 1.72 mmol, 1.0 equiv) in methanol:water 3:1 (9 mL, 0.2 M). The mixture was stirred for 4h at room temperature before concentrated to water under reduce pressure. The residue was diluted with a small amount of water before being acidify to pH 3 with a solution of HCl 1 M, a white precipitate appears. The suspension was extract twice with EtOAc (2x20 mL). The combined organic phases were washed with brine (20 mL), dried over Na_2SO_4, filtered and concentrated under reduce pressure. The white solid residue was used with no further purification step. In a 50 mL flask, DIPEA (2.0 equiv) was added to Boc–Ala–His(Trt)–OH (1.0 equiv), *L*–H-A.A–OMe•HCl (1.0 equiv) and HCTU or HATU (1.5 equiv) in DMF (0.2 M). The mixture was stirred for 16h at room temperature before being extracted twice with dichloromethane. The combined organic phases were successively washed with sat. aq. $NaHCO_3$ (2x20 mL), brine (2x20 mL), dried over Na_2SO_4, filtered and concentrated under reduce pressure. The resulting crude product was purified by column chromatography using the indicated eluent system to afford the desired pure product.

Methyl N^{α}-((*tert*-butoxycarbonyl)-*L*-alanyl)-N^{τ}-trityl-*L*-histidyl-*L*-valinate (4a)

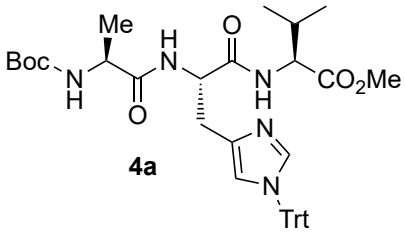

The general procedure was followed starting from Boc–Ala–His(Trt)–OH (640 mg, 1.13 mmol), *L*–H-Val–OMe•HCl (189 mg, 1.13 mmol), HCTU (698 mg, 1.69 mmol) and DiPEA (385 µL, 2.25 mmol) in DMF (6 mL). The resulting crude product was purified on silica gel (Hexane–EtOAc, gradient from 90:10 up to 20:80) to afford **4a** as a white solid (501 mg, 65%). **Mp** 79 – 81 °C; $\mathbf{R_f}$ = 0.42 (DCM–MeOH, 95:5).

IR (ATR)/$\bar{\nu}$: 3275, 2970, 1740, 1659, 1493, 1445, 1366, 1245, 1205, 1159, 1001, 841, 748, 701, 659, 638 cm^{-1}.

^{1}H-NMR (300 MHz, $CDCl_3$) δ 8.46 (d, *J* = 6.1 Hz, 1H), 7.52 (d, *J* = 8.2 Hz, 1H), 7.38 – 7.27 (m, 10H), 7.13 – 7.00 (m, 6H), 6.66 (s, 1H), 5.22 (d, *J* = 6.6 Hz, 1H), 4.78 – 4.65 (m, 1H), 4.39 (dd, *J* = 8.4, 5.3 Hz, 1H), 4.24 – 4.12 (m, 1H), 3.64 (s, 3H), 3.11 (A of ABX, *J* = 15.1, 4.3 Hz, 1H), 2.89 (B of ABX, *J* = 15.1, 5.9 Hz, 1H), 2.14 – 2.01 (m, 1H), 1.38 (d, *J* = 7.2 Hz, 3H), 1.35 (s, 9H), 0.80 (d, *J* = 6.8 Hz, 6H).

^{13}C-NMR (75 MHz, $CDCl_3$) δ 172.8, 171.9, 171.0, 155.4, 142.2, 138.2, 136.9, 129.8, 128.2, 128.1, 119.7, 79.8, 75.5, 57.6, 53.3, 52.0, 50.7, 30.9, 29.3, 28.4, 19.1, 18.0.

HRMS–ESI: *m/z* $[M + H]^+$ calcd. for $C_{39}H_{47}N_5O_6$: 682.3599, found 682.3594.

Methyl *N*$^\alpha$-((*tert*-butoxycarbonyl)-*L*-alanyl)-*N*$^\tau$-trityl-*L*-histidylglycinate (4b)

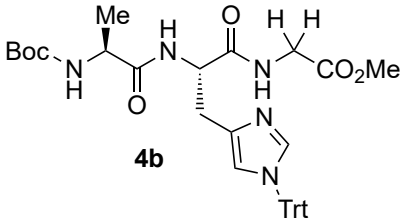

4b

The general procedure was followed starting from Boc–Ala–His(Trt)–OH (170 mg, 0.3 mmol), H-Gly–OMe•HCl (38 mg, 0.3 mmol), HCTU (186 mg, 0.45 mmol) and DiPEA (105 µL, 0.6 mmol) in DMF (2 mL). The resulting crude product was purified on silica gel (DCM–MeOH, gradient from 100:0 to 97:3) to afford **4b** as a white solid (119 mg, 62%). **Mp** 93 – 95 °C; **R_f** = 0.13 (DCM–MeOH, 95:5).

IR (ATR)/$\bar{\nu}$: 3290, 2977, 1753, 1660, 1520, 1492, 1445, 1365, 1245, 1203, 1162, 1133, 1036, 1001, 844, 748, 700, 660, 638 cm^{-1}.

^{1}H-NMR (300 MHz, $CDCl_3$) δ 8.61 (d, *J* = 7.7 Hz, 1H), 7.56 (t, *J* = 5.6 Hz, 1H), 7.33 (d, *J* = 1.4 Hz, 1H), 7.32 – 7.26 (m, 9H), 7.15 – 7.01 (m, 6H), 6.64 (s, 1H), 5.35 (d, *J* = 5.3 Hz, 1H), 4.70 (dt, *J* = 7.7, 5.0 Hz, 1H), 4.15 – 4.00 (m, 1H), 3.97 – 3.79 (m, 2H), 3.62 (s, 3H), 3.13 (dd, *J* = 14.1, 4.2 Hz, 1H), 2.87 (dd, *J* = 14.7, 5.4 Hz, 1H), 1.36 (d, *J* = 7.0 Hz, 3H), 1.29 (s, 9H).

^{13}C-NMR (75 MHz, $CDCl_3$) δ 172.8, 171.5, 169.6, 156.1, 142.3, 138.3, 136.8, 129.8, 128.1, 128.1, 119.9, 80.1, 75.4, 53.2, 52.0, 51.4, 41.1, 29.1, 28.3, 18.1.

HRMS–ESI: *m/z* $[M + H]^+$ calcd. for $C_{36}H_{41}N_5O_6$: 640.3130, found 640.3129.

Methyl *N*$^\alpha$-((*tert*-butoxycarbonyl)-*L*-alanyl)-*N*$^\tau$-trityl-*L*-histidyl-*L*-phenylalaninate (4c)

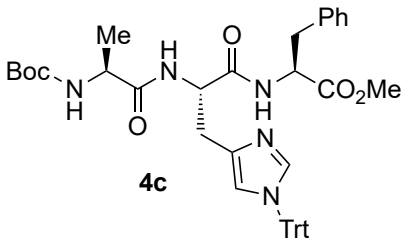

4c

The general procedure was followed starting from Boc–Ala–His(Trt)–OH (250 mg, 0.44 mmol), *L*–H-Phe–OMe•HCl (95 mg, 0.44 mmol), HCTU (273 mg, 0.66 mmol) and DiPEA (150 µL, 0.76 mmol) in DMF (2 mL). The resulting crude product was purified on silica gel (Hexane–EtOAc, gradient from

90:10 to 30:70) to afford **4c** as a white solid (212 mg, 66%). **Mp** 87 – 89 °C; $\mathbf{R_f}$ = 0.41 (DCM–MeOH, 95:5).

IR (ATR)/$\bar{\nu}$: 3290, 2976, 1744, 1657, 1493, 1444, 1365, 1243, 1212, 1163, 1131, 1087, 1031, 1001, 856, 747, 699, 659, 638 cm^{-1}.

^{1}H-NMR (300 MHz, $CDCl_3$) δ 8.09 (d, *J* = 7.3 Hz, 1H), 7.63 (d, *J* = 7.6 Hz, 1H), 7.34 – 7.24 (m, 9H), 7.21 – 7.13 (m, 3H), 7.12 – 6.99 (m, 9H), 6.64 (s, 1H), 5.44 (d, *J* = 6.9 Hz, 1H), 4.78 – 4.63 (m, 2H), 4.27 – 4.12 (m, 1H), 3.55 (s, 3H), 3.09 – 2.96 (m, 3H), 2.89 (dd, *J* = 14.8, 5.9 Hz, 1H), 1.36 (s, 9H), 1.28 (d, *J* = 7.1 Hz, 3H).

^{13}C-NMR (75 MHz, $CDCl_3$) δ 172.7, 171.4, 170.6, 155.4, 142.2, 138.2, 136.8, 136.1, 129.7, 129.2, 128.4, 128.0, 128.0, 126.9, 119.7, 79.6, 75.3, 53.7, 53.1, 52.0, 50.4, 37.9, 29.6, 28.3, 18.7.

HRMS–ESI: *m/z* $[M + H]^+$ calcd. for $C_{43}H_{47}N_5O_6$: 730.3599, found 730.3605.

Methyl *N*$^{\alpha}$-((*tert*-butoxycarbonyl)-*L*-alanyl)-*N*$^{\tau}$-trityl-*L*-histidyl-*L*-methioninate (4d)

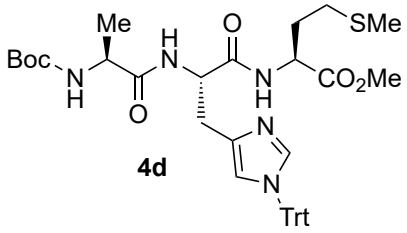

4d

The general procedure was followed starting from Boc–Ala–His(Trt)–OH (170 mg, 0.3 mmol), *L*–H-Met–OMe•HCl (60 mg, 0.3 mmol), HCTU (186 mg, 0.45 mmol) and DiPEA (105 µL, 0.6 mmol) in DMF (2 mL). The resulting crude product was purified on silica gel (DCM–MeOH, gradient from 100:0 to 97:3) to afford **4d** as a white solid (95 mg, 44%). **Mp** 118 – 120 °C; $\mathbf{R_f}$ = 0.14 (DCM–MeOH, 95:5).

IR (ATR)/$\bar{\nu}$: 3265, 2969, 2915, 1744, 1715, 1662, 1645, 1518, 1446, 1234, 1215, 1160, 1134, 1036, 1014, 837, 748, 700, 657 cm^{-1}.

^{1}H-NMR (300 MHz, $CDCl_3$) δ 8.39 (d, *J* = 7.4 Hz, 1H), 7.61 (d, *J* = 6.6 Hz, 1H), 7.36 – 7.27 (m, 10H), 7.13 – 7.00 (m, 6H), 6.65 (s, 1H), 5.22 (d, *J* = 5.9 Hz, 1H), 4.67 (dt, *J* = 7.5, 5.2 Hz, 1H), 4.58 – 4.45 (m, 1H), 4.10 (p, *J* = 6.9 Hz, 1H), 3.63 (s, 3H), 3.22 – 3.09 (m, 1H), 2.89 – 2.80 (m, 1H), 2.38 (t, *J* = 7.5 Hz, 2H), 2.06 – 2.01 (m, 1H), 1.99 (s, 3H), 1.95 – 1.89 (m, 1H), 1.38 (d, *J* = 6.9 Hz, 3H), 1.32 (s, 9H).

^{13}C-NMR (75 MHz, $CDCl_3$) δ 172.8, 171.9, 171.1, 155.8, 142.1, 138.3, 136.6, 129.8, 128.2, 128.1, 119.9, 80.1, 75.5, 53.3, 53.2, 52.4, 51.7, 31.3, 30.0, 28.4, 18.4, 15.4, 15.0.

HRMS–ESI: *m/z* $[M + H]^+$ calcd. for $C_{39}H_{47}N_5O_6S$: 714.3320, found 714.3323.

Methyl N$^{\alpha}$-((tert-butoxycarbonyl)-L-alanyl)-N$^{\tau}$-trityl-L-histidyl-L-prolinate (4e)

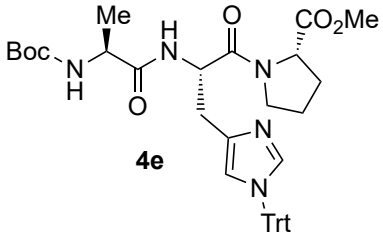

4e

The general procedure was followed starting from Boc–Ala–His(Trt)–OH (200 mg, 0.35 mmol), *L*–H-Pro–OMe•HCl (58 mg, 0.35 mmol), HATU (201 mg, 0.53 mmol) and DiPEA (120 µL, 0.7 mmol) in DMF (2 mL). The resulting crude product was purified on silica gel (DCM–MeOH, gradient from 100:0 to 97:3) to afford **4e** as a white solid (119 mg, 50%). **Mp** 92 – 94 °C; **R$_f$** = 0.25 (DCM–MeOH, 95:5).

IR (ATR)/$\bar{\nu}$: 3284, 2959, 1743, 1709, 1643, 1493, 1445, 1365, 1245, 1161, 1131, 1022, 1001, 837, 747, 701, 661, 638 cm^{-1}.

^{1}H-NMR (600 MHz, CDCl$_3$) δ 7.66 (s, 1H), 7.37 – 7.28 (m, 10H), 7.14 – 7.10 (m, 6H), 6.86 (s, 1H), 5.36 (d, *J* = 6.2 Hz, 1H), 4.99 – 4.91 (m, 1H), 4.50 (dd, *J* = 8.5, 3.7 Hz, 1H), 4.14 – 4.05 (m, 1H), 3.72 – 3.65 (m, 1H), 3.62 – 3.56 (m, 1H), 3.43 (s, 3H), 3.14 – 3.08 (m, 1H), 2.92 (dd, *J* = 14.8, 5.3 Hz, 1H), 2.20 – 2.12 (m, 1H), 1.99 – 1.87 (m, 3H), 1.35 (s, 9H), 1.26 (d, *J* = 7.0 Hz, 3H).

***Presence of conformers:* ^{13}C-NMR (150 MHz, CDCl$_3$)** δ 172.5, 172.5, 169.1, 155.6, 141.4, 137.1, 129.9, 129.7, 128.4, 128.3, 128.3, 128.2, 127.8, 121.4, 79.9, 76.8, 58.9, 55.8, 52.2, 50.8, 50.3, 47.0, 28.9, 28.4, 24.8, 18.4.

HRMS–ESI: *m/z* $[M + H]^+$ calcd. for $C_{39}H_{45}N_5O_6$: 680.3443, found 680.3443.

Methyl *N*$^{\alpha}$-((*tert*-butoxycarbonyl)-*L*-alanyl)-*N*$^{\tau}$-trityl-*L*-histidyl-*L*-serinate (4f)

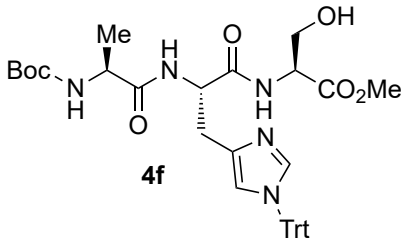

4f

The general procedure was followed starting from Boc–Ala–His(Trt)–OH (170 mg, 0.3 mmol), *L*–H-Ser–OMe•HCl (47 mg, 0.3 mmol), HCTU (186 mg, 0.53 mmol) and DiPEA (105 µL, 0.6 mmol) in DMF (2 mL). The resulting crude product was purified on silica gel (DCM–MeOH, gradient from 100:0 to 95:5) to afford **4f** as a white solid (107 mg, 53%). **Mp** 100 – 102 °C; **R$_f$** = 0.29 (DCM–MeOH, 95:5).

IR (ATR)/$\bar{\nu}$: 3292, 2977, 1743, 1655, 1492, 1445, 1365, 1239, 1205, 1161, 1132, 1068, 1036, 1001, 841, 748, 700, 660, 638 cm^{-1}.

^{1}H-NMR (300 MHz, CDCl$_3$) δ 7.88 (d, *J* = 6.1 Hz, 1H), 7.55 (d, *J* = 7.4 Hz, 1H), 7.37 – 7.34 (m, 1H), 7.33 – 7.27 (m, 9H), 7.14 – 7.00 (m, 6H), 6.65 (s, 1H), 5.31 (d, *J* = 6.0 Hz, 1H), 4.80 – 4.68 (m, 1H), 4.49 – 4.40 (m, 1H), 4.13 – 3.99 (m, 1H), 3.91 (dd, *J* = 11.7, 4.5 Hz, 1H), 3.84 (dd, *J* =

11.6, 3.5 Hz, 1H), 3.63 (s, 3H), 3.13 (dd, *J* = 14.5, 4.4 Hz, 1H), 2.94 (dd, *J* = 15.2, 4.6 Hz, 1H), 1.38 – 1.32 (m, 3H), 1.31 (s, 9H).

^{13}C-NMR (75 MHz, $CDCl_3$) δ 172.8, 171.0, 170.6, 155.9, 142.2, 138.5, 136.1, 129.8, 128.2, 128.2, 120.5, 80.3, 75.5, 62.0, 55.3, 52.9, 52.4, 51.0, 29.5, 28.4, 18.3.

HRMS–ESI: *m/z* $[M + H]^+$ calcd. for $C_{37}H_{43}N_5O_7$: 670.3235, found 670.3244.

c. Synthesis of tripeptides Boc–A.A–His(Trt)–Val–OMe (4g–j)

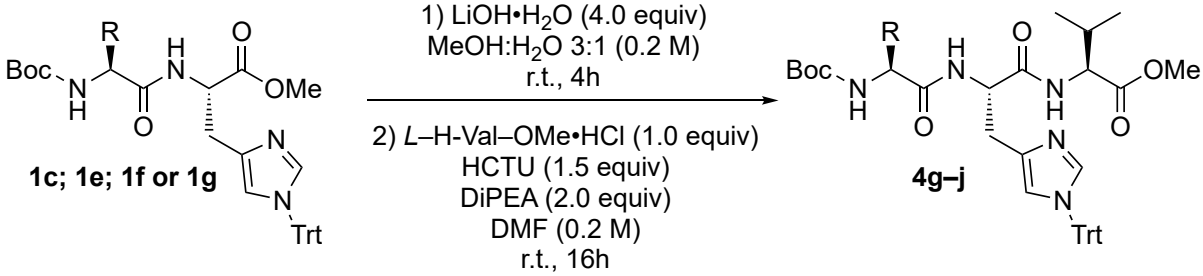

Manuscript, Scheme 5.: In a 50 mL flask, lithium hydroxide monohydrate (4.0 equiv) was added to a solution of methyl N^{α}-((*tert*-butoxycarbonyl)-*L*-Amino acid)-N^{τ}-trityl-*L*-histidinate (**1c; 1e; 1f or 1g**) (1.0 equiv) in methanol:water 3:1 (9 mL, 0.2 M). The mixture was stirred for 4h at room temperature before concentrated to water under reduce pressure. The residue was diluted with a small amount of water before being acidify to pH 3 with a solution of HCl 1 M, a white precipitate appears. The suspension was extract twice with EtOAc (2x20 mL). The combined organic phases were washed with brine (20 mL), dried over Na_2SO_4, filtered and concentrated under reduce pressure. The white solid residue was used with no further purification step. In a 50 mL flask, DIPEA (2.0 equiv) was added to Boc–A.A–His(Trt)–OH (1.0 equiv), *L*–H-Val–OMe•HCl (1.0 equiv) and HCTU (1.5 equiv) in DMF (0.2 M). The mixture was stirred for 16h at room temperature before being extracted twice with dichloromethane. The combined organic phases were successively washed with sat. aq. $NaHCO_3$ (2x20 mL), brine (2x20 mL), dried over Na_2SO_4, filtered and concentrated under reduce pressure. The resulting crude product was purified by column chromatography using the indicated eluent system to afford the desired pure product.

Methyl N^{α}-((*tert*-butoxycarbonyl)-*L*-phenylalanyl)-N^{τ}-trityl-*L*-histidyl-*L*-valinate (4g)

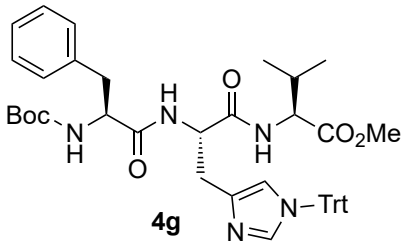

4g

The general procedure was followed starting from Boc–Phe–His(Trt)–OH (228 mg, 0.35 mmol), *L*–H-Val–OMe•HCl (60 mg, 0.35 mmol), HCTU (219 mg, 0.53 mmol) and DiPEA (120 µL, 0.71 mmol) in DMF (2 mL). The resulting crude product was purified on silica gel (DCM–MeOH, gradient from 100:0 to 95:5) to afford **4g** as a white solid (150 mg, 56%). **Mp** 83 – 85 °C; $\mathbf{R_f}$ = 0.43 (DCM–MeOH, 95:5).

IR (ATR)/$\bar{\nu}$: 3290, 2966, 1741, 1651, 1492, 1445, 1365, 1246, 1205, 1157, 1086, 1021, 1001, 870, 842, 747, 699, 660, 638 cm^{-1}.

^{1}H-NMR (300 MHz, $CDCl_3$) δ 8.34 (d, *J* = 6.0 Hz, 1H), 7.46 (d, *J* = 7.9 Hz, 1H), 7.35 – 7.25 (m, 10H), 7.23 – 7.12 (m, 5H), 7.11 – 7.02 (m, 6H), 6.64 (s, 1H), 5.18 (d, *J* = 6.8 Hz, 1H), 4.72 (q, *J* = 6.3 Hz, 1H), 4.46 – 4.33 (m, 2H), 3.63 (s, 3H), 3.17 (dd, *J* = 14.0, 5.0 Hz, 1H), 3.07 (dd, *J* = 14.9, 3.7 Hz, 1H), 3.03 – 2.90 (m, 1H), 2.87 – 2.78 (m, 1H), 2.16 – 2.03 (m, 1H), 1.28 (s, 9H), 0.83 (d, *J* = 3.3 Hz, 3H), 0.81 (d, *J* = 3.4 Hz, 3H).

^{13}C-NMR (75 MHz, $CDCl_3$) δ 172.0, 171.6, 171.0, 155.6, 142.2, 138.4, 136.8, 136.7, 129.7, 129.3, 128.6, 128.1, 128.1, 126.9, 119.6, 79.9, 75.4, 57.7, 56.0, 53.4, 52.0, 30.8, 29.5, 28.2, 19.0, 18.0.

HRMS–ESI: *m/z* $[M + H]^+$ calcd. for $C_{45}H_{51}N_5O_6$: 758.3912, found 758.3913.

Methyl N^{α}-((*tert*-butoxycarbonyl)-*L*-glycyl)-N^{τ}-trityl-*L*-histidyl-*L*-valinate (4h)

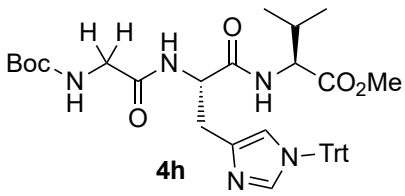

4h

The general procedure was followed starting from Boc–Gly–His(Trt)–OH (276 mg, 0.5 mmol), *L*–H-Val–OMe•HCl (83 mg, 0.5 mmol), HCTU (309 mg, 0.75 mmol) and DiPEA (170 µL, 1.0 mmol) in DMF (2.5 mL). The resulting crude product was purified on silica gel (DCM–MeOH, gradient from 100:0 to 95:5) to afford **4h** as a white solid (64 mg, 19%). **Mp** 78 – 80 °C; $\mathbf{R_f}$ = 0.64 (DCM–MeOH, 90:10).

IR (ATR)/$\bar{\nu}$: 3297, 2966, 2930, 1745, 1715, 1658, 1494, 1445, 1366, 1247, 1206, 1157, 1033, 1001, 870, 749, 702, 661, 639 cm^{-1}.

^{1}H-NMR (300 MHz, $CDCl_3$) δ 8.14 (d, *J* = 6.7 Hz, 1H), 7.67 (d, *J* = 8.3 Hz, 1H), 7.35 – 7.28 (m, 10H), 7.13 – 7.05 (m, 6H), 6.65 (s, 1H), 5.37 – 5.27 (m, 1H), 4.77 (q, *J* = 6.1 Hz, 1H), 4.41 (dd, *J* = 8.4, 5.1 Hz, 1H), 3.91 – 3.78 (m, 2H), 3.64 (s, 3H), 3.07 (dd, *J* = 15.0, 4.7 Hz, 1H), 2.95 – 2.85 (m, 1H), 2.18 – 2.06 (m, 1H), 1.38 (s, 9H), 0.84 (d, *J* = 1.5 Hz, 3H), 0.82 (d, *J* = 1.6 Hz, 3H).

^{13}C-NMR (75 MHz, $CDCl_3$) δ 172.0, 171.1, 169.5, 156.0, 142.4, 138.3, 137.0, 129.8, 128.2, 128.1, 119.7, 79.9, 75.4, 57.7, 53.1, 52.1, 38.7, 31.0, 29.9, 28.4, 19.2, 18.0.

HRMS–ESI: *m/z* $[M + H]^+$ calcd. for $C_{38}H_{45}N_5O_6$: 668.3443, found 668.3457.

Methyl *N*$^{\alpha}$-((*tert*-butoxycarbonyl)-*L*-methionyl)-*N*$^{\tau}$-trityl-*L*-histidyl-*L*-valinate (4i)

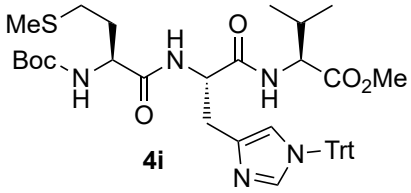

4i

The general procedure was followed starting from Boc–Met–His(Trt)–OH (226 mg, 0.36 mmol), *L*–H-Val–OMe•HCl (60 mg, 0.36 mmol), HCTU (223 mg, 0.54 mmol) and DiPEA (125 µL, 0.72 mmol) in DMF (2 mL). The resulting crude product was purified on silica gel (DCM–MeOH, gradient from 100:0 to 95:5) to afford **4i** as a white solid (64 mg, 19%). **Mp** 86 – 88 °C; $\mathbf{R_f}$ = 0.43 (DCM–MeOH, 95:5).

IR (ATR)/$\bar{\nu}$: 3285, 2967, 1740, 1657, 1493, 1445, 1390, 1366, 1246, 1208, 1158, 1024, 1001, 840, 748, 701, 660, 639 cm^{-1}.

^{1}H-NMR (300 MHz, $CDCl_3$) δ 8.32 (d, *J* = 6.3 Hz, 1H), 7.42 (d, *J* = 7.9 Hz, 1H), 7.36 – 7.27 (m, 10H), 7.13 – 7.01 (m, 6H), 6.65 (s, 1H), 5.47 (d, *J* = 7.1 Hz, 1H), 4.71 (q, *J* = 6.0 Hz, 1H), 4.39 (dd, *J* = 8.4, 5.2 Hz, 1H), 4.32 – 4.22 (m, 1H), 3.62 (s, 3H), 3.06 (dd, *J* = 14.8, 4.7 Hz, 1H), 2.92 – 2.85 (m, 1H), 2.54 (t, *J* = 7.4 Hz, 2H), 2.18 – 2.06 (m, 2H), 2.05 (s, 3H), 1.95 – 1.82 (m, 1H), 1.35 (s, 9H), 0.82 (d, *J* = 1.2 Hz, 3H), 0.80 (d, *J* = 1.3 Hz, 3H).

^{13}C-NMR (75 MHz, $CDCl_3$) δ 172.1, 171.9, 171.0, 155.7, 142.3, 138.4, 136.7, 129.8, 128.2, 128.1, 119.8, 80.0, 75.5, 57.6, 54.2, 53.4, 52.1, 32.1, 30.9, 30.2, 28.4, 19.1, 18.0, 15.3.

HRMS–ESI: *m/z* $[M + H]^+$ calcd. for $C_{41}H_{51}N_5O_6S$: 742.3633, found 742.3647.

Methyl *N*$^{\alpha}$-((*tert*-butoxycarbonyl)-*L*-seryl)-*N*$^{\tau}$-trityl-*L*-histidyl-*L*-valinate (4j)

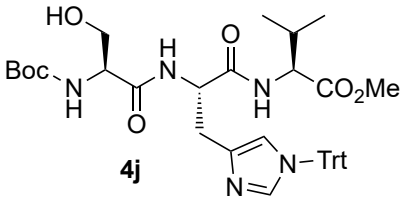

4j

The general procedure was followed starting from Boc–Ser–His(Trt)–OH (160 mg, 0.27 mmol), *L*–H-Val–OMe•HCl (46 mg, 0.27 mmol), HCTU (170 mg, 0.41 mmol) and DiPEA (95 µL, 0.55 mmol) in DMF (1.5 mL). The resulting crude product was purified on silica gel (DCM–MeOH, gradient from 100:0 to 95:5) to afford **4j** as a white solid (45 mg, 24%). **Mp** 104 – 106 °C; $\mathbf{R_f}$ = 0.34 (DCM–MeOH, 95:5).

IR (ATR)/$\bar{\nu}$: 3285, 2959, 1739, 1655, 1492, 1445, 1366, 1208, 1156, 1057, 1037, 1001, 841, 748, 700, 660 cm^{-1}.

^{1}H-NMR (300 MHz, $CDCl_3$) δ 7.82 (d, *J* = 6.6 Hz, 1H), 7.37 – 7.27 (m, 11H), 7.14 – 7.01 (m, 7H), 6.62 (s, 1H), 5.69 (d, *J* = 6.1 Hz, 1H), 4.77 (q, *J* = 5.9 Hz, 1H), 4.44 (dd, *J* = 8.6, 5.0 Hz, 1H), 4.15 (s(br), 1H), 4.01 (dd, *J* = 11.3, 2.0 Hz, 1H), 3.68 (dd, *J* = 11.3, 5.6 Hz, 1H), 3.56 (s, 3H), 3.11 (dd, *J* = 14.9, 4.2 Hz, 1H), 2.93 (dd, *J* = 15.2, 6.0 Hz, 1H), 2.20 – 2.02 (m, 1H), 1.40 (s, 9H), 0.84 (d, *J* = 4.3 Hz, 3H), 0.82 (d, *J* = 4.4 Hz, 3H).

^{13}C-NMR (150 MHz, $CDCl_3$) δ 172.4, 171.5, 170.7, 155.6, 142.2, 138.6, 136.4, 129.9, 128.2, 128.2, 120.1, 80.1, 75.6, 63.1, 57.4, 57.0, 53.9, 52.2, 31.1, 29.5, 28.4, 19.1, 17.9.

HRMS–ESI: *m/z* $[M + H]^+$ calcd. for $C_{39}H_{47}N_5O_7$: 698.3548, found 698.3556.

d. Synthesis of tripeptides Boc–A.A_1–A.A_2–His(Trt)–OMe (6a–e)

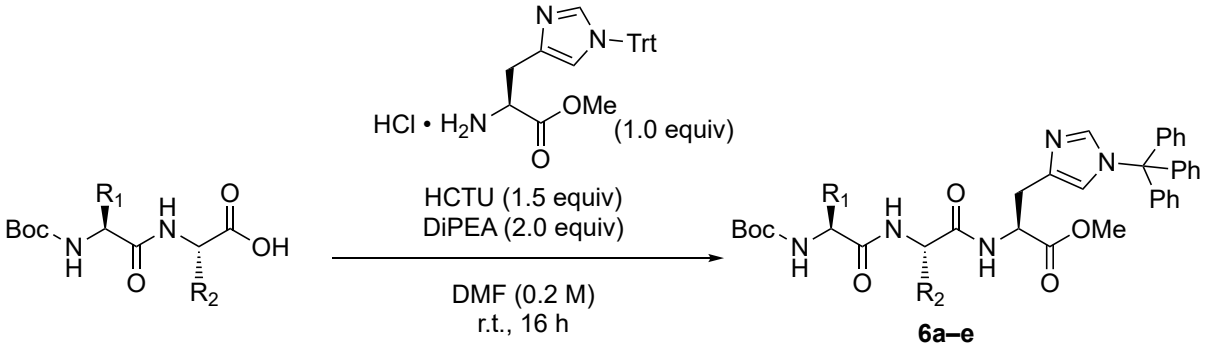

Manuscript, Scheme 6.: In a 50 mL flask, DIPEA (2.0 equiv) was added to Boc–A.A_1– A.A_2–OH (1.0 equiv), *L*–H-His(Trt)–OMe•HCl (1.0 equiv) and HCTU (1.5 equiv) in DMF (0.2 M). The mixture was stirred for 16h at room temperature before being extracted twice with dichloromethane. The combined organic phases were successively washed with sat. aq. $NaHCO_3$ (2x20 mL), brine (2x20 mL), dried over Na_2SO_4, filtered and concentrated under reduce pressure. The resulting crude product was purified by column chromatography using the indicated eluent system to afford the desired pure product.

Methyl N^{α}-(*tert*-butoxycarbonyl)-*L*-alanyl-*L*-valyl-N^{τ}-trityl-*L*-histidinate (6a)

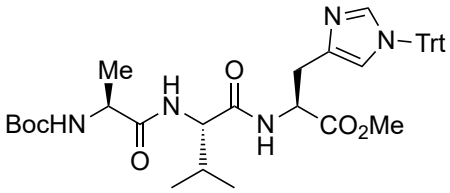

6a

This compound has been previously reported [1]: **Mp** 87 – 89 °C; $\mathbf{R_f}$ = 0.34 (DCM–MeOH, 95:5).

IR (ATR)/$\bar{\nu}$: 3292, 2972, 1650, 1493, 1445, 1162, 838, 748, 701, 660 cm^{-1}.

^{1}H-NMR (300 MHz, $CDCl_3$) δ 7.82 (d, *J* = 7.4 Hz, 1H), 7.43 (s, 1H), 7.35 – 7.25 (m, 9H), 7.15 – 7.09 (m, 1H), 7.09 – 7.01 (m, 6H), 6.58 (s, 1H), 5.44 (s, 1H), 4.79 – 4.63 (m, 1H), 4.31 (dd, *J* = 8.2, 5.7 Hz, 1H), 4.23 – 4.09 (m, 1H), 3.53 (s, 3H), 3.01 (dd, *J* = 14.6, 5.1 Hz, 1H), 2.94 (dd, *J* = 14.9, 5.0 Hz, 1H), 2.20 – 2.05 (m, 1H), 1.38 (s, 9H), 1.26 (d, *J* = 7.0 Hz, 3H), 0.90 (t, *J* = 6.1 Hz, 6H).

Methyl N^{α}-(*tert*-butoxycarbonyl)-*L*-valyl-*L*-alanyl -N^{τ}-trityl-*L*-histidinate (6b)

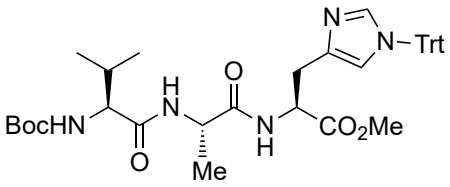

6b

This compound has been previously reported [1]: **Mp** 92 – 94 °C; $\mathbf{R_f}$ = 0.36 (DCM–MeOH, 95:5).

IR (ATR)/$\bar{\nu}$: 3275, 2972, 1745, 1651, 1493, 1445, 1366, 1160, 1132, 838, 748, 701, 660 cm^{-1}.

^{1}H-NMR (300 MHz, $CDCl_3$) δ 7.70 (d, *J* = 7.8 Hz, 1H), 7.45 (s, 1H), 7.34 – 7.27 (m, 9H), 7.13 – 7.00 (m, 7H), 6.56 (d, *J* = 1.0 Hz, 1H), 5.25 (d, *J* = 8.9 Hz, 1H), 4.80 – 4.70 (m, 1H), 4.48 (p, *J* = 6.9 Hz, 1H), 4.01 – 3.91 (m, 1H), 3.55 (s, 3H), 3.04 (dd, *J* = 14.9, 5.1 Hz, 1H), 2.94 (dd, *J* = 10.2, 5.6 Hz, 1H), 2.14 – 1.99 (m, 1H), 1.39 (s, 9H), 1.36 (d, *J* = 7.1 Hz, 3H), 0.85 (dd, *J* = 13.5, 6.8 Hz, 6H).

Methyl N^{α}-*(tert*-butoxycarbonyl*)-L*-alanylglycyl-N^{τ}-trityl-*L*-histidinate (6c)

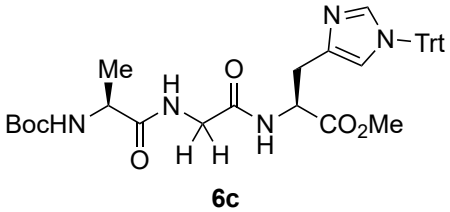

6c

The general procedure was followed starting from Boc–Ala–Gly–OH (100 mg, 0.41 mmol), *L*–H-His(Trt)–OMe•HCl (182 mg, 0.41 mmol), HCTU (252 mg, 0.61 mmol) and DiPEA (140 µL, 0.81 mmol) in DMF (2 mL). The resulting crude product was purified on silica gel (DCM–MeOH, gradient from 100:0 to 97:3) to afford **6c** as a white solid (146 mg, 56%). **Mp** 86 – 89 °C; $\mathbf{R_f}$ = 0.20 (DCM–MeOH, 95:5).

[1] Chan, H.-C..; Bueno, B.; Le Roch, A.; Gagnon, *Chem.Eur. J.* **2021**, *27*, 13330–13336

IR (ATR)/$\bar{\nu}$: 3298, 2978, 1743, 1662, 1493, 1445, 1365, 1241, 1210, 1162, 1132, 1025, 1001, 870, 842, 747, 700, 660, 638 cm^{-1}.

^{1}H-NMR (600 MHz, $CDCl_3$) δ 7.72 (d, *J* = 6.5 Hz, 1H), 7.39 (s, 1H), 7.33 – 7.27 (m, 9H), 7.12 (s, 1H), 7.10 – 7.04 (m, 6H), 6.53 (s, 1H), 5.54 (d, *J* = 7.8 Hz, 1H), 4.74 (dt, *J* = 7.6, 5.0 Hz, 1H), 4.24 (s(br), 1H), 4.00 (dd, *J* = 16.6, 3.4 Hz, 1H), 3.89 (dd, *J* = 17.0, 5.0 Hz, 1H), 3.54 (s, 3H), 3.01 (dd, *J* = 14.6, 5.4 Hz, 1H), 2.93 (dd, *J* = 14.6, 4.6 Hz, 1H), 1.36 (s, 9H), 1.31 (d, *J* = 7.1 Hz, 3H).

^{13}C-NMR (150 MHz, $CDCl_3$) δ 173.1, 171.4, 168.6, 155.5, 142.2, 138.8, 136.1, 129.7, 128.2, 128.1, 119.7, 79.9, 75.4, 52.7, 52.2, 50.1, 42.8, 29.6, 28.3, 18.7.

HRMS–ESI: *m/z* $[M + H]^+$ calcd. for $C_{36}H_{41}N_5O_6$: 640.3130, found 640.3139.

Methyl *N*$^\alpha$-(*tert*-butoxycarbonyl)glycyl-*L*-alanyl-*N*$^\tau$-trityl-*L*-histidinate (6d)

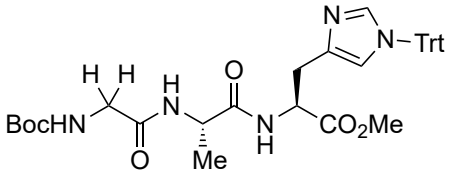

6d

The general procedure was followed starting from Boc–Gly–Ala–OH (100 mg, 0.41 mmol), *L*–H-His(Trt)–OMe•HCl (182 mg, 0.41 mmol), HCTU (252 mg, 0.61 mmol) and DiPEA (140 µL, 0.81 mmol) in DMF (2 mL). The resulting crude product was purified on silica gel (DCM–MeOH, gradient from 100:0 to 97:3) to afford **6d** as a white solid (120 mg, 46%). **Mp** 89 – 91 °C; **R_f** = 0.18 (DCM–MeOH, 95:5).

IR (ATR)/$\bar{\nu}$: 3291, 2978, 1652, 1494, 1445, 1366, 1241, 1209, 1159, 1088, 1034, 1001, 942, 842, 747, 700, 660, 638 cm^{-1}.

^{1}H-NMR (600 MHz, $CDCl_3$) δ ^{1}H 7.76 (d, *J* = 7.6 Hz, 1H), 7.37 (s, 1H), 7.34 – 7.28 (m, 9H), 7.11 – 7.04 (m, 7H), 6.54 (s, 1H), 5.54 (t, *J* = 5.1 Hz, 1H), 4.73 (dt, *J* = 7.6, 4.9 Hz, 1H), 4.59 – 4.49 (m, 1H), 3.82 (dd, *J* = 16.6, 4.3 Hz, 1H), 3.75 (dd, *J* = 16.2, 3.7 Hz, 1H), 3.55 (s, 3H), 3.02 (dd, *J* = 14.7, 5.4 Hz, 1H), 2.95 (dd, *J* = 14.7, 4.3 Hz, 1H), 1.39 (s, 9H), 1.36 (d, *J* = 7.0 Hz, 3H).

^{13}C-NMR (150 MHz, $CDCl_3$) δ 172.0, 171.4, 169.2, 156.0, 142.2, 138.7, 136.2, 129.7, 128.2, 128.2, 119.7, 78.0, 75.4, 52.7, 52.2, 48.8, 44.2, 29.4, 28.3, 18.6.

HRMS–ESI: *m/z* $[M + H]^+$ calcd. for $C_{36}H_{41}N_5O_6$: 640.3130, found 640.3150.

Methyl *N*$^\alpha$-(*tert*-butoxycarbonyl)glycylglycyl-*N*$^\tau$-trityl-*L*-histidinate (6e)

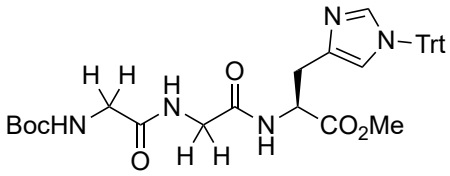

6e

The general procedure was followed starting from Boc–Gly–Gly–OH (229 mg, 0.99 mmol), *L*–H-His(Trt)–OMe•HCl (442 mg, 0.99 mmol), HCTU (612 mg, 1.48 mmol) and DiPEA (335 µL, 1.97 mmol) in DMF (5 mL). The

resulting crude product was purified on silica gel (DCM–MeOH, gradient from 100:0 to 97:3) to afford **6e** as a white solid (150 mg, 24%). **Mp** 85 – 87 °C; $\mathbf{R_f}$ = 0.17 (DCM–MeOH, 95:5).

IR (ATR)/$\bar{\nu}$: 3315, 2971, 1744, 1668, 1516, 1495, 1445, 1281, 1248, 1213, 1163, 1132, 1110, 950, 843, 749, 702, 661 cm^{-1}.

^{1}H-NMR (600 MHz, $CDCl_3$) δ 7.78 (d, *J* = 7.6 Hz, 1H), 7.45 (s, 1H), 7.32 – 7.27 (m, 10H), 7.11 – 7.04 (m, 6H), 6.57 (s, 1H), 5.80 (s, 1H), 4.74 – 4.69 (m, 1H), 3.95 (dd, *J* = 16.9, 5.3 Hz, 1H), 3.90 (dd, *J* = 16.9, 5.2 Hz, 1H), 3.79 (s(br), 2H), 3.53 (s, 3H), 2.99 (dd, *J* = 14.8, 5.7 Hz, 1H), 2.95 (dd, *J* = 14.9, 4.9 Hz, 1H), 1.36 (s, 9H).

^{13}C-NMR (150 MHz, $CDCl_3$) δ 171.5, 170.6, 168.9, 156.2, 142.0, 138.5, 135.7, 129.7, 128.2, 128.1, 119.9, 80.0, 75.6, 52.7, 52.2, 44.1, 42.7, 29.4, 28.3.

HRMS–ESI: *m/z* $[M + H]^+$ calcd. for $C_{35}H_{39}N_5O_6$: 626.2973, found 626.2994.

e. Synthesis of tetrapeptide Boc–Ala–His(Trt)–Val–Gly–OMe (8)

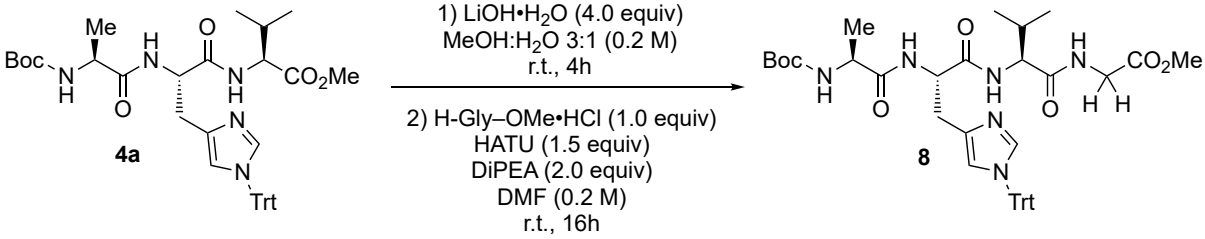

Methyl N^{α}-((*tert*-butoxycarbonyl)-*L*-alanyl)-N^{τ}-trityl-*L*-histidyl-*L*-valylglycinate (8)

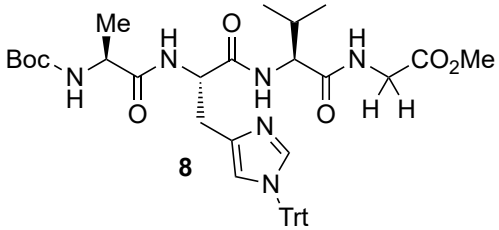

Manuscript, Scheme 7.: In a 50 mL flask, lithium hydroxide monohydrate (62 mg, 1.5 mmol, 4.0 equiv) was added to a solution of methyl N^{α}-((*tert*-butoxycarbonyl)-*L*-alanyl)-N^{τ}-trityl-*L*-histidyl-*L*-valinate (**4a**) (250 mg, 0.37 mmol, 1.0 equiv) in methanol:water 3:1 (3 mL, 0.1 M). The mixture was stirred for 4h at room temperature before concentrated to water under reduce pressure. The residue was diluted with a small amount of water before being acidify to pH 3 with a solution of HCl 1 M, a white precipitate appears. The suspension was extract twice with EtOAc (2x20 mL). The combined organic phases were washed with brine (20 mL), dried over Na_2SO_4, filtered and concentrated under reduce pressure. The white solid residue was used with no further purification step. In a 50 mL flask, DIPEA (115 µL, 0.67 mmol, 2.0 equiv) was added to

Boc–Ala–His(Trt)–Val–OH (223 mg, 0.33 mmol, 1.0 equiv), H-Gly–OMe•HCl (42 mg, 0.33 mmol, 1.0 equiv) and HATU (190 mg, 0,50 mmol, 1.5 equiv) in DMF (2 mL, 0.2 M). The mixture was stirred for 16h at room temperature before being extracted twice with dichloromethane. The combined organic phases were successively washed with sat. aq. $NaHCO_3$ (2x20 mL), brine (2x20 mL), dried over Na_2SO_4, filtered and concentrated under reduce pressure. The resulting crude product was purified on silica gel (DCM–MeOH, gradient from 100:0 to 97:3) to afford **8** as a white solid (143 mg, 58%). **Mp** 104 – 106 °C; $\mathbf{R_f}$ = 0.38 (DCM–MeOH, 95:5).

IR (ATR)/$\bar{\nu}$: 3285, 2970, 1751, 1639, 1493, 1445, 1366, 1206, 1161, 1132, 1036, 1001, 841, 747, 701, 659, 638 cm^{-1}.

^{1}H-NMR (600 MHz, $CDCl_3$) δ 8.71 (d, *J* = 4.9 Hz, 1H), 7.73 (s, 1H), 7.33 – 7.28 (m, 10H), 7.10 – 7.03 (m, 6H), 7.01 (d, *J* = 8.8 Hz, 1H), 6.68 (s, 1H), 5.12 (d, *J* = 4.4 Hz, 1H), 4.56 (q, *J* = 5.5 Hz, 1H), 4.36 (dd, *J* = 8.7, 5.0 Hz, 1H), 4.12 – 4.04 (m, 2H), 3.81 (dd, *J* = 17.7, 5.3 Hz, 1H), 3.63 (s, 3H), 3.13 – 3.07 (m, 1H), 2.95 (dd, *J* = 15.0, 5.9 Hz, 1H), 2.39 – 2.28 (m, 1H), 1.38 – 1.35 (m, 3H), 1.33 (s, 9H), 0.86 (d, *J* = 6.8 Hz, 3H), 0.83 (d, *J* = 6.8 Hz, 3H).

^{13}C-NMR (150 MHz, $CDCl_3$) δ 173.9, 171.8, 171.3, 170.4, 155.8, 142.2, 138.7, 136.6, 129.7, 128.3, 128.2, 120.0, 80.3, 75.5, 58.8, 54.5, 52.1, 51.4, 41.1, 29.6, 28.9, 28.4, 19.4, 17.4.

HRMS–ESI: *m/z* $[M + H]^+$ calcd. for $C_{41}H_{50}N_6O_7$: 739.3814, found 739.3818.

4. Procedure for the coupling between methyl ester N-protected histidine-containing peptides (1, 4, 6 and 8) and triarylbismuthines (2)

General method: In a sealed tube, *N*,*N*-diisopropylethylamine (1.0 equiv) was added to the N^{τ}-trityl-histidine-containing peptide (1.0 equiv), the corresponding triarylbismuthine (**2)** (1.0 equiv), copper(II) acetate (1.0 equiv) and phenanthroline (1.0 equiv) in CH_2Cl_2 (0.1 M). Oxygen was bubbled in the reaction mixture before stirred in an oil bath set at 50 °C for 16 hours. After cooled down at room temperature, the mixture was directly purified on silica gel chromatography using the corresponding eluent system to afford desired pure product.

a. Arylated compounds (3a–i) from dipeptides (1a–i) using tritolylbismuth (2a)

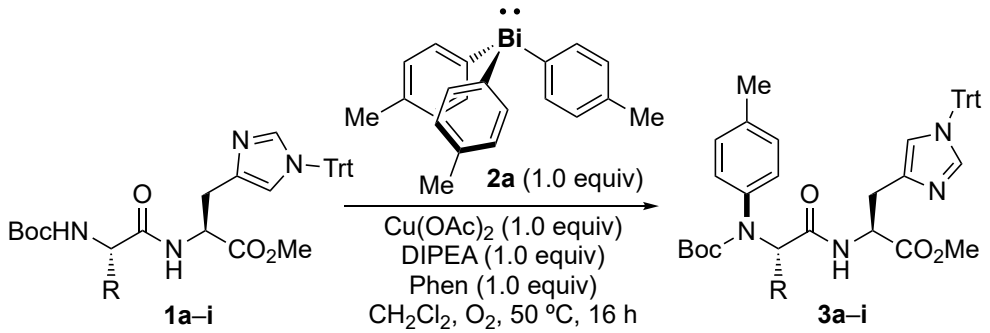

Methyl N^{α}-(*N*-(*tert*-butoxycarbonyl)-*N*-(*p*-tolyl)-*L*-alanyl)-N^{τ}-trityl-*L*-histidinate (3a)

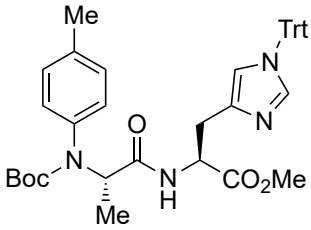

3a

This compound has been previously reported [1]: **Mp** 64 – 66 °C; **R_f** = 0.47 (DCM–MeOH, 95:5).

IR (ATR)/$\bar{\nu}$: 3288, 2972, 2928, 1746, 1687, 1514, 1494, 1445, 1366, 1323, 1159, 1132, 748, 701, 660, 637 cm^{-1}.

^{1}H-NMR (300 MHz, $CDCl_3$) δ 8.07 (s, 1H), 7.38 – 7.28 (m, 10H), 7.17 (d, *J* = 8.1 Hz, 2H), 7.12 – 7.00 (m, 8H), 6.58 (s, 1H), 4.85 – 4.75 (m, 1H), 4.67 – 4.57 (m, 1H), 3.60 (s, 3H), 3.12 (dd, *J* = 14.6, 5.1 Hz, 1H), 3.00 (dd, *J* = 14.6, 4.8 Hz, 1H), 2.29 (s, 3H), 1.36 (s, 9H), 1.30 (d, *J* = 7.1 Hz, 3H).

Methyl N^{α}-(*N*-(*tert*-butoxycarbonyl)-*N*-(*p*-tolyl)-*L*-leucyl)-N^{τ}-trityl-*L*-histidinate (3b)

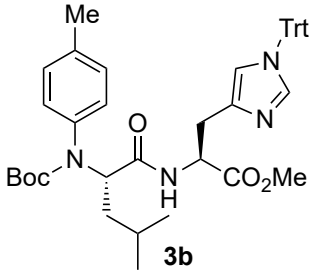

3b

The general procedure was followed starting from Boc–Leu–His(Trt)–OMe **1b** (65 mg, 0.10 mmol), tritolylbismuth **2a** (50 mg, 0.10 mmol), copper(II) acetate (19 mg, 0.10 mmol), phenanthroline (19 mg, 0.1 mmol) and DiPEA (18 µL, 0.1 mmol) in CH_2Cl_2 (1 mL). The resulting crude product was purified on silica gel (DCM–MeOH, gradient from 100:0 to 98:2) to afford **3b** as a white solid (41 mg, 55%). **Mp** 45 – 47 °C; **R_f** = 0.55 (DCM–MeOH, 95:5).

IR (ATR)/$\bar{\nu}$: 3319, 2953, 1747, 1687, 1513, 1493, 1445, 1366, 1321, 1238, 1163, 1132, 1036, 1002, 826, 747, 701, 660, 638 cm^{-1}.

^{1}H-NMR (600 MHz, $CDCl_3$) δ 7.96 (s(br), 1H), 7.24 – 7.17 (m, 10H), 7.04 – 6.95 (m, 8H), 6.92 (d, *J* = 8.1 Hz, 2H), 6.49 (s, 1H), 4.70 (q, *J* = 5.8 Hz, 1H), 4.53 (s(br), 1H), 3.51 (s, 3H), 3.01 (dd, *J*

= 14.7, 5.2 Hz, 1H), 2.90 (dd, *J* = 14.6, 5.0 Hz, 1H), 2.18 (s, 3H), 1.61 – 1.52 (m, 2H), 1.51 – 1.44 (m, 1H), 1.27 (s(br), 9H), 0.74 (d, *J* = 3.4 Hz, 3H), 0.73 (d, *J* = 3.5 Hz, 3H).

^{13}C-NMR (150 MHz, $CDCl_3$) δ 172.1, 171.9, 155.2, 142.4, 138.8, 136.5, 136.2, 129.9, 129.8, 129.2, 128.5, 128.1, 128.1, 119.4, 80.8, 75.4, 53.0, 52.2, 38.1, 30.0, 28.4, 24.9, 23.1, 22.1, 21.1.

HRMS–ESI: *m/z* $[M + H]^+$ calcd. for $C_{44}H_{50}N_4O_5$: 715.3854, found 715.3852.

Methyl *N*$^{\alpha}$-(*N*-(*tert*-butoxycarbonyl)-*N*-(*p*-tolyl)-*L*-phenylalanyl)-*N*$^{\tau}$-trityl-*L*-histidinate (3c)

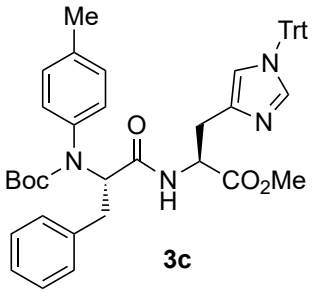

3c

The general procedure was followed starting from Boc–Phe–His(Trt)–OMe **1c** (62 mg, 94 µmol), tritolylbismuth **2a** (45 mg, 94 µmol), copper(II) acetate (17 mg, 94 µmol), phenanthroline (17 mg, 94 µmol) and DiPEA (16 µL, 94 µmol) in CH_2Cl_2 (1 mL). The resulting crude product was purified on silica gel (DCM–MeOH, gradient from 100:0 to 98:2) to afford **3c** as a white solid (35 mg, 50%). **Mp** 70 – 72 °C; **R_f** = 0.42 (Hexane–EtOAc, 50:50).

IR (ATR)/$\tilde{\nu}$: 3304, 2912, 1746, 1685, 1513, 1494, 1445, 1366, 1321, 1302, 1239, 1158, 1133, 1034, 828, 747, 700, 660 cm^{-1}.

^{1}H-NMR (600 MHz, $CDCl_3$) δ 8.26 (s, 1H), 7.37 – 7.25 (m, 9H), 7.24 – 7.19 (m, 3H), 7.19 – 7.15 (m, 1H), 7.12 (d, *J* = 7.4 Hz, 2H), 7.10 – 7.02 (m, 6H), 6.81 (d, *J* = 7.9 Hz, 2H), 6.69 – 6.46 (m, 3H), 4.85 – 4.79 (m, 1H), 4.63 – 4.55 (m, 1H), 3.59 (s, 3H), 3.34 – 3.14 (m, 2H), 3.10 (dd, *J* = 14.7, 5.1 Hz, 1H), 3.04 – 2.97 (m, 1H), 2.19 (s, 3H), 1.33 (s(br), 9H).

^{13}C-NMR (150 MHz, $CDCl_3$) δ 171.9, 171.3, 154.9, 142.5, 139.5, 138.8, 138.6, 136.5, 136.0, 129.9, 129.5, 129.0, 128.4, 128.1, 127.6, 126.5, 119.5, 80.9, 75.4, 65.6, 53.1, 52.2, 35.1, 30.0, 28.4, 21.0.

HRMS–ESI: *m/z* $[M + H]^+$ calcd. for $C_{47}H_{48}N_4O_5$: 749.3698, found 749.3706.

Methyl *N*$^{\alpha}$-(*N*-(*tert*-butoxycarbonyl)-*N*-(*p*-tolyl)glycyl)-*N*$^{\tau}$-trityl-*L*-histidinate (3d)

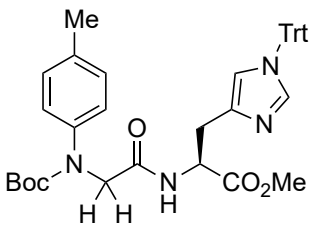

3d

The general procedure was followed starting from Boc–Gly–His(Trt)–OMe **1d** (60 mg, 0.11 mmol), tritolylbismuth **2a** (51 mg, 0.11 mmol), copper(II) acetate (19 mg, 0.11 mmol), phenanthroline (19 mg, 0.11 mmol) and DiPEA (18 µL, 0.11 mmol) in CH_2Cl_2 (1 mL). The resulting crude product was purified on silica gel (DCM–MeOH,

gradient from 100:0 to 98:2) to afford **3d** as a white solid (52 mg, 75%). **Mp** 57 – 59 °C; $\mathbf{R_f}$ = 0.35 (DCM–MeOH, 95:5).

IR (ATR)/$\bar{\nu}$: 3304, 2912, 1747, 1690, 1514, 1493, 1444, 1366, 1234, 1152, 1034, 1017, 824, 748, 701, 660, 638 cm^{-1}.

^{1}H-NMR (300 MHz, $CDCl_3$) δ 8.19 (s, 1H), 7.38 – 7.28 (m, 10H), 7.27 (s, 1H), 7.25 (s, 1H), 7.12 – 7.00 (m, 8H), 6.53 (s, 1H), 4.87 – 4.77 (m, 1H), 4.33 – 4.17 (m, 2H), 3.58 (s, 3H), 3.08 (dd, *J* = 14.6, 4.5 Hz, 1H), 2.95 (dd, *J* = 14.5, 4.4 Hz, 1H), 2.27 (s, 3H), 1.40 (s, 9H).

^{13}C-NMR (75 MHz, $CDCl_3$) δ 171.6, 169.4, 154.7, 142.4, 140.4, 138.8, 136.6, 135.8, 129.9, 129.4, 128.1, 126.3, 119.6, 81.1, 75.4, 54.4, 52.6, 52.1, 29.7, 28.3, 21.1.

HRMS–ESI: *m/z* $[M + H]^+$ calcd. for $C_{40}H_{42}N_4O_5$: 659.3228, found 659.3232.

Methyl N^{α}-(*N*-(*tert*-butoxycarbonyl)-*N*-(*p*-tolyl)-*L*-methionyl)-N^{τ}-trityl-*L*-histidinate (3e)

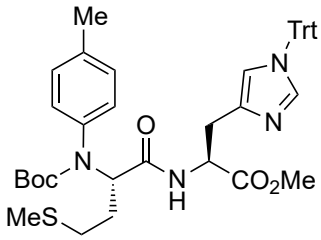

3e

The general procedure was followed starting from Boc–Met–His(Trt)–OMe **1e** (100 mg, 0.16 mmol), tritolylbismuth **2a** (75 mg, 0.16 mmol), copper(II) acetate (28 mg, 0.16 mmol), phenanthroline (28 mg, 0.16 mmol) and DiPEA (27 µL, 0.16 mmol) in CH_2Cl_2 (1.6 mL). The resulting crude product was purified on silica gel (Hexane–EtOAc, gradient from 100:0 to 60:40) to afford **3e** as a yellow solid (70 mg, 61%). **Mp** 51 – 53 °C; $\mathbf{R_f}$ = 0.70 (Hexane–EtOAc, 50:50).

IR (ATR)/$\bar{\nu}$: 3308, 2919, 1746, 1687, 1513, 1493, 1445, 1366, 1322, 1302, 1158, 1132, 1035, 828, 748, 700, 659, 638 cm^{-1}.

^{1}H-NMR (600 MHz, $CDCl_3$) δ 8.14 (s, 1H), 7.34 – 7.27 (m, 10H), 7.20 – 7.13 (m, 2H), 7.11 – 7.06 (m, 6H), 7.02 (d, *J* = 8.1 Hz, 2H), 6.58 (s, 1H), 4.79 (dt, *J* = 7.1, 5.2 Hz, 1H), 4.71 (t, *J* = 6.4 Hz, 1H), 3.60 (s, 3H), 3.11 (dd, *J* = 14.5, 5.5 Hz, 1H), 2.99 (dd, *J* = 14.6, 4.9 Hz, 1H), 2.52 (t, *J* = 7.2 Hz, 2H), 2.28 (s, 3H), 2.19 (s(br), 1H), 1.98 (s, 3H), 1.96 – 1.88 (m, 1H), 1.36 (s(br), 9H).

^{13}C-NMR (150 MHz, $CDCl_3$) δ 171.8, 171.4, 155.0, 142.3, 138.8, 138.0, 136.4, 135.0, 129.8, 129.3, 128.1, 128.0, 119.5, 81.1, 75.4, 61.0, 53.0, 52.1, 31.1, 29.8, 29.2, 28.4, 21.1, 15.3.

HRMS–ESI: *m/z* $[M + H]^+$ calcd. for $C_{43}H_{48}N_4O_5S$: 733.3418, found 733.3429.

Methyl N^{α}-(*N*-(*tert*-butoxycarbonyl)-*N*-(*p*-tolyl)-*L*-valyl)-N^{τ}-trityl-*L*-histidinate (3f)

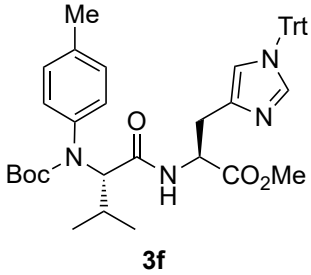

3f

The general procedure was followed starting from Boc–Val–His(Trt)–OMe **1f** (60 mg, 98 µmol), tritolylbismuth **2a** (47 mg, 98 µmol), copper(II) acetate (18 mg, 98 µmol), phenanthroline (18 mg, 98 µmol) and DiPEA (17 µL, 98 µmol) in CH_2Cl_2 (1 mL). The resulting crude product was purified on silica gel (Hexane–EtOAc, gradient from 100:0 to 60:40) to afford **3f** as a white solid (9 mg, 13%). **Mp** 67 – 69 °C; $\mathbf{R_f}$ = 0.48 (Hexane–EtOAc, 30:70).

IR (ATR)/$\bar{\nu}$: 3298, 2967, 2927, 1747, 1686, 1513, 1493, 1445, 1366, 1325, 1303, 1242, 1167, 1088, 1035, 1001, 870, 827, 748, 701, 660, 638 cm^{-1}.

^{1}H-NMR (300 MHz, $CDCl_3$) δ 8.12 (s(br), 1H), 7.38 – 7.28 (m, 10H), 7.17 – 7.10 (m, 6H), 7.10 – 7.01 (m, 4H), 6.63 (s, 1H), 4.83 – 4.75 (m, 1H), 3.86 – 3.70 (m, 1H), 3.64 (s, 3H), 3.62 – 3.57 (m, 1H), 3.11 (dd, *J* = 14.5, 5.7 Hz, 1H), 2.99 (dd, *J* = 15.5, 6.2 Hz, 1H), 2.29 (s, 3H), 1.33 (s, 9H), 1.00 (d, *J* = 6.6 Hz, 3H), 0.85 (d, *J* = 6.7 Hz, 3H).

HRMS–ESI: *m/z* $[M + H]^+$ calcd. for $C_{43}H_{48}N_4O_5$: 701.3698, found 701.3700.

Methyl N^{α}-(N^6-(((9*H*-fluoren-9-yl)methoxy)carbonyl)-N^2-(*tert*-butoxycarbonyl)-N^2-(*p*-tolyl)-*L*-lysyl)-N^{τ}-trityl-*L*-histidinate (3g)

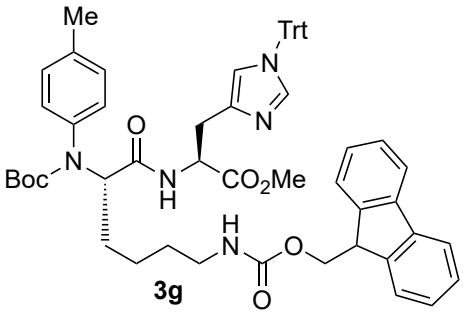

3g

The general procedure was followed starting from Boc–Lys–His(Trt)–OMe **1g** (50 mg, 58 µmol), tritolylbismuth **2a** (28 mg, 58 µmol), copper(II) acetate (11 mg, 58 µmol), phenanthroline (11 mg, 58 µmol) and DiPEA (10 µL, 58 µmol) in CH_2Cl_2 (0.6 mL). The resulting crude product was purified on silica gel (Hexane–EtOAc, gradient from 100:0 to 60:40) to afford **3g** as an white solid (12 mg, 22%). **Mp** 67 – 69 °C; $\mathbf{R_f}$ = 0.78 (Hexane–EtOAc, 30:70).

IR (ATR)/$\bar{\nu}$: 3269, 2924, 2853, 1687, 1513, 1447, 1366, 1325, 1244, 1162, 1133, 1001, 829, 758, 742, 701, 661, 638 cm^{-1}.

^{1}H-NMR (600 MHz, $CDCl_3$) δ 8.05 – 8.00 (m, 1H), 7.69 (d, *J* = 7.5 Hz, 2H), 7.51 (d, *J* = 7.6 Hz, 2H), 7.31 (t, *J* = 7.4 Hz, 2H), 7.27 – 7.21 (m, 12H), 7.04 (s(br), 2H), 7.03 – 6.99 (m, 6H), 6.94 (d, *J* = 8.3 Hz, 2H), 6.51 (s, 1H), 4.84 (s(br), 1H), 4.73 (dt, *J* = 7.4, 5.2 Hz, 1H), 4.61 (s, 2H), 4.45

(s(br), 1H), 4.32 – 4.26 (m, 2H), 4.12 (t, *J* = 7.1 Hz, 1H), 3.52 (s, 3H), 3.08 – 3.00 (m, 3H), 2.93 (dd, *J* = 14.4, 5.0 Hz, 1H), 2.20 (s, 3H), 1.41 – 1.32 (m, 4H), 1.18 (s, 9H).

HRMS–ESI: *m/z* $[M + H]^+$ calcd. for $C_{59}H_{61}N_5O_7$: 952.4644, found 952.4643.

Methyl N^{α}-(*N*-(*tert*-butoxycarbonyl)-*N*,*O*-di-*p*-tolyl-*L*-seryl)-N^{τ}-trityl-*L*-histidinate (3h)

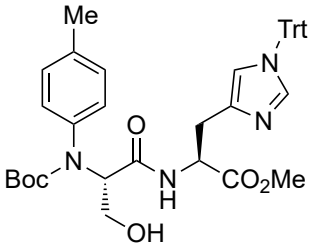

3h

The general procedure was followed starting from Boc–Ser–His(Trt)–OMe **1h** (52 mg, 87 µmol), tritolylbismuth **2a** (42 mg, 87 µmol), copper(II) acetate (16 mg, 87 µmol), phenanthroline (16 mg, 87 µmol) and DiPEA (15 µL, 87 µmol) in CH_2Cl_2 (1 mL). The resulting crude product was purified on silica gel (Hexane–EtOAc, gradient from 100:0 to 60:40) to afford **3h** as a white solid (33 mg, 49%). **Mp** 65 – 67 °C; $\mathbf{R_f}$ = 0.78 (Hexane–EtOAc, 50:50).

IR (ATR)/$\bar{\nu}$: 3304, 2919, 1747, 1688, 1510, 1445, 1366, 1324, 1239, 1205, 1156, 1133, 1036, 817, 747, 700, 660, 638 cm^{-1}.

^{1}H-NMR (300 MHz, $CDCl_3$) δ 8.36 (s(br), 1H), 7.38 – 7.26 (m, 12H), 7.13 – 7.05 (m, 6H), 7.02 (d, *J* = 7.5 Hz, 4H), 6.79 (d, *J* = 8.5 Hz, 2H), 6.58 (s, 1H), 4.84 (dt, *J* = 7.3, 4.9 Hz, 2H), 4.59 – 4.44 (m, 1H), 4.26 (t, *J* = 9.5 Hz, 1H), 3.59 (s, 3H), 3.14 (dd, *J* = 14.7, 5.1 Hz, 1H), 3.01 (dd, *J* = 14.7, 4.8 Hz, 1H), 2.28 (s, 3H), 2.26 (s, 3H), 1.36 (s(br), 9H).

^{13}C-NMR (75 MHz, $CDCl_3$) δ 171.7, 169.6, 156.3, 142.4, 138.8, 136.5, 130.3, 129.9, 129.9, 129.4, 128.3, 128.2, 119.5, 114.8, 81.0, 75.4, 66.0, 52.9, 52.2, 29.8, 29.7, 28.4, 21.1, 20.6.

HRMS–ESI: *m/z* $[M + H]^+$ calcd. for $C_{48}H_{50}N_4O_6$: 779.3803, found 779.3811.

Methyl N^{α}-(*N*-(*tert*-butoxycarbonyl)-*O*-(*p*-tolyl)-*L*-threonyl)-N^{τ}-trityl-*L*-histidinate (3i)

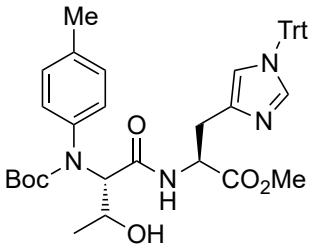

3i

The general procedure was followed starting from Boc–Thr–His(Trt)–OMe **1i** (60 mg, 98 µmol), tritolylbismuth **2a** (47 mg, 98 µmol), copper(II) acetate (18 mg, 98 µmol), phenanthroline (18 mg, 98 µmol) and DiPEA (17 µL, 98 µmol) in CH_2Cl_2 (1 mL). The resulting crude product was purified on silica gel (Hexane–EtOAc, gradient from 100:0 to 60:40) to afford **3i** as a white solid (30 mg, 44%). **Mp** 66 – 68 °C; $\mathbf{R_f}$ = 0.79 (Hexane–EtOAc, 30:70).

IR (ATR)/$\bar{\nu}$: 3354, 2973, 2919, 1746, 1715, 1675, 1508, 1492, 1445, 1366, 1229, 1166, 1132, 1034, 749, 702, 661 cm^{-1}.

^{1}H-NMR (600 MHz, $CDCl_3$) δ 7.89 (d, *J* = 7.6 Hz, 1H), 7.37 – 7.27 (m, 10H), 7.09 – 7.03 (m, 6H), 6.93 (d, *J* = 8.3 Hz, 2H), 6.83 (d, *J* = 8.2 Hz, 2H), 6.48 (s, 1H), 5.67 (d, *J* = 6.5 Hz, 1H), 4.92 – 4.84 (m, 1H), 4.83 – 4.77 (m, 1H), 4.41 (dd, *J* = 7.3, 2.3 Hz, 1H), 3.61 (s, 3H), 3.08 (dd, *J* = 14.6, 4.7 Hz, 1H), 2.94 (dd, *J* = 14.5, 4.2 Hz, 1H), 2.22 (s, 3H), 1.44 (s, 9H), 1.24 (d, *J* = 6.3 Hz, 3H).
^{13}C-NMR (150 MHz, $CDCl_3$) δ 171.6, 169.4, 155.7, 154.9, 142.4, 138.7, 136.2, 130.9, 130.0, 129.9, 129.9, 128.2, 119.8, 116.9, 80.0, 75.4, 74.0, 57.6, 52.7, 52.2, 30.2, 28.5, 20.6, 15.1.
HRMS–ESI: *m/z* $[M + H]^+$ calcd. for $C_{42}H_{46}N_4O_6$: 703.3490, found 703.3516.

b. Arylated compounds (5aa –an) from tripeptides (4a) using triarylbismuth (2)

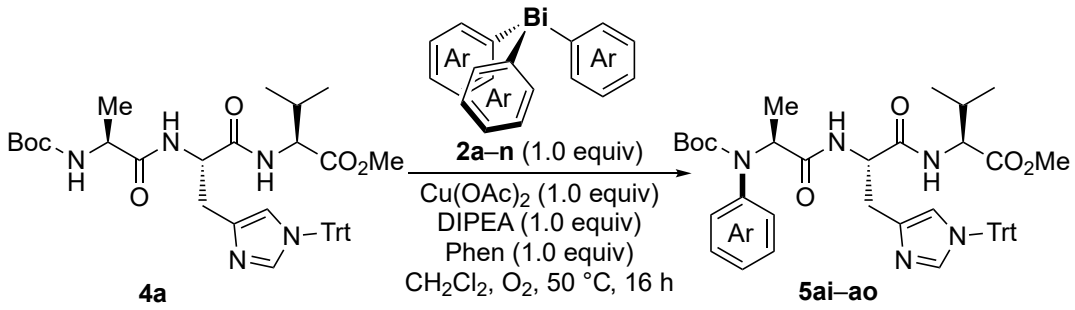

Methyl N^{α}-(*N*-(*tert*-butoxycarbonyl)-*N*-(*p*-tolyl)-*L*-alanyl)-N^{τ}-trityl-*L*-histidyl-*L*-valinate (5aa)

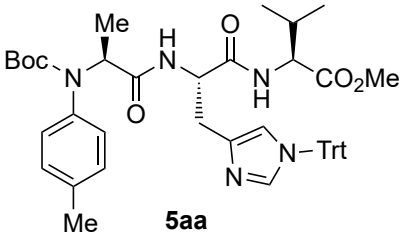

This compound has been previously reported[1]: **Mp** 134 – 136 °C; **R_f** = 0.46 (DCM–MeOH, 95:5)
IR (ATR)/$\bar{\nu}$: 3155, 2970, 1740, 1668, 1514, 1495, 1447, 1367, 1155, 1129, 1019, 1001, 839, 747, 701, 662, 640 cm^{-1}.
^{1}H-NMR (300 MHz, $CDCl_3$) δ 8.35 (d, *J* = 7.2 Hz, 1H), 8.08 (s, 1H), 7.74 (d, *J* = 5.9 Hz, 1H), 7.41 – 7.31 (m, 10H), 7.10 (dd, *J* = 5.9, 1.7 Hz, 8H), 7.04 (d, *J* = 8.2 Hz, 1H), 6.87 (s, 1H), 5.27 – 5.11 (m, 1H), 4.50 – 4.29 (m, 2H), 3.67 (s, 3H), 3.54 (d, *J* = 15.1 Hz, 1H), 2.96 – 2.81 (m, 1H), 2.27 (s, 3H), 2.26 – 2.20 (m, 1H), 1.31 (d, *J* = 6.6 Hz, 3H), 1.22 (s, 9H), 1.02 (dd, *J* = 15.7, 6.8 Hz, 6H).

Methyl N^{α}-(*N*-(*tert*-butoxycarbonyl)-*N*-(*m*-tolyl)-*L*-alanyl)-N^{τ}-trityl-*L*-histidyl-*L*-valinate (5ab)

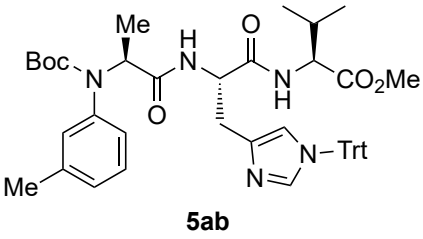

5ab

The general procedure was followed starting from Boc–Ala–His(Trt)–Val–OMe **4a** (50 mg, 73 µmol), tri-*m*-tolylbismuthane **2b** (35 mg, 73 µmol), copper(II) acetate (13 mg, 73 µmol), phenanthroline (13 mg, 73 µmol) and DiPEA (13 µL, 73 µmol) in CH_2Cl_2 (1 mL). The resulting crude product was purified on silica gel (DCM–MeOH, gradient from 100:0 to 98:2) to afford **5ab** as a white solid (35 mg, 61%). **Mp** 75 – 77 °C; $\mathbf{R_f}$ = 0.39 (DCM–MeOH, 95:5).

IR (ATR)/$\bar{\nu}$: 3315, 2972, 2923, 1741, 1674, 1491, 1445, 1367, 1317, 1253, 1202, 1154, 1088, 1036, 1001, 841, 748, 701, 660, 637 cm^{-1}.

^{1}H-NMR (600 MHz, $CDCl_3$) δ 8.64 (d, *J* = 4.6 Hz, 1H), 7.71 (d, *J* = 7.9 Hz, 1H), 7.34 – 7.28 (m, 10H), 7.19 – 7.14 (m, 2H), 7.12 – 7.07 (m, 7H), 7.02 (d, *J* = 7.5 Hz, 1H), 6.70 (s, 1H), 4.88 – 4.81 (m, 1H), 4.54 – 4.47 (m, 1H), 4.41 (dd, *J* = 7.9, 5.6 Hz, 1H), 3.64 (s, 3H), 3.25 – 3.17 (m, 1H), 2.92 (dd, *J* = 14.5, 5.4 Hz, 1H), 2.27 (s, 3H), 2.16 – 2.09 (m, 1H), 1.41 (d, *J* = 6.9 Hz, 3H), 1.34 (s, 9H), 0.83 (d, *J* = 6.8 Hz, 6H).

^{13}C-NMR (150 MHz, $CDCl_3$) δ 172.1, 172.1, 171.4, 154.7, 142.4, 141.3, 138.6, 138.2, 137.2, 129.9, 129.0, 128.6, 128.2, 128.2, 127.6, 125.2, 119.6, 80.9, 75.5, 57.7, 53.3, 52.0, 31.0, 29.6, 28.4, 21.4, 19.2, 18.1, 15.7.

HRMS–ESI: *m/z* $[M + H]^+$ calcd. for $C_{46}H_{53}N_5O_6$: 772.4069, found 772.4063.

Methyl N^{α}-(*N*-(*tert*-butoxycarbonyl)-*N*-phenyl-*L*-alanyl)-N^{τ}-trityl-*L*-histidyl-*L*-valinate (5ad)

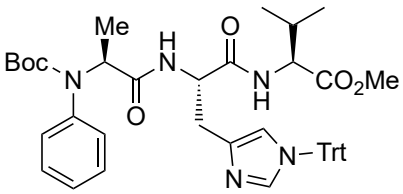

5ad

The general procedure was followed starting from Boc–Ala–His(Trt)–Val–OMe **4a** (70 mg, 0.10 mmol), triphenylbismuthane **2d** (45 mg, 0.10 mmol), copper(II) acetate (19 mg, 0.10 mmol), phenanthroline (18 mg, 0.10 mmol) and DiPEA (18 µL, 0.10 mmol) in CH_2Cl_2 (1 mL). The resulting crude product was purified on silica gel (DCM–MeOH, gradient from 100:0 to 98:2) to afford **5ad** as a white solid (38 mg, 49%). **Mp** 76 – 78 °C; $\mathbf{R_f}$ = 0.50 (DCM–MeOH, 95:5).

IR (ATR)/$\bar{\nu}$: 3315, 2972, 1741, 1674, 1494, 1446, 1368, 1310, 1256, 1156, 1002, 838, 749, 701, 660, 637 cm^{-1}.

^{1}H-NMR (300 MHz, $CDCl_3$) δ 8.56 (d, *J* = 6.6 Hz, 1H), 7.67 (d, *J* = 8.3 Hz, 1H), 7.35 – 7.27 (m, 14H), 7.25 – 7.18 (m, 1H), 7.12 – 7.05 (m, 6H), 6.71 (s, 1H), 4.81 (q, *J* = 5.6 Hz, 1H), 4.56 (q, *J* =

7.1 Hz, 1H), 4.39 (dd, *J* = 8.3, 5.4 Hz, 1H), 3.64 (s, 3H), 3.22 – 3.17 (m, 1H), 2.93 (dd, *J* = 14.5, 6.0 Hz, 1H), 2.18 – 2.06 (m, 1H), 1.36 (d, *J* = 7.1 Hz, 3H), 1.32 (s, 9H), 0.84 (d, *J* = 6.8 Hz, 6H).

Presence of conformers: **^{13}C-NMR (150 MHz, $CDCl_3$)** δ 172.2, 172.1, 171.4, 154.9, 142.3, 141.0, 138.2, 136.9, 129.9, 128.8, 128.5, 128.2, 128.2, 127.0, 119.8, 81.0, 75.6, 57.8, 55.5, 53.4, 52.1, 47.3, 43.5, 30.9, 29.6, 28.4, 19.8, 18.1.

HRMS–ESI: *m/z* $[M + H]^+$ calcd. for $C_{45}H_{51}N_5O_6$: 758.3912, found 758.3909.

Methyl *N*$^{\alpha}$-(*N*-(tert-butoxycarbonyl)-*N*-(4-methoxyphenyl)-*L*-alanyl)-*N*$^{\tau}$-trityl-*L*-histidyl-*L*-valinate (5ae)

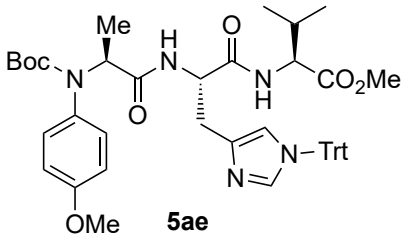

5ae

The general procedure was followed starting from Boc–Ala–His(Trt)–Val–OMe **4a** (60 mg, 88 µmol), tris(4-methoxyphenyl)bismuthane **2e** (47 mg, 88 µmol), copper(II) acetate (16 mg, 88 µmol), phenanthroline (16 mg, 88 µmol) and DiPEA (15 µL, 88 µmol) in CH_2Cl_2 (1 mL). The resulting crude product was purified on silica gel (DCM–MeOH, gradient from 100:0 to 98:2) to afford **5ae** as a white solid (35 mg, 50%). **Mp** 89 – 91 °C; **R_f** = 0.46 (Hexane–EtOAc, 20:80).

IR (ATR)/$\bar{\nu}$: 3315, 2972, 2928, 1741, 1673, 1511, 1445, 1366, 1321, 1294, 1244, 1205, 1155, 1033, 1001, 839, 748, 701, 660 cm^{-1}.

^{1}H-NMR (600 MHz, $CDCl_3$) δ 8.49 (d, *J* = 6.1 Hz, 1H), 7.68 (d, *J* = 7.2 Hz, 1H), 7.35 – 7.27 (m, 10H), 7.23 – 7.14 (m, 2H), 7.13 – 7.05 (m, 6H), 6.79 (d, *J* = 8.8 Hz, 2H), 6.70 (s, 1H), 4.85 – 4.77 (m, 1H), 4.58 (s(br), 1H), 4.40 (dd, *J* = 8.2, 5.5 Hz, 1H), 3.76 (s, 3H), 3.64 (s, 3H), 3.18 (dd, *J* = 14.9, 4.3 Hz, 1H), 2.92 (dd, *J* = 14.9, 6.4 Hz, 1H), 2.15 – 2.09 (m, 1H), 1.31 (s(br), 12H), 0.84 (d, *J* = 6.8 Hz, 6H).

^{13}C-NMR (150 MHz, $CDCl_3$) δ 172.4, 172.1, 171.4, 158.3, 155.3, 142.4, 138.3, 137.1, 129.9, 129.8, 128.2, 128.2, 119.7, 113.9, 80.8, 75.5, 57.8, 55.5, 53.4, 52.1, 30.9, 29.6, 28.4, 19.2, 18.1, 15.8, 14.3.

HRMS–ESI: *m/z* $[M + H]^+$ calcd. for $C_{46}H_{53}N_5O_7$: 788.4018, found 788.4020.

Methyl N^{α}-(*N*-(tert-butoxycarbonyl)-*N*-(4-fluorophenyl)-*L*-alanyl)-N^{τ}-trityl-*L*-histidyl-*L*-valinate (5af)

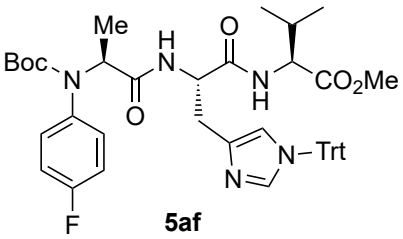

5af

The general procedure was followed starting from Boc–Ala–His(Trt)–Val–OMe **4a** (50 mg, 73 µmol), tris(4-fluorophenyl)bismuthane **2f** (36 mg, 73 µmol), copper(II) acetate (13 mg, 73 µmol), phenanthroline (13 mg, 73 µmol) and DiPEA (13 µL, 73 µmol) in CH_2Cl_2 (1 mL). The resulting crude product was purified on silica gel (DCM–MeOH, gradient from 100:0 to 98:2) to afford **5af** as a white solid (33 mg, 58%). **Mp** 81 – 83 °C; $\mathbf{R_f}$ = 0.65 (Hexane–EtOAc, 30:70).

IR (ATR)/$\bar{\nu}$: 3301, 2959, 2914, 1741, 1682, 1508, 1445, 1367, 1318, 1215, 1152, 1036, 1001, 843, 748, 701, 660 cm^{-1}.

^{1}H-NMR (600 MHz, $CDCl_3$) δ 8.47 (s, 1H), 7.69 (d, *J* = 6.7 Hz, 1H), 7.37 – 7.23 (m, 12H), 7.16 – 7.04 (m, 6H), 6.96 (t, *J* = 8.6 Hz, 2H), 6.71 (s, 1H), 4.81 (q, *J* = 5.7 Hz, 1H), 4.64 – 4.53 (m, 1H), 4.41 (dd, *J* = 7.9, 5.5 Hz, 1H), 3.65 (s, 3H), 3.18 (dd, *J* = 14.8, 3.2 Hz, 1H), 2.93 (dd, *J* = 14.4, 5.5 Hz, 1H), 2.17 – 2.08 (m, 1H), 1.32 (s(br), 12H), 0.84 (d, *J* = 6.8 Hz, 6H).

^{13}C-NMR (150 MHz, $CDCl_3$) δ 172.1, 171.29, 161.41 (d, *J* = 244.7 Hz), 154.89, 142.33, 138.18, 136.94, 136.70, 130.52 (d, *J* = 8.4 Hz), 129.87, 128.25, 128.20, 119.78, 115.5 (d, *J* = 22.4 Hz), 81.11, 75.62, 57.77, 53.39, 52.05, 30.94, 29.61, 28.34, 19.16, 18.09, 15.89.

^{19}F NMR (564 MHz, $CDCl_3$) δ -115.24.

HRMS–ESI: *m/z* $[M + H]^+$ calcd. for $C_{45}H_{50}FN_5O_6$: 776.3818, found 776.3818.

Methyl N^{α}-(*N*-(tert-butoxycarbonyl)-*N*-(4-(trifluoromethyl)phenyl)-*L*-alanyl)-N^{τ}-trityl-*L*-histidyl-*L*-valinate (5ag)

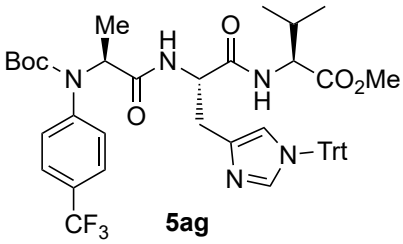

5ag

The general procedure was followed starting from Boc–Ala–His(Trt)–Val–OMe **4a** (43 mg, 63 µmol), tris(4-(trifluoromethyl)phenyl)bismuthane **2g** (41 mg, 63 µmol), copper(II) acetate (12 mg, 63 µmol), phenanthroline (11 mg, 63 µmol) and DiPEA (11 µL, 63 µmol) in CH_2Cl_2 (700 µL). The resulting crude product was purified on silica gel (DCM–MeOH, gradient from 100:0 to 98:2) to afford **5ag** as a white solid (11 mg, 21%). **Mp** 82 – 84 °C; $\mathbf{R_f}$ = 0.46 (DCM–MeOH, 95:5).

IR (ATR)/$\bar{\nu}$: 3315, 2963, 2928, 1743, 1689, 1519, 1494, 1446, 1369, 1324, 1254, 1162, 1123, 1068, 1018, 1002, 854, 748, 701, 660 cm^{-1}.

^{1}H-NMR (600 MHz, $CDCl_3$) δ 8.52 (d, *J* = 5.2 Hz, 1H), 7.70 (d, *J* = 7.5 Hz, 1H), 7.54 (d, *J* = 8.4 Hz, 2H), 7.45 (d, *J* = 8.3 Hz, 2H), 7.37 – 7.29 (m, 10H), 7.12 – 7.06 (m, 6H), 6.71 (s, 1H), 4.83 (q, *J* = 5.6 Hz, 1H), 4.62 (q, *J* = 7.1 Hz, 1H), 4.41 (dd, *J* = 8.3, 5.3 Hz, 1H), 3.65 (s, 3H), 3.17 (dd, *J* = 15.0, 4.4 Hz, 1H), 2.98 – 2.89 (m, 1H), 2.16 – 2.09 (m, 1H), 1.39 (d, *J* = 7.1 Hz, 3H), 1.34 (s, 9H), 0.84 (d, *J* = 6.8 Hz, 6H).

^{13}C-NMR (150 MHz, $CDCl_3$) δ 172.1, 171.7, 171.2, 154.2, 144.3, 142.3, 138.1, 129.9, 128.8, 128.3, 128.2, 125.9 (q, *J* = 3.5 Hz), 124.1 (d, *J* = 270.6 Hz), 119.8, 81.7, 58.2, 57.8, 53.5, 52.1, 31.0, 29.7, 28.3, 19.2, 18.1, 15.9.

^{19}F NMR (282 MHz, $CDCl_3$) δ -62.40.

HRMS–ESI: *m/z* $[M + H]^+$ calcd. for $C_{46}H_{50}F_3N_5O_6$: 826.3786, found 826.3797.

Methyl N^{α}-(*N*-(tert-butoxycarbonyl)-*N*-(4-chlorophenyl)-*L*-alanyl)-N^{τ}-trityl-*L*-histidyl-*L*-valinate (5ai)

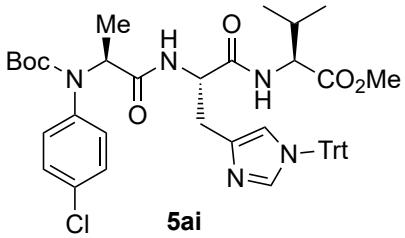

5ai

The general procedure was followed starting from Boc–Ala–His(Trt)–Val–OMe **4a** (50 mg, 73 µmol), tris(4-chlorophenyl)bismuthane **2i** (40 mg, 73 µmol), copper(II) acetate (13 mg, 73 µmol), phenanthroline (13 mg, 73 µmol) and DiPEA (13 µL, 73 µmol) in CH_2Cl_2 (740 µL). The resulting crude product was purified on silica gel (DCM–MeOH, gradient from 100:0 to 98:2) to afford **5ai** as a white solid (27 mg, 47%). **Mp** 74 – 76 °C; **R_f** = 0.68 (Hexane–EtOAc, 30:70).

IR (ATR)/$\bar{\nu}$: 3310, 2959, 2928, 1741, 1683, 1493, 1446, 1367, 1317, 1255, 1156, 1091, 1015, 840, 748, 701, 660 cm^{-1}.

^{1}H-NMR (600 MHz, $CDCl_3$) δ 8.46 (d, *J* = 5.5 Hz, 1H), 7.68 (d, *J* = 8.2 Hz, 1H), 7.42 – 7.27 (m, 10H), 7.25 (s, 4H), 7.10 – 7.04 (m, 6H), 6.71 (s, 1H), 4.81 (q, *J* = 5.9 Hz, 1H), 4.59 (q, *J* = 6.7 Hz, 1H), 4.41 (dd, *J* = 8.3, 5.3 Hz, 1H), 3.65 (s, 3H), 3.17 (dd, *J* = 15.0, 4.4 Hz, 1H), 2.94 (dd, *J* = 14.9, 5.9 Hz, 1H), 2.17 – 2.09 (m, 1H), 1.34 (d, *J* = 7.8 Hz, 3H), 1.33 (s, 9H), 0.84 (d, *J* = 6.8 Hz, 6H).

^{13}C-NMR (150 MHz, $CDCl_3$) δ 172.1, 172.0, 171.2, 154.6, 142.3, 139.4, 138.1, 136.8, 132.6, 130.1, 129.9, 128.9, 128.3, 128.2, 119.8, 81.3, 75.7, 57.8, 53.4, 52.1, 30.9, 29.5, 28.3, 19.2, 18.1, 15.9.

HRMS–ESI: *m/z* $[M + H]^+$ calcd. for $C_{45}H_{50}ClN_5O_6$: 792.3522, found 792.3516.

Methyl N^{α}-(*N*-(tert-butoxycarbonyl)-*N*-(4-bromophenyl)-*L*-alanyl)-N^{τ}-trityl-*L*-histidyl-*L*-valinate (5aj)

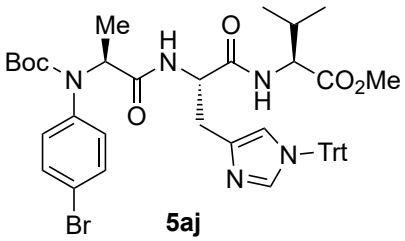

5aj

The general procedure was followed starting from Boc–Ala–His(Trt)–Val–OMe **4a** (50 mg, 73 µmol), tris(4-bromophenyl)bismuthane **2j** (50 mg, 73 µmol), copper(II) acetate (13 mg, 73 µmol), phenanthroline (13 mg, 73 µmol) and DiPEA (13 µL, 73 µmol) in CH_2Cl_2 (740 µL). The resulting crude product was purified on silica gel (DCM–MeOH, gradient from 100:0 to 98:2) to afford **5aj** as a white solid (29 mg, 48%). **Mp** 85 – 87 °C; $\mathbf{R_f}$ = 0.44 (DCM–MeOH, 95:5).

IR (ATR)/$\bar{\nu}$: 3319, 2963, 2919, 1742, 1683, 1489, 1445, 1367, 1318, 1254, 1156, 1070, 1012, 837, 748, 701, 661 cm^{-1}.

^{1}H-NMR (600 MHz, $CDCl_3$) δ 8.45 (d, *J* = 5.7 Hz, 1H), 7.64 (d, *J* = 8.0 Hz, 1H), 7.33 (d, *J* = 8.5 Hz, 2H), 7.28 – 7.22 (m, 10H), 7.12 (d, *J* = 8.3 Hz, 2H), 7.06 – 6.98 (m, 6H), 6.63 (s, 1H), 4.78 – 4.72 (m, 1H), 4.52 (q, *J* = 6.8 Hz, 1H), 4.34 (dd, *J* = 8.2, 5.4 Hz, 1H), 3.58 (s, 3H), 3.10 (dd, *J* = 14.8, 3.5 Hz, 1H), 2.91 – 2.80 (m, 1H), 2.14 – 1.99 (m, 1H), 1.26 (s, 12H), 0.77 (d, *J* = 6.8 Hz, 6H).

^{13}C-NMR (150 MHz, $CDCl_3$) δ 172.1, 171.9, 171.3, 154.5, 142.3, 140.0, 138.2, 137.1, 131.9, 130.4, 129.9, 128.2, 128.2, 120.6, 119.7, 81.3, 75.6, 57.7, 53.4, 52.1, 30.9, 29.6, 28.3, 19.2, 18.1, 15.8.

HRMS–ESI: *m/z* $[M + H]^+$ calcd. for $C_{45}H_{50}BrN_5O_6$: 836.3018, found 836.3026.

Methyl N^{α}-(*N*-(tert-butoxycarbonyl)-*N*-(4-(dimethoxymethyl)phenyl)-*L*-alanyl)-N^{τ}-trityl-*L*-histidyl-*L*-valinate (5ak)

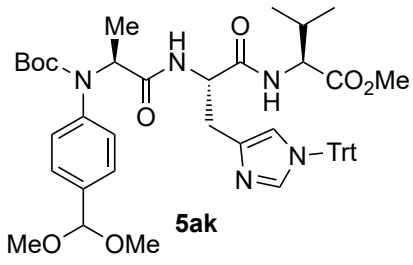

5ak

The general procedure was followed starting from Boc–Ala–His(Trt)–Val–OMe **4a** (50 mg, 73 µmol), tris(4-(dimethoxymethyl)phenyl)bismuthane **2k** (49 mg, 73 µmol), copper(II) acetate (13 mg, 73 µmol), phenanthroline (13 mg, 73 µmol) and DiPEA (13 µL, 73 µmol) in CH_2Cl_2 (740 µL). The resulting crude product was purified on basified silica gel (DCM–MeOH, gradient from 100:0 to 98:2) to afford **5ak** as a white solid (39 mg, 64%). **Mp** 64 – 66 °C; $\mathbf{R_f}$ = 0.29 (DCM–MeOH, 95:5).

IR (ATR)/$\bar{\nu}$: 3315, 2924, 2852, 1740, 1682, 1512, 1494, 1445, 1366, 1319, 1254, 1156, 1099, 1052, 1020, 984, 828, 748, 701, 660 cm^{-1}.

^{1}H-NMR (300 MHz, $CDCl_3$) δ 8.58 (d, *J* = 7.0 Hz, 1H), 7.76 (d, *J* = 8.5 Hz, 1H), 7.37 (d, *J* = 8.4 Hz, 2H), 7.34 – 7.27 (m, 12H), 7.15 – 7.02 (m, 6H), 6.69 (s, 1H), 5.37 (s, 1H), 4.82 (dt, *J* = 6.6, 4.4 Hz, 1H), 4.56 (q, *J* = 7.1 Hz, 1H), 4.41 (dd, *J* = 8.4, 5.4 Hz, 1H), 3.64 (s, 3H), 3.29 (s, 6H), 3.19 (dd, *J* = 15.0, 4.2 Hz, 1H), 2.90 (dd, *J* = 14.9, 6.2 Hz, 1H), 2.23 – 2.04 (m, 1H), 1.37 (d, *J* = 9.1 Hz, 3H), 1.32 (s, 9H), 0.83 (d, *J* = 6.8 Hz, 6H).

^{13}C-NMR (75 MHz, $CDCl_3$) δ 172.1, 172.0, 171.4, 154.7, 142.4, 141.2, 138.2, 137.2, 136.6, 129.9, 128.2, 128.2, 127.2, 119.6, 102.8, 81.1, 75.5, 57.8, 53.4, 52.7, 52.0, 45.9, 30.9, 29.8, 28.3, 19.2, 18.1, 15.7.

HRMS–ESI: *m/z* $[M + H]^+$ calcd. for $C_{48}H_{57}N_5O_8$: 832.4280, found 832.4291.

Methyl *N*$^\alpha$-(*N*-(tert-butoxycarbonyl)-*N*-(4-((tetrahydro-2*H*-pyran-2-yl)oxy)phenyl))-*L*-alanyl-*N*$^\tau$-trityl-*L*-histidyl-*L*-valinate (5al)

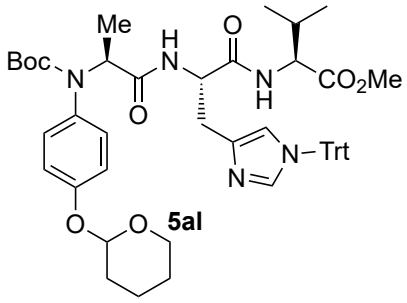

The general procedure was followed starting from Boc–Ala–His(Trt)–Val–OMe **4a** (50 mg, 73 µmol), tris(4-((tetrahydro-2*H*-pyran-2-yl)oxy)phenyl)bismuthane **2l** (54 mg, 73 µmol), copper(II) acetate (13 mg, 73 µmol), phenanthroline (13 mg, 73 µmol) and DiPEA (13 µL, 73 µmol) in CH_2Cl_2 (740 µL). The resulting crude product was purified on basified silica gel (DCM–MeOH, gradient from 100:0 to 98:2) to afford **5al** as a white solid (33 mg, 52%). **Mp** 69 – 71 °C; **R_f** = 0.31 (DCM–MeOH, 95:5).

IR (ATR)/$\tilde{\nu}$: 3310, 2929, 1740, 1681, 1509, 1445, 1367, 1321, 1233, 1202, 1156, 1112, 1075, 1035, 960, 920, 841, 748, 701, 660 cm^{-1}.

^{1}H-NMR (600 MHz, $CDCl_3$) δ 8.55 (d, *J* = 6.7 Hz, 1H), 7.79 – 7.71 (m, 1H), 7.35 – 7.28 (m, 10H), 7.22 – 7.13 (m, 2H), 7.12 – 7.05 (m, 6H), 6.94 (d, *J* = 8.8 Hz, 2H), 6.69 (s, 1H), 5.34 (q, *J* = 2.9 Hz, 1H), 4.84 – 4.77 (m, 1H), 4.57 (s(br), 1H), 4.41 (dd, *J* = 8.2, 5.5 Hz, 1H), 3.90 – 3.84 (m, 1H), 3.64 (s, 3H), 3.59 – 3.54 (m, 1H), 3.19 (dd, *J* = 15.0, 4.2 Hz, 1H), 2.90 (dd, *J* = 15.0, 6.5 Hz, 1H), 2.85 (q, *J* = 7.1 Hz, 1H), 2.16 – 2.09 (m, 1H), 2.02 – 1.95 (m, 1H), 1.89 – 1.79 (m, 2H), 1.70 – 1.62 (m, 1H), 1.60 – 1.55 (m, 1H), 1.32 (s(br), 12H), 0.83 (d, *J* = 6.8 Hz, 6H).

^{13}C-NMR (150 MHz, $CDCl_3$) δ 172.2, 172.2, 172.1, 171.4, 171.4, 155.9, 142.5, 138.3, 137.3, 129.9, 129.6, 128.1, 119.6, 116.5, 96.6, 80.8, 75.4, 62.2, 57.8, 53.4, 52.0, 45.9, 31.0, 30.5, 29.8, 29.6, 28.4, 25.3, 19.2, 18.9, 18.1, 15.7.

HRMS–ESI: *m/z* $[M + H]^+$ calcd. for $C_{50}H_{59}N_5O_8$: 858.4436, found 858.4443.

Methyl N^{α}-(*N*-(tert-butoxycarbonyl)-*N*-(3-formylphenyl))-*L*-alanyl-N^{τ}-trityl-*L*-histidyl-*L*-valinate (5am)

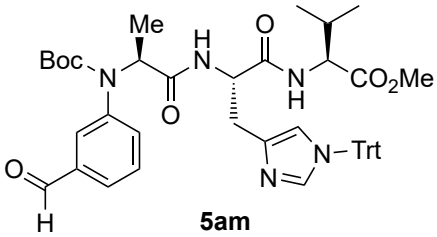

5am

The general procedure was followed starting from Boc–Ala–His(Trt)–Val–OMe **4a** (50 mg, 73 µmol), 3,3',3''-bismuthanetriyltribenzaldehyde **2m** (38 mg, 73 µmol), copper(II) acetate (13 mg, 73 µmol), phenanthroline (13 mg, 73 µmol) and DiPEA (13 µL, 73 µmol) in CH_2Cl_2 (740 µL). The resulting crude product was purified on silica gel (DCM–MeOH, gradient from 100:0 to 98:2) to afford **5am** as a yellow solid (27 mg, 47%). **Mp** 63 – 65 °C; $\mathbf{R_f}$ = 0.26 (DCM–MeOH, 95:5).

IR (ATR)/$\bar{\nu}$: 3301, 2968, 2923, 1740, 1690, 1519, 1490, 1445, 1368, 1315, 1254, 1151, 1035, 1001, 839, 748, 700, 660 cm^{-1}.

^{1}H-NMR (600 MHz, $CDCl_3$) δ 9.95 (s, 1H), 8.69 – 8.55 (m, 1H), 7.89 (s, 1H), 7.75 (d, *J* = 7.6 Hz, 1H), 7.63 (d, *J* = 7.9 Hz, 1H), 7.59 (d, *J* = 8.0 Hz, 1H), 7.47 (t, *J* = 7.8 Hz, 1H), 7.35 – 7.29 (m, 10H), 7.12 – 7.05 (m, 6H), 6.72 (s, 1H), 4.83 (q, *J* = 5.5 Hz, 1H), 4.61 (q, *J* = 6.9 Hz, 1H), 4.40 (dd, *J* = 8.2, 5.4 Hz, 1H), 3.63 (s, 3H), 3.21 (dd, *J* = 14.9, 3.5 Hz, 1H), 2.94 (dd, *J* = 14.8, 5.8 Hz, 1H), 2.17 – 2.08 (m, 1H), 1.40 (d, *J* = 7.2 Hz, 3H), 1.33 (s, 9H), 0.82 (d, *J* = 6.7 Hz, 6H).

^{13}C-NMR (150 MHz, $CDCl_3$) δ 191.8, 172.1, 171.9, 171.2, 154.4, 142.3, 138.2, 137.2, 134.7, 130.0, 129.9, 129.5, 128.3, 128.2, 128.0, 127.9, 127.3, 119.9, 81.6, 75.7, 57.7, 55.6, 53.4, 52.1, 43.6, 30.9, 28.3, 19.2, 18.1, 16.1.

HRMS–ESI: *m/z* $[M + H]^+$ calcd. for $C_{46}H_{51}N_5O_7$: 786.3861, found 786.3878.

Methyl (6*S*,9*S*,12*S*)-12-isopropyl-5-(4-(methoxycarbonyl)phenyl)-2,2,6-trimethyl-4,7,10-trioxo-9-((1-trityl-1*H*-imidazol-4-yl)methyl)-3-oxa-5,8,11-triazatridecan-13-oate (5an)

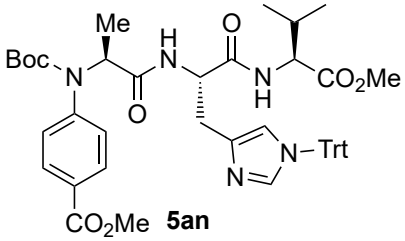

5an

The general procedure was followed starting from Boc–Ala–His(Trt)–Val–OMe **4a** (50 mg, 73 µmol), trimethyl 4,4',4''-bismuthanetriyltribenzoate **2n** (45 mg, 73 µmol), copper(II) acetate (13 mg, 73 µmol), phenanthroline (13 mg, 73 µmol) and DiPEA (13 µL, 73 µmol) in CH_2Cl_2 (740 µL). The resulting crude product was purified on silica gel (DCM–MeOH, gradient from 100:0 to 98:2) to afford **5an** as a white solid (22 mg, 37%). **Mp** 84 – 86 °C; $\mathbf{R_f}$ = 0.24 (DCM–MeOH, 95:5).

IR (ATR)/$\bar{\nu}$: 3199, 2963, 1683, 1511, 1493, 1445, 1392, 1369, 1321, 1277, 1156, 1113, 1019, 836, 749, 701, 660 cm^{-1}.

^{1}H-NMR (600 MHz, $CDCl_3$) δ 8.57 (s, 1H), 7.97 (d, *J* = 8.5 Hz, 2H), 7.61 (d, *J* = 7.6 Hz, 1H), 7.39 (d, *J* = 8.4 Hz, 2H), 7.35 – 7.29 (m, 10H), 7.14 – 7.02 (m, 6H), 6.71 (s, 1H), 4.85 – 4.77 (m, 1H), 4.60 (q, *J* = 7.1 Hz, 1H), 4.39 (dd, *J* = 8.0, 5.5 Hz, 1H), 3.90 (s, 3H), 3.64 (s, 3H), 3.18 (q, *J* = 7.4 Hz, 1H), 2.92 (dd, *J* = 13.7, 4.4 Hz, 1H), 2.16 – 2.07 (m, 1H), 1.39 (d, *J* = 7.1 Hz, 3H), 1.33 (s, 9H), 0.83 (d, *J* = 6.7 Hz, 6H).

***Presence of conformers*: ^{13}C-NMR (150 MHz, $CDCl_3$)** δ 172.1, 171.9, 166.7, 154.2, 145.4, 142.3, 138.1, 130.2, 129.9, 128.4, 128.3, 128.2, 128.1, 128.0, 127.4, 119.9, 81.6, 75.7, 58.4, 57.8, 55.9, 53.4, 52.3, 52.1, 43.8, 30.9, 28.3, 19.8, 18.1, 15.8, 12.7.

HRMS–ESI: *m/z* $[M + H]^+$ calcd. for $C_{47}H_{53}N_5O_8$: 816.3967, found 816.3978.

Methyl N^{α}-(*N*-(*tert*-butoxycarbonyl)-*N*-(naphthalen-2-yl)-*L*-alanyl)-N^{τ}-trityl-*L*-histidyl-*L*-valinate (5ao)

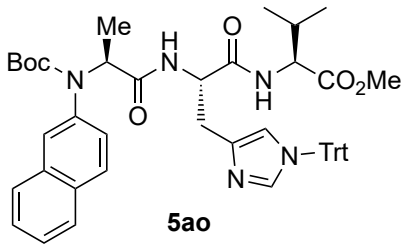

5ao

The general procedure was followed starting from Boc–Ala–His(Trt)–Val–OMe **4a** (50 mg, 73 µmol), tri(naphthalen-2-yl)bismuthane **2o** (43 mg, 73 µmol), copper(II) acetate (13 mg, 73 µmol), phenanthroline (13 mg, 73 µmol) and DiPEA (13 µL, 73 µmol) in CH_2Cl_2 (740 µL). The resulting crude product was purified on silica gel (DCM–MeOH, gradient from 100:0 to 98:2) to afford **5ao** as a white solid (30 mg, 51%). **Mp** 67 – 69 °C; **R_f** = 0.47 (DCM–MeOH, 95:5).

IR (ATR)/$\bar{\nu}$: 3310, 2963, 2928, 1741, 1682, 1493, 1445, 1391, 1367, 1312, 1254, 1202, 1155, 1129, 1036, 1001, 858, 818, 747, 700, 660 cm^{-1}.

^{1}H-NMR (600 MHz, $CDCl_3$) δ 8.71 (d, *J* = 5.7 Hz, 1H), 7.84 – 7.78 (m, 2H), 7.75 (d, *J* = 8.7 Hz, 1H), 7.72 (d, *J* = 7.8 Hz, 2H), 7.47 – 7.39 (m, 3H), 7.35 – 7.27 (m, 10H), 7.12 – 7.05 (m, 6H), 6.71 (s, 1H), 4.88 (q, *J* = 5.4 Hz, 1H), 4.67 (q, *J* = 6.8 Hz, 1H), 4.42 (dd, *J* = 8.3, 5.4 Hz, 1H), 3.64 (s, 3H), 3.23 (dd, *J* = 14.9, 3.5 Hz, 1H), 2.96 (dd, *J* = 14.6, 5.4 Hz, 1H), 2.17 – 2.09 (m, 1H), 1.43 (d, *J* = 7.0 Hz, 3H), 1.34 (s, 9H), 0.84 (d, *J* = 4.3 Hz, 3H), 0.83 (d, *J* = 4.1 Hz, 3H).

^{13}C-NMR (150 MHz, $CDCl_3$) δ 172.1, 172.1, 171.4, 154.8, 153.2, 142.4, 138.7, 138.2, 133.6, 132.1, 129.9, 128.4, 128.2, 128.2, 128.1, 127.6, 127.3, 126.3, 126.2, 126.1, 119.7, 81.1, 75.5, 58.7, 57.8, 53.4, 52.0, 31.0, 29.6, 28.4, 19.2, 18.1, 15.9.

HRMS–ESI: *m/z* $[M + H]^+$ calcd. for $C_{49}H_{53}N_5O_6$: 808.4069, found 808.4071.

c. Arylated compounds (5a –f) from tripeptides (4a–f) using tritolylbismuth (2a)

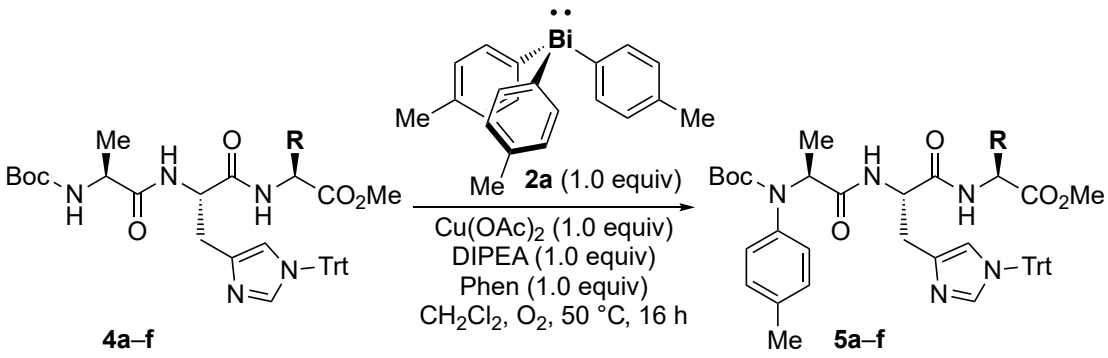

Methyl N^{α}-(*N*-(*tert*-butoxycarbonyl)-*N*-(*p*-tolyl)-*L*-alanyl)-N^{τ}-trityl-*L*-histidyl-*L*-valinate (5a)

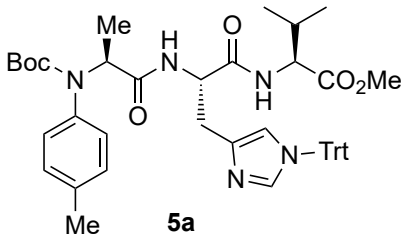

This compound has been previously reported[1]: **Mp** 134 – 136 °C; $\mathbf{R_f}$ = 0.46 (DCM–MeOH, 95:5)

IR (ATR)/$\bar{\nu}$: 3155, 2970, 1740, 1668, 1514, 1495, 1447, 1367, 1155, 1129, 1019, 1001, 839, 747, 701, 662, 640 cm^{-1}.

^{1}H-NMR (300 MHz, $CDCl_3$) δ 8.35 (d, *J* = 7.2 Hz, 1H), 8.08 (s, 1H), 7.74 (d, *J* = 5.9 Hz, 1H), 7.41 – 7.31 (m, 10H), 7.10 (dd, *J* = 5.9, 1.7 Hz, 8H), 7.04 (d, *J* = 8.2 Hz, 1H), 6.87 (s, 1H), 5.27 – 5.11 (m, 1H), 4.50 – 4.29 (m, 2H), 3.67 (s, 3H), 3.54 (d, *J* = 15.1 Hz, 1H), 2.96 – 2.81 (m, 1H), 2.27 (s, 3H), 2.26 – 2.20 (m, 1H), 1.31 (d, *J* = 6.6 Hz, 3H), 1.22 (s, 9H), 1.02 (dd, *J* = 15.7, 6.8 Hz, 6H).

Methyl N^{α}-(*N*-(*tert*-butoxycarbonyl)-*N*-(*p*-tolyl)-*L*-alanyl)-N^{τ}-trityl-*L*-histidyglycinate (5b)

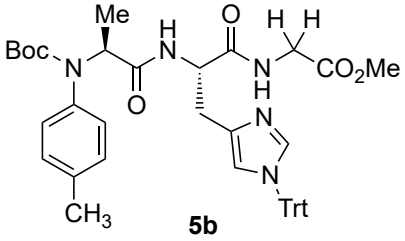

The general procedure was followed starting from Boc–Ala–His(Trt)–Gly–OMe **4b** (70 mg, 0.11 mmol), tri-*p*-tolylbismuthane **2a** (53 mg, 0.11 mmol), copper(II) acetate (20 mg, 0.11 mmol), phenanthroline (20 mg, 0.11 mmol) and DiPEA (19 µL, 0.11 mmol) in CH_2Cl_2 (1 mL). The resulting crude product was purified on silica gel (DCM–MeOH, gradient from 100:0 to 98:2) to afford **5b** as a yellowish solid (59 mg, 74%). **Mp** 75 – 77 °C; $\mathbf{R_f}$ = 0.26 (DCM–MeOH, 95:5).

IR (ATR)/$\bar{\nu}$: 3323, 2977, 2919, 1754, 1668, 1513, 1494, 1445, 1366, 1322, 1237, 1201, 1132, 1036, 1001, 851, 829, 747, 700, 660 cm^{-1}.

^{1}H-NMR (600 MHz, $CDCl_3$) δ 8.72 (s, 1H), 7.83 (s, 1H), 7.38 – 7.28 (m, 10H), 7.20 (d, *J* = 8.0 Hz, 2H), 7.14 – 7.07 (m, 8H), 6.70 (s, 1H), 4.77 (s, 1H), 4.40 (q, *J* = 7.2 Hz, 1H), 3.99 (dd, *J* = 17.7, 5.7 Hz, 1H), 3.87 (dd, *J* = 17.7, 5.3 Hz, 1H), 3.65 (s, 3H), 3.25 (d, *J* = 14.5 Hz, 1H), 2.92 (d, *J* = 14.6 Hz, 1H), 2.31 (s, 3H), 1.36 (d, *J* = 7.3 Hz, 3H), 1.27 (s, 9H).

^{13}C-NMR (150 MHz, $CDCl_3$) δ 172.2, 171.7, 169.9, 155.4, 142.4, 138.5, 138.3, 136.9, 136.7, 129.9, 129.4, 128.3, 128.1, 120.0, 80.9, 75.5, 59.2, 53.6, 52.1, 41.3, 29.2, 28.4, 21.1, 15.8.

HRMS–ESI: *m/z* $[M + H]^+$ calcd. for $C_{43}H_{47}N_5O_6$: 730.3599, found 730.3617.

Methyl N^{α}-(*N*-(*tert*-butoxycarbonyl)-*N*-(*p*-tolyl)-*L*-alanyl)-N^{τ}-trityl-*L*-histidyl-*L*-phenylalaninate (5c)

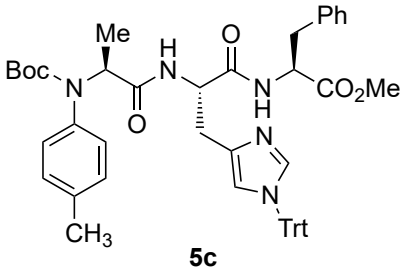

5c

The general procedure was followed starting from Boc–Ala–His(Trt)–Phe–OMe **4c** (70 mg, 96 µmol), tri-*p*-tolylbismuthane **2a** (46 mg, 96 µmol), copper(II) acetate (17 mg, 96 µmol), phenanthroline (17 mg, 96 µmol) and DiPEA (16 µL, 96 µmol) in CH_2Cl_2 (1 mL). The resulting crude product was purified on silica gel (DCM–MeOH, gradient from 100:0 to 98:2) to afford **5c** as a white solid (56 mg, 72%). **Mp** 85 – 87 °C; **R_f** = 0.24 (DCM–MeOH, 95:5).

IR (ATR)/$\bar{\nu}$: 3292, 2923, 1744, 1669, 1514, 1494, 1445, 1366, 1322, 1250, 1203, 1158, 1131, 1031, 854, 830, 747, 700, 660 cm^{-1}.

^{1}H-NMR (300 MHz, $CDCl_3$) δ 8.40 (d, *J* = 6.9 Hz, 1H), 7.84 (d, *J* = 7.7 Hz, 1H), 7.38 – 7.27 (m, 10H), 7.21 – 7.02 (m, 15H), 6.66 (s, 1H), 4.86 – 4.77 (m, 1H), 4.72 (q, *J* = 6.9 Hz, 1H), 4.45 (q, *J* = 7.0 Hz, 1H), 3.60 (s, 3H), 3.24 – 3.10 (m, 1H), 3.05 (d, *J* = 6.4 Hz, 2H), 2.88 (dd, *J* = 15.0, 5.3 Hz, 1H), 2.31 (s, 3H), 1.38 – 1.32 (m, 12H).

^{13}C-NMR (75 MHz, $CDCl_3$) δ 172.0, 171.7, 171.2, 154.9, 142.4, 138.6, 136.5, 129.9, 129.4, 129.3, 128.5, 128.1, 126.9, 119.7, 80.8, 75.4, 58.6, 54.0, 53.2, 52.2, 37.8, 29.5, 28.4, 21.1, 15.5.

HRMS–ESI: *m/z* $[M + H]^+$ calcd. for $C_{50}H_{53}N_5O_6$: 820.4069, found 820.4069.

Methyl N^{α}-(*N*-(*tert*-butoxycarbonyl)-*N*-(*p*-tolyl)-*L*-alanyl)-N^{τ}-trityl-*L*-histidyl-*L*-methioninate (5d)

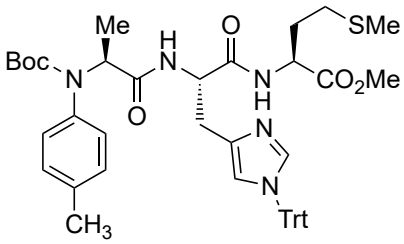

5d

The general procedure was followed starting from Boc–Ala–His(Trt)–Met–OMe **4d** (88 mg, 0.12 mmol), tri-*p*-tolylbismuthane **2a** (60 mg, 0.12 mmol), copper(II) acetate (22 mg, 0.12 mmol), phenanthroline (22 mg, 0.12 mmol) and DiPEA (21 µL, 0.12 mmol) in CH_2Cl_2 (1.2 mL). The resulting crude product was purified on silica gel (DCM–MeOH, gradient from 100:0 to 98:2) to afford **5d** as a yellow solid (65 mg, 65%). **Mp** 80 – 82 °C; $\mathbf{R_f}$ = 0.29 (DCM–MeOH, 95:5).

IR (ATR)/$\bar{\nu}$: 3331, 2977, 2915, 1742, 1668, 1514, 1494, 1445, 1158, 1131, 1001, 839, 748, 701, 660 cm^{-1}.

^{1}H-NMR (600 MHz, $CDCl_3$) δ 8.58 (s, 1H), 7.83 (d, *J* = 7.7 Hz, 1H), 7.36 – 7.28 (m, 10H), 7.15 (d, *J* = 8.2 Hz, 2H), 7.12 – 7.06 (m, 8H), 6.70 (s, 1H), 4.78 (q, *J* = 5.9 Hz, 1H), 4.54 (dt, *J* = 8.0, 5.1 Hz, 1H), 4.45 (q, *J* = 7.2 Hz, 1H), 3.65 (s, 3H), 3.21 (dd, *J* = 14.6, 4.1 Hz, 1H), 2.91 (dd, *J* = 15.2, 6.0 Hz, 1H), 2.41 (t, *J* = 7.6 Hz, 2H), 2.31 (s, 3H), 2.15 – 2.07 (m, 1H), 2.03 – 1.97 (m, 1H), 2.00 (s, 3H), 1.35 (d, *J* = 7.3 Hz, 3H), 1.30 (s, 9H).

***Presence of conformers:* ^{13}C-NMR (150 MHz, $CDCl_3$)** δ 172.1, 172.1, 171.4, 155.1, 142.3, 138.5, 138.2, 137.0, 136.6, 129.9, 129.4, 128.2, 128.2, 119.9, 80.9, 75.6, 58.8, 55.6, 53.3, 52.3, 51.9, 31.3, 30.2, 29.2, 28.4, 21.1, 15.6, 15.4.

HRMS–ESI: *m/z* $[M + H]^+$ calcd. for $C_{46}H_{53}N_5O_6S$: 804.3789, found 804.3795.

Methyl N^{α}-(*N*-(*tert*-butoxycarbonyl)-*N*-(*p*-tolyl)-*L*-alanyl)-N^{τ}-trityl-*L*-histidyl-*L*-prolinate (5e)

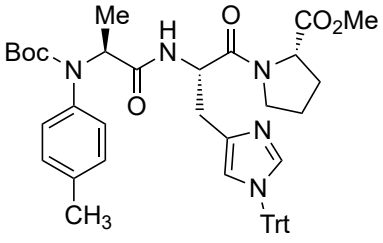

5e

The general procedure was followed starting from Boc–Ala–His(Trt)–Pro–OMe **4e** (70 mg, 0.10 mmol), tri-*p*-tolylbismuthane **2a** (50 mg, 0.10 mmol), copper(II) acetate (19 mg, 0.10 mmol), phenanthroline (19 mg, 0.10 mmol) and DiPEA (18 µL, 0.10 mmol) in CH_2Cl_2 (1.2 mL). The resulting crude product was purified preparative TLC (DCM–MeOH, 96:4) to afford **5e** as a white solid (52 mg, 66%). **Mp** 66 – 68 °C; $\mathbf{R_f}$ = 0.29 (DCM–MeOH, 95:5).

IR (ATR)/$\bar{\nu}$: 2925, 1743, 1689, 1651, 1514, 1494, 1444, 1366, 1323, 1248, 1159, 1131, 1036, 1020, 1001, 841, 747, 701, 660 cm^{-1}.

^{1}H-NMR (600 MHz, $CDCl_3$) δ 7.57 (s, 1H), 7.31 – 7.27 (m, 10H), 7.15 – 7.10 (m, 6H), 7.08 (d, *J* = 10.9 Hz, 2H), 7.01 (d, *J* = 8.0 Hz, 2H), 6.76 (s, 1H), 4.99 (q, *J* = 6.1 Hz, 1H), 4.60 – 4.47 (m, 2H), 3.83 (q, *J* = 7.9 Hz, 1H), 3.62 (dt, *J* = 9.4, 6.3 Hz, 1H), 3.47 (s, 3H), 3.07 (dd, *J* = 14.6, 5.6 Hz, 1H), 2.91 (dd, *J* = 14.6, 6.2 Hz, 1H), 2.28 (s, 3H), 2.19 – 2.11 (m, 1H), 2.00 – 1.93 (m, 2H), 1.93 – 1.86 (m, 1H), 1.42 – 1.35 (m, 3H), 1.34 (s, 9H).

***Presence of conformers:* ^{13}C-NMR (150 MHz, $CDCl_3$)** δ 172.6, 172.0, 170.3, 154.9, 142.6, 138.5, 136.4, 130.0, 129.8, 129.3, 128.3, 128.2, 128.1, 128.0, 120.2, 80.9, 75.5, 58.7, 52.1, 51.3, 47.0, 30.5, 29.8, 29.1, 28.4, 25.0, 21.1, 15.5.

HRMS–ESI: *m/z* $[M + H]^+$ calcd. for $C_{46}H_{51}N_5O_6$: 770.3912, found 770.3910.

Methyl *N*-(*N*$^\alpha$-(*N*-(*tert*-butoxycarbonyl)-*N*-(*p*-tolyl)-*L*-alanyl)-*N*$^\tau$-trityl-*L*-histidyl)-*O*-(*p*-tolyl)-*L*-serinate (5f)

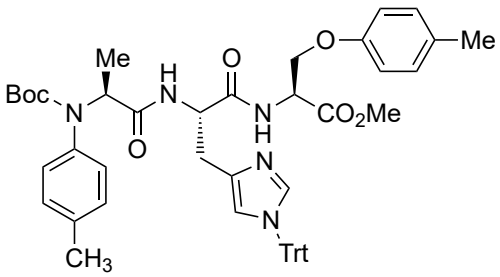

5f

The general procedure was followed starting from Boc–Ala–His(Trt)–Ser–OMe **4f** (55 mg, 82 µmol), tri-*p*-tolylbismuthane **2a** (40 mg, 82 µmol), copper(II) acetate (15 mg, 82 µmol), phenanthroline (15 mg, 82 µmol) and DiPEA (14 µL, 82 µmol) in CH_2Cl_2 (1 mL). The resulting crude product was purified on silica gel (Hexane–EtOAc, gradient from 80:20 to 30:70) to afford **5f** as a white solid (32 mg, 45%). **Mp** 80 – 82 °C; **R_f** = 0.63 (Hexane–EtOAc, 20:80).

IR (ATR)/$\tilde{\nu}$: 3299, 2921, 1748, 1671, 1511, 1445, 1366, 1323, 1237, 1204, 1157, 1132, 1087, 1036, 1001, 816, 748, 701, 660 cm^{-1}.

^{1}H-NMR (600 MHz, $CDCl_3$) δ 8.25 (s, 1H), 8.17 – 8.09 (m, 1H), 7.38 – 7.26 (m, 10H), 7.13 (d, *J* = 6.7 Hz, 2H), 7.10 – 7.06 (m, 6H), 7.05 (d, *J* = 8.1 Hz, 2H), 6.97 (d, *J* = 8.3 Hz, 2H), 6.70 (s, 1H), 6.68 (d, *J* = 8.3 Hz, 2H), 4.91 – 4.78 (m, 2H), 4.54 (s, 1H), 4.31 (dd, *J* = 9.3, 3.6 Hz, 1H), 4.13 (dd, *J* = 9.3, 3.6 Hz, 1H), 3.66 (s, 3H), 3.20 – 3.13 (m, 1H), 3.02 – 2.93 (m, 1H), 2.30 (s, 3H), 2.24 (s, 3H), 1.31 (s(br), 12H).

^{13}C-NMR (150 MHz, $CDCl_3$) δ 172.2, 171.6, 170.1, 156.3, 154.5, 142.4, 138.3, 138.2, 136.6, 130.6, 129.9, 129.9, 129.4, 128.3, 128.2, 119.8, 114.9, 80.9, 75.6, 68.0, 53.9, 53.4, 52.7, 52.6, 30.0, 28.4, 21.1, 20.6, 15.7.

HRMS–ESI: *m/z* $[M + H]^+$ calcd. for $C_{51}H_{55}N_5O_7$: 850.4174, found 850.4187.

d. Arylated compounds (5g–j) from tripeptides (4g–j) using tritolylbismuth (2a)

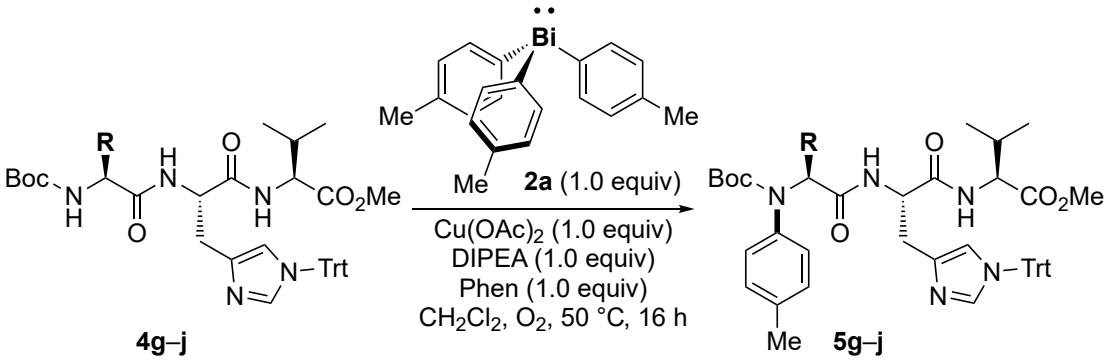

Methyl N^{α}-(*N*-(*tert*-butoxycarbonyl)-*N*-(*p*-tolyl)-*L*-phenylalanyl)-N^{τ}-trityl-*L*-histidyl-*L*-valinate (5g)

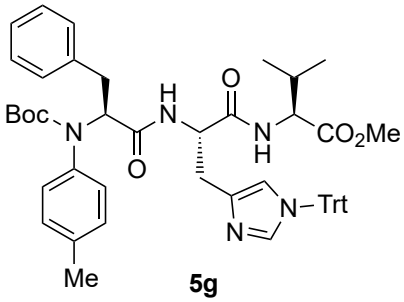

The general procedure was followed starting from Boc–Phe–His(Trt)–Val–OMe **4g** (70 mg, 92 µmol), tri-*p*-tolylbismuthane **2a** (45 mg, 92 µmol), copper(II) acetate (17 mg, 92 µmol), phenanthroline (17 mg, 92 µmol) and DiPEA (16 µL, 92 µmol) in CH_2Cl_2 (1 mL). The resulting crude product was purified on silica gel (DCM–MeOH, gradient from 100:0 to 98:2) to afford **5g** as a yellow solid (28 mg, 36%). **Mp** 74 – 76 °C; $\mathbf{R_f}$ = 0.36 (DCM–MeOH, 95:5).

IR (ATR)/$\bar{\nu}$: 3295, 2965, 2928, 1740, 1674, 1513, 1495, 1445, 1367, 1319, 1303, 1253, 1203, 1154, 1033, 1001, 827, 747, 700, 660 cm^{-1}.

^{1}H-NMR (600 MHz, $CDCl_3$) δ 8.61 (s, 1H), 7.73 (d, *J* = 8.2 Hz, 1H), 7.33 – 7.28 (m, 10H), 7.24 (d, *J* = 7.4 Hz, 2H), 7.21 (d, *J* = 7.1 Hz, 1H), 7.15 (d, *J* = 7.2 Hz, 2H), 7.11 – 7.06 (m, 6H), 6.87 (d, *J* = 8.0 Hz, 2H), 6.71 (s, 1H), 6.59 (s(br), 2H), 4.90 – 4.84 (m, 1H), 4.63 – 4.56 (m, 1H), 4.47 – 4.40 (m, 1H), 3.64 (s, 3H), 3.37 (s(br), 1H), 3.27 (s(br), 1H), 3.21 – 3.14 (m, 1H), 2.98 – 2.90 (m, 1H), 2.22 (s, 3H), 2.19 – 2.09 (m, 1H), 1.33 (s(br), 9H), 0.84 (d, *J* = 6.7 Hz, 6H).

^{13}C-NMR (150 MHz, $CDCl_3$) δ 172.1, 171.4, 171.2, 165.9, 154.7, 142.5, 141.1, 139.6, 139.0, 138.5, 136.1, 129.9, 129.6, 129.1, 128.5, 128.1, 127.5, 126.6, 119.6, 80.9, 75.5, 65.6, 57.7, 53.4, 52.0, 31.0, 29.8, 28.4, 21.0, 19.2, 18.0.

HRMS–ESI: *m/z* $[M + H]^+$ calcd. for $C_{52}H_{57}N_5O_6$: 848.4382, found 848.4387.

Methyl N^{α}-(*N*-(*tert*-butoxycarbonyl)-*N*-(*p*-tolyl)glycyl)-N^{τ}-trityl-*L*-histidyl-*L*-valinate (5h)

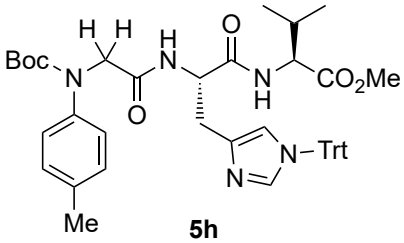

5h

The general procedure was followed starting from Boc–Gly–His(Trt)–Val–OMe **4h** (54 mg, 81 µmol), tri-*p*-tolylbismuthane **2a** (39 mg, 81 µmol), copper(II) acetate (15 mg, 81 µmol), phenanthroline (15 mg, 81 µmol) and DiPEA (14 µL, 81 µmol) in CH_2Cl_2 (1 mL). The resulting crude product was purified on silica gel (DCM–MeOH, gradient from 100:0 to 98:2) to afford **5h** as a white solid (37 mg, 61%). **Mp** 83 – 85 °C; $\mathbf{R_f}$ = 0.36 (Hexane–EtOAc, 30:70).

IR (ATR)/$\bar{\nu}$: 3292, 2965, 2931, 1742, 1683, 1514, 1494, 1445, 1367, 1206, 1152, 1035, 1017, 1001, 868, 824, 748, 701, 659 cm^{-1}.

^{1}H-NMR (300 MHz, $CDCl_3$) δ 8.54 (d, *J* = 7.1 Hz, 1H), 7.60 (d, *J* = 8.4 Hz, 1H), 7.36 – 7.28 (m, 10H), 7.23 (d, *J* = 8.2 Hz, 2H), 7.13 – 7.03 (m, 8H), 6.67 (s, 1H), 4.85 – 4.76 (m, 1H), 4.41 (dd, *J* = 8.5, 5.3 Hz, 1H), 4.31 (d, *J* = 17.0 Hz, 1H), 4.24 (d, *J* = 17.0 Hz, 1H), 3.64 (s, 3H), 3.15 (dd, *J* = 15.0, 4.2 Hz, 1H), 2.87 (dd, *J* = 15.0, 6.1 Hz, 1H), 2.29 (s, 3H), 2.18 – 2.04 (m, 1H), 1.36 (s, 9H), 0.83 (d, *J* = 3.0 Hz, 3H), 0.81 (d, *J* = 3.0 Hz, 3H).

^{13}C-NMR (75 MHz, $CDCl_3$) δ 172.0, 171.1, 169.5, 154.9, 142.4, 140.3, 138.3, 137.1, 136.0, 129.9, 129.6, 128.2, 128.2, 126.3, 119.7, 81.2, 75.5, 57.7, 54.6, 53.2, 52.0, 31.0, 29.7, 28.3, 21.1, 19.2, 18.0.

HRMS–ESI: *m/z* $[M + H]^+$ calcd. for $C_{45}H_{51}N_5O_6$: 758.3912, found 758.3920.

Methyl N^{α}-(*N*-(*tert*-butoxycarbonyl)-*N*-(*p*-tolyl)-*L*-methionyl)-N^{τ}-trityl-*L*-histidyl-*L*-valinate (5i)

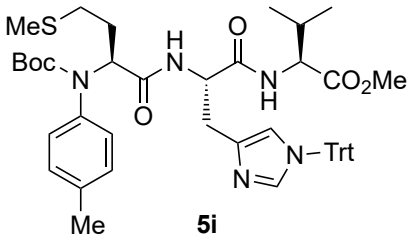

5i

The general procedure was followed starting from Boc–Met–His(Trt)–Val–OMe **4i** (84 mg, 0.11 mmol), tri-*p*-tolylbismuthane **2a** (55 mg, 0.11 mmol), copper(II) acetate (21 mg, 0.11 mmol), phenanthroline (20 mg, 0.11 mmol) and DiPEA (19 µL, 0.11 mmol) in CH_2Cl_2 (1.1 mL). The resulting crude product was purified on silica gel (Hexane–EtOAc, gradient from 80:20 to 30:70) to afford **5i** as a yellow solid (48 mg, 51%). **Mp** 71 – 73 °C; $\mathbf{R_f}$ = 0.35 (DCM–MeOH, 95:5).

IR (ATR)/$\bar{\nu}$: 3306, 2965, 2925, 1741, 1683, 1513, 1494, 1445, 1367, 1323, 1303, 1255, 1204, 1155, 1037, 1001, 870, 828, 748, 701, 660 cm^{-1}.

^{1}H-NMR (600 MHz, $CDCl_3$) δ 8.45 (s, 1H), 7.70 (d, *J* = 7.2 Hz, 1H), 7.36 – 7.27 (m, 10H), 7.17 – 7.06 (m, 8H), 7.04 (d, *J* = 7.9 Hz, 2H), 6.70 (s(br), 1H), 4.82 (s, 1H), 4.76 – 4.68 (m, 1H), 4.48 – 4.40 (m, 1H), 3.63 (s, 3H), 3.17 – 3.08 (m, 1H), 2.96 – 2.89 (m, 1H), 2.54 (t, *J* = 7.1 Hz, 2H), 2.28 (s, 4H), 2.16 – 2.08 (m, 1H), 1.99 (s, 3H), 1.98 – 1.91 (m, 1H), 1.35 (s, 9H), 0.85 (d, *J* = 2.9 Hz, 3H), 0.84 (d, *J* = 2.9 Hz, 3H).

^{13}C-NMR (150 MHz, $CDCl_3$) δ 172.0, 171.3, 171.3, 165.8, 154.9, 142.4, 138.1, 136.5, 129.8, 129.4, 128.1, 127.8, 119.4, 81.2, 75.5, 61.2, 57.6, 53.4, 52.0, 31.2, 31.0, 29.8, 29.0, 28.3, 21.1, 19.1, 18.0, 15.3.

HRMS–ESI: *m/z* $[M + H]^+$ calcd. for $C_{48}H_{57}N_5O_6S$: 832.4102, found 832.4113.

Methyl *N*$^\alpha$-(*N*-(*tert*-butoxycarbonyl)-*N*,*O*-di-*p*-tolyl-*L*-seryl)-*N*$^\tau$-trityl-*L*-histidyl-*L*-valinate (5j)

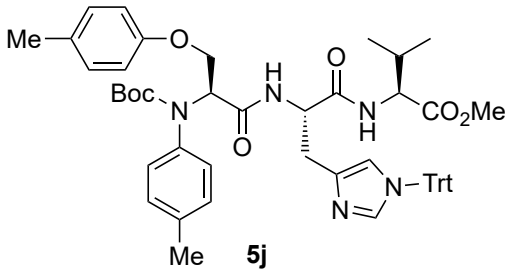

5j

The general procedure was followed starting from Boc–Ser–His(Trt)–Val–OMe **4j** (45 mg, 65 µmol), tri-*p*-tolylbismuthane **2a** (31 mg, 65 µmol), copper(II) acetate (12 mg, 65 µmol), phenanthroline (12 mg, 65 µmol) and DiPEA (11 µL, 65 µmol) in CH_2Cl_2 (650 µL). The resulting crude product was purified on silica gel (Hexane–EtOAc, gradient from 80:20 to 30:70) to afford **5j** as a white solid (19 mg, 33%). **Mp** 72 – 74 °C; **R_f** = 0.57 (Hexane–EtOAc, 20:80).

IR (ATR)/$\bar{\nu}$: 3334, 2965, 2929, 1742, 1683, 1511, 1445, 1368, 1324, 1241, 1209, 1156, 1037, 818, 749, 702, 660 cm^{-1}.

^{1}H-NMR (600 MHz, $CDCl_3$) δ 7.34 – 7.28 (m, 12H), 7.12 – 7.07 (m, 8H), 7.05 (d, *J* = 7.9 Hz, 2H), 7.02 (d, *J* = 7.9 Hz, 2H), 6.78 (d, *J* = 7.3 Hz, 2H), 6.71 (s, 1H), 4.91 – 4.84 (m, 1H), 4.85 – 4.81 (m, 1H), 4.57 – 4.51 (m, 1H), 4.44 (dd, *J* = 8.0, 5.2 Hz, 1H), 4.28 (t, *J* = 9.5 Hz, 1H), 3.64 (s, 3H), 3.21 – 3.15 (m, 1H), 3.00 – 2.91 (m, 1H), 2.29 (s, 3H), 2.25 (s, 3H), 2.15 – 2.06 (m, 1H), 1.33 (s, 9H), 0.85 – 0.79 (m, 6H).

^{13}C-NMR (150 MHz, $CDCl_3$) δ 172.1, 171.2, 169.6, 156.3, 142.4, 136.7, 130.3, 130.3, 130.0, 129.9, 129.8, 129.5, 128.7, 128.5, 128.2, 126.9, 119.6, 114.7, 80.8, 75.5, 53.3, 52.1, 36.8, 31.0, 29.8, 28.4, 24.8, 23.5, 21.2, 20.6, 19.2, 18.0.

HRMS–ESI: *m/z* $[M + H]^+$ calcd. for $C_{53}H_{59}N_5O_7$: 878.4487, found 878.4479.

e. Arylated compounds (7) from tripeptides (6) using tritolylbismuth (2a)

Methyl N^{α}-(*N*-((*tert*-butoxycarbonyl)glycyl)-*N*-(*p*-tolyl)glycyl)-N^{τ}-trityl-*L*-histidinate (7e)

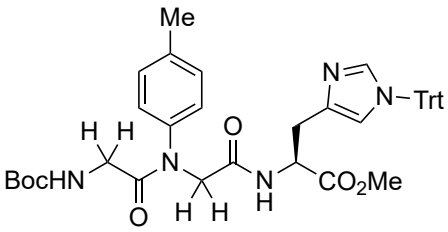

7e

The general procedure was followed starting from Boc–Gly–Gly–His(Trt)–OMe **6e** (60 mg, 96 µmol), tri-*p*-tolylbismuthane **2a** (69 mg, 144 µmol, 1.5 equiv.), copper(II) acetate (26 mg, 144 µmol, 1.5 equiv.), phenanthroline (26 mg, 144 µmol, 1.5 equiv.) and DiPEA (24.5 µL, 144 µmol, 1.5 equiv.) in CH_2Cl_2 (1 mL). The resulting crude product was purified on silica gel (DCM–MeOH, gradient from 100:0 to 98:2) to afford **7e** as a white solid (17 mg, 25%).

Mp 74 – 76 °C; **R_f** = 0.24 (DCM–MeOH, 95:5).

IR (ATR)/$\bar{\nu}$: 3322, 2975, 2930, 1746, 1674, 1514, 1494, 1445, 1391, 1366, 1245, 1210, 1169, 1133, 1034, 870, 829, 750, 703, 661 cm^{-1}.

^{1}H-NMR (600 MHz, $CDCl_3$) δ 7.93 (s, 1H), 7.37 – 7.29 (m, 10H), 7.25 (d, *J* = 8.3 Hz, 2H), 7.13 (d, *J* = 8.3 Hz, 2H), 7.11 – 7.07 (m, 6H), 6.56 (s, 1H), 5.36 (s(br), 1H), 4.82 – 4.76 (m, 1H), 4.43 (d, *J* = 16.3 Hz, 1H), 4.22 (d, *J* = 16.9 Hz, 1H), 3.76 – 3.67 (m, 2H), 3.59 (s, 3H), 3.07 (dd, *J* = 14.6, 4.9 Hz, 1H), 2.98 (dd, *J* = 14.5, 4.6 Hz, 1H), 2.32 (s, 3H), 1.36 (s, 9H).

^{13}C-NMR (150 MHz, $CDCl_3$) δ 171.4, 169.7, 167.9, 155.6, 142.2, 138.8, 138.3, 136.2, 130.6, 130.0, 129.7, 128.1, 127.6, 119.7, 115.1, 79.4, 75.4, 53.5, 52.6, 52.1, 43.2, 29.6, 28.3, 21.0.

HRMS–ESI: *m/z* $[M + H]^+$ calcd. for $C_{42}H_{45}N_5O_6$: 716.3443, found 716.3471.

f. Arylated compounds (9) from tetrapeptide (8) using tritolylbismuth (2a)

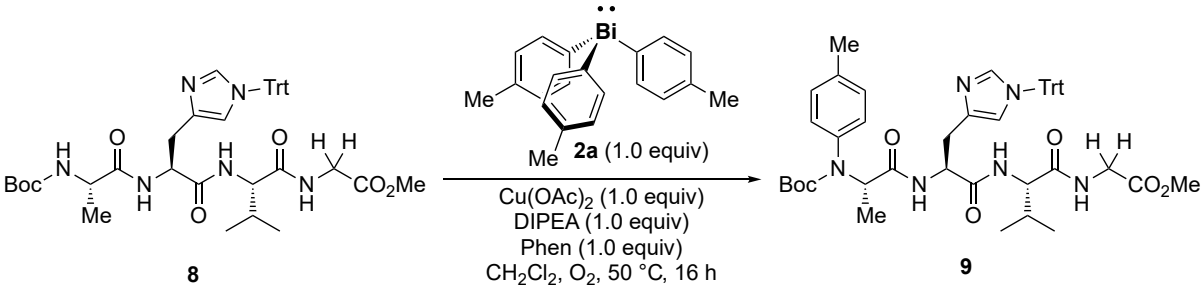

8 **9**

Methyl N^{α}-(*N*-(*tert*-butoxycarbonyl)-*N*-(*p*-tolyl)-*L*-alanyl)-N^{τ}-trityl-*L*-histidyl-*L*-valylglycinate (9)

The general procedure was followed starting from Boc–Ala–His(Trt)–Val–Gly–OMe **8** (70 mg, 95 µmol), tri-*p*-tolylbismuthane **2a** (46 mg, 95 µmol), copper(II) acetate (17 mg, 95 µmol), phenanthroline (17 mg, 95 µmol) and DiPEA (16 µL, 95 µmol) in CH_2Cl_2 (1 mL). The resulting

crude product was purified on silica gel (DCM–MeOH, gradient from 100:0 to 98:2) to afford **9** as a white solid (50 mg, 64%). **Mp** 95 – 97 °C; **R_f** = 0.36 (DCM–MeOH, 95:5).

IR (ATR)/$\bar{\nu}$: 3315, 2968, 2923, 1752, 1667, 1513, 1494, 1445, 1367, 1323, 1203, 1157, 1131, 1036, 1001, 988, 842, 748, 701, 660 cm^{-1}.

^{1}H-NMR (600 MHz, $CDCl_3$) δ 8.76 (s(br), 1H), 7.83 (s, 1H), 7.36 – 7.28 (m, 11H), 7.15 (d, *J* = 8.0 Hz, 2H), 7.10 – 7.05 (m, 8H), 6.75 (s, 1H), 4.59 (q, *J* = 5.5 Hz, 1H), 4.46 (q, *J* = 7.2 Hz, 1H), 4.39 (dd, *J* = 8.8, 4.9 Hz, 1H), 4.09 (dd, *J* = 17.7, 6.1 Hz, 1H), 3.83 (dd, *J* = 17.7, 5.3 Hz, 1H), 3.64 (s, 3H), 3.17 (dd, *J* = 14.8, 4.2 Hz, 1H), 3.00 (dd, *J* = 14.8, 6.3 Hz, 1H), 2.43 – 2.38 (m, 1H), 2.32 (s, 3H), 1.28 (s, 12H), 0.91 – 0.86 (m, 6H).

^{13}C-NMR (150 MHz, $CDCl_3$) δ 173.5, 171.8, 171.5, 170.3, 155.2, 142.3, 138.6, 137.9, 136.8, 136.7, 129.8, 129.4, 128.5, 128.3, 128.2, 120.0, 81.0, 75.6, 59.0, 58.5, 54.9, 52.1, 41.2, 29.4, 28.3, 21.2, 19.6, 17.4, 16.0.

HRMS–ESI: *m/z* $[M + H]^+$ calcd. for $C_{48}H_{56}N_6O_7$: 829.4283, found 829.4301.

5. Procedure for selective deprotection of 5a

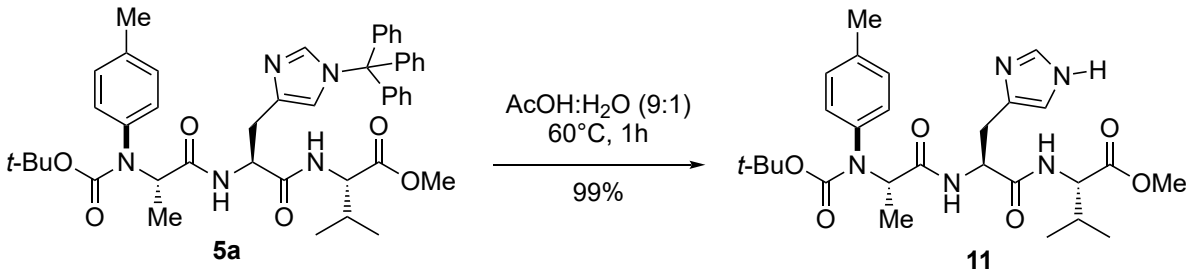

Methyl *N*-(*tert*-butoxycarbonyl)-*N*-(*p*-tolyl)-*L*-alanyl-*L*-histidyl-*L*-valinate (11)

In a flask, Boc–*N*(Tolyl)–Ala–His(trt)–Val–OMe **5a** (50 mg, 0.65 mmol) in AcOH:H_2O (9:1, 0.35 M) was stirred for 1h30 at 60 °C. After cooling down at room temperature, the solvent was co-evaporated with cyclohexane under reduce pressure. The white solid residue was purified on silica gel chromatography (5% MeOH/CH_2Cl_2) to afford **11** as a white solid (35 mg, 99%): This compound has been previously reported[1]: **Mp** 154 – 157 °C; **R_f** = 0.46 (6% MeOH/CH_2Cl_2); **^{1}H-NMR (600 MHz, $CDCl_3$)** δ 7.86 (s(br), 1H), 7.62 (s(br), 1H), 7.56 (s, 1H), 7.14 – 7.08 (m, 4H), 6.83 (s, 1H), 4.80 – 4.75 (m, 1H), 4.57 – 4.51 (m, 1H), 4.39 (dd, *J* = 8.3, 5.2 Hz, 1H), 3.71 (s, 3H), 3.16 (dd, *J* = 15.1, 4.7 Hz, 1H), 3.09 (dd, *J* = 15.2, 5.9 Hz, 1H), 2.33 (s, 3H), 2.18 – 2.11 (m, 1H), 1.36 (s, 9H), 1.30 (d, *J* = 6.9 Hz, 3H), 0.86 (dd, *J* = 6.8, 3.5 Hz, 6H).

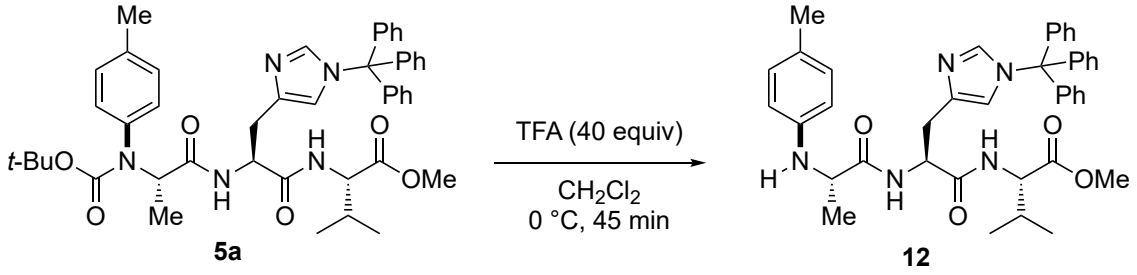

Methyl N$^{\alpha}$-(p-tolyl-L-alanyl)-N$^{\tau}$-trityl-L-histidyl-L-valinate (12)

In a flask, trifluoroacetic acid (450 µL, 5.8 mmol, 40 equiv.) was added slowly to a solution of methyl *N*$^{\alpha}$-(*N*-(*tert*-butoxycarbonyl)-*N*-(*p*-tolyl)-*L*-alanyl)-*N*$^{\tau}$-trityl-*L*-histidyl-*L*-valinate (**5a**) (112 mg, 0.15 mmol, 1.0 equiv.) in dichloromethane (3 mL, 0.5 M) at 0 °C. After stirred at 0 °C for 45 min (followed by TLC), the mixture was purred in a sat. solution of $NaHCO_3$. The combined organic phases were washed with brine (20 mL), dried over Na_2SO_4, filtered and concentrated under reduce pressure. The white solid residue was purified on silica gel chromatography (2% MeOH/CH_2Cl_2) to afford **12** as a white solid (67 mg, 69%). **Mp** 74 – 76 °C; **R$_f$** = 0.36 (CH_2Cl_2–MeOH, 93:7).

IR (ATR)/$\bar{\nu}$: 3324, 2965, 1743, 1667, 1521, 1494, 1446, 1318, 1205, 1155, 749, 702, 661 cm^{-1}.

^{1}H-NMR (600 MHz, CDCl$_3$) δ 8.70 (d, *J* = 7.3 Hz, 1H), 7.35 – 7.28 (m, 9H), 7.20 (d, *J* = 1.0 Hz, 1H), 7.10 (d, *J* = 8.7 Hz, 1H), 7.06 – 7.00 (m, 6H), 6.91 (d, *J* = 8.2 Hz, 2H), 6.64 (s, 1H), 6.52 (d, *J* = 8.3 Hz, 2H), 4.70 – 4.64 (m, 1H), 4.36 (dd, *J* = 8.7, 5.3 Hz, 1H), 3.95 (s(br), 1H), 3.89 (q, *J* = 6.8 Hz, 1H), 3.70 (s, 3H), 3.10 (dd, *J* = 14.6, 5.0 Hz, 1H), 2.88 (dd, *J* = 14.8, 5.6 Hz, 1H), 2.16 (s, 3H), 1.97 – 1.88 (m, 1H), 1.47 (d, *J* = 7.0 Hz, 3H), 0.71 (d, *J* = 6.8 Hz, 3H), 0.60 (d, *J* = 6.8 Hz, 3H).

^{13}C-NMR (150 MHz, CDCl$_3$) δ 175.0, 172.0, 171.0, 144.3, 142.4, 138.4, 136.8, 130.1, 129.8, 128.2, 128.14, 127.6, 119.7, 113.2, 75.4, 57.4, 54.7, 53.4, 52.1, 31.1, 29.3, 20.5, 19.7, 19.2, 17.9.

HRMS–ESI: *m/z* $[M + H]^+$ calcd. for $C_{41}H_{45}N_5O_4$: 672.3544, found 672.3575.

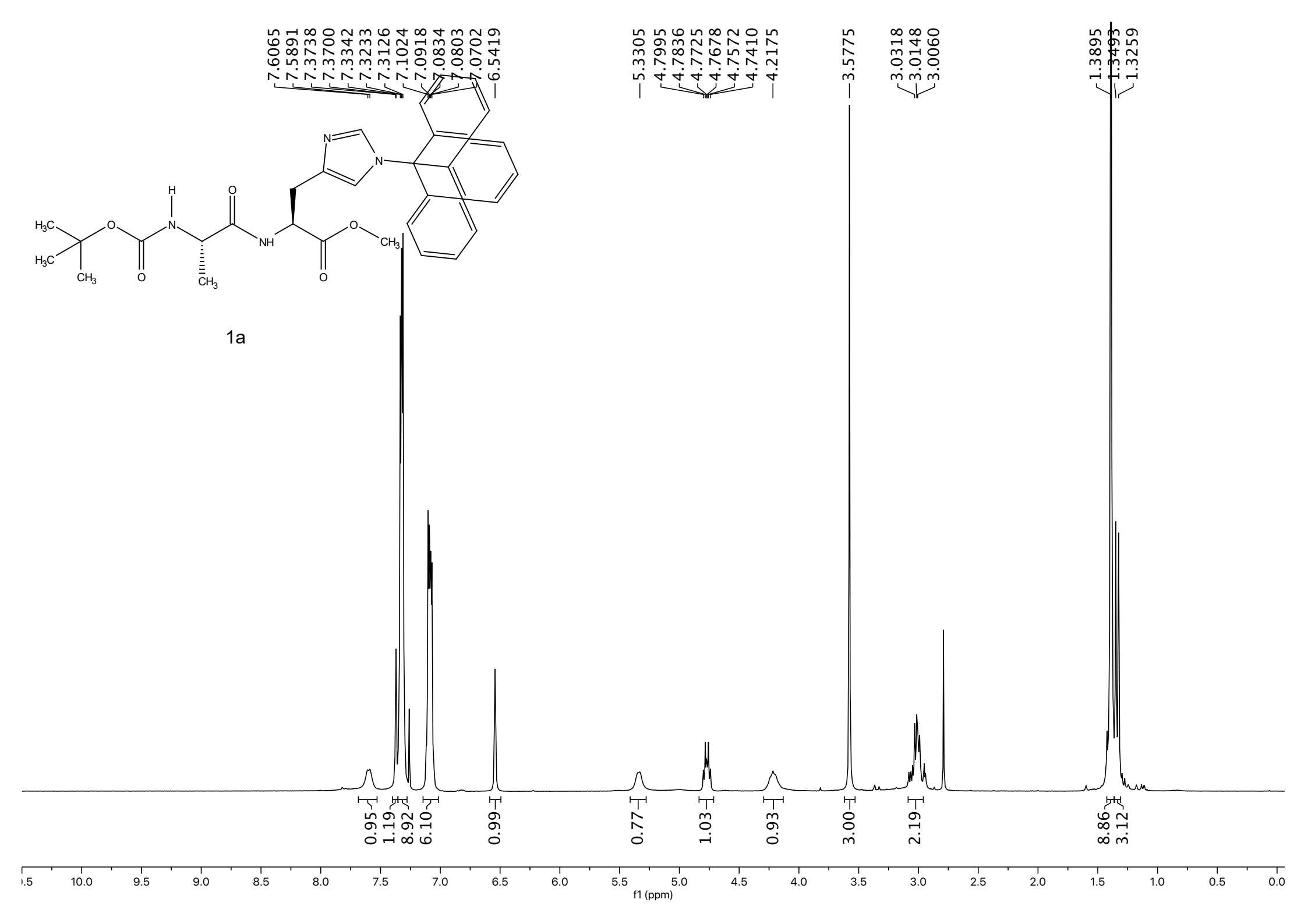
7.6065
7.5891
7.3738
7.3700
7.3342
7.3233
7.3126
7.1024
7.0918
7.0834
7.0803
7.0702
6.5419
5.3305
4.7995
4.7836
4.7725
4.7678
4.7572
4.7410
4.2175
3.5775
3.0318
3.0148
3.0060
1.3895
1.3493
1.3259
0.95
1.19
8.92
6.10
0.99
0.77
1.03
0.93
3.00
2.19
8.86
3.12
f1 (ppm)

1a

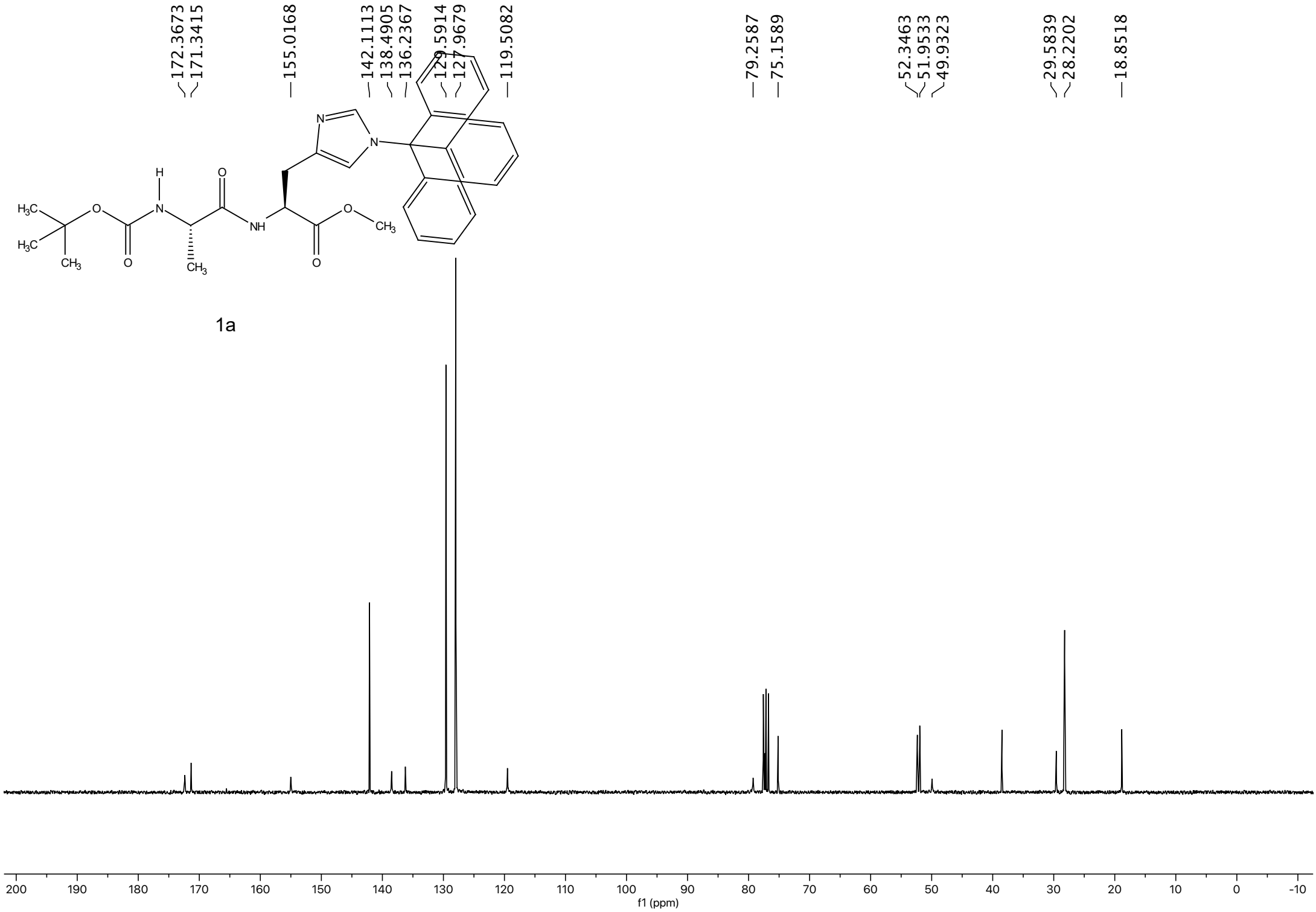
172.3673
171.3415
155.0168
142.1113
138.4905
136.2367
129.5914
127.9679
119.5082
79.2587
75.1589
52.3463
51.9533
49.9323
29.5839
28.2202
18.8518
1a
f1 (ppm)

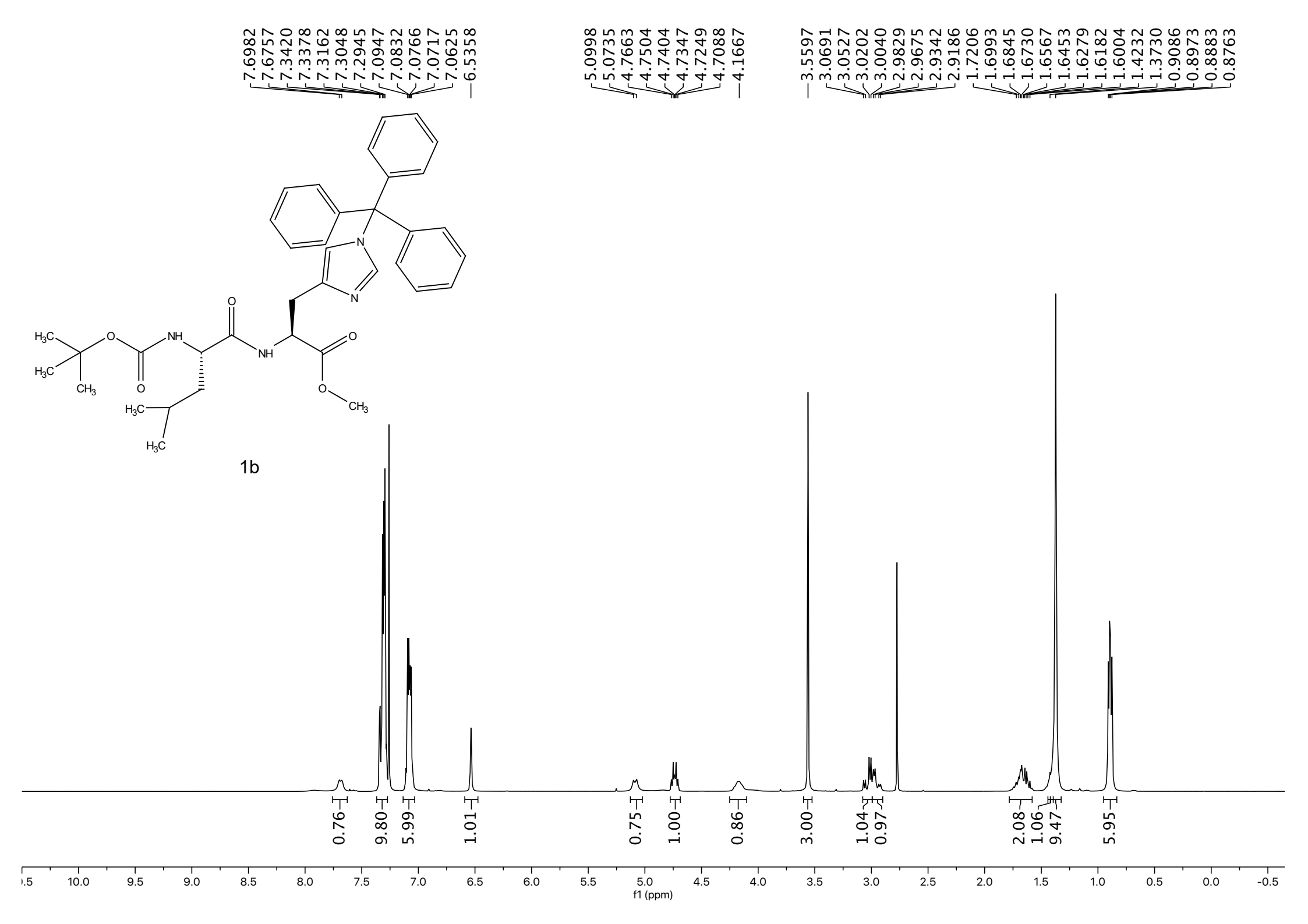
7.6982
7.6757
7.3420
7.3378
7.3162
7.3048
7.2945
7.0947
7.0832
7.0766
7.0717
7.0625
6.5358
5.0998
5.0735
4.7663
4.7504
4.7404
4.7347
4.7249
4.7088
4.1667
3.5597
3.0691
3.0527
3.0202
3.0040
2.9829
2.9675
2.9342
2.9186
1.7206
1.6993
1.6845
1.6730
1.6567
1.6453
1.6279
1.6182
1.6004
1.4232
1.3730
0.9086
0.8973
0.8883
0.8763
1b
0.76
9.80
5.99
1.01
0.75
1.00
0.86
3.00
1.04
0.97
2.08
1.06
9.47
5.95
f1 (ppm)

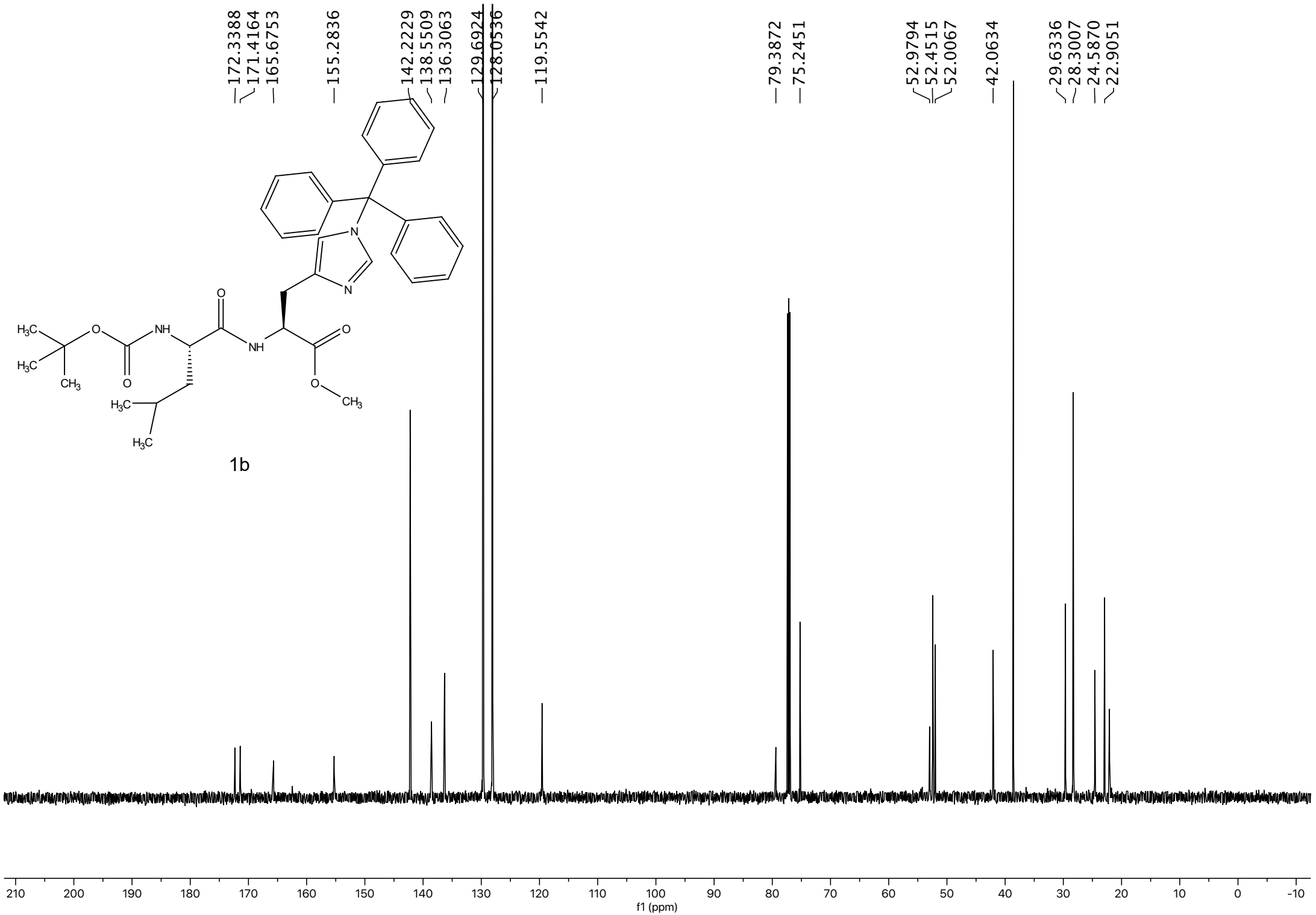
172.3388
171.4164
165.6753
155.2836
142.2229
138.5509
136.3063
129.6924
128.0536
119.5542
79.3872
75.2451
52.9794
52.4515
52.0067
42.0634
29.6336
28.3007
24.5870
22.9051
1b
f1 (ppm)

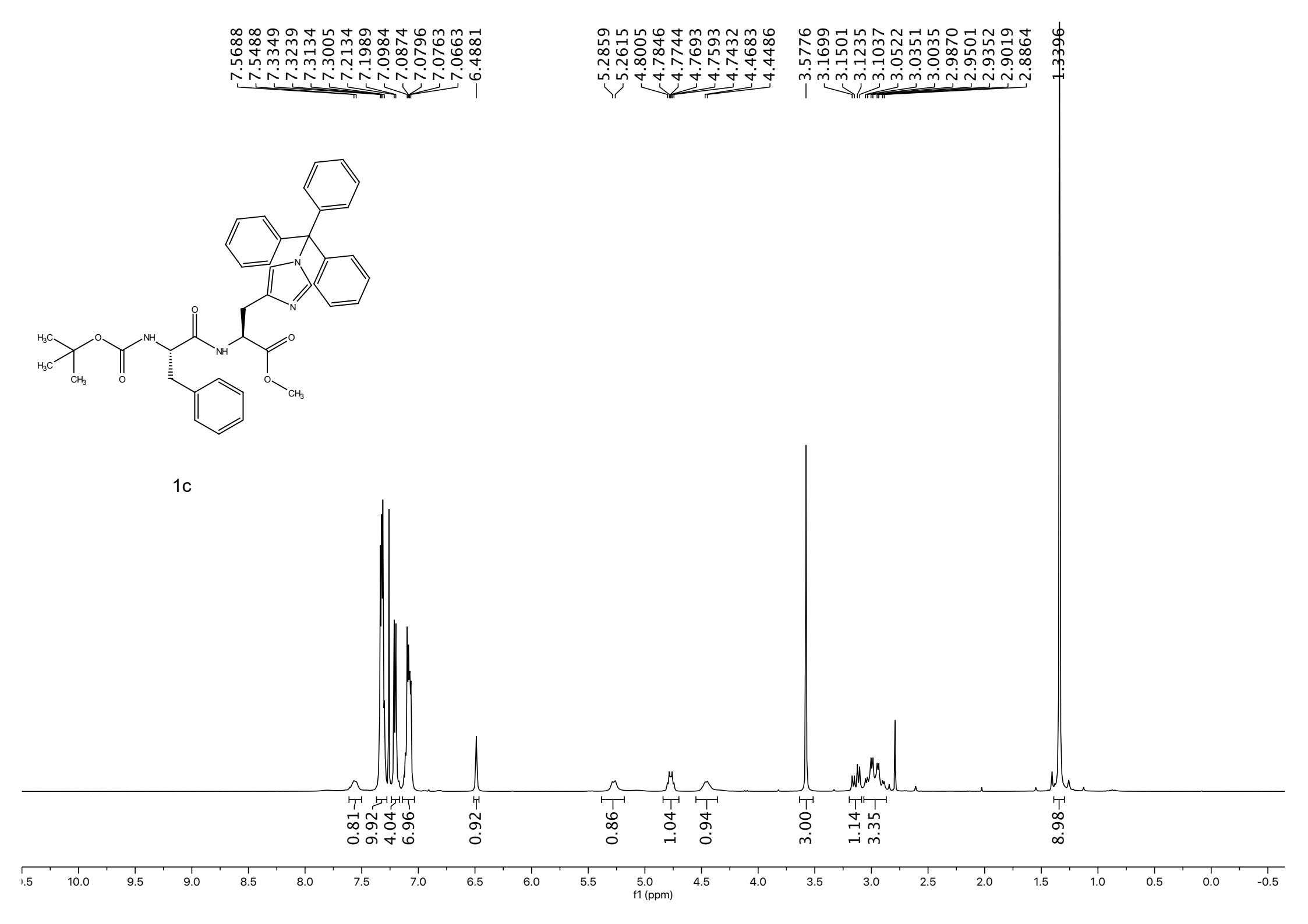
7.5688
7.5488
7.3349
7.3239
7.3134
7.3005
7.2134
7.1989
7.0984
7.0874
7.0796
7.0763
7.0663
6.4881
5.2859
5.2615
4.8005
4.7846
4.7744
4.7693
4.7593
4.7432
4.4683
4.4486
3.5776
3.1699
3.1501
3.1235
3.1037
3.0522
3.0351
3.0035
2.9870
2.9501
2.9352
2.9019
2.8864
1.3396
1c
0.81
9.92
4.04
6.96
0.92
0.86
1.04
0.94
3.00
1.14
3.35
8.98
f1 (ppm)

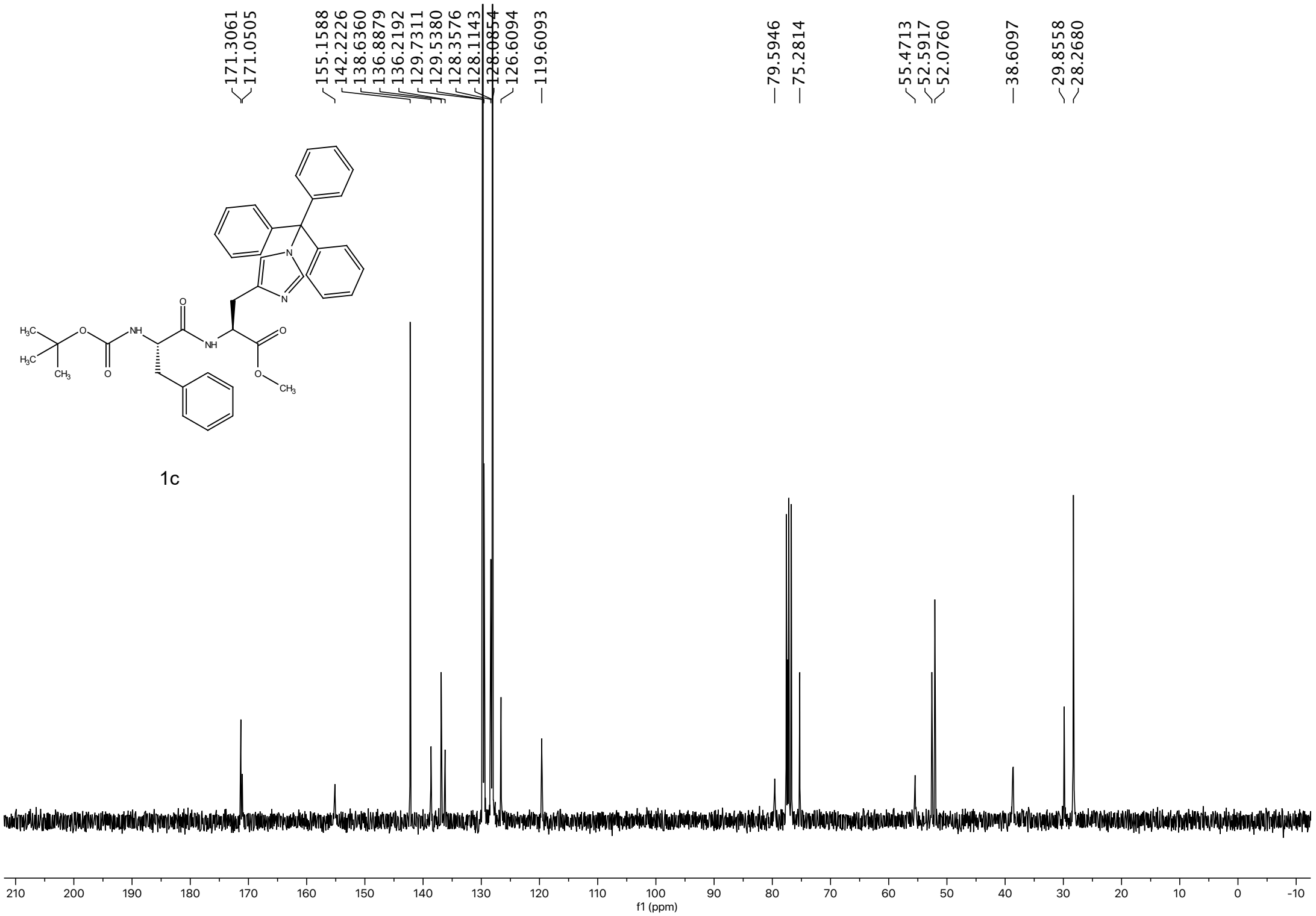
171.3061
171.0505
155.1588
142.2226
138.6360
136.8879
136.2192
129.7311
129.5380
128.3576
128.1143
128.0854
126.6094
119.6093
79.5946
75.2814
55.4713
52.5917
52.0760
38.6097
29.8558
28.2680
1c
f1 (ppm)

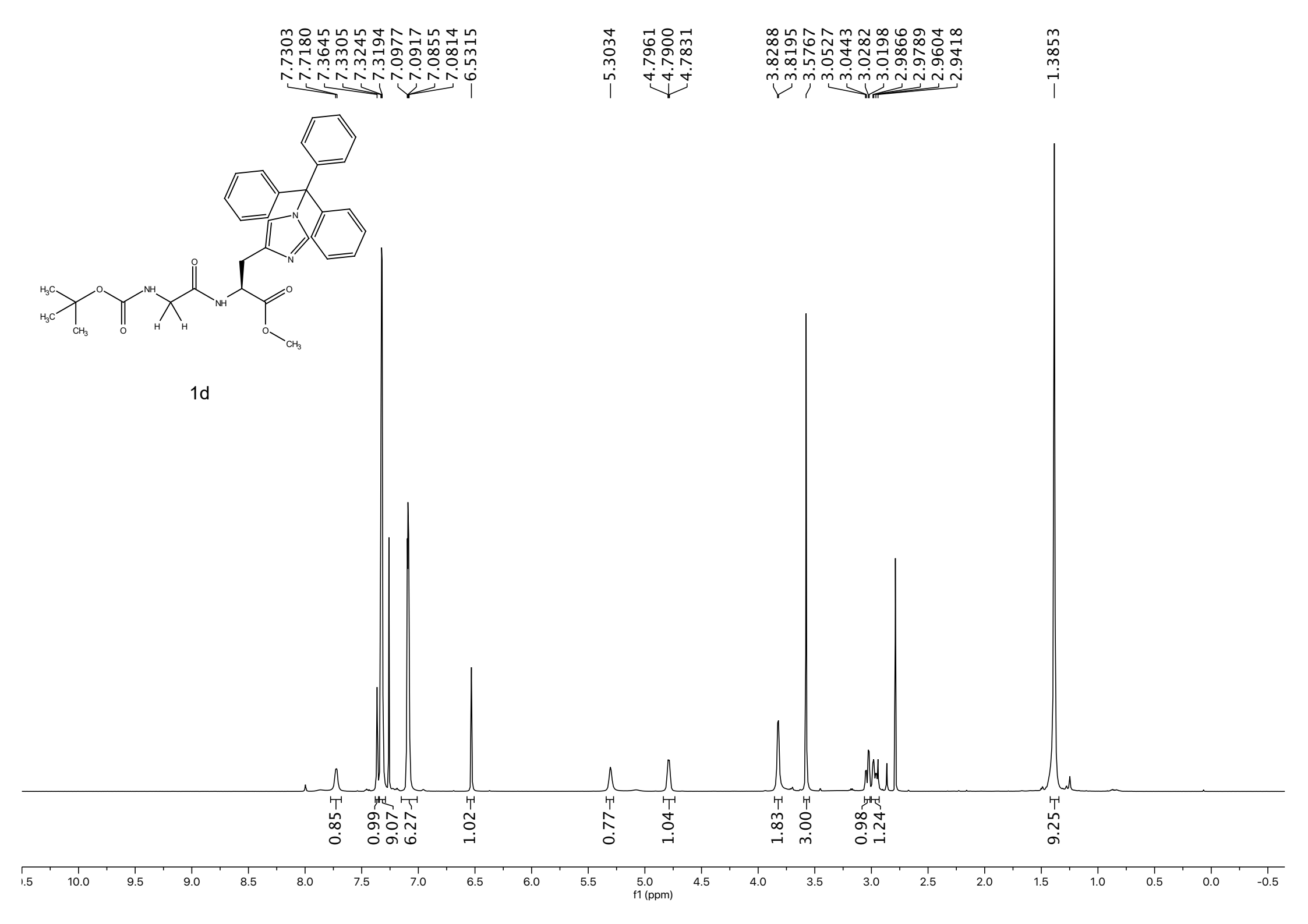
7.7303
7.7180
7.3645
7.3305
7.3245
7.3194
7.0977
7.0917
7.0855
7.0814
6.5315
5.3034
4.7961
4.7900
4.7831
3.8288
3.8195
3.5767
3.0527
3.0443
3.0282
3.0198
2.9866
2.9789
2.9604
2.9418
1.3853
0.85
0.99
9.07
6.27
1.02
0.77
1.04
1.83
3.00
0.98
1.24
9.25
f1 (ppm)

1d

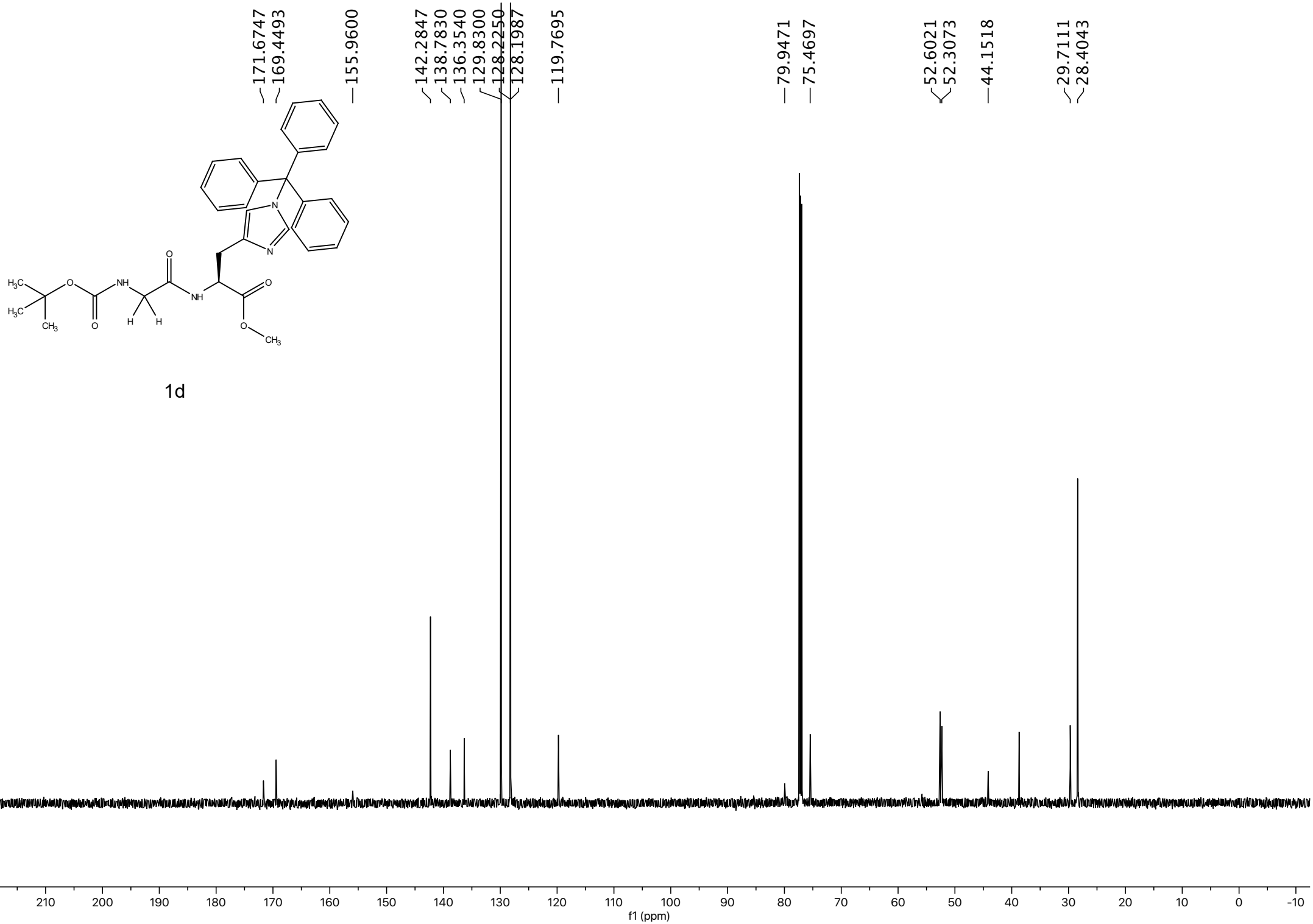
171.6747
169.4493
155.9600
142.2847
138.7830
136.3540
129.8300
128.2250
128.1987
119.7695
79.9471
75.4697
52.6021
52.3073
44.1518
29.7111
28.4043
1d
f1 (ppm)

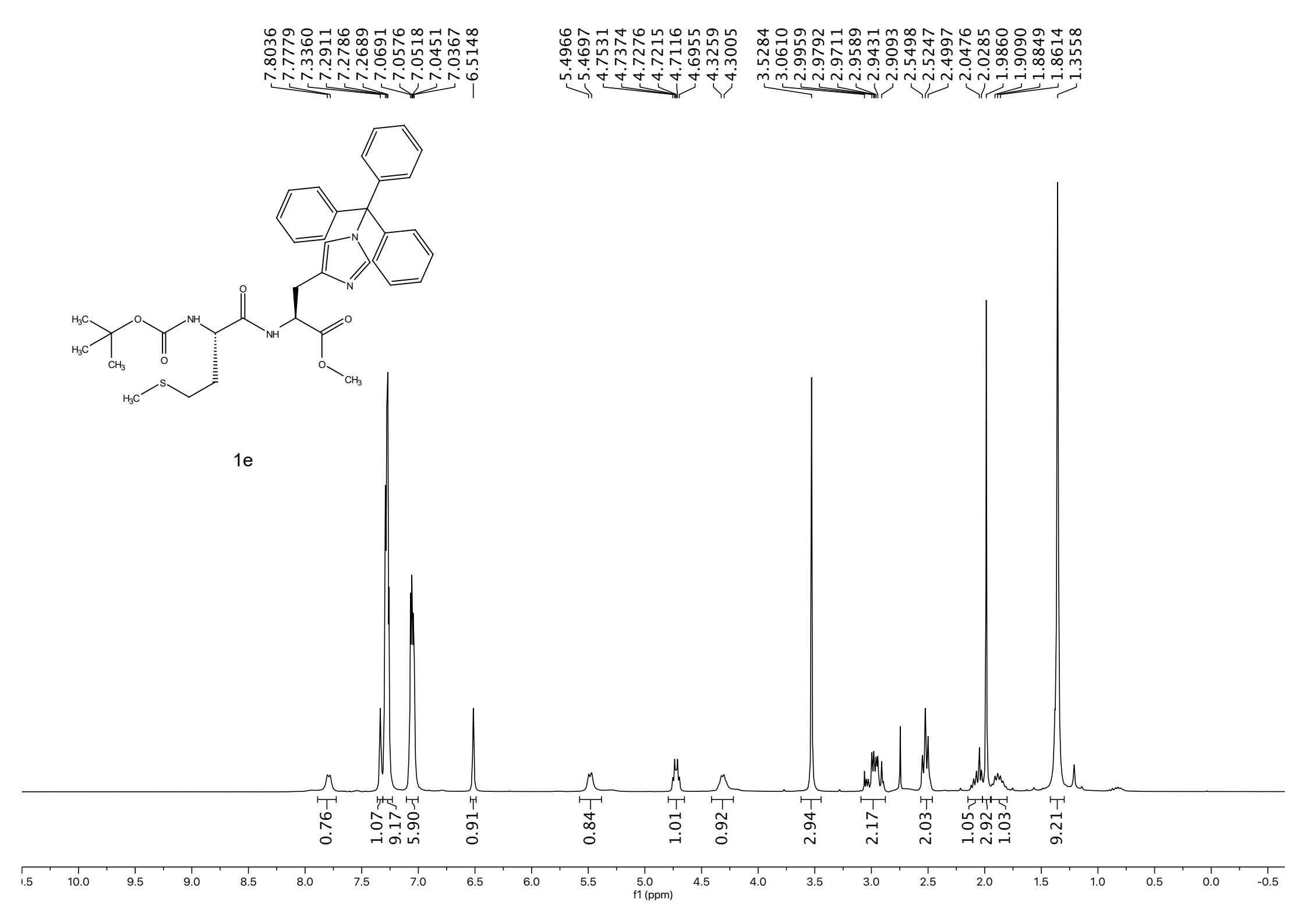
7.8036
7.7779
7.3360
7.2911
7.2786
7.2689
7.0691
7.0576
7.0518
7.0451
7.0367
6.5148
5.4966
5.4697
4.7531
4.7374
4.7276
4.7215
4.7116
4.6955
4.3259
4.3005
3.5284
3.0610
2.9959
2.9792
2.9711
2.9589
2.9431
2.9093
2.5498
2.5247
2.4997
2.0476
2.0285
1.9860
1.9090
1.8849
1.8614
1.3558
1e
0.76
1.07
9.17
5.90
0.91
0.84
1.01
0.92
2.94
2.17
2.03
1.05
2.92
1.03
9.21
f1 (ppm)

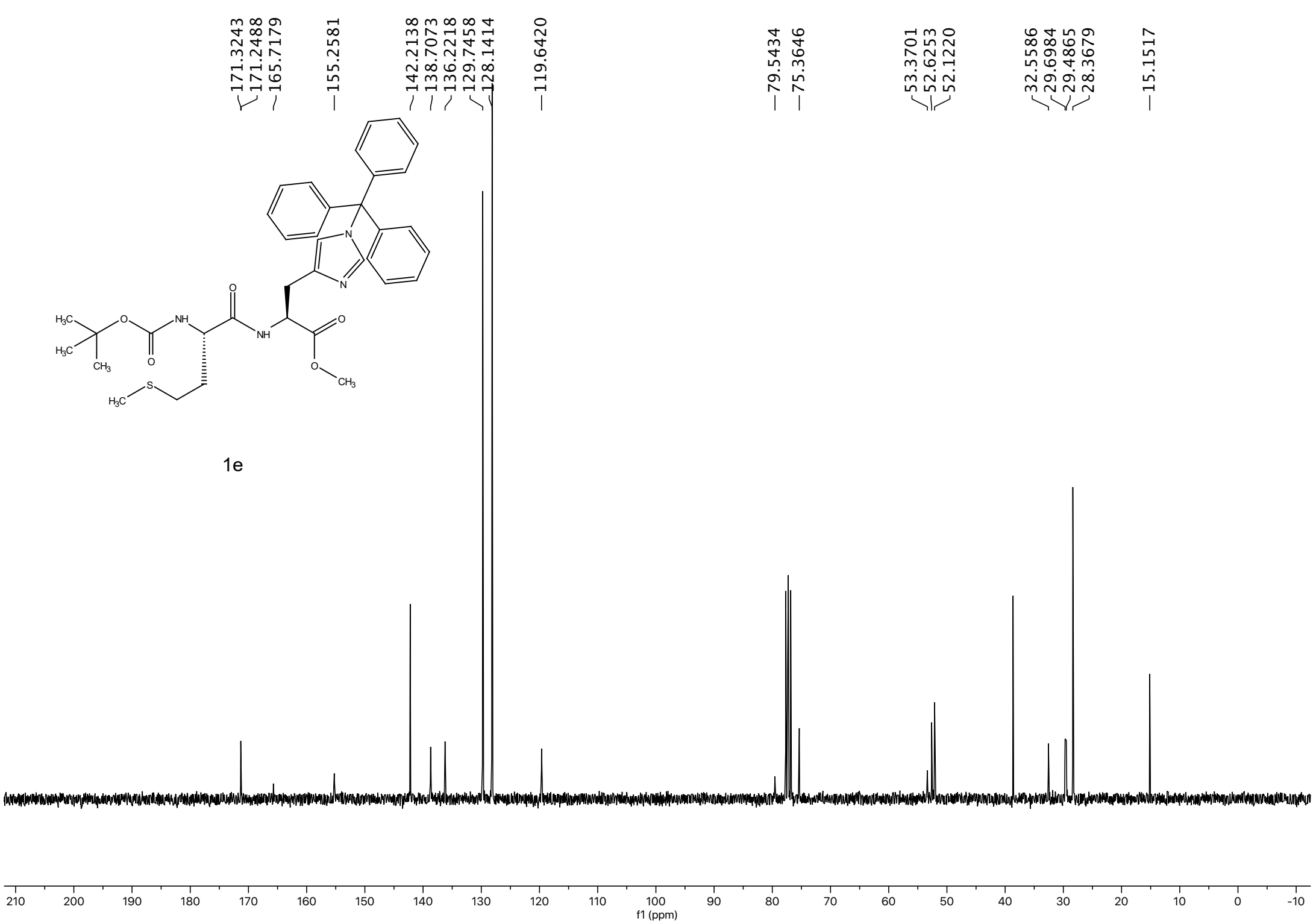
171.3243
171.2488
165.7179
155.2581
142.2138
138.7073
136.2218
129.7458
128.1414
119.6420
79.5434
75.3646
53.3701
52.6253
52.1220
32.5586
29.6984
29.4865
28.3679
15.1517
1e
f1 (ppm)

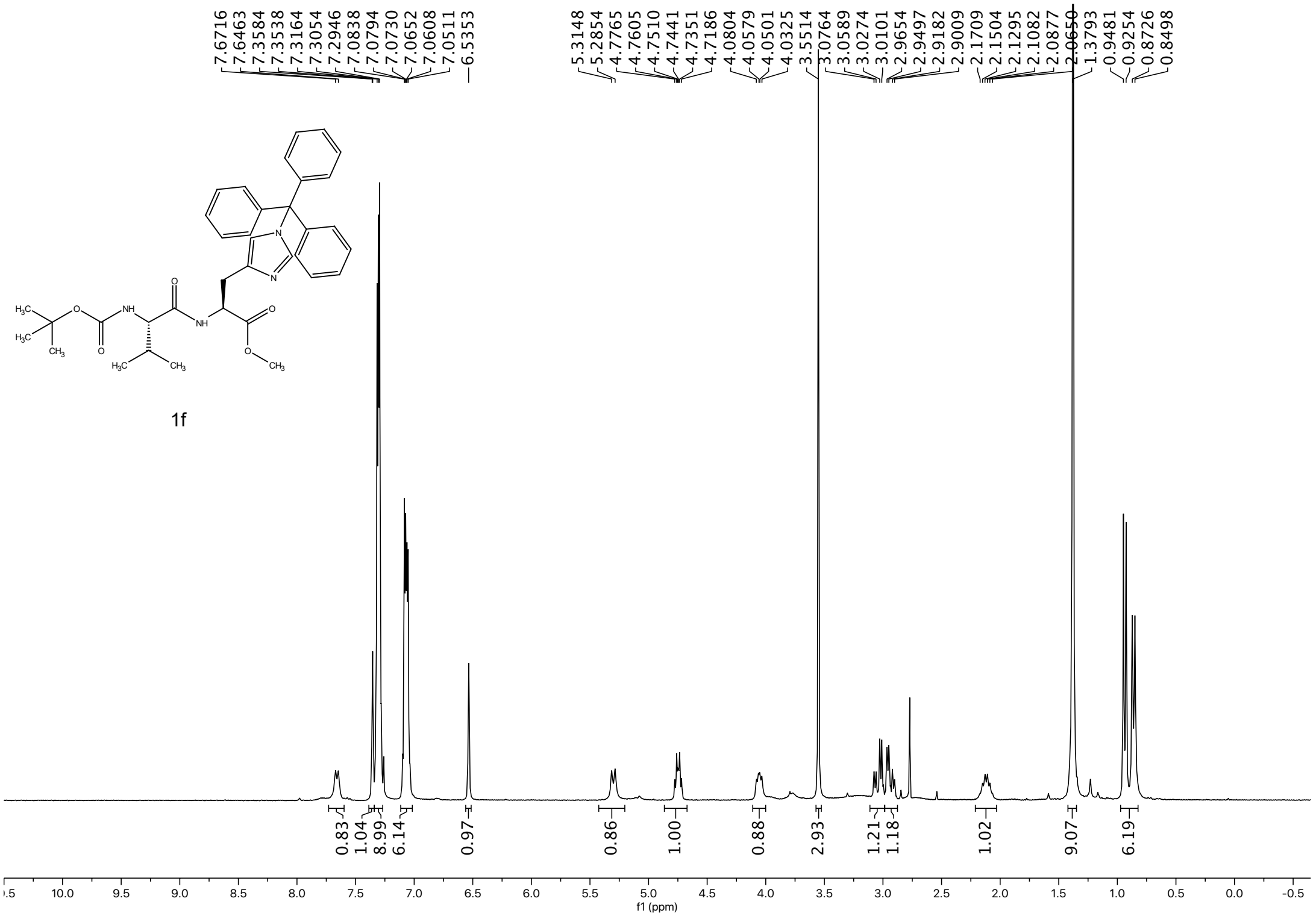
7.6716
7.6463
7.3584
7.3538
7.3164
7.3054
7.2946
7.0838
7.0794
7.0730
7.0652
7.0608
7.0511
6.5353
5.3148
5.2854
4.7765
4.7605
4.7510
4.7441
4.7351
4.7186
4.0804
4.0579
4.0501
4.0325
3.5514
3.0764
3.0589
3.0274
3.0101
2.9654
2.9497
2.9182
2.9009
2.1709
2.1504
2.1295
2.1082
2.0877
2.0650
1.3793
0.9481
0.9254
0.8726
0.8498
0.83
1.04
8.99
6.14
0.97
0.86
1.00
0.88
2.93
1.21
1.18
1.02
9.07
6.19
f1 (ppm)

1f

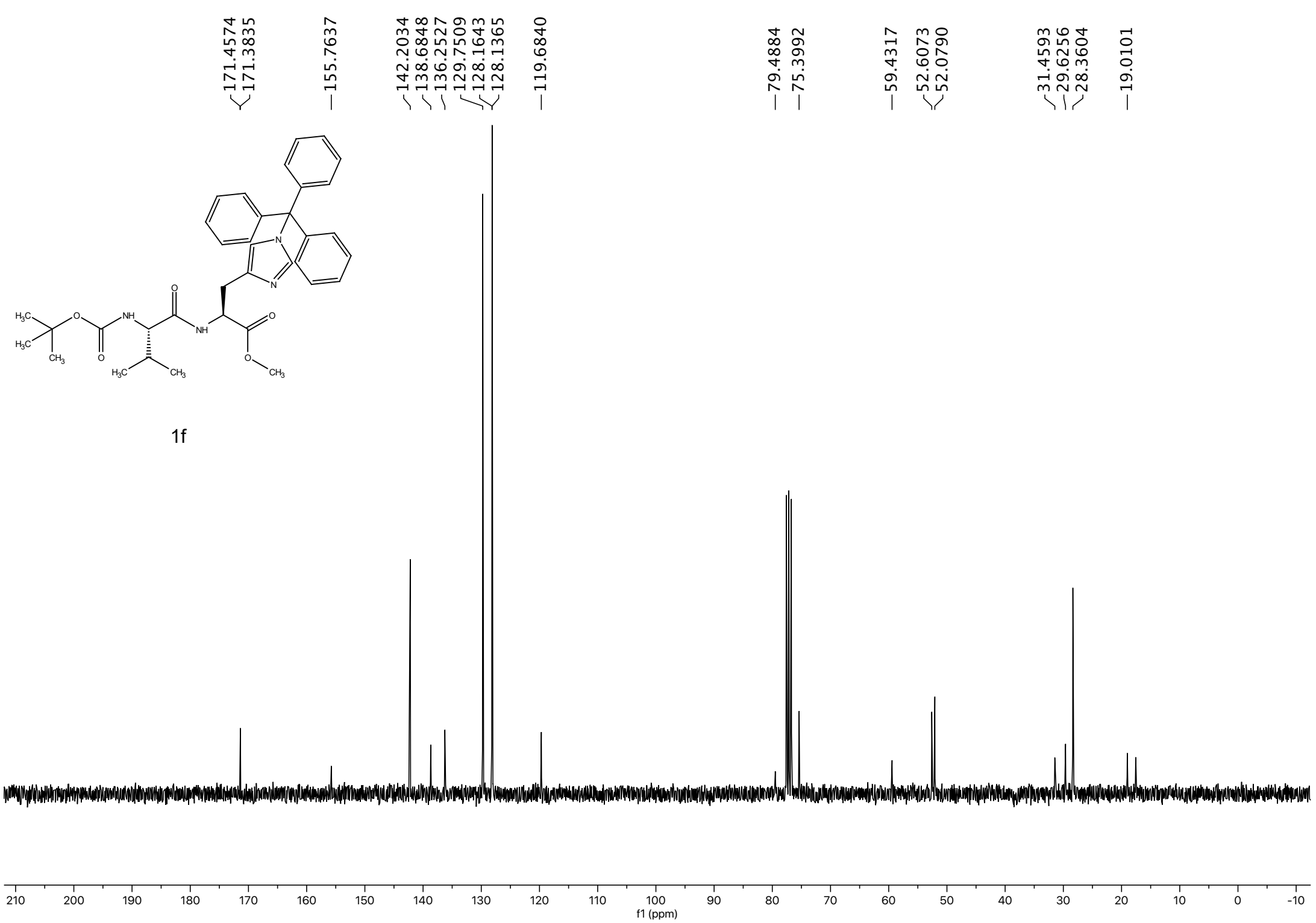
171.4574
171.3835
155.7637
142.2034
138.6848
136.2527
129.7509
128.1643
128.1365
119.6840
79.4884
75.3992
59.4317
52.6073
52.0790
31.4593
29.6256
28.3604
19.0101
1f
f1 (ppm)

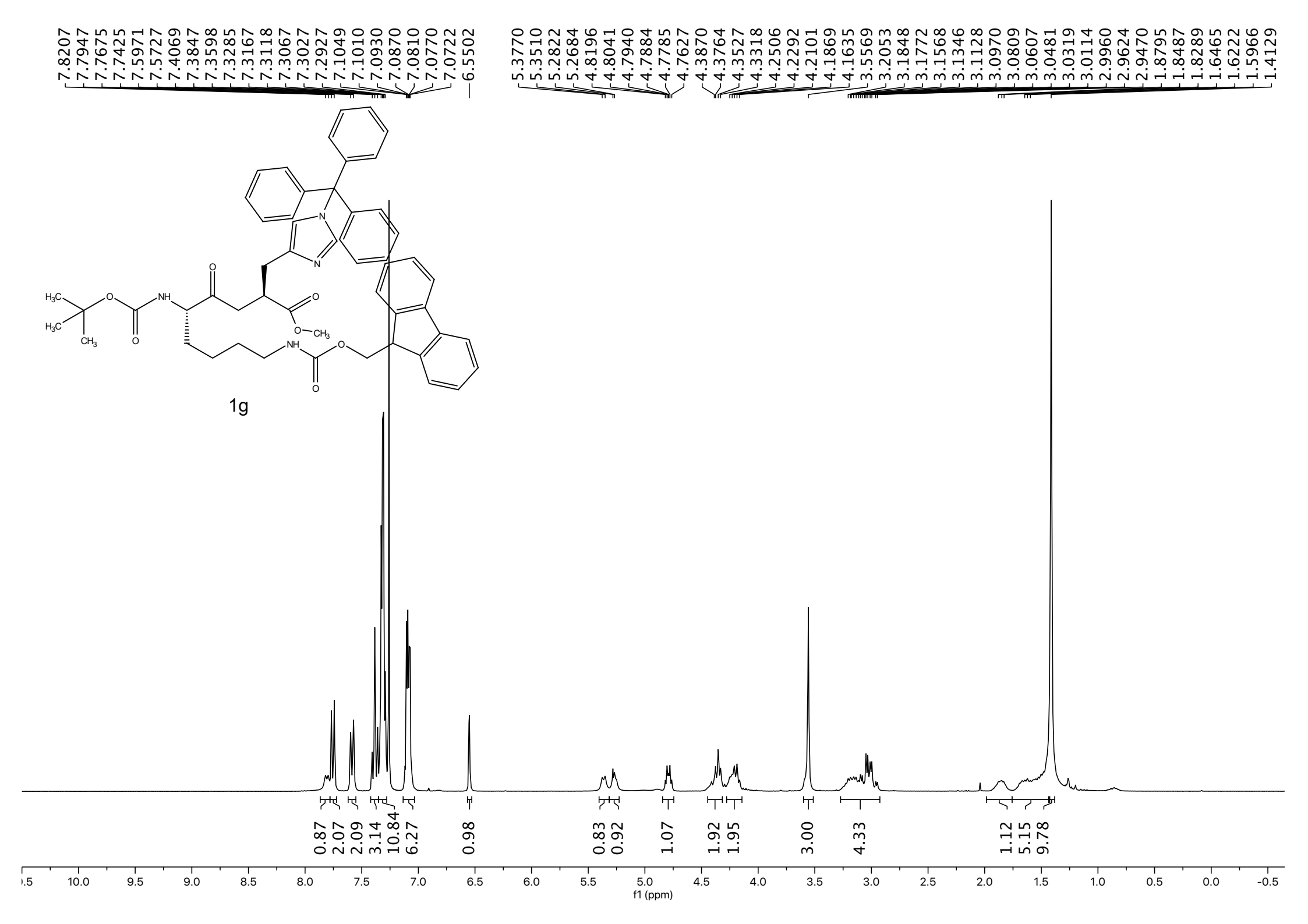
7.8207
7.7947
7.7675
7.7425
7.5971
7.5727
7.4069
7.3847
7.3598
7.3285
7.3167
7.3118
7.3067
7.3027
7.2927
7.1049
7.1010
7.0930
7.0870
7.0810
7.0770
7.0722
6.5502
5.3770
5.3510
5.2822
5.2684
4.8196
4.8041
4.7940
4.7884
4.7785
4.7627
4.3870
4.3764
4.3527
4.3318
4.2506
4.2292
4.2101
4.1869
4.1635
3.5569
3.2053
3.1848
3.1772
3.1568
3.1346
3.1128
3.0970
3.0809
3.0607
3.0481
3.0319
3.0114
2.9960
2.9624
2.9470
1.8795
1.8487
1.8289
1.6465
1.6222
1.5966
1.4129
1g
0.87
2.07
2.09
3.14
10.84
6.27
0.98
0.83
0.92
1.07
1.92
1.95
3.00
4.33
1.12
5.15
9.78
f1 (ppm)

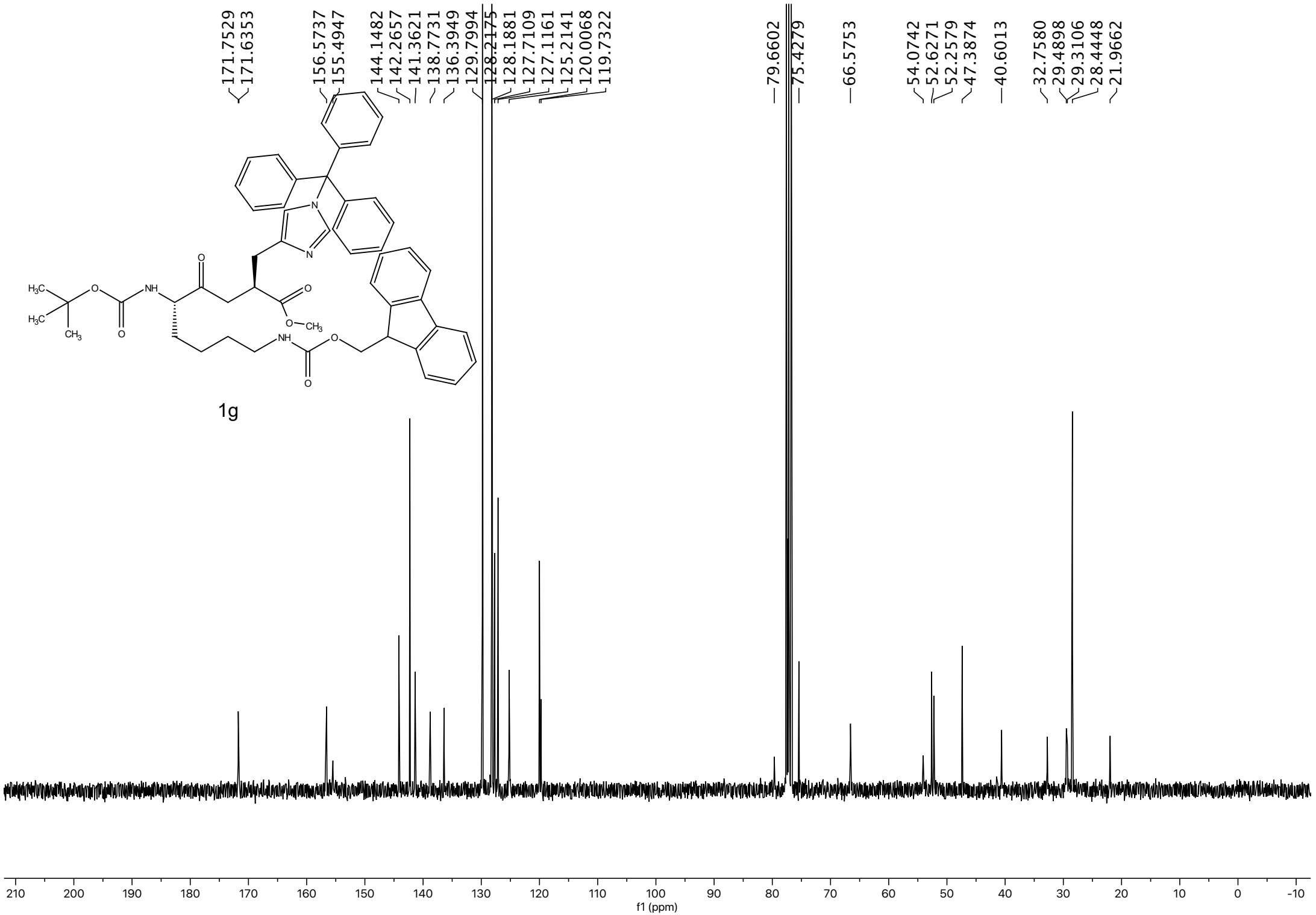
171.7529
171.6353
156.5737
155.4947
144.1482
142.2657
141.3621
138.7731
136.3949
129.7994
128.2175
128.1881
127.7109
127.1161
125.2141
120.0068
119.7322
79.6602
75.4279
66.5753
54.0742
52.6271
52.2579
47.3874
40.6013
32.7580
29.4898
29.3106
28.4448
21.9662
1g
f1 (ppm)

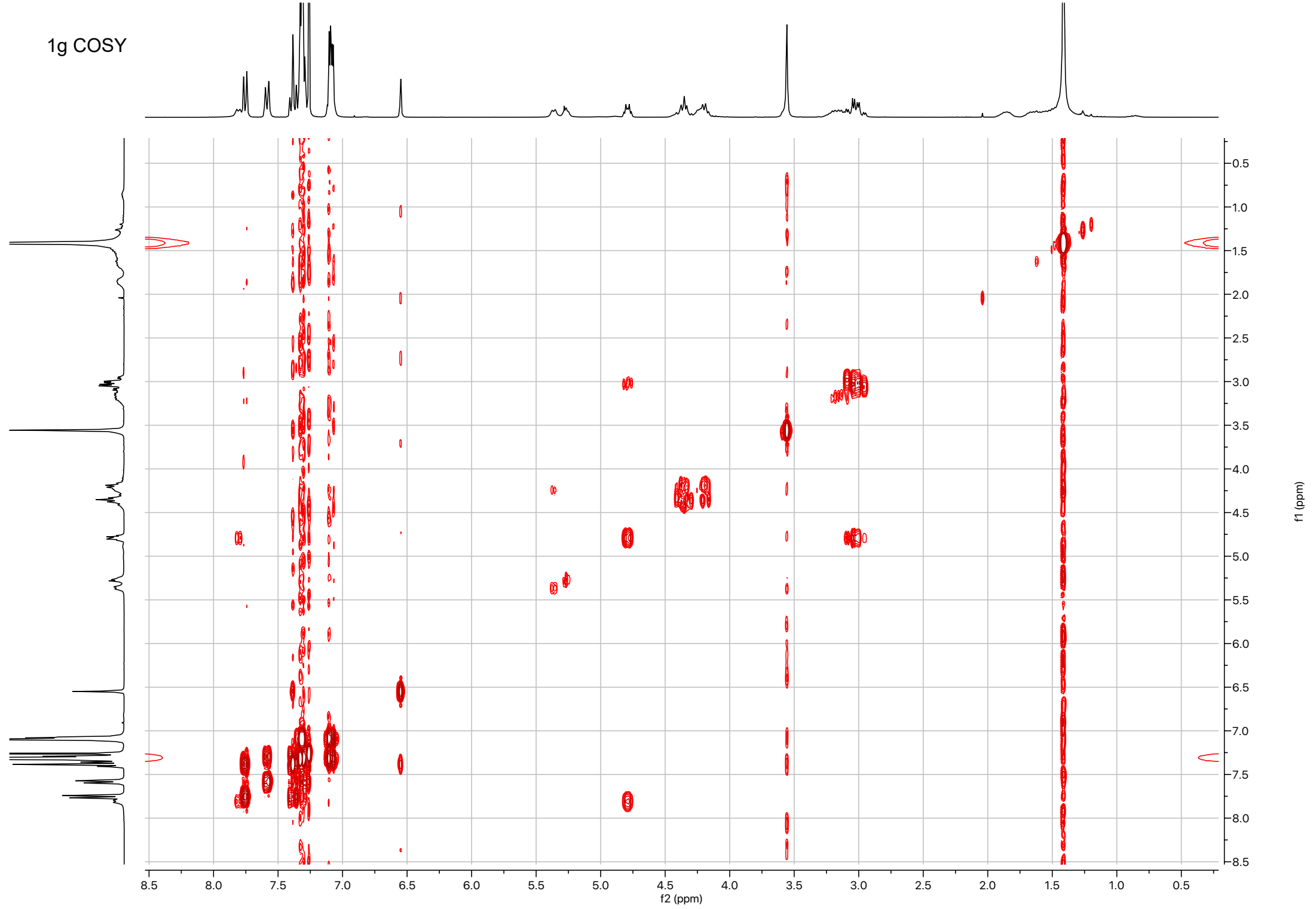
1g COSY
8.5
8.0
7.5
7.0
6.5
6.0
5.5
5.0
4.5
4.0
3.5
3.0
2.5
2.0
1.5
1.0
0.5
f2 (ppm)
0.5
1.0
1.5
2.0
2.5
3.0
3.5
4.0
4.5
5.0
5.5
6.0
6.5
7.0
7.5
8.0
8.5
f1 (ppm)

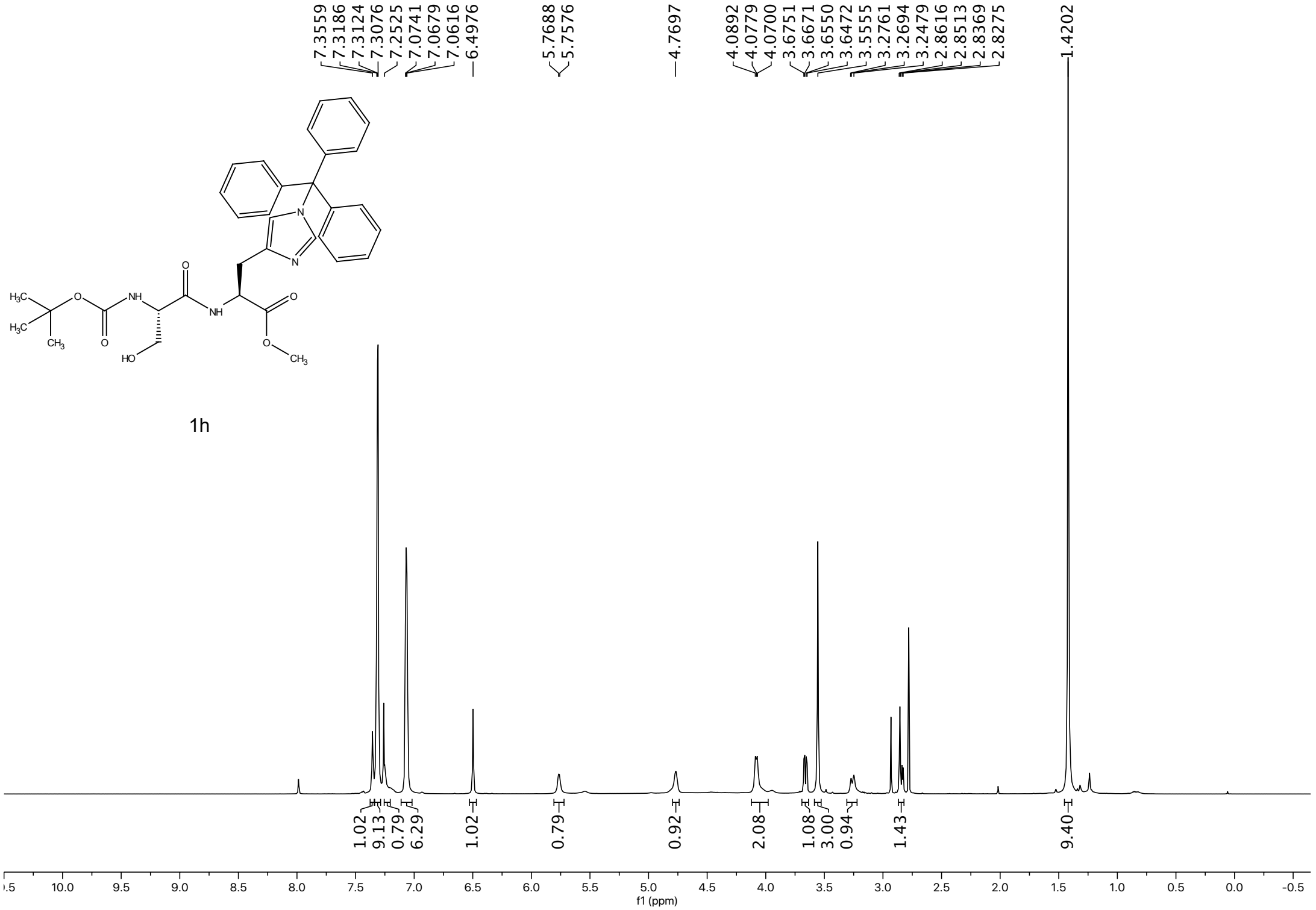
7.3559
7.3186
7.3124
7.3076
7.2525
7.0741
7.0679
7.0616
6.4976
5.7688
5.7576
4.7697
4.0892
4.0779
4.0700
3.6751
3.6671
3.6550
3.6472
3.5555
3.2761
3.2694
3.2479
2.8616
2.8513
2.8369
2.8275
1.4202
1.02
9.13
0.79
6.29
1.02
0.79
0.92
2.08
1.08
3.00
0.94
1.43
9.40
f1 (ppm)

1h

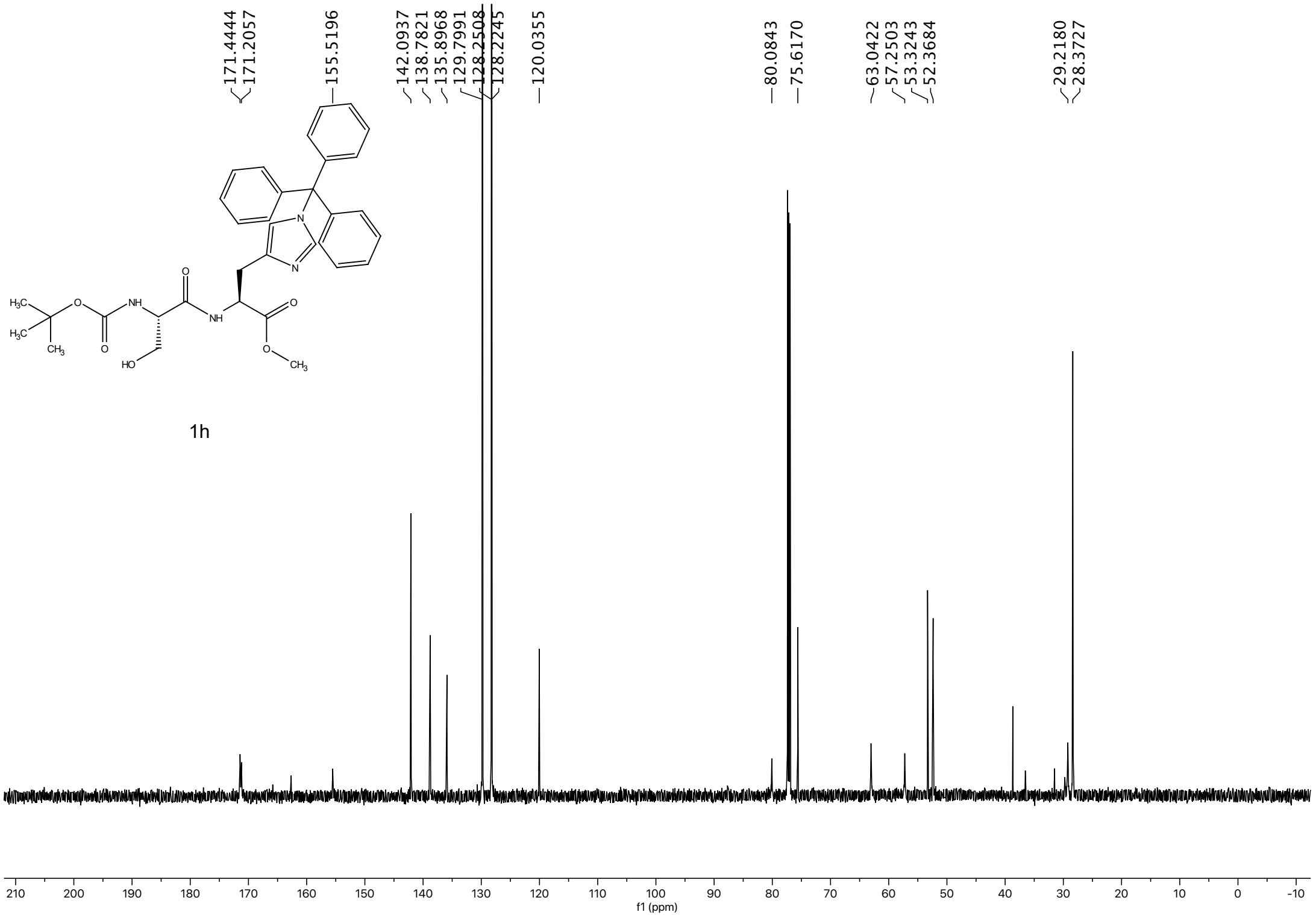
171.4444
171.2057
155.5196
142.0937
138.7821
135.8968
129.7991
128.2508
128.2245
120.0355
80.0843
75.6170
63.0422
57.2503
53.3243
52.3684
29.2180
28.3727
1h
f1 (ppm)

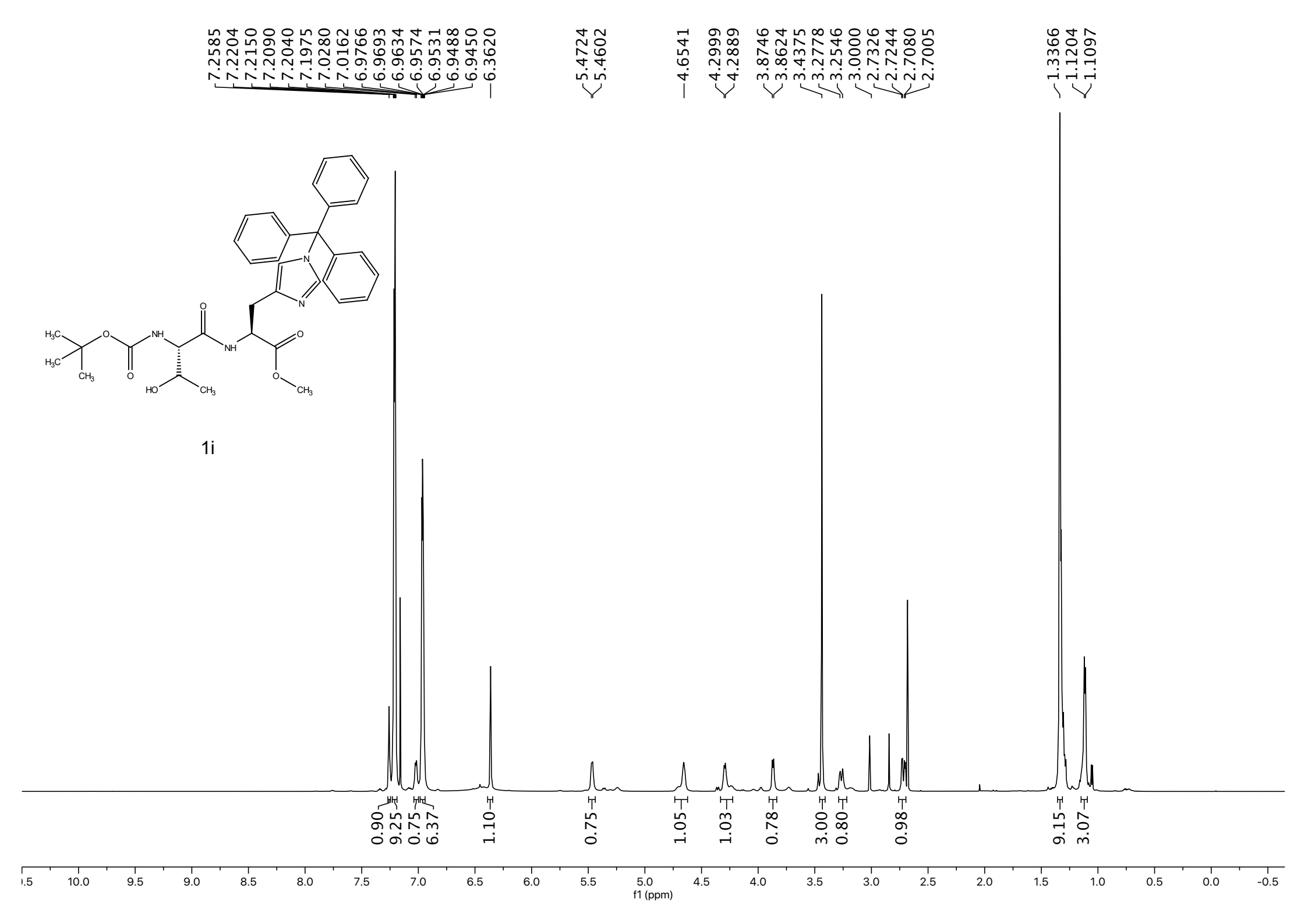
7.2585
7.2204
7.2150
7.2090
7.2040
7.1975
7.0280
7.0162
6.9766
6.9693
6.9634
6.9574
6.9531
6.9488
6.9450
6.3620
5.4724
5.4602
4.6541
4.2999
4.2889
3.8746
3.8624
3.4375
3.2778
3.2546
3.0000
2.7326
2.7244
2.7080
2.7005
1.3366
1.1204
1.1097
0.90
9.25
0.75
6.37
1.10
0.75
1.05
1.03
0.78
3.00
0.80
0.98
9.15
3.07
f1 (ppm)

1i

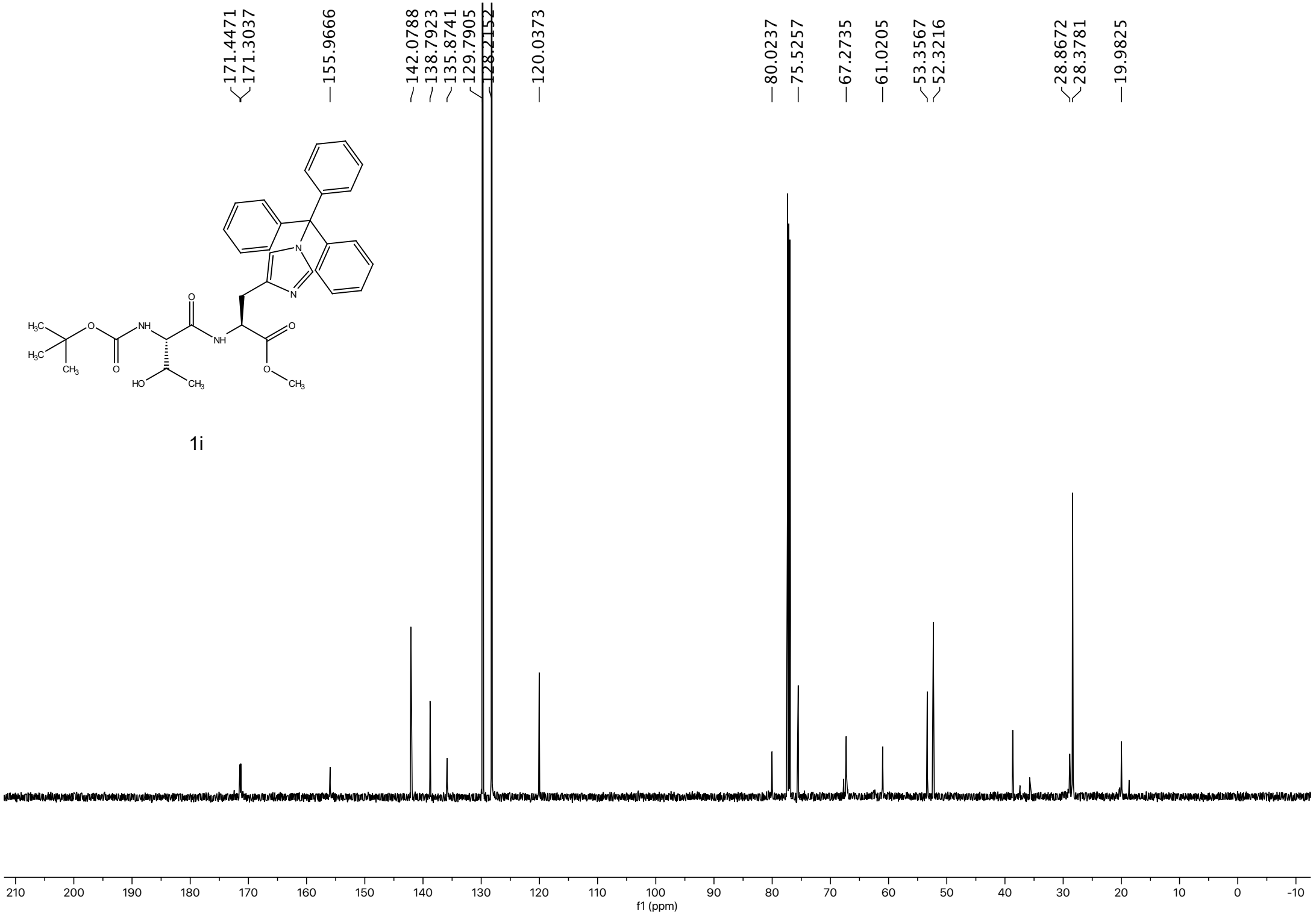
171.4471
171.3037
155.9666
142.0788
138.7923
135.8741
129.7905
128.2152
120.0373
80.0237
75.5257
67.2735
61.0205
53.3567
52.3216
28.8672
28.3781
19.9825
1i
f1 (ppm)

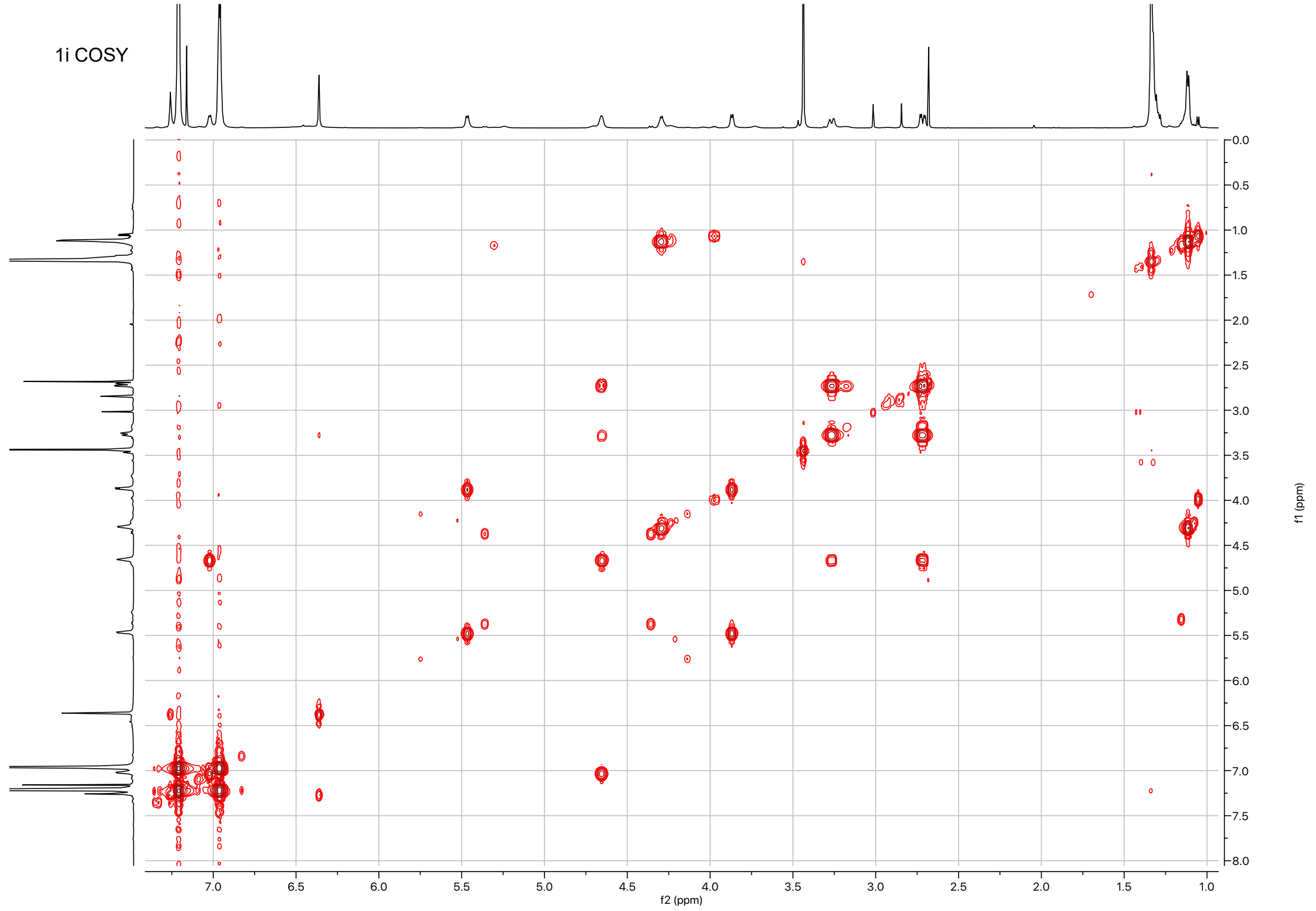
1i COSY
f2 (ppm)
f1 (ppm)

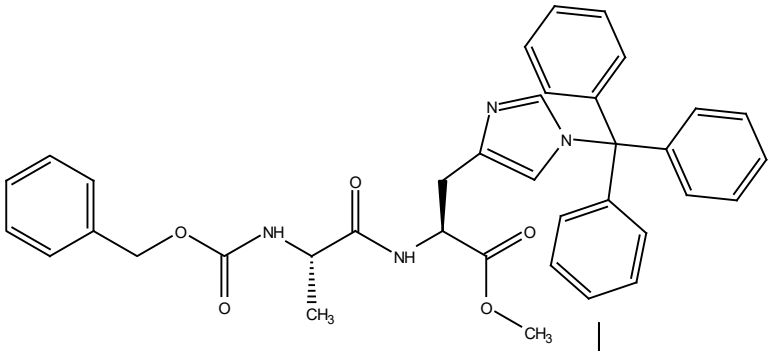
N
N
O
NH
O
NH
O
O
O
CH3
CH3

1j

7.7567
7.7317
7.3492
7.3454
7.2916
7.2548
7.0967
7.0860
6.5422
5.7913
5.7673
5.0923
5.0522
5.0286
4.9867
4.7905
4.7747
4.7639
4.7589
4.7487
4.7324
4.3470
4.3269
4.3038
4.2804
3.5636
2.9998
1.3856
1.3624
0.97
1.28
12.97
0.99
6.30
1.01
0.92
2.06
1.03
0.95
3.00
1.96
3.16
f1 (ppm)

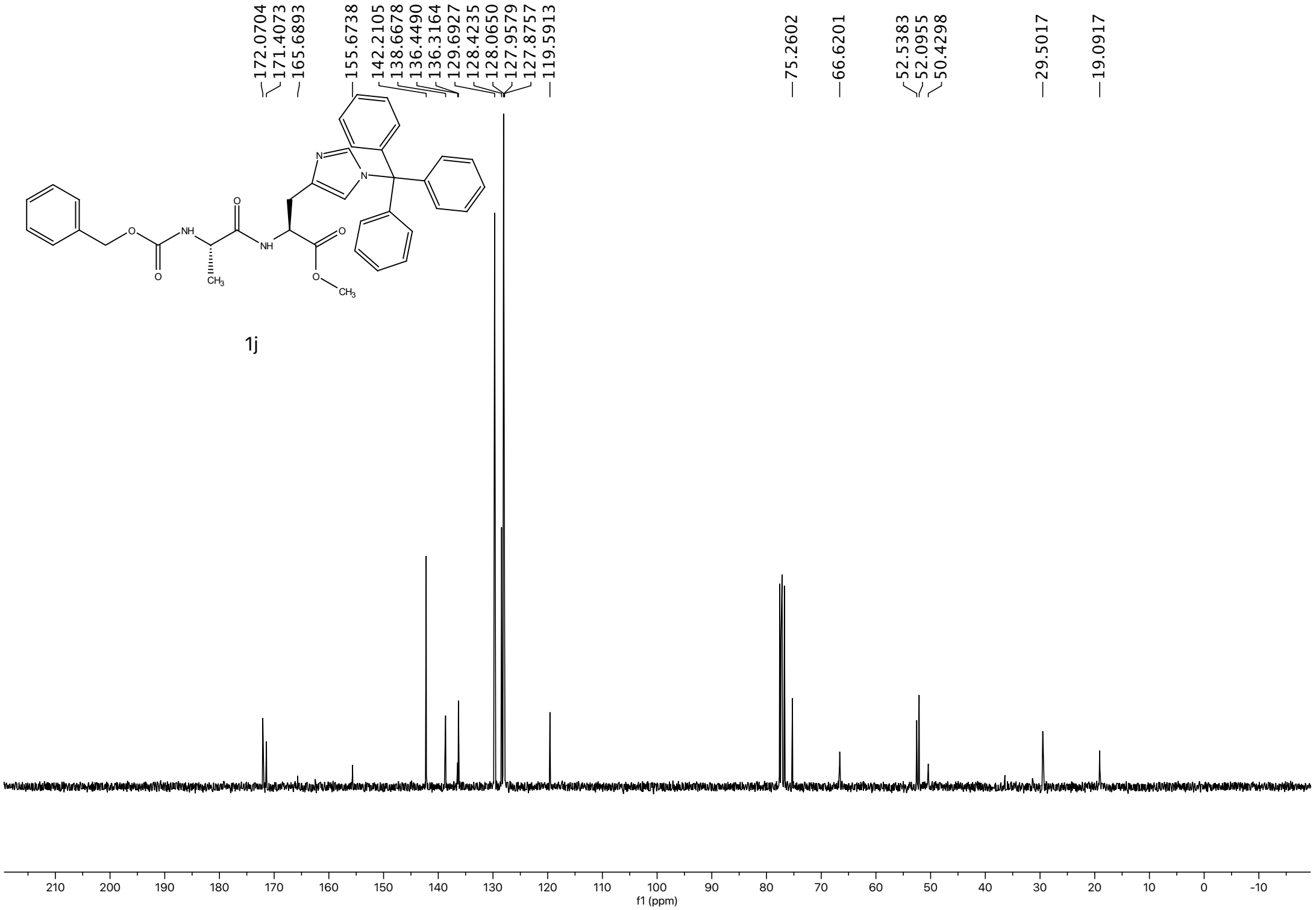
172.0704
171.4073
165.6893
155.6738
142.2105
138.6678
136.4490
136.3164
129.6927
128.4235
128.0650
127.9579
127.8757
119.5913
75.2602
66.6201
52.5383
52.0955
50.4298
29.5017
19.0917
1j
f1 (ppm)

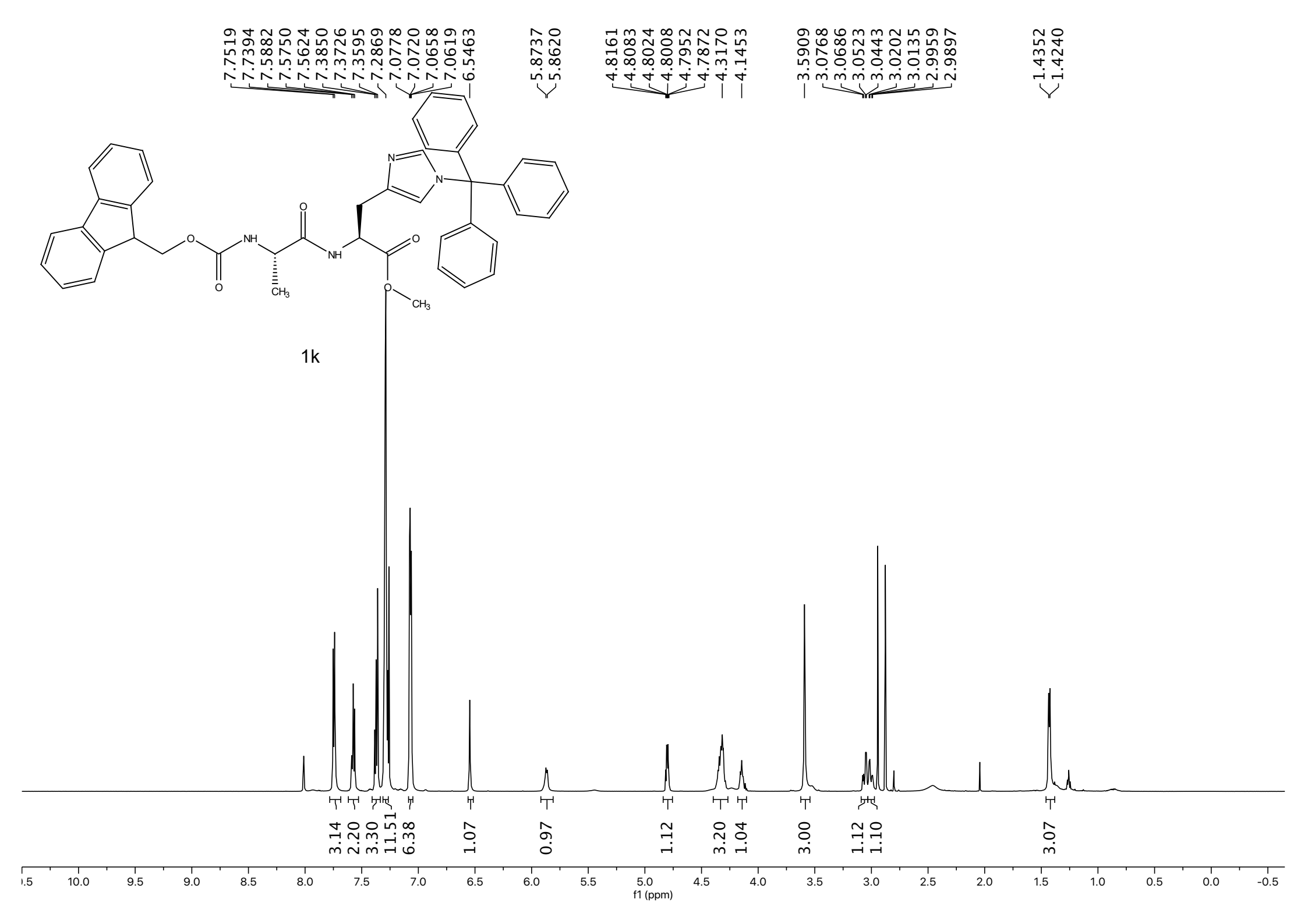
7.7519
7.7394
7.5882
7.5750
7.5624
7.3850
7.3726
7.3595
7.2869
7.0778
7.0720
7.0658
7.0619
6.5463
5.8737
5.8620
4.8161
4.8083
4.8024
4.8008
4.7952
4.7872
4.3170
4.1453
3.5909
3.0768
3.0686
3.0523
3.0443
3.0202
3.0135
2.9959
2.9897
1.4352
1.4240
1k
3.14
2.20
3.30
11.51
6.38
1.07
0.97
1.12
3.20
1.04
3.00
1.12
1.10
3.07
f1 (ppm)

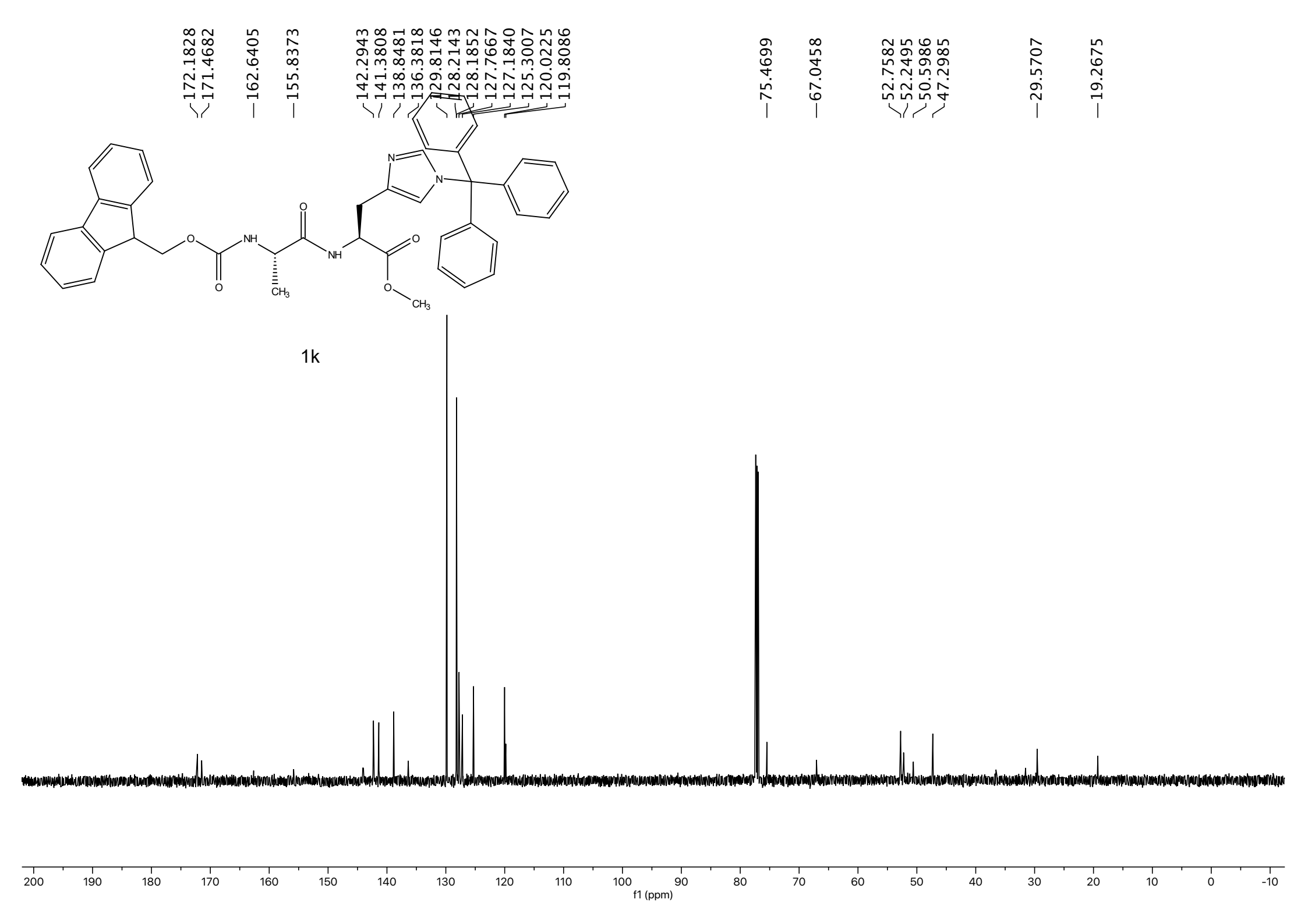
172.1828
171.4682
162.6405
155.8373
142.2943
141.3808
138.8481
136.3818
129.8146
128.2143
128.1852
127.7667
127.1840
125.3007
120.0225
119.8086
75.4699
67.0458
52.7582
52.2495
50.5986
47.2985
29.5707
19.2675
1k
f1 (ppm)

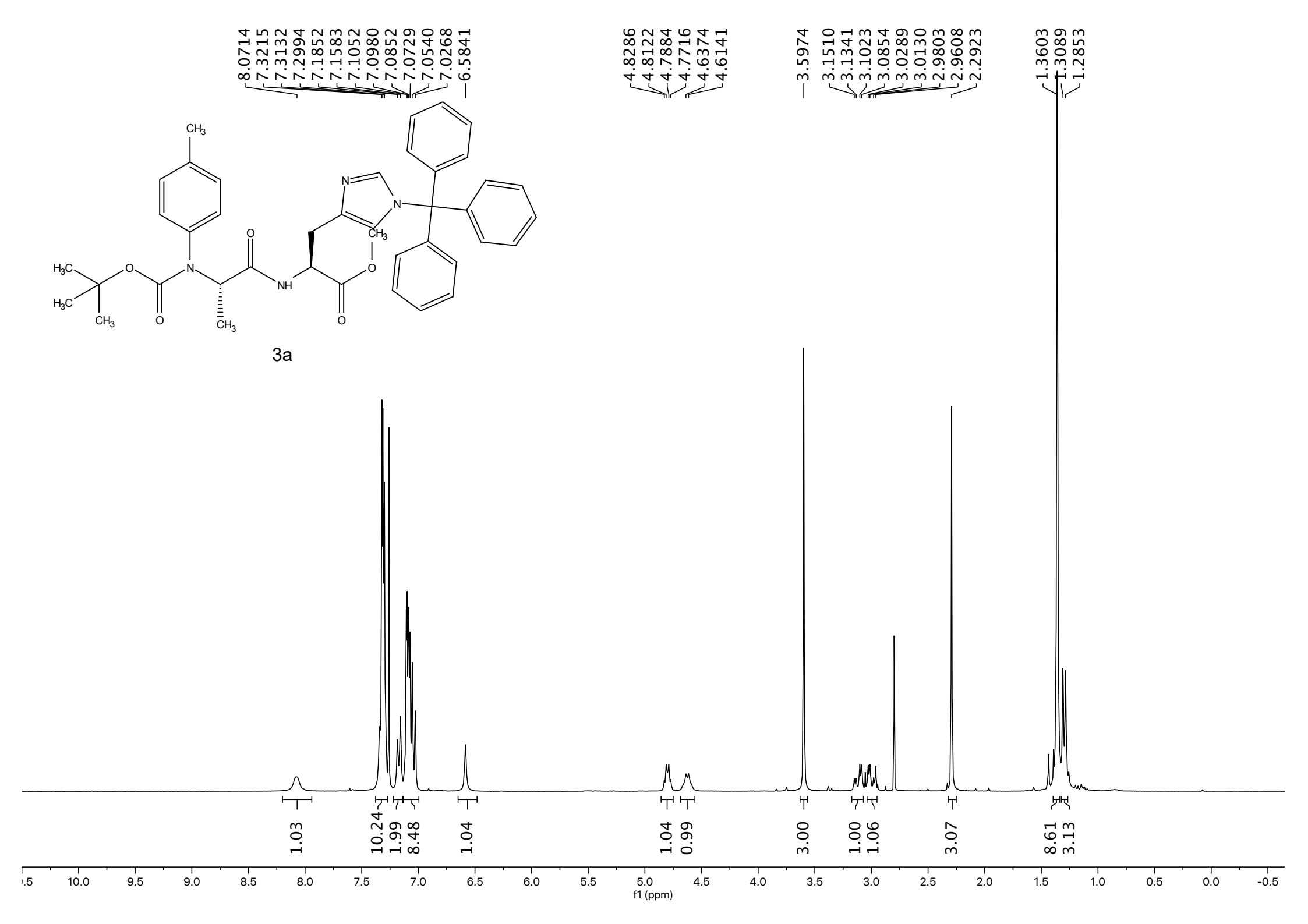
8.0714
7.3215
7.3132
7.2994
7.1852
7.1583
7.1052
7.0980
7.0852
7.0729
7.0540
7.0268
6.5841
4.8286
4.8122
4.7884
4.7716
4.6374
4.6141
3.5974
3.1510
3.1341
3.1023
3.0854
3.0289
3.0130
2.9803
2.9608
2.2923
1.3603
1.3089
1.2853
1.03
10.24
1.99
8.48
1.04
1.04
0.99
3.00
1.00
1.06
3.07
8.61
3.13
f1 (ppm)

3a

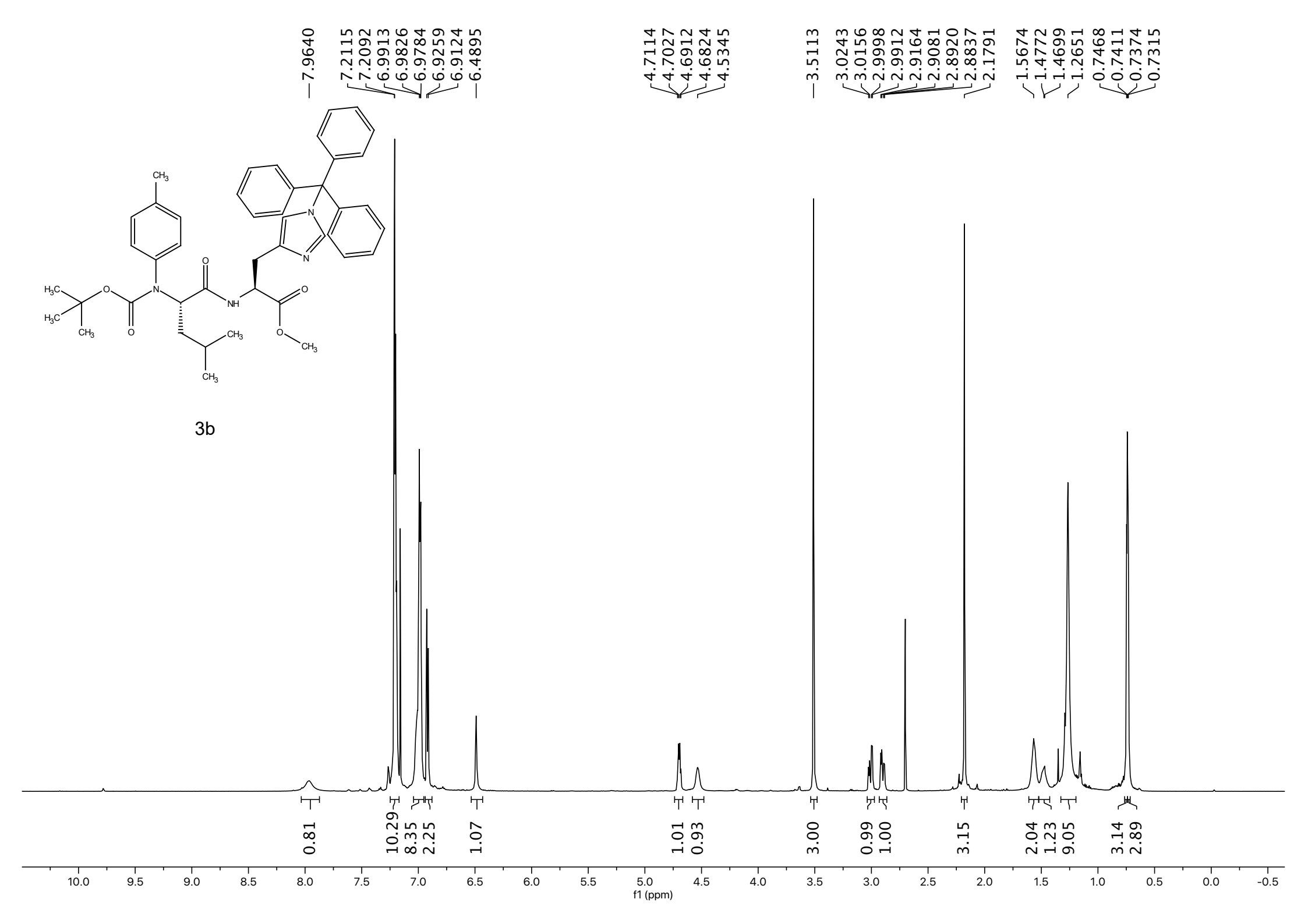
7.9640
7.2115
7.2092
6.9913
6.9826
6.9784
6.9259
6.9124
6.4895
4.7114
4.7027
4.6912
4.6824
4.5345
3.5113
3.0243
3.0156
2.9998
2.9912
2.9164
2.9081
2.8920
2.8837
2.1791
1.5674
1.4772
1.4699
1.2651
0.7468
0.7411
0.7374
0.7315
0.81
10.29
8.35
2.25
1.07
1.01
0.93
3.00
0.99
1.00
3.15
2.04
1.23
9.05
3.14
2.89
f1 (ppm)

3b

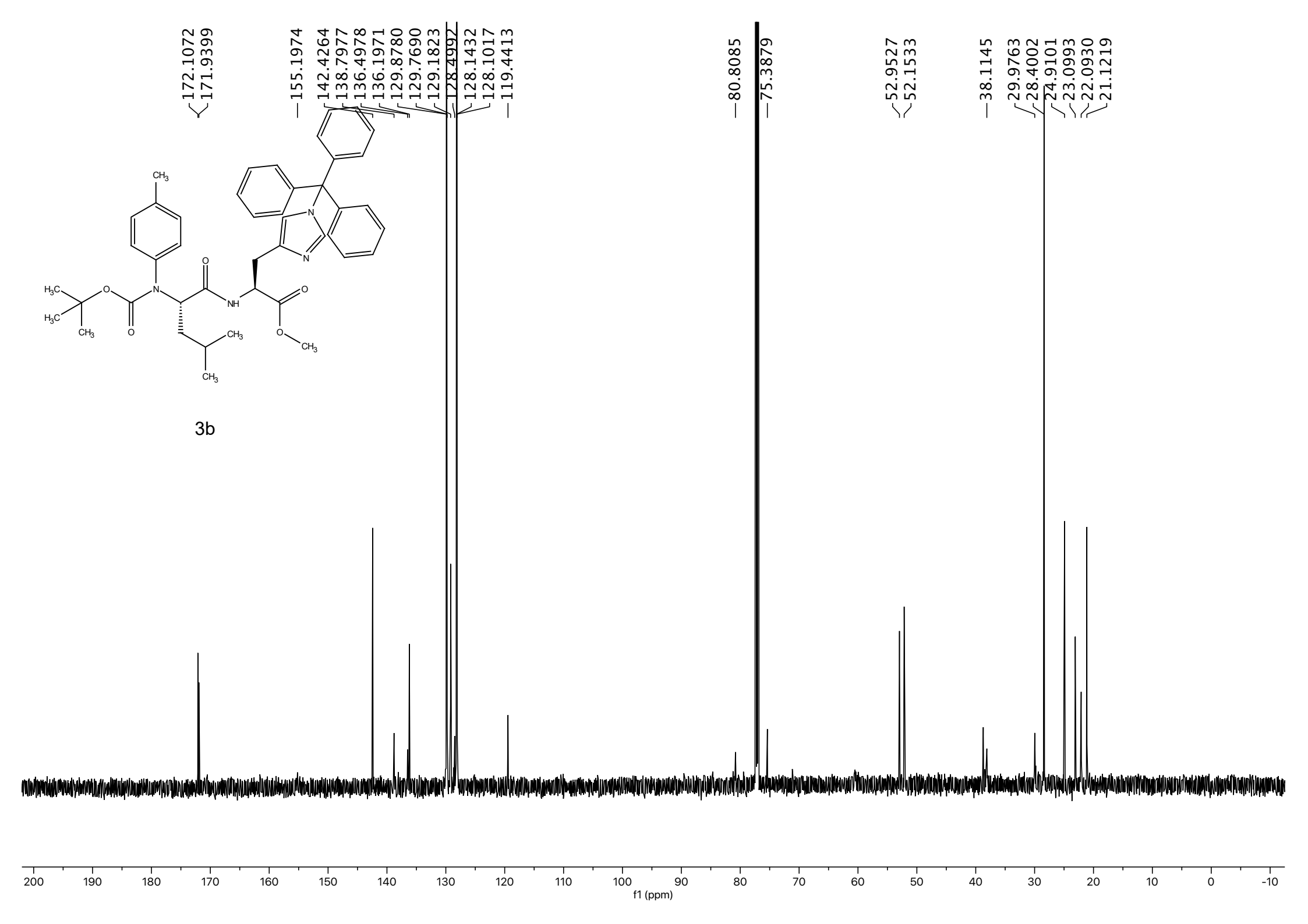
172.1072
171.9399
155.1974
142.4264
138.7977
136.4978
136.1971
129.8780
129.7690
129.1823
128.4992
128.1432
128.1017
119.4413
80.8085
75.3879
52.9527
52.1533
38.1145
29.9763
28.4002
24.9101
23.0993
22.0930
21.1219
3b
f1 (ppm)

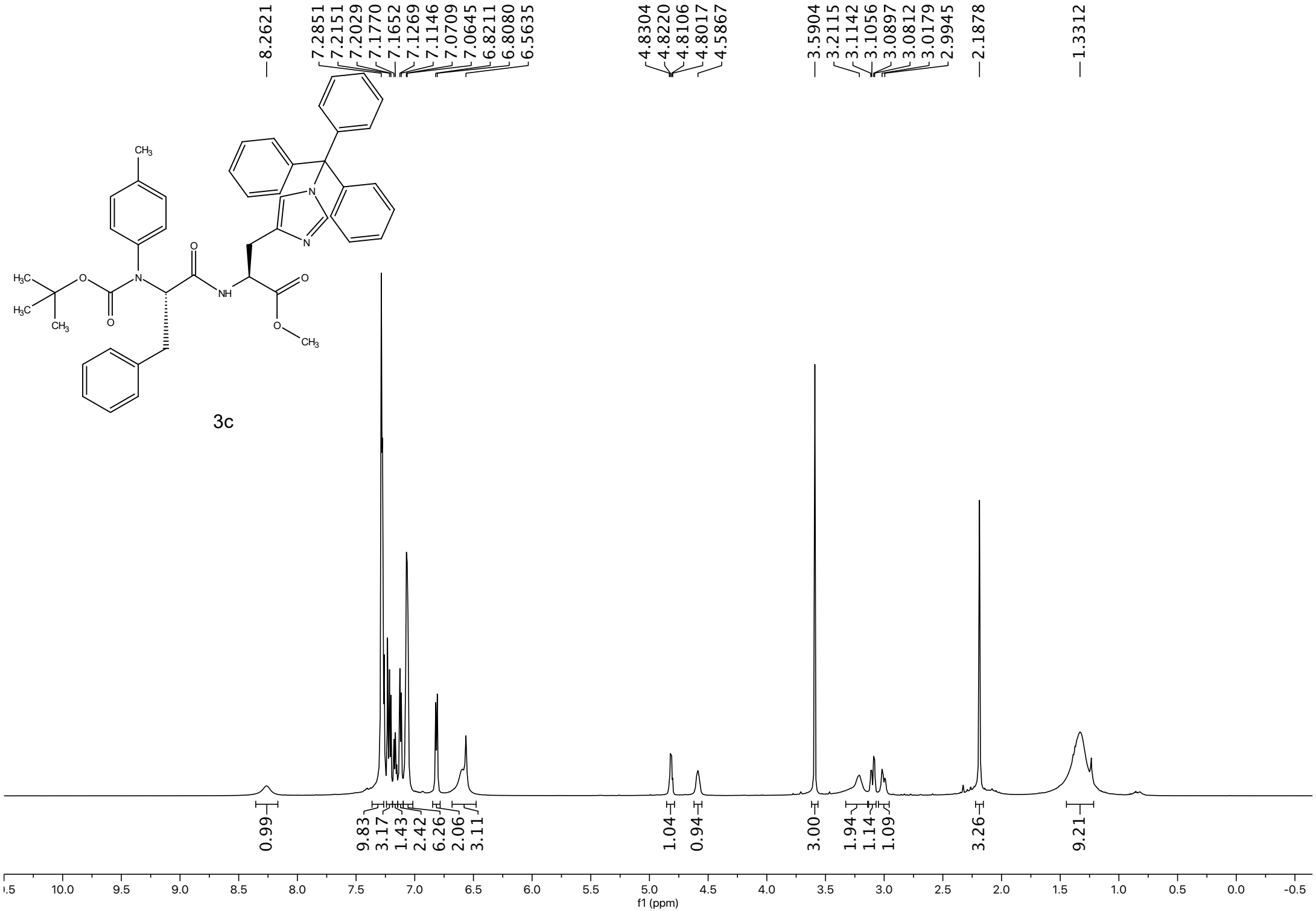
8.2621
7.2851
7.2151
7.2029
7.1770
7.1652
7.1269
7.1146
7.0709
7.0645
6.8211
6.8080
6.5635
4.8304
4.8220
4.8106
4.8017
4.5867
3.5904
3.2115
3.1142
3.1056
3.0897
3.0812
3.0179
2.9945
2.1878
1.3312
0.99
9.83
3.17
1.43
2.42
6.26
2.06
3.11
1.04
0.94
3.00
1.94
1.14
1.09
3.26
9.21
f1 (ppm)

3c

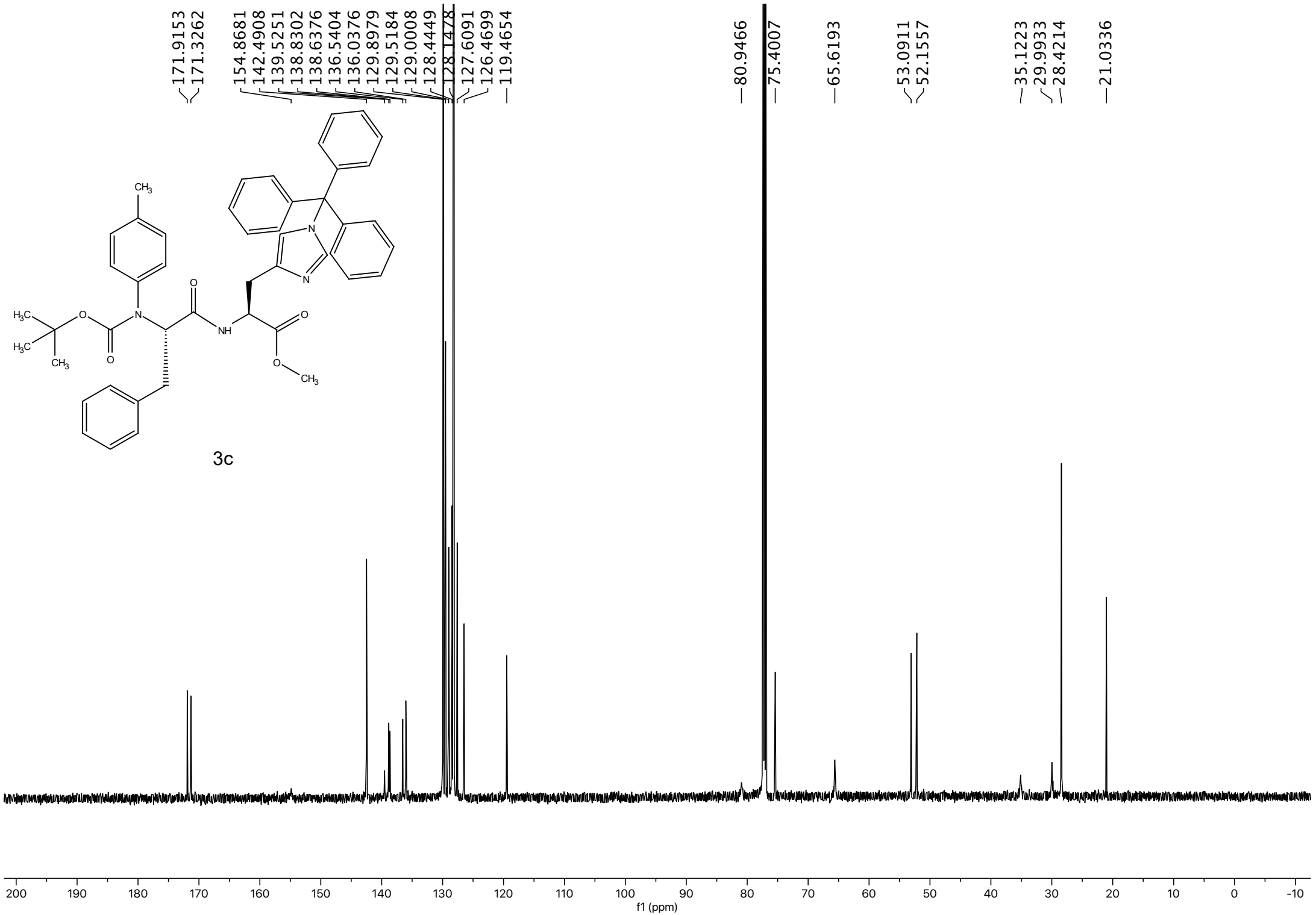
171.9153
171.3262
154.8681
142.4908
139.5251
138.8302
138.6376
136.5404
136.0376
129.8979
129.5184
129.0008
128.4449
128.1478
127.6091
126.4699
119.4654
80.9466
75.4007
65.6193
53.0911
52.1557
35.1223
29.9933
28.4214
21.0336
CH3
N
N
O
O
H3C
O
N
NH
O
H3C
CH3
O
O
CH3
3c
200
190
180
170
160
150
140
130
120
110
100
90
80
70
60
50
40
30
20
10
0
-10
f1 (ppm)

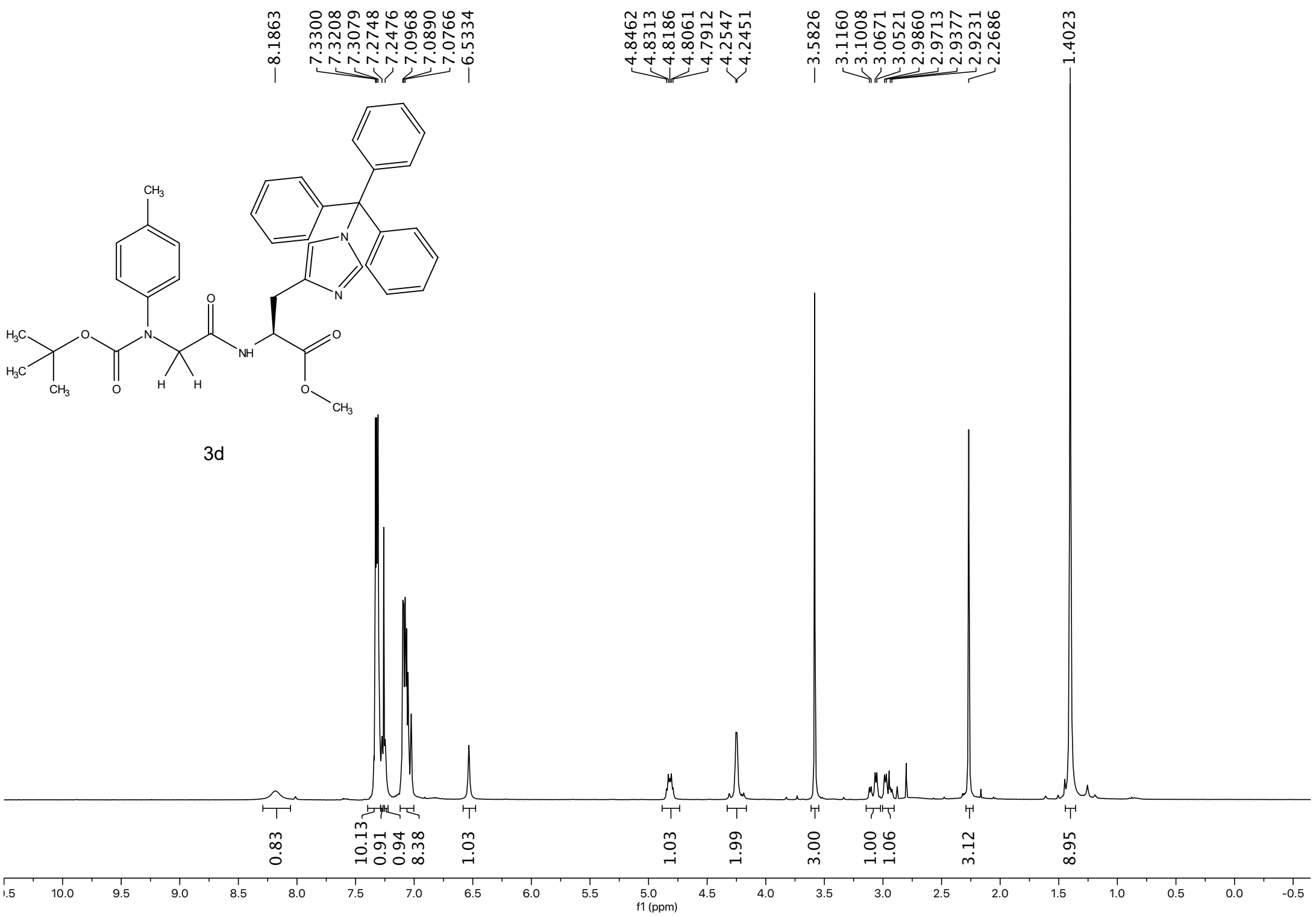
8.1863
7.3300
7.3208
7.3079
7.2748
7.2476
7.0968
7.0890
7.0766
6.5334
4.8462
4.8313
4.8186
4.8061
4.7912
4.2547
4.2451
3.5826
3.1160
3.1008
3.0671
3.0521
2.9860
2.9713
2.9377
2.9231
2.2686
1.4023
0.83
10.13
0.91
0.94
8.38
1.03
1.03
1.99
3.00
1.00
1.06
3.12
8.95
f1 (ppm)

3d

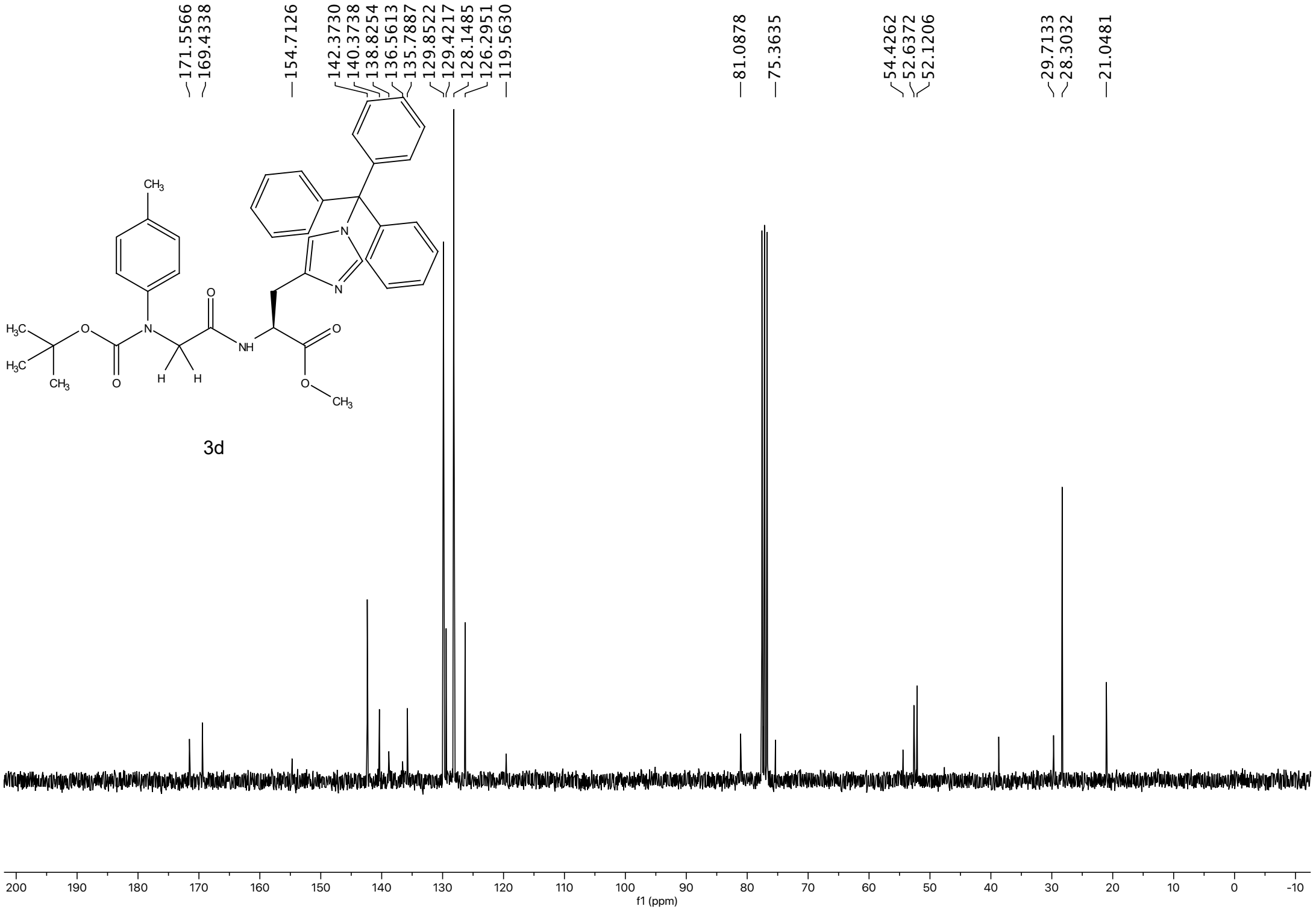
171.5566
169.4338
154.7126
142.3730
140.3738
138.8254
136.5613
135.7887
129.8522
129.4217
128.1485
126.2951
119.5630
81.0878
75.3635
54.4262
52.6372
52.1206
29.7133
28.3032
21.0481
CH3
N
N
O
O
NH
O
O
H3C
H3C
CH3
O
H
H
O
CH3
3d
200
190
180
170
160
150
140
130
120
110
100
90
80
70
60
50
40
30
20
10
0
-10
f1 (ppm)

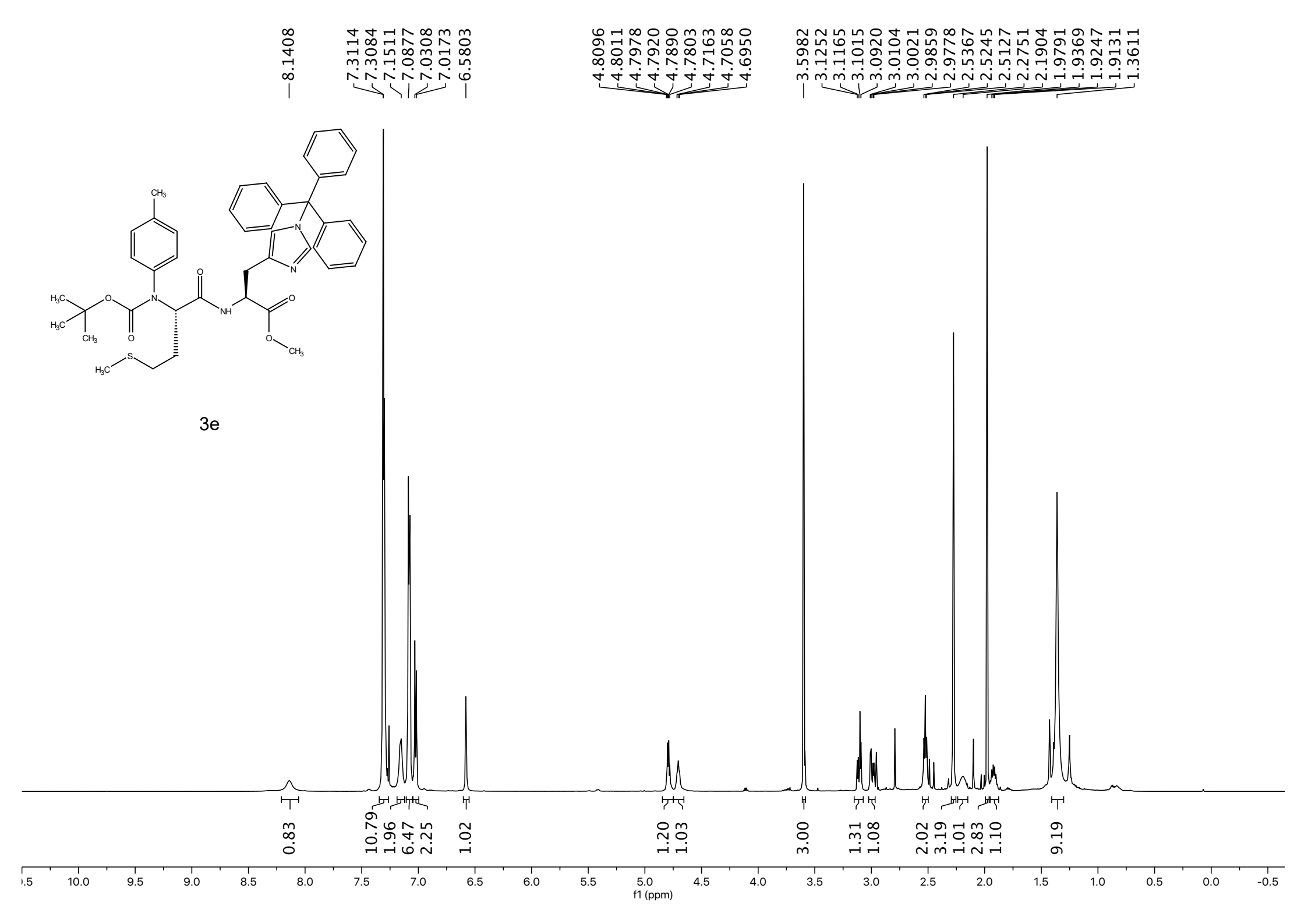
8.1408
7.3114
7.3084
7.1511
7.0877
7.0308
7.0173
6.5803
4.8096
4.8011
4.7978
4.7920
4.7890
4.7803
4.7163
4.7058
4.6950
3.5982
3.1252
3.1165
3.1015
3.0920
3.0104
3.0021
2.9859
2.9778
2.5367
2.5245
2.5127
2.2751
2.1904
1.9791
1.9369
1.9247
1.9131
1.3611
0.83
10.79
1.96
6.47
2.25
1.02
1.20
1.03
3.00
1.31
1.08
2.02
3.19
1.01
2.83
1.10
9.19
f1 (ppm)

3e

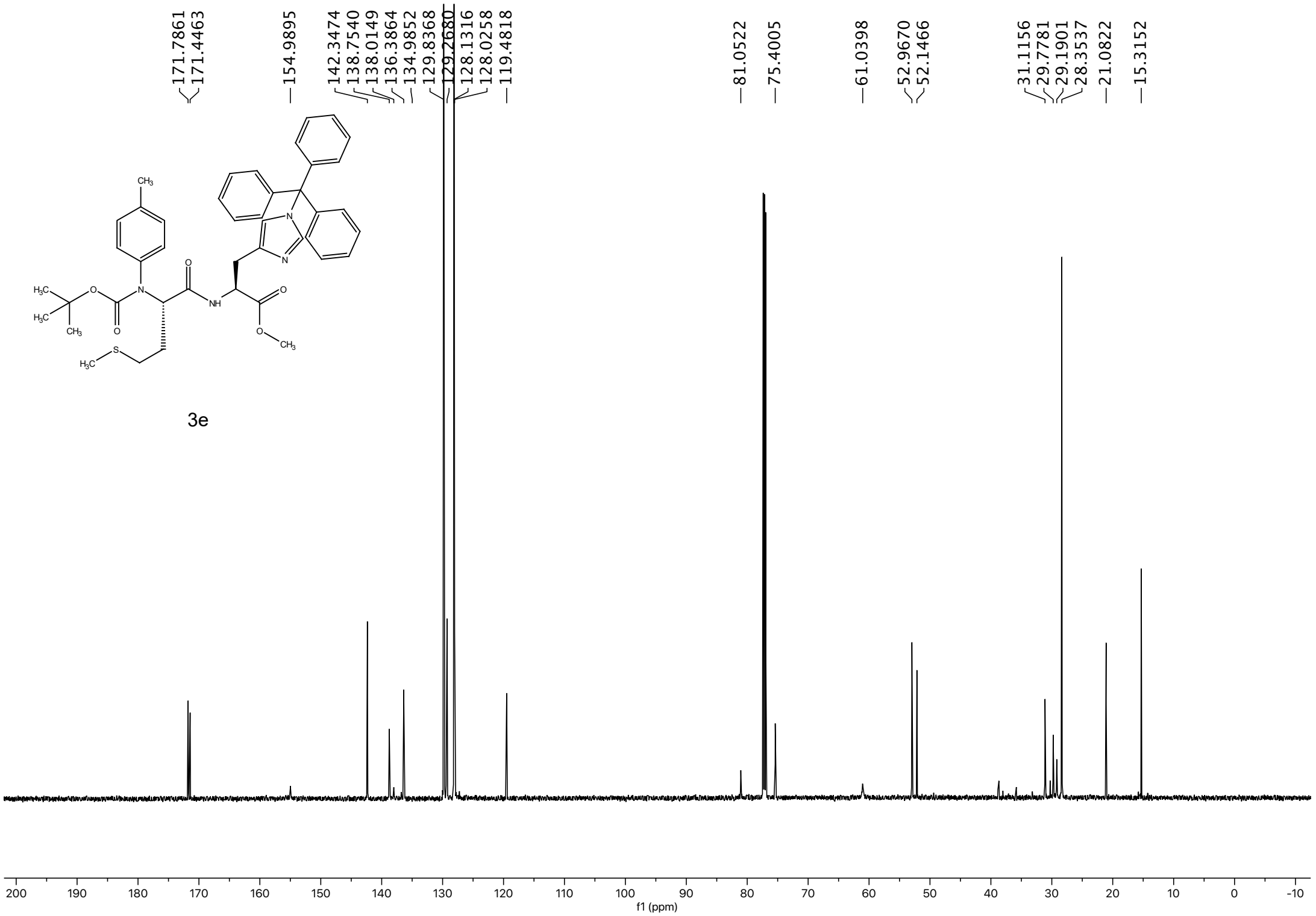
171.7861
171.4463
154.9895
142.3474
138.7540
138.0149
136.3864
134.9852
129.8368
129.2680
128.1316
128.0258
119.4818
81.0522
75.4005
61.0398
52.9670
52.1466
31.1156
29.7781
29.1901
28.3537
21.0822
15.3152
3e
200
190
180
170
160
150
140
130
120
110
100
90
80
70
60
50
40
30
20
10
0
-10
f1 (ppm)

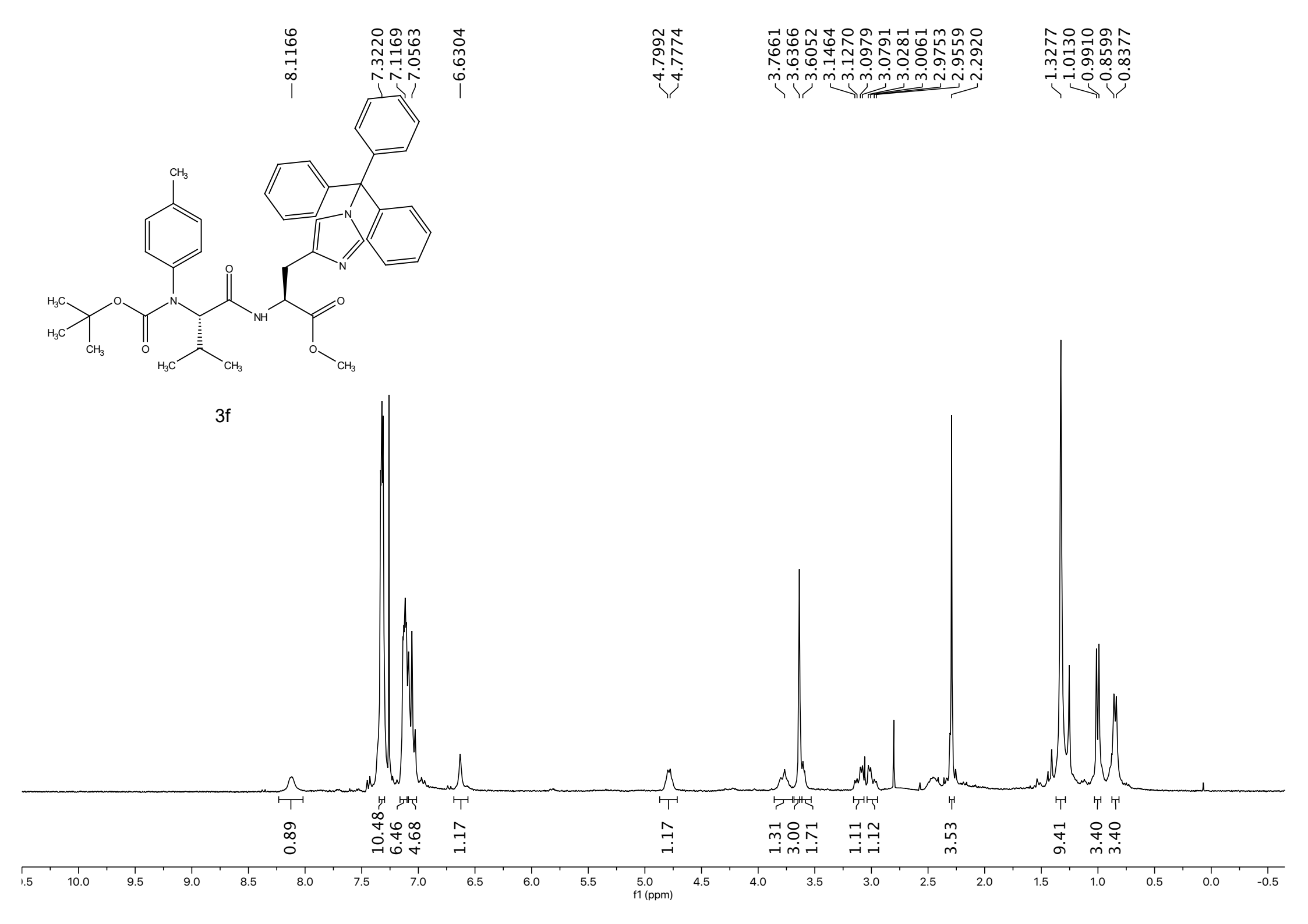
8.1166
7.3220
7.1169
7.0563
6.6304
4.7992
4.7774
3.7661
3.6366
3.6052
3.1464
3.1270
3.0979
3.0791
3.0281
3.0061
2.9753
2.9559
2.2920
1.3277
1.0130
0.9910
0.8599
0.8377
0.89
10.48
6.46
4.68
1.17
1.17
1.31
3.00
1.71
1.11
1.12
3.53
9.41
3.40
3.40
f1 (ppm)

3f

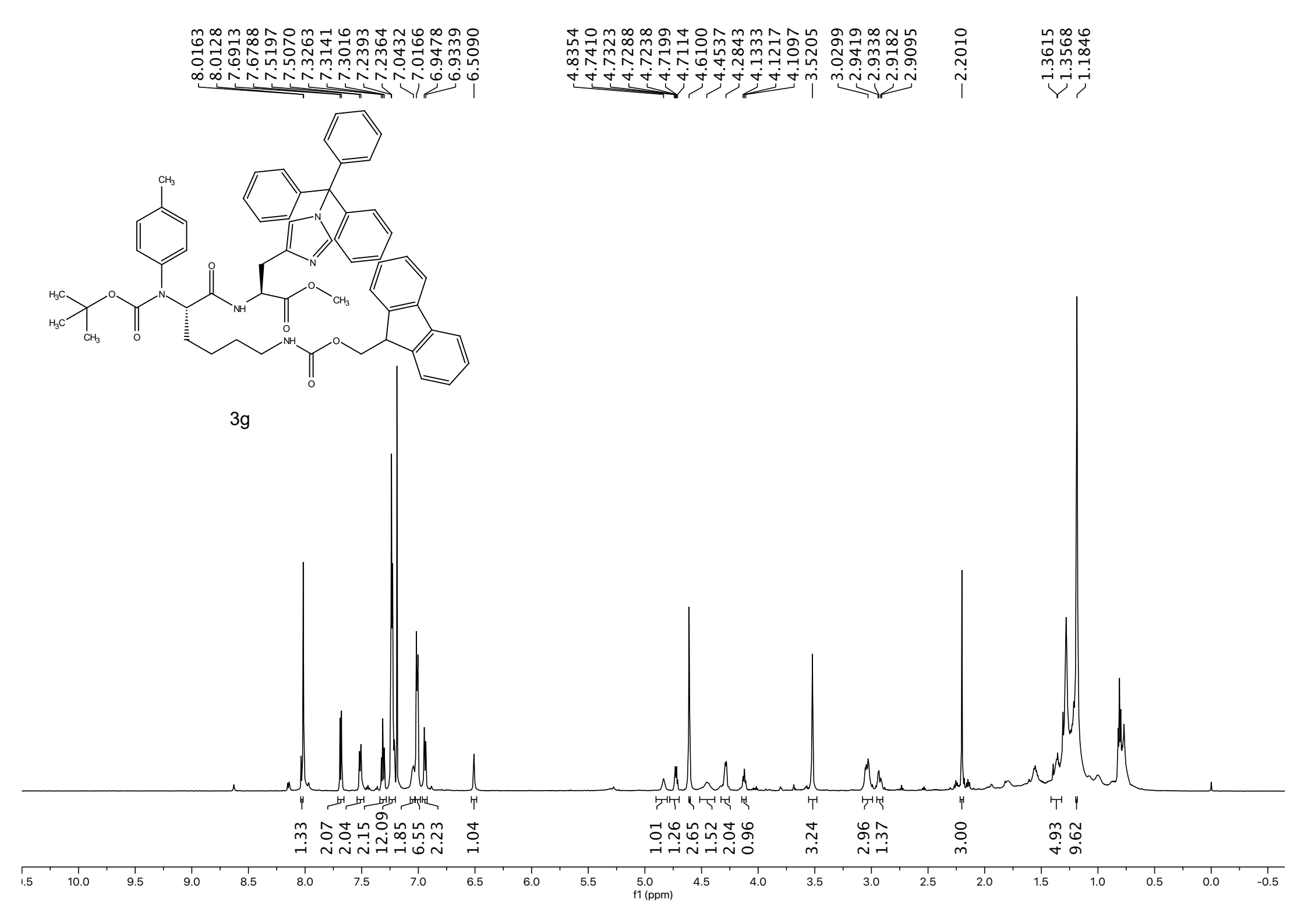
8.0163
8.0128
7.6913
7.6788
7.5197
7.5070
7.3263
7.3141
7.3016
7.2393
7.2364
7.0432
7.0166
6.9478
6.9339
6.5090
4.8354
4.7410
4.7323
4.7288
4.7238
4.7199
4.7114
4.6100
4.4537
4.2843
4.1333
4.1217
4.1097
3.5205
3.0299
2.9419
2.9338
2.9182
2.9095
2.2010
1.3615
1.3568
1.1846
3g
1.33
2.07
2.04
2.15
12.09
1.85
6.55
2.23
1.04
1.01
1.26
2.65
1.52
2.04
0.96
3.24
2.96
1.37
3.00
4.93
9.62
f1 (ppm)

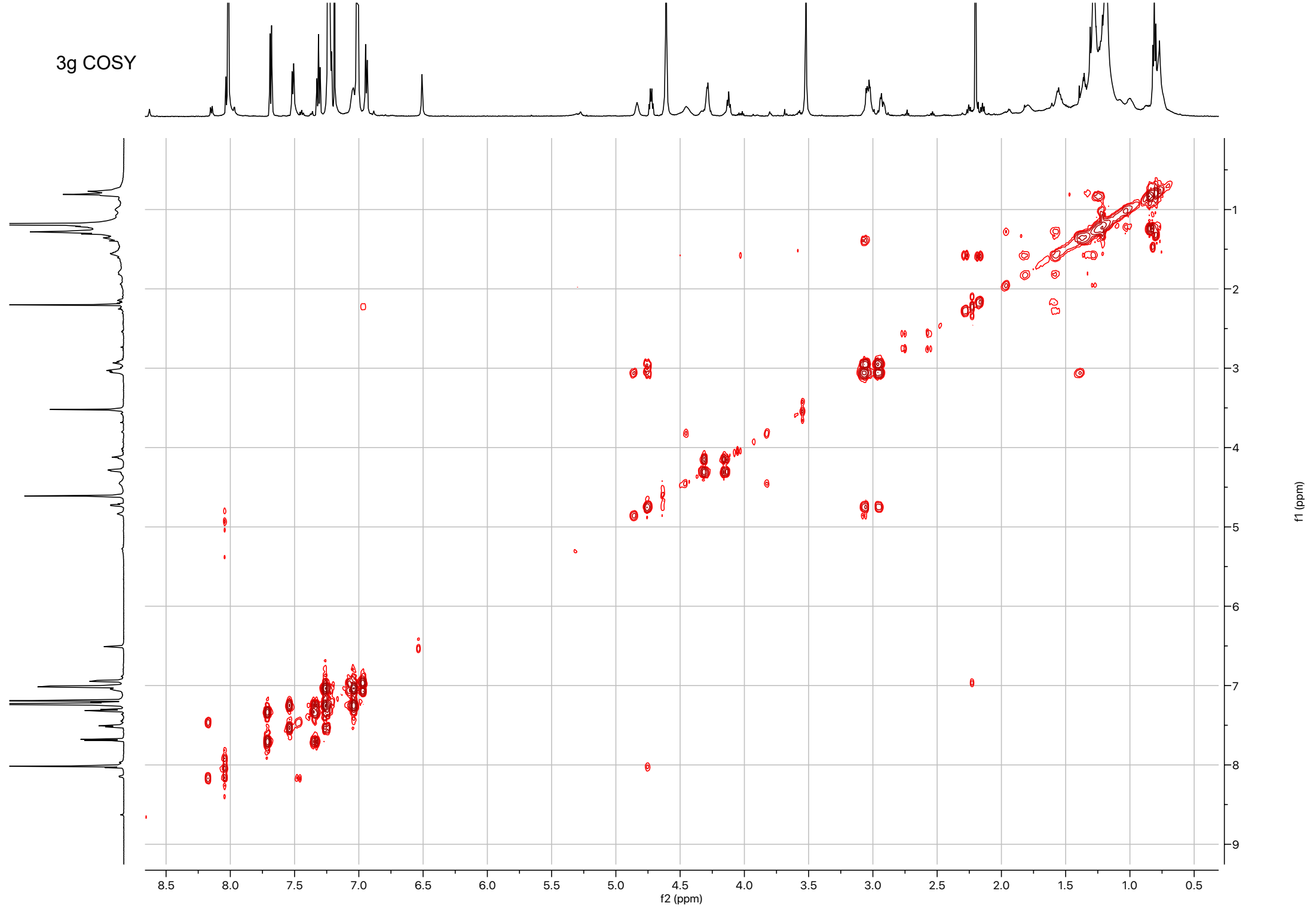
3g COSY
8.5
8.0
7.5
7.0
6.5
6.0
5.5
5.0
4.5
4.0
3.5
3.0
2.5
2.0
1.5
1.0
0.5
f2 (ppm)
1
2
3
4
5
6
7
8
9
f1 (ppm)

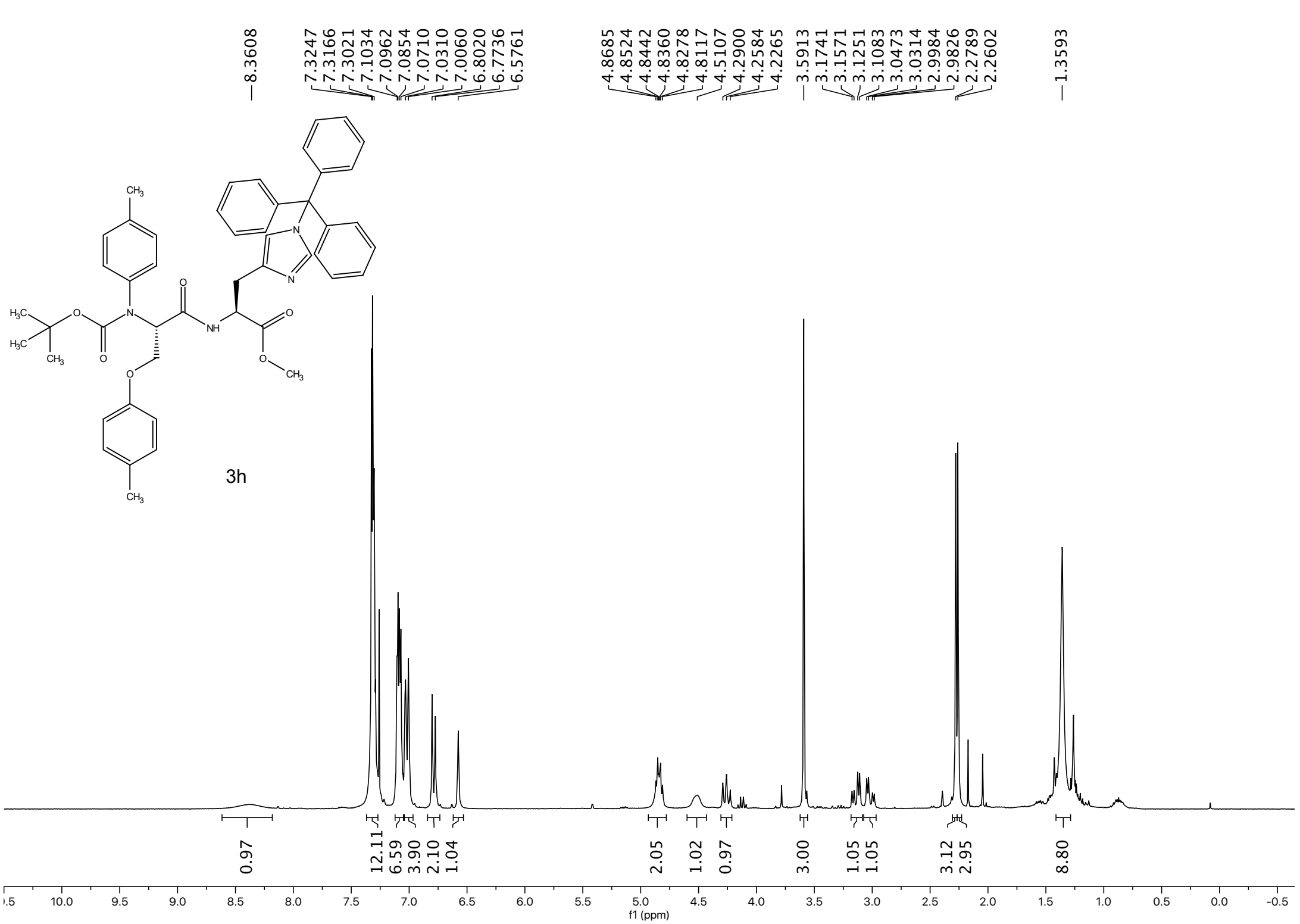
8.3608
7.3247
7.3166
7.3021
7.1034
7.0962
7.0854
7.0710
7.0310
7.0060
6.8020
6.7736
6.5761
4.8685
4.8524
4.8442
4.8360
4.8278
4.8117
4.5107
4.2900
4.2584
4.2265
3.5913
3.1741
3.1571
3.1251
3.1083
3.0473
3.0314
2.9984
2.9826
2.2789
2.2602
1.3593
3h
0.97
12.11
6.59
3.90
2.10
1.04
2.05
1.02
0.97
3.00
1.05
1.05
3.12
2.95
8.80
f1 (ppm)

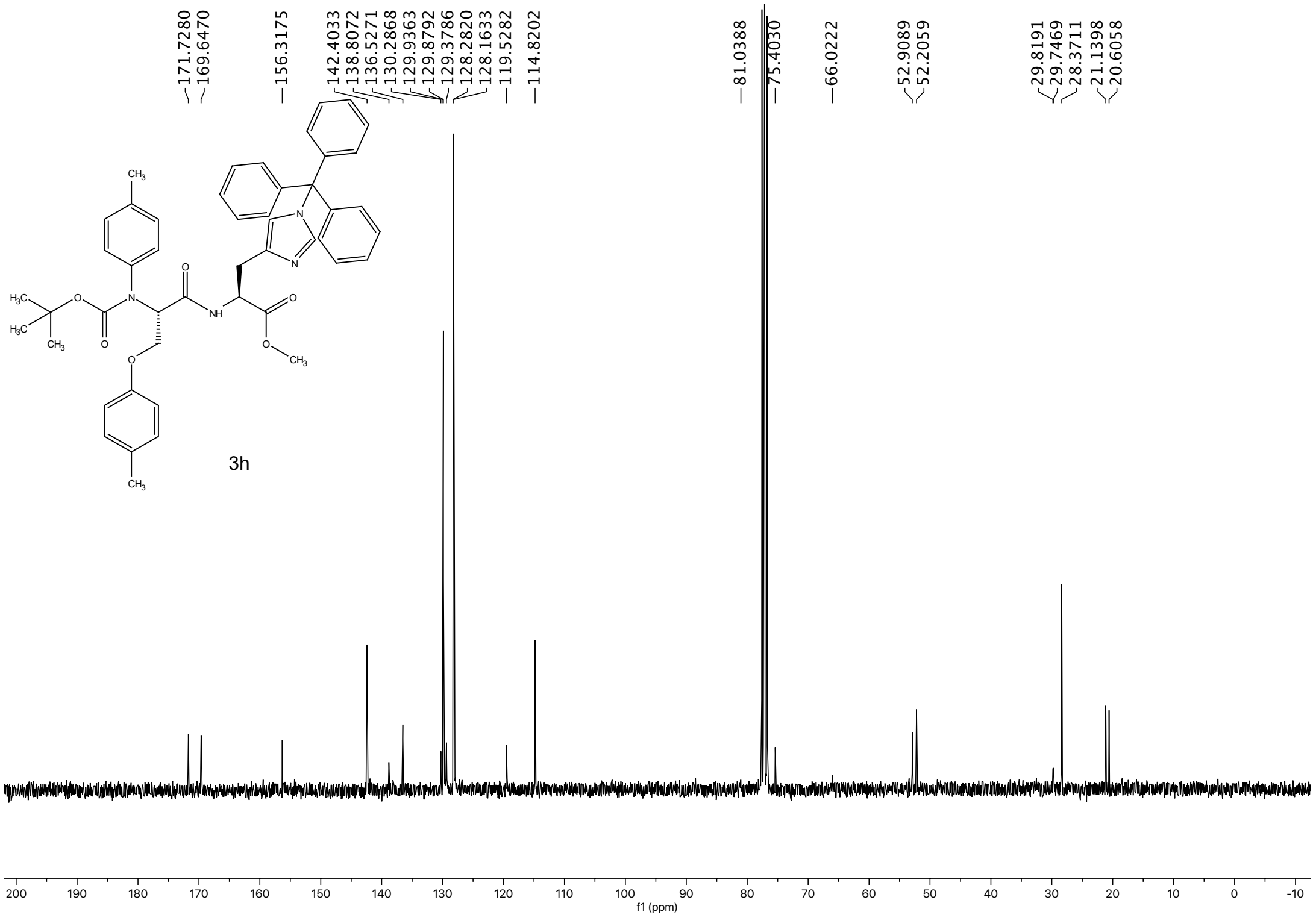
171.7280
169.6470
156.3175
142.4033
138.8072
136.5271
130.2868
129.9363
129.8792
129.3786
128.2820
128.1633
119.5282
114.8202
81.0388
75.4030
66.0222
52.9089
52.2059
29.8191
29.7469
28.3711
21.1398
20.6058
3h
f1 (ppm)

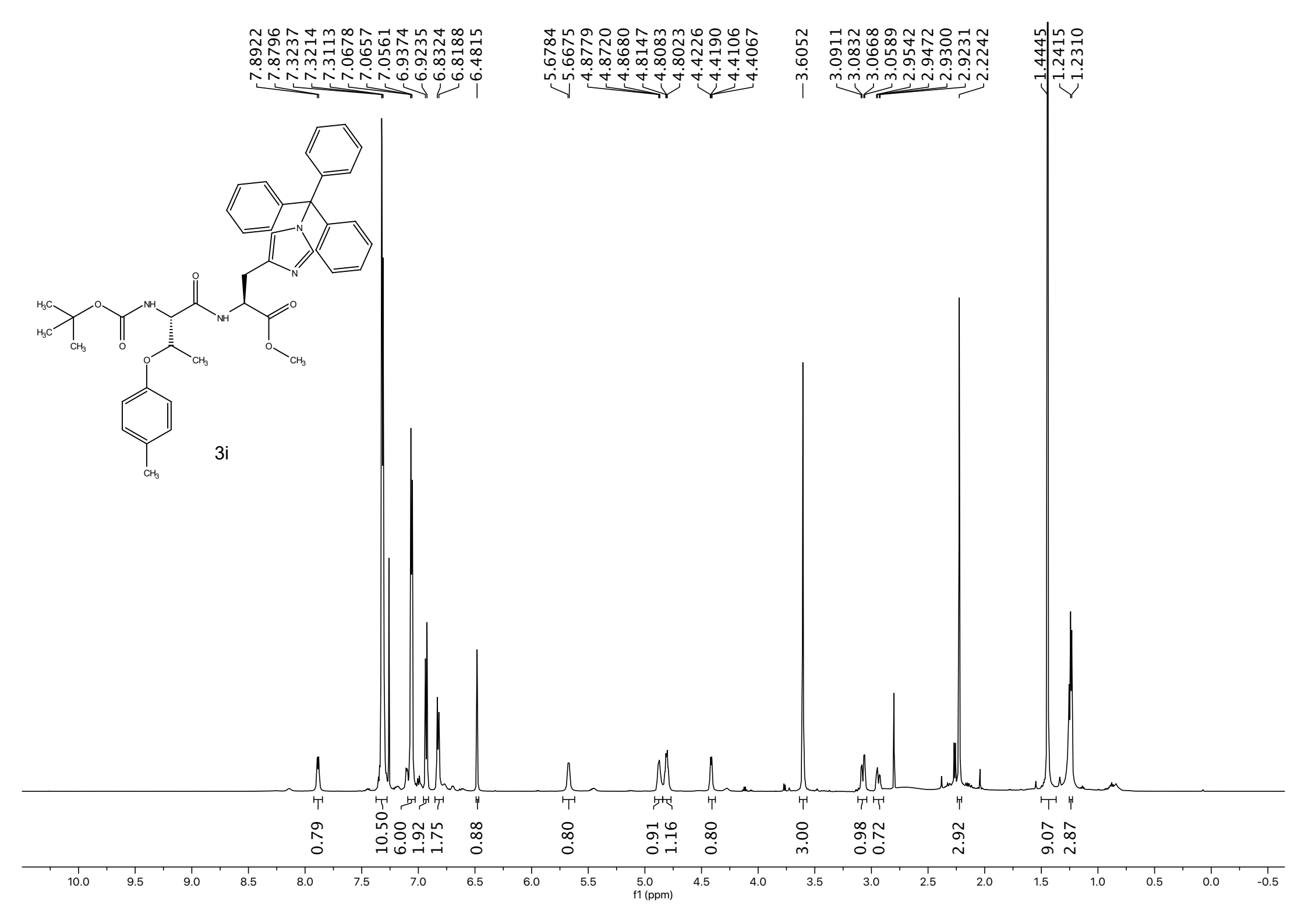
7.8922
7.8796
7.3237
7.3214
7.3113
7.0678
7.0657
7.0561
6.9374
6.9235
6.8324
6.8188
6.4815
5.6784
5.6675
4.8779
4.8720
4.8680
4.8147
4.8083
4.8023
4.4226
4.4190
4.4106
4.4067
3.6052
3.0911
3.0832
3.0668
3.0589
2.9542
2.9472
2.9300
2.9231
2.2242
1.4445
1.2415
1.2310
0.79
10.50
6.00
1.92
1.75
0.88
0.80
0.91
1.16
0.80
3.00
0.98
0.72
2.92
9.07
2.87
f1 (ppm)
3i

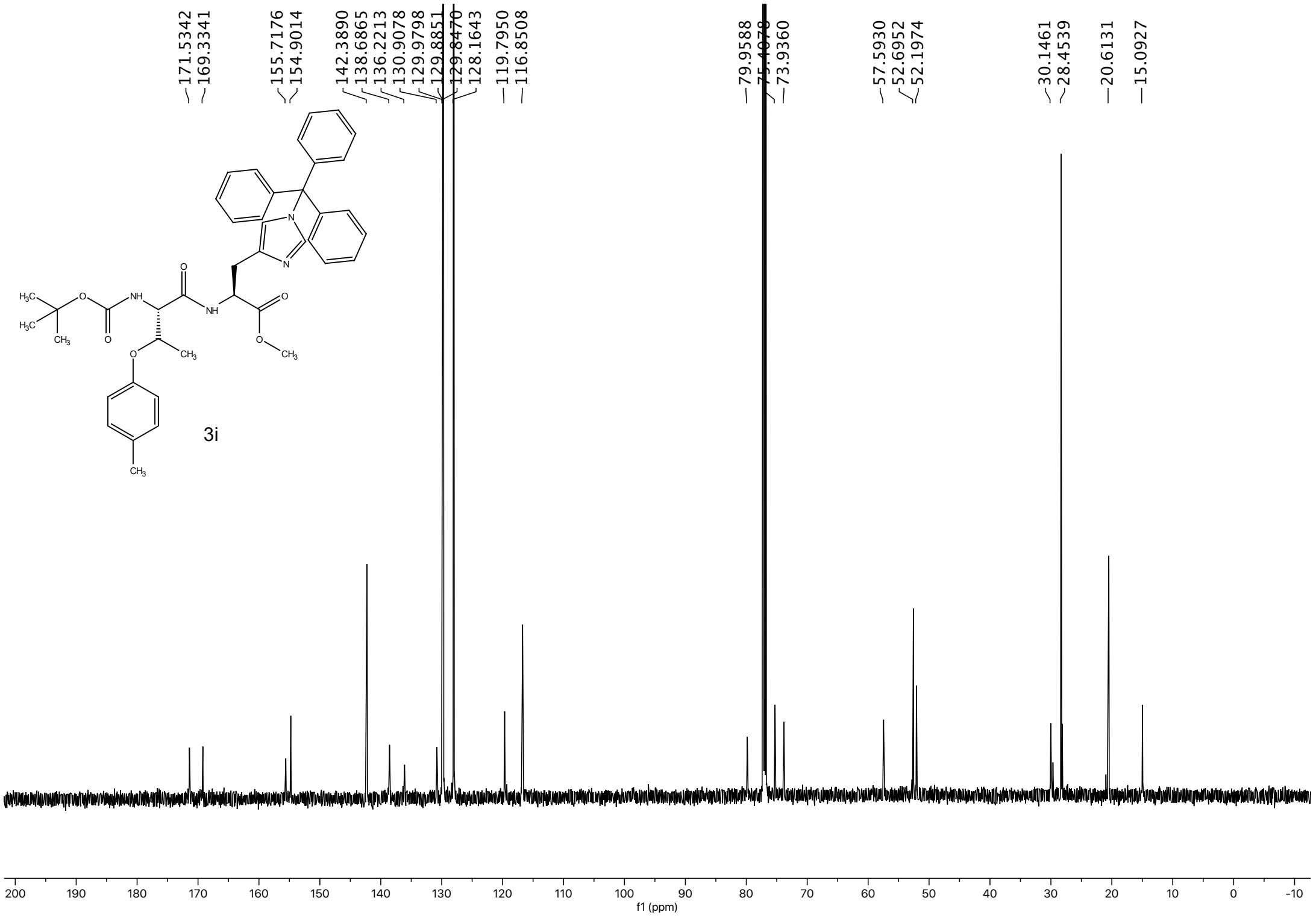
171.5342
169.3341
155.7176
154.9014
142.3890
138.6865
136.2213
130.9078
129.9798
129.8851
129.8470
128.1643
119.7950
116.8508
79.9588
75.4078
73.9360
57.5930
52.6952
52.1974
30.1461
28.4539
20.6131
15.0927
3i
200
190
180
170
160
150
140
130
120
110
100
90
80
70
60
50
40
30
20
10
0
-10
f1 (ppm)

3i COSY

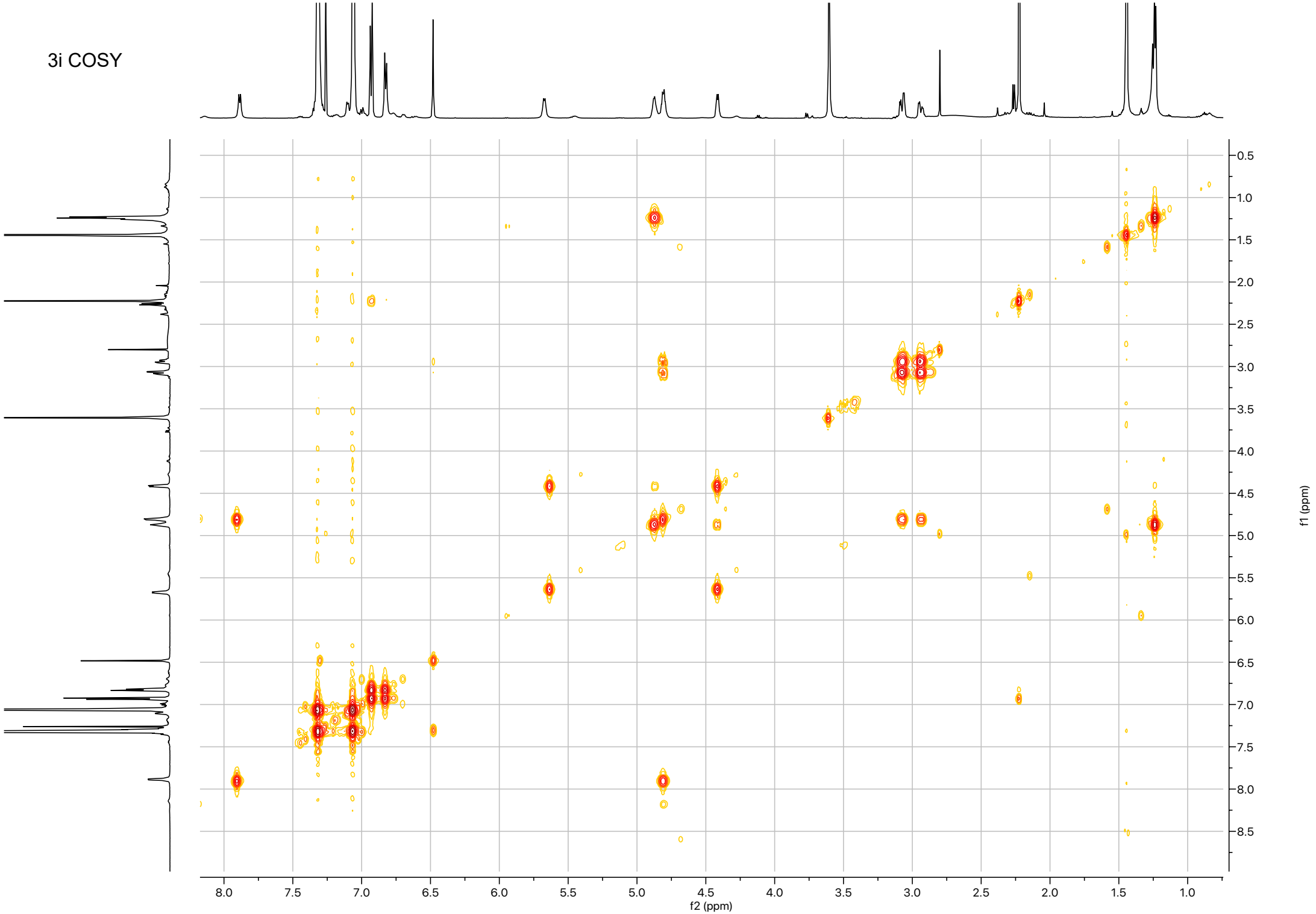

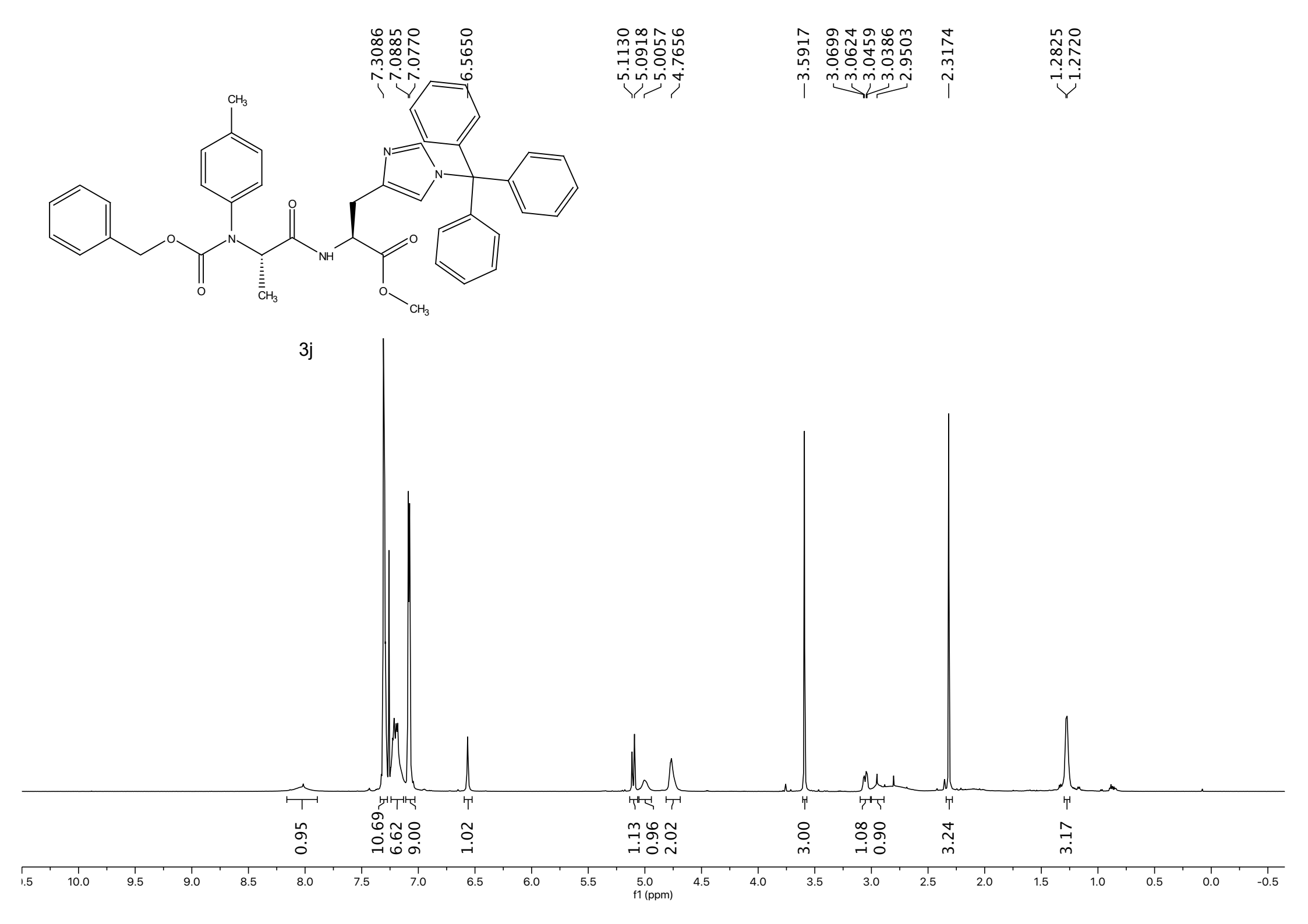
7.3086
7.0885
7.0770
6.5650
5.1130
5.0918
5.0057
4.7656
3.5917
3.0699
3.0624
3.0459
3.0386
2.9503
2.3174
1.2825
1.2720
3j
0.95
10.69
6.62
9.00
1.02
1.13
0.96
2.02
3.00
1.08
0.90
3.24
3.17
f1 (ppm)

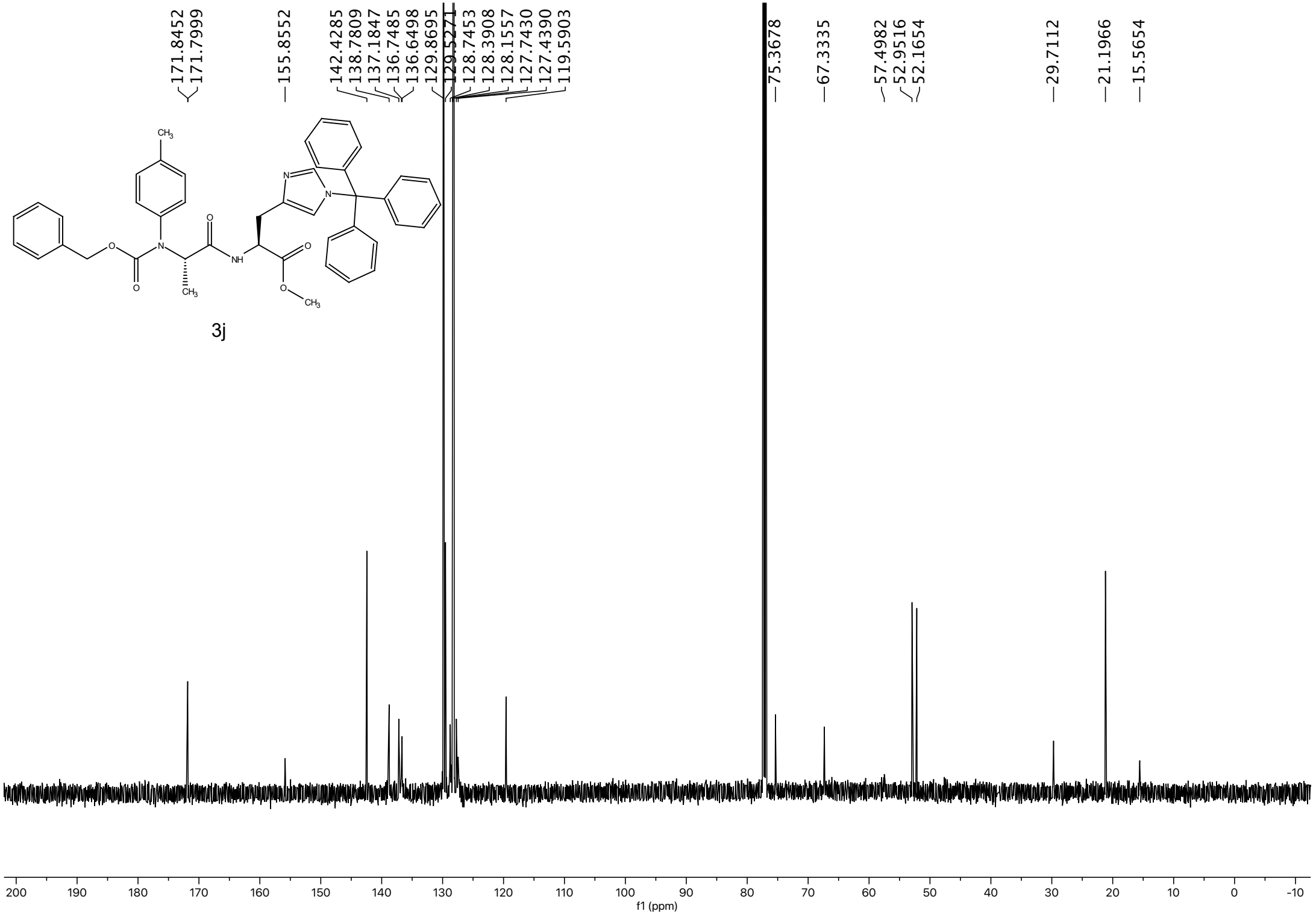
171.8452
171.7999
155.8552
142.4285
138.7809
137.1847
136.7485
136.6498
129.8695
129.5271
128.7453
128.3908
128.1557
127.7430
127.4390
119.5903
75.3678
67.3335
57.4982
52.9516
52.1654
29.7112
21.1966
15.5654
CH3
O
N
NH
O
O
CH3
O
N
N
O
O
CH3
3j
200
190
180
170
160
150
140
130
120
110
100
90
80
70
60
50
40
30
20
10
0
-10
f1 (ppm)

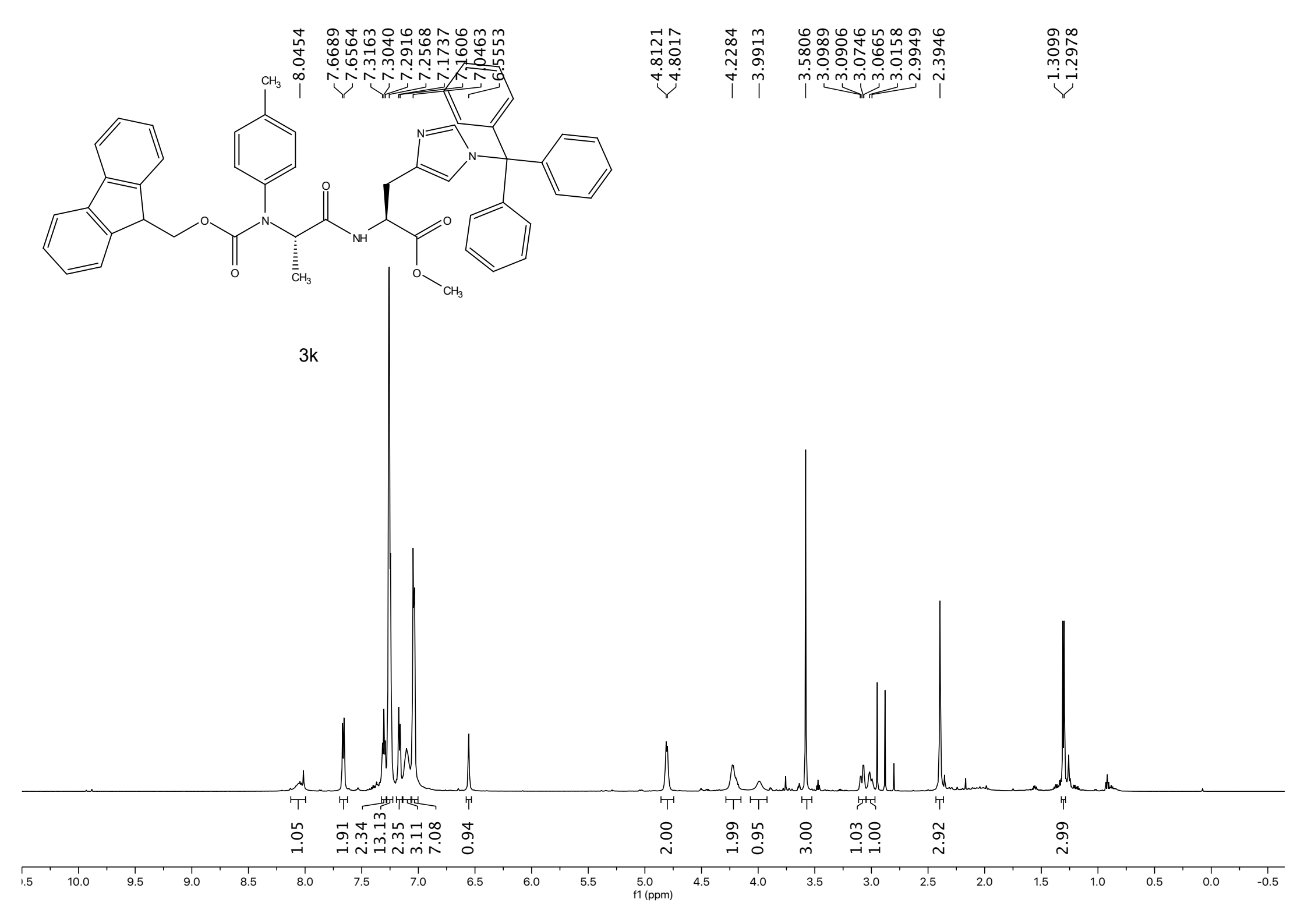
8.0454
7.6689
7.6564
7.3163
7.3040
7.2916
7.2568
7.1737
7.1606
7.0463
6.5553
4.8121
4.8017
4.2284
3.9913
3.5806
3.0989
3.0906
3.0746
3.0665
3.0158
2.9949
2.3946
1.3099
1.2978
3k
1.05
1.91
2.34
13.13
2.35
3.11
7.08
0.94
2.00
1.99
0.95
3.00
1.03
1.00
2.92
2.99
f1 (ppm)

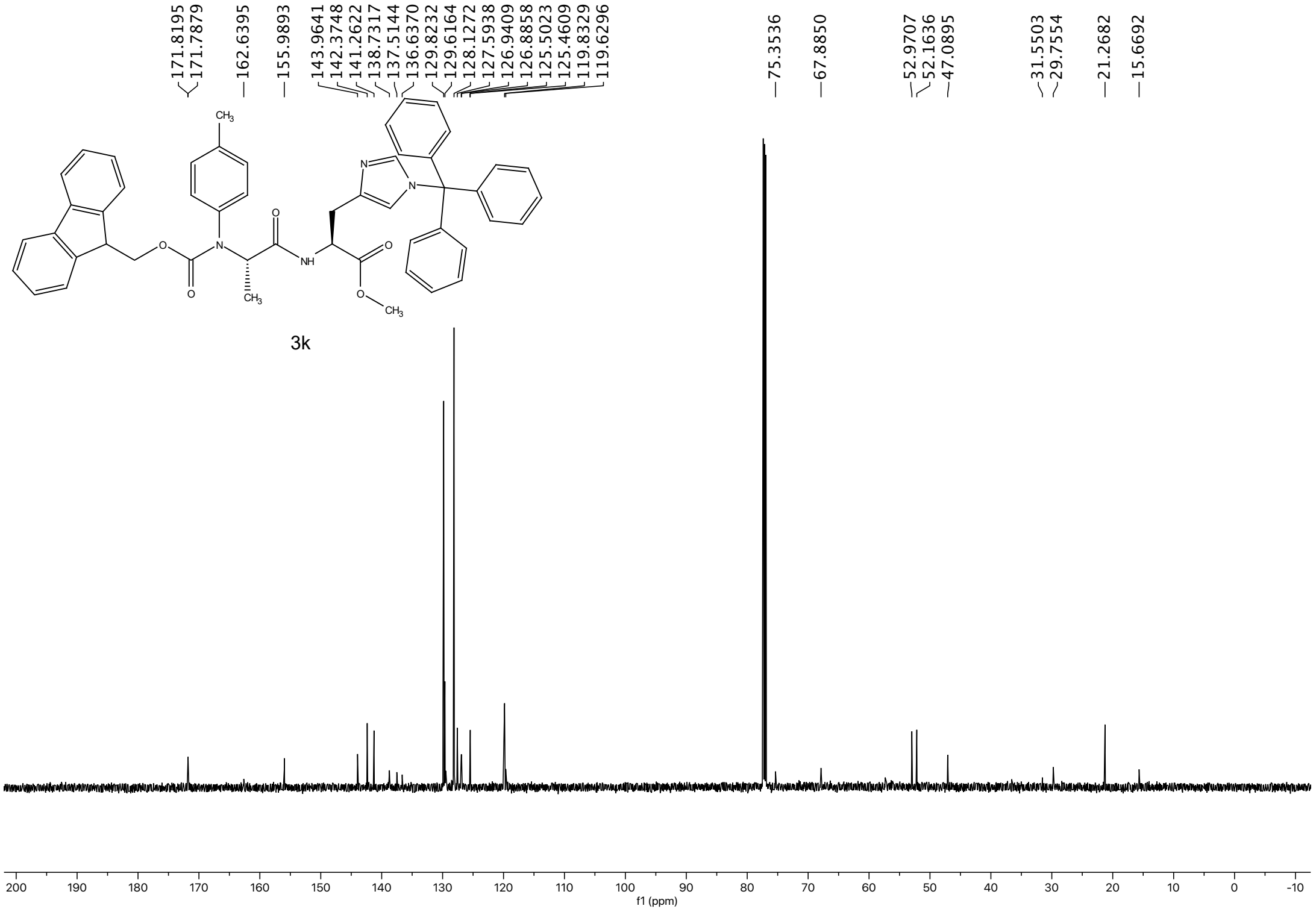
171.8195
171.7879
162.6395
155.9893
143.9641
142.3748
141.2622
138.7317
137.5144
136.6370
129.8232
129.6164
128.1272
127.5938
126.9409
126.8858
125.5023
125.4609
119.8329
119.6296
75.3536
67.8850
52.9707
52.1636
47.0895
31.5503
29.7554
21.2682
15.6692
CH3
N
N
O
O
N
NH
O
O
O
CH3
CH3
3k
200
190
180
170
160
150
140
130
120
110
100
90
80
70
60
50
40
30
20
10
0
-10
f1 (ppm)

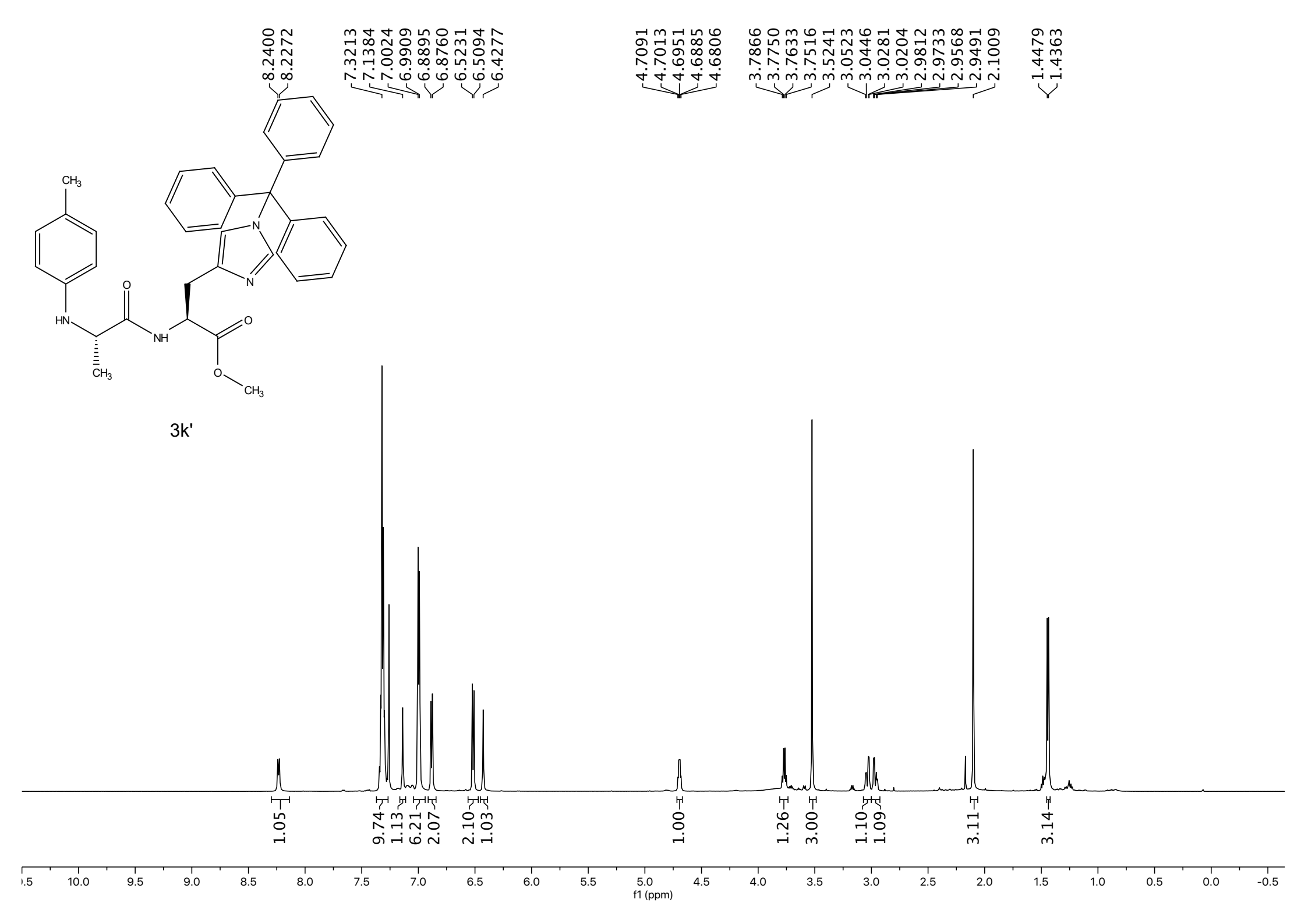
8.2400
8.2272
7.3213
7.1384
7.0024
6.9909
6.8895
6.8760
6.5231
6.5094
6.4277
4.7091
4.7013
4.6951
4.6885
4.6806
3.7866
3.7750
3.7633
3.7516
3.5241
3.0523
3.0446
3.0281
3.0204
2.9812
2.9733
2.9568
2.9491
2.1009
1.4479
1.4363
CH3
HN
O
NH
O
O
CH3
CH3
N
N
3k'
1.05
9.74
1.13
6.21
2.07
2.10
1.03
1.00
1.26
3.00
1.10
1.09
3.11
3.14
f1 (ppm)

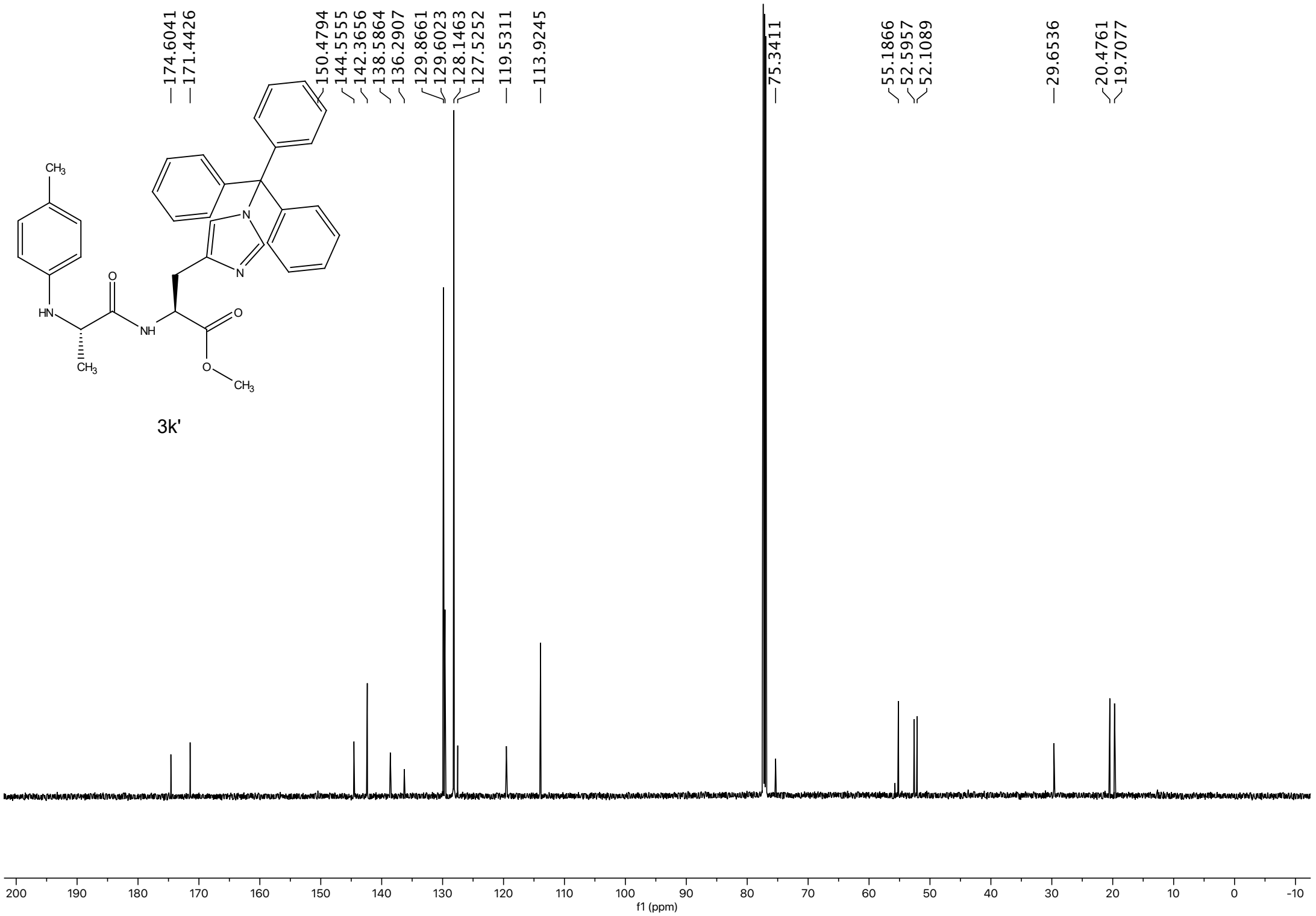
174.6041
171.4426
150.4794
144.5555
142.3656
138.5864
136.2907
129.8661
129.6023
128.1463
127.5252
119.5311
113.9245
75.3411
55.1866
52.5957
52.1089
29.6536
20.4761
19.7077
CH3
HN
O
NH
O
O
CH3
CH3
N
N
200
190
180
170
160
150
140
130
120
110
100
90
80
70
60
50
40
30
20
10
0
-10
f1 (ppm)

3k'

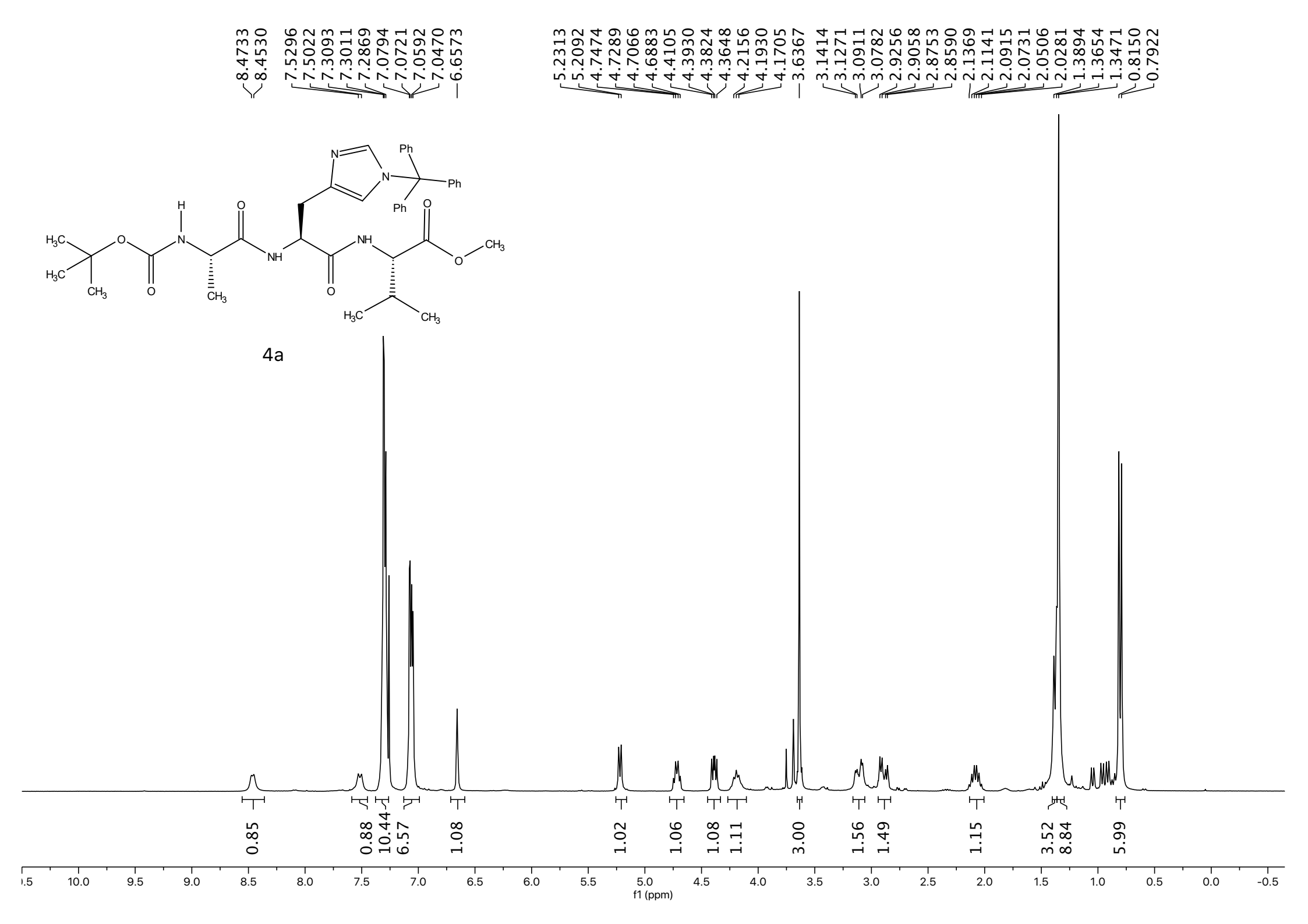
8.4733
8.4530
7.5296
7.5022
7.3093
7.3011
7.2869
7.0794
7.0721
7.0592
7.0470
6.6573
5.2313
5.2092
4.7474
4.7289
4.7066
4.6883
4.4105
4.3930
4.3824
4.3648
4.2156
4.1930
4.1705
3.6367
3.1414
3.1271
3.0911
3.0782
2.9256
2.9058
2.8753
2.8590
2.1369
2.1141
2.0915
2.0731
2.0506
2.0281
1.3894
1.3654
1.3471
0.8150
0.7922
Ph
Ph
Ph
N
N
H
O
O
NH
NH
O
O
O
O
CH3
H3C
H3C
CH3
CH3
H3C
CH3
4a
0.85
0.88
10.44
6.57
1.08
1.02
1.06
1.08
1.11
3.00
1.56
1.49
1.15
3.52
8.84
5.99
f1 (ppm)

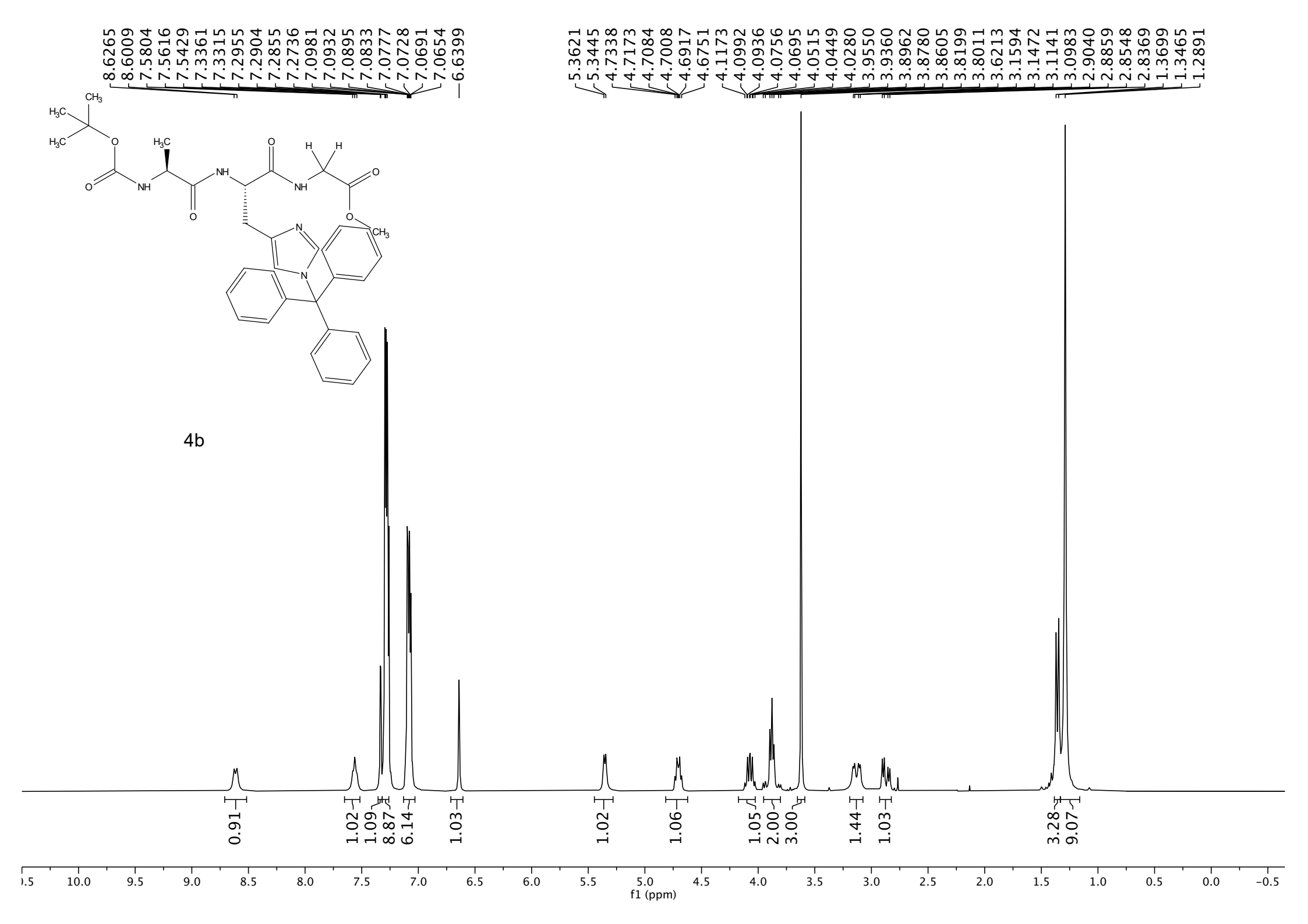
8.6265
8.6009
7.5804
7.5616
7.5429
7.3361
7.3315
7.2955
7.2904
7.2855
7.2736
7.0981
7.0932
7.0895
7.0833
7.0777
7.0728
7.0691
7.0654
6.6399
5.3621
5.3445
4.7338
4.7173
4.7084
4.7008
4.6917
4.6751
4.1173
4.0992
4.0936
4.0756
4.0695
4.0515
4.0449
4.0280
3.9550
3.9360
3.8962
3.8780
3.8605
3.8199
3.8011
3.6213
3.1594
3.1472
3.1141
3.0983
2.9040
2.8859
2.8548
2.8369
1.3699
1.3465
1.2891
4b
0.91
1.02
1.09
8.87
6.14
1.03
1.02
1.06
1.05
2.00
3.00
1.44
1.03
3.28
9.07
f1 (ppm)

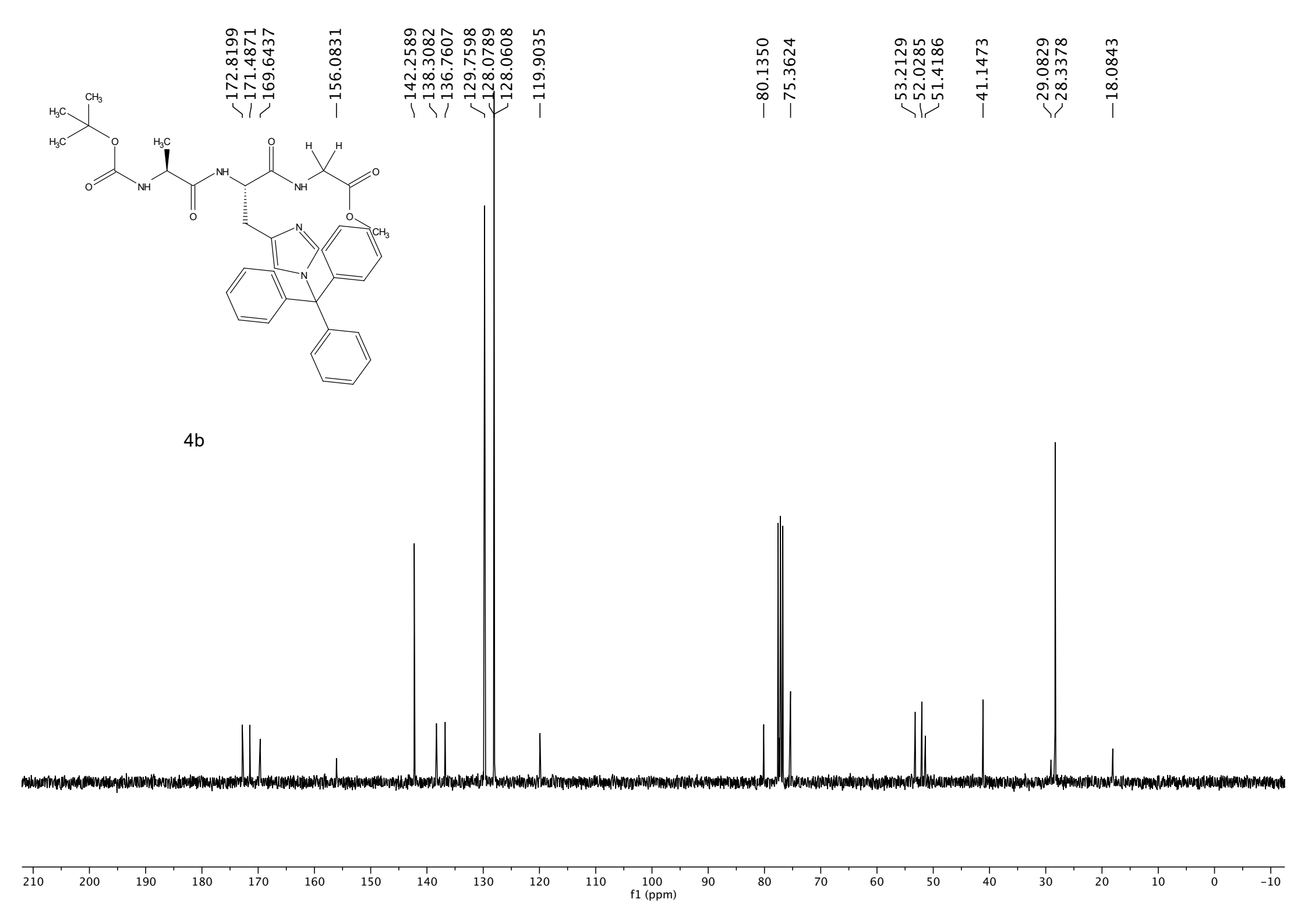
172.8199
171.4871
169.6437
156.0831
142.2589
138.3082
136.7607
129.7598
128.0789
128.0608
119.9035
80.1350
75.3624
53.2129
52.0285
51.4186
41.1473
29.0829
28.3378
18.0843
4b
f1 (ppm)

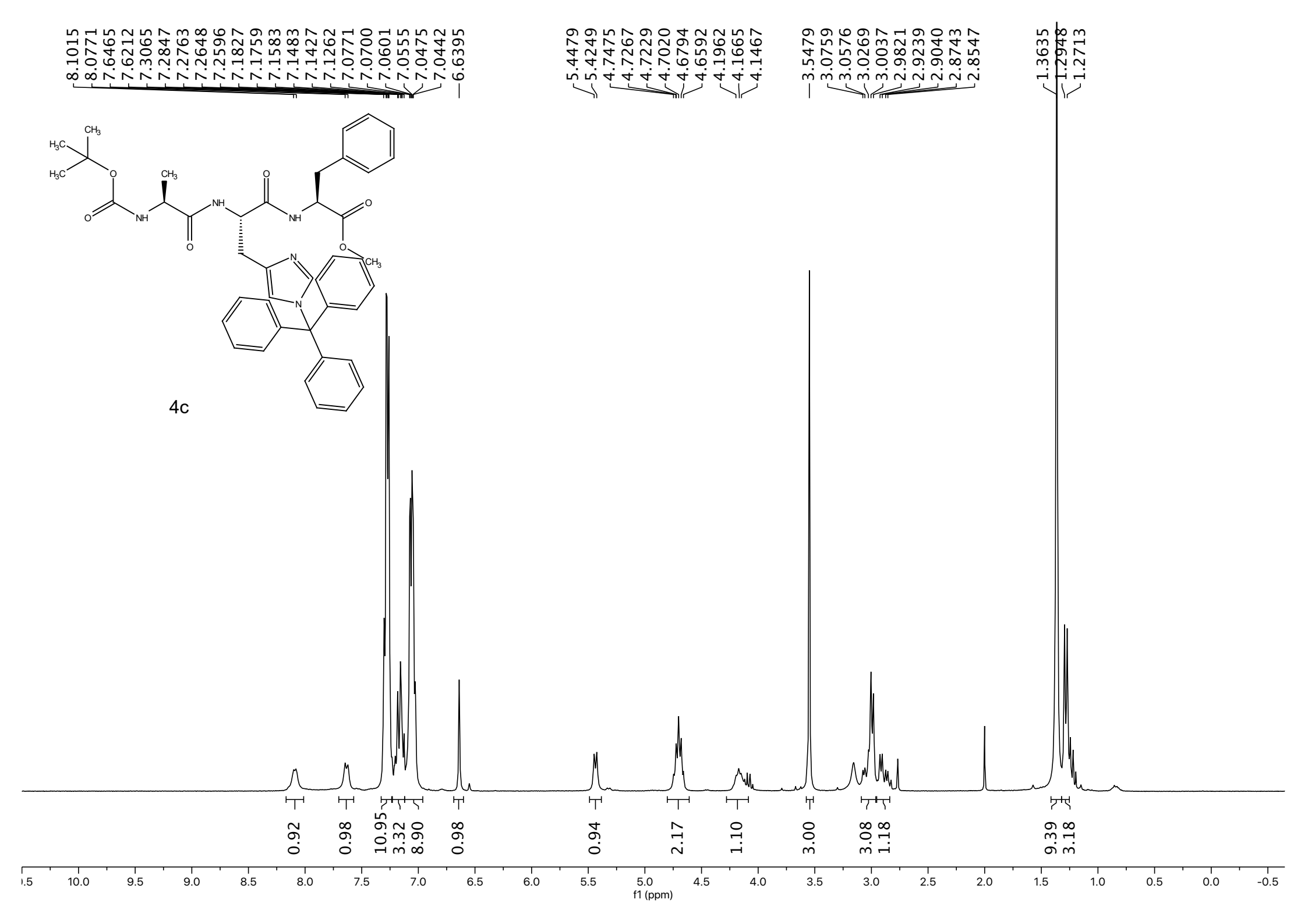
8.1015
8.0771
7.6465
7.6212
7.3065
7.2847
7.2763
7.2648
7.2596
7.1827
7.1759
7.1583
7.1483
7.1427
7.1262
7.0771
7.0700
7.0601
7.0555
7.0475
7.0442
6.6395
5.4479
5.4249
4.7475
4.7267
4.7229
4.7020
4.6794
4.6592
4.1962
4.1665
4.1467
3.5479
3.0759
3.0576
3.0269
3.0037
2.9821
2.9239
2.9040
2.8743
2.8547
1.3635
1.2948
1.2713
4c
0.92
0.98
10.95
3.32
8.90
0.98
0.94
2.17
1.10
3.00
3.08
1.18
9.39
3.18
f1 (ppm)

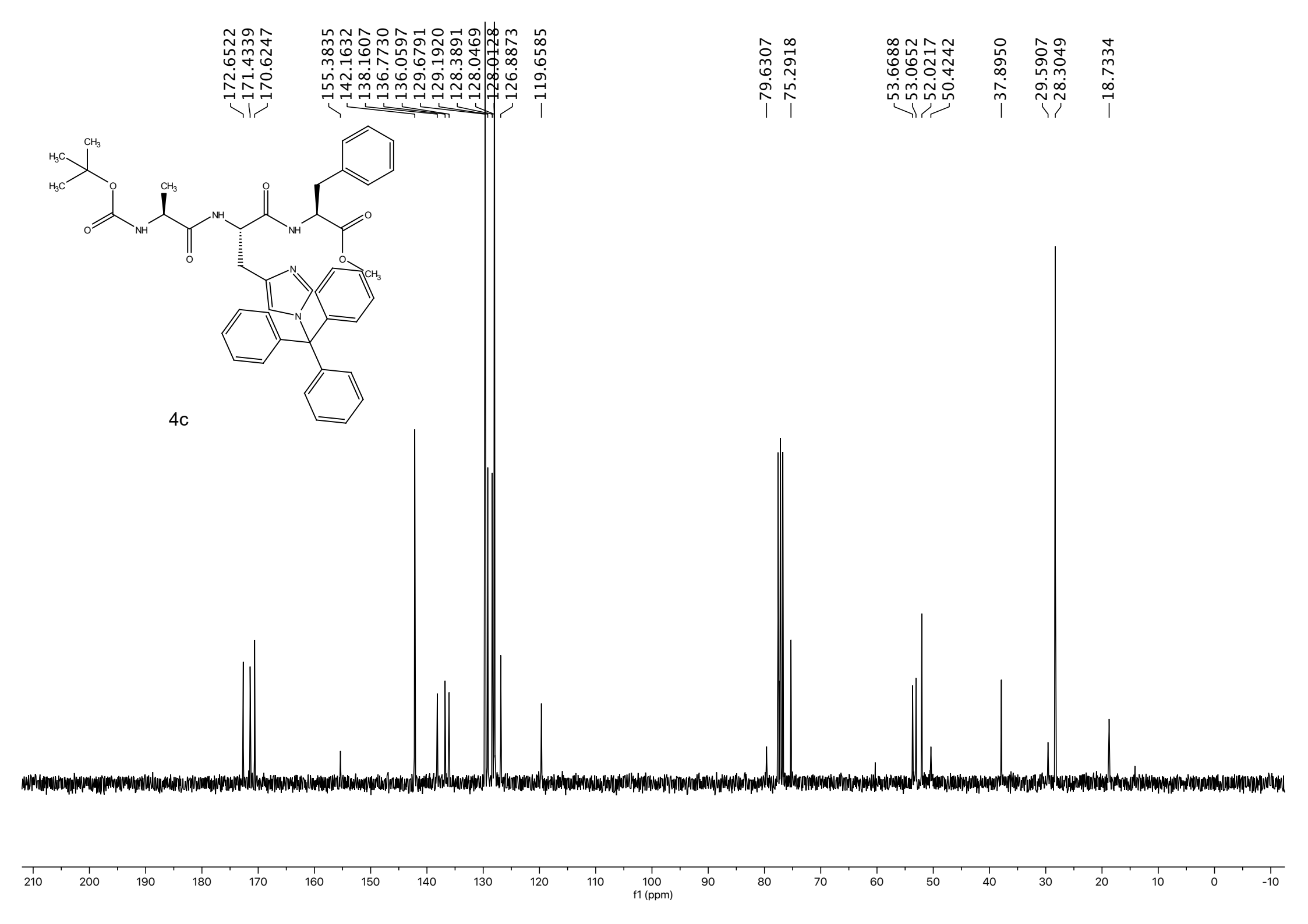
172.6522
171.4339
170.6247
155.3835
142.1632
138.1607
136.7730
136.0597
129.6791
129.1920
128.3891
128.0469
128.0128
126.8873
119.6585
79.6307
75.2918
53.6688
53.0652
52.0217
50.4242
37.8950
29.5907
28.3049
18.7334
4c
f1 (ppm)

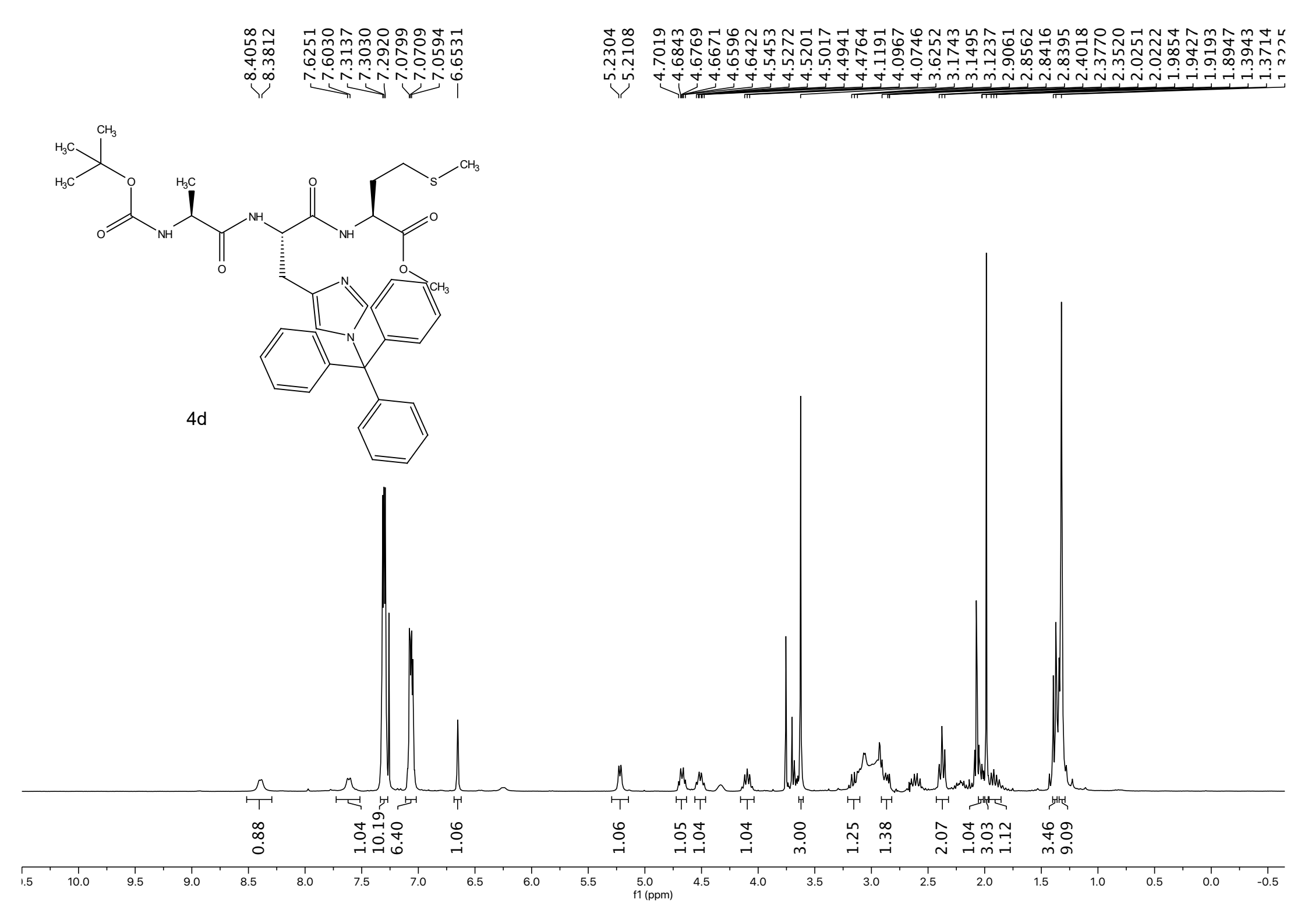
8.4058
8.3812
7.6251
7.6030
7.3137
7.3030
7.2920
7.0799
7.0709
7.0594
6.6531
5.2304
5.2108
4.7019
4.6843
4.6769
4.6671
4.6596
4.6422
4.5453
4.5272
4.5201
4.5017
4.4941
4.4764
4.1191
4.0967
4.0746
3.6252
3.1743
3.1495
3.1237
2.9061
2.8562
2.8416
2.8395
2.4018
2.3770
2.3520
2.0251
2.0222
1.9854
1.9427
1.9193
1.8947
1.3943
1.3714
4d
0.88
1.04
10.19
6.40
1.06
1.06
1.05
1.04
1.04
3.00
1.25
1.38
2.07
1.04
3.03
1.12
3.46
9.09
f1 (ppm)

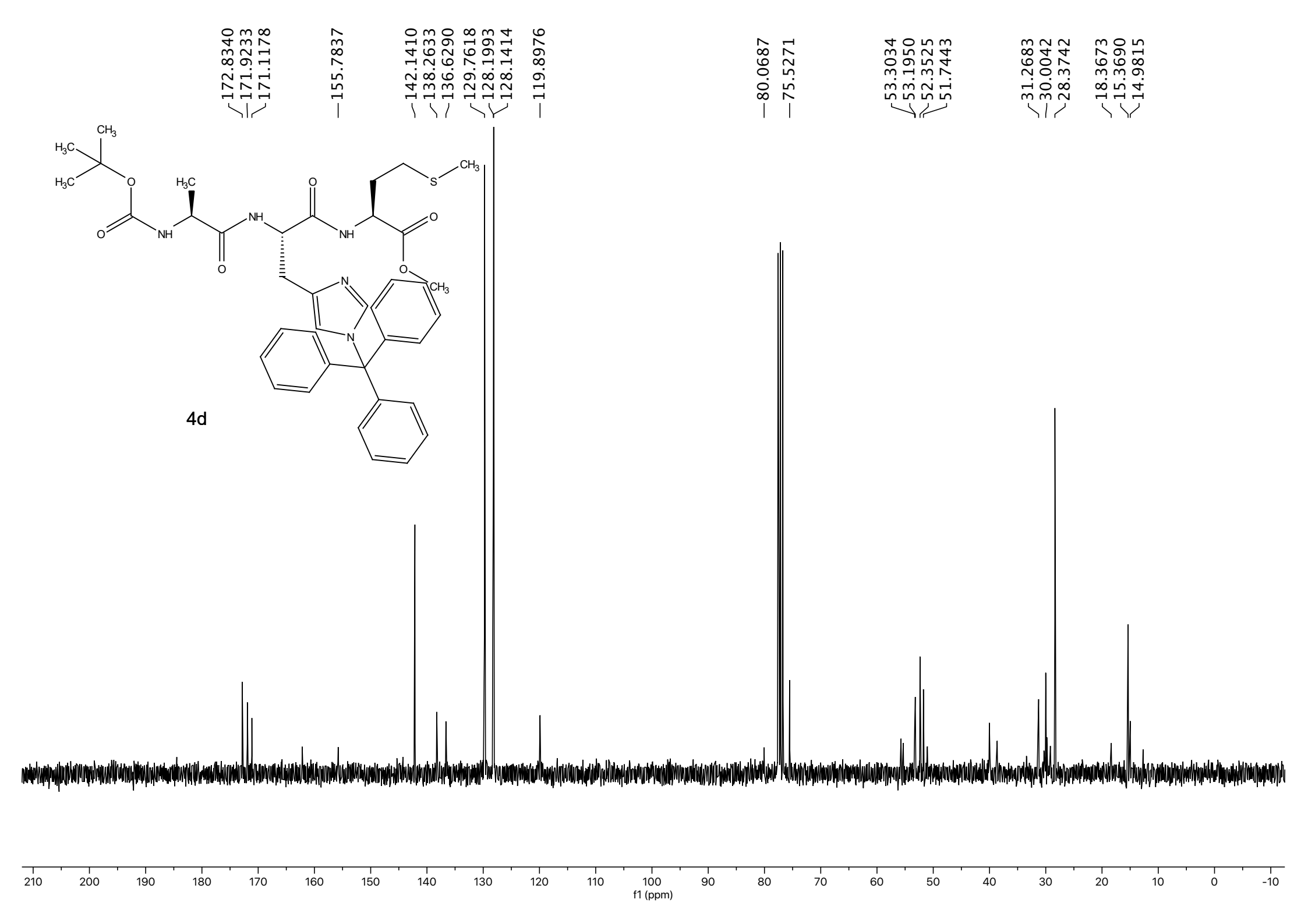
172.8340
171.9233
171.1178
155.7837
142.1410
138.2633
136.6290
129.7618
128.1993
128.1414
119.8976
80.0687
75.5271
53.3034
53.1950
52.3525
51.7443
31.2683
30.0042
28.3742
18.3673
15.3690
14.9815
4d
f1 (ppm)

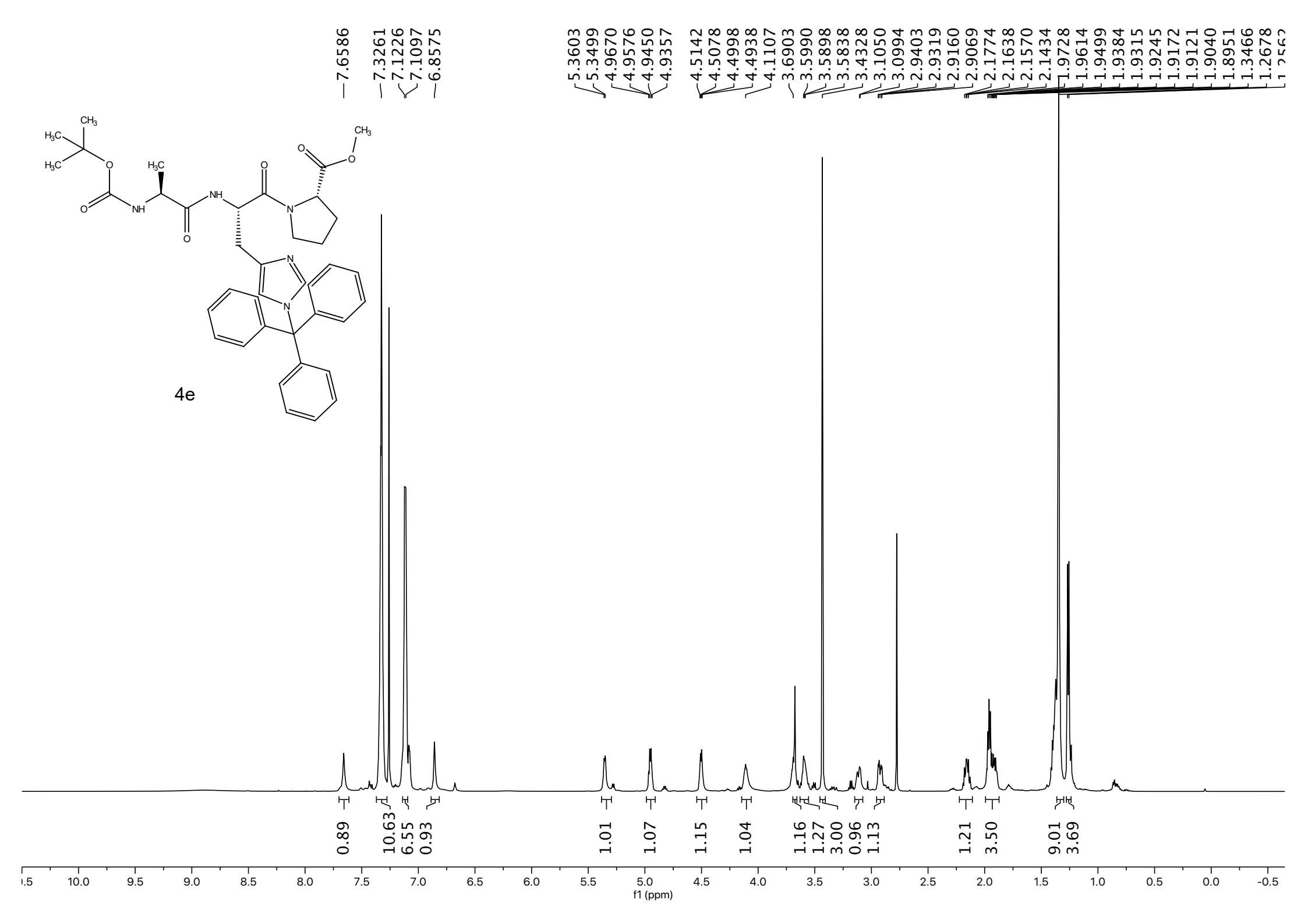
7.6586
7.3261
7.1226
7.1097
6.8575
5.3603
5.3499
4.9670
4.9576
4.9450
4.9357
4.5142
4.5078
4.4998
4.4938
4.1107
3.6903
3.5990
3.5898
3.5838
3.4328
3.1050
3.0994
2.9403
2.9319
2.9160
2.9069
2.1774
2.1638
2.1570
2.1434
1.9728
1.9614
1.9499
1.9384
1.9315
1.9245
1.9172
1.9121
1.9040
1.8951
1.3466
1.2678
4e
0.89
10.63
6.55
0.93
1.01
1.07
1.15
1.04
1.16
1.27
3.00
0.96
1.13
1.21
3.50
9.01
3.69
f1 (ppm)

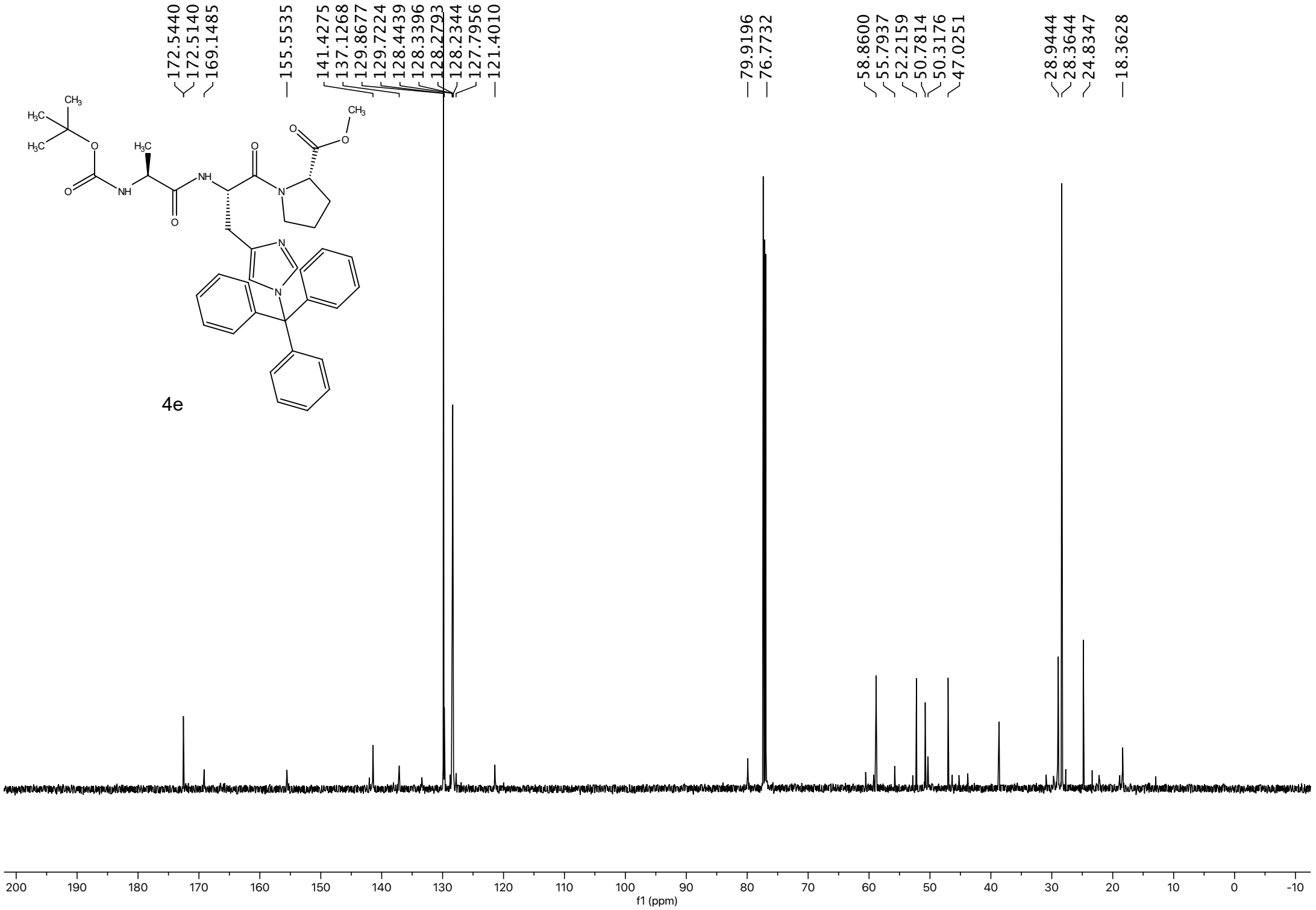
172.5440
172.5140
169.1485
155.5535
141.4275
137.1268
129.8677
129.7224
128.4439
128.3396
128.2793
128.2344
127.7956
121.4010
79.9196
76.7732
58.8600
55.7937
52.2159
50.7814
50.3176
47.0251
28.9444
28.3644
24.8347
18.3628
4e
f1 (ppm)

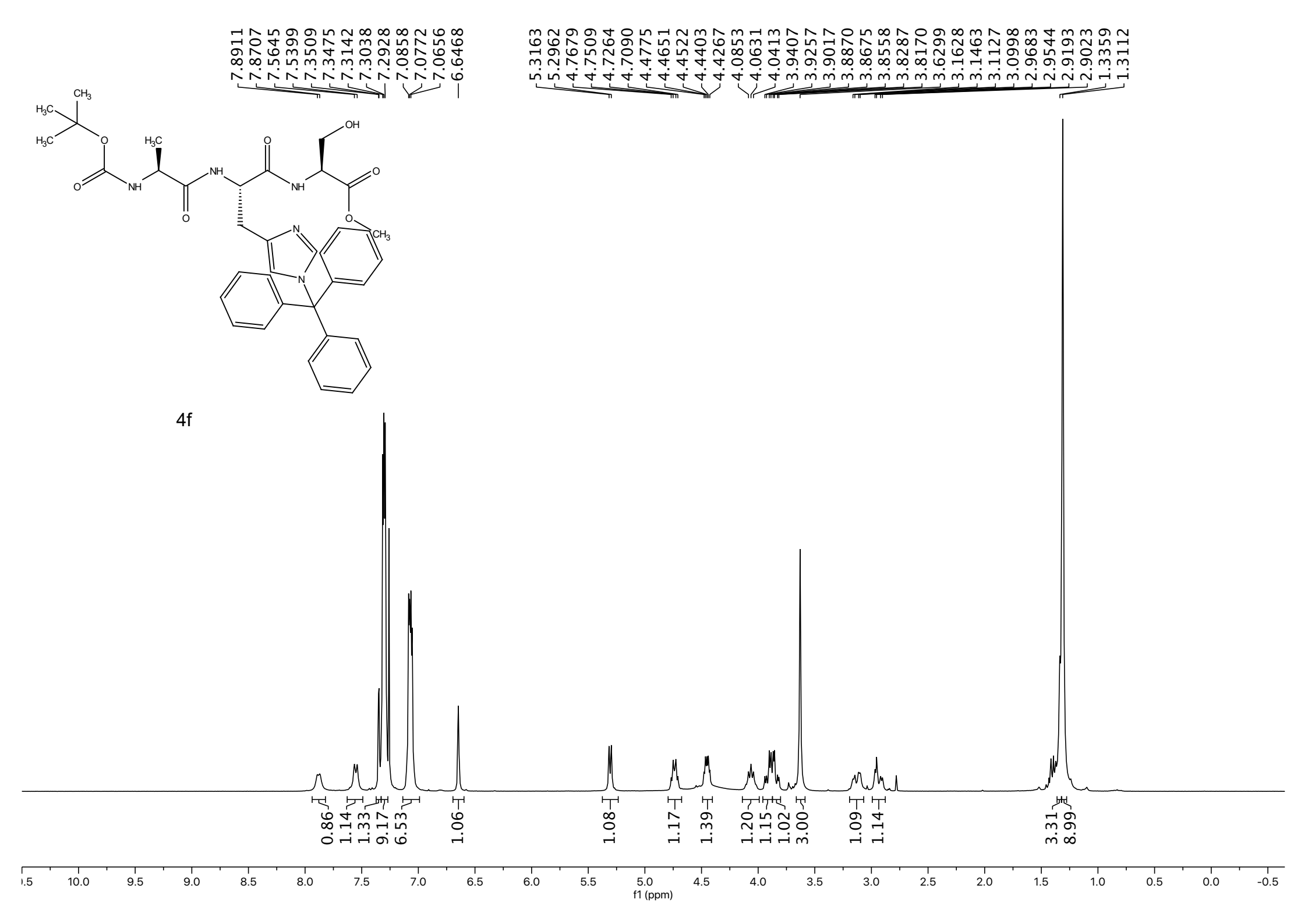
7.8911
7.8707
7.5645
7.5399
7.3509
7.3475
7.3142
7.3038
7.2928
7.0858
7.0772
7.0656
6.6468
5.3163
5.2962
4.7679
4.7509
4.7264
4.7090
4.4775
4.4651
4.4522
4.4403
4.4267
4.0853
4.0631
4.0413
3.9407
3.9257
3.9017
3.8870
3.8675
3.8558
3.8287
3.8170
3.6299
3.1628
3.1463
3.1127
3.0998
2.9683
2.9544
2.9193
2.9023
1.3359
1.3112
4f
0.86
1.14
1.33
9.17
6.53
1.06
1.08
1.17
1.39
1.20
1.15
1.02
3.00
1.09
1.14
3.31
8.99
f1 (ppm)

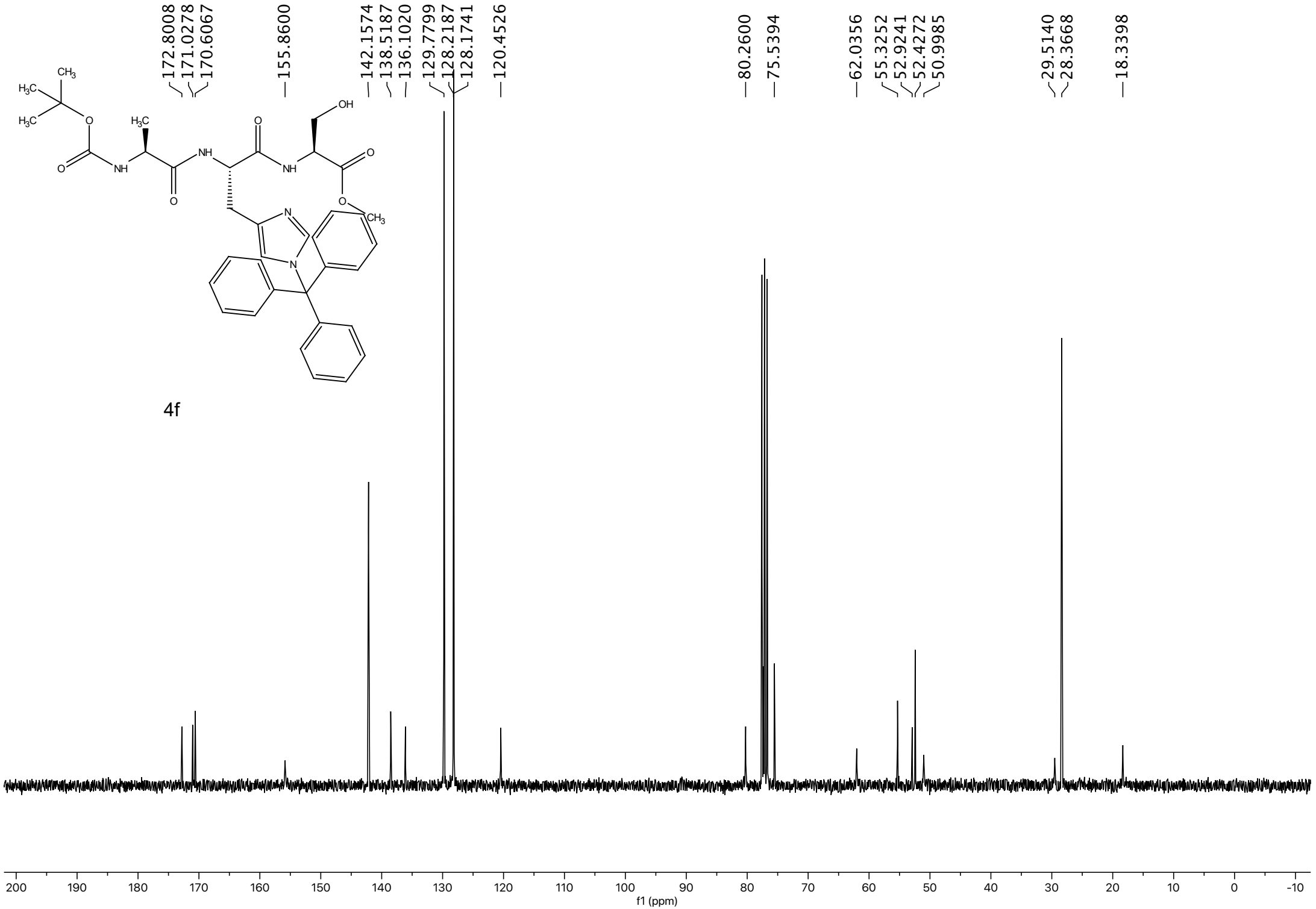
172.8008
171.0278
170.6067
155.8600
142.1574
138.5187
136.1020
129.7799
128.2187
128.1741
120.4526
80.2600
75.5394
62.0356
55.3252
52.9241
52.4272
50.9985
29.5140
28.3668
18.3398
4f
f1 (ppm)

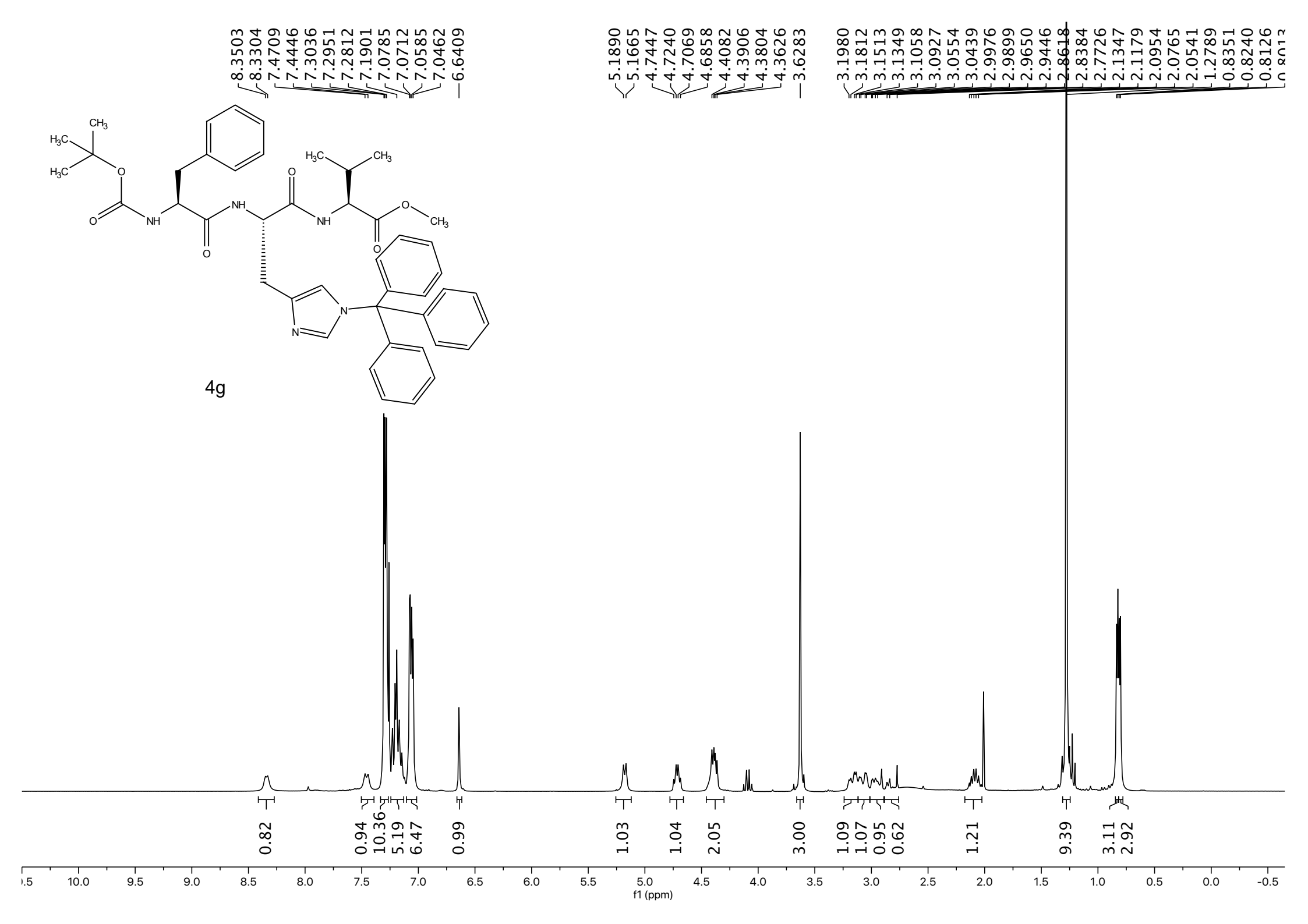
8.3503
8.3304
7.4709
7.4446
7.3036
7.2951
7.2812
7.1901
7.0785
7.0712
7.0585
7.0462
6.6409
5.1890
5.1665
4.7447
4.7240
4.7069
4.6858
4.4082
4.3906
4.3804
4.3626
3.6283
3.1980
3.1812
3.1513
3.1349
3.1058
3.0927
3.0554
3.0439
2.9976
2.9899
2.9650
2.9446
2.8618
2.8384
2.7726
2.1347
2.1179
2.0954
2.0765
2.0541
1.2789
0.8351
0.8240
0.8126
4g
0.82
0.94
10.36
5.19
6.47
0.99
1.03
1.04
2.05
3.00
1.09
1.07
0.95
0.62
1.21
9.39
3.11
2.92
f1 (ppm)

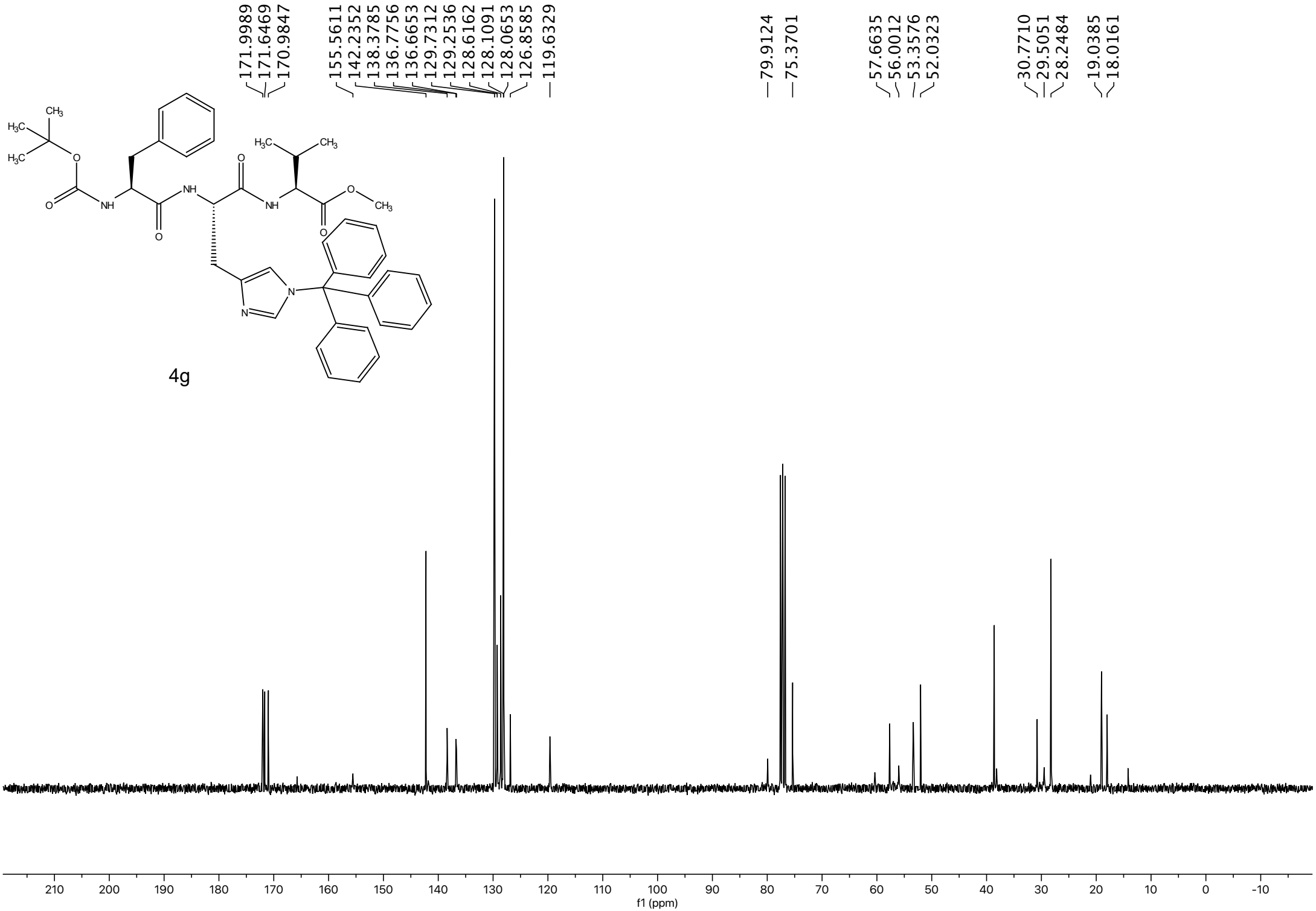
171.9989
171.6469
170.9847
155.5611
142.2352
138.3785
136.7756
136.6653
129.7312
129.2536
128.6162
128.1091
128.0653
126.8585
119.6329
79.9124
75.3701
57.6635
56.0012
53.3576
52.0323
30.7710
29.5051
28.2484
19.0385
18.0161
4g
f1 (ppm)

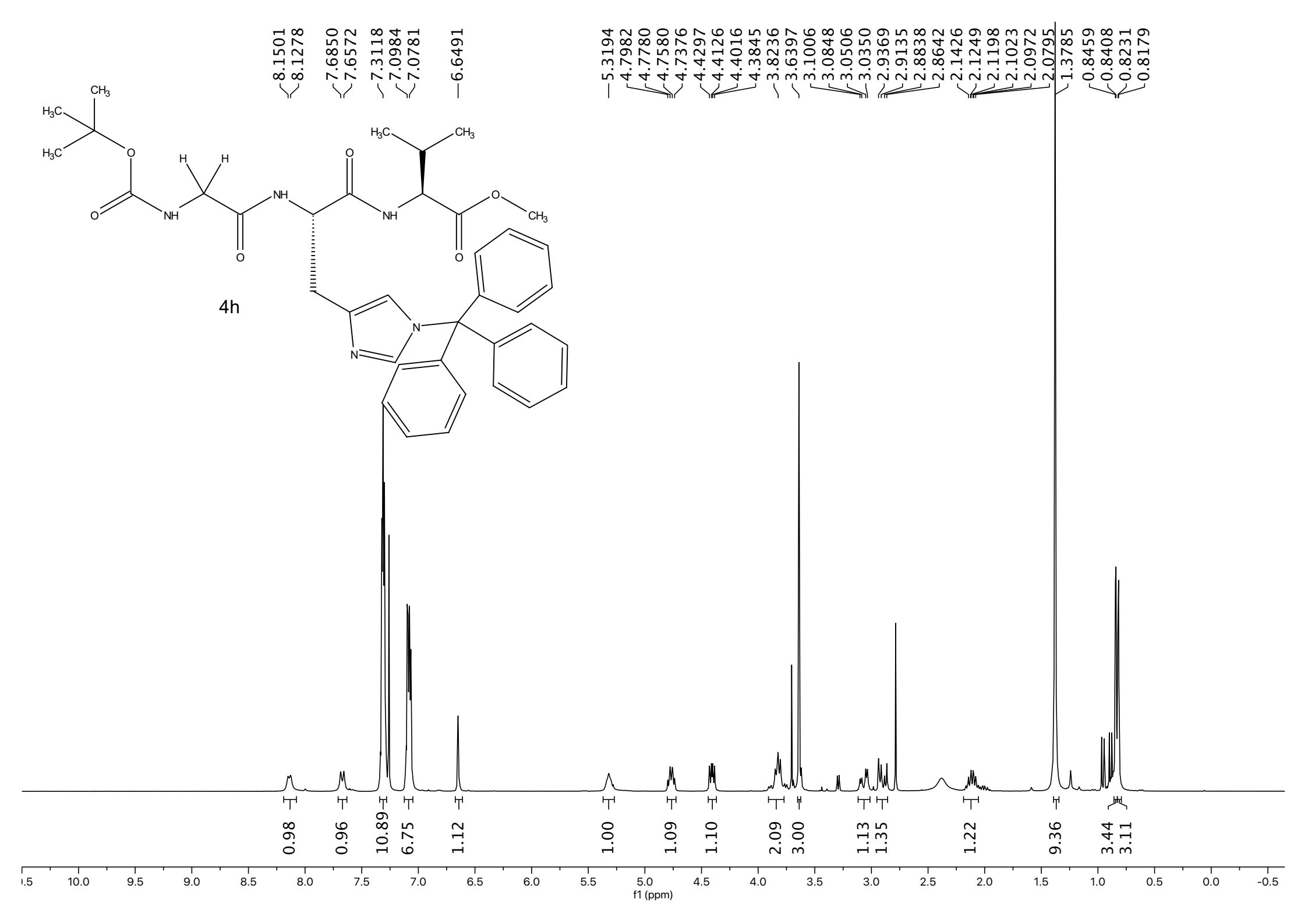
8.1501
8.1278
7.6850
7.6572
7.3118
7.0984
7.0781
6.6491
5.3194
4.7982
4.7780
4.7580
4.7376
4.4297
4.4126
4.4016
4.3845
3.8236
3.6397
3.1006
3.0848
3.0506
3.0350
2.9369
2.9135
2.8838
2.8642
2.1426
2.1249
2.1198
2.1023
2.0972
2.0795
1.3785
0.8459
0.8408
0.8231
0.8179
4h
0.98
0.96
10.89
6.75
1.12
1.00
1.09
1.10
2.09
3.00
1.13
1.35
1.22
9.36
3.44
3.11
f1 (ppm)

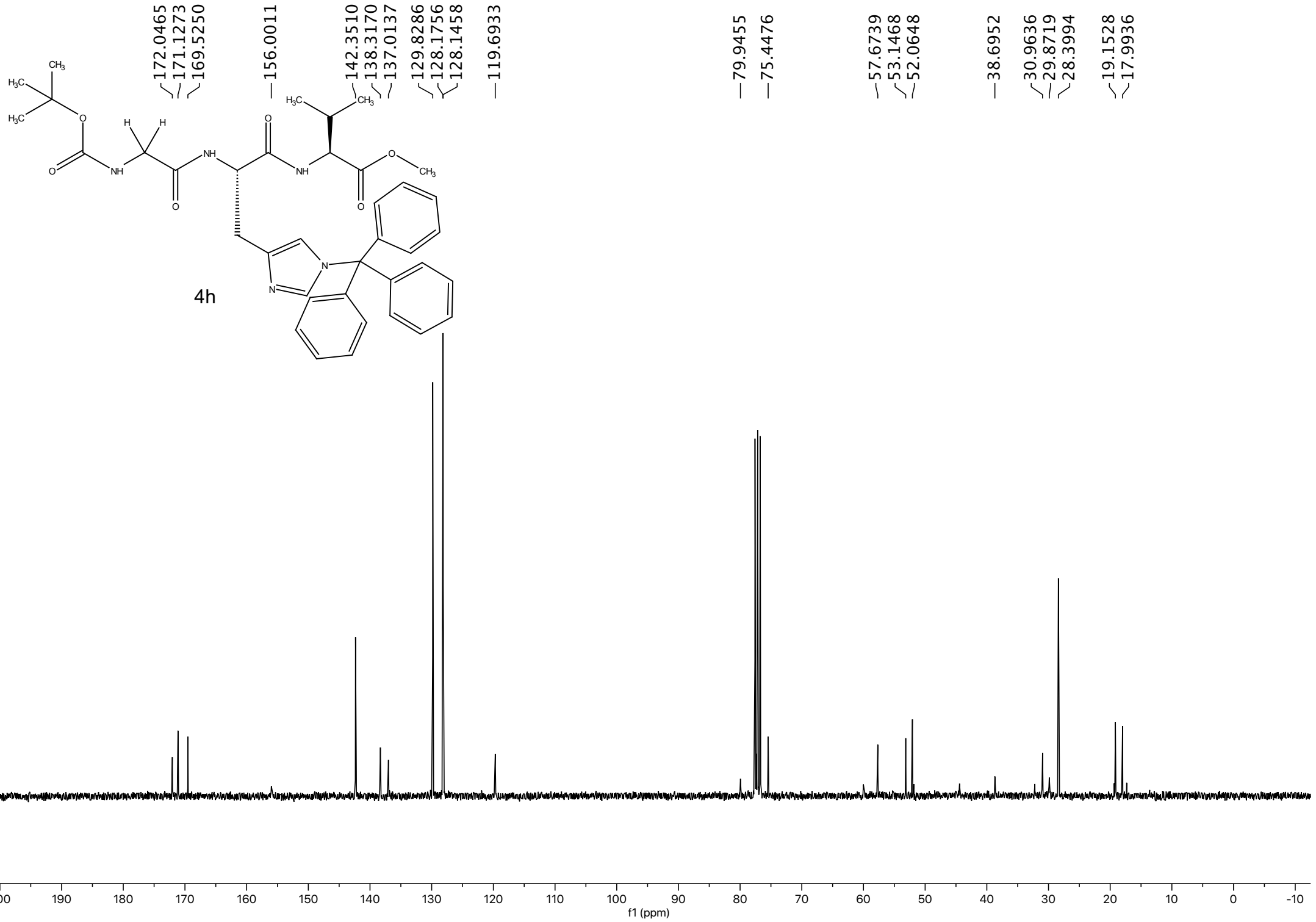
172.0465
171.1273
169.5250
156.0011
142.3510
138.3170
137.0137
129.8286
128.1756
128.1458
119.6933
79.9455
75.4476
57.6739
53.1468
52.0648
38.6952
30.9636
29.8719
28.3994
19.1528
17.9936
4h
200
190
180
170
160
150
140
130
120
110
100
90
80
70
60
50
40
30
20
10
0
-10
f1 (ppm)

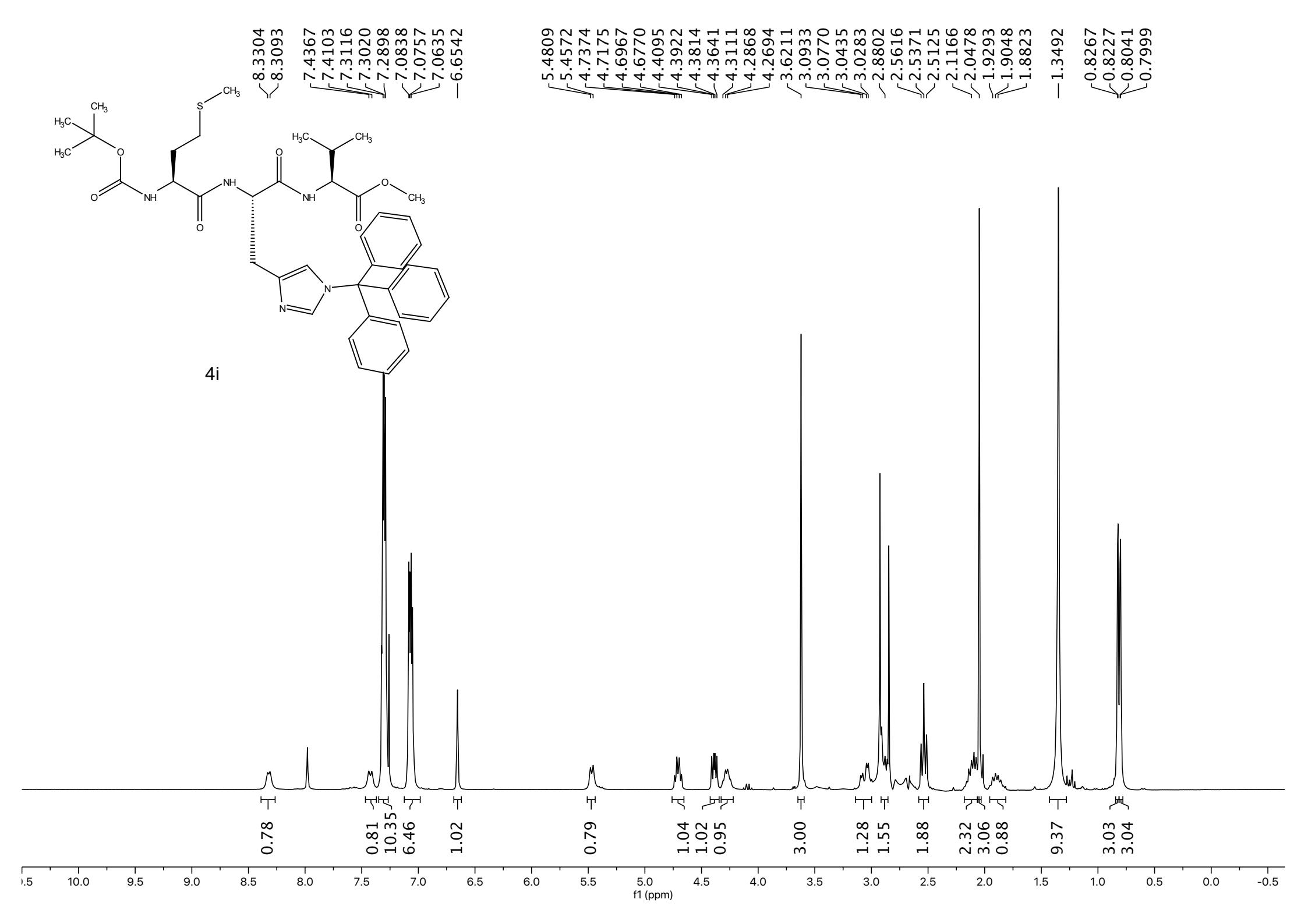
8.3304
8.3093
7.4367
7.4103
7.3116
7.3020
7.2898
7.0838
7.0757
7.0635
6.6542
5.4809
5.4572
4.7374
4.7175
4.6967
4.6770
4.4095
4.3922
4.3814
4.3641
4.3111
4.2868
4.2694
3.6211
3.0933
3.0770
3.0435
3.0283
2.8802
2.5616
2.5371
2.5125
2.1166
2.0478
1.9293
1.9048
1.8823
1.3492
0.8267
0.8227
0.8041
0.7999
4i
0.78
0.81
10.35
6.46
1.02
0.79
1.04
1.02
0.95
3.00
1.28
1.55
1.88
2.32
3.06
0.88
9.37
3.03
3.04
f1 (ppm)

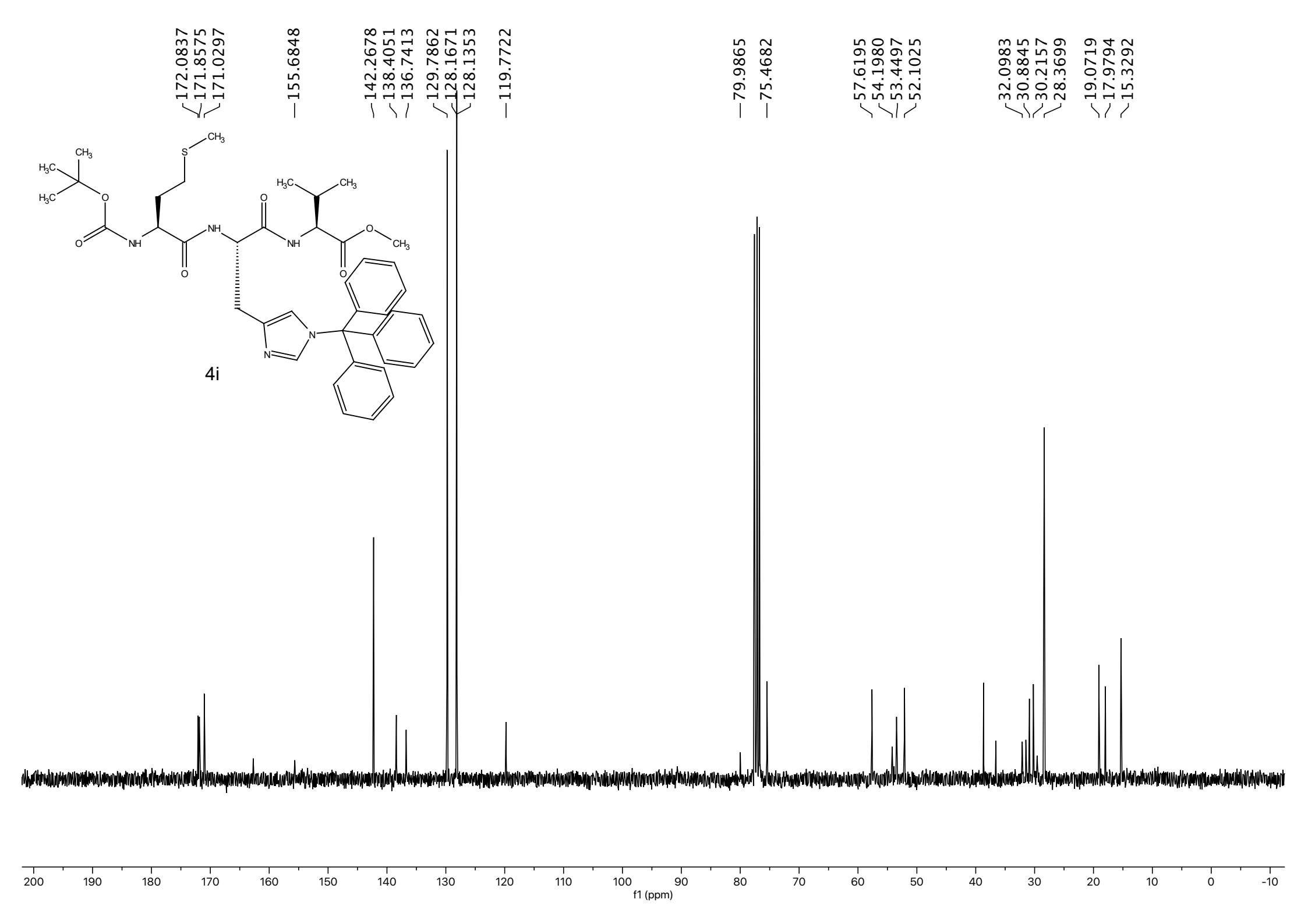
172.0837
171.8575
171.0297
155.6848
142.2678
138.4051
136.7413
129.7862
128.1671
128.1353
119.7722
79.9865
75.4682
57.6195
54.1980
53.4497
52.1025
32.0983
30.8845
30.2157
28.3699
19.0719
17.9794
15.3292
4i
200
190
180
170
160
150
140
130
120
110
100
90
80
70
60
50
40
30
20
10
0
-10
f1 (ppm)

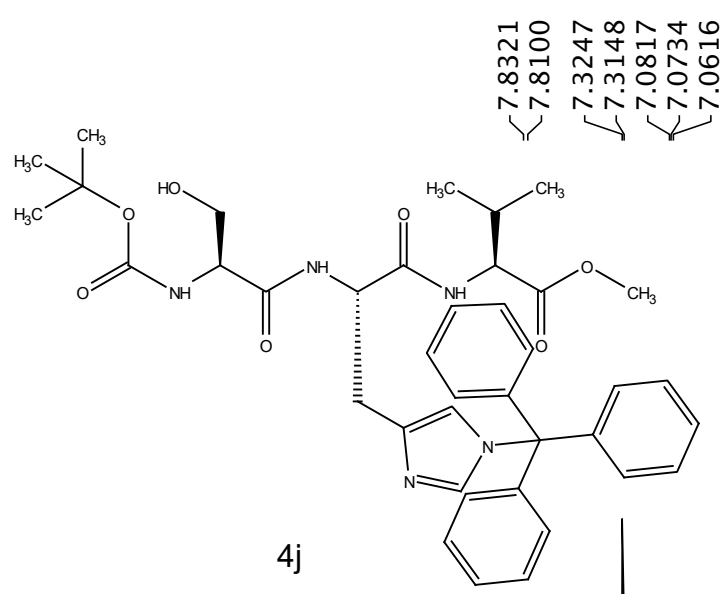
4j

7.8321
7.8100
7.3247
7.3148
7.0817
7.0734
7.0616
6.6166
5.7011
5.6808
4.7996
4.7796
4.7615
4.7402
4.4603
4.4435
4.4315
4.4147
4.1478
4.0329
4.0259
3.9950
3.9885
3.7065
3.6884
3.6693
3.6504
3.5601
3.1400
3.1260
3.0901
3.0764
2.9619
2.9425
2.9120
2.8912
2.1099
2.0926
1.3970
0.8498
0.8354
0.8273
0.8126
0.87
10.87
7.53
1.11
1.01
1.14
1.13
1.09
1.15
1.24
3.00
1.08
1.41
1.22
9.82
3.29
3.34
f1 (ppm)

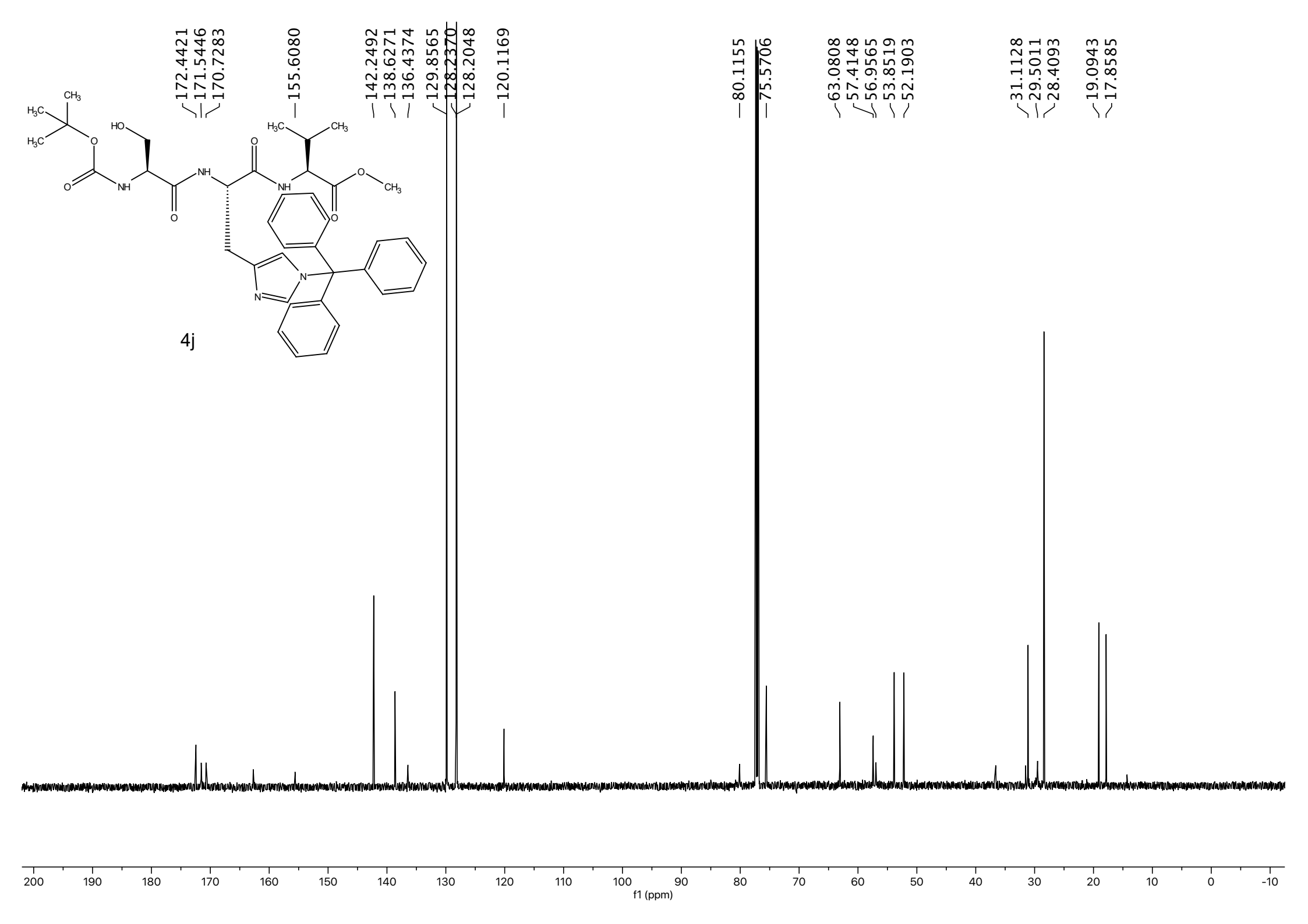
172.4421
171.5446
170.7283
155.6080
142.2492
138.6271
136.4374
129.8565
128.2370
128.2048
120.1169
80.1155
75.5706
63.0808
57.4148
56.9565
53.8519
52.1903
31.1128
29.5011
28.4093
19.0943
17.8585
4j
200
190
180
170
160
150
140
130
120
110
100
90
80
70
60
50
40
30
20
10
0
-10
f1 (ppm)

4j COSY

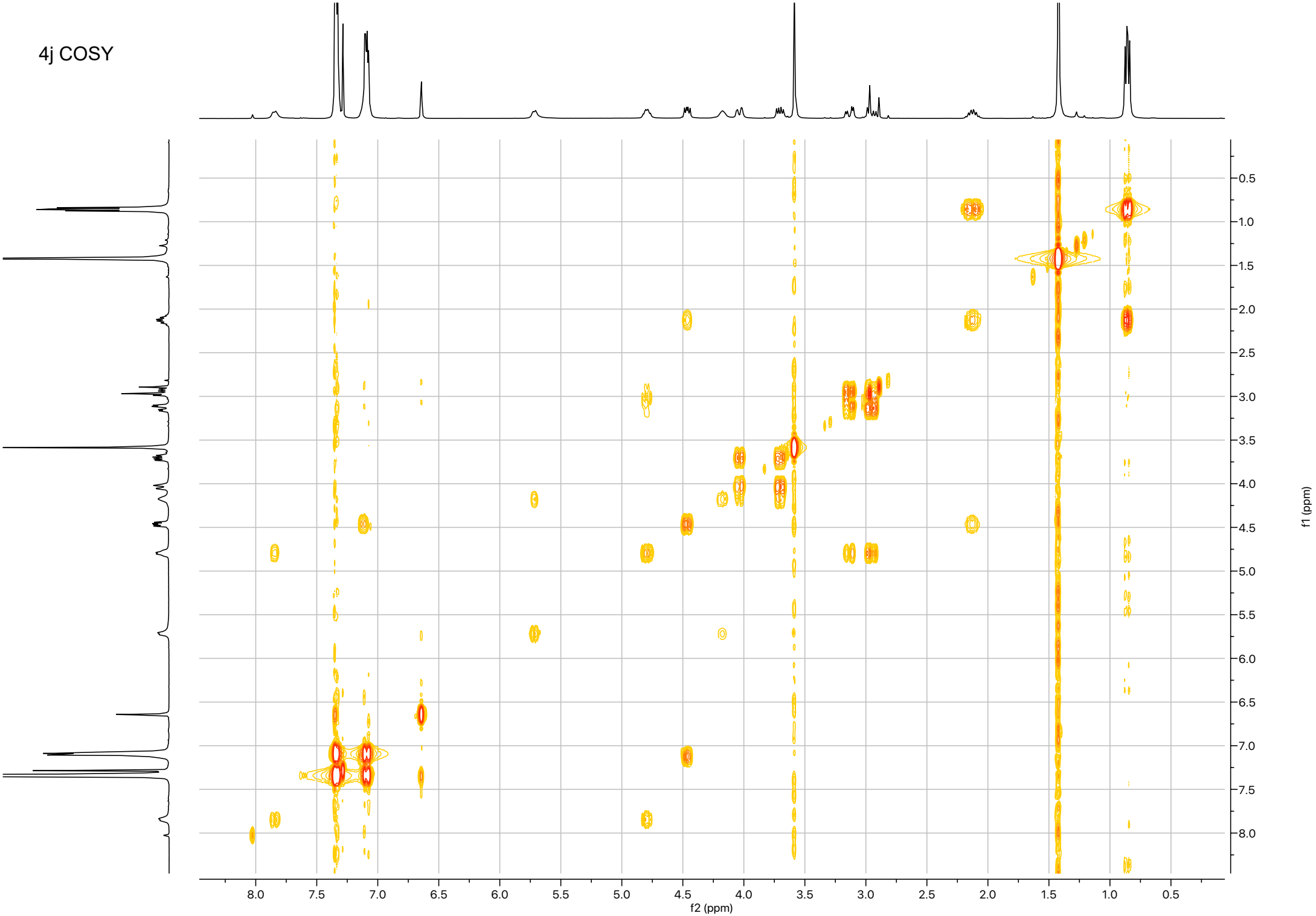
8.0
7.5
7.0
6.5
6.0
5.5
5.0
4.5
4.0
3.5
3.0
2.5
2.0
1.5
1.0
0.5
f2 (ppm)
0.5
1.0
1.5
2.0
2.5
3.0
3.5
4.0
4.5
5.0
5.5
6.0
6.5
7.0
7.5
8.0
f1 (ppm)

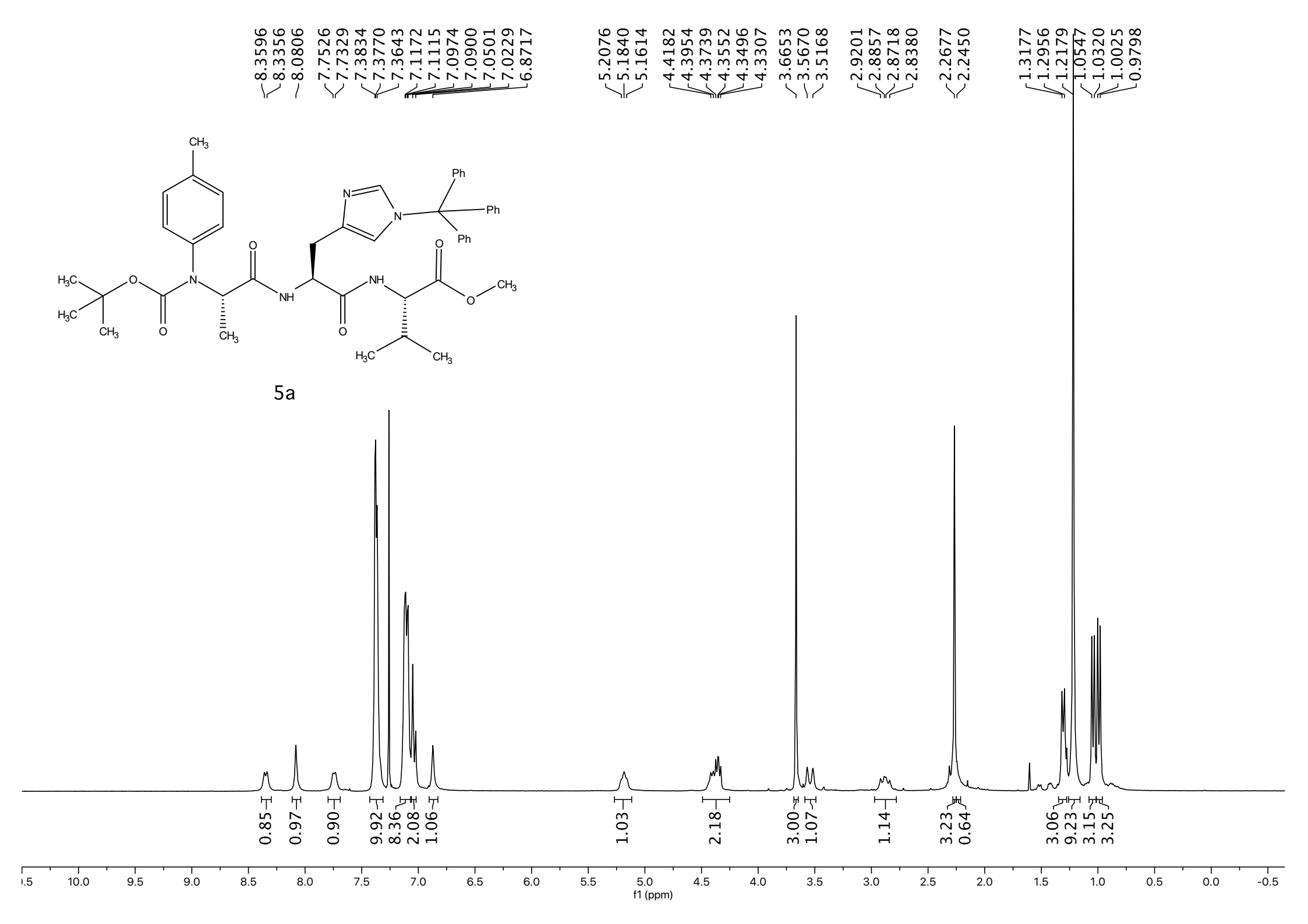
8.3596
8.3356
8.0806
7.7526
7.7329
7.3834
7.3770
7.3643
7.1172
7.1115
7.0974
7.0900
7.0501
7.0229
6.8717
5.2076
5.1840
5.1614
4.4182
4.3954
4.3739
4.3552
4.3496
4.3307
3.6653
3.5670
3.5168
2.9201
2.8857
2.8718
2.8380
2.2677
2.2450
1.3177
1.2956
1.2179
1.0547
1.0320
1.0025
0.9798
0.85
0.97
0.90
9.92
8.36
2.08
1.06
1.03
2.18
3.00
1.07
1.14
3.23
0.64
3.06
9.23
3.15
3.25
f1 (ppm)

5a

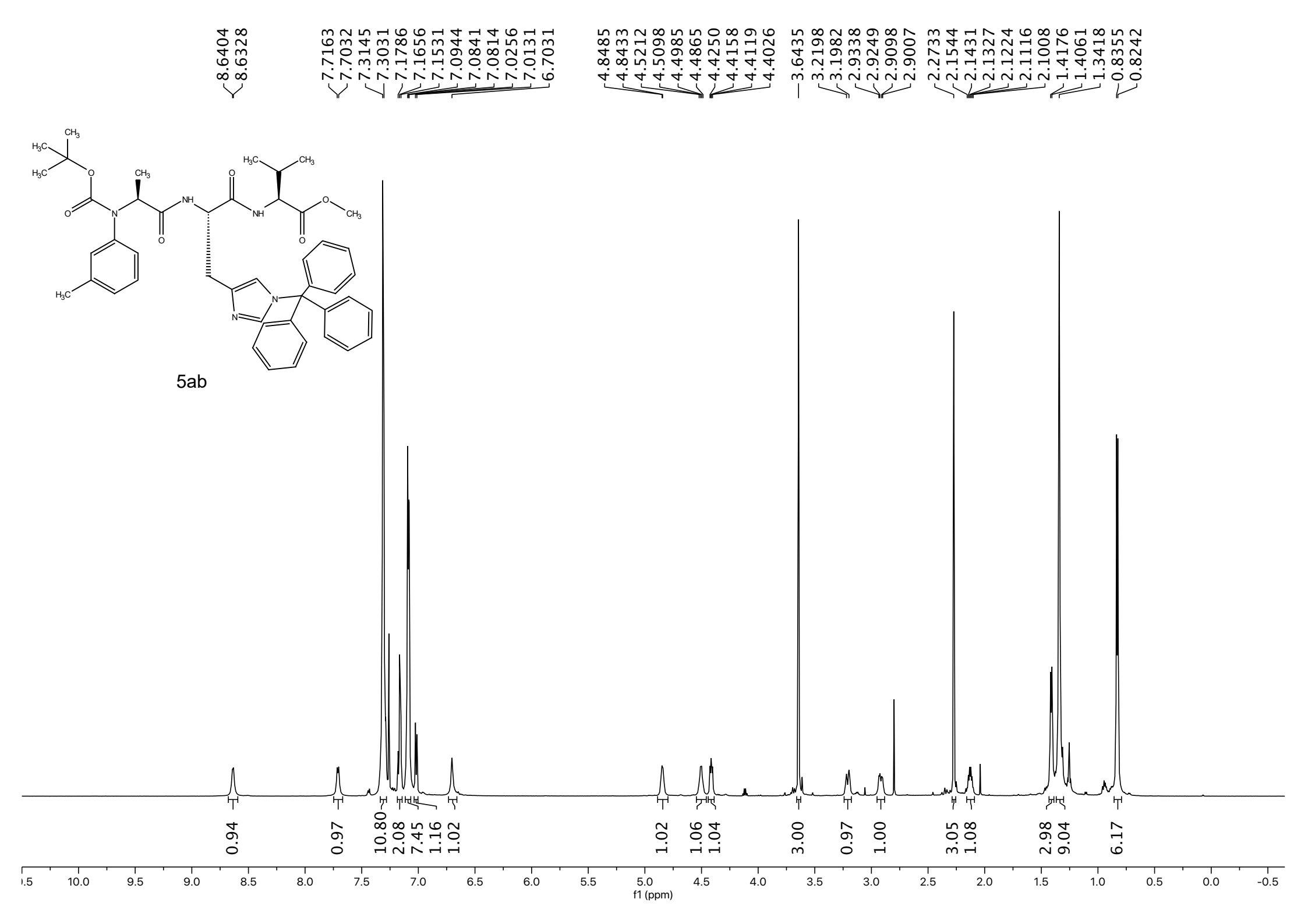
8.6404
8.6328
7.7163
7.7032
7.3145
7.3031
7.1786
7.1656
7.1531
7.0944
7.0841
7.0814
7.0256
7.0131
6.7031
4.8485
4.8433
4.5212
4.5098
4.4985
4.4865
4.4250
4.4158
4.4119
4.4026
3.6435
3.2198
3.1982
2.9338
2.9249
2.9098
2.9007
2.2733
2.1544
2.1431
2.1327
2.1224
2.1116
2.1008
1.4176
1.4061
1.3418
0.8355
0.8242
5ab
0.94
0.97
10.80
2.08
7.45
1.16
1.02
1.02
1.06
1.04
3.00
0.97
1.00
3.05
1.08
2.98
9.04
6.17
f1 (ppm)

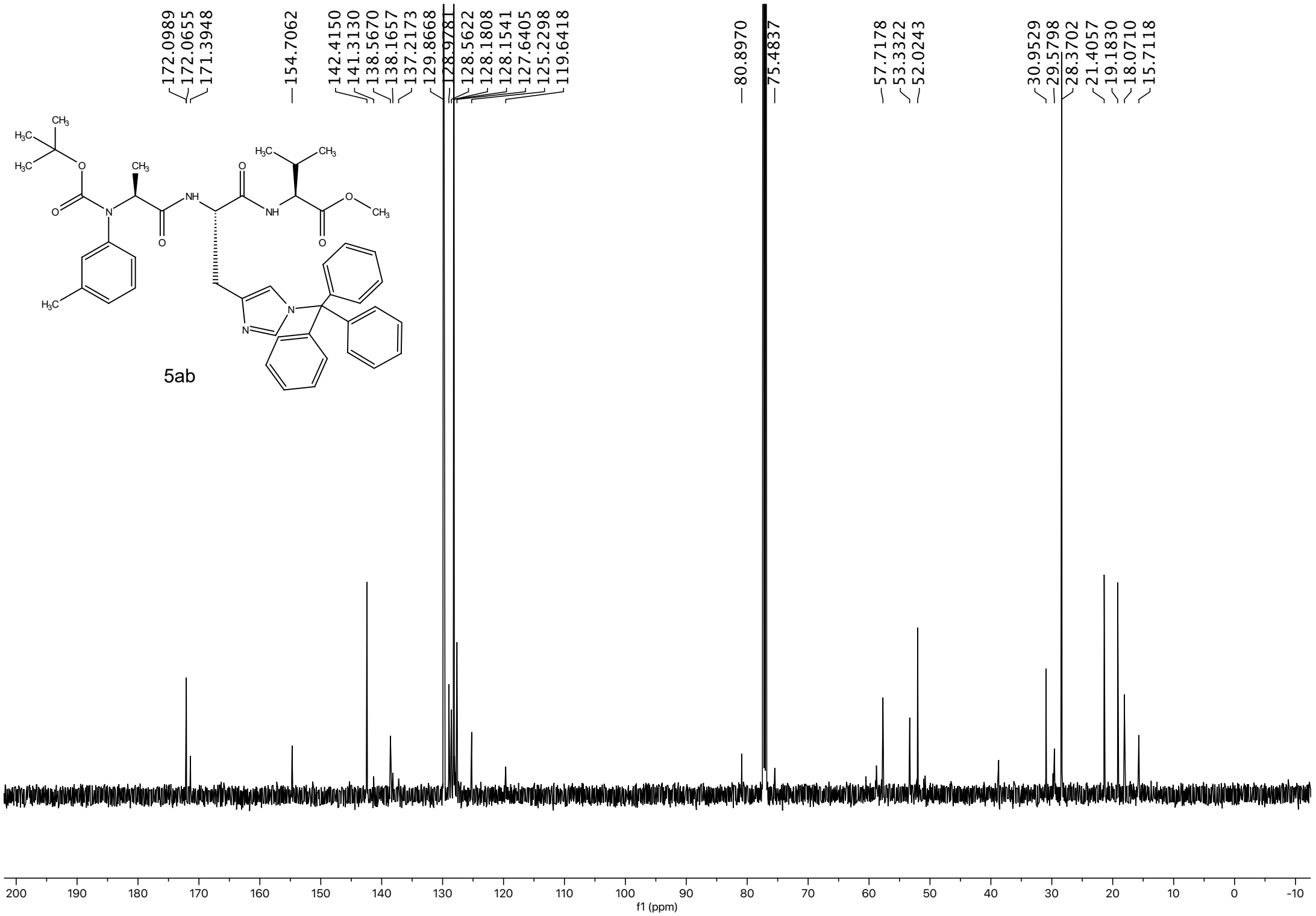
172.0989
172.0655
171.3948
154.7062
142.4150
141.3130
138.5670
138.1657
137.2173
129.8668
128.9781
128.5622
128.1808
128.1541
127.6405
125.2298
119.6418
80.8970
75.4837
57.7178
53.3322
52.0243
30.9529
29.5798
28.3702
21.4057
19.1830
18.0710
15.7118
5ab
f1 (ppm)

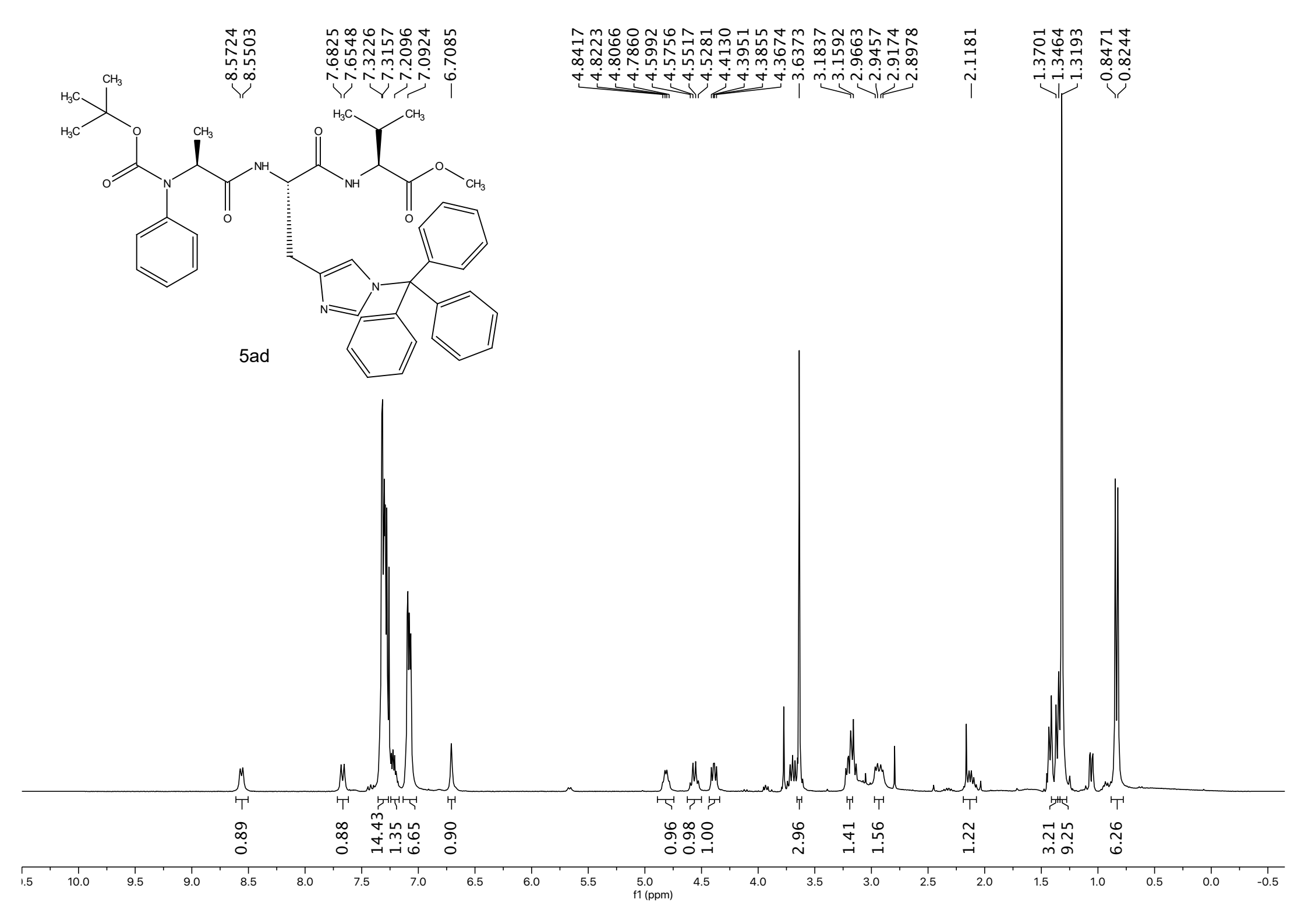
8.5724
8.5503
7.6825
7.6548
7.3226
7.3157
7.2096
7.0924
6.7085
4.8417
4.8223
4.8066
4.7860
4.5992
4.5756
4.5517
4.5281
4.4130
4.3951
4.3855
4.3674
3.6373
3.1837
3.1592
2.9663
2.9457
2.9174
2.8978
2.1181
1.3701
1.3464
1.3193
0.8471
0.8244
5ad
0.89
0.88
14.43
1.35
6.65
0.90
0.96
0.98
1.00
2.96
1.41
1.56
1.22
3.21
9.25
6.26
f1 (ppm)

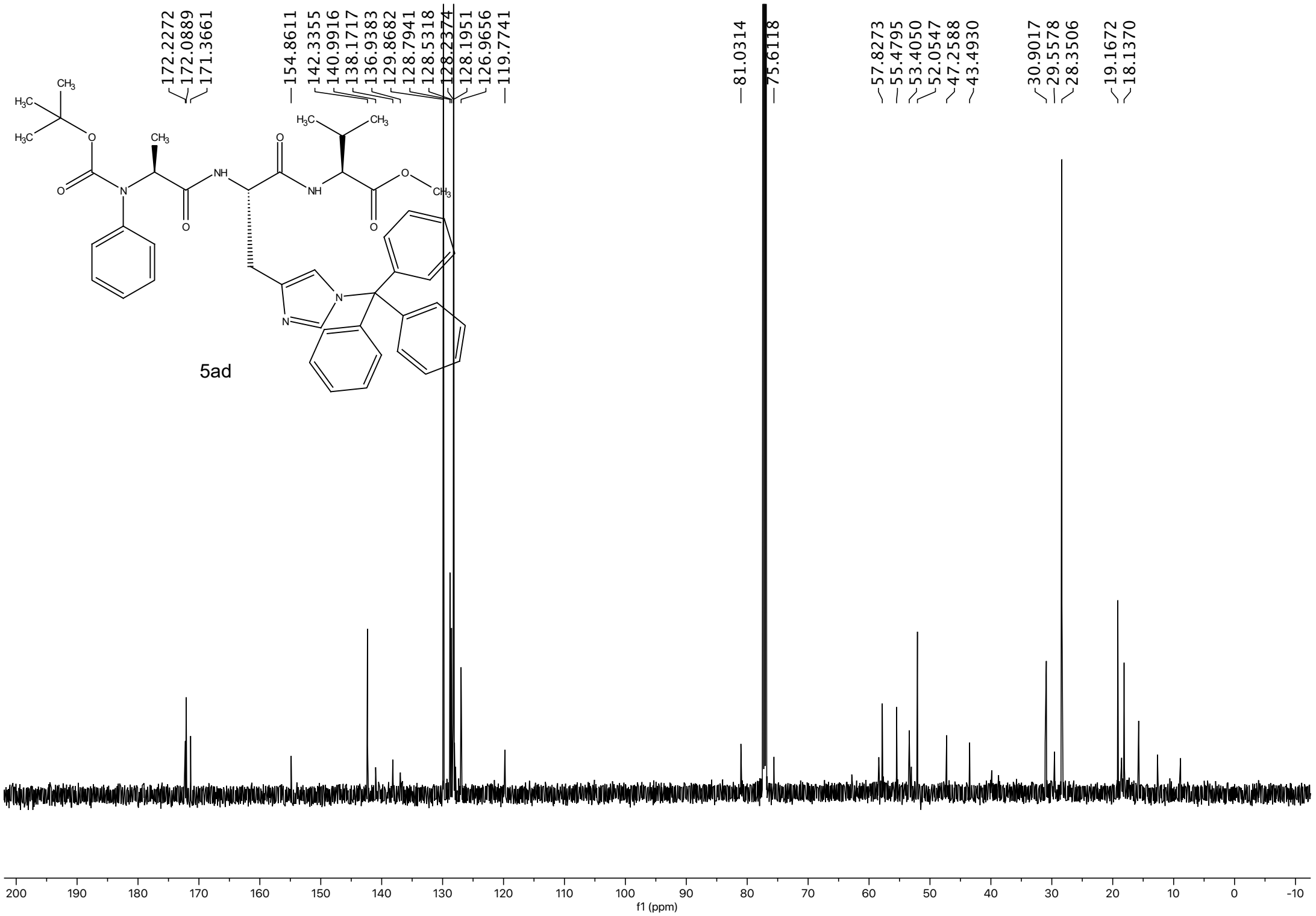
172.2272
172.0889
171.3661
154.8611
142.3355
140.9916
138.1717
136.9383
129.8682
128.7941
128.5318
128.2374
128.1951
126.9656
119.7741
81.0314
75.6118
57.8273
55.4795
53.4050
52.0547
47.2588
43.4930
30.9017
29.5578
28.3506
19.1672
18.1370
5ad
200
190
180
170
160
150
140
130
120
110
100
90
80
70
60
50
40
30
20
10
0
-10
f1 (ppm)

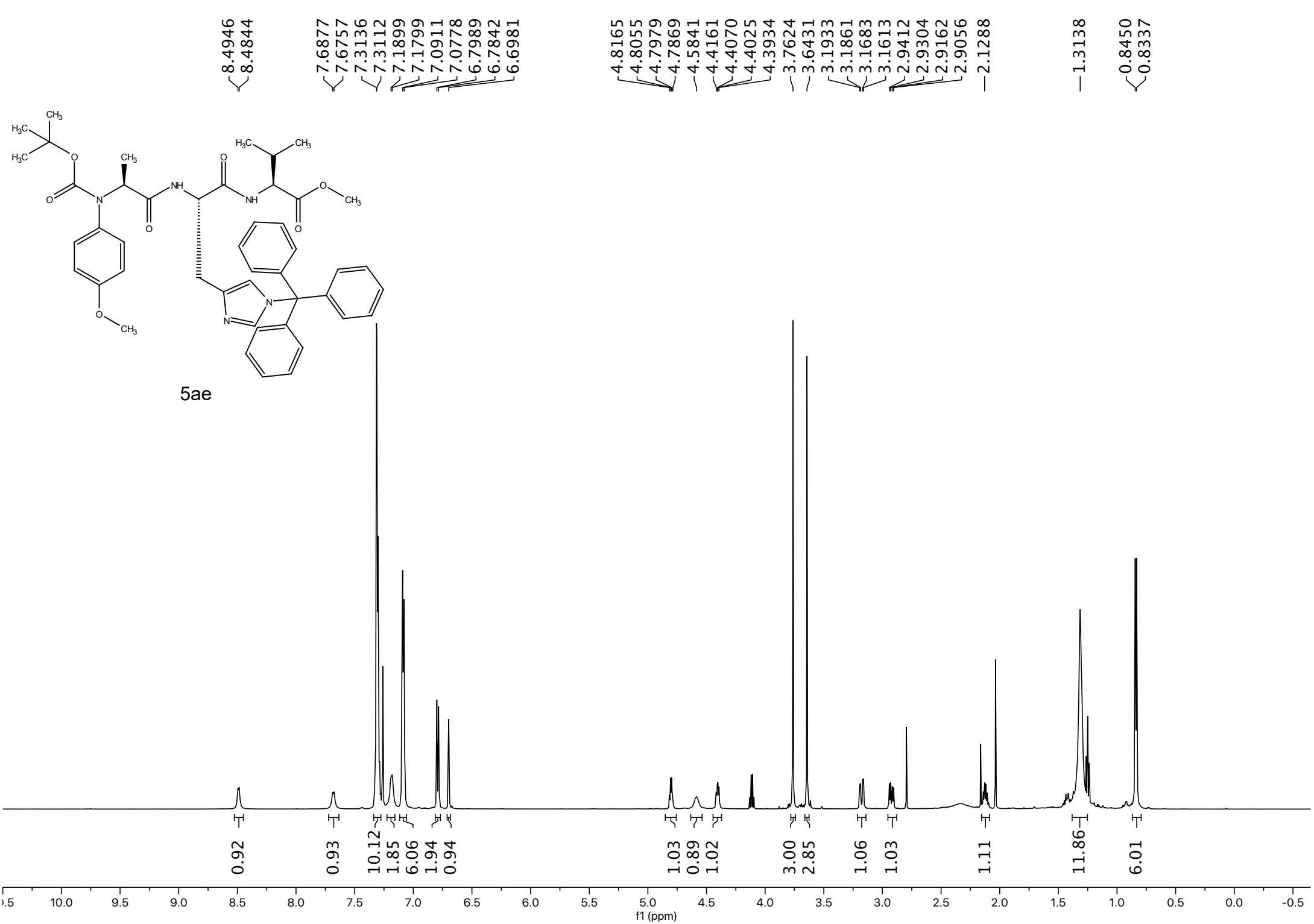
8.4946
8.4844
7.6877
7.6757
7.3136
7.3112
7.1899
7.1799
7.0911
7.0778
6.7989
6.7842
6.6981
4.8165
4.8055
4.7979
4.7869
4.5841
4.4161
4.4070
4.4025
4.3934
3.7624
3.6431
3.1933
3.1861
3.1683
3.1613
2.9412
2.9304
2.9162
2.9056
2.1288
1.3138
0.8450
0.8337
5ae
0.92
0.93
10.12
1.85
6.06
1.94
0.94
1.03
0.89
1.02
3.00
2.85
1.06
1.03
1.11
11.86
6.01
f1 (ppm)

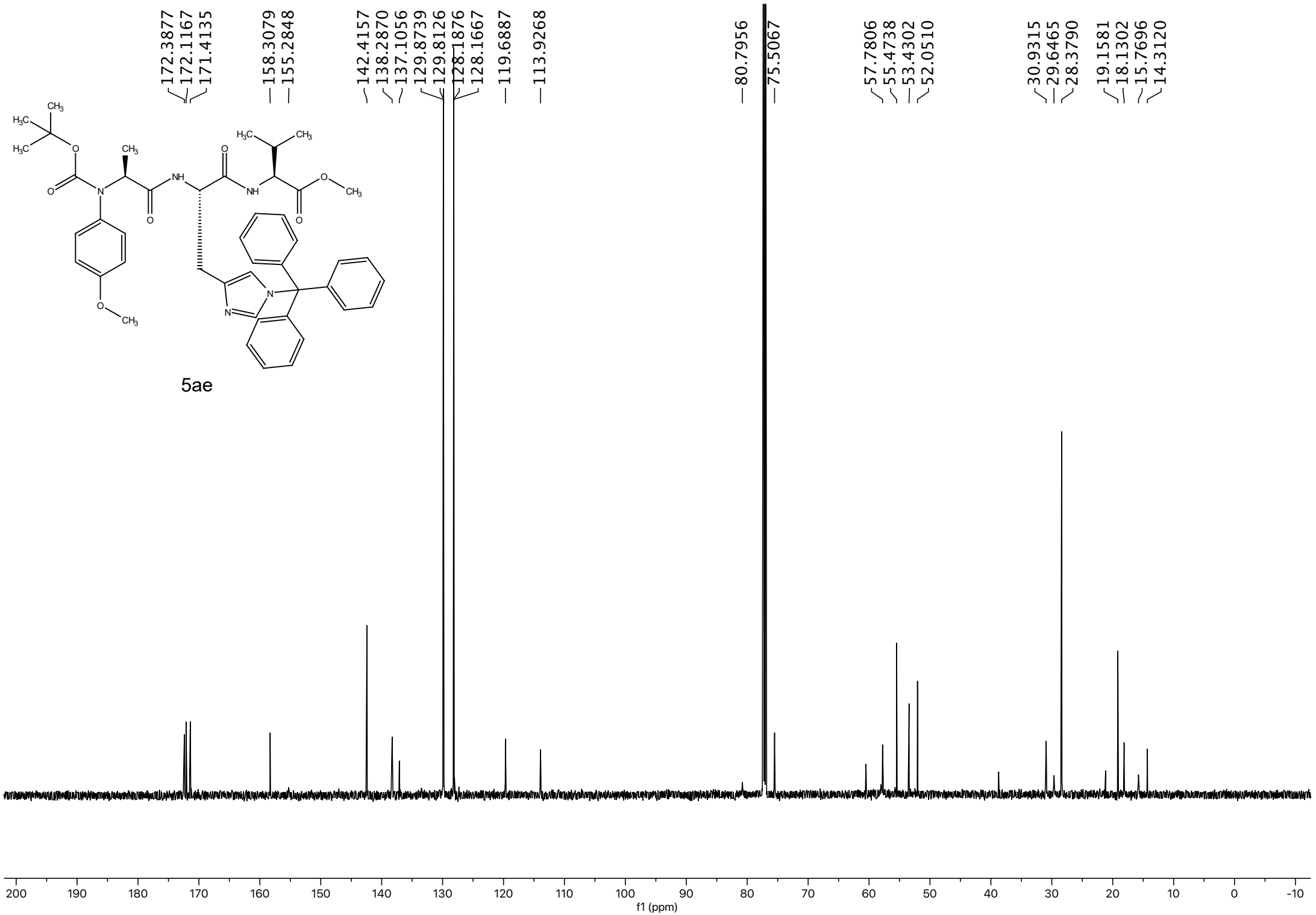
172.3877
172.1167
171.4135
158.3079
155.2848
142.4157
138.2870
137.1056
129.8739
129.8126
128.1876
128.1667
119.6887
113.9268
80.7956
75.5067
57.7806
55.4738
53.4302
52.0510
30.9315
29.6465
28.3790
19.1581
18.1302
15.7696
14.3120
5ae
200
190
180
170
160
150
140
130
120
110
100
90
80
70
60
50
40
30
20
10
0
-10
f1 (ppm)

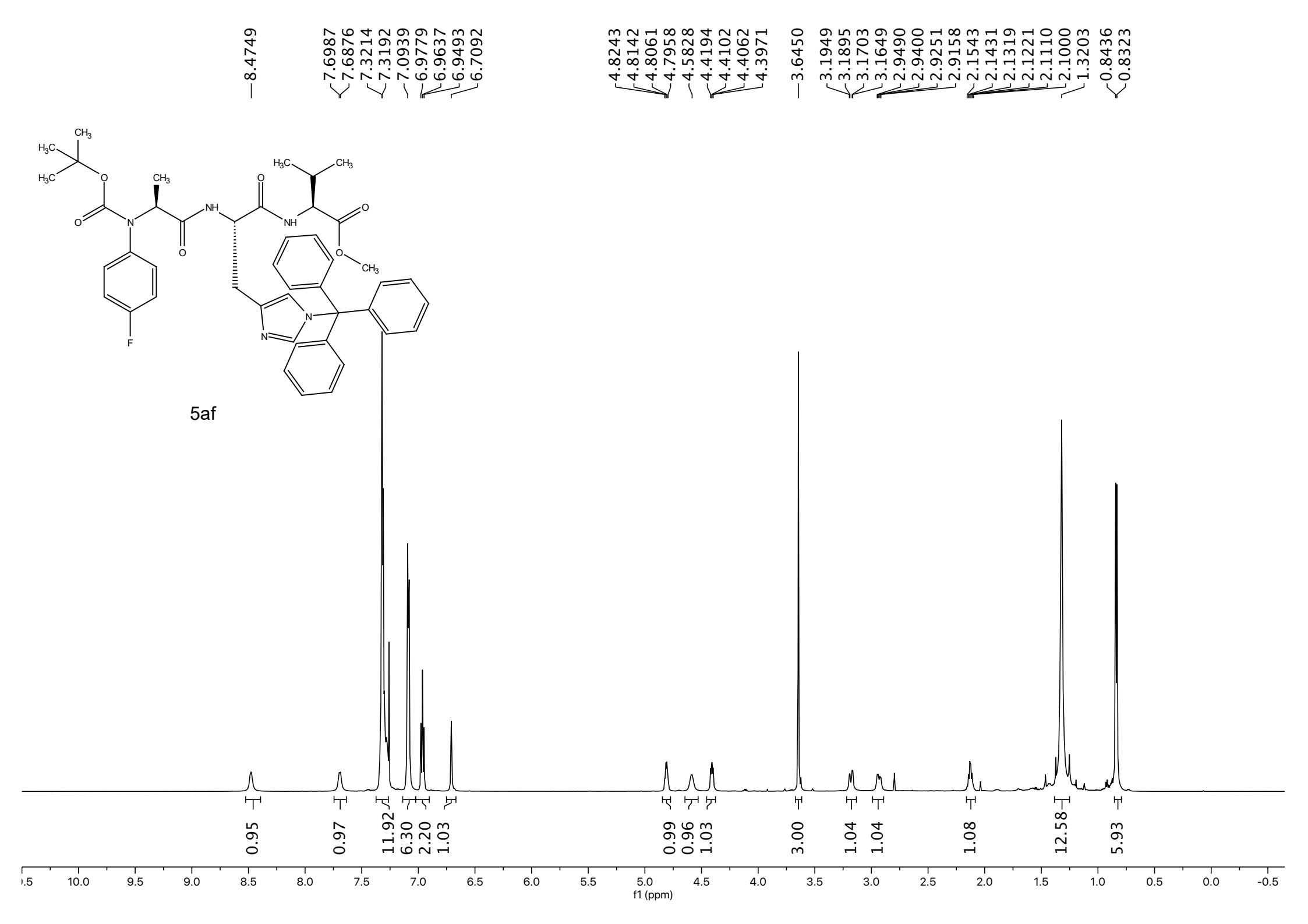
8.4749
7.6987
7.6876
7.3214
7.3192
7.0939
6.9779
6.9637
6.9493
6.7092
4.8243
4.8142
4.8061
4.7958
4.5828
4.4194
4.4102
4.4062
4.3971
3.6450
3.1949
3.1895
3.1703
3.1649
2.9490
2.9400
2.9251
2.9158
2.1543
2.1431
2.1319
2.1221
2.1110
2.1000
1.3203
0.8436
0.8323
5af
0.95
0.97
11.92
6.30
2.20
1.03
0.99
0.96
1.03
3.00
1.04
1.04
1.08
12.58
5.93
f1 (ppm)

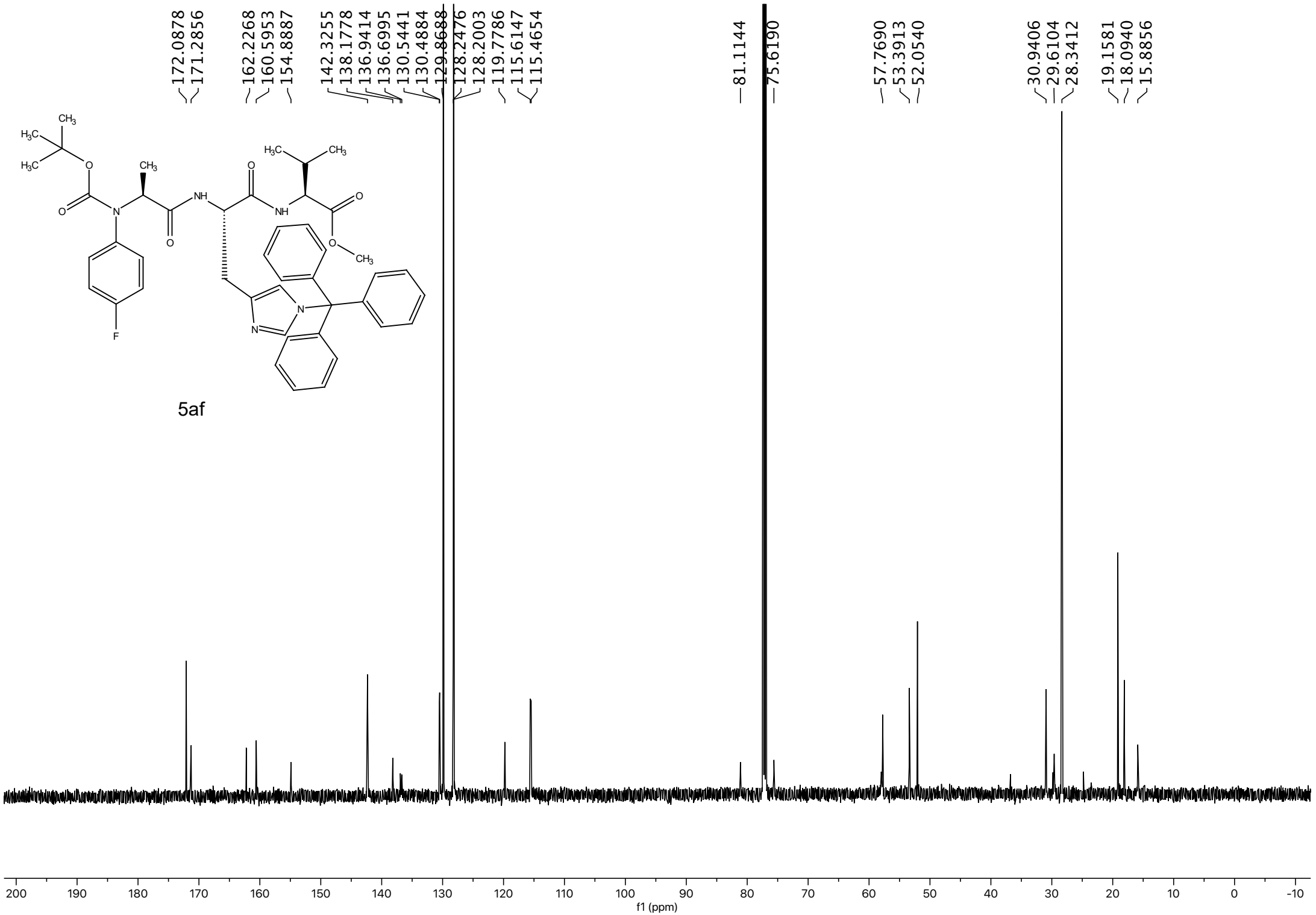
172.0878
171.2856
162.2268
160.5953
154.8887
142.3255
138.1778
136.9414
136.6995
130.5441
130.4884
129.8688
128.2476
128.2003
119.7786
115.6147
115.4654
81.1144
75.6190
57.7690
53.3913
52.0540
30.9406
29.6104
28.3412
19.1581
18.0940
15.8856
5af
f1 (ppm)

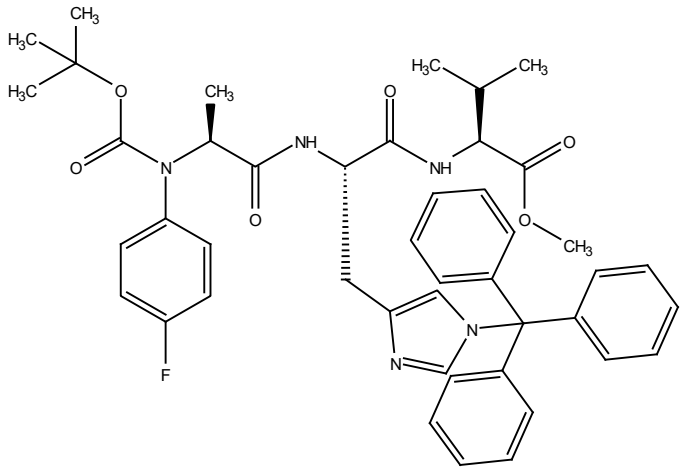

5af

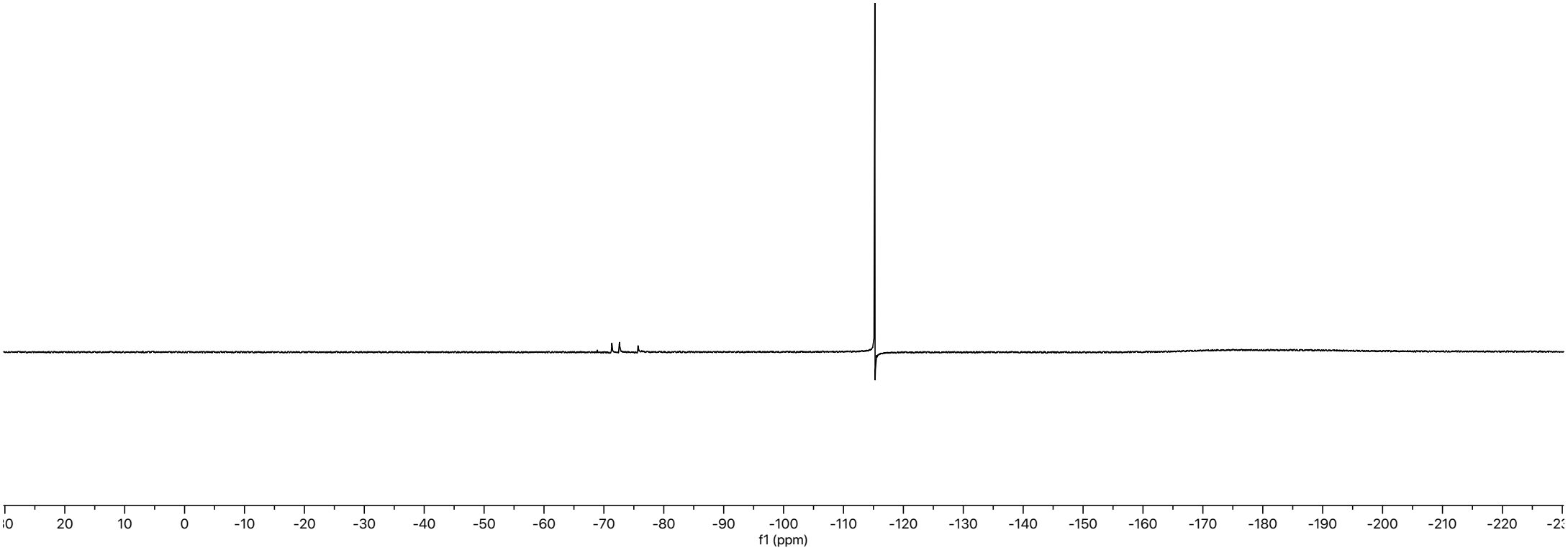

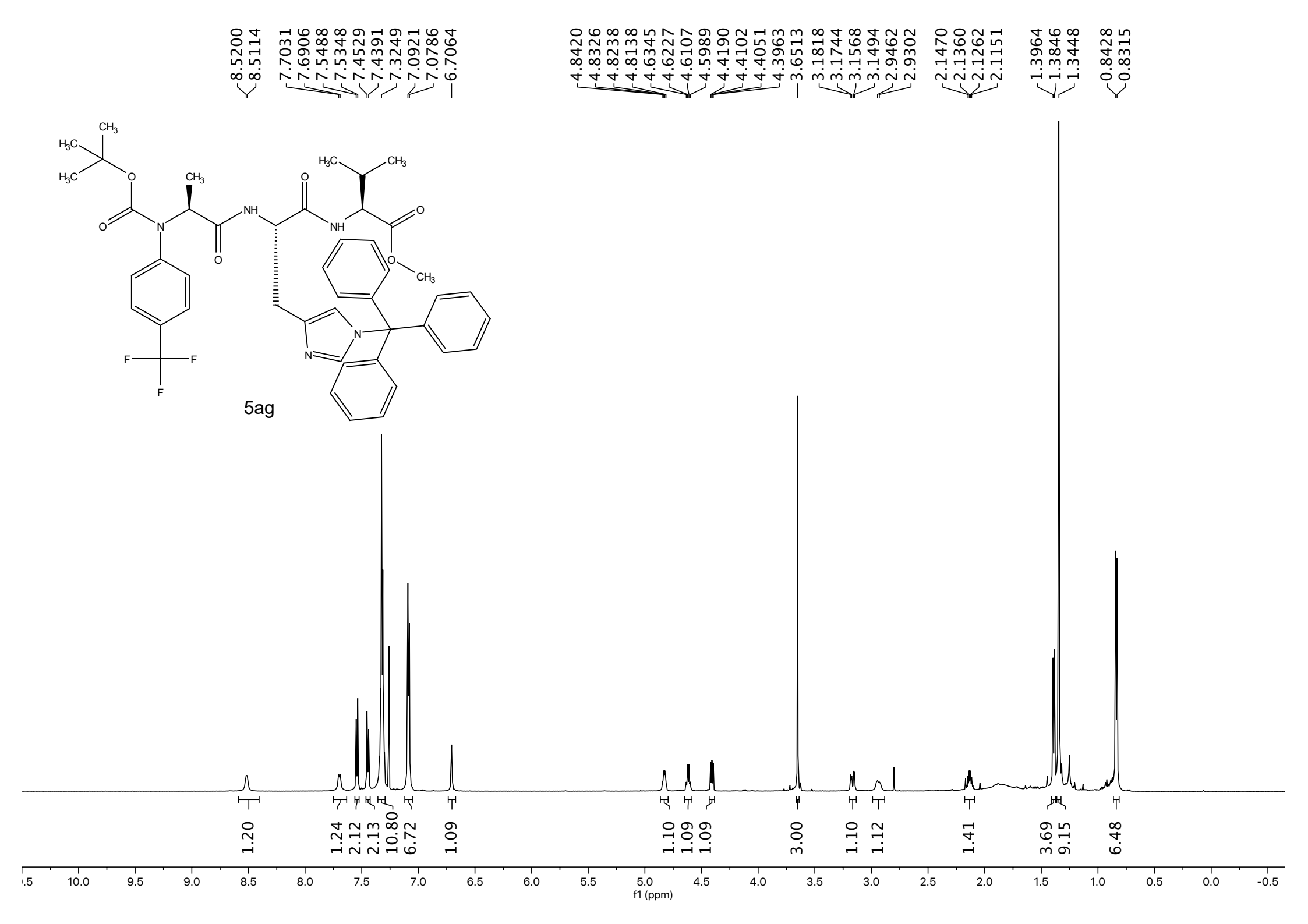
8.5200
8.5114
7.7031
7.6906
7.5488
7.5348
7.4529
7.4391
7.3249
7.0921
7.0786
6.7064
4.8420
4.8326
4.8238
4.8138
4.6345
4.6227
4.6107
4.5989
4.4190
4.4102
4.4051
4.3963
3.6513
3.1818
3.1744
3.1568
3.1494
2.9462
2.9302
2.1470
2.1360
2.1262
2.1151
1.3964
1.3846
1.3448
0.8428
0.8315
5ag
1.20
1.24
2.12
2.13
10.80
6.72
1.09
1.10
1.09
1.09
3.00
1.10
1.12
1.41
3.69
9.15
6.48
f1 (ppm)

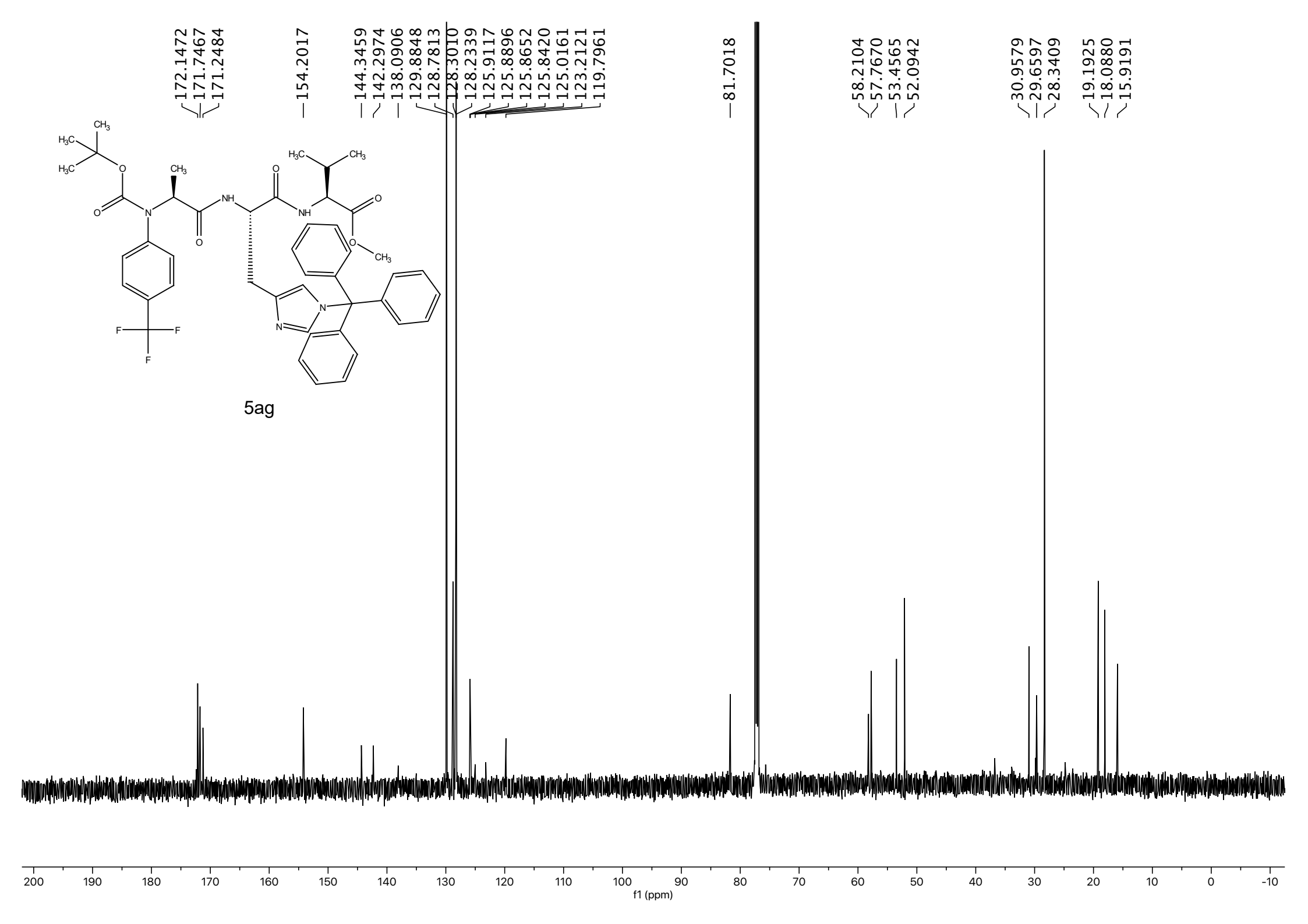
172.1472
171.7467
171.2484
154.2017
144.3459
142.2974
138.0906
129.8848
128.7813
128.3010
128.2339
125.9117
125.8896
125.8652
125.8420
125.0161
123.2121
119.7961
81.7018
58.2104
57.7670
53.4565
52.0942
30.9579
29.6597
28.3409
19.1925
18.0880
15.9191
5ag
f1 (ppm)

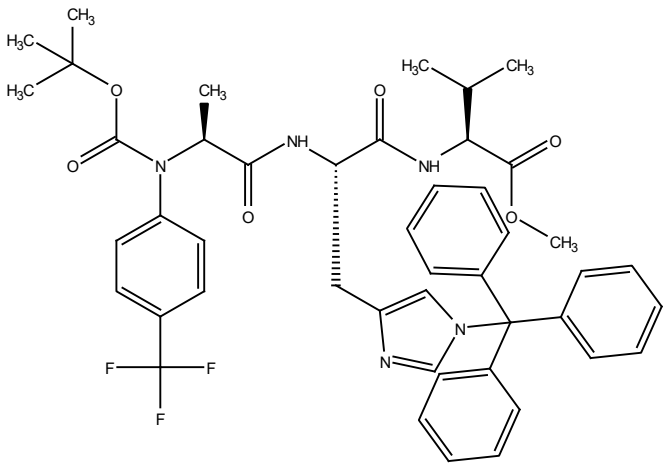

5ah

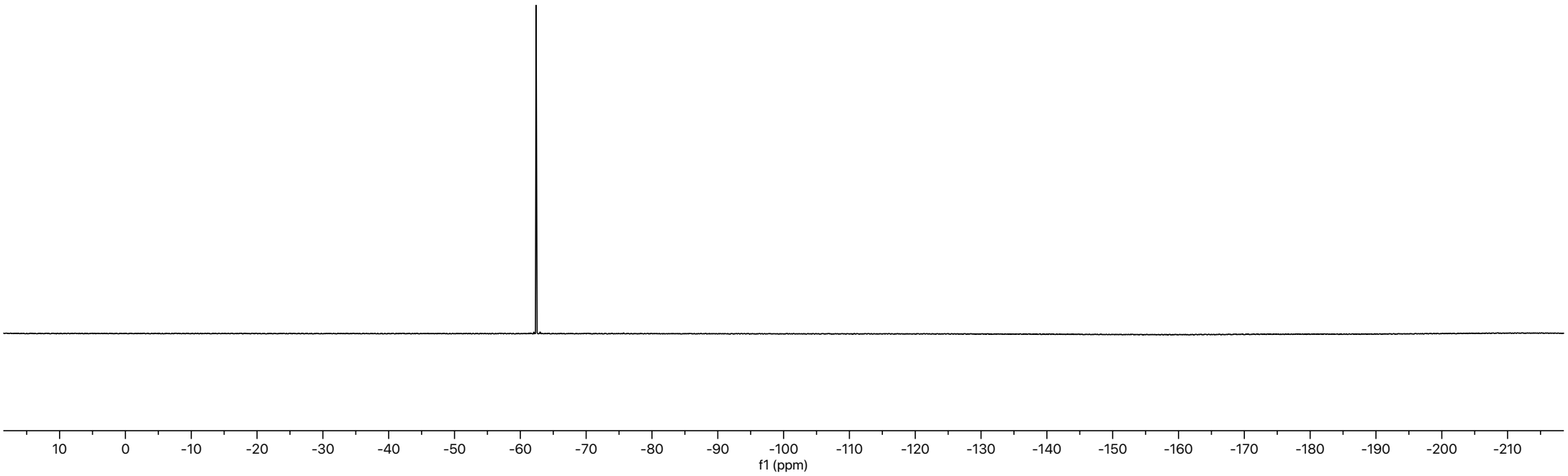
−62.3989
10
0
-10
-20
-30
-40
-50
-60
-70
-80
-90
-100
-110
-120
-130
-140
-150
-160
-170
-180
-190
-200
-210
f1 (ppm)

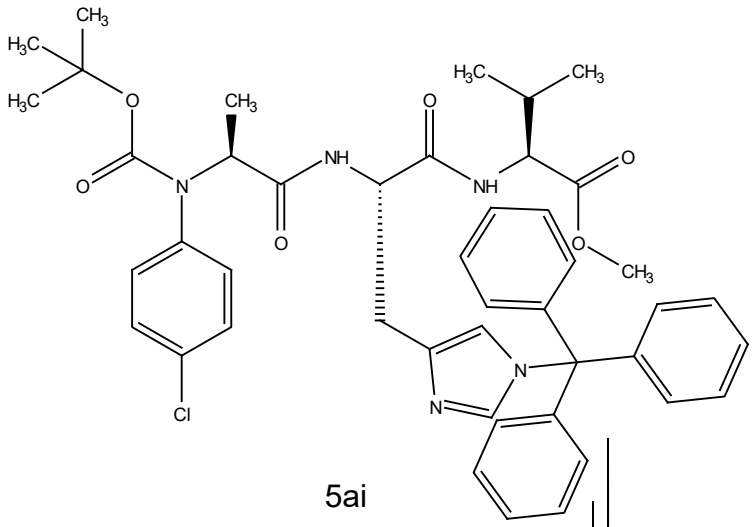

5ai

8.4635
8.4544
7.6821
7.6685
7.3253
7.3236
7.2477
7.0939
7.0842
7.0806
6.7114
4.8289
4.8184
4.8099
4.7994
4.6038
4.5929
4.5812
4.5705
4.4181
4.4092
4.4043
4.3954
3.6481
3.1910
3.1837
3.1660
3.1588
2.9547
2.9449
2.9300
2.9201
2.1344
2.1244
2.1133
1.3436
1.3256
0.8461
0.8347

1.01
1.13
10.82
3.94
6.56
1.06
1.06
1.02
1.08
3.00
1.06
1.14
1.10
11.94
6.16

f1 (ppm)

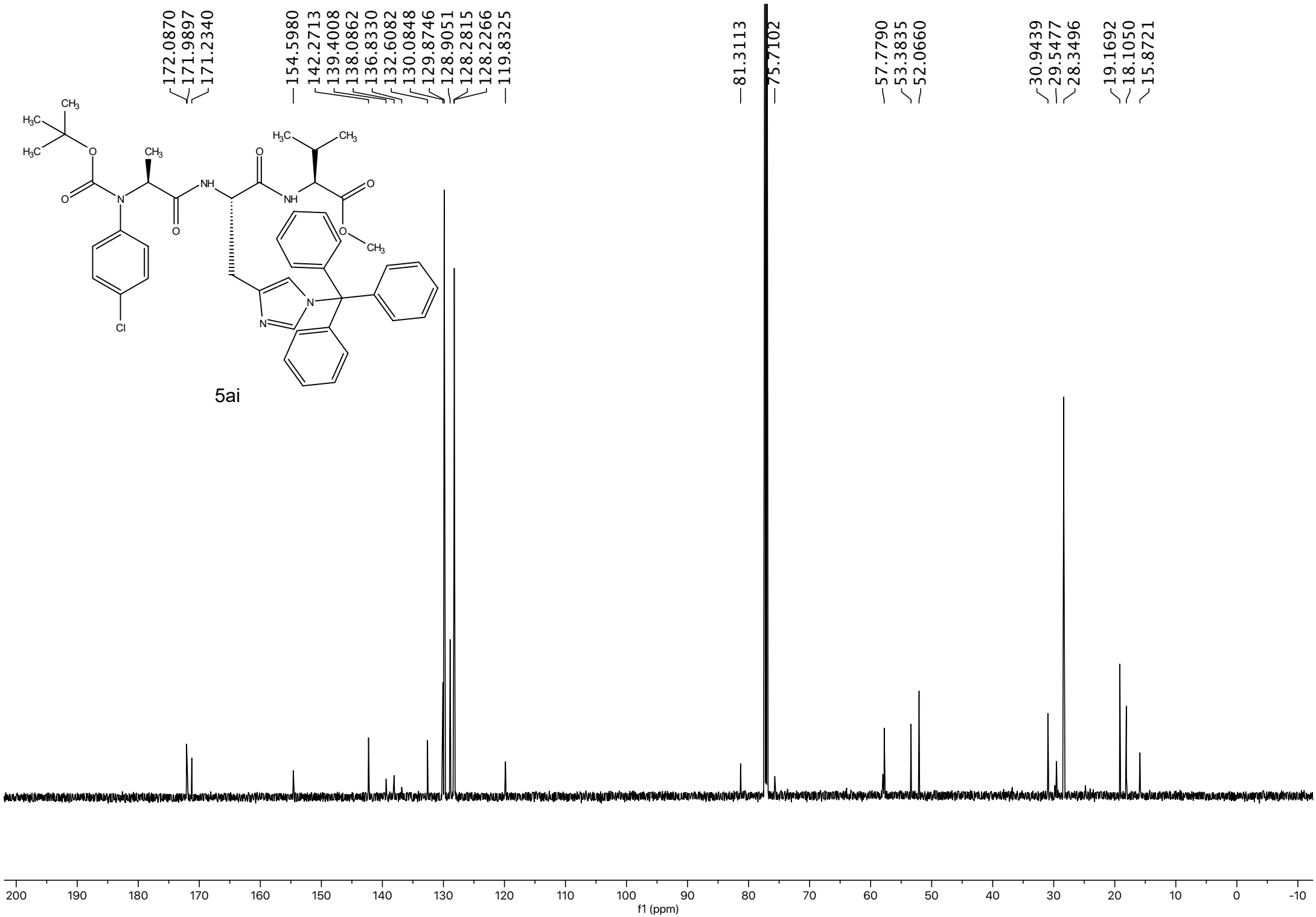
172.0870
171.9897
171.2340
154.5980
142.2713
139.4008
138.0862
136.8330
132.6082
130.0848
129.8746
128.9051
128.2815
128.2266
119.8325
81.3113
75.7102
57.7790
53.3835
52.0660
30.9439
29.5477
28.3496
19.1692
18.1050
15.8721
5ai
f1 (ppm)

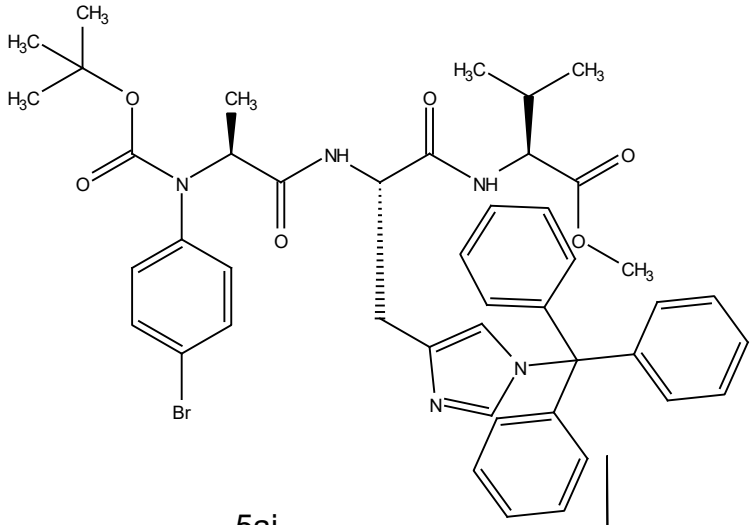

5aj

8.4499
8.4404
7.6452
7.6319
7.3330
7.3189
7.2530
7.2416
7.1292
7.1153
7.0220
7.0119
7.0090
6.6308
4.7460
4.7387
4.5364
4.5254
4.5136
4.5024
4.3496
4.3407
4.3360
4.3270
3.5809
3.1188
3.1129
3.0941
3.0883
2.8656
2.8571
2.8416
2.0628
2.0525
1.2602
0.7726
0.7613

0.96
0.97
2.08
10.67
2.08
6.31
0.98
0.93
0.94
1.11
3.00
1.10
1.11
1.13
12.27
6.34

f1 (ppm)

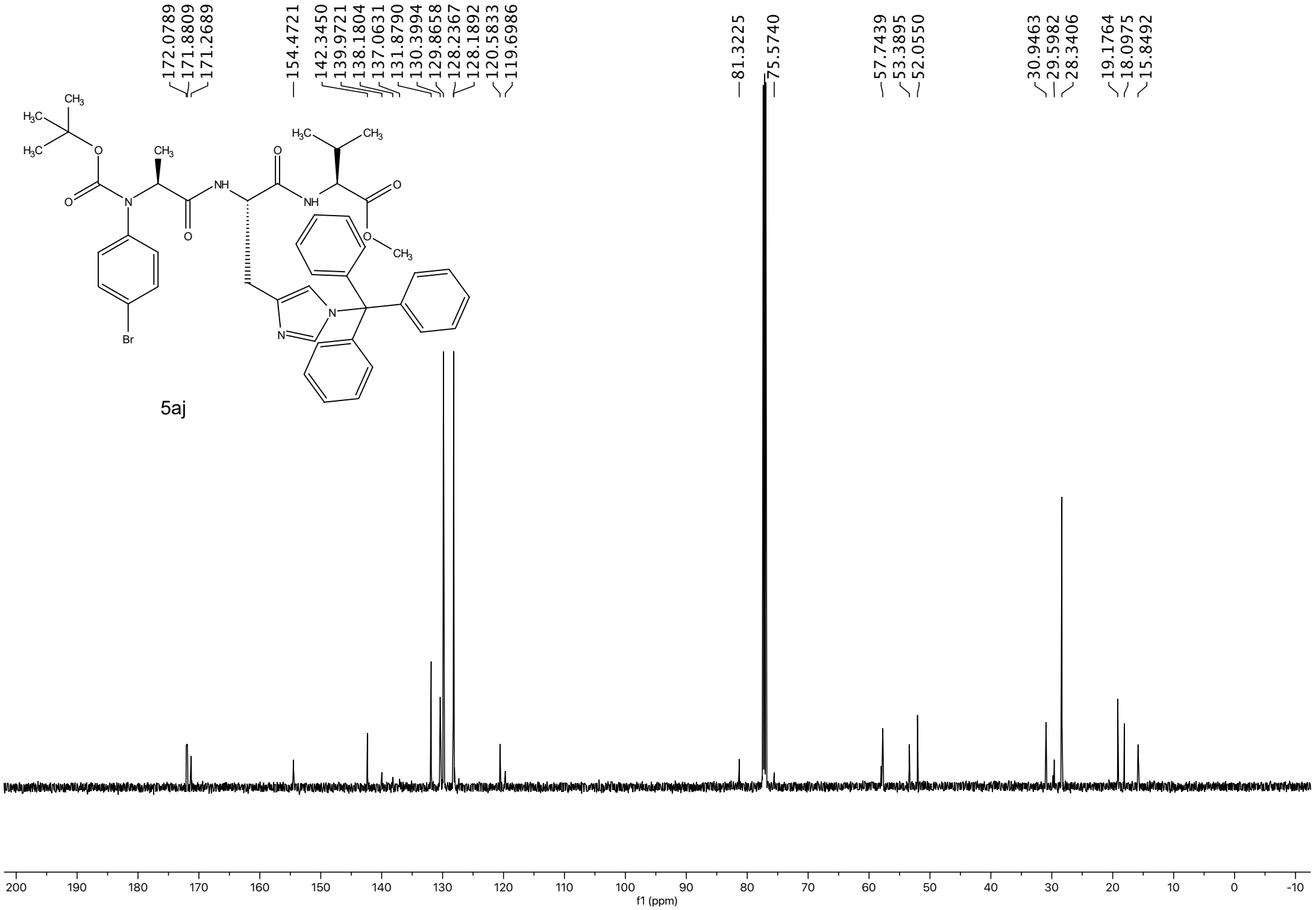
172.0789
171.8809
171.2689
154.4721
142.3450
139.9721
138.1804
137.0631
131.8790
130.3994
129.8658
128.2367
128.1892
120.5833
119.6986
81.3225
75.5740
57.7439
53.3895
52.0550
30.9463
29.5982
28.3406
19.1764
18.0975
15.8492
5aj
200
190
180
170
160
150
140
130
120
110
100
90
80
70
60
50
40
30
20
10
0
-10
f1 (ppm)

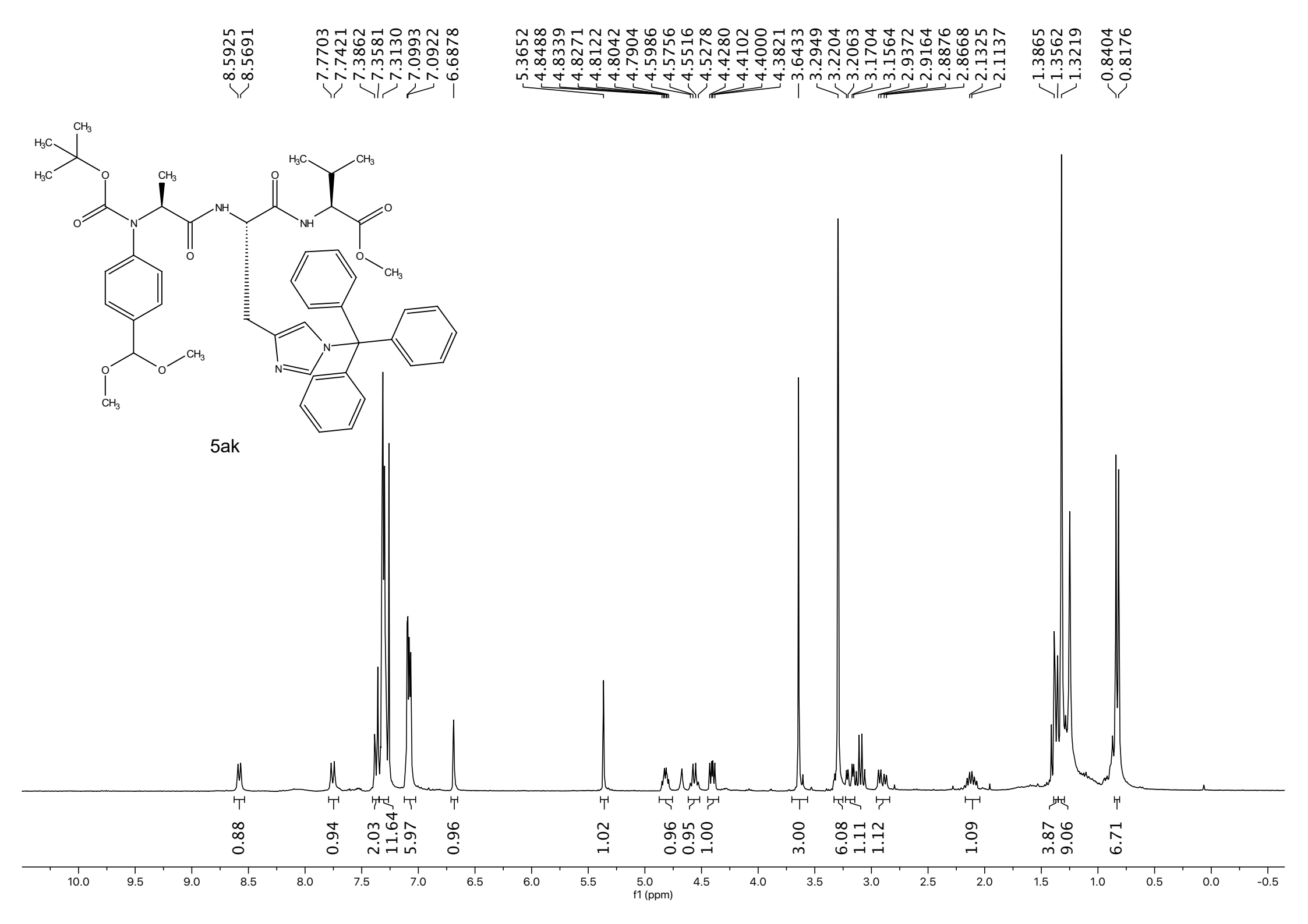
8.5925
8.5691
7.7703
7.7421
7.3862
7.3581
7.3130
7.0993
7.0922
6.6878
5.3652
4.8488
4.8339
4.8271
4.8122
4.8042
4.7904
4.5986
4.5756
4.5516
4.5278
4.4280
4.4102
4.4000
4.3821
3.6433
3.2949
3.2204
3.2063
3.1704
3.1564
2.9372
2.9164
2.8876
2.8668
2.1325
2.1137
1.3865
1.3562
1.3219
0.8404
0.8176
5ak
0.88
0.94
2.03
11.64
5.97
0.96
1.02
0.96
0.95
1.00
3.00
6.08
1.11
1.12
1.09
3.87
9.06
6.71
f1 (ppm)

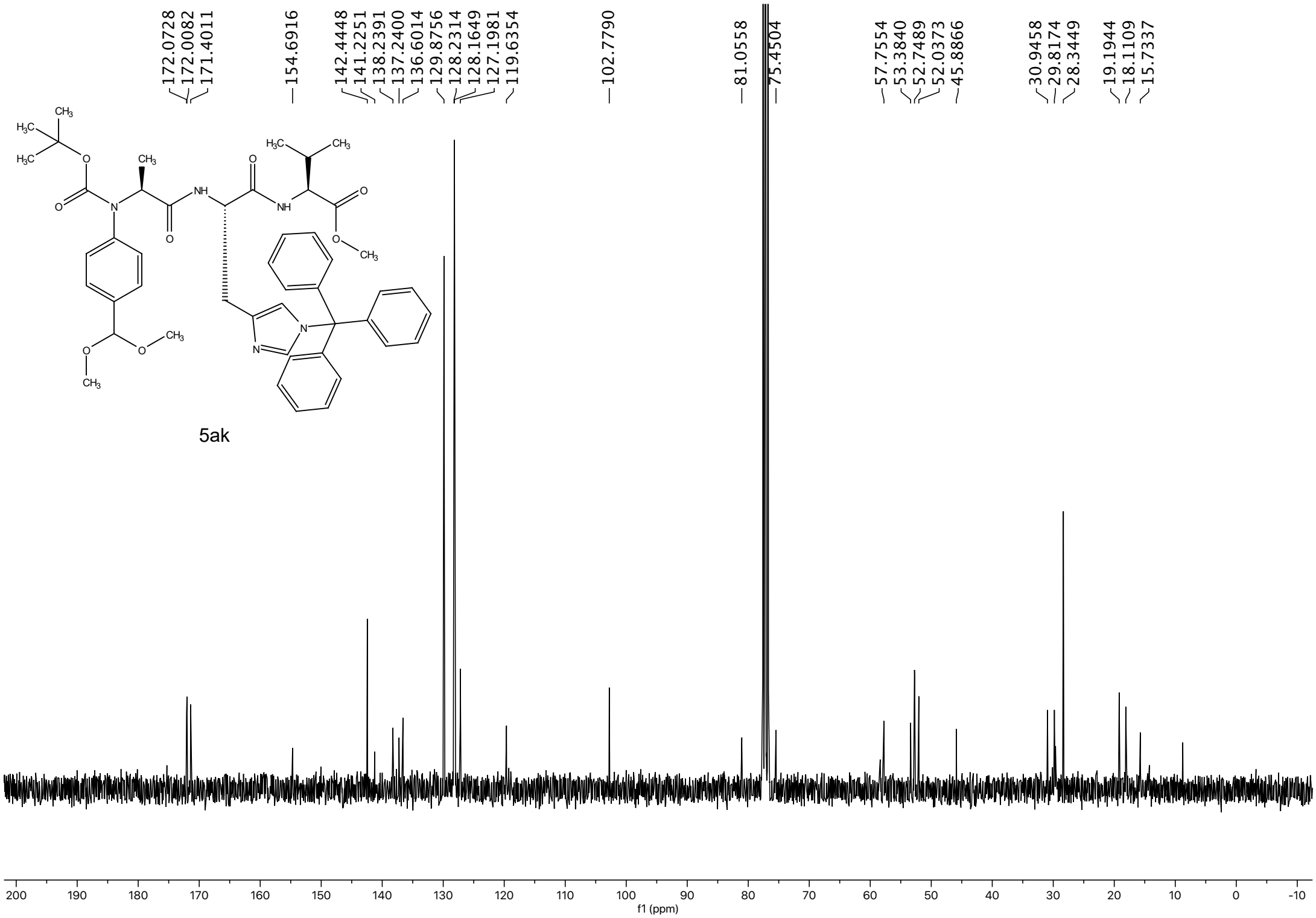
172.0728
172.0082
171.4011
154.6916
142.4448
141.2251
138.2391
137.2400
136.6014
129.8756
128.2314
128.1649
127.1981
119.6354
102.7790
81.0558
75.4504
57.7554
53.3840
52.7489
52.0373
45.8866
30.9458
29.8174
28.3449
19.1944
18.1109
15.7337
5ak
200
190
180
170
160
150
140
130
120
110
100
90
80
70
60
50
40
30
20
10
0
-10
f1 (ppm)

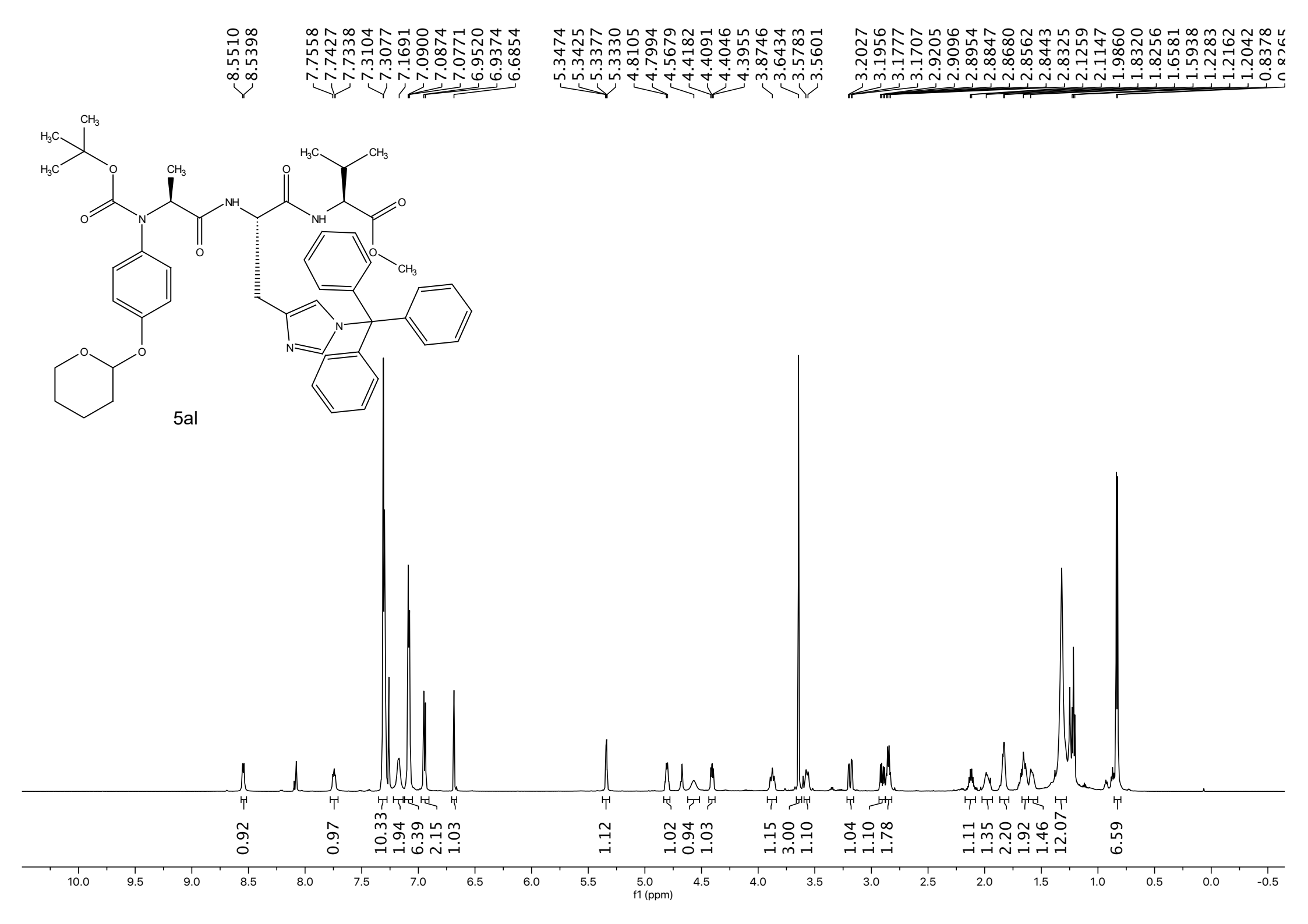
8.5510
8.5398
7.7558
7.7427
7.7338
7.3104
7.3077
7.1691
7.0900
7.0874
7.0771
6.9520
6.9374
6.6854
5.3474
5.3425
5.3377
5.3330
4.8105
4.7994
4.5679
4.4182
4.4091
4.4046
4.3955
3.8746
3.6434
3.5783
3.5601
3.2027
3.1956
3.1777
3.1707
2.9205
2.9096
2.8954
2.8847
2.8680
2.8562
2.8443
2.8325
2.1259
2.1147
1.9860
1.8320
1.8256
1.6581
1.5938
1.2283
1.2162
1.2042
0.8378
5al
0.92
0.97
10.33
1.94
6.39
2.15
1.03
1.12
1.02
0.94
1.03
1.15
3.00
1.10
1.04
1.10
1.78
1.11
1.35
2.20
1.92
1.46
12.07
6.59
f1 (ppm)

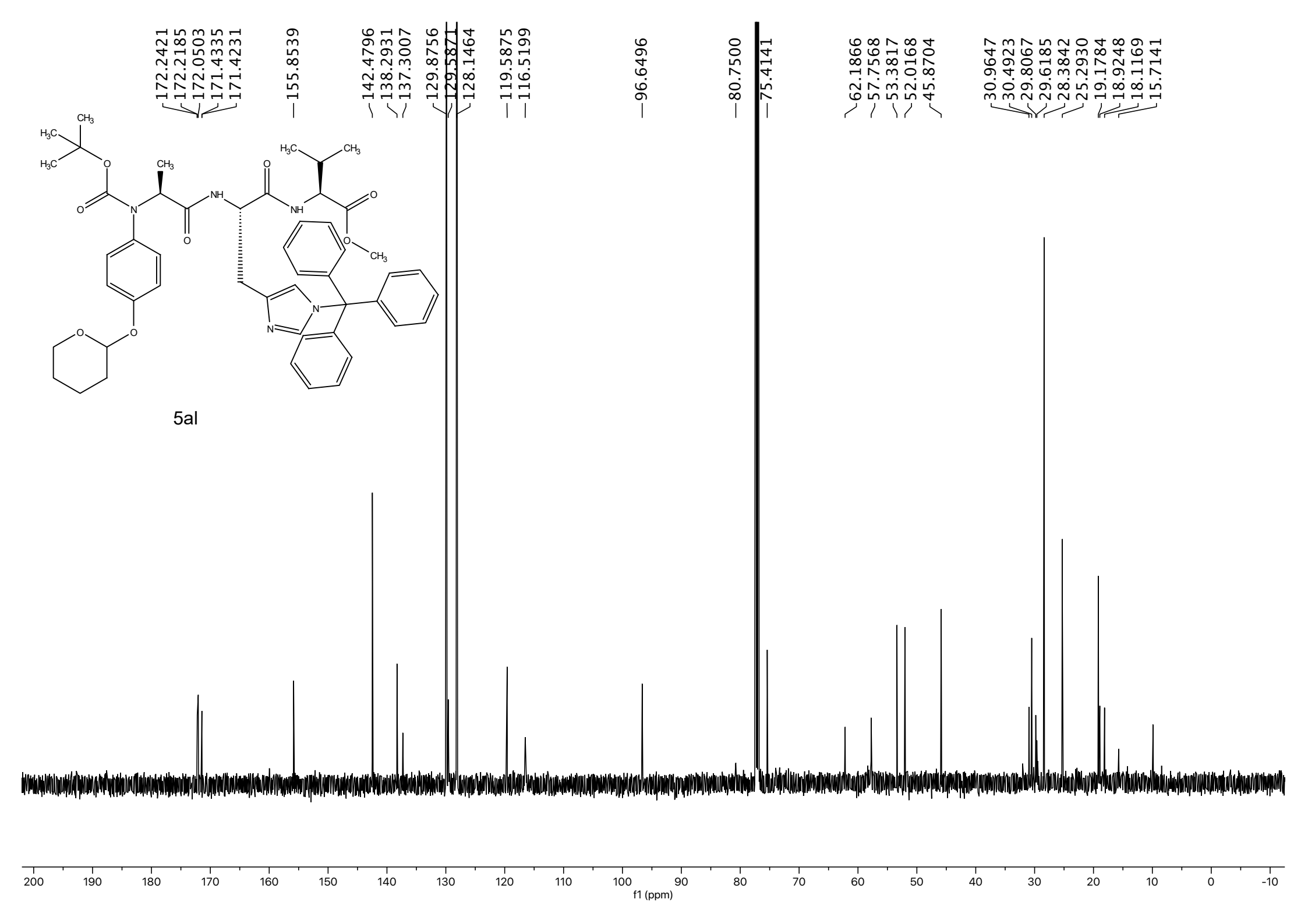
172.2421
172.2185
172.0503
171.4335
171.4231
155.8539
142.4796
138.2931
137.3007
129.8756
129.5871
128.1464
119.5875
116.5199
96.6496
80.7500
75.4141
62.1866
57.7568
53.3817
52.0168
45.8704
30.9647
30.4923
29.8067
29.6185
28.3842
25.2930
19.1784
18.9248
18.1169
15.7141
5al
f1 (ppm)

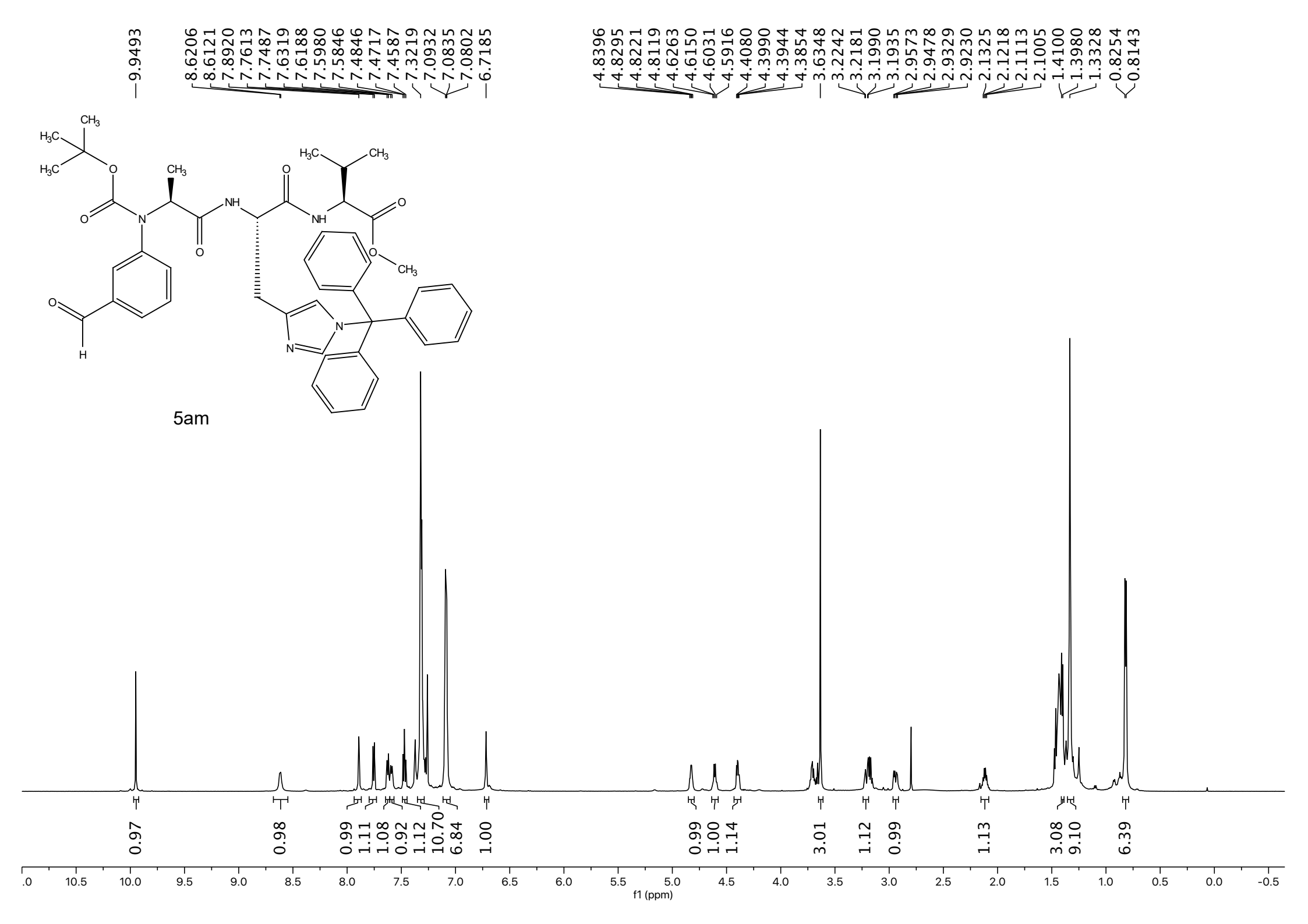
9.9493
8.6206
8.6121
7.8920
7.7613
7.7487
7.6319
7.6188
7.5980
7.5846
7.4846
7.4717
7.4587
7.3219
7.0932
7.0835
7.0802
6.7185
4.8396
4.8295
4.8221
4.8119
4.6263
4.6150
4.6031
4.5916
4.4080
4.3990
4.3944
4.3854
3.6348
3.2242
3.2181
3.1990
3.1935
2.9573
2.9478
2.9329
2.9230
2.1325
2.1218
2.1113
2.1005
1.4100
1.3980
1.3328
0.8254
0.8143
5am
0.97
0.98
0.99
1.11
1.08
0.92
1.12
10.70
6.84
1.00
0.99
1.00
1.14
3.01
1.12
0.99
1.13
3.08
9.10
6.39
f1 (ppm)

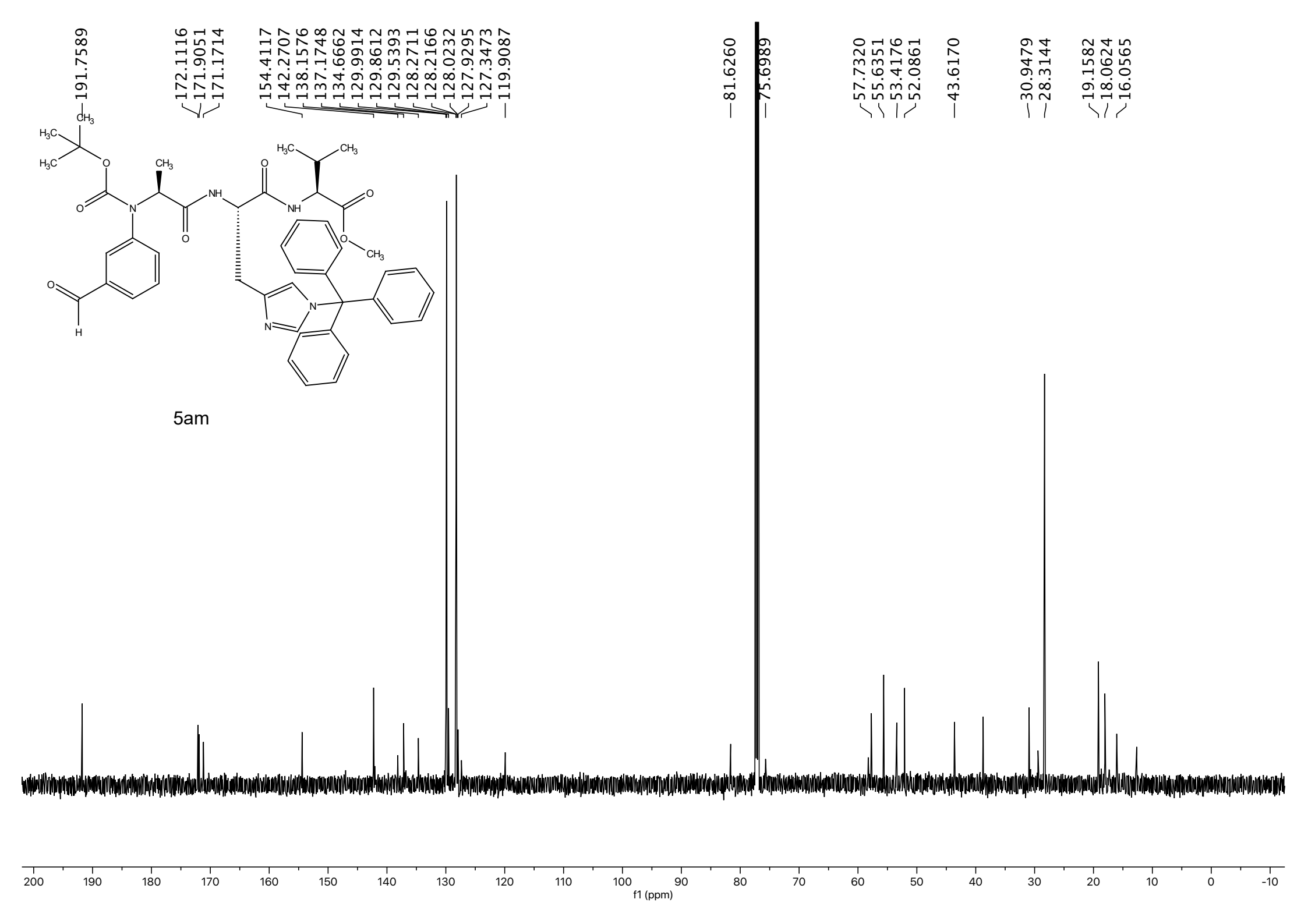
191.7589
172.1116
171.9051
171.1714
154.4117
142.2707
138.1576
137.1748
134.6662
129.9914
129.8612
129.5393
128.2711
128.2166
128.0232
127.9295
127.3473
119.9087
81.6260
75.6989
57.7320
55.6351
53.4176
52.0861
43.6170
30.9479
28.3144
19.1582
18.0624
16.0565
5am
200
190
180
170
160
150
140
130
120
110
100
90
80
70
60
50
40
30
20
10
0
-10
f1 (ppm)

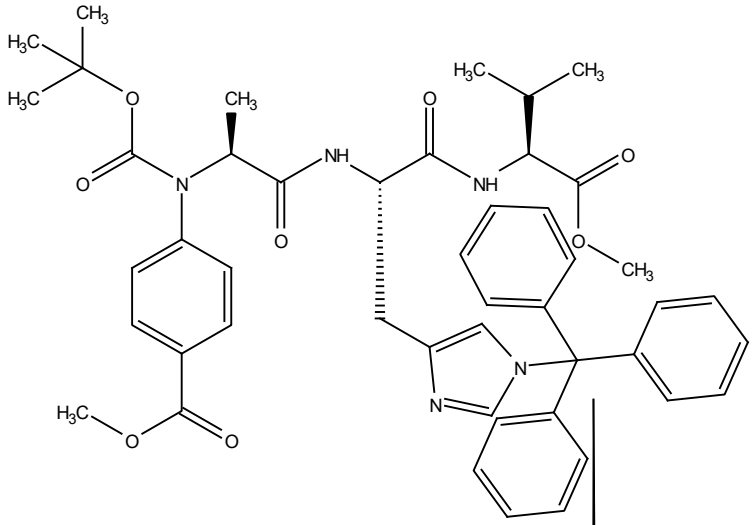

5an

8.5744
7.9734
7.9593
7.6200
7.6073
7.3942
7.3802
7.3232
7.0887
7.0789
7.0760
6.7104
4.8122
4.8052
4.6127
4.6010
4.5891
4.5773
4.4002
4.3910
4.3869
4.3777
3.9020
3.6435
3.2015
3.1891
3.1768
3.1646
2.9338
2.9282
2.9126
2.9036
2.1300
2.1194
1.3976
1.3857
1.3286
0.8358
0.8246

0.89
1.94
0.99
2.18
10.95
6.49
1.10
1.02
1.07
1.04
3.00
2.89
1.25
1.19
1.32
3.77
8.94
6.07

f1 (ppm)

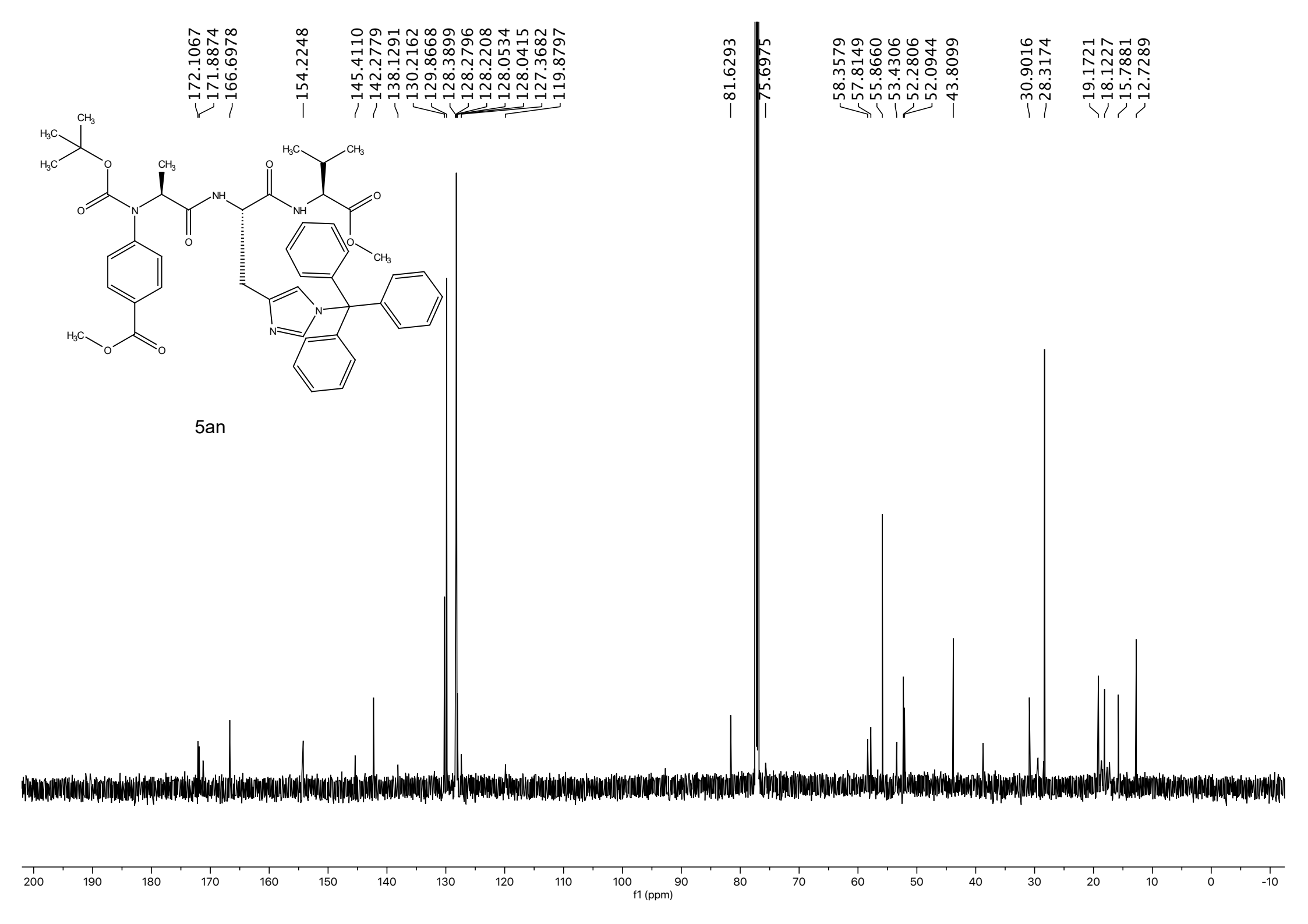
172.1067
171.8874
166.6978
154.2248
145.4110
142.2779
138.1291
130.2162
129.8668
128.3899
128.2796
128.2208
128.0534
128.0415
127.3682
119.8797
81.6293
75.6975
58.3579
57.8149
55.8660
53.4306
52.2806
52.0944
43.8099
30.9016
28.3174
19.1721
18.1227
15.7881
12.7289
5an
f1 (ppm)

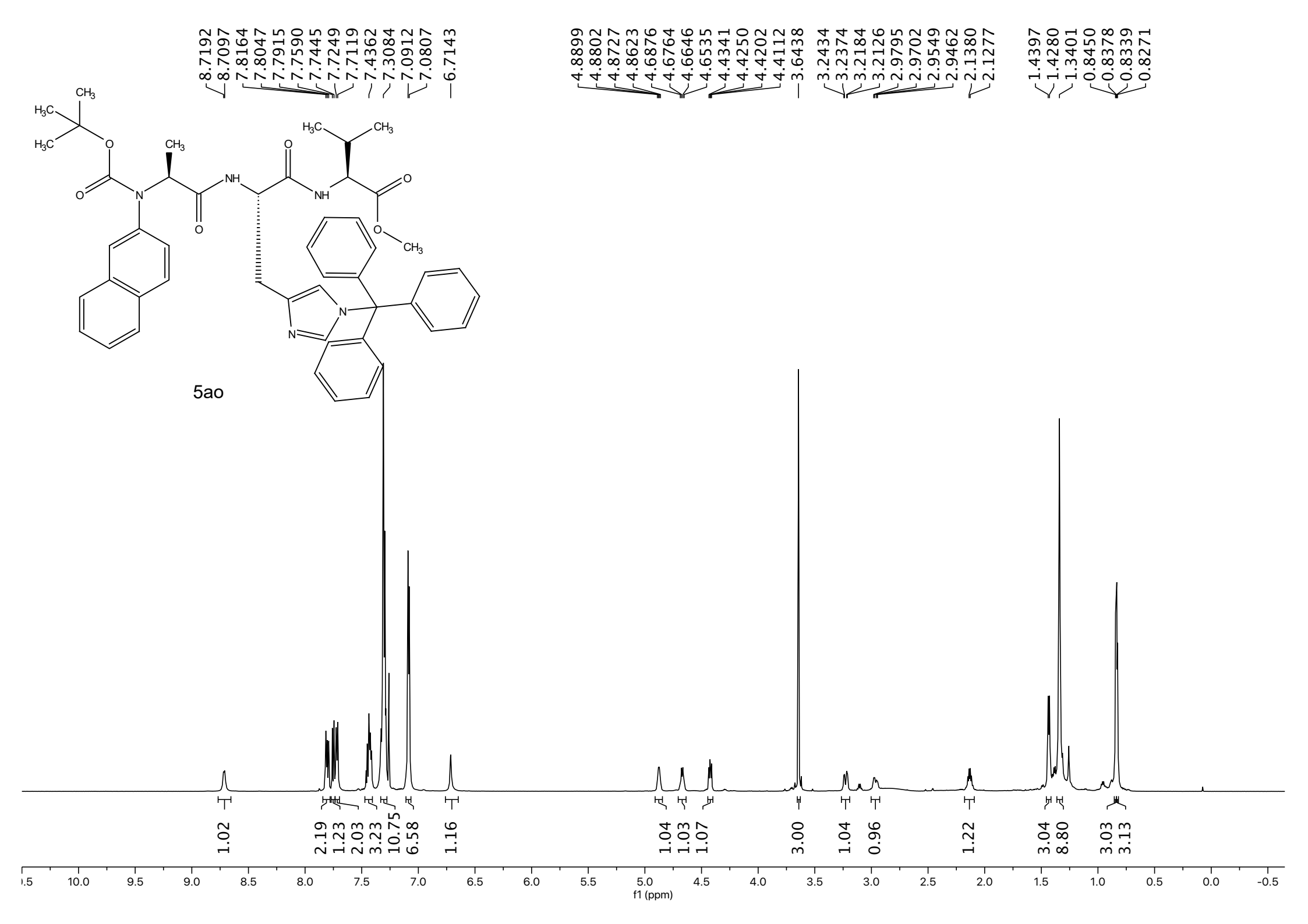
8.7192
8.7097
7.8164
7.8047
7.7915
7.7590
7.7445
7.7249
7.7119
7.4362
7.3084
7.0912
7.0807
6.7143
4.8899
4.8802
4.8727
4.8623
4.6876
4.6764
4.6646
4.6535
4.4341
4.4250
4.4202
4.4112
3.6438
3.2434
3.2374
3.2184
3.2126
2.9795
2.9702
2.9549
2.9462
2.1380
2.1277
1.4397
1.4280
1.3401
0.8450
0.8378
0.8339
0.8271
5ao
1.02
2.19
1.23
2.03
3.23
10.75
6.58
1.16
1.04
1.03
1.07
3.00
1.04
0.96
1.22
3.04
8.80
3.03
3.13
f1 (ppm)

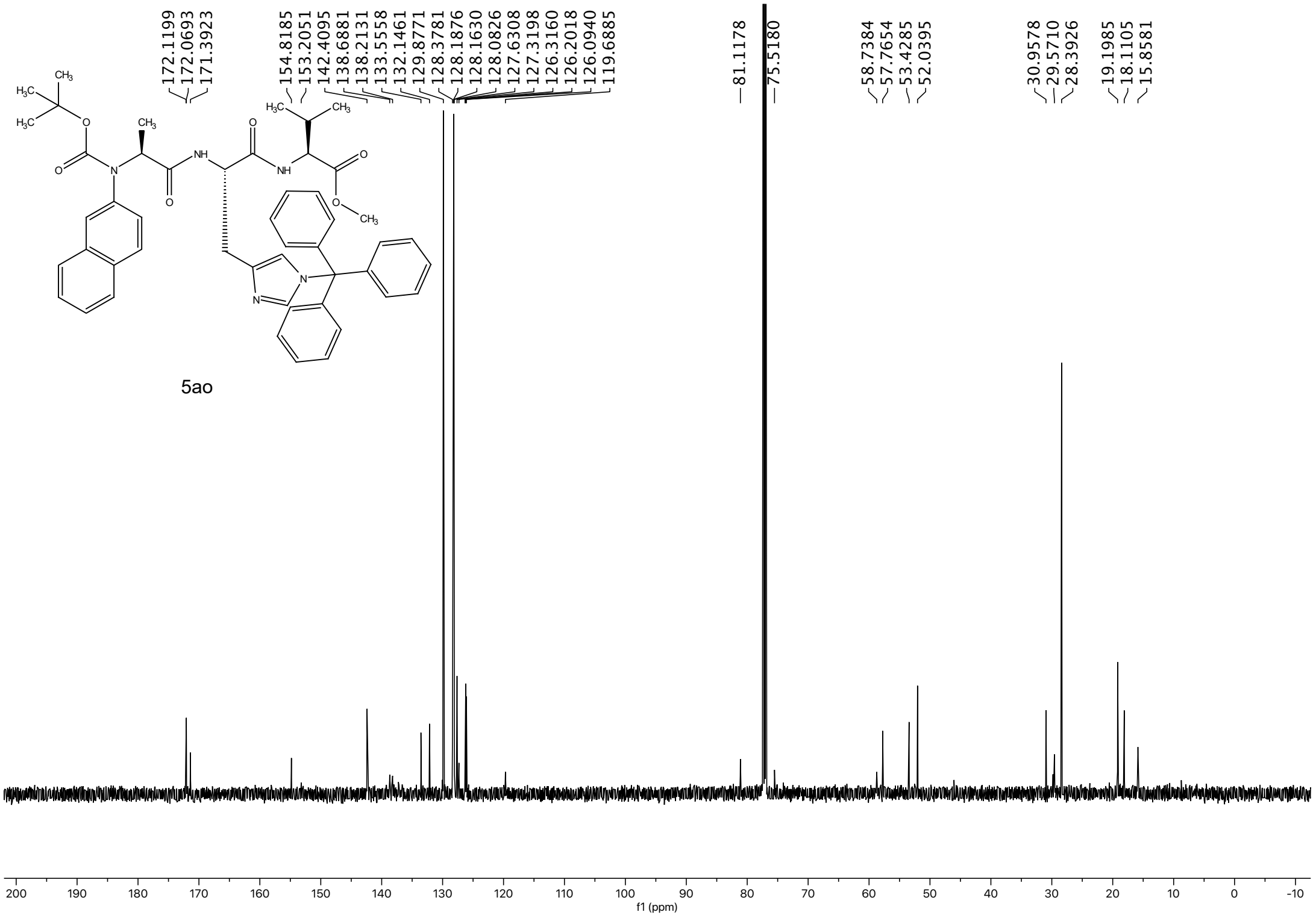
172.1199
172.0693
171.3923
154.8185
153.2051
142.4095
138.6881
138.2131
133.5558
132.1461
129.8771
128.3781
128.1876
128.1630
128.0826
127.6308
127.3198
126.3160
126.2018
126.0940
119.6885
81.1178
75.5180
58.7384
57.7654
53.4285
52.0395
30.9578
29.5710
28.3926
19.1985
18.1105
15.8581
5ao
200
190
180
170
160
150
140
130
120
110
100
90
80
70
60
50
40
30
20
10
0
-10
f1 (ppm)

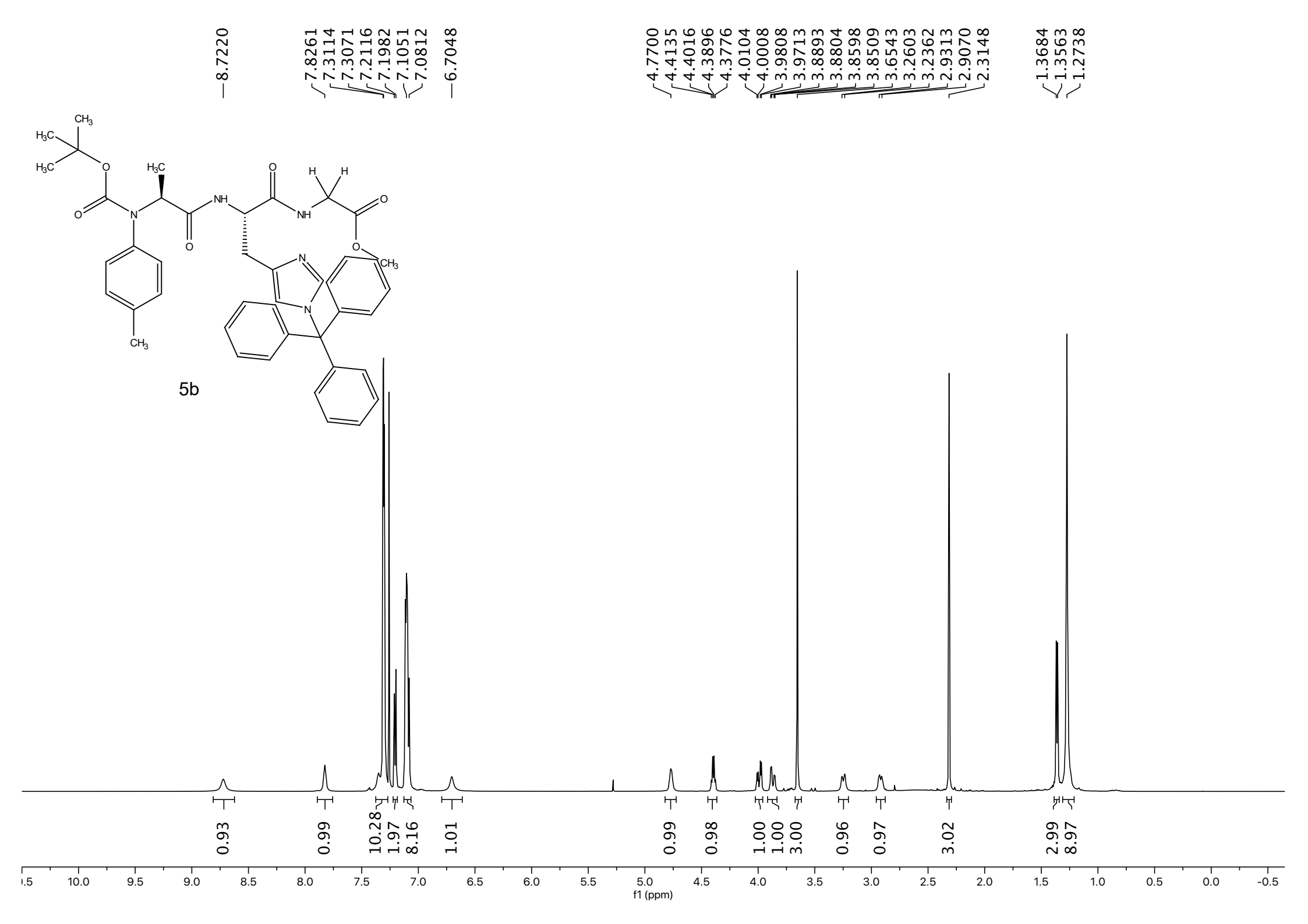
8.7220
7.8261
7.3114
7.3071
7.2116
7.1982
7.1051
7.0812
6.7048
4.7700
4.4135
4.4016
4.3896
4.3776
4.0104
4.0008
3.9808
3.9713
3.8893
3.8804
3.8598
3.8509
3.6543
3.2603
3.2362
2.9313
2.9070
2.3148
1.3684
1.3563
1.2738
5b
0.93
0.99
10.28
1.97
8.16
1.01
0.99
0.98
1.00
1.00
3.00
0.96
0.97
3.02
2.99
8.97
f1 (ppm)

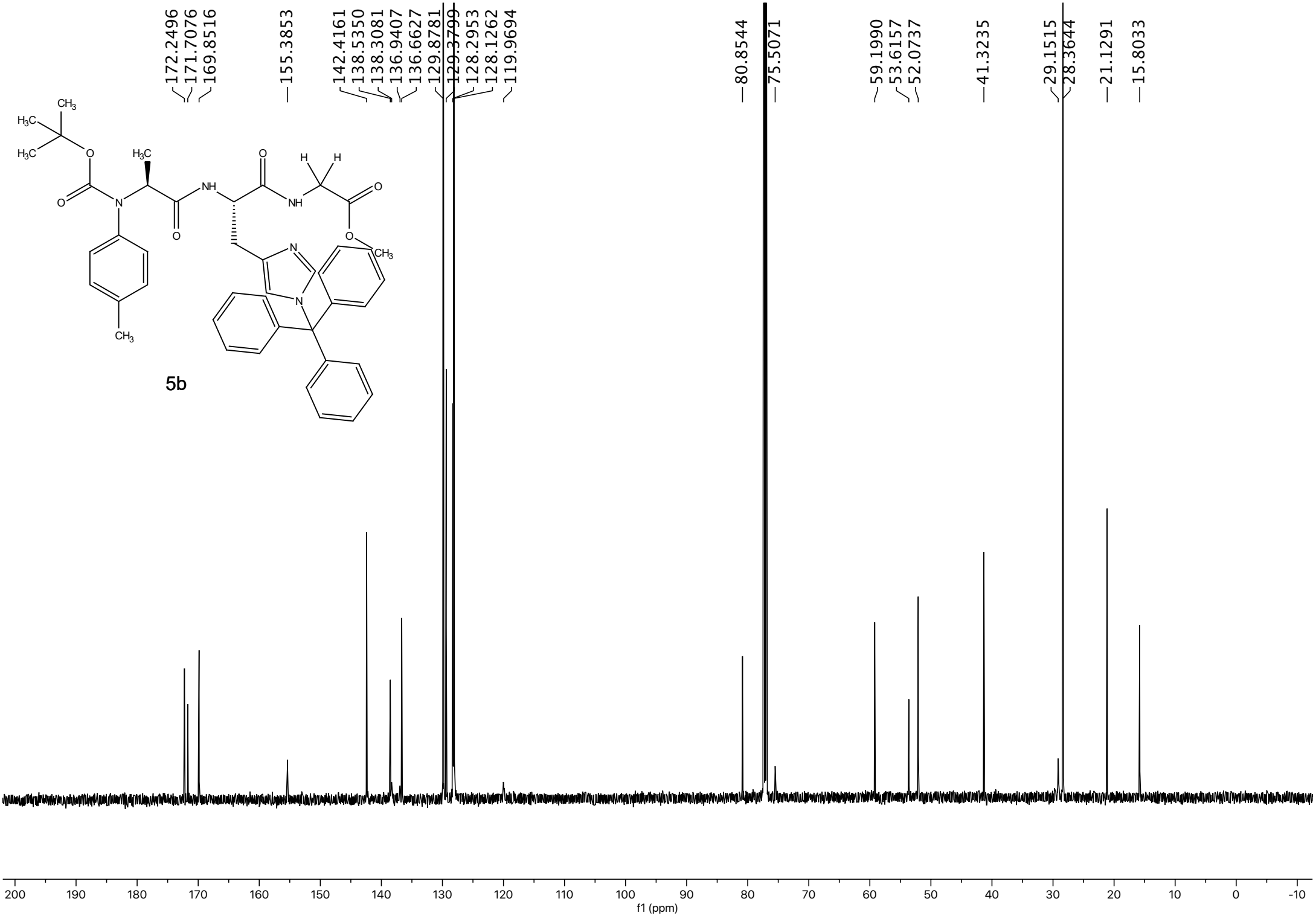
172.2496
171.7076
169.8516
155.3853
142.4161
138.5350
138.3081
136.9407
136.6627
129.8781
129.3799
128.2953
128.1262
119.9694
80.8544
75.5071
59.1990
53.6157
52.0737
41.3235
29.1515
28.3644
21.1291
15.8033
5b
f1 (ppm)

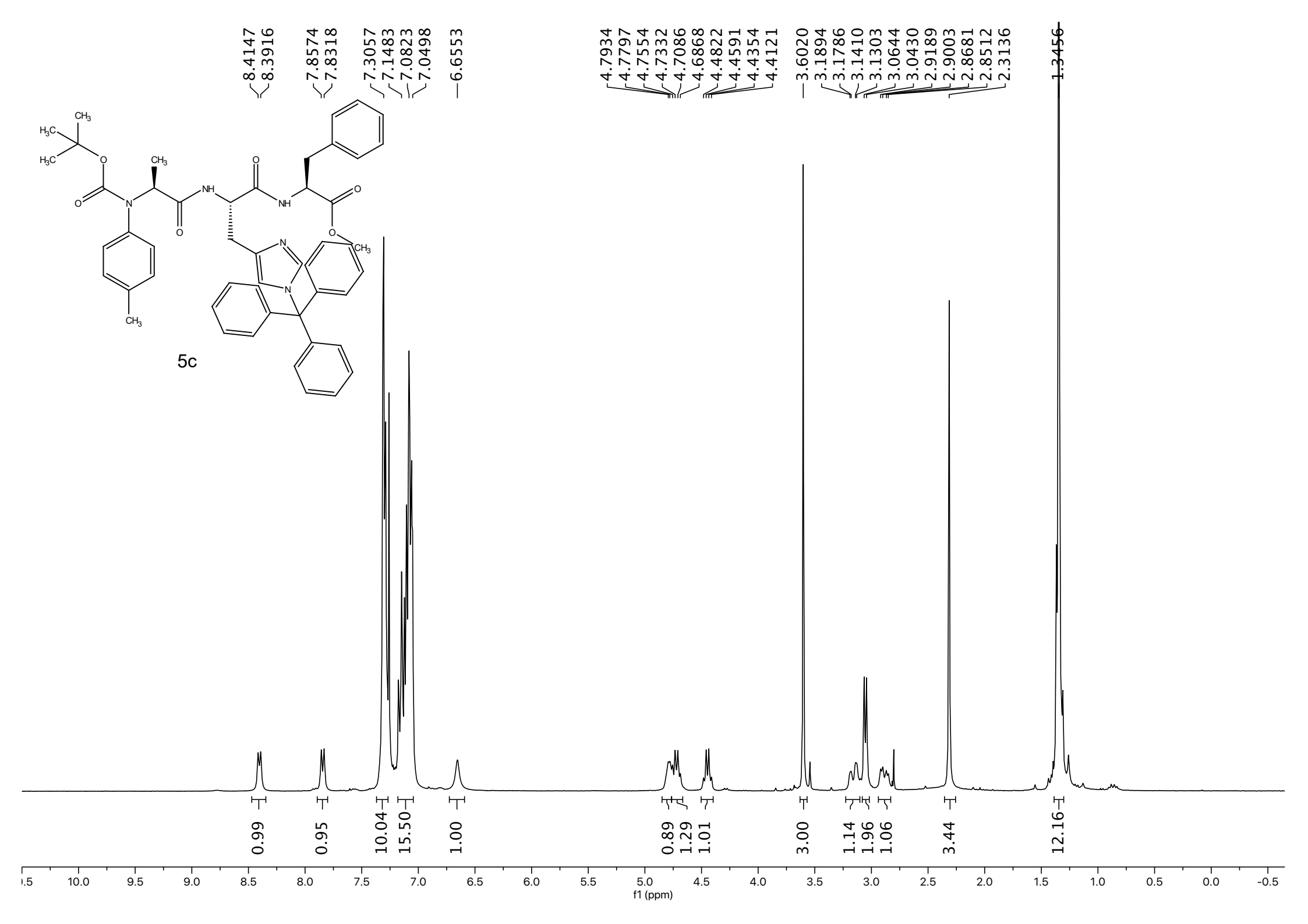
8.4147
8.3916
7.8574
7.8318
7.3057
7.1483
7.0823
7.0498
6.6553
4.7934
4.7797
4.7554
4.7332
4.7086
4.6868
4.4822
4.4591
4.4354
4.4121
3.6020
3.1894
3.1786
3.1410
3.1303
3.0644
3.0430
2.9189
2.9003
2.8681
2.8512
2.3136
1.3456
0.99
0.95
10.04
15.50
1.00
0.89
1.29
1.01
3.00
1.14
1.96
1.06
3.44
12.16
f1 (ppm)

5c

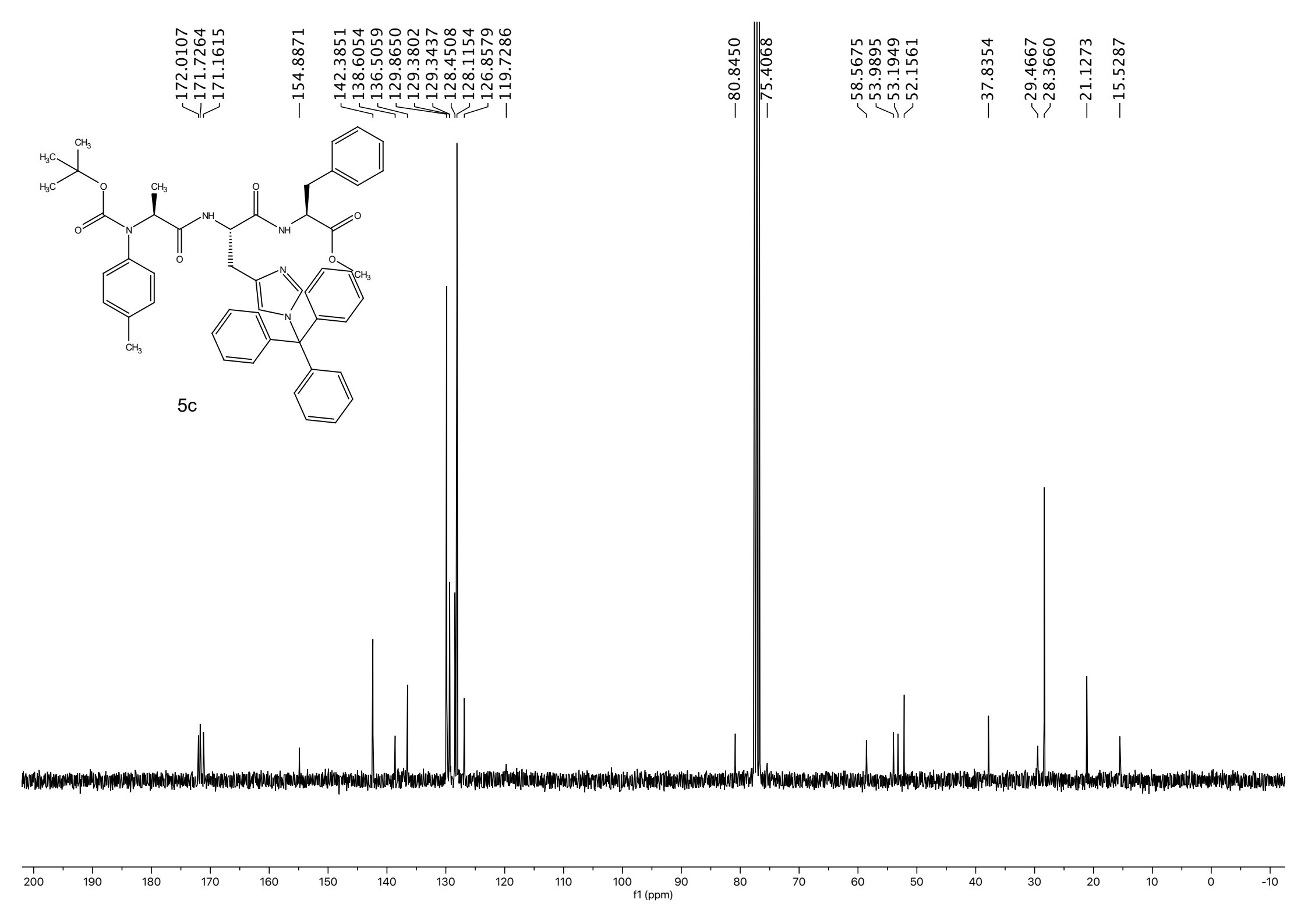
172.0107
171.7264
171.1615
154.8871
142.3851
138.6054
136.5059
129.8650
129.3802
129.3437
128.4508
128.1154
126.8579
119.7286
80.8450
75.4068
58.5675
53.9895
53.1949
52.1561
37.8354
29.4667
28.3660
21.1273
15.5287
5c
f1 (ppm)

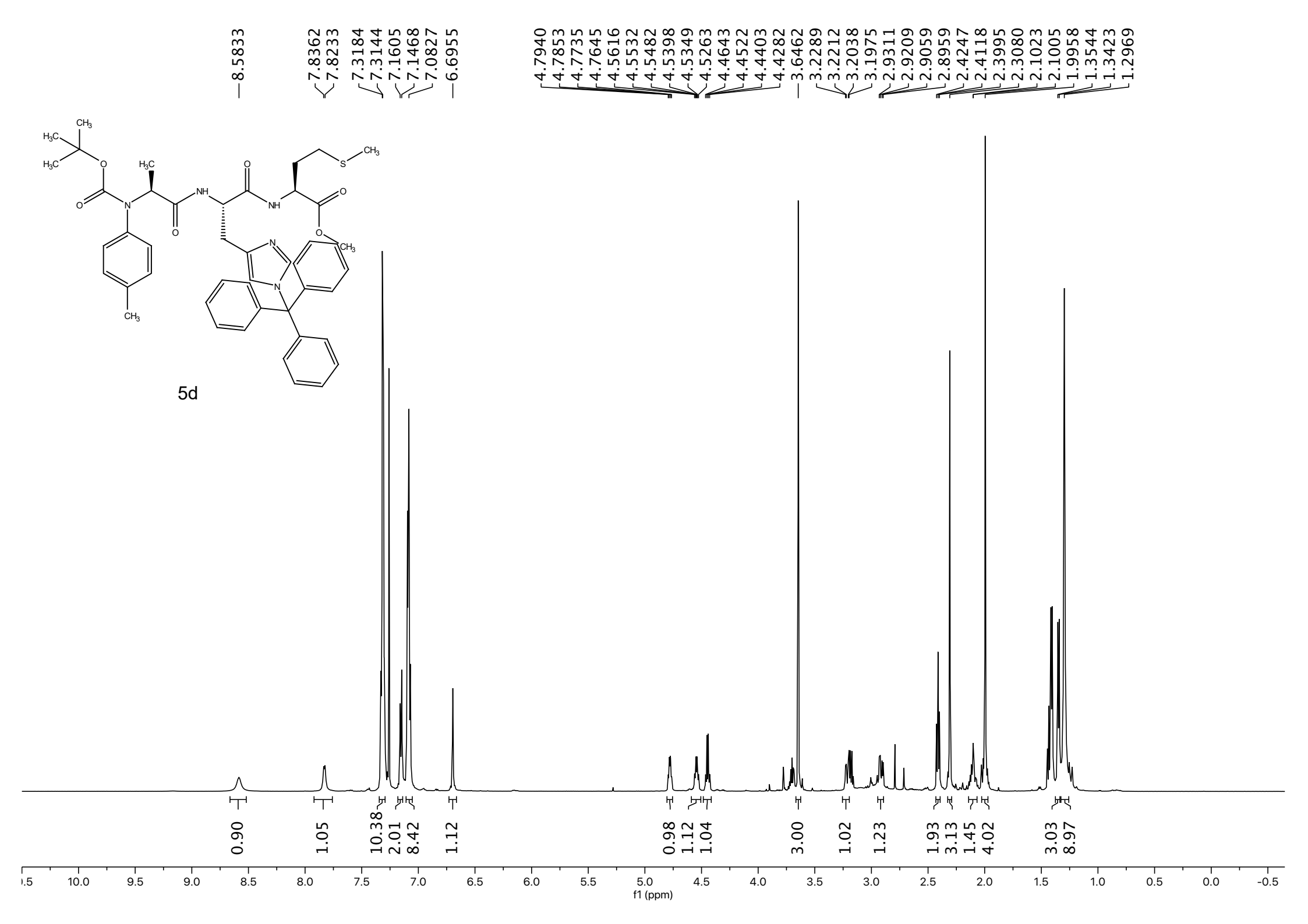
8.5833
7.8362
7.8233
7.3184
7.3144
7.1605
7.1468
7.0827
6.6955
4.7940
4.7853
4.7735
4.7645
4.5616
4.5532
4.5482
4.5398
4.5349
4.5263
4.4643
4.4522
4.4403
4.4282
3.6462
3.2289
3.2212
3.2038
3.1975
2.9311
2.9209
2.9059
2.8959
2.4247
2.4118
2.3995
2.3080
2.1023
2.1005
1.9958
1.3544
1.3423
1.2969
5d
0.90
1.05
10.38
2.01
8.42
1.12
0.98
1.12
1.04
3.00
1.02
1.23
1.93
3.13
1.45
4.02
3.03
8.97
f1 (ppm)

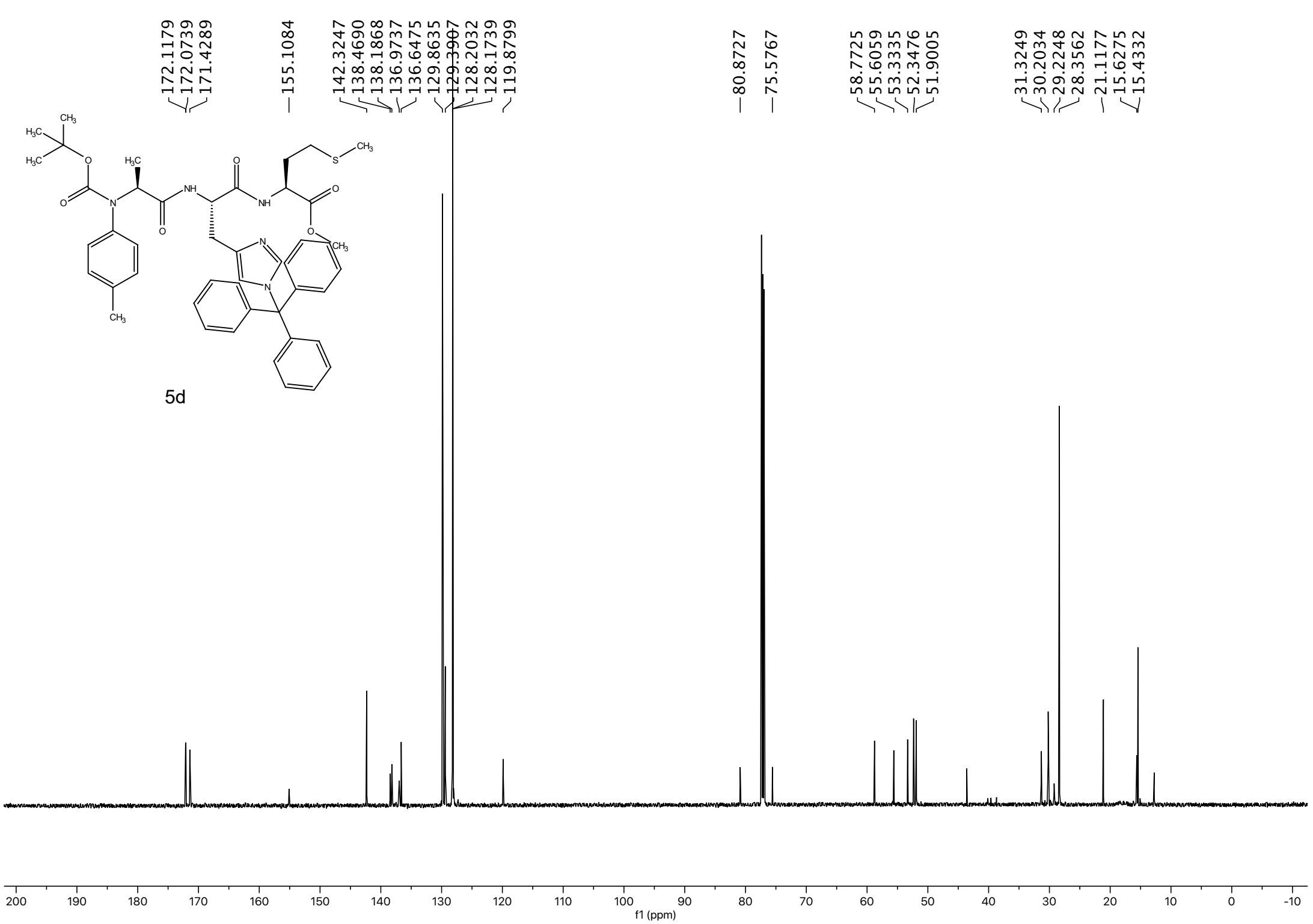
172.1179
172.0739
171.4289
155.1084
142.3247
138.4690
138.1868
136.9737
136.6475
129.8635
129.3907
128.2032
128.1739
119.8799
80.8727
75.5767
58.7725
55.6059
53.3335
52.3476
51.9005
31.3249
30.2034
29.2248
28.3562
21.1177
15.6275
15.4332
5d
f1 (ppm)

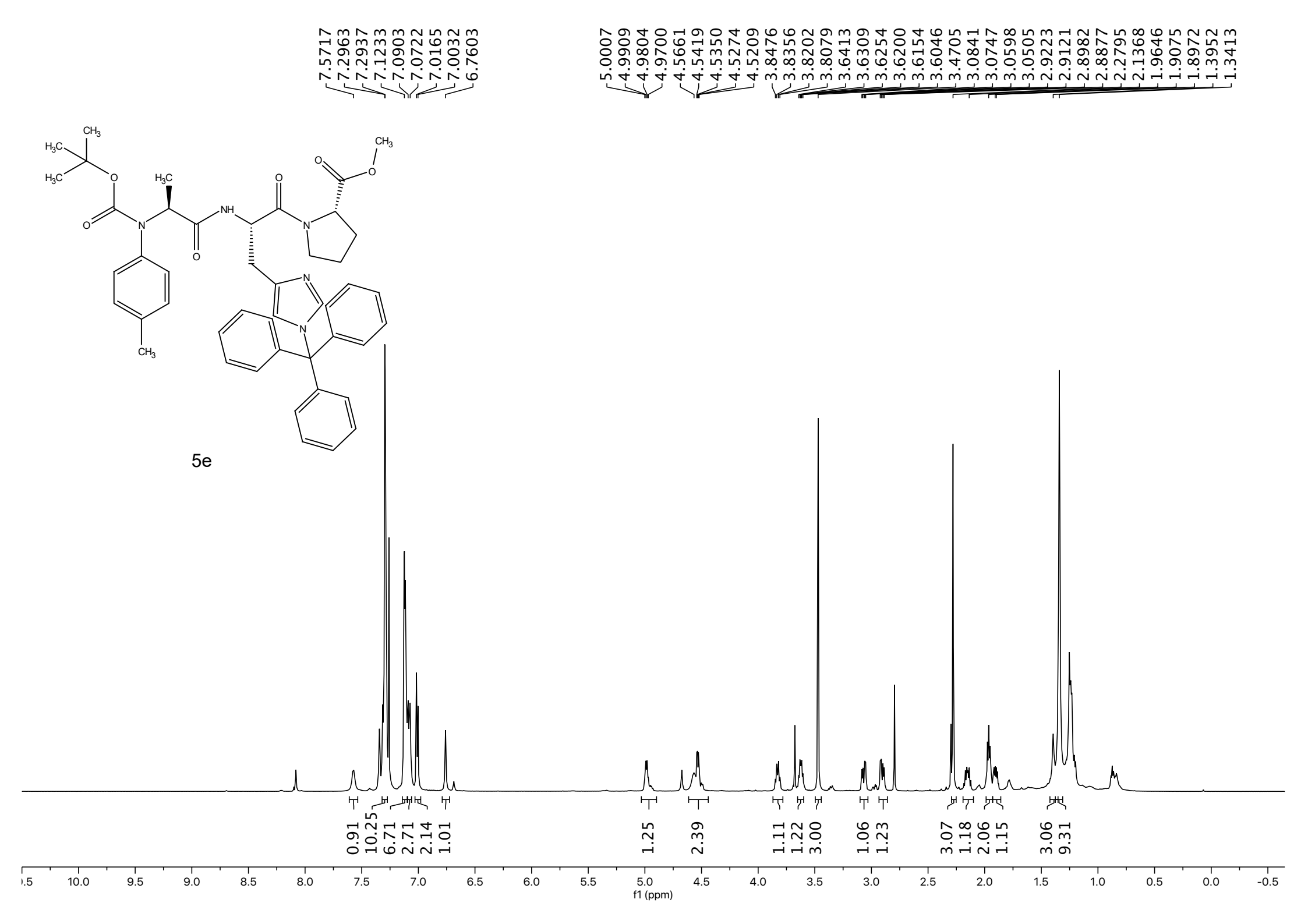
7.5717
7.2963
7.2937
7.1233
7.0903
7.0722
7.0165
7.0032
6.7603
5.0007
4.9909
4.9804
4.9700
4.5661
4.5419
4.5350
4.5274
4.5209
3.8476
3.8356
3.8202
3.8079
3.6413
3.6309
3.6254
3.6200
3.6154
3.6046
3.4705
3.0841
3.0747
3.0598
3.0505
2.9223
2.9121
2.8982
2.8877
2.2795
2.1368
1.9646
1.9075
1.8972
1.3952
1.3413
5e
0.91
10.25
6.71
2.71
2.14
1.01
1.25
2.39
1.11
1.22
3.00
1.06
1.23
3.07
1.18
2.06
1.15
3.06
9.31
f1 (ppm)

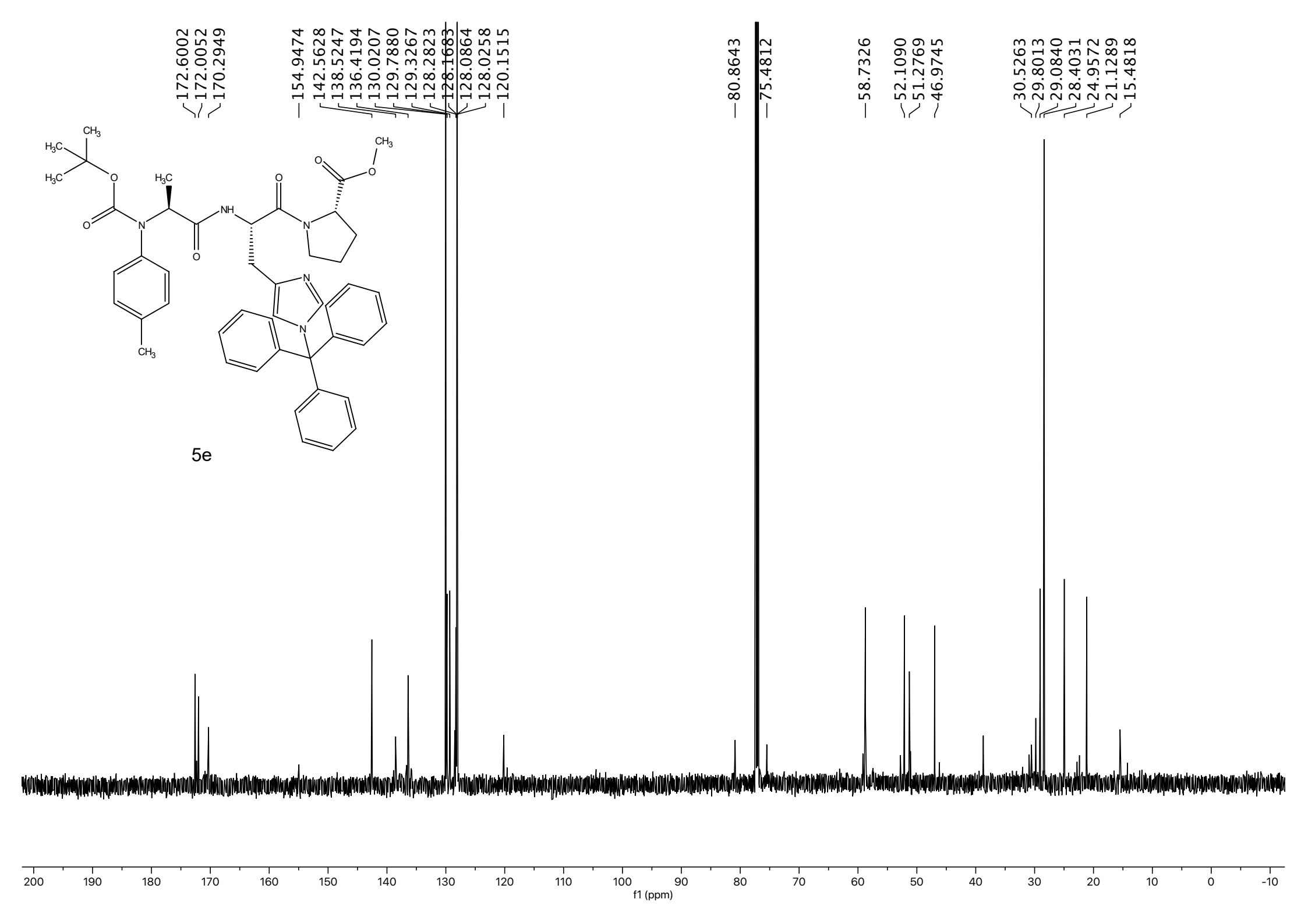
172.6002
172.0052
170.2949
154.9474
142.5628
138.5247
136.4194
130.0207
129.7880
129.3267
128.2823
128.1683
128.0864
128.0258
120.1515
80.8643
75.4812
58.7326
52.1090
51.2769
46.9745
30.5263
29.8013
29.0840
28.4031
24.9572
21.1289
15.4818
5e
f1 (ppm)

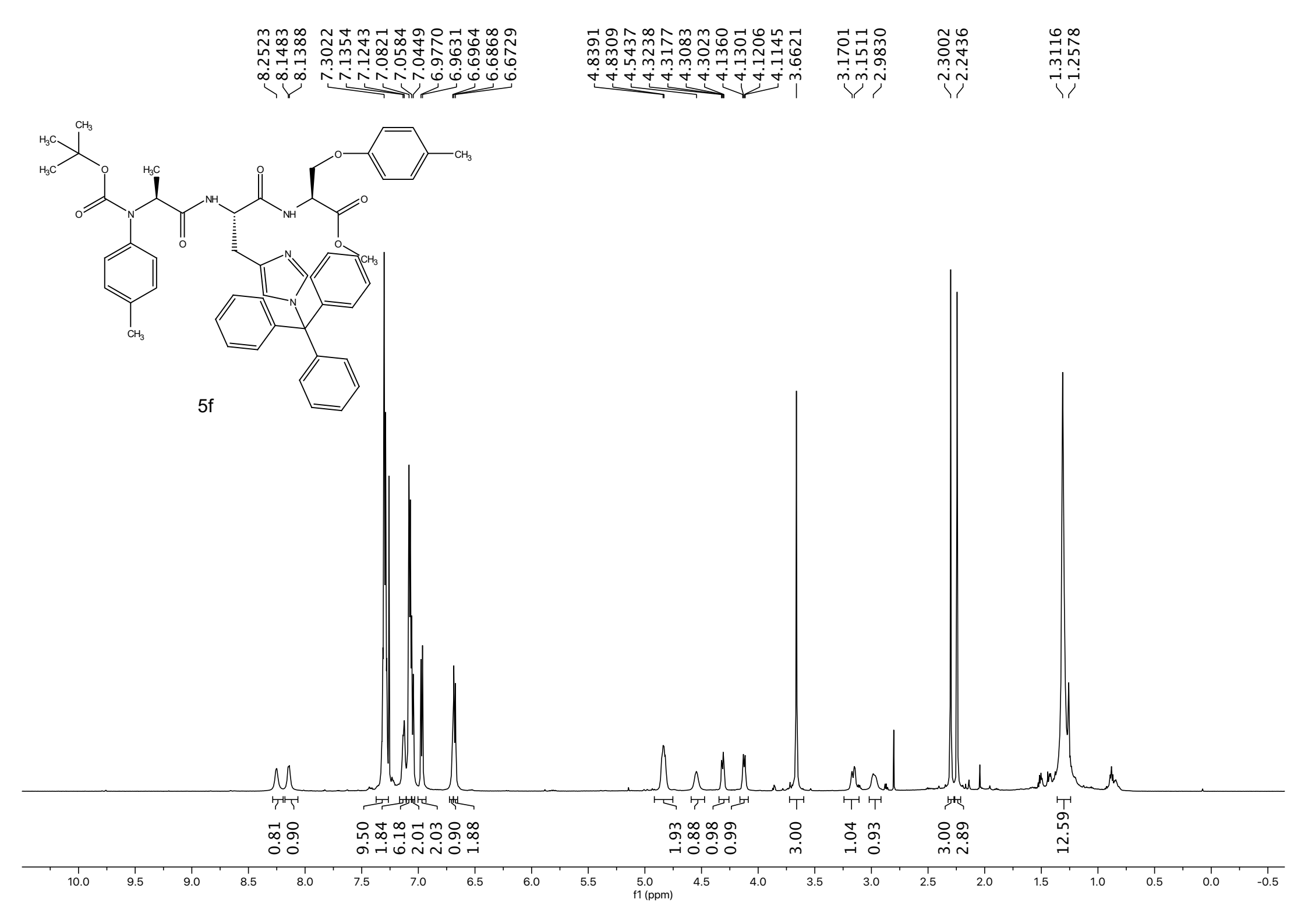
8.2523
8.1483
8.1388
7.3022
7.1354
7.1243
7.0821
7.0584
7.0449
6.9770
6.9631
6.6964
6.6868
6.6729
4.8391
4.8309
4.5437
4.3238
4.3177
4.3083
4.3023
4.1360
4.1301
4.1206
4.1145
3.6621
3.1701
3.1511
2.9830
2.3002
2.2436
1.3116
1.2578
5f
0.81
0.90
9.50
1.84
6.18
2.01
2.03
0.90
1.88
1.93
0.88
0.98
0.99
3.00
1.04
0.93
3.00
2.89
12.59
f1 (ppm)

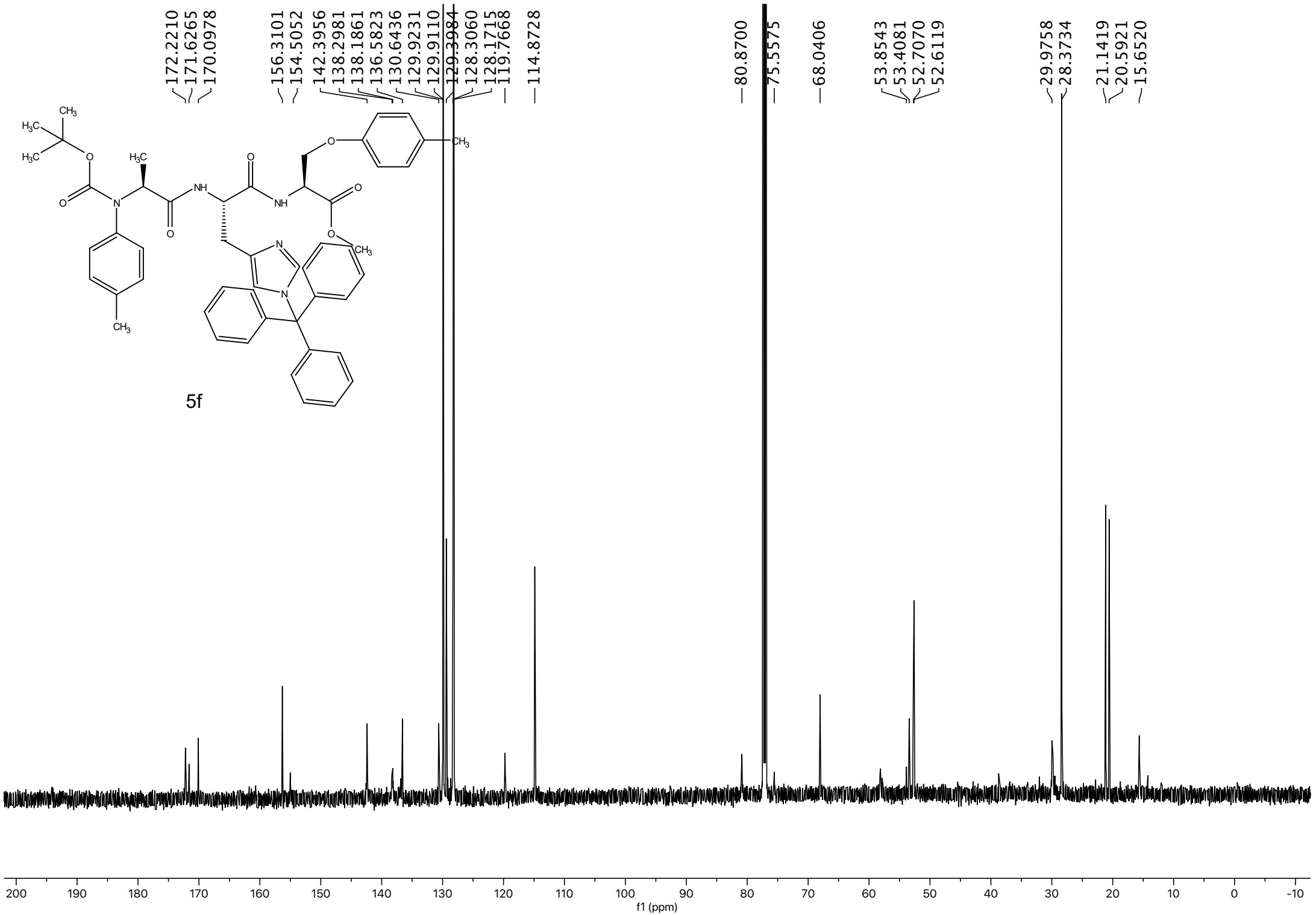
172.2210
171.6265
170.0978
156.3101
154.5052
142.3956
138.2981
138.1861
136.5823
130.6436
129.9231
129.9110
129.3984
128.3060
128.1715
119.7668
114.8728
80.8700
75.5575
68.0406
53.8543
53.4081
52.7070
52.6119
29.9758
28.3734
21.1419
20.5921
15.6520
5f
200
190
180
170
160
150
140
130
120
110
100
90
80
70
60
50
40
30
20
10
0
-10
f1 (ppm)

5f COSY

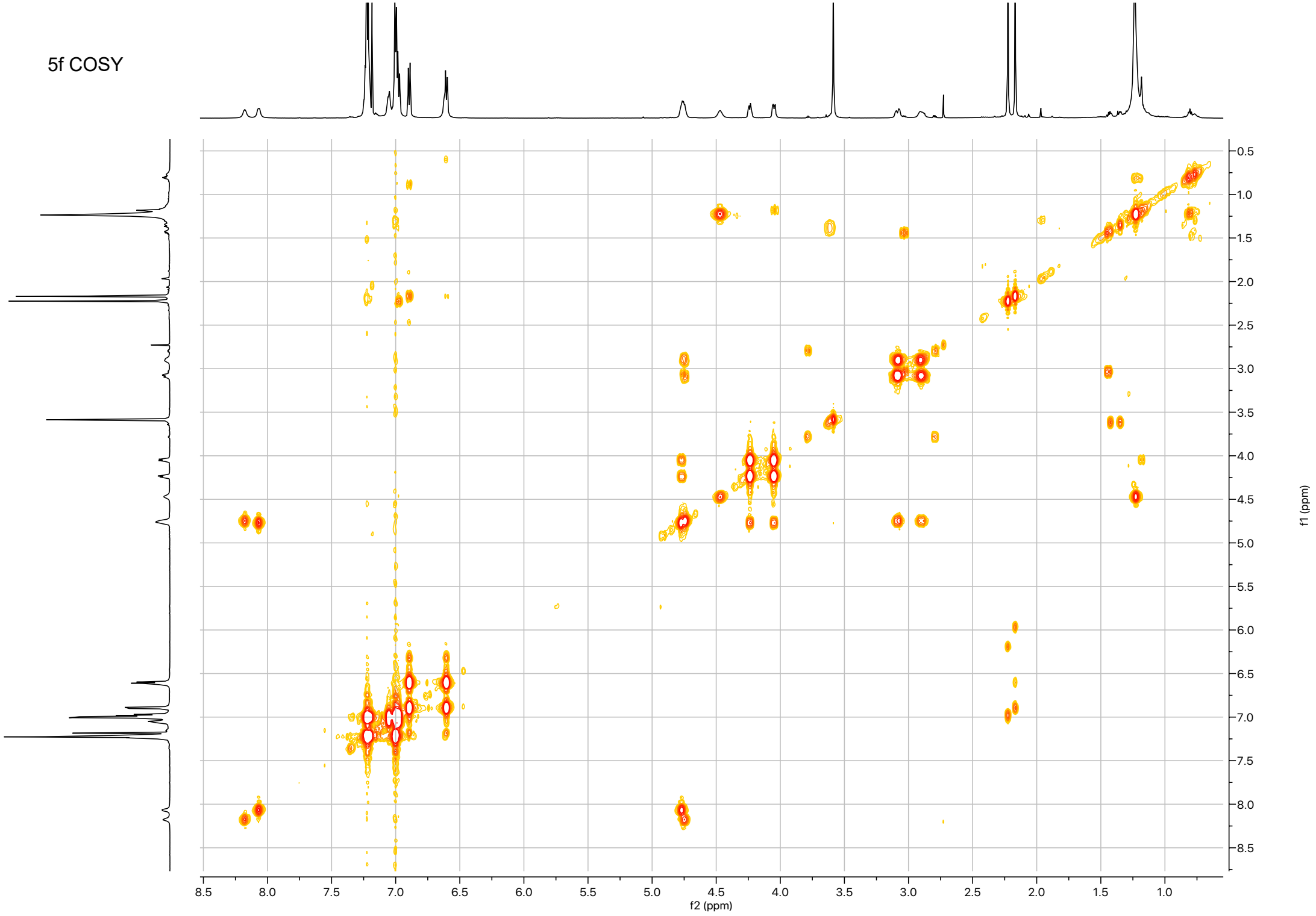
8.5
8.0
7.5
7.0
6.5
6.0
5.5
5.0
4.5
4.0
3.5
3.0
2.5
2.0
1.5
1.0
f2 (ppm)
0.5
1.0
1.5
2.0
2.5
3.0
3.5
4.0
4.5
5.0
5.5
6.0
6.5
7.0
7.5
8.0
8.5
f1 (ppm)

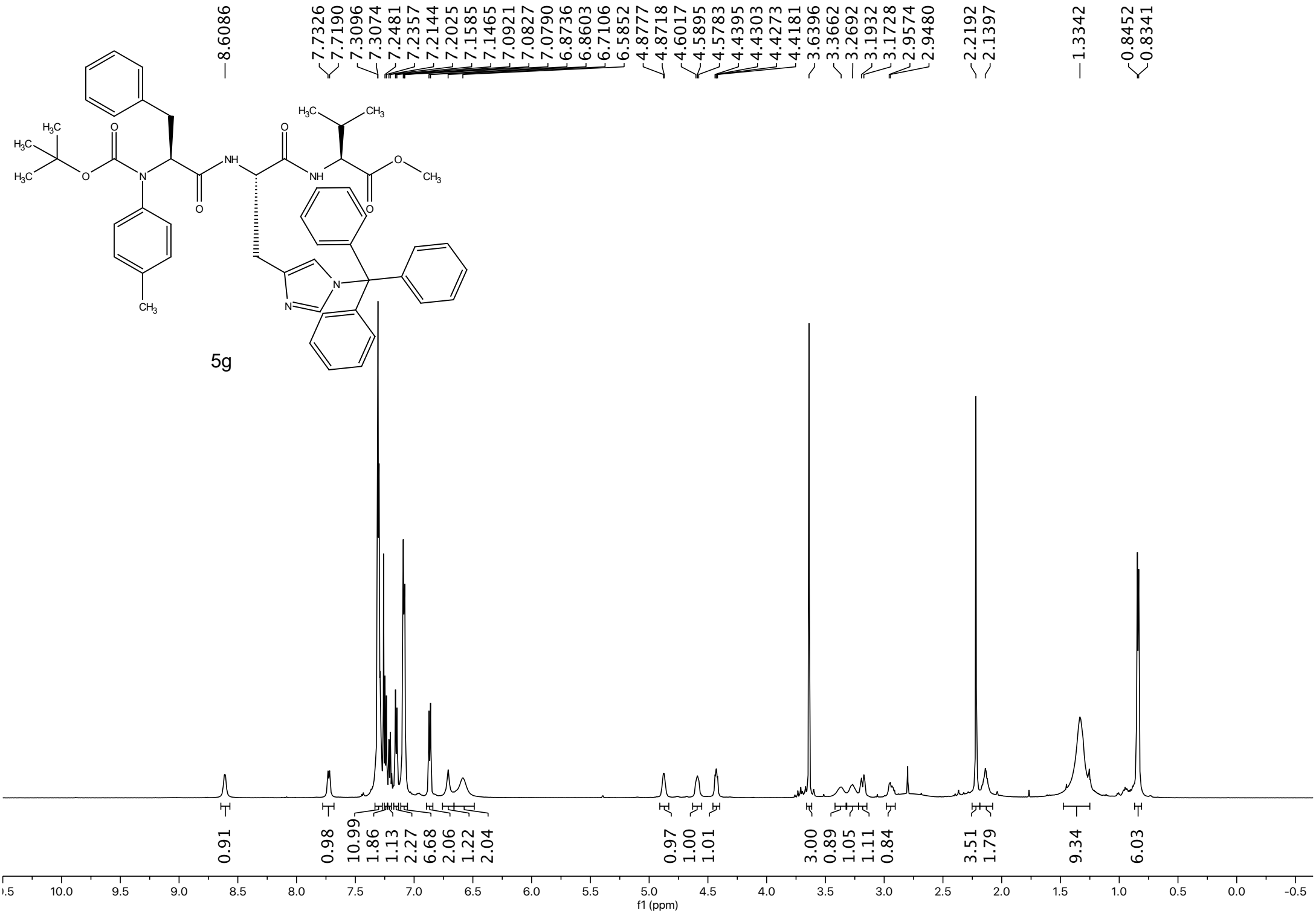
8.6086
7.7326
7.7190
7.3096
7.3074
7.2481
7.2357
7.2144
7.2025
7.1585
7.1465
7.0921
7.0827
7.0790
6.8736
6.8603
6.7106
6.5852
4.8777
4.8718
4.6017
4.5895
4.5783
4.4395
4.4303
4.4273
4.4181
3.6396
3.3662
3.2692
3.1932
3.1728
2.9574
2.9480
2.2192
2.1397
1.3342
0.8452
0.8341
5g
0.91
0.98
10.99
1.86
1.13
2.27
6.68
2.06
1.22
2.04
0.97
1.00
1.01
3.00
0.89
1.05
1.11
0.84
3.51
1.79
9.34
6.03
f1 (ppm)

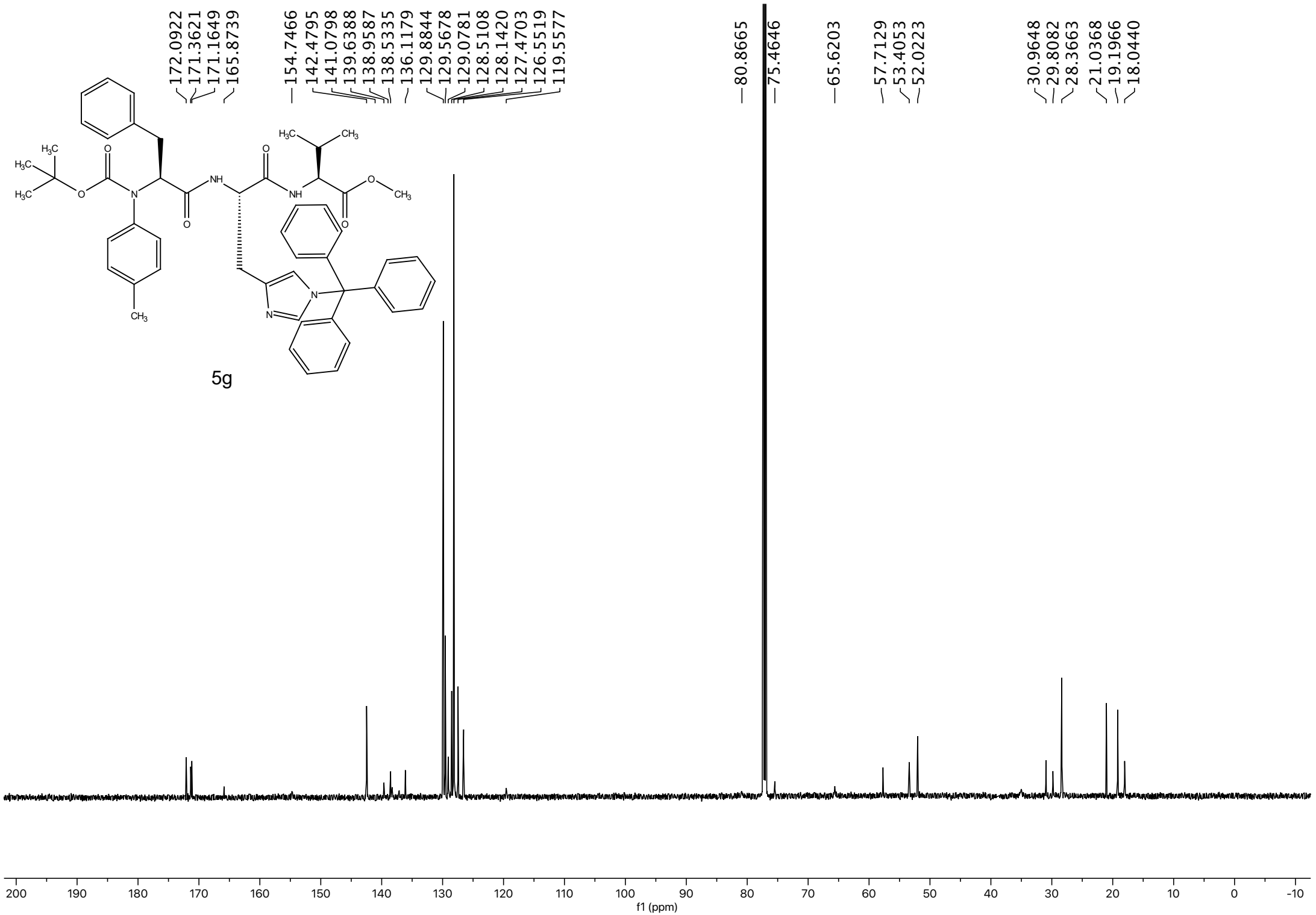
172.0922
171.3621
171.1649
165.8739
154.7466
142.4795
141.0798
139.6388
138.9587
138.5335
136.1179
129.8844
129.5678
129.0781
128.5108
128.1420
127.4703
126.5519
119.5577
80.8665
75.4646
65.6203
57.7129
53.4053
52.0223
30.9648
29.8082
28.3663
21.0368
19.1966
18.0440
5g
200
190
180
170
160
150
140
130
120
110
100
90
80
70
60
50
40
30
20
10
0
-10
f1 (ppm)

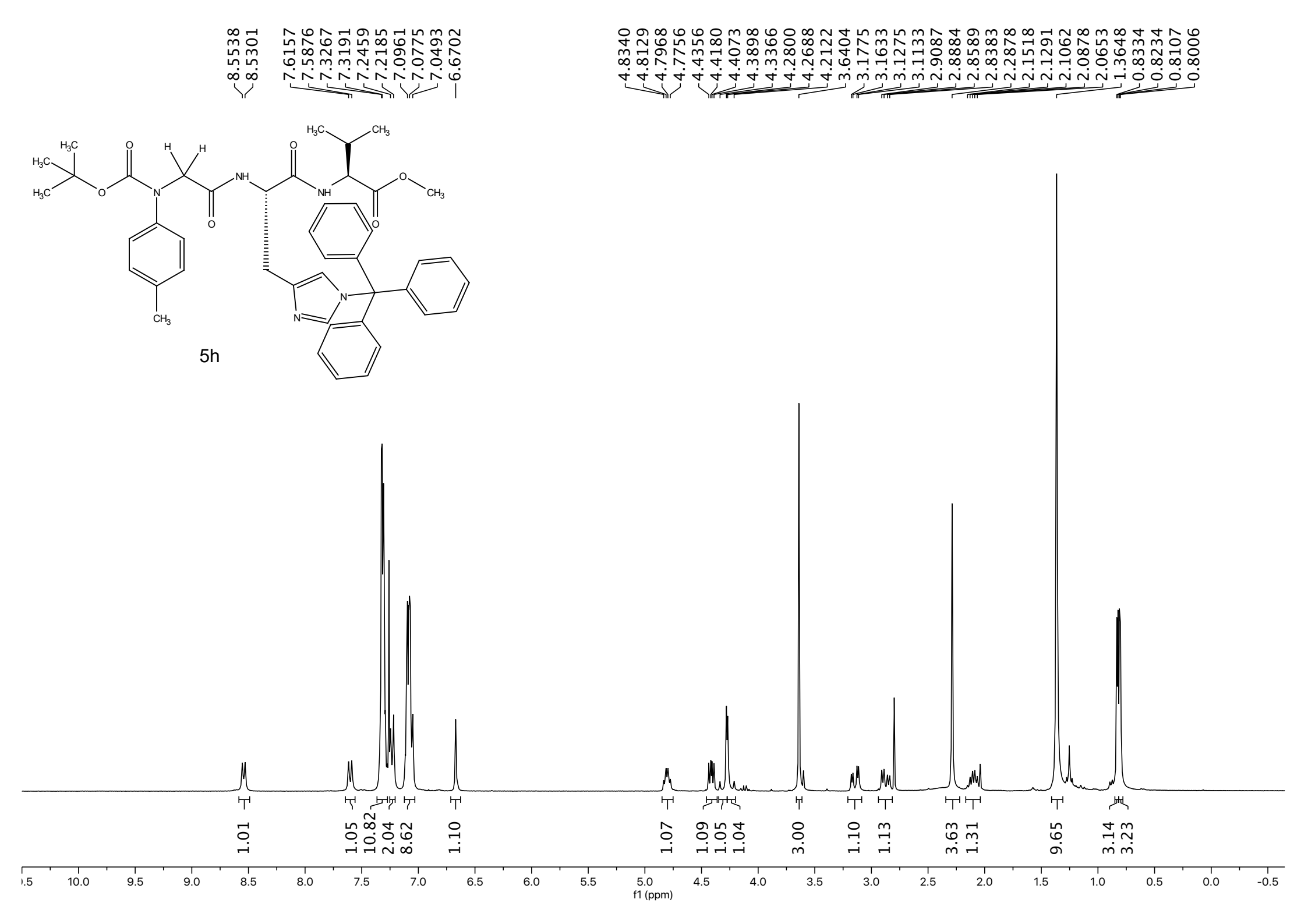
8.5538
8.5301
7.6157
7.5876
7.3267
7.3191
7.2459
7.2185
7.0961
7.0775
7.0493
6.6702
4.8340
4.8129
4.7968
4.7756
4.4356
4.4180
4.4073
4.3898
4.3366
4.2800
4.2688
4.2122
3.6404
3.1775
3.1633
3.1275
3.1133
2.9087
2.8884
2.8589
2.8383
2.2878
2.1518
2.1291
2.1062
2.0878
2.0653
1.3648
0.8334
0.8234
0.8107
0.8006
5h
1.01
1.05
10.82
2.04
8.62
1.10
1.07
1.09
1.05
1.04
3.00
1.10
1.13
3.63
1.31
9.65
3.14
3.23
f1 (ppm)

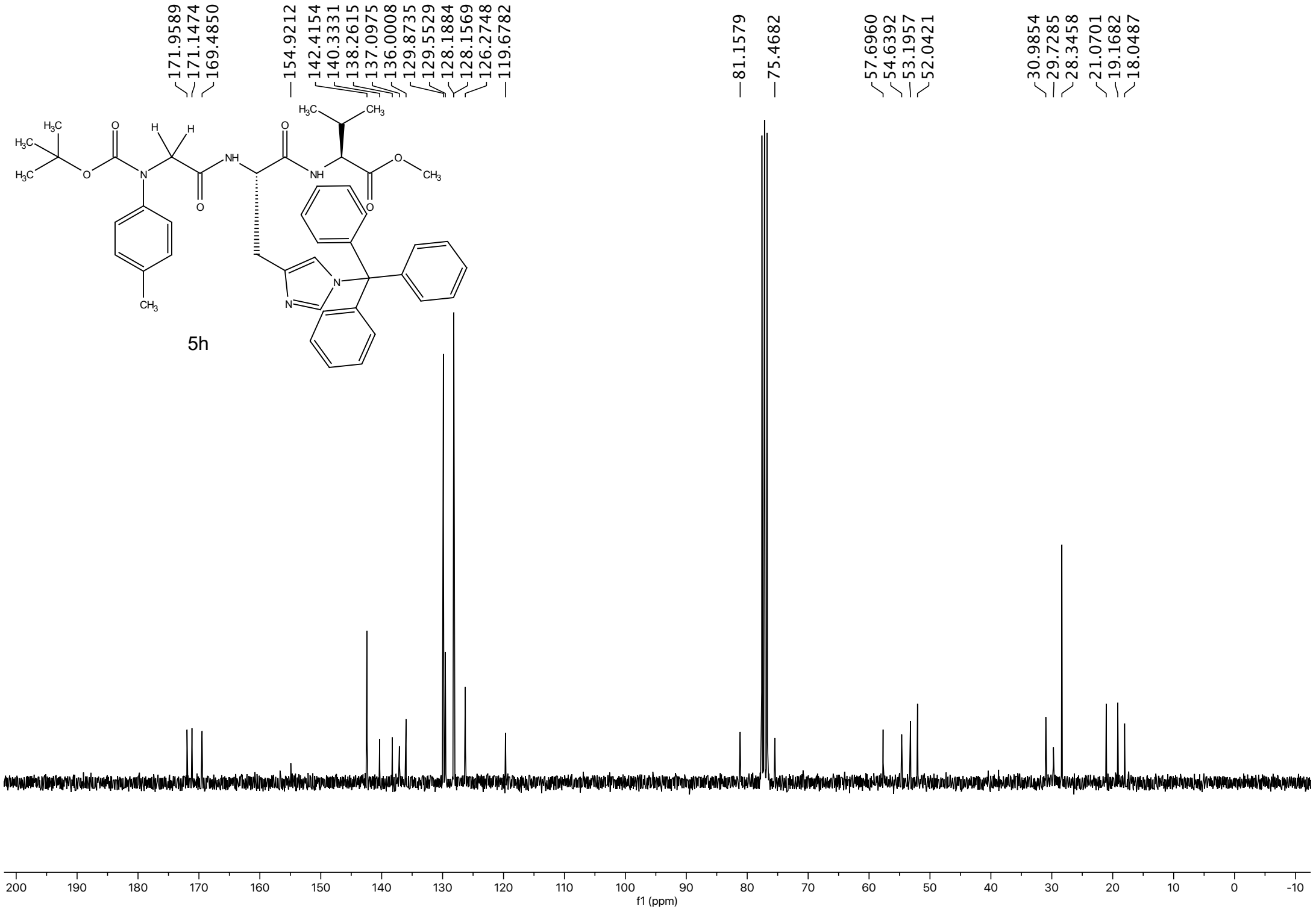
171.9589
171.1474
169.4850
154.9212
142.4154
140.3331
138.2615
137.0975
136.0008
129.8735
129.5529
128.1884
128.1569
126.2748
119.6782
81.1579
75.4682
57.6960
54.6392
53.1957
52.0421
30.9854
29.7285
28.3458
21.0701
19.1682
18.0487
5h
200
190
180
170
160
150
140
130
120
110
100
90
80
70
60
50
40
30
20
10
0
-10
f1 (ppm)

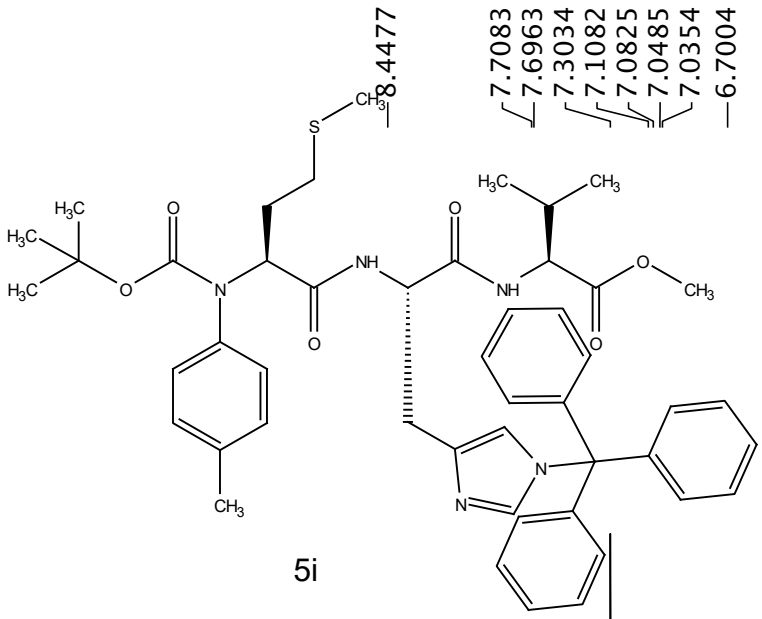

5i

8.4477
7.7083
7.6963
7.3034
7.1082
7.0825
7.0485
7.0354
6.7004
4.8199
4.7218
4.4367
3.6327
3.1167
2.9384
2.5481
2.5363
2.5246
2.2778
2.1273
2.1171
1.9926
1.9577
1.9460
1.9339
1.3463
0.8490
0.8442
0.8384
0.8336

0.85
0.99
10.38
8.30
2.13
0.95
0.88
0.97
0.98
3.00
0.85
0.88
2.08
3.93
1.33
3.00
1.04
9.16
3.05
2.62

f1 (ppm)

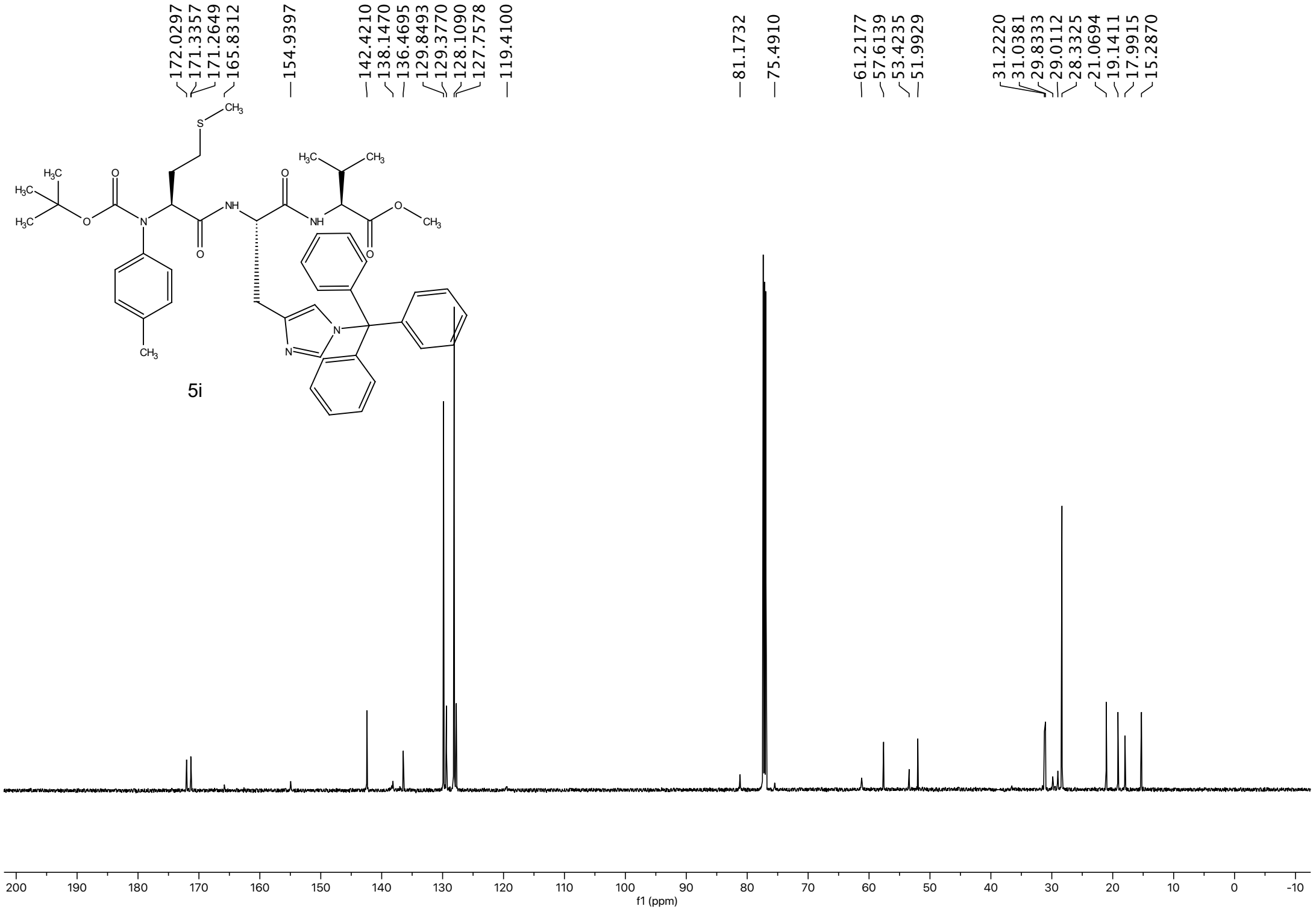
172.0297
171.3357
171.2649
165.8312
154.9397
142.4210
138.1470
136.4695
129.8493
129.3770
128.1090
127.7578
119.4100
81.1732
75.4910
61.2177
57.6139
53.4235
51.9929
31.2220
31.0381
29.8333
29.0112
28.3325
21.0694
19.1411
17.9915
15.2870
5i
200
190
180
170
160
150
140
130
120
110
100
90
80
70
60
50
40
30
20
10
0
-10
f1 (ppm)

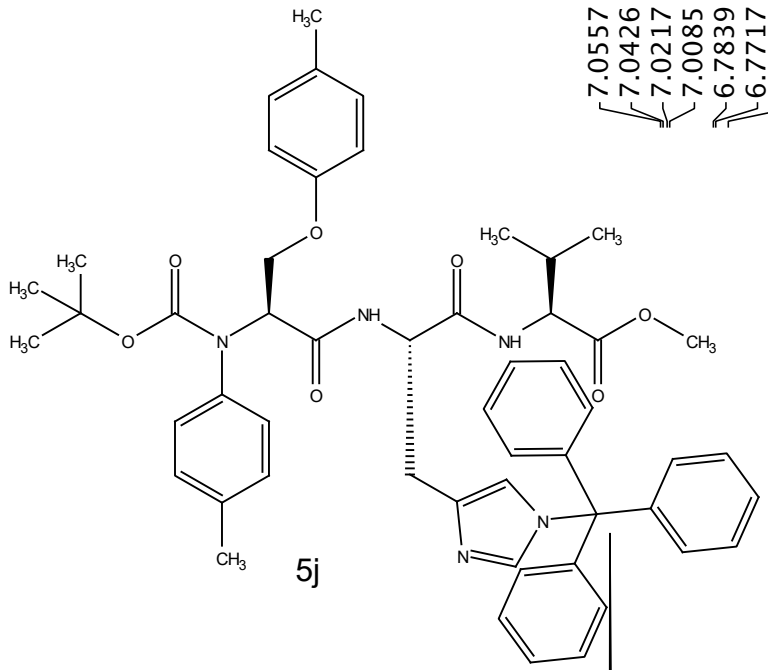

5j

7.0557
7.0426
7.0217
7.0085
6.7839
6.7717
6.7072
4.8681
4.8269
4.5463
4.5392
4.4474
4.4388
4.4340
4.4254
4.2975
4.2818
4.2660
3.6408
3.1892
3.1711
2.9617
2.2884
2.2548
2.1159
1.3277
0.8224

12.84
8.07
2.49
1.97
2.01
1.04
1.04
1.01
1.08
1.18
1.01
3.00
0.99
1.07
3.42
3.34
1.69
9.59
6.01

f1 (ppm)

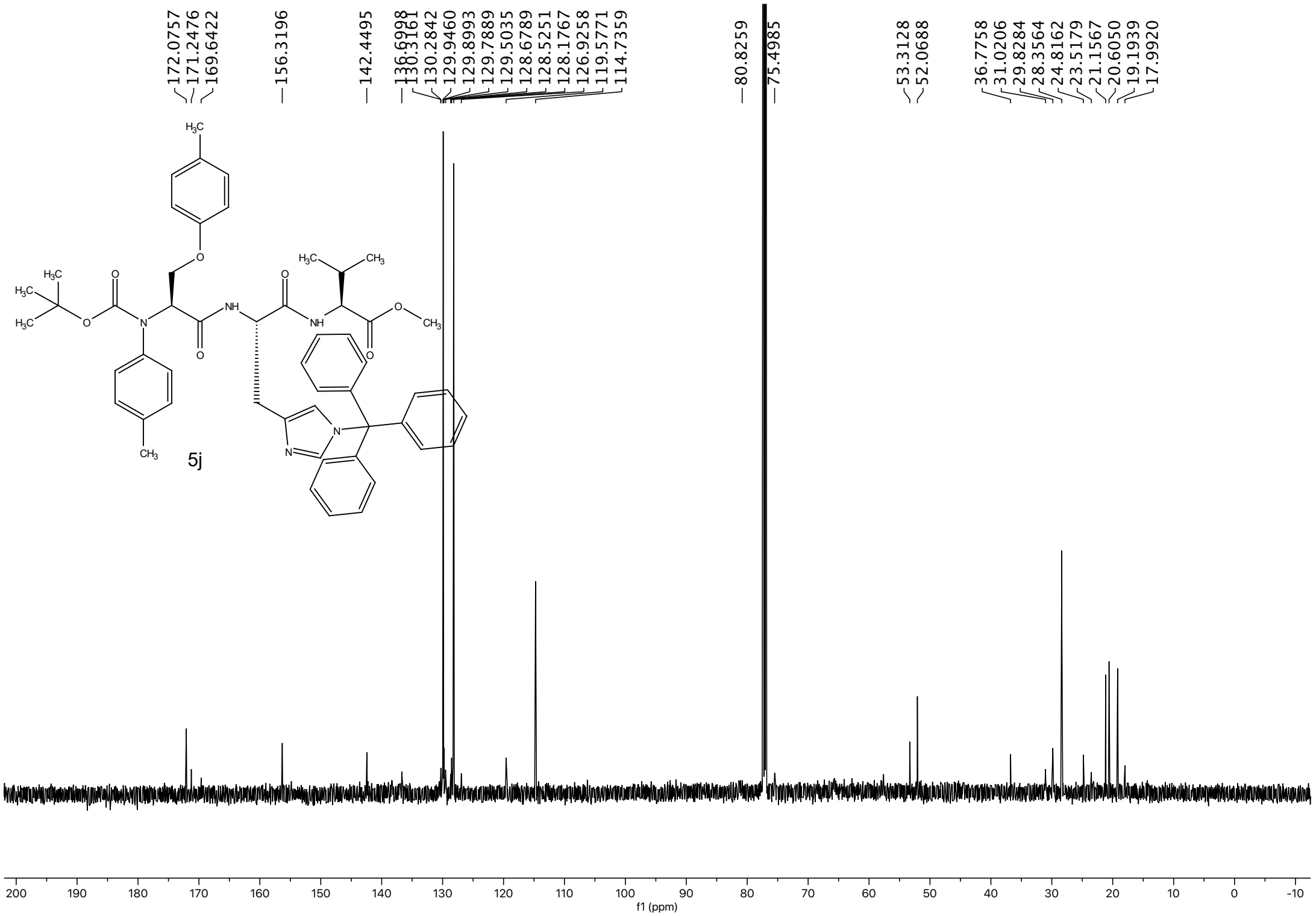
172.0757
171.2476
169.6422
156.3196
142.4495
136.6998
130.3161
130.2842
129.9460
129.8993
129.7889
129.5035
128.6789
128.5251
128.1767
126.9258
119.5771
114.7359
80.8259
75.4985
53.3128
52.0688
36.7758
31.0206
29.8284
28.3564
24.8162
23.5179
21.1567
20.6050
19.1939
17.9920
5j
200
190
180
170
160
150
140
130
120
110
100
90
80
70
60
50
40
30
20
10
0
-10
f1 (ppm)

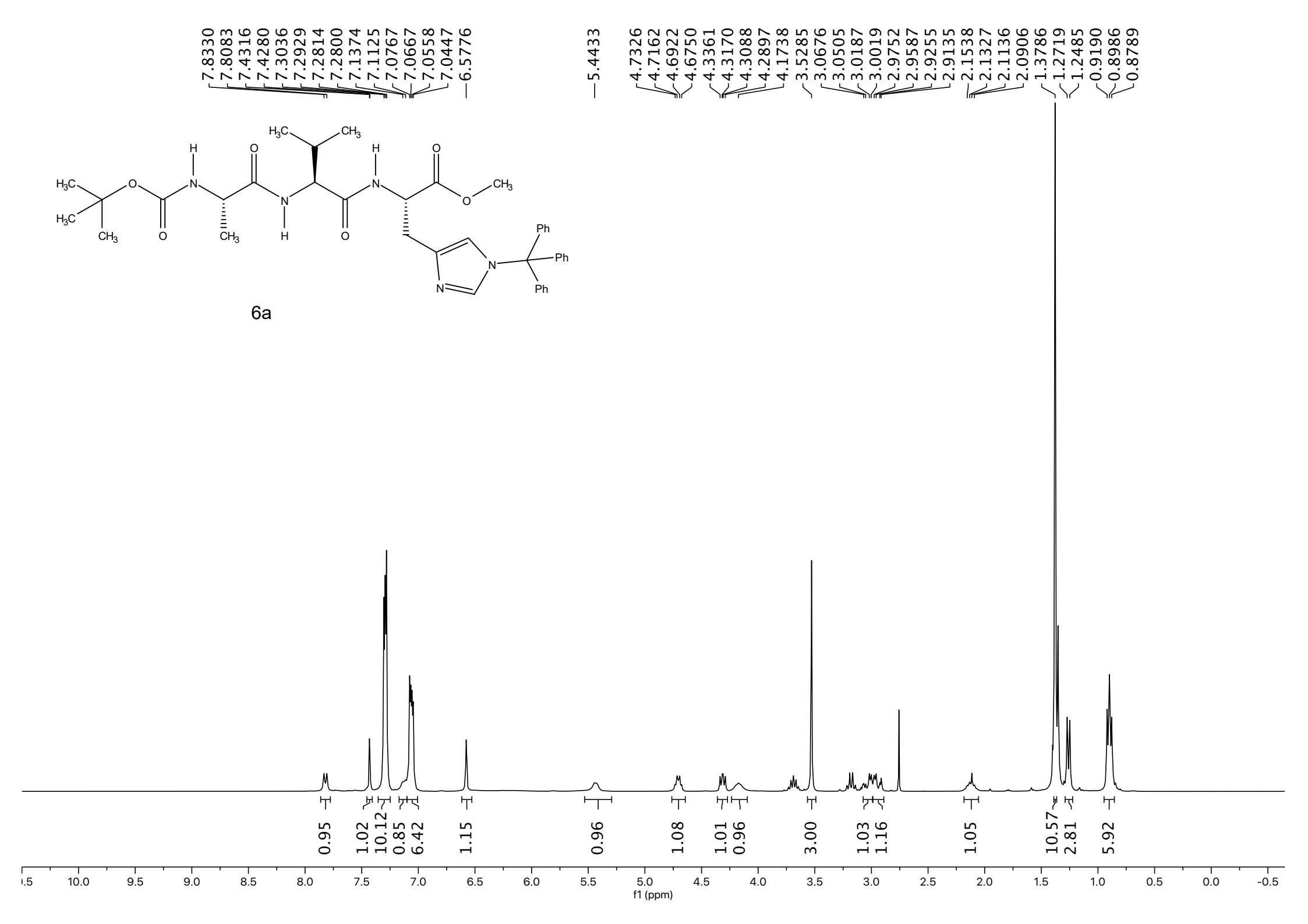
7.8330
7.8083
7.4316
7.4280
7.3036
7.2929
7.2814
7.2800
7.1374
7.1125
7.0767
7.0667
7.0558
7.0447
6.5776
5.4433
4.7326
4.7162
4.6922
4.6750
4.3361
4.3170
4.3088
4.2897
4.1738
3.5285
3.0676
3.0505
3.0187
3.0019
2.9752
2.9587
2.9255
2.9135
2.1538
2.1327
2.1136
2.0906
1.3786
1.2719
1.2485
0.9190
0.8986
0.8789
0.95
1.02
10.12
0.85
6.42
1.15
0.96
1.08
1.01
0.96
3.00
1.03
1.16
1.05
10.57
2.81
5.92
f1 (ppm)

6a

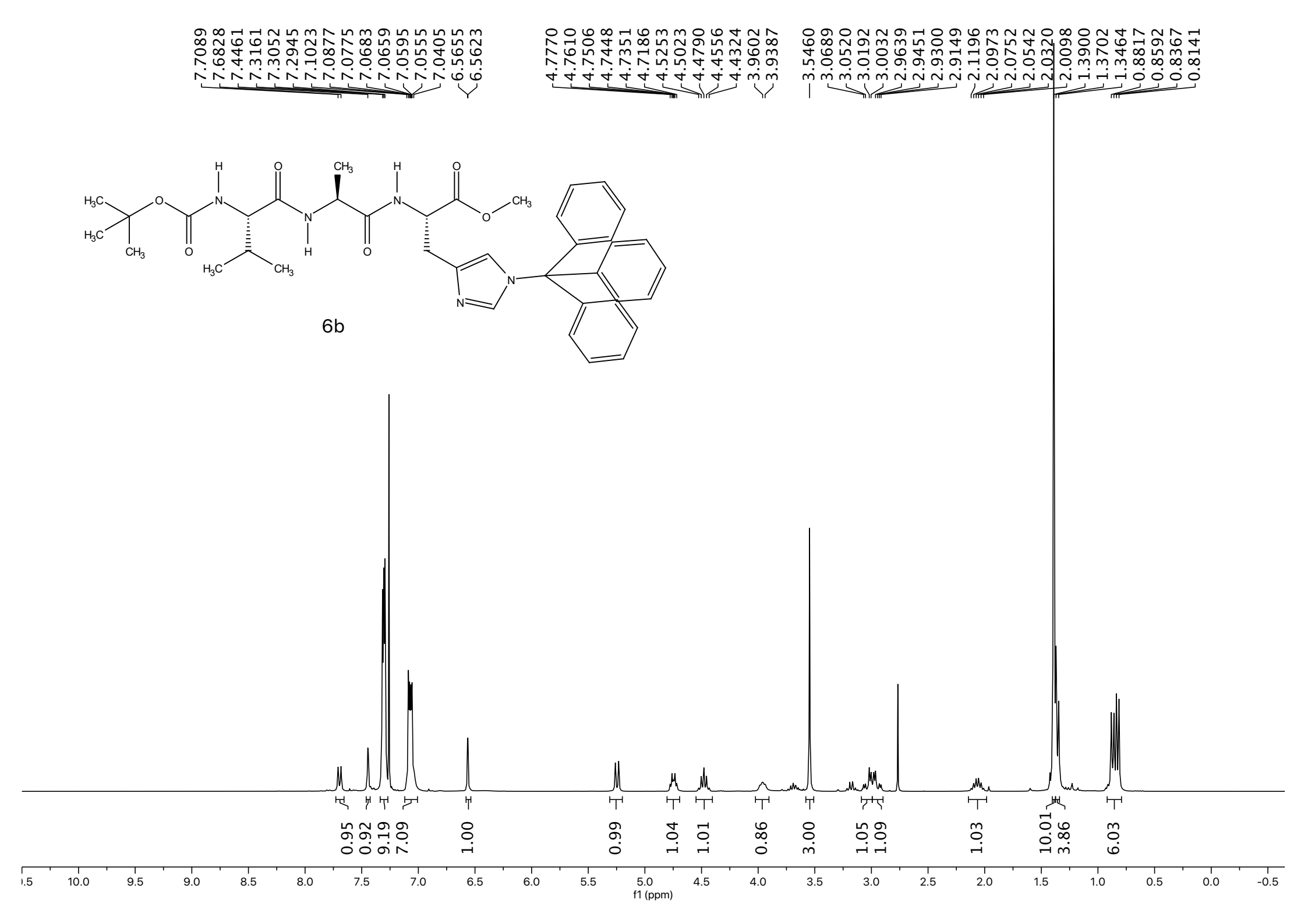
7.7089
7.6828
7.4461
7.3161
7.3052
7.2945
7.1023
7.0877
7.0775
7.0683
7.0659
7.0595
7.0555
7.0405
6.5655
6.5623
4.7770
4.7610
4.7506
4.7448
4.7351
4.7186
4.5253
4.5023
4.4790
4.4556
4.4324
3.9602
3.9387
3.5460
3.0689
3.0520
3.0192
3.0032
2.9639
2.9451
2.9300
2.9149
2.1196
2.0973
2.0752
2.0542
2.0320
2.0098
1.3900
1.3702
1.3464
0.8817
0.8592
0.8367
0.8141
6b
0.95
0.92
9.19
7.09
1.00
0.99
1.04
1.01
0.86
3.00
1.05
1.09
1.03
10.01
3.86
6.03
f1 (ppm)

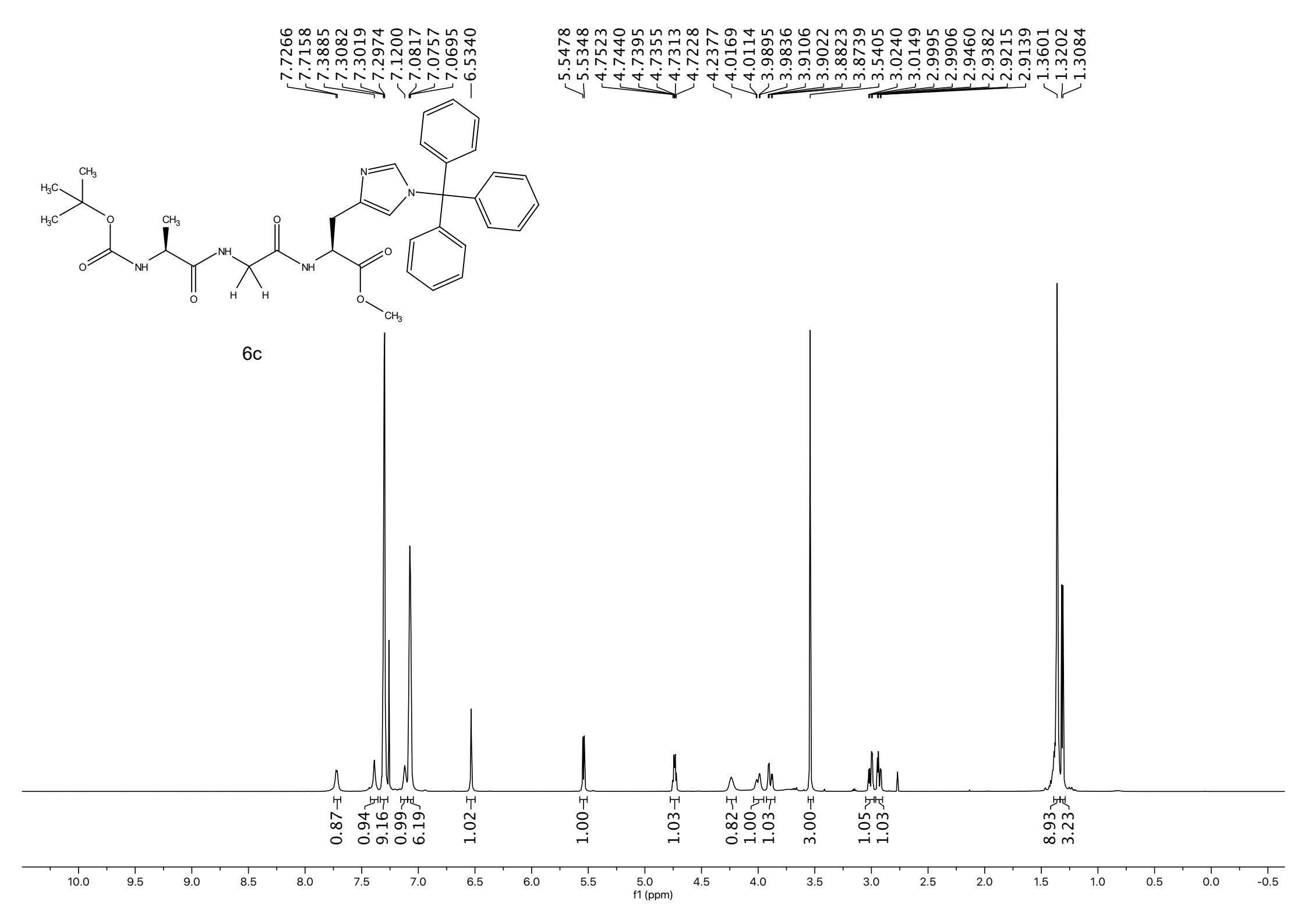
7.7266
7.7158
7.3885
7.3082
7.3019
7.2974
7.1200
7.0817
7.0757
7.0695
6.5340
5.5478
5.5348
4.7523
4.7440
4.7395
4.7355
4.7313
4.7228
4.2377
4.0169
4.0114
3.9895
3.9836
3.9106
3.9022
3.8823
3.8739
3.5405
3.0240
3.0149
2.9995
2.9906
2.9460
2.9382
2.9215
2.9139
1.3601
1.3202
1.3084
6c
0.87
0.94
9.16
0.99
6.19
1.02
1.00
1.03
0.82
1.00
1.03
3.00
1.05
1.03
8.93
3.23
f1 (ppm)

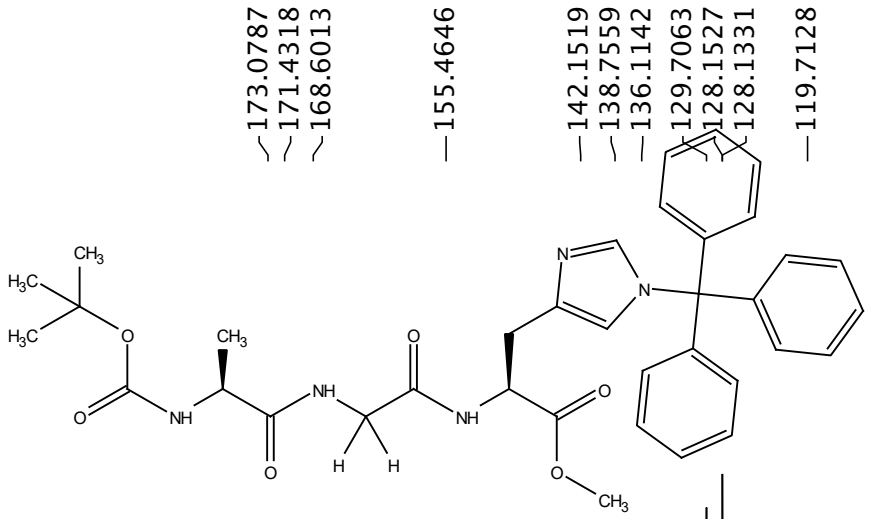

6c

173.0787
171.4318
168.6013
155.4646
142.1519
138.7559
136.1142
129.7063
128.1527
128.1331
119.7128
79.9004
75.4055
52.6585
52.1834
50.0690
42.8169
29.6393
28.3331
18.6595
200
190
180
170
160
150
140
130
120
110
100
90
80
70
60
50
40
30
20
10
0
-10
f1 (ppm)

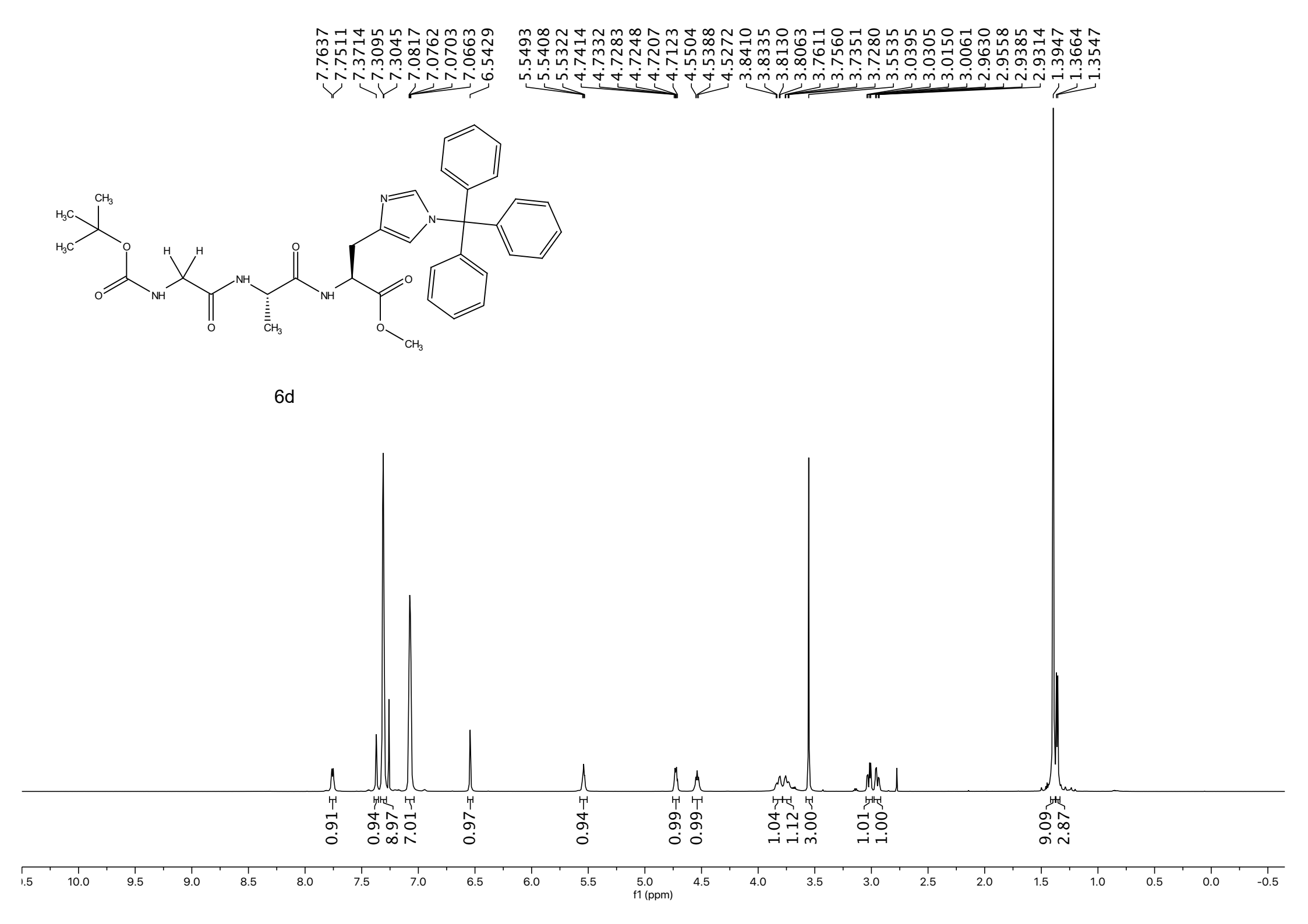
7.7637
7.7511
7.3714
7.3095
7.3045
7.0817
7.0762
7.0703
7.0663
6.5429
5.5493
5.5408
5.5322
4.7414
4.7332
4.7283
4.7248
4.7207
4.7123
4.5504
4.5388
4.5272
3.8410
3.8335
3.8130
3.8063
3.7611
3.7560
3.7351
3.7280
3.5535
3.0395
3.0305
3.0150
3.0061
2.9630
2.9558
2.9385
2.9314
1.3947
1.3664
1.3547
6d
0.91
0.94
8.97
7.01
0.97
0.94
0.99
0.99
1.04
1.12
3.00
1.01
1.00
9.09
2.87
f1 (ppm)

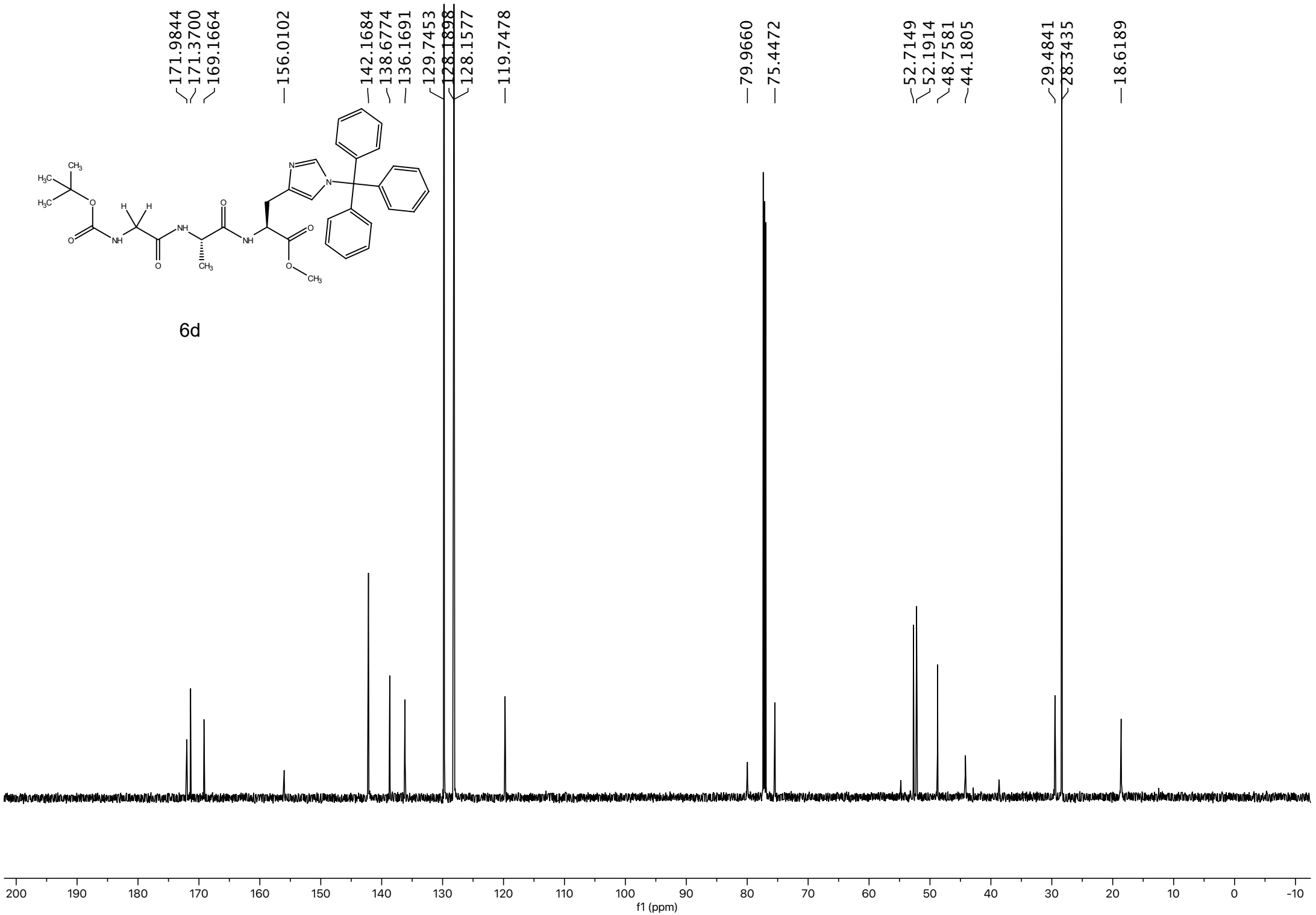
171.9844
171.3700
169.1664
156.0102
142.1684
138.6774
136.1691
129.7453
128.1898
128.1577
119.7478
79.9660
75.4472
52.7149
52.1914
48.7581
44.1805
29.4841
28.3435
18.6189
6d
f1 (ppm)

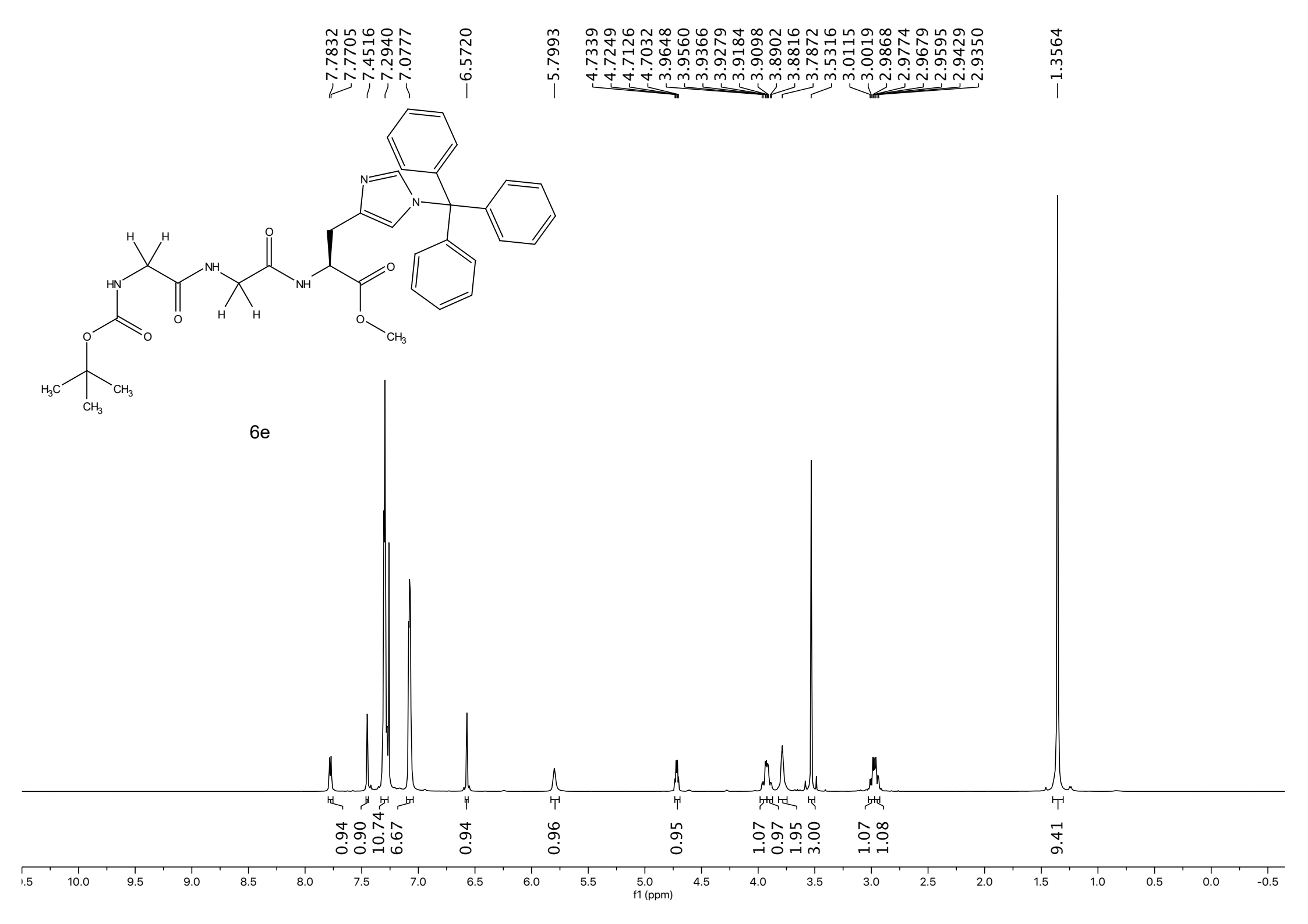
7.7832
7.7705
7.4516
7.2940
7.0777
6.5720
5.7993
4.7339
4.7249
4.7126
4.7032
3.9648
3.9560
3.9366
3.9279
3.9184
3.9098
3.8902
3.8816
3.7872
3.5316
3.0115
3.0019
2.9868
2.9774
2.9679
2.9595
2.9429
2.9350
1.3564
6e
0.94
0.90
10.74
6.67
0.94
0.96
0.95
1.07
0.97
1.95
3.00
1.07
1.08
9.41
f1 (ppm)

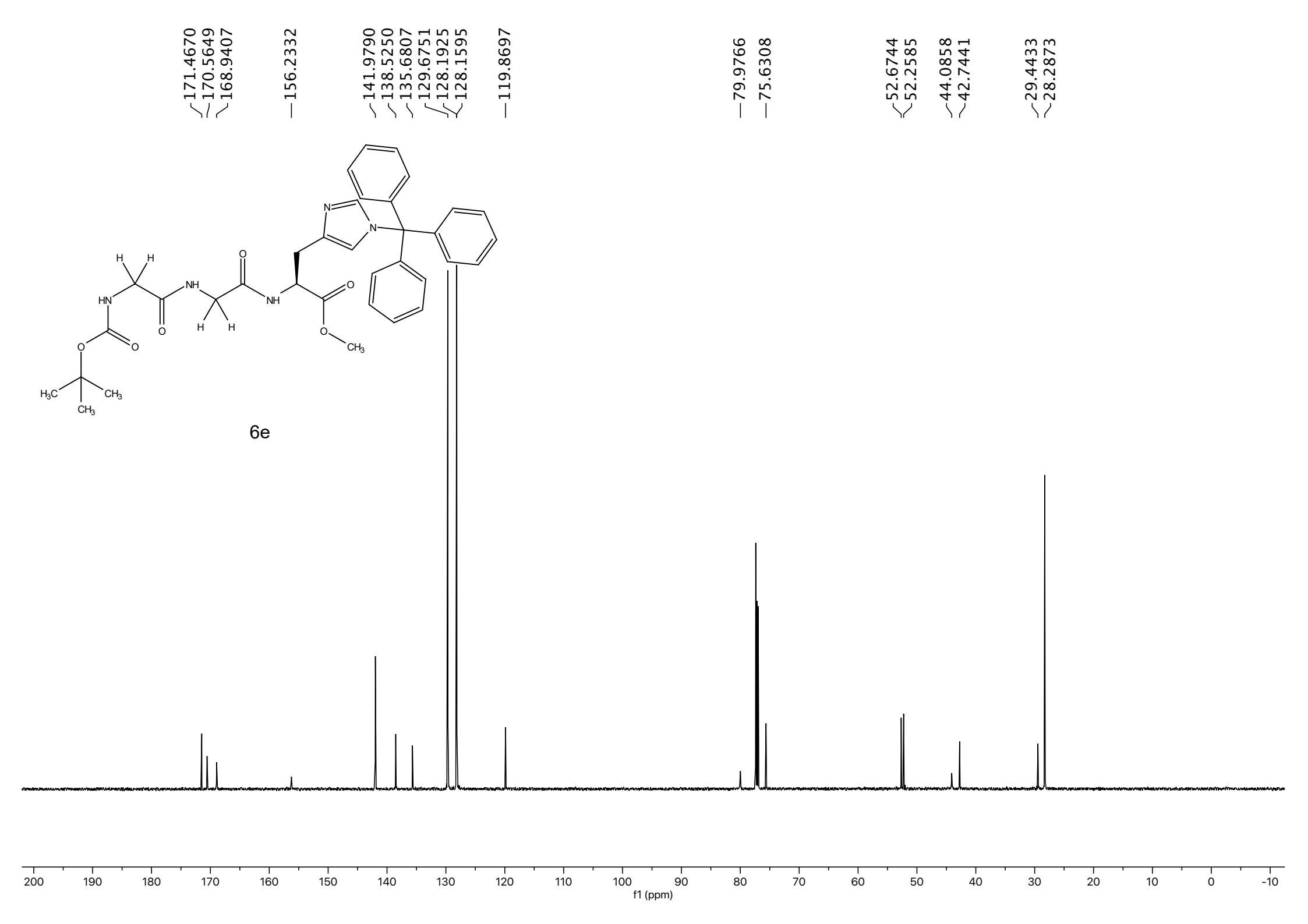
171.4670
170.5649
168.9407
156.2332
141.9790
138.5250
135.6807
129.6751
128.1925
128.1595
119.8697
79.9766
75.6308
52.6744
52.2585
44.0858
42.7441
29.4433
28.2873
6e
f1 (ppm)

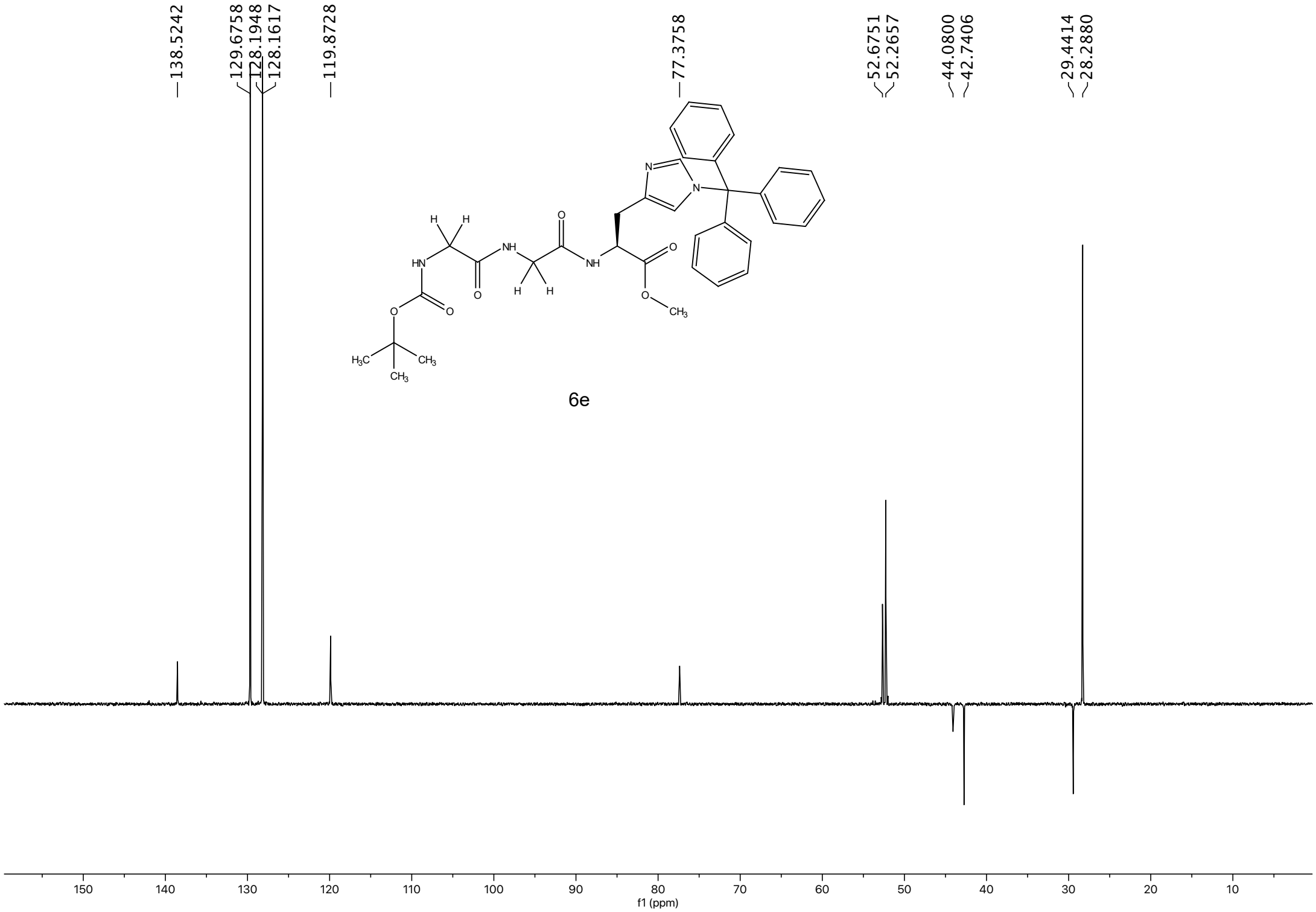
138.5242
129.6758
128.1948
128.1617
119.8728
77.3758
52.6751
52.2657
44.0800
42.7406
29.4414
28.2880
150
140
130
120
110
100
90
80
70
60
50
40
30
20
10
f1 (ppm)

6e

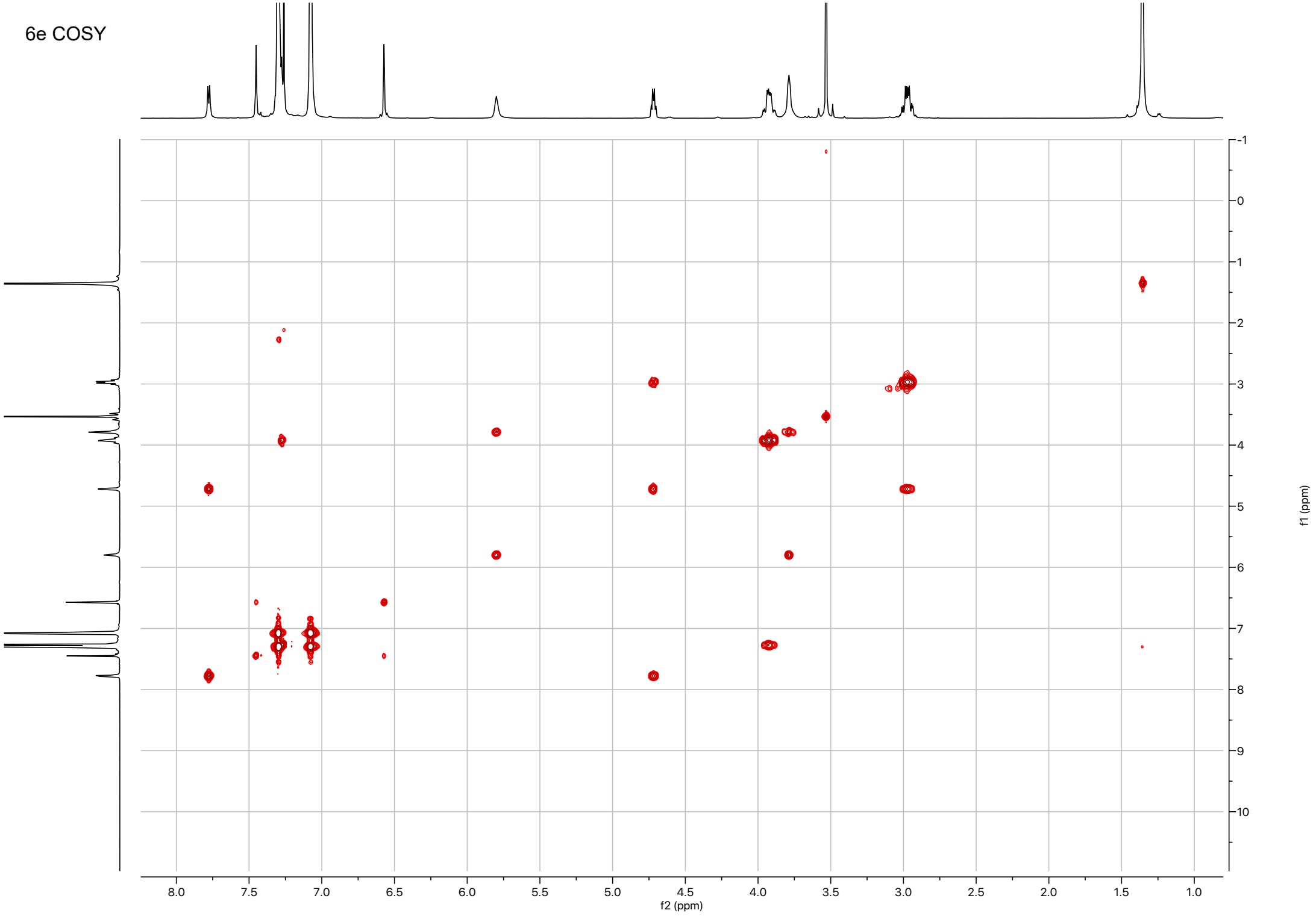
6e COSY
8.0
7.5
7.0
6.5
6.0
5.5
5.0
4.5
4.0
3.5
3.0
2.5
2.0
1.5
1.0
f2 (ppm)
-1
0
1
2
3
4
5
6
7
8
9
10
f1 (ppm)

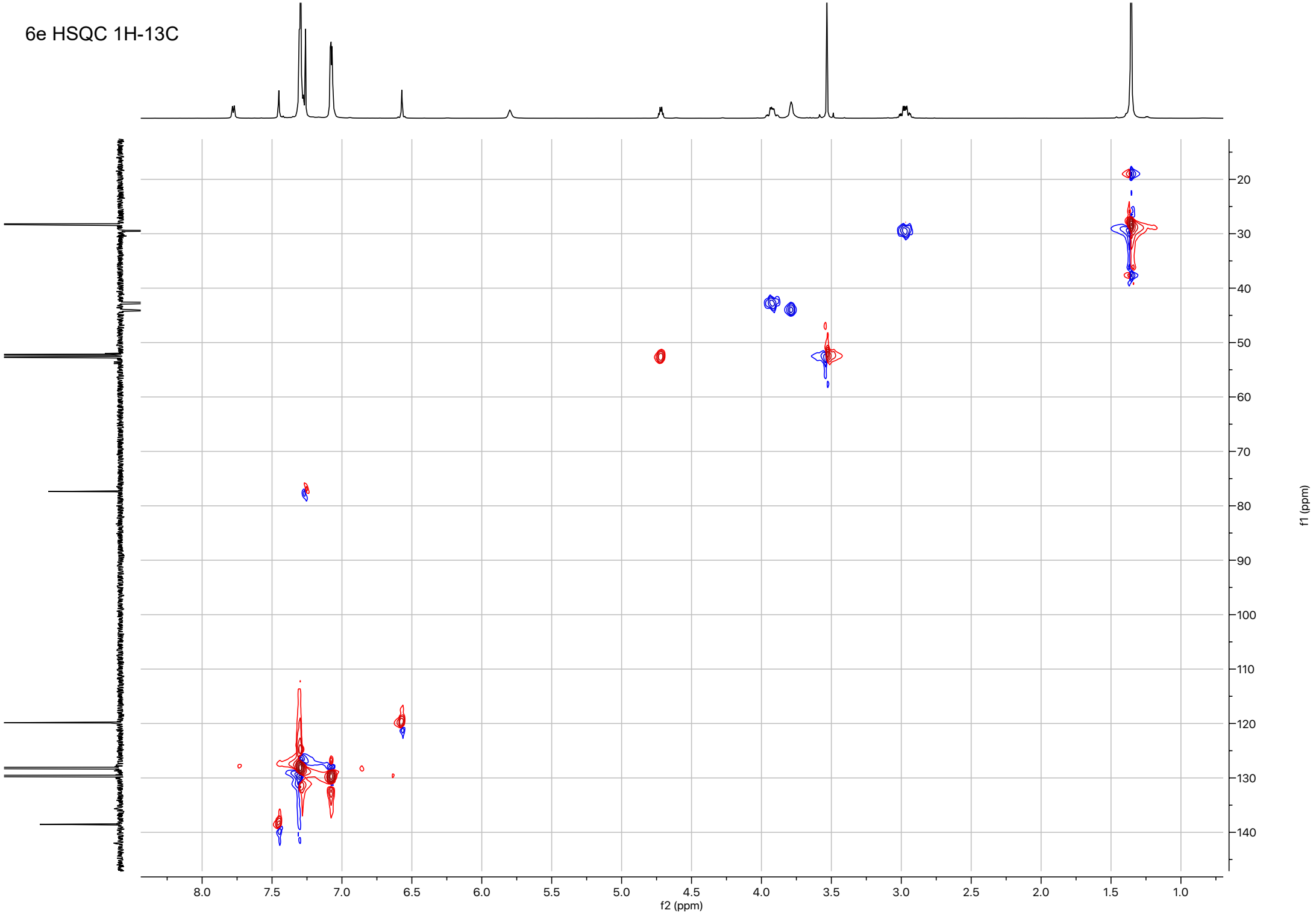
6e HSQC 1H-13C
8.0
7.5
7.0
6.5
6.0
5.5
5.0
4.5
4.0
3.5
3.0
2.5
2.0
1.5
1.0
f2 (ppm)
20
30
40
50
60
70
80
90
100
110
120
130
140
f1 (ppm)

6e HSQC 1H-15N

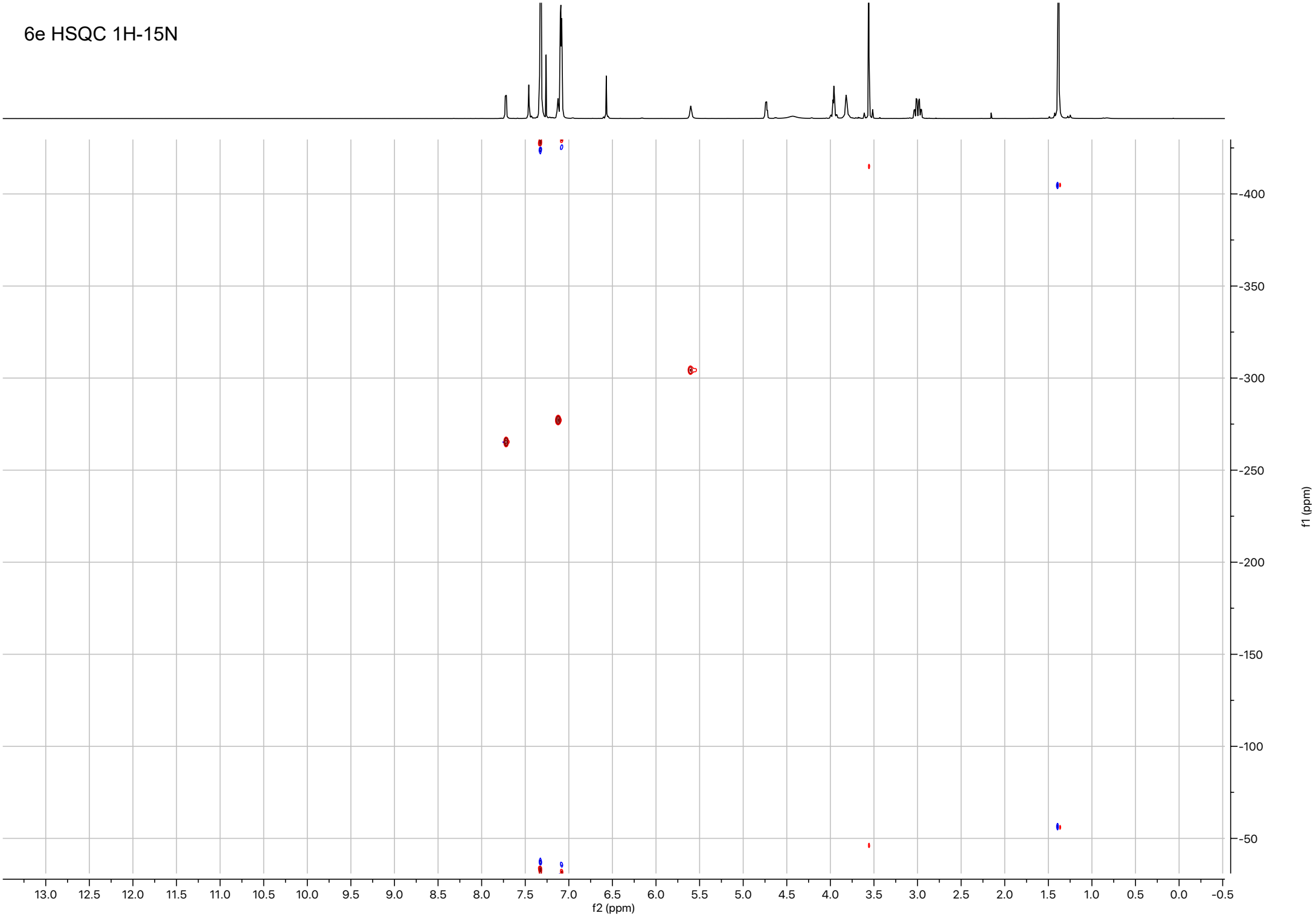


6e HMBC 1H-15N
12.0
11.5
11.0
10.5
10.0
9.5
9.0
8.5
8.0
7.5
7.0
6.5
6.0
5.5
5.0
4.5
4.0
3.5
3.0
2.5
2.0
1.5
1.0
0.5
0.0
-0.5
f2 (ppm)
-400
-350
-300
-250
-200
-150
-100
-50
f1 (ppm)

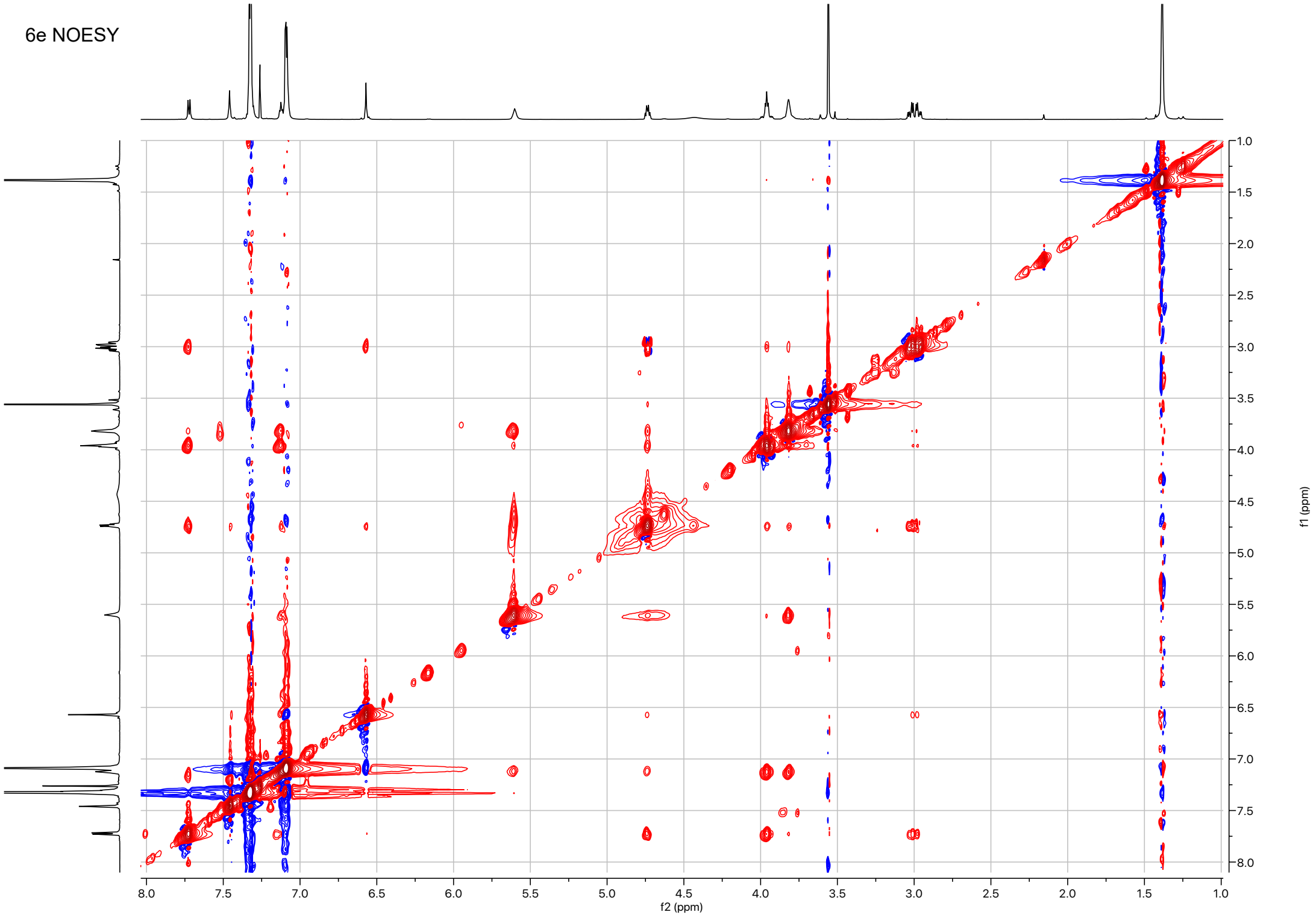
6e NOESY
8.0
7.5
7.0
6.5
6.0
5.5
5.0
4.5
4.0
3.5
3.0
2.5
2.0
1.5
1.0
f2 (ppm)
1.0
1.5
2.0
2.5
3.0
3.5
4.0
4.5
5.0
5.5
6.0
6.5
7.0
7.5
8.0
f1 (ppm)

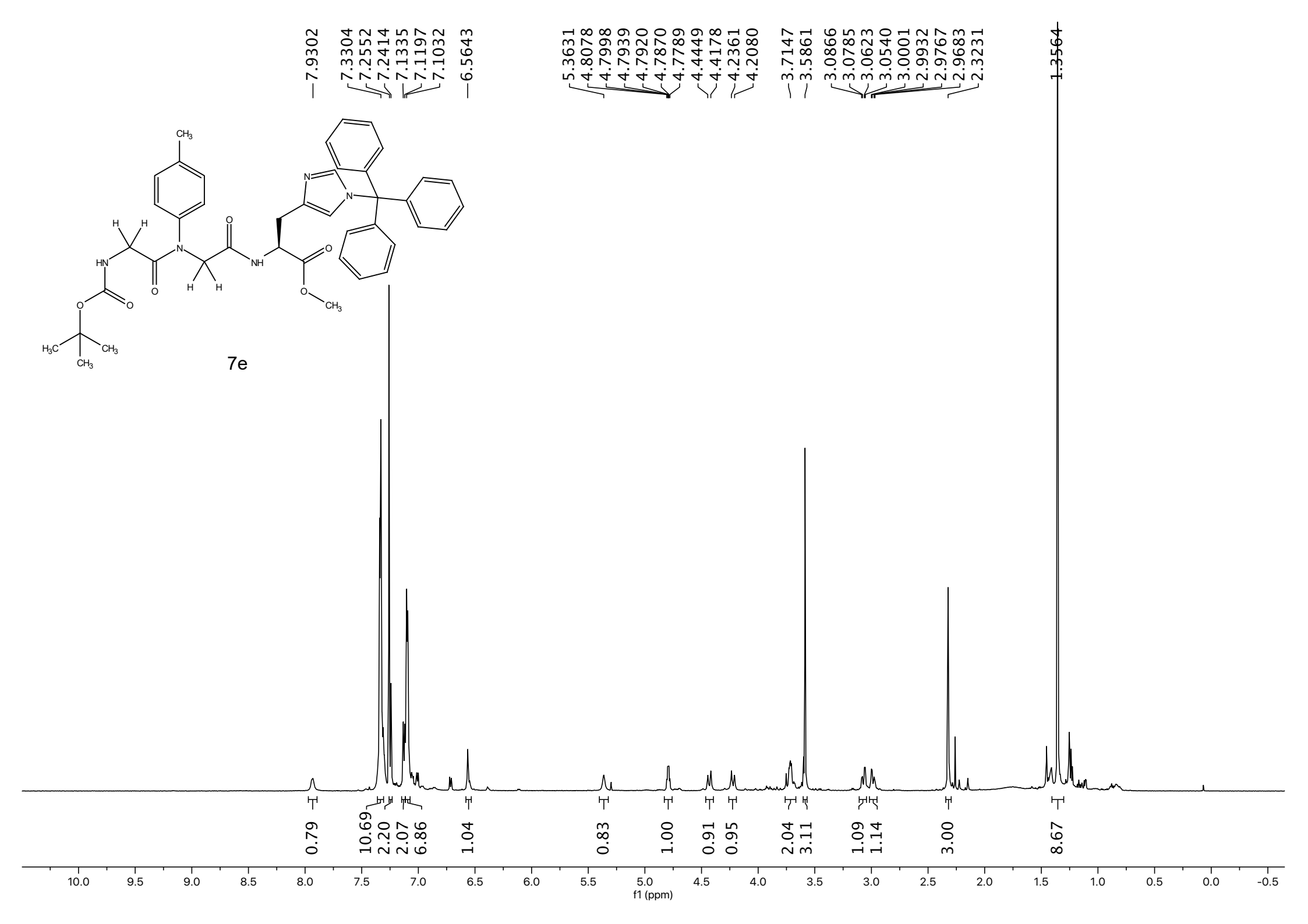
7.9302
7.3304
7.2552
7.2414
7.1335
7.1197
7.1032
6.5643
5.3631
4.8078
4.7998
4.7939
4.7920
4.7870
4.7789
4.4449
4.4178
4.2361
4.2080
3.7147
3.5861
3.0866
3.0785
3.0623
3.0540
3.0001
2.9932
2.9767
2.9683
2.3231
1.3564
0.79
10.69
2.20
2.07
6.86
1.04
0.83
1.00
0.91
0.95
2.04
3.11
1.09
1.14
3.00
8.67
f1 (ppm)

7e

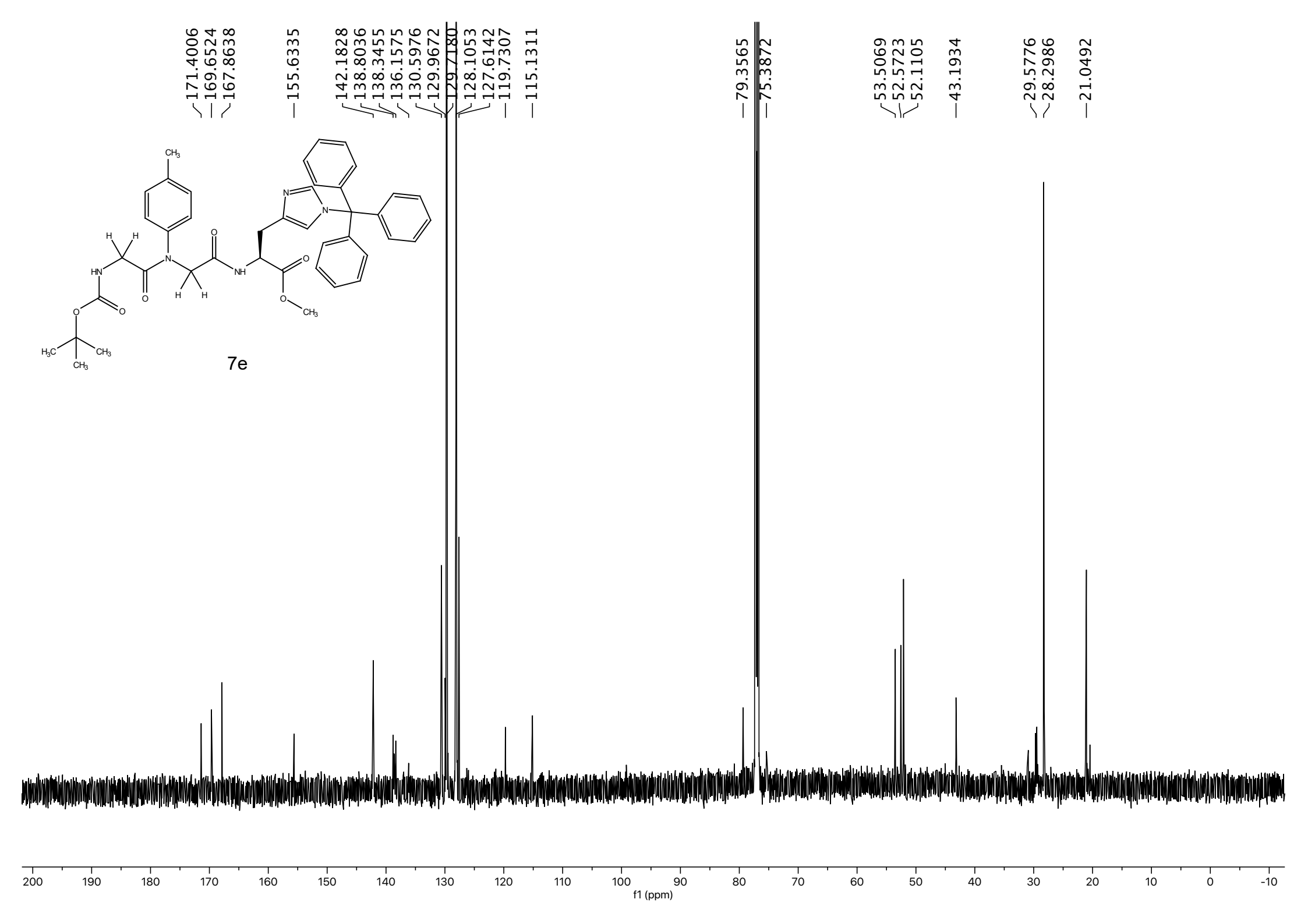
171.4006
169.6524
167.8638
155.6335
142.1828
138.8036
138.3455
136.1575
130.5976
129.9672
129.7180
128.1053
127.6142
119.7307
115.1311
79.3565
75.3872
53.5069
52.5723
52.1105
43.1934
29.5776
28.2986
21.0492
7e
200
190
180
170
160
150
140
130
120
110
100
90
80
70
60
50
40
30
20
10
0
-10
f1 (ppm)

7e COSY

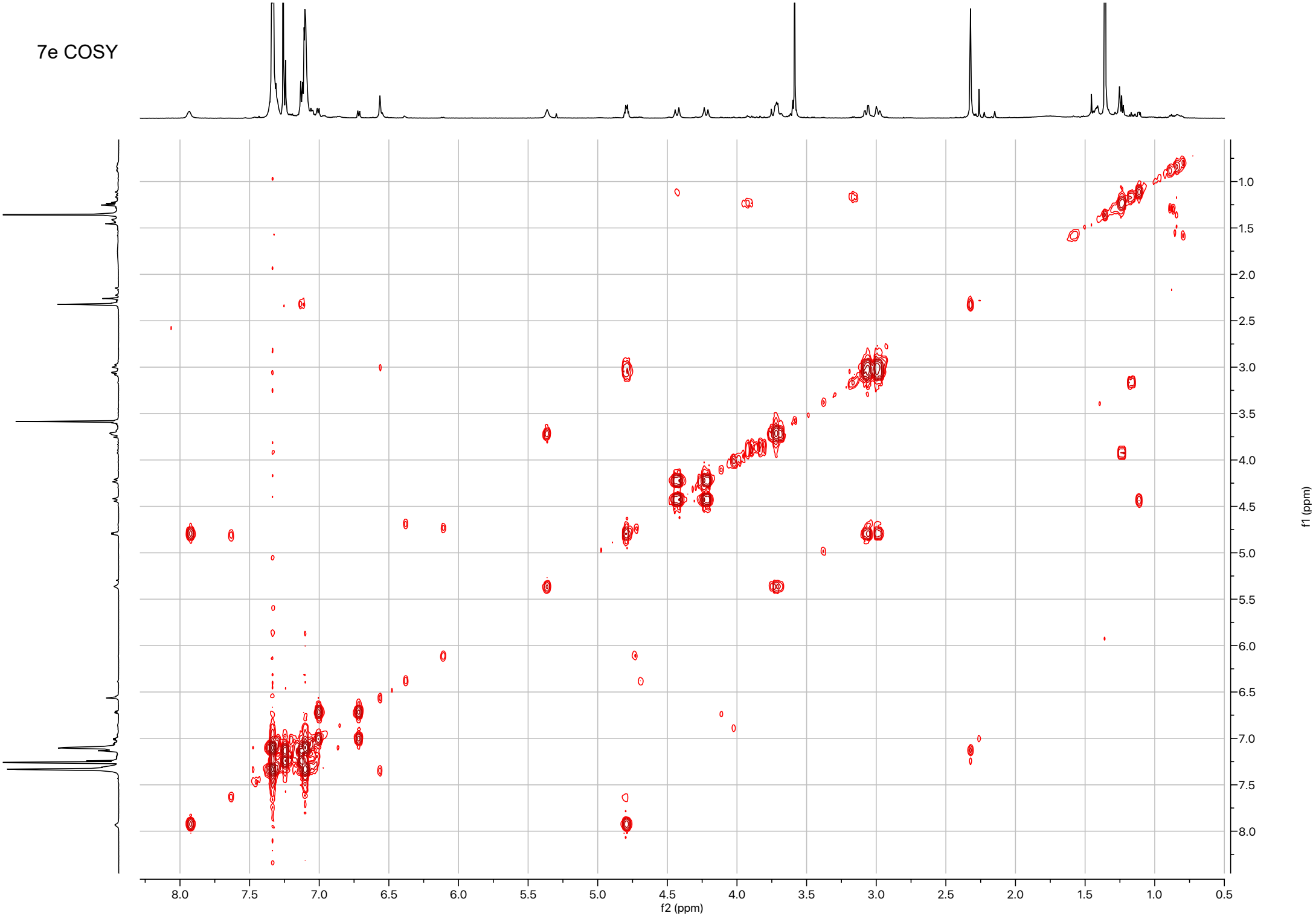
8.0
7.5
7.0
6.5
6.0
5.5
5.0
4.5
4.0
3.5
3.0
2.5
2.0
1.5
1.0
0.5
f2 (ppm)
1.0
1.5
2.0
2.5
3.0
3.5
4.0
4.5
5.0
5.5
6.0
6.5
7.0
7.5
8.0
f1 (ppm)

7e NOESY

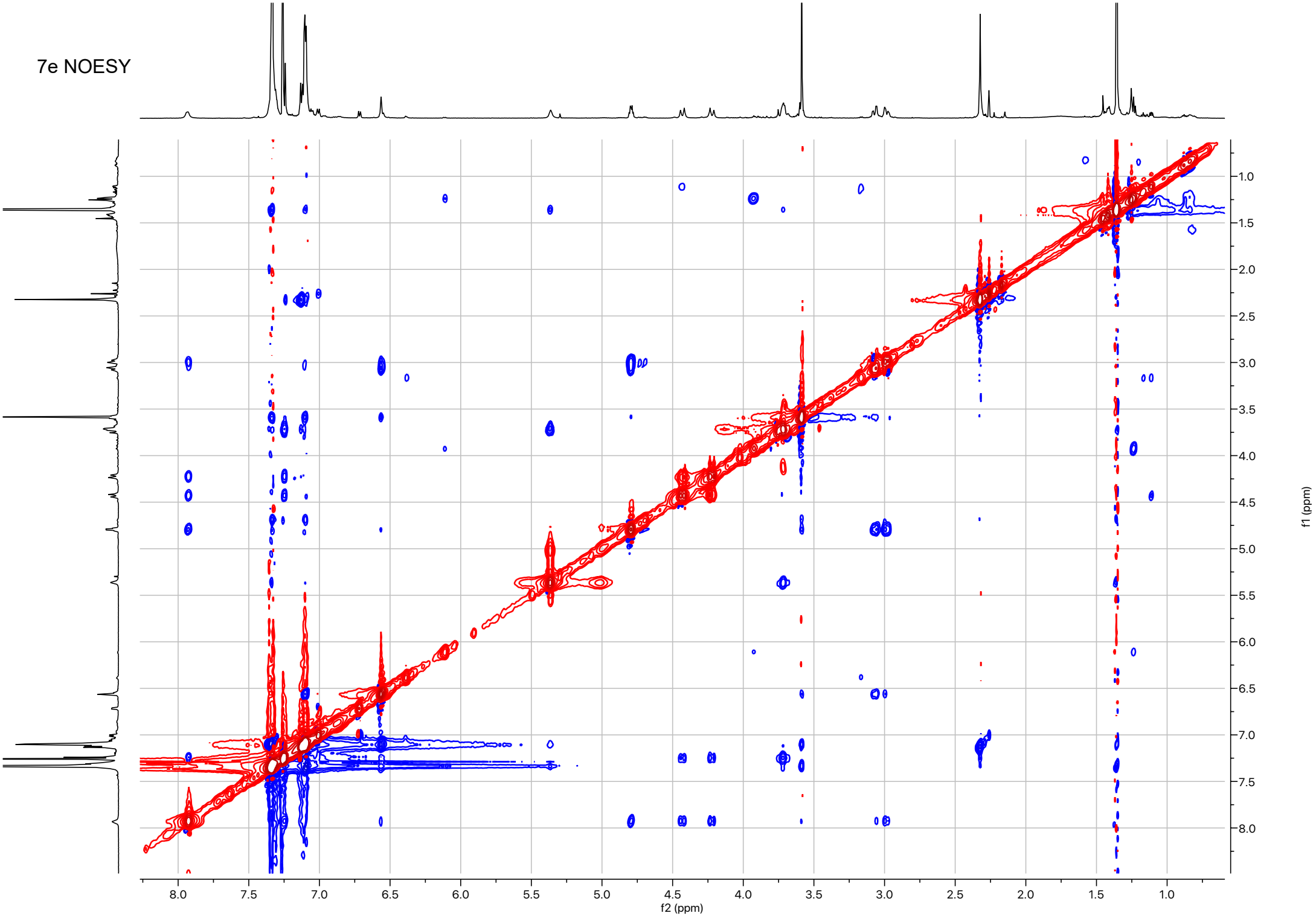
8.0
7.5
7.0
6.5
6.0
5.5
5.0
4.5
4.0
3.5
3.0
2.5
2.0
1.5
1.0
f2 (ppm)
1.0
1.5
2.0
2.5
3.0
3.5
4.0
4.5
5.0
5.5
6.0
6.5
7.0
7.5
8.0
f1 (ppm)

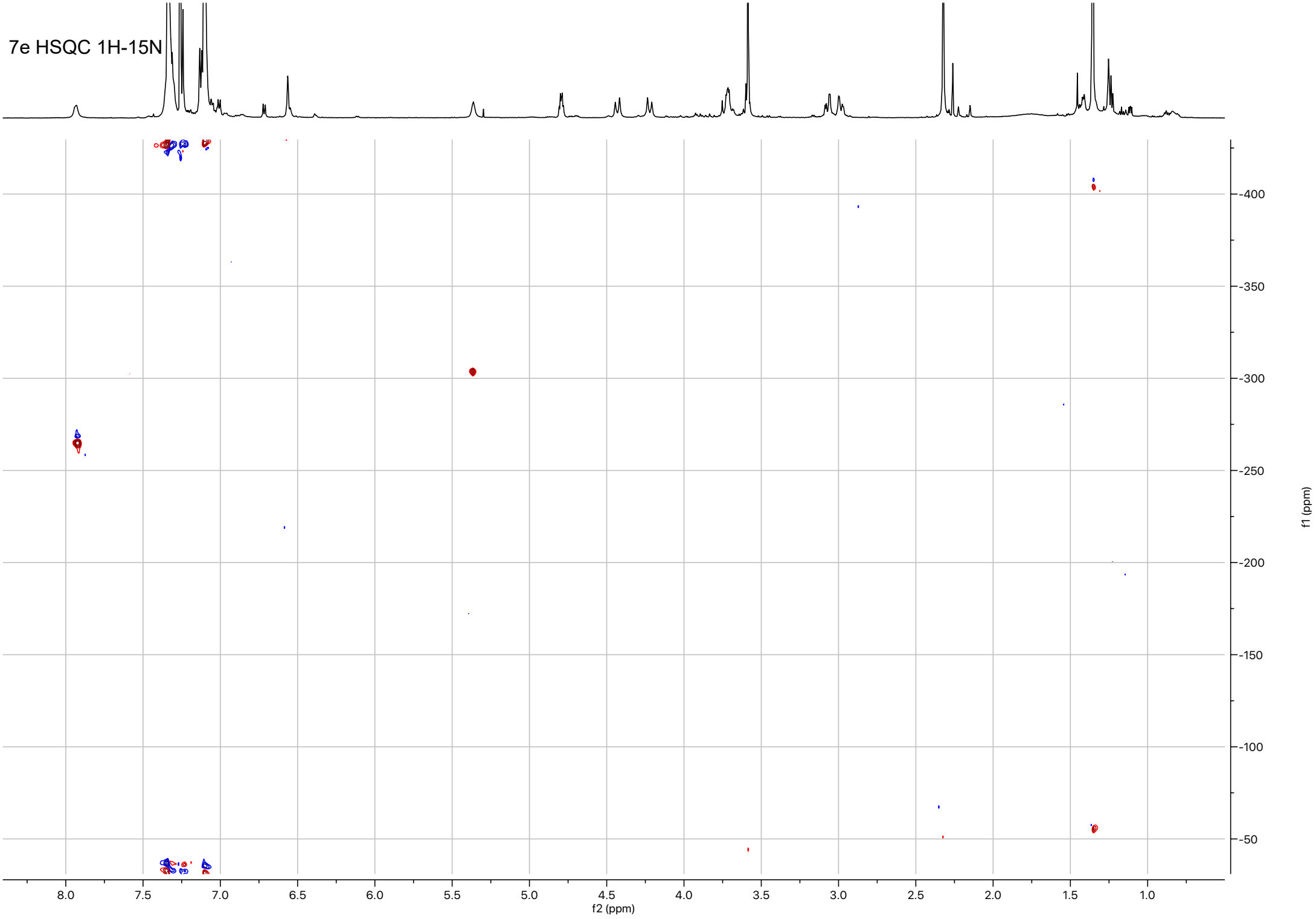
7e HSQC 1H-15N
-400
-350
-300
-250
-200
-150
-100
-50
f1 (ppm)
8.0
7.5
7.0
6.5
6.0
5.5
5.0
4.5
4.0
3.5
3.0
2.5
2.0
1.5
1.0
f2 (ppm)

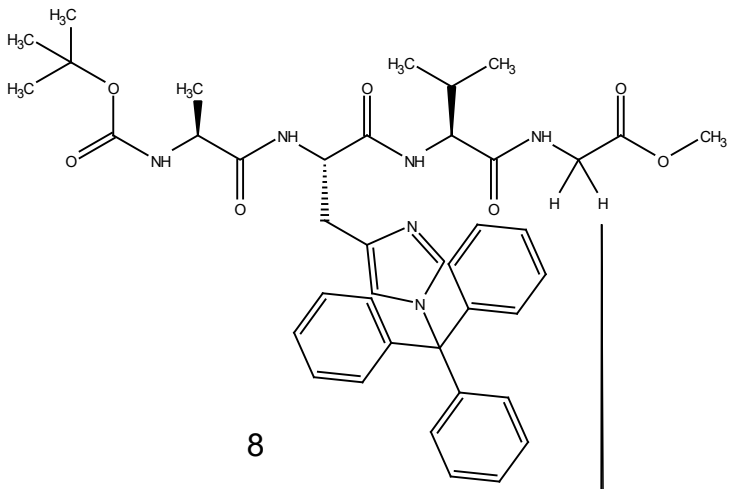

8

8.7093
8.7011
7.7287
7.3122
7.3100
7.0629
7.0136
6.9990
6.6791
5.1250
5.1177
4.5759
4.5663
4.5581
4.5485
4.3720
4.3637
4.3575
4.3492
4.0951
4.0850
4.0653
4.0552
3.8333
3.8244
3.8037
3.7950
3.6347
1.3668
1.3554
1.3272
0.8660
0.8546
0.8404
0.8290
0.94
1.04
10.88
6.66
1.04
1.02
0.99
1.05
1.07
2.15
1.10
3.00
1.08
1.14
1.16
3.44
9.11
3.20
3.30
f1 (ppm)

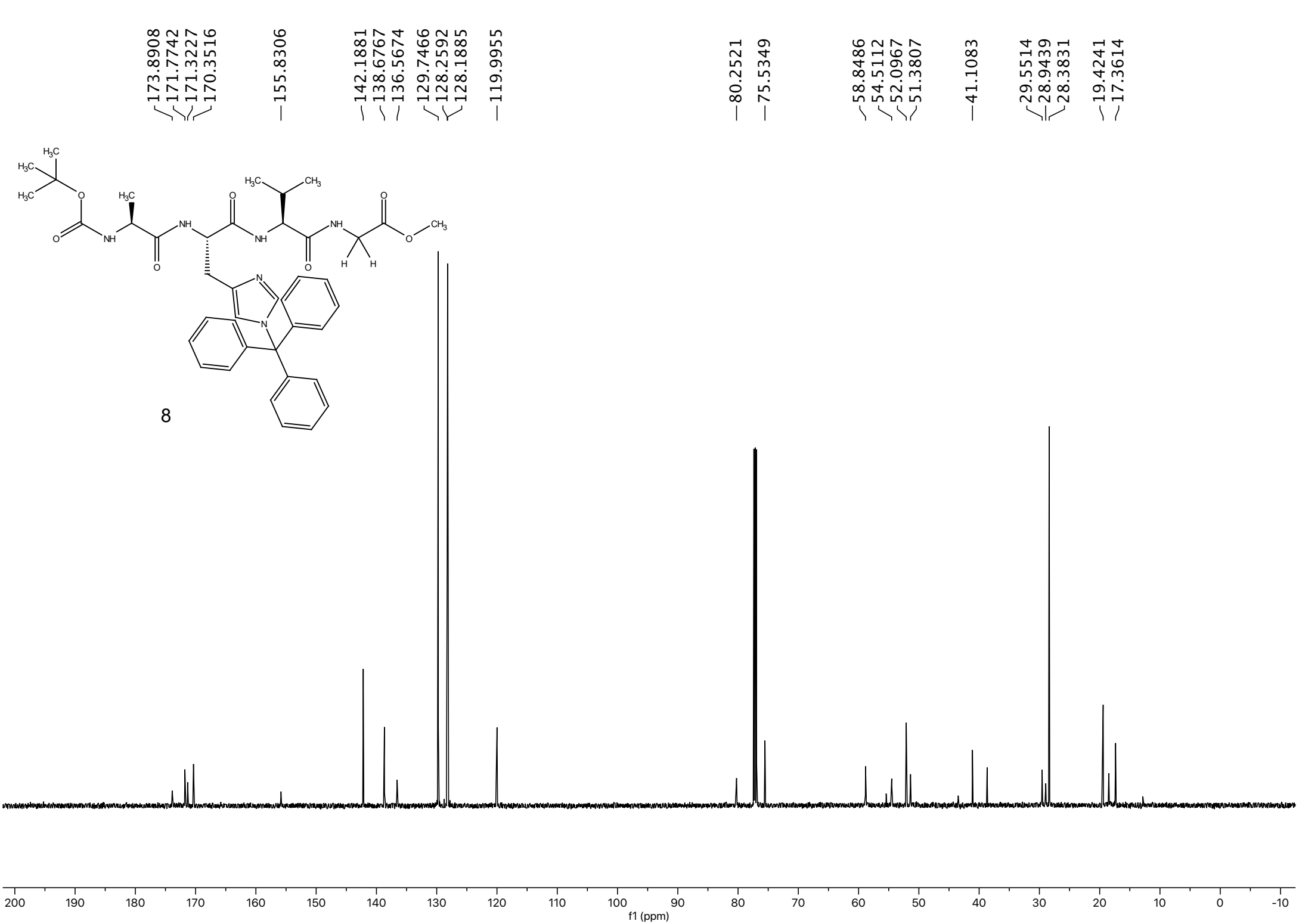
173.8908
171.7742
171.3227
170.3516
155.8306
142.1881
138.6767
136.5674
129.7466
128.2592
128.1885
119.9955
80.2521
75.5349
58.8486
54.5112
52.0967
51.3807
41.1083
29.5514
28.9439
28.3831
19.4241
17.3614
8
200
190
180
170
160
150
140
130
120
110
100
90
80
70
60
50
40
30
20
10
0
-10
f1 (ppm)

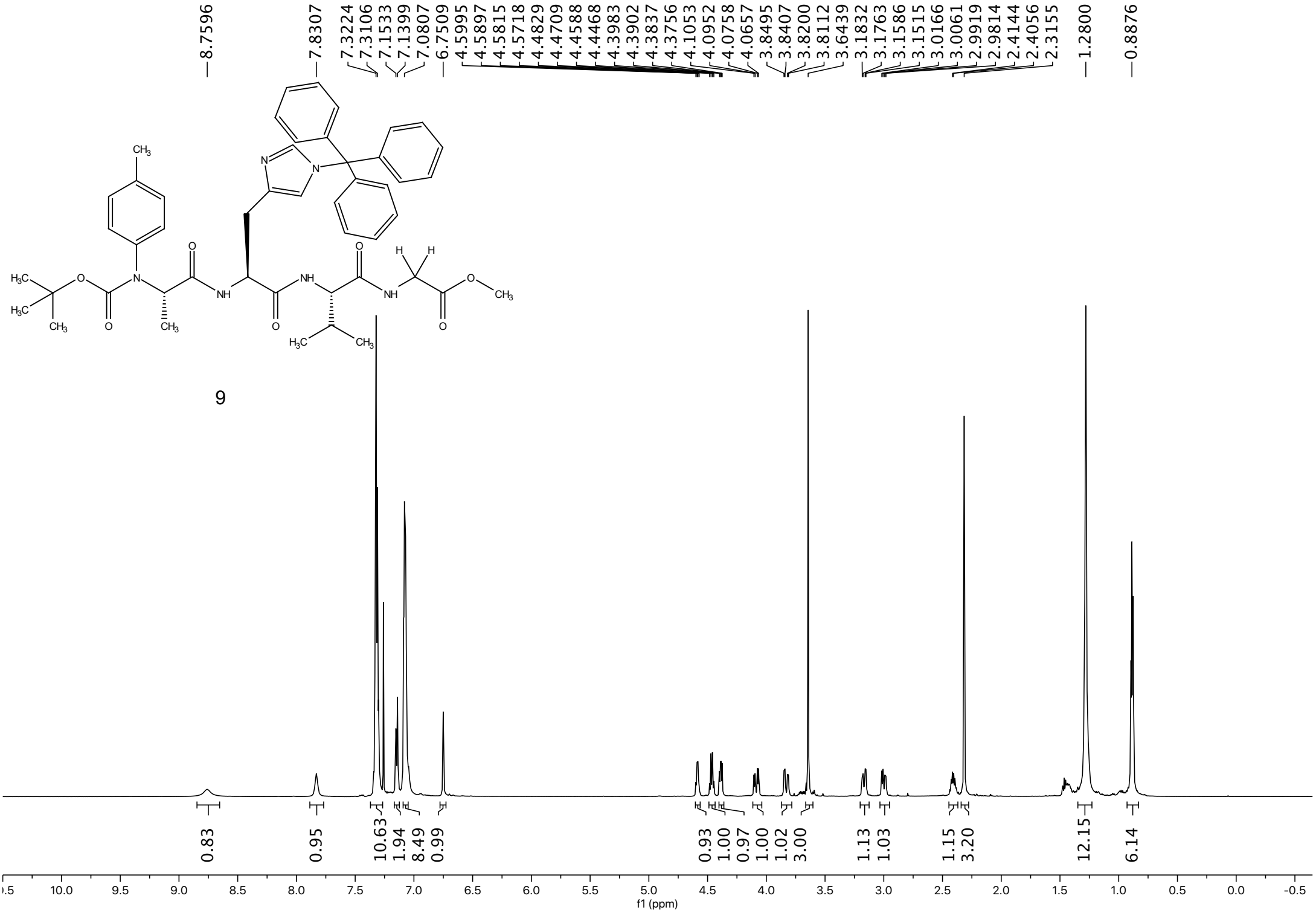
8.7596
7.8307
7.3224
7.3106
7.1533
7.1399
7.0807
6.7509
4.5995
4.5897
4.5815
4.5718
4.4829
4.4709
4.4588
4.4468
4.3983
4.3902
4.3837
4.3756
4.1053
4.0952
4.0758
4.0657
3.8495
3.8407
3.8200
3.8112
3.6439
3.1832
3.1763
3.1586
3.1515
3.0166
3.0061
2.9919
2.9814
2.4144
2.4056
2.3155
1.2800
0.8876
0.83
0.95
10.63
1.94
8.49
0.99
0.93
1.00
0.97
1.00
1.02
3.00
1.13
1.03
1.15
3.20
12.15
6.14
f1 (ppm)

9

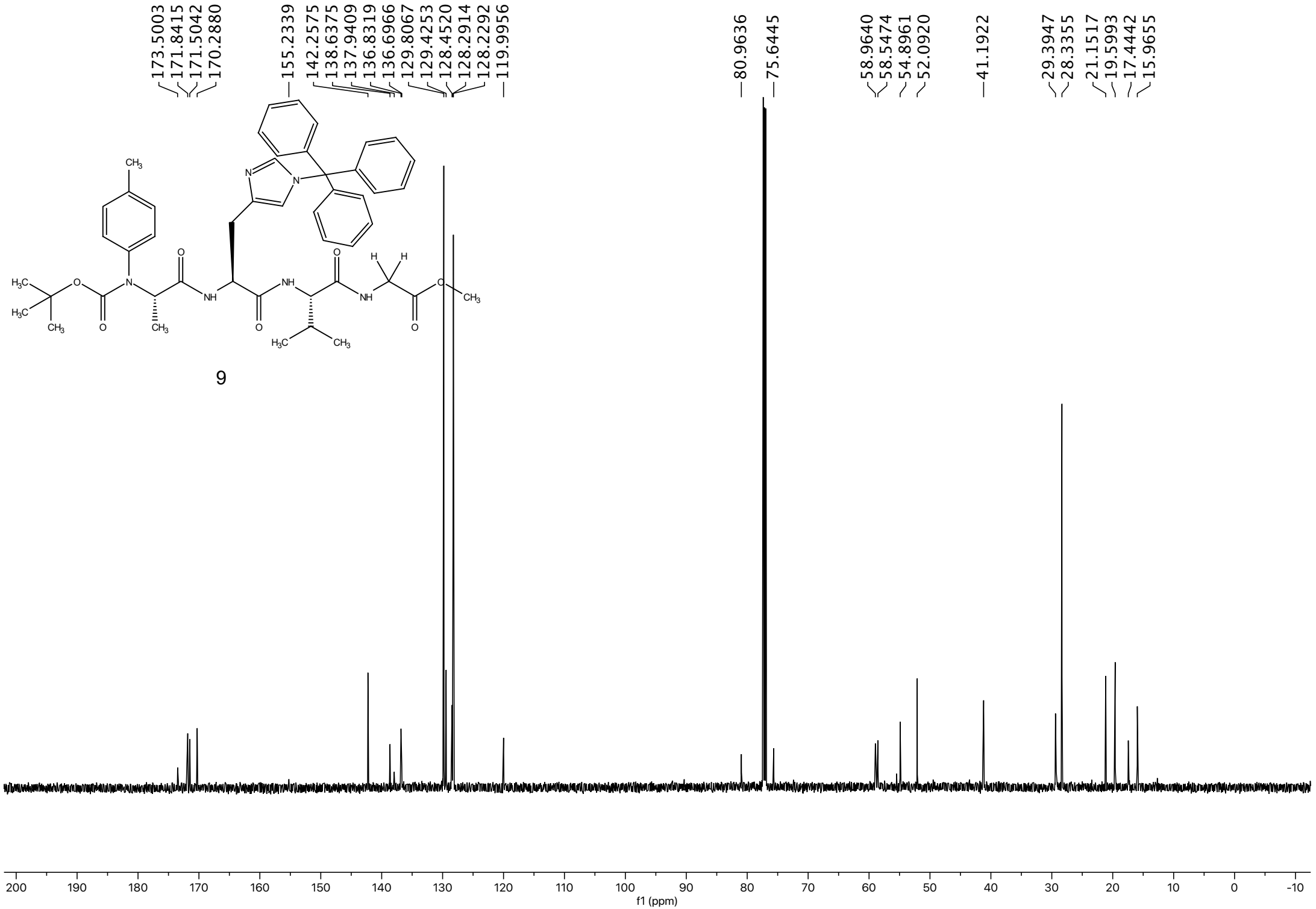
173.5003
171.8415
171.5042
170.2880
155.2339
142.2575
138.6375
137.9409
136.8319
136.6966
129.8067
129.4253
128.4520
128.2914
128.2292
119.9956
80.9636
75.6445
58.9640
58.5474
54.8961
52.0920
41.1922
29.3947
28.3355
21.1517
19.5993
17.4442
15.9655
9
f1 (ppm)

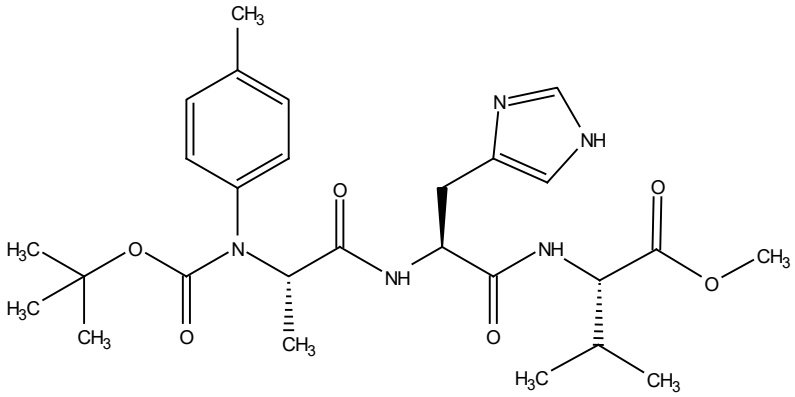

11

7.8628
7.6177
7.5564
7.1347
7.1289
7.1232
7.1084
7.0934
6.8323
4.7880
4.7783
4.7680
4.7581
4.5536
4.5416
4.5296
4.5176
4.4046
4.3959
4.3908
4.3821
3.7081
3.1751
3.1672
3.1500
3.1421
3.1111
3.1012
3.0858
3.0759
2.3284
2.1648
2.1557
2.1530
2.1442
2.1414
2.1322
1.3602
1.3048
1.2933
0.8643
0.8585
0.8529
0.8470
0.85
0.90
1.12
4.40
1.08
1.04
1.07
1.07
3.00
1.07
1.07
3.02
1.12
9.69
3.26
3.05
3.04
f1 (ppm)

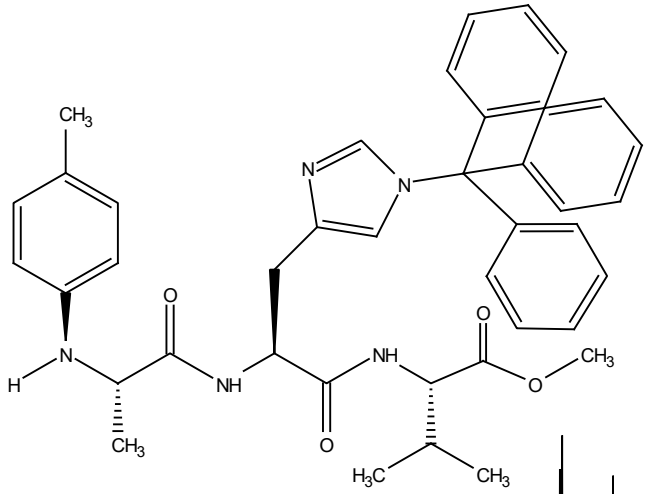

12

8.7021
8.6899
7.2985
7.1056
7.0911
7.0370
7.0256
6.9205
6.9068
6.6385
6.5274
6.5135
4.6819
4.6730
4.6610
4.6520
4.3734
4.3646
4.3589
4.3500
3.9515
3.9043
3.8930
3.8815
3.8703
3.6984
3.1208
3.1124
3.0960
3.0877
2.8973
2.8880
2.8726
2.8633
2.1642
1.9262
1.9168
1.4791
1.4675
0.7197
0.7083
0.6076
0.5962
0.97
9.21
1.01
1.08
6.07
2.02
0.98
2.00
1.00
1.00
0.91
1.05
3.00
1.00
0.99
3.01
1.07
3.11
2.96
2.95
f1 (ppm)

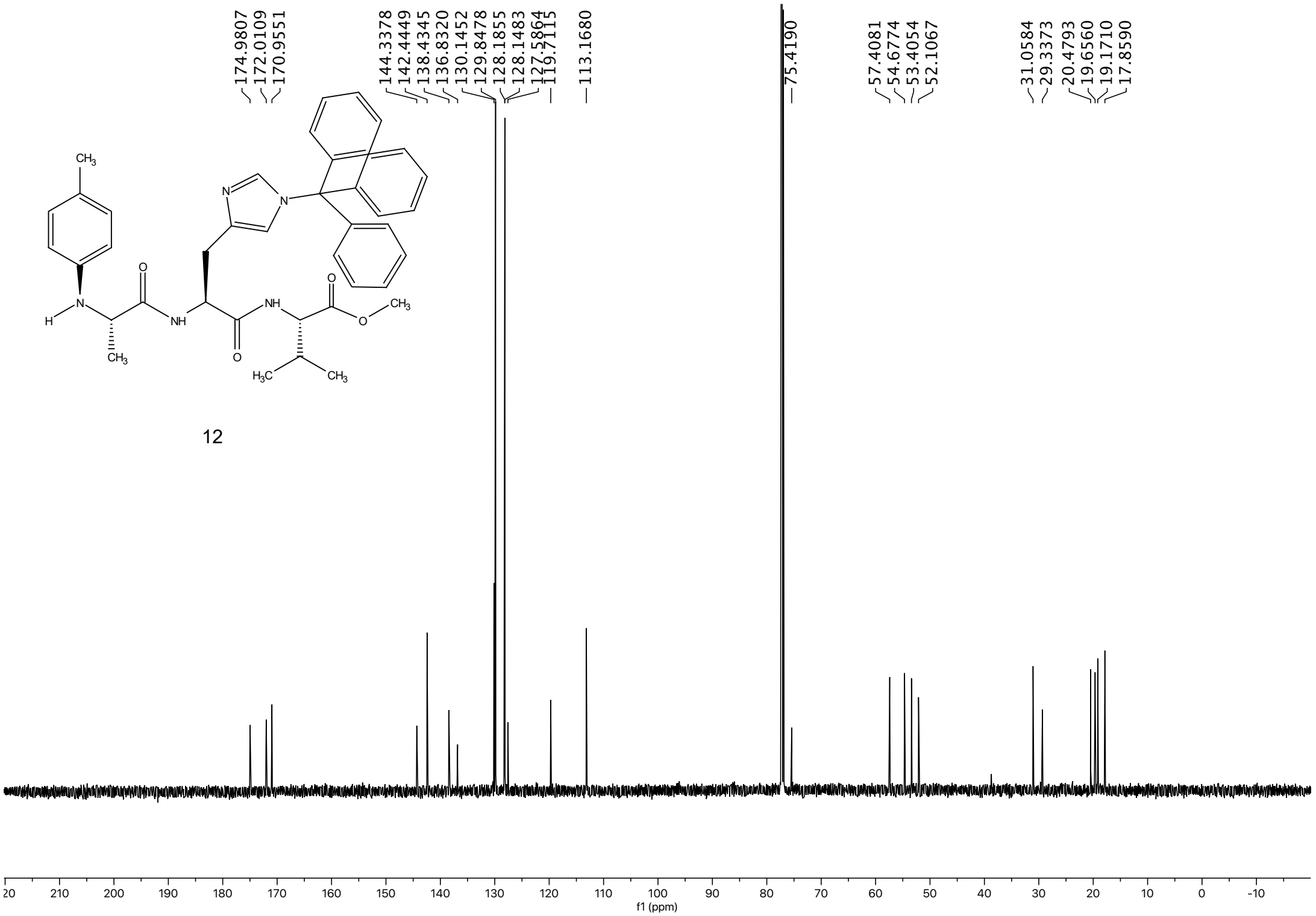
174.9807
172.0109
170.9551
144.3378
142.4449
138.4345
136.8320
130.1452
129.8478
128.1855
128.1483
127.5864
119.7115
113.1680
75.4190
57.4081
54.6774
53.4054
52.1067
31.0584
29.3373
20.4793
19.6560
19.1710
17.8590
f1 (ppm)

12